MAGNETIC RESONANCE SPECTROSCOPY OF GABA AND GLUTAMATE IN MENTAL HEALTH

EDITED BY: Maria Concepcion Garcia Otaduy,
Marcio Gerhardt Soeiro-de-Souza and Richard Edden

PUBLISHED IN: Frontiers in Psychiatry and Frontiers in Human Neuroscience

frontiers Research Topics

frontiers

ISSN 1664-8714
ISBN 978-2-88974-546-3
DOI 10.3389/978-2-88974-546-3

About Frontiers

Frontiers is more than just an open-access publisher of scholarly articles: it is a pioneering approach to the world of academia, radically improving the way scholarly research is managed. The grand vision of Frontiers is a world where all people have an equal opportunity to seek, share and generate knowledge. Frontiers provides immediate and permanent online open access to all its publications, but this alone is not enough to realize our grand goals.

Frontiers Journal Series

The Frontiers Journal Series is a multi-tier and interdisciplinary set of open-access, online journals, promising a paradigm shift from the current review, selection and dissemination processes in academic publishing. All Frontiers journals are driven by researchers for researchers; therefore, they constitute a service to the scholarly community. At the same time, the Frontiers Journal Series operates on a revolutionary invention, the tiered publishing system, initially addressing specific communities of scholars, and gradually climbing up to broader public understanding, thus serving the interests of the lay society, too.

Dedication to Quality

Each Frontiers article is a landmark of the highest quality, thanks to genuinely collaborative interactions between authors and review editors, who include some of the world's best academicians. Research must be certified by peers before entering a stream of knowledge that may eventually reach the public - and shape society; therefore, Frontiers only applies the most rigorous and unbiased reviews.
Frontiers revolutionizes research publishing by freely delivering the most outstanding research, evaluated with no bias from both the academic and social point of view. By applying the most advanced information technologies, Frontiers is catapulting scholarly publishing into a new generation.

What are Frontiers Research Topics?

Frontiers Research Topics are very popular trademarks of the Frontiers Journals Series: they are collections of at least ten articles, all centered on a particular subject. With their unique mix of varied contributions from Original Research to Review Articles, Frontiers Research Topics unify the most influential researchers, the latest key findings and historical advances in a hot research area! Find out more on how to host your own Frontiers Research Topic or contribute to one as an author by contacting the Frontiers Editorial Office: frontiersin.org/about/contact

MAGNETIC RESONANCE SPECTROSCOPY OF GABA AND GLUTAMATE IN MENTAL HEALTH

Topic Editors:
Maria Concepcion Garcia Otaduy, University of São Paulo, Brazil
Marcio Gerhardt Soeiro-de-Souza, University of São Paulo, Brazil
Richard Edden, Johns Hopkins University, United States

Citation: Otaduy, M. C. G., Soeiro-de-Souza, M. G., Edden, R., eds. (2022). Magnetic Resonance Spectroscopy of GABA and Glutamate in Mental Health. Lausanne: Frontiers Media SA. doi: 10.3389/978-2-88974-546-3

Table of Contents

frontiers in Psychiatry

EDITORIAL
published: 11 March 2022
doi: 10.3389/fpsyt.2022.866356

Editorial: Magnetic Resonance Spectroscopy of GABA and Glutamate in Mental Health

*Maria Concepcion Garcia Otaduy**

LIM44, Instituto e Departamento de Radiologia, Faculdade de Medicina, Universidade de São Paulo, São Paulo, Brazil

Keywords: magnetic resonance spectroscopy, GABA, glutamate, mental health, MEGA-PRESS

Editorial on the Research Topic

Magnetic Resonance Spectroscopy of GABA and Glutamate in Mental Health

This Research Topic presents a variety of studies that illustrate the vast potential that magnetic resonance spectroscopy (MRS) offers to investigate glutamate (Glu) and/or gamma aminobutyric acid (GABA) metabolism related to different psychiatric conditions. GABA is the primary inhibitory neurotransmitter in the brain, and Glu the principal excitatory transmitter. For several aspects of mental health, it is important that there is a balance between both of these molecules, and it is already known that in several psychiatric conditions (i.e., schizophrenia, depression, bipolar disorder, autism), one or both of these metabolites are altered. Currently, MRS is the only non-invasive neuroimaging technique that allows *in vivo* investigation of glutamatergic and GABAergic abnormalities within brain regions of interest.

Four thorough reviews, eight original research papers, three brief research reports, and one methods paper compose the present Research Topic, in an attempt to bring a diverse overview about the current possibilities to study the roles of GABA and Glu in mental health by MRS.

The review *Glutamate and GABA Homeostasis and Neurometabolism in Major Depressive Disorder* presents a comprehensive introduction about the role of Glu and GABA in brain homeostasis and metabolism, and describes briefly how these metabolites can be measured by 1H- and 13C-MRS. It then summarizes how these processes appear to be unbalanced in several psychiatric diseases, with an emphasis in major depressive disorder, and how antidepressant treatment affects the glutamatergic and GABAergic systems (Sarawagi et al.).

Four of the original research articles in this topic focus on investigating Glu/Glx and/or GABA alterations in different psychiatric disorders: Obsessive-compulsive disorder, schizophrenia, bipolar disorder, and depression. Interestingly all of them studied a large group of patients ($\geq$40), allowing the researchers to investigate possible associations with disease duration or other clinical variables, in an attempt to contribute robust and reproducible results to the field.

The methodologies used in these four studies are very diverse. In *Higher levels of pro-inflammatory cytokines are associated with higher levels of glutamate in the anterior cingulate cortex in depressed adolescents*, the authors used a single voxel PRESS sequence, a robust and fast acquisition, with the main focus of quantifying Glu and ascorbate (Ho et al.). In *Increased Glutamate plus Glutamine in the Right Middle Cingulate in Early Schizophrenia but not in Bipolar Psychosis: A Whole Brain 1H-MRS Study*, a more time-demanding (about 17 min) 3D-MRSI EPSI sequence was used, which allows the construction of whole-brain metabolite maps that can be compared between groups to identify the location of individual voxels presenting statistical significant differences (Bustillo et al.). This is a very interesting approach, as metabolic changes can occur at different regions, and

OPEN ACCESS

Edited and reviewed by:
Michael Kluge,
University Hospital Leipzig, Germany

***Correspondence:**
Maria Concepcion Garcia Otaduy
maria.otaduy@hc.fm.usp.br

Specialty section:
This article was submitted to Molecular Psychiatry, a section of the journal Frontiers in Psychiatry

Received: *31 January 2022*
Accepted: *03 February 2022*
Published: *11 March 2022*

Citation:
Otaduy MCG (2022) Editorial: Magnetic Resonance Spectroscopy of GABA and Glutamate in Mental Health. Front. Psychiatry 13:866356. doi: 10.3389/fpsyt.2022.866356

conventional single voxel spectroscopy also suffers from partial volume effects due to larger voxel sizes. But none of these techniques at 3T allow for quantification of GABA. For this purpose the use of editing techniques like MEGA-PRESS or 2D-JPRESS, as adopted in *Lower ventromedial prefrontal cortex glutamate levels in patients with obsessive-compulsive disorder*, is necessary (Batistuzzo et al.). At ultra-high fields (≥7T), the chemical shift dispersion is large enough to enable the distinction of GABA, Glu, and glutamine from the other overlapping metabolites, without the need of using editing pulses, as shown in *Metabolite alterations in adults with schizophrenia, first degree relatives, and healthy controls: a multi-region 7T MRS study* (Wijtenburg, Wang, et al.). There is no doubt that the MRS field in psychiatry will hugely benefit from the slowly increasing number of MRS studies conducted at 7T.

In *GABA, glutamate, and neural activity: a systematic review with meta-analysis of multimodal 1H-MRS-fMRI studies*, the authors successfully gather evidence to elucidate the relationship between GABA/Glu and brain activation, in the resting state and during stimulation (Kiemes et al.).

This Research Topic also includes several examples of how multimodal 1H-MRS-fMRI studies can enhance our understanding of brain function and metabolism. In *Simultaneous measurement of the BOLD effect and metabolic changes in response to visual stimulation using the MEGA-PRESS sequence at 3 T*, the authors implement an interesting method, using an MEGA-edited GABA-PRESS sequence at 3T, to measure simultaneously the BOLD effect from the linewidth of the unsuppressed water spectrum, and the changes in both Glx and GABA levels in the occipital cortex during visual stimulation (Dwyer et al.). The method proved to be very reliable for measuring the BOLD effect from the water signal linewidth, but still needs further validation for proper metabolite quantification. In *Multimodal Neuroimaging Study of Visual Plasticity in Schizophrenia*, the authors are able to demonstrate, by using a paradigm-based fMRI experiment, that visual plasticity in schizophrenia is impaired and that it is related to basal GABA levels (Wijtenburg, West, et al.). In a different approach, the authors of *Glutamate- and GABA-modulated connectivity in auditory hallucinations—a combined resting state fMRI and MR spectroscopy study* use functional connectivity results from resting state fMRI data to show that its association with metabolic levels of Glu and GABA is different according to auditory verbal hallucination severity in patients with psychosis (Weber et al.). And in *Unaltered Brain GABA concentrations and Resting fMRI Activity in Functional Dyspepsia with and without Comorbid Depression*, the authors also use resting state fMRI data to evaluate possible differences in brain activation and metabolism between patients with functional dyspepsia with and without major depression disorder (Mak et al.).

The review *Local and Interregional Neurochemical Associations Measured by Magnetic Resonance Spectroscopy for Studying Brain Functions and Psychiatric Disorders* presents the basis for neurochemical association of glutamate with GABA, NAA, and glutamine and discusses the importance of observing this association, as it can be altered in specific mental health disorders (Shen et al.). In such an endeavor, they highlight the role of spectral editing spectroscopy techniques in eliminating unwanted correlations caused by spectral overlapping. The paper ends with a review of the methods available to correctly quantify the strength of these neurometabolic associations, not only locally but also between different brain regions by using chemical shift imaging (CSI). For CSI, the combination of ultra-high field strengths (7T) is desired, as it allows the researchers to resolve Glu and GABA without the use of highly selective editing pulses and simplifies the multivoxel acquisition process.

In the review paper *Elevated brain glutamate levels in bipolar disorder and pyruvate carboxylase-mediated anaplerosis*, the authors show supporting evidence for the interesting hypothesis that elevated Glu levels in bipolar disorder can be explained by increased pyruvate carboxylase-mediated anaplerosis in the brain (Shen and Tomar).

This Research Topic includes also three brief research reports that bring very promising preliminary results about the use of MEGA-PRESS at 3T in longitudinal studies to monitor treatment or intervention effects: *Intermittent theta-burst stimulation transcranial magnetic stimulation increases GABA in the medial prefrontal cortex: a preliminary sham-controlled magnetic resonance spectroscopy study in acute bipolar depression* (Diederichs et al.); *Left dorsolateral prefrontal cortex Glx/tCr predicts efficacy of high frequency 4- to 6-week rTMS treatment and is associated with symptom improvement in adults with major depressive disorder: Findings from a pilot study* (Bhattacharyya et al.); and *Cortical Glutamate and GABA changes during Early Abstinence in Alcohol Dependence and their Associations with Benzodiazepine Medication* (Wang et al.).

As a final remark, the importance of the methods paper *Feasibility of measuring GABA levels in the upper brainstem in healthy volunteers using edited MRS* needs to be highlighted, since it opens up a new scope of research to address some important brain functions in the brainstem, and their relation to mental health (Song et al.). The upper brainstem contains many integrative nuclei that mediate physiological functions, known to be disrupted in neurodegenerative diseases. In this paper, the authors show the feasibility of acquiring high-quality 3T GABA-specific MEGA-PRESS spectra in the upper brainstem.

Throughout the Research Topic, methodological rigor, especially in relation to spectroscopy acquisition techniques, was one of the top priorities in the preparation of this volume, as we understand this is necessary for obtaining meaningful results that can contribute to the field. In the last few years, the MRS scientific community has been making a huge effort to establish useful guidelines for MRS acquisition and reports (1–5). Hopefully this will also facilitate large-scale collaborative MRS studies about Glu and GABA in psychiatric conditions similar to that proposed by the ENIGMA consortium for genetic and neuroimaging data.

AUTHOR CONTRIBUTIONS

The author confirms being the sole contributor of this work and has approved it for publication.

REFERENCES

1. Wilson M, Andronesi O, Barker PB, Bartha R, Bizzi A, Bolan PJ, et al. Methodological consensus on clinical proton MRS of the brain: Review and recommendations. *Magn Reson Med*. (2019) 82:527–50. doi: 10.1002/mrm.27742
2. Lin A, Andronesi O, Bogner W, Choi IY, Coello E, Cudalbu C, et al. Experts' Working group on reporting standards for mr spectroscopy. minimum reporting standards for *in vivo* magnetic resonance spectroscopy (MRSinMRS): experts' consensus recommendations. *NMR Biomed*. (2021) 34:e4484. doi: 10.1002/nbm.4484
3. Choi IY, Andronesi OC, Barker P, Bogner W, Edden RAE, Kaiser LG, et al. Spectral editing in ^{1} H magnetic resonance spectroscopy: Experts' consensus recommendations. *NMR Biomed*. (2021) 34:e4411. doi: 10.1002/nbm.4411
4. Near J, Harris AD, Juchem C, Kreis R, Marjańska M, Öz G, et al. Preprocessing, analysis and quantification in single-voxel magnetic resonance spectroscopy: experts' consensus recommendations. *NMR Biomed*. (2021) 34:e4257. doi: 10.1002/nbm.4257
5. Öz G, Deelchand DK, Wijnen JP, Mlynárik V, Xin L, Mekle R, et al. Experts' Working Group on Advanced Single Voxel 1H MRS. Advanced single voxel ^{1}H magnetic resonance spectroscopy techniques in humans: experts' consensus recommendations. *NMR Biomed*. (2020) 10:e4236. doi: 10.1002/nbm.4236

Conflict of Interest: The author declares that the research was conducted in the absence of any commercial or financial relationships that could be construed as a potential conflict of interest.

Publisher's Note: All claims expressed in this article are solely those of the authors and do not necessarily represent those of their affiliated organizations, or those of the publisher, the editors and the reviewers. Any product that may be evaluated in this article, or claim that may be made by its manufacturer, is not guaranteed or endorsed by the publisher.

frontiers in Psychiatry

REVIEW
published: 11 August 2020
doi: 10.3389/fpsyt.2020.00802

Local and Interregional Neurochemical Associations Measured by Magnetic Resonance Spectroscopy for Studying Brain Functions and Psychiatric Disorders

Jun Shen, Dina Shenkar, Li An and Jyoti Singh Tomar*

Molecular Imaging Branch, National Institute of Mental Health, Bethesda, MD, United States

Magnetic resonance spectroscopy (MRS) studies have found significant correlations among neurometabolites (*e.g.*, between glutamate and GABA) across individual subjects and altered correlations in neuropsychiatric disorders. In this article, we discuss neurochemical associations among several major neurometabolites which underpin these observations by MRS. We also illustrate the role of spectral editing in eliminating unwanted correlations caused by spectral overlapping. Finally, we describe the prospects of mapping macroscopic neurochemical associations across the brain and characterizing excitation–inhibition balance of neural networks using glutamate- and GABA-editing MRS imaging.

Keywords: glutamate, GABA, neurochemical correlations, magnetic resonance spectroscopy, spectral editing, psychiatric disorders

OPEN ACCESS

Edited by:
Maria Concepcion Garcia Otaduy, University of São Paulo, Brazil

Reviewed by:
Mark Mikkelsen, Johns Hopkins University, United States
Stefania Schiavone, University of Foggia, Italy

****Correspondence:***
Jun Shen
shenj@intra.nimh.nih.gov

Specialty section:
This article was submitted to Molecular Psychiatry, a section of the journal Frontiers in Psychiatry

Received: *08 June 2020*
Accepted: *27 July 2020*
Published: *11 August 2020*

Citation:
Shen J, Shenkar D, An L and Tomar JS (2020) Local and Interregional Neurochemical Associations Measured by Magnetic Resonance Spectroscopy for Studying Brain Functions and Psychiatric Disorders. Front. Psychiatry 11:802. doi: 10.3389/fpsyt.2020.00802

INTRODUCTION

In vivo MRS is the only noninvasive technique that can directly measure brain chemicals *in vivo*. Using techniques similar to MRI, MRS can measure concentrations of many neurometabolites as well as metabolic fluxes from localized brain regions (1). Over the past decades, MRS studies have found biochemical abnormalities in essentially all neuropsychiatric disorders, providing important insights into our understanding of etiologies and treatments of various brain diseases. These studies have, in most cases, focused on alterations in the concentrations of individual brain neurometabolites by comparing them among different cohorts and/or effects of treatments.

Many significant correlations among neurometabolites and between individual neurometabolites and non-MRS measures of brain function and disorders have been reported more recently. Altered correlations have been found in neuropsychiatric disorders, revealing abnormal neurochemical associations under pathophysiological conditions [e.g., (2–12)]. The strong correlations among N-acetylaspartate (NAA)/choline in precentral gyrus, midcingulate cortex, and thalamus found in healthy subjects were absent in patients with amyotrophic lateral sclerosis (4). Correlation between hippocampal Glx (glutamate + glutamine) and NAA has been demonstrated to be a more sensitive biomarker differentiating between healthy controls and schizophrenia patients than either neurometabolite alone (6, 7). In patients with subclinical hepatic encephalopathy the occipital

lobe phosphodiester measured by ^{31}P MRS and Glx levels were found to be negatively correlated (13). Interregional correlations of glutamate and GABA levels have also been reported in many studies [e.g., (8, 14–17)]. These studies have clearly demonstrated that neurochemical associations are abnormally altered in many brain disorders, but the absolute strengths of these correlations measured by different MRS methodologies have been inconsistent or controversial [e.g., (5, 14, 15, 18–23)]. In particular, the effects of spectral overlap on the observed neurometabolite correlations have yet to be illustrated although they can significantly confound the intrinsic neurochemical correlations of interest.

Many studies of neurochemical associations rely on spectral fitting [e.g., (24)] to extract neurometabolite concentrations from overlapping signals. When there is significant spectral overlap between two signals overestimate of one signal is statistically correlated with underestimate of the other signal and *vice versa*, even when there exists no neurochemical correlation between the two signals. In addition, this type of statistical correlations can propagate due to the intensity constraints imposed by LCModel (24) or overlapping with neurochemically correlated signals. When neurometabolite concentrations are correlated with other measurements (e.g., behavior, resting state fMRI functional connectivity, or gene expression), statistical correlations due to spectral overlap among MRS measurements can also affect correlations between MRS measurements and non-MRS measurements.

In this article we review dominant metabolic pathways connecting major neurometabolites (25–27) which underpin the neurochemical associations detected by MRS correlation studies. Non-MRS neurochemical studies of animal models that found correlated changes in neurometabolite concentrations under various pathophysiological conditions are also discussed. Monte Carlo simulations are performed to demonstrate the existence of statistical correlations that originated from spectral overlap. Finally, we discuss MRS techniques that eliminate spectral overlap and associated statistical correlations. We hope that these discussions will spur interest in developing MRS techniques for mapping neurochemical associations across the brain to facilitate a variety of clinical investigations. In particular, since glutamate and GABA play dominant roles in the excitation–inhibition balance (28, 29) and in many neuropsychiatric disorders (30–33), MRS characterization of glutamate–GABA associations among the nodes of neural networks may provide considerable insight into the interactions between glutamatergic and GABAergic systems and their abnormalities.

METABOLIC PATHWAYS UNDERLYING NEUROCHEMICAL ASSOCIATIONS

Predominant metabolic pathways connecting NAA, glutamate, glutamine, and GABA are reviewed in detail. For clarity, a table summarizing these pathways is provided (**Table 1**).

NAA-Glutamate Association

NAA is the most abundant free amino acid derivative in the CNS. NAA is found almost exclusively within the nervous system. In the adult brain, it is mostly confined to neurons. As such, it is of great clinical interest as it has been considered as a neuronal marker for assessment of neuronal viability in a variety of neuropsychiatric disorders using proton MRS. For example, NAA level is markedly reduced within the infarct of stroke patients (34), while a higher NAA level is associated with a better clinical outcome (35). Despite the intense interest in NAA, both its physiological and metabolic roles in normal brain functions as well as in neuropsychiatric disorders remain poorly understood [for a review of the putative role of NAA, see (36)].

TABLE 1 | Predominant metabolic pathways of NAA, glutamate, glutamine and GABA in brain.

Neurometabolites	Anabolic enzymes	Catabolic enzymes
NAA	NAA synthase	aspartoacylase
glutamate	aspartate aminotransferase, glutaminase, glutamate dehydrogenase	aspartate aminotransferase, glutamine synthetase, glutamate dehydrogenase, glutamic acid decarboxylase
glutamine	glutamine synthetase	glutaminase
GABA	glutamic acid decarboxylase	GABA transaminase

Important metabolic associations exist among major neurometabolites observable by MRS through precursor–product relationships and sharing common substrates (26, 37, 38). Glutamate, the most abundant intracellular amino acids in mammals, is a key component of intermediary metabolism and a precursor of numerous cellular components including proteins as well as neurometabolites such as GABA, N-acetylaspartylglutamate (NAAG), and glutathione (26). As glutamate is also the primary excitatory neurotransmitter in the CNS, it is not surprising that the proton MRS has found abnormal glutamate levels in many neuropsychiatric disorders including multiple sclerosis (39), major depression (40), and bipolar disorder (41) where glutamatergic dysfunction is broadly implicated.

Glutamate is primarily synthesized by transamination from α-ketoglutarate catalyzed by aspartate aminotransferase (25):

$$\text{glutamate} + \text{oxaloacetate} \leftrightarrow \alpha - \text{ketoglutarate} + \text{aspartate}$$

Glutamate also is produced, to a much lesser extent, from α-ketoglutarate and ammonium *via* glutamate dehydrogenase, from glutamine *via* hydrolysis catalyzed by phosphate-activated glutaminase, by other transamination reactions that use α-ketoglutarate as receptor of the amino group, and during protein turnover (42).

The transaminases of importance for maintenance of glutamate homeostasis in the brain are mainly aspartate aminotransferase, branched-chain aminotransferase, and alanine aminotransferase with aspartate aminotransferase dominating overwhelmingly, representing >97% of the glutamate-related aminotransferase activities (26). ^{13}C magnetization transfer MRS experiments have shown that the aspartate aminotransferase reaction is extremely fast in the brain *in vivo* (43). This rapid transamination by aspartate aminotransferase predominates in the formation of glutamate in the CNS, forming strong metabolic coupling between glutamate and aspartate (25). The tight connection between glutamate and

aspartate becomes conspicuous under many pathophysiological conditions where the brain is challenged or perturbed metabolically. For example, during hypoglycemia a decrease in glutamate concentration was accompanied by an increase in aspartate concentration (44–46). Similarly, barbiturate anesthesia and hypothermia were also found to lower the concentration of α-ketoglutarate accompanied by reduced glutamate concentration and increased aspartate concentration (47–49). These correlated changes in glutamate and aspartate were explained by a sizable shift in the aspartate aminotransferase reaction towards aspartate formation at the cost of a reduction in glutamate concentration (25, 26). In contrast, both hypocapnia and hypoxic hypoxia are associated with an increase in glutamate concentration and a reduction in aspartate concentration with the aspartate aminotransferase reaction shifting in the opposite direction (25, 26, 50).

A strong metabolic coupling between glutamate and aspartate mediated by the rapid and ubiquitous aspartate aminotransferase reaction also affects NAA, the dominant signal in proton MRS, as NAA is primarily synthesized from acetyl coenzyme A (CoA) and aspartate by NAA synthase (51):

$$\text{acetyl} - \text{CoA} + \text{aspartate} \rightarrow \text{CoA} + \text{H}^+ + \text{NAA}$$

In addition to this indirect connection from glutamate to NAA synthesis *via* aspartate, both glutamate and NAA are products of NAAG catabolism catalyzed by N-acetylated-α-linked-amino dipeptidase (52–54). The deacetylation of NAA catalyzed by aspartoacylase has also been proposed as a significant metabolic pathway for NAA to act as a reservoir for glutamate in brain (55).

Glutamate–Glutamine Association

In contrast to glutamate, which is predominantly located in glutamatergic neurons, glutamine is primarily an astrocytic chemical. In the MRS literature glutamate + glutamine is often collectively referred to as Glx as at lower magnetic fields it has been difficult to separate the two spectroscopically. Abnormal glutamine concentrations have been found in several brain disorders including cancer, hepatic encephalopathy, and other neuropsychiatric disorders (56, 57).

Although the overall glutamate pool in neural tissues rapidly turns over fueled by primarily glucose under normal physiological conditions, glutamate released from nerve terminals is replenished by astroglial glutamine *via* the glutamate–glutamine neurotransmitter cycle [**Figure 1**; (26, 59)]. The negatively charged highly hydrophilic glutamate cannot diffuse across cell membranes. The concentration of glutamate in the extracellular space is extremely low due to its rapid uptake into the astroglia facilitated by high-affinity Na^+-dependent transport systems against a large concentration gradient (60–62). Once taken up into the astroglial cells, glutamate is converted into glutamine by glutamine synthetase:

$$\text{glutamate} + \text{NH}_3 + \text{adenosin triphosphate}$$

$$\rightarrow \text{glutamine} + \text{adenosine diphosphate} + \text{P}_\text{i}$$

or oxidized by assimilation into the tricarboxylic acid cycle of astroglial cells (26, 63). Once formed, glutamine readily enters nerve terminals by its own low affinity transport system or by simple diffusion. There the phosphate-activated glutaminase converts it into glutamate (26):

$$\text{glutamine} + \text{H}_2\text{O} \rightarrow \text{glutamate} + \text{NH}_4^+$$

A large number of neurochemical as well as autoradiographic studies have confirmed that glutamate is selectively taken up by astroglial cells and then converted into glutamine, while glutamine preferentially enters the neurons and is converted into glutamate there (64). *In vivo* ^{13}C and ^{15}N MRS studies have quantitatively measured the glutamate–glutamine cycling flux in rodent and human brains [e.g., (58, 65–69)]. Results from these studies have demonstrated that the glutamate–glutamine cycle

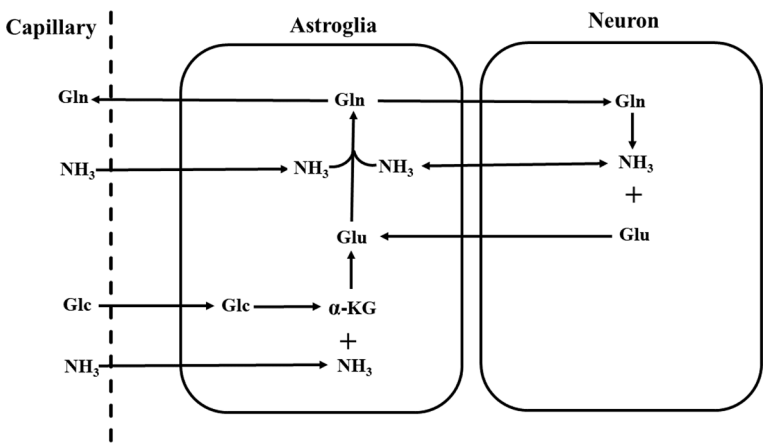

FIGURE 1 | Schematic diagram of the glutamate–glutamine neurotransmitter cycle between neurons and astroglia (58). Glutamate (Glu) is taken up from the synaptic cleft into astroglia. There glutamate is converted to glutamine (Gln) by glutamine synthetase. The inactive glutamine is released by the astroglia, enters the neurons, and then is converted into glutamate by phosphate-activated glutaminase. Glc, glucose; α-KG, α-ketoglutarate; NH_3, ammonia.

between glutamatergic neurons and astroglia is metabolically significant, providing a major connection between glutamate and glutamine in the brain (70). In addition, over the range of glutamate concentrations found in the nerve terminals, product inhibition appears to be the main mechanism of control of glutaminase activity with glutamate significantly attenuating the activity of glutaminase (71).

The metabolic connection between glutamate and glutamine is manifested in many brain disorders and animal models. For example, elevated ammonia level in the brain is associated with increased glutamine synthesis for ammonia detoxification (67). It has been reported that in hyperammonemia and hepatic encephalopathy the elevation of glutamine level in the brain is accompanied by a reduced glutamate level as glutamate acts as a receptor for the excessive ammonia (72). The changes in glutamate and glutamine levels, however, do not necessarily go in opposite directions. Both glutamate and glutamine are abundant in the brain. Despite efforts to understand the roles of glutamate and glutamine, the reason for maintaining relatively high concentrations of glutamate and glutamine in the brain is still poorly understood. It is possible that a high concentration of glutamate and glutamine facilitates the generally high metabolic activities in the brain because glutamate and glutamine are key components of intermediary metabolism (25). They are also precursors of many other cellular components (26). Their role as "energy reservoirs" is particularly clear when the brain is under metabolic stress. For example, when glucose is scarce, such as in hypoglycemia, both glutamate and glutamine act as energy fuels. As a result, the concentrations of both glutamate and glutamine are reduced in synchrony during hypoglycemia and in many other pathophysiological conditions when normal oxidative metabolism is impaired (45, 73).

Glutamate–GABA Association

While glutamate is the major excitatory neurotransmitter in the mammalian brain, GABA is the major inhibitory neurotransmitter. Since the initial detection of reduced GABA levels in epilepsy patients by MRS (74) and a strong correlation between GABA levels and seizure control in epilepsy patients treated by vigabatrin (75), MRS of GABA has greatly advanced both in terms of MRS methodologies and their clinical applications in studying GABAergic abnormalities in neuropsychiatric disorders.

Like glutamate, GABA metabolism proceeds through important intermediates of the tricarboxylic acid cycle. When GABA was first discovered (76) it was realized that GABA was formed from glutamate. Later studies identified that the principal pathway of GABA goes through α-decarboxylation of glutamate *via* glutamic acid decarboxylase which converts glutamate directly into GABA (77):

$$\text{glutamate} \rightarrow \text{GABA} + \text{CO}_2$$

The source of the GABA precursor is believed to be dominated by neuronal glucose with astroglial glutamine playing a smaller role (78–80). GABA synthesis from putrescine and other polyamines is metabolically insignificant in the brain although polyamines play an important role in the developing brain (81).

A fundamental aspect of glutamate–GABA association is the excitation–inhibition balance in the brain (32, 82) because of their roles as the dominant excitatory and inhibitory neurotransmitters, respectively, in the CNS. Glutamatergic neurons (e.g., cortical pyramidal neurons) receive a significant degree of $GABA_A$-mediated inhibition through interneurons (83). Balanced excitation and inhibition facilitate normal brain functions, and failure to maintain excitation–inhibition balance underlies dysfunction in many brain disorders (32, 33, 84). Many studies have also revealed altered glutamate and GABA. For example, GABA levels were found to decrease, whereas Glx levels increased with increasing visual input in the occipital cortex of healthy subjects (85). Both glutamate and GABA increased following vigorous exercise (86). In autistic patients the frontal lobe [GABA]/[Glu] ratio was found to be significantly lower, suggesting abnormality in the regulation between GABA and glutamate (87). Abnormalities in MRS measures of glutamate and/or GABA in many other neuropsychiatric disorders have also been reported and reviewed [e.g., (40, 88–90)].

Long range excitatory and inhibitory interactions between functionally connected brain regions are well established (91–93). The strong coupling between glutamatergic neurotransmission and total GABA level is supported by a large body of *in vitro* and *in vivo* evidence [e.g., (16, 75, 94–100)]. A large number of neuroimaging studies have also shown that total glutamate or Glx concentration is significantly correlated with neural activity or glutamatergic neurotransmission [e.g., (28, 101–103)]. Correlations of total glutamate and total GABA levels locally and among regions functionally connected in a specific neural network have also been reported [e.g., (15–17, 19)].

STATISTICAL CORRELATIONS AMONG MRS SIGNALS DUE TO SPECTRAL OVERLAP

Many neurometabolites have similar resonant frequencies, leading to spectral overlap among MRS signals. Effects of spectral overlap on the Cremer–Rao lower bounds of extracted neurometabolites have been analyzed previously (104). Extracting the concentrations of neurometabolites by spectral fitting is essentially mapping the acquired MRS spectrum (**spec**) into a vector (**conc**) consisting of concentrations by inverting the matrix equation **spec** = **basis** • **conc** (24). Here, **basis** is a matrix consisting of basis spectra of the component neurometabolites, which transforms the concentration vector **conc** into the fitted spectrum that approximates **spec** in the sense of least squares. Overlapping neurometabolites become statistically correlated through the covariance matrix (COV) of **conc** (105):

$$\text{COV}(\mathbf{conc}) = \sigma^2(\mathbf{basis}^\dagger \bullet \mathbf{basis})^{-1}$$

where † denotes Hermitian transposition and σ^2 is the noise variance of the measured spectrum **spec**. The off-diagonal elements (proportional to the square of cross-correlation coefficients) of COV(**conc**) depend on the frequency separation

among the resonances of the neurometabolites in **basis**. **Figure 2** shows Monte Carlo simulations of the correlation between two singlet peaks as a function of their separation in the frequency domain. **Figure 2A** shows the correlation between $conc_1$ and $conc_2$ across individual fits when spectral overlap between the two signals is minimal. The correlation between $conc_1$ and $conc_2$ when their frequency separation equals their half-height linewidth is plotted in **Figure 2B**. Finally, the correlation between $conc_1$ and $conc_2$ when their frequency separation equals 0.5* half-height linewidth is plotted in **Figure 2C**. As shown by **Figure 2** statistical correlation between these two neurochemically unrelated signals increases as their spectral overlap increases. Here the large correlation values occur when the two signals happen to exhibit similar chemical shifts, not because one signal influences the other neurochemically. This simple example of two overlapping singlets illustrates a point of caution in the interpretation of neurometabolite correlation results. For multiplets and neurometabolites with multiple resonances, spectral overlap occurs when two resonance lines overlap each other even when the chemical shifts are not very close.

The off-diagonal elements of the covariance matrix become highly significant in the presence of severe spectral overlap such as in short echo time MRS spectra. In addition to overlapping neurometabolites, a strong baseline can also cause statistical correlations (106, 107) because the baseline, which arises from macromolecules and/or lipids and residual water, overlaps with essentially all neurometabolite signals. **Figure 3** compares spectral fitting of two 3 T short echo time single voxel *in vivo* spectra by the commercial LCModel software. The spectrum on the left was acquired using short echo time Point RESolved Spectroscopy (PRESS) technique from a cubic voxel in the anterior cingulate cortex of a healthy subject at 3 T (echo time = 35 ms, voxel size = 8 ml). The spectrum on the right was generated by broadening the linewidths of the spectrum on the left by 2.0 Hz and adding random noise to maintain the same signal-to-noise ratio (107). Both spectra in **Figure 3** were fitted using LCModel with the same default settings (24). With 2.0 Hz line-broadening the LCModel baseline was conspicuously stronger around the spectral region near 2.35 ppm where glutamate and the aspartyl moiety of NAA resonate. Both NAA and glutamate levels reported by LCModel were lowered by approximately the same amount (~11%) after the line-broadening [n = 10; (107)]. This reduction in the extracted metabolite concentrations was found to be generally more pronounced with greater line-broadening. Although the concentrations of neurometabolites in the two spectra of **Figure 3** are identical, the LCModel produced lower neurometabolite levels and a more intense baseline after 2.0 Hz line-broadening. Because of the spectral overlap between baseline and neurometabolites, overestimating (underestimating) the baseline causes underestimating (overestimating) neurometabolites and *vice versa*. Neurometabolites overlapping with the same broad baseline peak are similarly underestimated (overestimated) due to the broad baseline signals. This in turn, contributes to positive statistical correlations among those neurometabolites regardless of the underlying neurochemical associations.

Spectral fitting techniques such as the LCModel heavily rely on the linewidth difference between neurometabolites and background signals to separate them. Broad neurometabolite peaks in the presence of a strong baseline, as often seen in clinical short echo time MRS data, can lead to significant quantification errors and unwanted statistical correlations because of the large baseline-metabolite covariances. The results in **Figure 3** are also corroborated by an earlier study which quantitatively analyzed the estimation uncertainties caused by the baseline using Cramer–Rao lower bound (CRLB) of the baseline (106), confirming that the estimation uncertainty significantly increases with decreased baseline smoothness and increased spectral linewidths.

PROSPECTS FOR MAPPING MACROSCOPIC NEUROCHEMICAL ASSOCIATIONS BY MRS IMAGING

Although group comparison of neurometabolite correlations between healthy controls and patients reveals altered neurochemical associations in brain disorders, determining the absolute strength

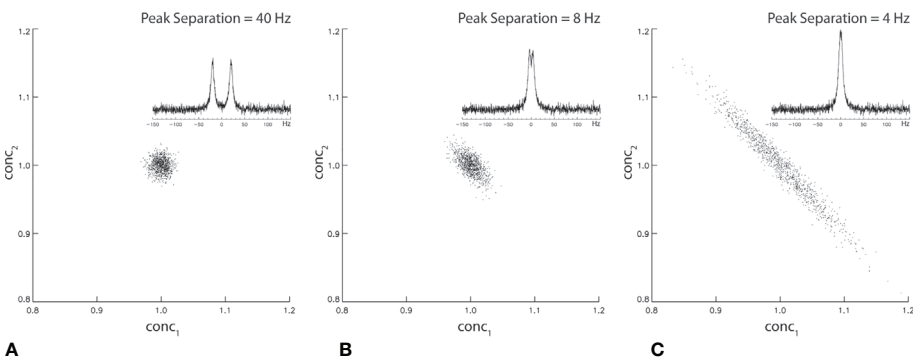

FIGURE 2 | Monte Carlo simulation of statistical correlation between two unrelated Lorentzian singlets with signal-to-noise ratio = 20. The half-height linewidth of the two peaks is 8 Hz. The same spectral fitting process was repeated 1,000 times with the same noise level but different noise realizations. For 40 Hz **(A)**, 8 Hz **(B)**, and 4 Hz **(C)** frequency separations between the two singlets, the correlation coefficient was found to be –0.04, –0.63, and –0.98, respectively.

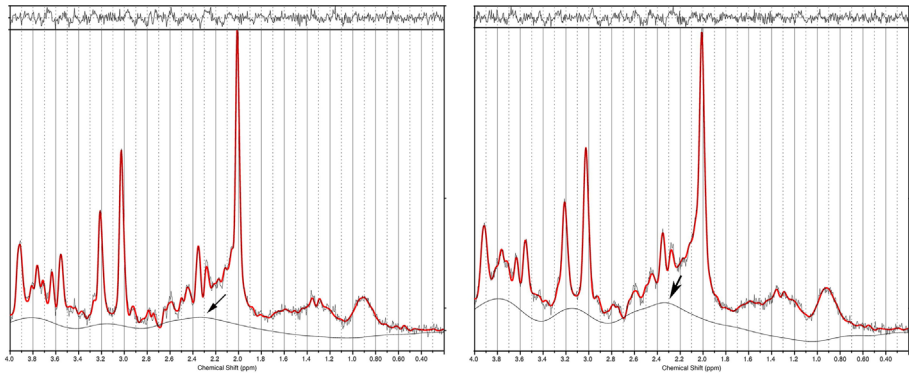

FIGURE 3 | (A) Single voxel short echo time spectrum acquired from the anterior cingulate cortex of a healthy subject at 3 T. Data was fitted using LCModel. **(B)** LCModel generated a different baseline from the same data after 2.0 Hz line-broadening and noise injection to maintain the same signal-to-noise ratio. The large change in baseline around 2.35 ppm (marked by an arrow) simultaneously reduced fitted NAA and glutamate concentrations, therefore, causing positive correlation between NAA and glutamate even though the only difference between the two spectra is their linewidth (*i.e.*, no correlations). Reprinted from reference (107) with permission from Elsevier.

of these correlations is important for interpreting clinical findings (20, 21) and for potentially relaying interregional associations across the brain. As linewidth variations in clinical MRS studies are very common, our analysis of statistical correlations that originated from the spectral overlap in the section *Statistical Correlations Among MRS Signals Due to Spectral Overlap* has demonstrated that spectral overlap should be eliminated or minimized when the absolute strength of neurometabolite correlations is to be determined. To facilitate measurement of the absolute strength of neurochemical associations, MRS techniques that result in flat baselines and isolated signals of interest would be ideal. Many existing single voxel spectral editing techniques generate flat or weak baselines while eliminating or minimizing overlapping resonances (74, 108–115), which are likely suited for measuring local or intraregional neurochemical associations.

Mapping macroscopic neurochemical associations across the human brain has the exciting potential to broadly impact studies of normal brain functions as well as neuropsychiatric disorders (32, 116, 117). Here we discuss the prospects for measuring interregional excitation–inhibition balance (32, 118–120) by spectroscopic imaging of spectrally resolved glutamate and GABA. Participant motion is a major issue in scanning many patients of neuropsychiatric disorders. Studying these patients using chemical shift imaging is technically challenging because of the relatively long scan time required for phase encoding. As artifacts in chemical shift images caused by motion are hard to detect, they can lead to erroneous diagnosis and data interpretation (121). It is well-known that participant motion inside a magnetic field causes changes in resonant frequencies. Incorporating spectral editing techniques based on highly selective radiofrequency pulses into chemical shift imaging therefore can lead to even larger errors due to the additional effects of carrier frequency mismatch on spectral editing yield.

To minimize error due to unavoidable patient movement during extended scan time necessary for phase encoding, we focus on techniques that can resolve glutamate or GABA in a single shot with relatively weak baselines at 7 T. Spectral isolation of glutamate or GABA accompanied with a weak baseline will minimize the unwanted correlations that originated from spectral overlap (107). The emphasis on minimizing spectral overlap for measuring interregional neurometabolite correlations may seem counterintuitive. However, it is necessary because, for example, overlapping with interregionally correlated signals can relay the correlation to overlapped signals. To spectrally resolve glutamate or GABA over an extended brain region, highly frequency-selective pulses popular for single voxel spectral editing cannot be used because of the unavoidable and significant residual B_0 inhomogeneity across a large volume in the brain, especially at high magnetic field strength. Highly frequency-selective pulses are sensitive to patient movement, system instability, and B_0 inhomogeneity as they will miss or partially miss the editing target in part of the slice(s) where resonance frequencies are shifted away (122, 123).

Weak or nearly flat baselines are automatically produced at long echo times because of the shorter T_2 values of macromolecules (1). Serendipitously, the strongly coupled glutamate H4 (2.35 ppm) forms an intense pseudo singlet at a relatively long echo time (~100 ms) at 7 T (111, 112). The resonances of glutamine H4 at 2.45 ppm and glutathione glutamyl H4 at 2.49 ppm also form pseudo singlets at ~100 ms echo time (see **Figure 4**). Therefore, glutamate can be spectrally resolved in a single shot without using any spectrally selective pulses at ~100 ms echo time at 7 T (111). At 7 T the multiplet signal of the aspartyl moiety of NAA at 2.49 ppm still overlaps with glutamine H4 and glutathione glutamyl H4 at ~100 ms echo time (111). The overlapping NAA aspartyl moiety signals can be eliminated using a J-suppression pulse acting on the α-H of the aspartyl moiety of NAA at 4.38 ppm (112). The J suppression pulse can be made band-selective with a flat top frequency profile (124) to accommodate variations in B_0. Either because no frequency selective pulses are needed (111) or

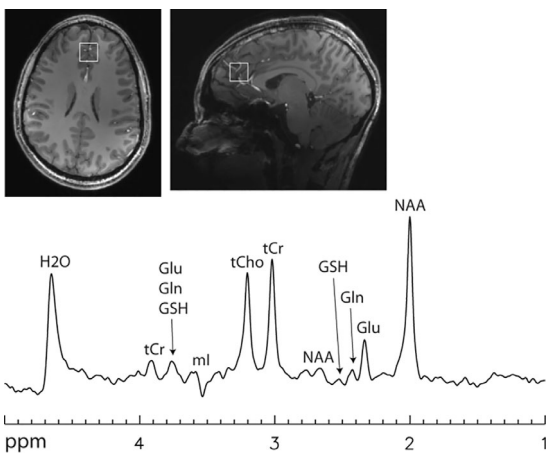

FIGURE 4 | Single voxel 7 T spectrum acquired using a single-shot echo time optimized PRESS sequence (112) without signal averaging. Voxel size = $2 \times 2 \times 2$ cm^3. Echo time = 106 ms. Line broadening = 8 Hz. Number of averages = 1. NAA, N-acetylaspartate; Glu, glutamate; Gln, glutamine; GSH, glutathione; tCr, total creatine; tCho, total choline; mI, myo-inositol. Glutamate H4 at 2.35 ppm was spectrally resolved with an approximately flat baseline.

with band-selective J suppression (112), chemical shift imaging of glutamate is feasible at 7 T in the presence of significant patient motion and residual static magnetic field inhomogeneity across the slice(s).

Multiple quantum filtering can be used to edit GABA in a single shot (125–128). It is also possible to generate a flat baseline using multiple quantum filtering (127). Chemical shift imaging of GABA over a large volume in the brain is challenging even at the high magnetic field strength of 7 T as all available GABA editing techniques rely on frequency selective pulses that differentially act on GABA H3 at 1.91 ppm and GABA H4 at 3.02 ppm. At 7 T, the chemical shift dispersion between GABA H3 and GABA H4 is 328 Hz. This relatively large chemical shift difference makes it possible to use band-selective pulses with a flat top (124) to accommodate changes in B_0 due to patient movement, system instability, and residual B_0 inhomogeneity while still affording a close to uniform editing yield. **Figure 5** proposes a band-selective multiple quantum filtering scheme that combines spectral selectivity while allowing signal to shift within the flat passband. This multiple quantum GABA editing scheme is expected to tolerate a large frequency shift with GABA H3 lying within the flat bandwidth and GABA H4 staying outside of the downfield transition band of the band-selective pulse acting on GABA H3.

Although we have focused on discussing chemical shift imaging of spectrally resolved glutamate and GABA without using highly selective editing pulses for the magnetic field strength of 7 T, similar ideas may also be developed for lower magnetic field strengths such as 3 T. For example, multiecho time averaging at 3 T can isolate glutamate with a nearly flat baseline without using any spectral editing pulses (109). Directly combining this approach with conventional phase-encoding for chemical shift imaging would not be feasible due to the large number [e.g., (32)] of echoes required for each phase encoding step. Instead of using evenly spaced echo times, the averaging effect may be obtained using fewer echo times with numerical optimization. Many fast imaging strategies such as echo-planar readout can also greatly accelerate data acquisition of chemical shift imaging experiments.

The coordinated variations of glutamate and GABA across the brain can be assessed using chemical shift images of spectrally resolved glutamate and GABA. The absolute strengths of interregional correlations of spectrally resolved glutamate and GABA have the exciting potential for characterizing excitatory–inhibitory connections among the nodes of neural networks, therefore providing novel

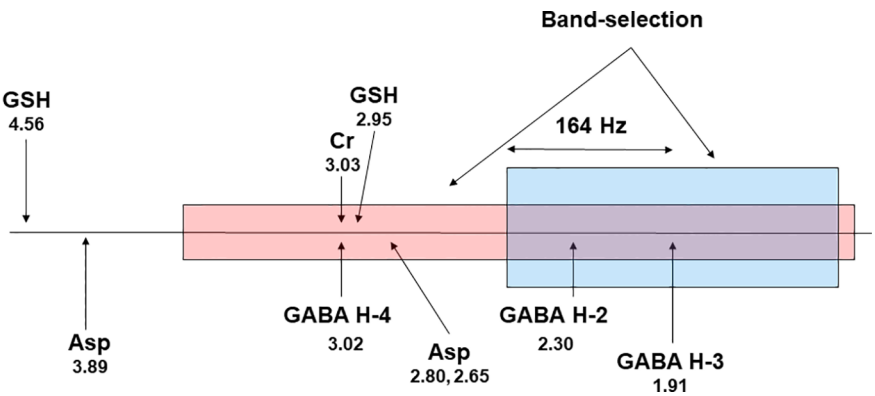

FIGURE 5 | A proposed scheme for band-selective multiple quantum filtering of GABA. A band-selective refocusing pulse prepares GABA into multiple quantum state while leaving glutathione in single quantum state by avoiding refocusing its cysteinyl α-H at 4.56 ppm. A band-selective 90° pulse converts the double quantum coherence into observable single quantum coherence. The frequency separation between GABA H4 and GABA H3 at 7 T is $164 \times 2 = 328$ Hz. Asp, aspartate; GSH, glutathione; Cr, creatine. The chemical shifts (in ppm) of the resonance signals are placed below their labels.

parameters for gauging interregional excitation–inhibition balance, the disruption of which is implicated in many neuropsychiatric disorders [e.g., (33, 103, 117, 129, 130)].

CONCLUSIONS

Previous neurochemical studies of animal models have revealed coordinated changes in major neurometabolites under various pathophysiological conditions which were attributed to the well-studied metabolic pathways connecting them. Recent MRS findings of neurometabolite correlations in healthy subjects and altered correlations in patients have further corroborated these associations, and their disruption is a hallmark of many neuropsychiatric disorders. To measure the absolute strength of these correlations, it is necessary to use spectral editing techniques to minimize or eliminate statistical correlations among MRS signals that originated from spectral overlap. Finally, chemical shift imaging of spectrally resolved glutamate and GABA is technically feasible at 7 T. It is hoped that the prospects for eliminating the confounding statistical correlations due to spectral overlap will reduce controversies in the field and generate further interest in characterizing local and interregional neurochemical associations especially glutamate–GABA interactions in the brain for studying neuropsychiatric disorders.

AUTHOR CONTRIBUTIONS

JS conceived the paper and performed literature search. DS and LA conducted laboratory research. JST performed literature search. JS, LA, and JST wrote the paper. All authors contributed to the article and approved the submitted version.

FUNDING

This work was supported by the Intramural Research Program of National Institute of Mental Health, NIH.

REFERENCES

1. de Graaf RA. *In vivo NMR spectroscopy*. John Wiley & Sons: Chichester, UK (1998).
2. Kleinhans NM, Schweinsburg BC, Cohen DN, Müller RA, Courchesne E. N-acetyl aspartate in autism spectrum disorders: regional effects and relationship to fMRI activation. *Brain Res* (2007) 1162:85–97. doi: 10.1016/j.brainres.2007.04.081
3. Walter M, Henning A, Grimm S, Schulte RF, Beck J, Dydak U, et al. The relationship between aberrant neuronal activation in the pregenual anterior cingulate, altered glutamatergic metabolism, and anhedonia in major depression. *Arch Gen Psychiatry* (2009) 66:478–86. doi: 10.1001/archgenpsychiatry.2009.39
4. Sudharshan N, Hanstock C, Hui B, Pyra T, Johnston W, Kalra S. Degeneration of the mid-cingulate cortex in amyotrophic lateral sclerosis detected in vivo with MR spectroscopy. *AJNR Am J Neuroradiol* (2011) 32:403–7. doi: 10.3174/ajnr.A2289
5. Waddell KW, Zanjanipour P, Pradhan S, Xu L, Welch EB, Joers JM, et al. Anterior cingulate and cerebellar GABA and Glu correlations measured by ^{1}H J-difference spectroscopy. *Magn Reson Imaging* (2011) 29:19–24. doi: 10.1016/j.mri.2010.07.005
6. Kraguljac NV, Reid MA, White DM, den Hollander J, Lahti AC. Regional decoupling of N-acetyl-aspartate and glutamate in schizophrenia. *Neuropsychopharmacology* (2012) 37:2635–42. doi: 10.1038/npp.2012.126
7. Kraguljac NV, White DM, Reid MA, Lahti AC. Increased hippocampal glutamate and volumetric deficits in unmedicated patients with schizophrenia. *JAMA Psychiatry* (2013) 70:1294–302. doi: 10.1001/jamapsychiatry.2013.2437
8. Gussew A, Borys C, Janetzki L, Cleve M, Malessa R, Habenicht U, et al. Altered regional and interregional interrelations of glutamate and GABA in patients with chronic low back pain – A ^{1}H-MR spectroscopic study, Clin. *Neurophysiology* (2015) 126:e109–10. doi: 10.1016/j.clinph.2015.04.165
9. Plitman E, de la Fuente-Sandoval C, Reyes-Madrigal F, Chavez S, Gómez-Cruz G, León-Ortiz P, et al. Elevated myo-inositol, choline, and glutamate levels in the associative striatum of antipsychotic-naive patients with first-episode psychosis: a proton magnetic resonance spectroscopy study with implications for glial dysfunction. *Schizophr Bull* (2016) 42:415–24. doi: 10.1093/schbul/sbv118
10. Cleve M, Gussew A, Wagner G, Bär KJ, Reichenbach JR. Assessment of intra- and inter-regional interrelations between GABA+, Glx and BOLD during pain perception in the human brain - A combined ^{1}H fMRS and fMRI study. *Neuroscience* (2017) 365:125–36. doi: 10.1016/j.neuroscience.2017.09.037
11. Sala A, Caminiti SP, Presotto L, Premi E, Pilotto A, Turrone R, et al. Altered brain metabolic connectivity at multiscale level in early Parkinson's disease. *Sci Rep* (2017) 7:4256. doi: 10.1038/s41598-017-04102-z
12. Niddam DM, Lai KL, Tsai SY, Lin YR, Chen WT, Fuh JL, et al. Neurochemical changes in the medial wall of the brain in chronic migraine. *Brain* (2018) 141:377–90. doi: 10.1093/brain/awx331
13. Taylor-Robinson SD, Buckley C, Changani KK, Hodgson HJ, Bell JD. Cerebral proton and phosphorus-31 magnetic resonance spectroscopy in patients with subclinical hepatic encephalopathy. *Liver* (1999) 19:389–98. doi: 10.1111/j.1478-3231.1999.tb00067.x
14. Grachev ID, Apkarian AV. Chemical network of the living human brain. Evidence of reorganization with aging. *Brain Res Cognit Brain Res* (2001) 11:185–97. doi: 10.1016/S0926-6410(00)00068-9
15. Cleve M, Gussew A, Janetzki L, Borys C, Reichenbach JR. Interregional associations between excitatory and inhibitory neurotransmitters in the resting human brain. *Proc ISMRM* (2015) 2348.
16. Just N, Sonnay S. Investigating the Role of Glutamate and GABA in the Modulation of Transthalamic Activity: A Combined fMRI-fMRS Study. *Front Physiol* (2017) 8:30. doi: 10.3389/fphys.2017.00030
17. van Veenendaal TM, Backes WH, Tse DHY, Scheenen TWJ, Klomp DW, Hofman PAM, et al. High field imaging of large-scale neurotransmitter networks: Proof of concept and initial application to epilepsy. *NeuroImage Clin* (2018) 19:47–55. doi: 10.1016/j.nicl.2018.04.006
18. Kim HJ, Kim JE, Cho G, IC S, Bae S, SJ H, et al. Associations between anterior cingulate cortex glutamate and gamma-aminobutyric acid concentrations and the harm avoidance temperament. *Neurosci Lett* (2009) 464:103–7. doi: 10.1016/j.neulet.2009.07.087
19. Tremblay S, Beaulé V, Proulx S, de Beaumont L, Marjanska M, Doyon J, et al. Relationship between transcranial magnetic stimulation measures of intracortical inhibition and spectroscopy measures of GABA and glutamate +glutamine. *J Neurophysiol* (2013) 109:1343–9. doi: 10.1152/jn.00704.2012
20. Kraguljac NV, Cutter GR, Morgan C, Lahti AC. In reply. *JAMA Psychiatry* (2014) 71:339–40. doi: 10.1001/jamapsychiatry.2014.22
21. Maddock R. The problem of spurious correlations between pairs of brain metabolite values measured in the same voxel with magnetic resonance spectroscopy. *JAMA Psychiatry* (2014) 71:338–9. doi: 10.1001/jamapsychiatry.2013.4343
22. Ende G, Cackowski S, Van Eijk J, Sack M, Demirakca T, Kleindienst N, et al. Impulsivity and aggression in female BPD and ADHD patients: association

with ACC glutamate and GABA concentrations. *Neuropsycho-pharmacology* (2016) 41:410–8. doi: 10.1038/npp.2015.153
23. Scholl J, Kolling N, Nelissen N, Stagg CJ, Harmer CJ, Rushworth MF. Excitation and inhibition in anterior cingulate predict use of past experiences. *elife* (2017) 6:e20365. doi: 10.7554/eLife.20365
24. Provencher SW. Estimation of Metabolite Concentrations from Localized in-Vivo Proton Nmr Spectra. *Magn Reson Med* (1993) 30(6):672–9. doi: 10.1002/mrm.1910300604
25. Siesjö BK. *Brain Energy Metabolism*. John Wiley & Sons: Chichester, UK (1978).
26. Erecinska M, Silver IA. Metabolism and role of glutamate in mammalian brain. *Prog Neurobiol* (1990) 35:245–96. doi: 10.1016/0301-0082(90)90013-7
27. Watts ME, Pocock R, Claudianos C. Brain energy and oxygen metabolism: emerging role in normal function and disease. *Front Mol Neurosci* (2018) 11:216. doi: 10.3389/fnmol.2018.00216
28. Duncan NW, Wiebking C, Northoff G. Associations of regional GABA and glutamate with intrinsic and extrinsic neural activity in humans - a review of multimodal imaging studies. *Neurosci Biobehav Rev* (2014) 47:36–52. doi: 10.1016/j.neubiorev.2014.07.016
29. Ajram LA, Pereira AC, Durieux AMS, Velthius HE, Petrinovic MM, McAlonan GM. The contribution of [^{1}H] magnetic resonance spectroscopy to the study of excitation-inhibition in autism. *Prog Neuropsychopharmacol Biol Psychiatry* (2019) 89:236–44. doi: 10.1016/j.pnpbp.2018.09.010
30. Yildiz-Yesiloglu A, Ankerst DP. Review of ^{1}H magnetic resonance spectroscopy findings in major depressive disorder: a meta-analysis. *Psychiatry Res* (2006) 147:1–25. doi: 10.1016/j.pscychresns.2005.12.004
31. Duman RS, Sanacora G, Krystal JH. Altered connectivity in depression: GABA and glutamate neurotransmitter deficits and reversal by novel treatments. *Neuron* (2019) 102:75–90. doi: 10.1016/j.neuron.2019.03.013
32. Sohal VS, Rubenstein JLR. Excitation-inhibition balance as a framework for investigating mechanisms in neuropsychiatric disorders. *Mol Psychiatry* (2019) 24:1248–57. doi: 10.1038/s41380-019-0426-0
33. Hjelmervik H, Craven AR, Sinceviciute I, Johnsen E, Kompus K, Bless JJ, et al. Intra-Regional Glu-GABA vs Inter-Regional Glu-Glu Imbalance: A ^{1}H-MRS Study of the Neurochemistry of Auditory Verbal Hallucinations in Schizophrenia. *Schizophr Bull* (2020) 46:633–42. doi: 10.1093/schbul/sbz099
34. Bruhn H, Frahm J, Gyngell ML, Merboldt KD, Hanicke W, Sauter R. Cerebral metabolism in man after acute stroke: new observations using localized proton NMR spectroscopy. *Magn Reson Med* (1989) 9:126–31. doi: 10.1002/mrm.1910090115
35. Lemesle M, Walker P, Guy F, D'Athis P, Billiar T, Giroud M, et al. Multivariate analysis predicts clinical outcome 30 days after middle cerebral artery infarction. *Acta Neurol Scand* (2000) 102:1–17. doi: 10.1034/j.1600-0404.2000.102001011.x
36. Moffett JR, Ross B, Arun P, Madhavarao CN, Namboodiri AM. N-Acetylaspartate in the CNS: from neurodiagnostics to neurobiology. *Prog Neurobiol* (2007) 81:89–131. doi: 10.1016/j.pneurobio.2006.12.003
37. Magistretti PJ. Cellular bases of functional brain imaging: insights from neuron-glia metabolic coupling. *Brain Res* (2000) 886:108–12. doi: 10.1016/S0006-8993(00)02945-0
38. Rothman DL, de Graaf RA, Hyder F, Mason GF, Behar KL, De Feyter HM. In vivo ^{13}C and ^{1}H-[^{13}C] MRS studies of neuroenergetics and neurotransmitter cycling, applications to neurological and psychiatric disease and brain cancer. *NMR Biomed* (2019) 32:e4172. doi: 10.1002/nbm.4172
39. Srinivasan R, Sailasuta N, Hurd R, Nelson S, Daniel Pelletier D. Evidence of elevated glutamate in multiple sclerosis using magnetic resonance spectroscopy at 3 T. *Brain* (2005) 128:1016–25. doi: 10.1093/brain/awh467
40. Hasler G, van der Veen JW, Tumonis T, Meyers N, Shen J, Drevets WC. Reduced prefrontal glutamate/glutamine and gamma-aminobutyric acid levels in major depression determined using proton magnetic resonance spectroscopy. *Arch Gen Psychiatry* (2007) 64:193–200. doi: 10.1001/archpsyc.64.2.193
41. Strawn JR, Patel NC, Chu W-J, Lee J-H, Adler CM, Kim M-J, et al. Glutamatergic effects of divalproex in adolescents with mania: a proton magnetic resonance spectroscopy study. *J Am Acad Child Adolesc Psychiatry* (2012) 51:642–51. doi: 10.1016/j.jaac.2012.03.009
42. Yelamanchi SD, Jayaram S, Thomas JK, Gundimeda S, Khan AA, Singhal A, et al. A pathway map of glutamate metabolism. *J Cell Commun Signal* (2016) 10:69–75. doi: 10.1007/s12079-015-0315-5
43. Shen J. In vivo carbon-13 magnetization transfer effect. Detection of aspartate aminotransferase reaction. *Magn Reson Med* (2005) 54:1321–6. doi: 10.1002/mrm.20709
44. Lewis LD, Ljunggren B, Norberg K, Siesjö BK. Changes in carbohydrate substrates, amino acids and ammonia in the brain during insulin-induced hypoglycemia. *J Neurochem* (1974) 23:659–71. doi: 10.1111/j.1471-4159.1974.tb04389.x
45. Engelsen B, Fonnum F. Effects of hypoglycemia on the transmitter pool and the metabolic pool of glutamate in rat brain. *Neurosci Lett* (1983) 42:317–22. doi: 10.1016/0304-3940(83)90281-1
46. Wong KL, Tyce GM. Glucose and amino acid metabolism in rat brain during sustained hypoglycemia. *Neurochem Res* (1983) 8:401–15. doi: 10.1007/BF00965097
47. Betz AL, Gilboe DD. Effect of pentobarbital on amino acid and urea flux in the isolated dog brain. *Am J Physiol* (1973) 224:580–7. doi: 10.1152/ajplegacy.1973.224.3.580
48. Hägerdal M, Harp J, Siesjö BK. Effect of hypothermia upon organic phosphates, glycolytic metabolites, citric acid cycle intermediates and associated amino acids in rat cerebral cortex. *J Neurochem* (1975) 24:743–8. doi: 10.1111/j.1471-4159.1975.tb11673.x
49. Chapman AG, Nordström CH, Siesjö BK. Influence of phenobarbital anesthesia on carbohydrate and amino acid metabolism in rat brain. *Anesthesiology* (1978) 48:175–82. doi: 10.1097/00000542-197803000-00003
50. MacMillan V, Siesjö BK. The influence of hypocapnia upon intracellular pH and upon some carbohydrate substrates, amino acids and organic phosphates in the brain. *J Neurochem* (1973) 21:1283–99. doi: 10.1111/j.1471-4159.1973.tb07582.x
51. Patel TB, Clark JB. Synthesis of N-acetyl-L-aspartate by rat brain mitochondria and its involvement in mitochondrial/cytosolic carbon transport. *Biochem J* (1979) 184(3):539–46. doi: 10.1042/bj1840539
52. Robinson MB, Blakely RD, Couto R, Coyle JT. Hydrolysis of the brain dipeptide N-acetyl-L-aspartyl-L-glutamate. Identification and characterization of a novel N-acetylated alpha-linked acidic dipeptidase activity from rat brain. *J Biol Chem* (1987) 262:14498–506.
53. Bzdega T, Turi T, Wroblewska B, She D, Chung HS, Kim H, et al. Molecular cloning of a peptidase against N-acetylaspartylglutamate from a rat hippocampal cDNA library. *J Neurochem* (1997) 69(6):2270–7. doi: 10.1046/j.1471-4159.1997.69062270.x
54. Luthi-Carter R, Berger UV, Barczak AK, Enna M, Coyle JT. Isolation and expression of a rat brain cDNA encoding glutamate carboxypeptidase II. *Proc Natl Acad Sci USA* (1998) 95:3215–20. doi: 10.1073/pnas.95.6.3215
55. Clark JF, Doepke A, Filosa JA, Wardle RL, Lu A, Meeker TJ, et al. N-acetylaspartate as a reservoir for glutamate. *Med Hypotheses* (2006) 67:506–12. doi: 10.1016/j.mehy.2006.02.047
56. Chavarria L, Cordoba J. Magnetic resonance imaging and spectroscopy in hepatic encephalopathy. *J Clin Exp Hepatol* (2015) 5:S69–74. doi: 10.1016/j.jceh.2013.10.001
57. Natarajan SK, Venneti S. Glutamine metabolism in brain tumors. *Cancers* (2019) 11:1628. doi: 10.3390/cancers11111628
58. Sibson NR, Dhankhar A, Mason GF, Behar KL, Rothman DL, Shulman RG. In vivo ^{13}C NMR measurements of cerebral glutamine synthesis as evidence for glutamate-glutamine cycling. *Proc Natl Acad Sci U S A* (1997) 94:2699–704. doi: 10.1073/pnas.94.6.2699
59. Rothman DL, De Feyter HM, de Graaf RA, Mason GF, Behar KL. ^{13}C MRS studies of neuroenergetics and neurotransmitter cycling in humans. *NMR Biomed* (2011) 24:943–57. doi: 10.1002/nbm.1772
60. Greene JG, Greenamyre JT. Bioenergetics and glutamate excitotoxicity. *Prog Neurobiol* (1996) 48:613–34. doi: 10.1016/0301-0082(96)00006-8
61. Rothstein JD, Dykes-Hoberg M, Pardo CA, Bristol LA, Jin L, Kuncl RW, et al. Knockout of glutamate transporters reveals a major role for astroglial transport in excitotoxicity and clearance of glutamate. *Neuron* (1996) 16:675–86. doi: 10.1016/S0896-6273(00)80086-0

62. Gether U, Andersen PH, Larsson OM, Schousboe A. Neurotransmitter transporters: molecular function of important drug targets. *Trends Pharmacol Sci* (2006) 27:375–83. doi: 10.1016/j.tips.2006.05.003
63. Hertz L. Intercellular metabolic compartmentation in the brain. *Past Present Future Neurochem Int* (2004) 45:285–96. doi: 10.1016/j.neuint.2003.08.016
64. Duce IR, Keen P. Selective uptake of [^{3}H]glutamine and [^{3}H]glutamate into neurons and satellite cells of dorsal root ganglia in vitro. *Neuroscience* (1983) 8:861–6. doi: 10.1016/0306-4522(83)90016-7
65. Sibson NR, Mason GF, Shen J, Cline GW, Herskovits AZ, Wall JE, et al. In vivo ^{13}C NMR measurement of neurotransmitter glutamate cycling, anaplerosis and TCA cycle flux in rat brain during. *J Neurochem* (2001) 76:975–89. doi: 10.1046/j.1471-4159.2001.00074.x
66. Gruetter R, Seaquist ER, Kim S, Ugurbil K. Localized in vivo ^{13}C-NMR of glutamate metabolism in the human brain: initial results at 4 Tesla. *Dev Neurosci* (1998) 20:380–8. doi: 10.1159/000017334
67. Shen J, Sibson NR, Cline G, Behar KL, Rothman DL, Shulman RG. ^{15}N-NMR spectroscopy studies of ammonia transport and glutamine synthesis in the hyperammonemic rat brain. *Dev Neurosci* (1998) 20:434–43. doi: 10.1159/000017341
68. Shen J, Petersen KF, Behar KL, Brown P, Nixon TW, Mason GF, et al. Determination of the rate of the glutamate/glutamine cycle in the human brain by in vivo ^{13}C NMR. *Proc Natl Acad Sci USA* (1999) 96:8235–40. doi: 10.1073/pnas.96.14.8235
69. Lebon V, Petersen KF, Cline GW, Shen J, Mason GF, Dufour S, et al. Astroglial contribution to brain energy metabolism in humans revealed by ^{13}C nuclear magnetic resonance spectroscopy. Elucidation of the dominant pathway for neurotransmitter glutamate repletion and measurement of astrocytic oxidative metabolism. *J Neurosci* (2002) 22:1523–31. doi: 10.1523/JNEUROSCI.22-05-01523.2002
70. Shen J. Modeling the glutamate-glutamine neurotransmitter cycle. *Front Neuroenergetics* (2013) 5(1). doi: 10.3389/fnene.2013
71. Bradford HF, Ward HK, Thomas AJ. Glutamine — a major substrate for nerve endings. *J Neurochem* (1978) 30:1453–9. doi: 10.1111/j.1471-4159.1978.tb10477.x
72. de Graaf AA, Deutz NE, Bosman DK, Chamuleau RA, de Haan JG, Bovee WM. The use of in vivo proton NMR to study the effects of hyperammonemia in the rat cerebral cortex. *NMR Biomed* (1991) 4:31–7. doi: 10.1002/nbm.1940040106
73. Stelmashook EV, Isaev NK, Lozier ER, Goryacheva ES, Khaspekov LG. Role of glutamine in neuronal survival and death during brain ischemia and hypoglycemia. *Int J Neurosci* (2011) 121:415–22. doi: 10.3109/00207454.2011.570464
74. Rothman DL, Petroff OA, Behar KL, Mattson RH. Localized ^{1}H NMR measurements of gamma-aminobutyric acid in human brain in vivo. *Proc Nat Acad Sci USA* (1993) 90:5662–6. doi: 10.1073/pnas.90.12.5662
75. Petroff OA, Behar KL, Mattson RH, Rothman DL. Human brain gamma-aminobutyric acid levels and seizure control following initiation of vigabatrin therapy. *J Neurochem* (1996) 67:2399–404. doi: 10.1046/j.1471-4159.1996.67062399.x
76. Roberts E, Frankel S. γ-Aminobutyric acid in brain: Its formation from glutamic acid. *J Biol Chem* (1950) 187:55–63.
77. Price NC, Stevens L. *Fundamentals of Enzymology*, *3rd ed*. Oxford University Press: Oxford, UK (1999).
78. Preece NE, Cerdán S. Metabolic precursors and compartmentation of cerebral GABA in vigabatrin-treated rats. *J Neurochem* (1996) 67:1718–25. doi: 10.1046/j.1471-4159.1996.67041718.x
79. Olsen RW, DeLorey TM. GABA Synthesis, Uptake and Release. In: Siegel GJ, Agranoff BW, Albers RW, Fisher SK, Uhler MD, editors. *Basic Neurochemistry: Molecular, Cellular and Medical Aspects*, *6th ed*. Philadelphia, USA: Lippincott-Raven (1999).
80. Yang J, Li SS, Bacher J, Shen J. Quantification of cortical GABA-glutamine cycling rate using in vivo magnetic resonance signal of [2-^{13}C]GABA derived from glia-specific substrate [2-^{13}C]acetate. *Neurochem Int* (2007) 50:371–8. doi: 10.1016/j.neuint.2006.09.011
81. Sequerra EB, Gardino P, Hedin-Pereira C, de Mello FG. Putrescine as an important source of GABA in the postnatal rat subventricular zone. *Neuroscience* (2007) 146:489–93. doi: 10.1016/j.neuroscience.2007.01.062
82. Tatti R, Haley MS, Swanson OK, Tselha T, Maffei A. Neurophysiology and regulation of the balance between excitation and inhibition in neocortical circuits. *Biol Psychiatry* (2017) 81:821–31. doi: 10.1016/j.biopsych.2016.09.017
83. Shepherd GM. *Neurobiology*. *3rd ed*. Oxford University Press: Oxford, UK (1994).
84. Rubenstein JL, Merzenich MM. Model of autism: increased ratio of excitation/inhibition in key neural systems. *Genes Brain Behav* (2003) 2:255–67. doi: 10.1034/j.1601-183X.2003.00037.x
85. Kurcyus K, Annac E, Hanning NM, Harris AD, Oeltzschner G, Edden R, et al. Opposite dynamics of GABA and glutamate levels in the occipital cortex during visual processing. *J Neurosci* (2018) 38:9967–76. doi: 10.1523/JNEUROSCI.1214-18.2018
86. Maddock RJ, Casazza GA, Fernandez DH, Maddock MI. Acute modulation of cortical glutamate and GABA content by physical activity. *J Neurosci* (2016) 36:2449–57. doi: 10.1523/JNEUROSCI.3455-15.2016
87. Harada M, Taki MM, Nose A, Kubo H, Mori K, Nishitani H, et al. Non-invasive evaluation of the GABAergic/glutamatergic system in autistic patients observed by MEGA-editing proton MR spectroscopy using a clinical 3 tesla instrument. *J Autism Dev Disord* (2011) 41:447–54. doi: 10.1007/s10803-010-1065-0
88. Sanacora G, Gueorguieva R, Epperson CN, Wu YT, Appel M, Rothman DL, et al. Subtype-specific alterations of gamma-aminobutyric acid and glutamate in patients with major depression. *Arch Gen Psychiatry* (2004) 61:705–13. doi: 10.1001/archpsyc.61.7.705
89. Pollack MH, Jensen JE, Simon NM, Kaufman RE, Renshaw PF. High-field MRS study of GABA, glutamate and glutamine in social anxiety disorder: response to treatment with levetiracetam. *Prog Neuropsychopharmacol Biol Psychiatry* (2008) 32:739–43. doi: 10.1016/j.pnpbp.2007.11.023
90. Maddock RJ, Buonocore MH. MR spectroscopic studies of the brain in psychiatric disorders. *Curr Top Behav Neurosci* (2012) 11:199–251. doi: 10.1007/7854_2011_197
91. Thomson AM, Lamy C. Functional maps of neocortical local circuitry. *Front Neurosci* (2007) 1:19–42. doi: 10.3389/neuro.01.1.1.002.2007
92. Caputi A, Melzer S, Michael M, Monyer H. The long and short of GABAergic neurons. *Curr Opin Neurobiol* (2013) 23:179–86. doi: 10.1016/j.conb.2013.01.021
93. Zikopoulos B, Barbas H. Altered neural connectivity in excitatory and inhibitory cortical circuits in autism. *Front Hum Neurosci* (2013) 7:609. doi: 10.3389/fnhum.2013.00609
94. Wood JD, Kurylo E, Lane R. gamma-Aminobutyric acid release from synaptosomes prepared from rats treated with isonicotinic acid hydrazide and gabaculine. *J Neurochem* (1988) 50:1839–43. doi: 10.1111/j.1471-4159.1988.tb02486.x
95. Golan H, Talpalar AE, Schleifstein-Attias D, Grossman Y. GABA metabolism controls inhibition efficacy in the mammalian CNS. *Neurosci Lett* (1996) 217:25–8. doi: 10.1016/0304-3940(96)13061-5
96. Jackson MF, Esplin B, Capek R. Reversal of the activity-dependent suppression of GABA-mediated inhibition in hippocampal slices from gamma-vinyl GABA (vigabatrin)-pretreated rats. *Neuropharmacology* (2000) 39:65–74. doi: 10.1016/S0028-3908(99)00075-1
97. Wu Y, Wang W, Richerson GB. GABA transaminase inhibition induces spontaneous and enhances depolarization-evoked GABA efflux via reversal of the GABA transporter. *J Neurosci* (2001) 21:2630–9. doi: 10.1523/JNEUROSCI.21-08-02630.2001
98. Chen Z, Silva AC, Yang J, Shen J. Elevated endogenous GABA level correlates with decreased fMRI signals in the rat brain during acute inhibition of GABA transaminase. *J Neurosci Res* (2005) 79:383–91. doi: 10.1002/jnr.20364
99. Yang J, Shen J. Elevated endogenous GABA concentration attenuates glutamate-glutamine cycling between neurons and astroglia. *J Neural Transm* (2009) 116:291–300. doi: 10.1007/s00702-009-0186-0
100. Rae CD. A guide to the metabolic pathways and function of metabolites observed in human brain ^{1}H magnetic resonance spectra. *Neurochem Res* (2014) 39:1–36. doi: 10.1007/s11064-013-1199-5
101. Boumezbeur F, Mason GF, de Graaf RA, Behar KL, Cline GW, Shulman GI, et al. Altered brain mitochondrial metabolism in healthy aging as assessed by

in vivo magnetic resonance spectroscopy. *J Cereb Blood Flow Metab* (2010) 30:211–21. doi: 10.1038/jcbfm.2009.197
102. Wagner G, Gussew A, Köhler S, de la Cruz F, Smesny S, Reichenbach JR, et al. Resting state functional connectivity of the hippocampus along the anterior-posterior axis and its association with glutamatergic metabolism. *Cortex* (2016) 81:104–17. doi: 10.1016/j.cortex.2016.03.022
103. Shukla DK, Wijtenburg SA, Chen H, Chiappelli JJ, Kochunov P, Hong LE, et al. Anterior cingulate glutamate and GABA associations on functional connectivity in schizophrenia. *Schizophr Bull* (2019) 45:647–58. doi: 10.1093/schbul/sby075
104. Cavassila S, Deval S, Huegen C, van Ormondt D, Graveron-Demilly D. Cramer-Rao bounds an evaluation tool for quantitation. *NMR Biomed* (2001) 14:278–83. doi: 10.1002/nbm.701
105. Draper NR, Smith H. *Applied regression analysis. 3rd ed*. Wiley, New York: USA (1998). p. 135–139.
106. Zhang Y, Shen J. Smoothness of in vivo spectral baseline determined by mean-square error. *Magn Reson Med* (2014) 72:913–22. doi: 10.1002/mrm.25013
107. Zhang Y, Shen J. Effects of noise and linewidth on in vivo analysis of glutamate at 3 T. *J Magn Reson* (2020) 314:106732. doi: 10.1016/j.jmr.2020.106732
108. Mescher M, Merkle H, Kirsch J, Garwood M, Gruetter R. Simultaneous in vivo spectral editing and water suppression. *NMR Biomed* (1998) 11:266–72. doi: 10.1002/(SICI)1099-1492(199810)11:6<266::AID-NBM530>3.0.CO;2-J
109. Hurd R, Sailasuta N, Srinivasan R, Vigneron DB, Pelletier D, Nelson SJ. Measurement of brain glutamate using TE-averaged PRESS at 3T. *Magn Reson Med* (2004) 51:435–40. doi: 10.1002/mrm.20007
110. Schubert F, Galliant J, Seifert F, Rinneberg H. Glutamate concentrations in human brain using single voxel proton magnetic resonance spectroscopy at 3 Tesla. *Neuroimage* (2004) 21:1762–71. doi: 10.1016/j.neuroimage.2003.11.014
111. Choi CH, Dimitrov IE, Douglas D, Patel A, Kaiser LG, Amezcua CA, et al. Improvement of resolution for brain coupled metabolites by optimized H-1 MRS at 7 T. *NMR BioMed* (2010) 23:1044–52. doi: 10.1002/nbm.1529
112. An L, Li S, Murdoch JB, Araneta MF, Johnson C, Shen J. Detection of glutamate, glutamine, and glutathione by radiofrequency suppression and echo time optimization at 7 Tesla. *Magn Reson Med* (2015) 73:451–8. doi: 10.1002/mrm.25150
113. Zhang Y, Shen J. Simultaneous quantification of glutamate and glutamine by J-modulated spectroscopy at 3 Tesla. *Magn Reson Med* (2016) 76:725–32. doi: 10.1002/mrm.25922
114. Saleh MG, Oeltzschner G, Chan KL, Puts NAJ, Mikkelsen M, Schär M, et al. Simultaneous edited MRS of GABA and glutathione. *Neuroimage* (2016) 142:576–82. doi: 10.1016/j.neuroimage.2016.07.056
115. Oeltzschner G, Saleh MG, Rimbault D, Mikkelsen M, Chan KL, Puts NAJ, et al. Advanced Hadamard-encoded editing of seven low-concentration brain metabolites: Principles of HERCULES. *Neuroimage* (2019) 185:181–90. doi: 10.1016/j.neuroimage.2018.10.002
116. Medford N, Critchley HD. Conjoint activity of anterior insular and anterior cingulate cortex: awareness and response. *Brain Struct Funct* (2010) 214:535–49. doi: 10.1007/s00429-010-0265-x
117. Lee E, Lee J, Kim E. Excitation/inhibition imbalance in animal models of autism spectrum disorders. *Biol Psychiatry* (2017) 81:838–47. doi: 10.1016/j.biopsych.2016.05.011
118. Sridharan D, Levitin DJ, Menon V. A critical role for the right fronto-insular cortex in switching between central-executive and default-mode networks. *Proc Natl Acad Sci U S A* (2008) 105:12569–74. doi: 10.1073/pnas.0800005105
119. Taylor KS, Seminowicz DA, Davis KD. Two systems of resting state connectivity between the insula and cingulate cortex. *Hum Brain Mapp* (2009) 30:2731–45. doi: 10.1002/hbm.20705
120. Horn DI, Yu C, Steiner J, Buchmann J, Kaufmann J, Osoba A, et al. Glutamatergic and resting-state functional connectivity correlates of severity in major depression - the role of pregenual anterior cingulate cortex and anterior insula. *Front Syst Neurosci* (2010) 4:33. doi: 10.3389/fnsys.2010.00033
121. Maclaren J, Herbst M, Speck O, Zaitsev M. Prospective motion correction in brain imaging: a review. *Magn Reson Med* (2013) 69:621–36. doi: 10.1002/mrm.24314
122. Evans CJ, Puts NA, Robson SE, Boy F, McGonigle DJ, Sumner P, et al. Subtraction artifacts and frequency (mis-)alignment in J-difference GABA editing. *J Magn Reson Imaging* (2013) 38:970–5. doi: 10.1002/jmri.23923
123. An L, Araneta MF, Johnson C, Shen J. Effects of carrier frequency mismatch on frequency-selective spectral editing. *MAGMA* (2019) 32:237–46. doi: 10.1007/s10334-018-0717-5
124. Geen H, Freeman R. Band-selective radiofrequency pulses J. *Magn Reson* (1991) 93:93–141. doi: 10.1016/0022-2364(91)90034-Q
125. McLean MA, Busza AL, Wald LL, Simister RJ, Barker GJ, Williams SR. In vivo GABA+ measurement at 1.5T using a PRESS-localized double quantum filter. *Magn Reson Med* (2002) 48:233–41. doi: 10.1002/mrm.10208
126. Choi C, Coupland NJ, Hanstock CC, Ogilvie CJ, Higgins AC, Gheorghiu D, et al. Brain gamma-aminobutyric acid measurement by proton double-quantum filtering with selective J rewinding. *Magn Reson Med* (2005) 54:272–9. doi: 10.1002/mrm.20563
127. Choi IY, Lee SP, Merkle H, Shen J. In vivo detection of gray and white matter differences in GABA concentration in the human brain. *Neuroimage* (2006) 33:85–93. doi: 10.1016/j.neuroimage.2006.06.016
128. Simister RJ, McLean MA, Barker GJ, Duncan JS. Proton MR spectroscopy of metabolite concentrations in temporal lobe epilepsy and effect of temporal lobe resection. *Epilepsy Res* (2009) 83:168–76. doi: 10.1016/j.eplepsyres.2008.11.006
129. Coyle JT. The GABA-glutamate connection in schizophrenia: which is the proximate cause? *Biochem Pharmacol* (2004) 68:1507–14. doi: 10.1016/j.bcp.2004.07.034
130. Cherlyn SY, Woon PS, Liu JJ, Ong WY, Tsai GC, Sim K. Genetic association studies of glutamate, GABA and related genes in schizophrenia and bipolar disorder: a decade of advance. *Neurosci Biobehav Rev* (2010) 34:958–77. doi: 10.1016/j.neubiorev.2010.01.002

Conflict of Interest: The authors declare that the research was conducted in the absence of any commercial or financial relationships that could be construed as a potential conflict of interest.

frontiers in Psychiatry

METHODS
published: 14 August 2020
doi: 10.3389/fpsyt.2020.00813

Feasibility of Measuring GABA Levels in the Upper Brainstem in Healthy Volunteers Using Edited MRS

*Yulu Song[1], Tao Gong[1], Richard A. E. Edden[2,3] and Guangbin Wang[1]**

[1] Department of Imaging and Nuclear Medicine, Shandong Medical Imaging Research Institute, Cheeloo College of Medicine, Shandong University, Jinn, China, [2] Russell H. Morgan Department of Radiology and Radiological Science, The Johns Hopkins University School of Medicine, Baltimore, MD, United States, [3] FM Kirby Center for Functional Brain Imaging, Kennedy Krieger Institute, Baltimore, MD, United States

Purpose: To assess the feasibility of small-voxel MEGA-PRESS in detecting gamma-aminobutyric acid (GABA) levels of the upper brainstem in healthy volunteers.

Materials and Methods: Forty-two healthy volunteers, aged between 20 and 76 years were enrolled in this study, and underwent a 3.0T MRI scan using an eight-channel phased-array head coil. The MEGA-PRESS sequence was used to edit GABA signal from a 10x25x30 mm^3 voxel in the upper brain stem. The detected signal includes contributions from macromolecules (MM) and homocarnosine and is therefore referred to as GABA+. All the data were processed using Gannet.

Results: Thirty-four cases were successful in measuring GABA in the upper brainstem and 8 cases failed (based on poor modeling of spectra). The GABA+ levels were 2.66 ± 0.75 i.u. in the upper brainstem of healthy volunteers, ranging from 1.50 to 4.40 i.u. The normalized fitting residual (FitErr in Gannet) was 12.1 ± 2.8%, ranging from 7.4% to 19.1%; it was below 15.5% in 30 cases (71%).

Conclusions: It is possible to measure GABA levels in the upper brainstem using MEGA-PRESS with a relatively small ROI, with a moderate between-subject variance of under 30%.

Keywords: GABA, MRI, MEGA-PRESS, brainstem, spectroscopy

OPEN ACCESS

Edited by:
Guido van Wingen, University of Amsterdam, Netherlands

Reviewed by:
Frank P. MacMaster, University of Calgary, Canada
Nithya Ramakrishnan, Baylor College of Medicine, United States

***Correspondence:**
Guangbin Wang
cjr.wangguangbin@vip.163.com

Specialty section:
This article was submitted to Neuroimaging and Stimulation, a section of the journal Frontiers in Psychiatry

Received: *31 January 2020*
Accepted: *28 July 2020*
Published: *14 August 2020*

Citation:
Song Y, Gong T, Edden RAE and Wang G (2020) Feasibility of Measuring GABA Levels in the Upper Brainstem in Healthy Volunteers Using Edited MRS. Front. Psychiatry 11:813. doi: 10.3389/fpsyt.2020.00813

INTRODUCTION

γ-aminobutyric acid (GABA) is the major inhibitory neurotransmitter in the developmentally mature mammalian central nervous system. GABA acts at inhibitory synapses in the brain by binding to specific transmembrane receptors in both pre- and postsynaptic neuronal processes. ^{1}H magnetic resonance spectroscopy (MRS) is a noninvasive technique that can be used to measure neurotransmitter levels in vivo (1). However, GABA is difficult to detect due to its low concentration and the presence of overlapping signals from other compounds such as creatine and N-acetyl aspartate (NAA) (2). Mescher-Garwood point-resolved spectroscopy (MEGA-PRESS) is able to estimate GABA levels reliably using an editing technique based on refocusing J-couplings (3). To date, MEGA-PRESS has been measured both in the healthy brain (4–8) and in various

neurodegenerative disorders, such as Alzheimer's disease (AD) (9, 10), multiple sclerosis (MS) (11, 12), as well as psychiatric diseases (13–16).

In the human brain, the brainstem includes the midbrain and the pons and medulla oblongata of the hindbrain. The midbrain is the recipient of projections from cortex, limbic structures, and striatum, and exerts essential modulating influences on those descending and ascending projections (17, 18). The upper brainstem (19) is under-studied by MRS, even though it contains many integrative nuclei that mediate physiological functions disrupted in neurological disease (18). Numerous studies have been performed on the pathological brainstem involvement in patients with neurodegenerative disorders (20–22). One QSM study showed that the pathological changes in the midbrain (elevated iron) have a direct relevance to the development of Parkinson's Disease (PD) (23). Zarow et al. found that for both PD and AD the greatest neuronal loss was found in the pons (Locus coeruleus, LC), and demonstrated that neural loss in the pons and midbrain was correlated with the duration of these neurodegenerative disorders (24). Some found that the sites in the upper brainstem that are damaged are likely to contribute to the physiological deficits emerging in PD and obstructive sleep apnea (OSA) (18, 25). One study of GABA+ at 7 T in PD showed a correlation between GABA levels in the pons and the putamen (22). To our knowledge, no study has yet sought to measure GABA+ levels in the upper brainstem at 3T using MEGA-PRESS, likely because the small volume in upper brainstem makes voxel sizes (~27ml) used in most previous studies impossible (6, 26–29). The objectives of this preliminary study were to measure the GABA+ levels of the upper brainstem in a small voxel (10 x 25 x 30 mm^3) with MEGA-PRESS in healthy volunteers.

METHODS

Participants

Between April 2018 and April 2019, 42 healthy volunteers (55% males and 45% females aged 20–76 years) were recruited to be scanned by 3T MRI. Written informed consent was obtained from each participant. The study was approved by the local institutional ethical review board. For all participants, exclusion criteria included contraindications for MRI and a history of alcohol or substance misuse.

MRS Acquisition

All MRI and MRS experiments were carried out using a 3T scanner (Achieva TX, Philips, Best, Netherlands) equipped with an eight-channel phased-array head coil.

Magnetic Resonance Spectroscopy

The MEGA-PRESS sequence generates two subspectra with the editing pulse ON in one and OFF in the other for GABA detection. The edited spectrum, which reveals the GABA+ signal, is obtained by subtracting one subspectrum from the other (30). MEGA-PRESS spectra were acquired from a 10 x 25 x 30 mm^3 voxel in the upper brainstem. Based on axial images, the voxel was centered left-right and in the midbrain, with the posterior face aligned to the posterior face of the midbrain. Based on sagittal images, the voxel was positioned cranially/caudally so as to maximize inclusion of midbrain and pontine tissue, and minimizing the inclusion of cerebrospinal fluid, as shown in **Figure 1**. **Figure 1D** illustrates the typical voxel placement across 15 subjects.

Sequence parameters were as follows: repetition time (TR) = 2 s; echo time (TE) = 68 ms; 320 averages; acquisition bandwidth =

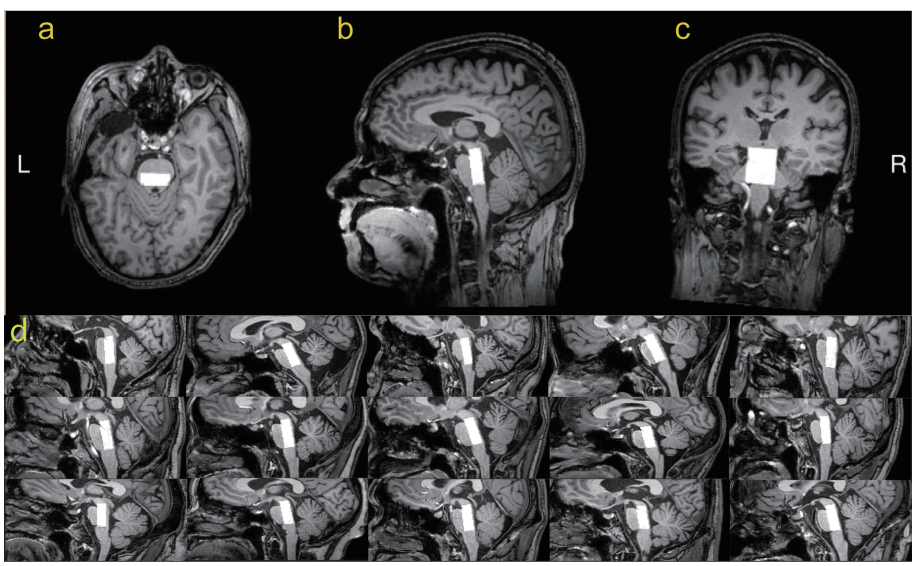

FIGURE 1 | T1-weighted TFE images show the ROI's position in the upper brainstem in a healthy volunteer. The white box represents the location of the ROI (10mm*25mm*30mm) in the axial **(A)**, sagittal **(B)**, and coronal **(C)** planes. Sagittal placement in 15 subjects illustrates the variable geometry and adjusted placement **(D)**.

2,000 Hz; Total acquisition time 10 min 56 sec; MOIST water suppression (31) and Philips pencil-beam (PB-auto) shimming (32) were used. Because the signals detected at 3.02 ppm using these experimental parameters is also expected to contain contributions from both macromolecules (MM) and homocarnosine, in this study the signal is labeled GABA+ rather than GABA (22).

Structural Magnetic Resonance

A whole-brain structural 3-dimensional MPRAGE (magnetization-prepared rapid-acquisition gradient echo) scan was acquired with 1 x 1 x 1 mm^3 isotropic resolution (TR = 8.2 ms; TE = 3.7 ms; flip angle = 8°, matrix = 256 × 256; field of view = 24 × 24 cm^2).

Magnetic Resonance Spectroscopy Data Analysis

MRS data were analyzed using the Gannet 3.1 software toolkit, a GABA-MRS analysis tool that is coded within MATLAB (The MathWorks, Inc., Natick, MA, USA) using the Optimization and Statistics toolboxes and is distributed as open-source software (33, 34). The analysis consisted of the following steps: (1) frequency-and-phase alignment of FIDs with robust spectral correction (35); (2) averaging and subtraction of aligned spectra to produce GABA+ spectra; (3) fitting a Gaussian to the 3-ppm GABA+ peak to quantify GABA+ based on the area under the curve. GABA+ levels were quantified in institutional units (i.u.) relative to the unsuppressed water signal. The version of Gannet used for this analysis has been archived on OSF at: https://osf.io/q92mb/.

The primary data quality metric generated by Matlab is fitting error (FitErr,%), calculated as the ratio of the standard deviation of the fitting residual to the GABA+ signal amplitude. A data quality cut-off of 15% (11, 27, 36) has been applied previously for brain applications with good SNR. In this study, we used a cut-off of 20% (37) to reject spectra of poor quality, using a less stringent criterion to reflect the lower SNR of the smaller-VOI (voxel of interest) brainstem acquisition. Using a 20% cut-off allows us to retain a larger number of datasets in the analysis, at the cost of increasing the variability of data to include poorer-quality data. The choice of an appropriate cut-off for future *in vivo* studies is a trade-off between variance and sample size (which both impact statistical power) and possible inclusion bias, e.g. only including data from more compliant subjects.

Metrics of GABA+ SNR and creatine signal linewidth are also calculated by Gannet and reported.

Statistical Analysis

Due to the large age-range of subjects, a secondary statistical analysis was performed to investigate whether the midbrain GABA+ level was correlated with age. The average GABA+ concentrations for the male and female participants were compared with a two-tailed unpaired *t*-test, using the concentrations derived with Gannet 3.1. Statistical analysis was performed in the Statistical Package for Social Sciences (SPSS version 20.0; IBM Corp., Armonk, NY). To evaluate age-related differences in GABA+ of upper brainstem, the Pearson correlation coefficient was calculated and a Fisher R-to-z transforms to assess significance with a *p*-threshold of 0.05.

RESULTS

MRI scans were obtained on 42 healthy volunteers. **Table 1** shows the demographics of these participants. The volunteer group is with mean age: 45.7 ± 14.7 years (19 females, 45.2%; 23 males, 54.8%).

GABA+ levels were 2.66 ± 0.75 i.u. in the healthy volunteers, ranging from 1.50 to 4.40 i.u (as shown in **Table 2**). The mean GABA FitErr for upper brainstem voxel of volunteers was 12.1 ± 2.8% (spectra with fitting error below 20% are shown in **Figure 2**). The median FitErr was 11.7%, and as can be seen in **Figure 3A**, the distribution of fitting errors is only moderately skewed (skewness = 0.772). 8 cases have a fitting error below 10%, 20 between 10 and 15%, 6 cases 15-20% and 8 cases over 20%, which were omitted from the analysis.

The SNR is highly dependent on the experimental conditions and is modified by such factors as the field strength, voxel size, total acquisition time, TR, TE, J-coupling modulation, coil

TABLE 1 | Demographics of all subjects.

Demographics of the participants.	**HC**
Total number of subjects	42
Age in years	45.7 ± 14.7
No.of female (%)	19 (45.2%)
No.of male (%)	23 (54.8%)

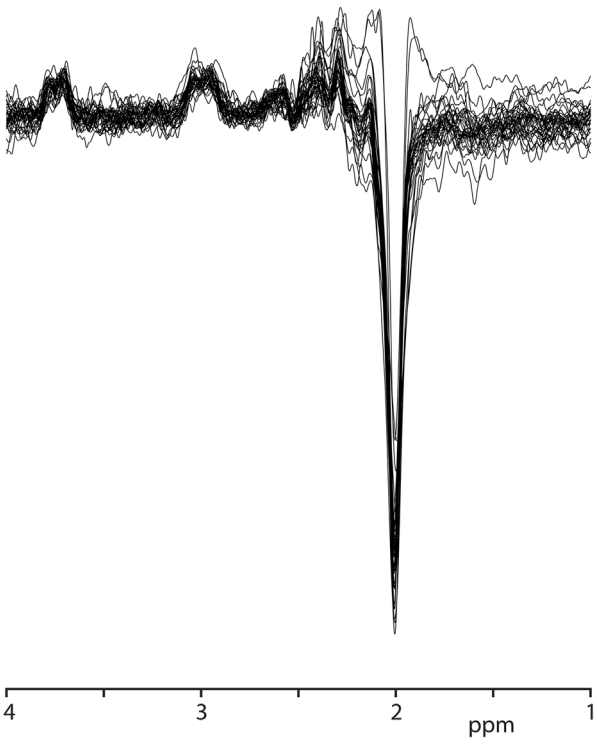

FIGURE 2 | In vivo GABA-edited spectra from the upper brainstem from 34 subjects (overlaid).

TABLE 2 | Subject demographics and MRS results.

	number	gender	Age	[GABA+]/i.u.	GABA+/Cr	FitErr (%)	GABA+ SNR	Cr.FWHM (linewidth)
1	MH-90*	F	55	61.89	2.024	2.4	47.3397	11.5112
2	MH-34	M	76	3.66	0.275	7.4	6.7847	6.6656
3	MH-116	M	57	4.397	0.228	8.4	3.8804	7.4313
4	MH-100	F	24	3.69	0.211	8.6	6.83	11.4299
5	MH-47	M	66	2.278	0.159	8.9	5.4383	7.3013
6	MH-95	M	48	2.892	0.148	9.3	6.5632	8.3427
7	MH-99	F	24	3.539	0.219	9.4	5.6473	6.8646
8	MH-107	M	56	2.623	0.124	9.7	3.8066	8.3243
9	MH-114	M	59	4.055	0.209	9.7	5.8652	7.349
10	MH-103	F	24	2.58	0.134	10	7.2623	9.7712
11	MH-104	M	56	2.731	0.156	10.2	4.5534	7.4724
12	MH-66	F	27	1.674	0.09	10.6	6.4	7.9068
13	MH-69	M	29	2.38	0.11	10.7	5.189	13.21
14	MH-27	F	50	3.375	0.092	10.7	7.0929	15.2452
15	MH-94	M	60	2.796	0.148	10.9	4.8486	7.187
16	MH-106	F	52	3.455	0.169	11.1	4.6792	9.2192
17	MH-37	F	36	2.586	0.203	11.4	5.7647	6.2624
18	MH-97	F	24	2.294	0.088	11.7	4.6513	10.9155
19	MH-92	M	56	2.537	0.143	11.7	4.5603	7.5527
20	MH-23	F	25	3.271	0.188	11.9	5.1726	7.7503
21	MH-101	M	24	3.374	0.299	12	5.433	6.4064
22	MH-110	F	58	3.318	0.179	12.4	6.4166	7.049
23	MH-61	M	56	2.209	0.119	12.7	4.0212	7.703
24	MH-73	F	24	1.52	0.01	12.8	5.0426	8.74
25	MH-115	F	50	2.937	0.112	13.2	5.6654	10.2316
26	MH-78	F	24	1.971	0.086	13.6	5.0123	10.00081
27	MH-117	F	59	2.329	0.122	13.8	6.2853	7.601
28	MH-112	M	36	2.209	0.114	14	3.7992	8.0255
29	MH-113	M	49	2.608	0.143	14.2	6.0098	7.7374
30	MH-108	M	52	1.678	0.065	15.1	4.1782	12.8079
31	MH-86	F	47	1.712	0.068	15.4	3.7966	12.3237
32	MH-109	M	60	2.131	0.101	15.6	4.0376	8.3851
33	MH-96	F	24	1.503	0.085	17.5	3.2026	7.5706
34	MH-53	M	61	2	0.106	18.1	4.6171	7.6339
35	MH-111	M	38	2.012	0.102	19.1	4.085	7.8425
36	MH-105*	M	57	2.042	0.118	20.1	3.3165	12.0987
37	MH-93*	M	53	1.815	0.078	23.6	3.9638	9.027
38	MH-89*	M	44	1.11	0.006	25	1.4629	7.8561
39	MH-91*	F	61	1.71	0.009	26	2.3535	6.5642
40	MH-87*	M	55	1.001	0.004	33	1.2958	7.0623
41	MH-98*	M	40	2.12	0.111	33	1.2958	7.0623
42	MH-88*	F	45	2.11	0.077	45.4	1.1705	6.8163

**Denotes low-quality data with FitErr >20%.*

loading, and the number of nuclei in the sample. In this study the mean SNR for upper brainstem voxel of volunteers was 5.19 ± 1.09 (as seen in **Figure 3**). The median SNR was 5.11. The distribution of SNR is only moderately skewed (skewness = 0.164 > 0). The linewidth is determined by a combination of the inherent T2 of the spin system under consideration and the loss of phase coherence in the sample volume from B_0 inhomogeneity caused by local differences in magnetic susceptibility. In our study the mean Cr linewidth was 8.7 ± 2.2 Hz. The median linewidth was 7.8 Hz (as seen in **Figure 3**). The distribution of linewidths is only moderately skewed (skewness = 1.5 > 0).

No significant correlations (p=0.215 > 0.05) with age were observed. There is no significant gender-related differences in the GABA+ levels in upper midbrain in the healthy volunteers (p=0.735>0.05).

DISCUSSION

This study demonstrates the feasibility of GABA-edited MEGA-PRESS in the upper brainstem in a moderately sized cohort of healthy volunteers and serves as an important foundation for future patient studies in movement disorders.

The brainstem is a midline structure formed by the midbrain, pons, and medulla containing a number of critical substructures (38). The major dopaminergic (DA) neuronal population of the mammalian brain is located in the ventral midbrain (VM) (39). The role of the brainstem as a route for all major efferent and afferent pathways to the periphery relies heavily on GABAergic connectivity (17). Brainstem pathology is implicated in many neurodegenerative disorders, including PD (20, 21). Postmortem evidence in PD indicates that pathological changes in the pons and medulla precede those in the substantia nigra, a key area of

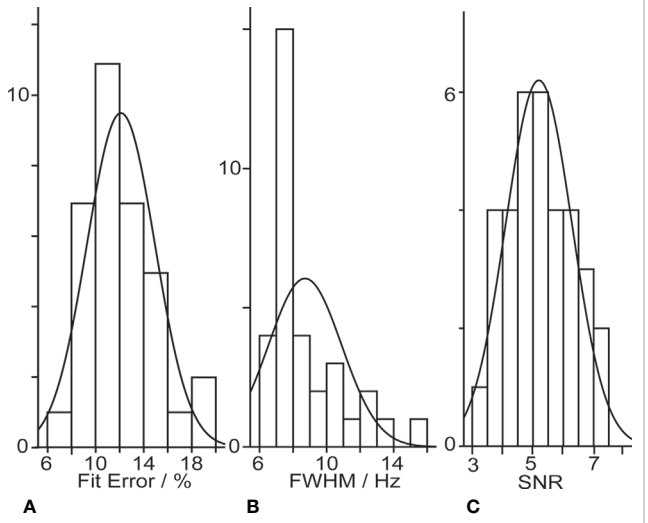

FIGURE 3 | Histograms of the distributions of fitting errors **(A)**, linewidth **(B)**, SNR **(C)**.

neuronal loss (22). It is therefore desirable to develop an MRS measure of GABA in the brainstem.

Edited MRS of GABA is made challenging by the relatively low concentration of GABA, signal overlap, and large typical voxel sizes. In order to measure GABA levels in the brainstem, a small-region of interest (ROI) MEGA-PRESS protocol has been developed. In spite of the relatively unfavorable anatomy, the linewidth achieved (median 7.8 Hz) is comparable to that seen in parietal lobe of the Big GABA multi-site study (mean 7.7 Hz (31)). This narrow linewidth is aided by the small voxel size (10 x 25 x 30 mm^3, compared to typical volumes of 30 x 30 x 30 mm^3 in the brain (31)). The GABA SNR is substantially lower than the SNR in that study (5.1 vs. 25), which reduction is largely explained by the 72% reduction in acquisition volume. The remaining reduction in SNR is likely attributable to the greater distance between the midbrain and the receive coil elements.

While the brainstem is under-studied with MRS compared to many cortical regions, there is some literature applying conventional (unedited) MRS there. For example, one MRS study at 1.5T showed higher N-acetylaspartate (NAA)/creatine (Cr) ratios in a 7.5 x 7.5 x 10 mm^3 voxel in bilateral rostral dorsal pons in patients with episodic migraine (EM) than those in patients with chronic migraine (CM) and normal controls (40). This study initiated the MRS scan if the water linewidth reported by the prescan process was less than 6 Hz. The ability of linear-combination modeling of conventional spectra and to resolve GABA signals without editing at 3T (and 7T) remains the subject of discussion. Macky et al. conducted conventional (unedited) PRESS-localized MRS at 3T in the midbrain (15 x 15 x 15 mm^3 voxel) and reported no differences in the ratio of GABA:creatine in patients with OSA compared with controls (18). Uzay et al. performed unedited MRS at 7T in the midbrain (30 x 10 x 15 mm^3 voxel), and showed the GABA+ level was increased in the pons in 11 patients with PD. In controls, the GABA+ level was 1.0 ± 0.2 mmol/g, with substantially larger relative variance than our study. One prior MEGA-PRESS pilot study showed GABA+ levels were significantly lower in the brainstems (25×18×30) of 12 possible Sleep Bruxism (SB) patients compared with 12 controls (41). This study conducted higher-order shimming to achieve linewidths of <25 Hz.

A number of studies have suggested that there is an age-related decrease of GABA+ levels in frontal and parietal regions in healthy control subjects (4, 42–44). While this effect is largely driven by bulk tissue changes, GABA+ levels still correlate with cognitive function (42). No MRS studies have investigated age-related changes in GABA+ concentrations in the upper brainstem of HC. The current study found no significant relationship between GABA+ levels and age. It is not currently possible to determine whether this negative result is due to reduced sample size, increased measurement variance or reduced neurodegenerative aging of the brainstem. Previous studies examining age-related volumetric decline in the brainstem have found no age effects for the volume of the whole brainstem, metencephalon or medulla, with only the midbrain showing a trend for age-related shrinkage (45, 46). In our study, the ROI mainly consists of midbrain and pons. Besides, a number of studies have suggested that there is a gender-related difference of GABA+ levels in dorso-lateral prefrontal cortex (4, 47). However, one edited-MRS study (48) showed that there is no gender differences were detected in anterior cingulate cortex, which was consistent with our study. The current study found no significant relationship between GABA+ levels and gender.

An eight-channel head coil was employed in our study. It is likely that higher-order, e.g. 32-channel, coils and other hardware innovations such as digital receiver chain would deliver higher SNR data that reported here. Measures of gray and white matter volume, white matter connectivity (fractional anisotropy and diffusivity measures) and functional connectivity in resting state networks are improved with 32- rather than 8-channel receive hardware (49). One MRS study showed that 32-channel would be better than 8 or 16-channel in SNR variations due to different hardware, pulse sequences, and post-processing between imaging and spectral scans (50). However, in our results, the SNR (mean: 5.19 ± 1.09; median: 5.11) is acceptable. We are confident that this demonstration of feasibility on an 8-channel head coil is applicable to other scanners with 32-channel hardware.

This study has several limitations. Firstly, the MEGA-PRESS sequence parameters give a GABA+ signal contaminated with MM and homocarnosine signals. Editing-based methods have been proposed to suppress the MM contribution (51), but the degree of MM suppression (and the polarity of the MM residual signal) is highly dependent on changes in the scanner frequency associated with motion and gradient heating (6). Secondly, the small size of the brainstem requires a small voxel. This results in a GABA+ measurement that has substantially lower SNR than is commonly achieved for brain measurements using a larger voxel. However, even though the voxel size is small for GABA MRS, it is large relative to the complex internal anatomy of the brainstem and includes a number of distinct structures without differentiation. This is a limitation inherent to MRS of low-concentration metabolites. We also recognize that the lack of a

gold standard for validation is a general concern for MRS measurements. Phantom validation of MRS protocols can be performed (and will indicate good linearity of measurements), but the challenges of MRS in the brainstem mostly center around subject and physiological motion, and local magnetic inhomogeneity, which phantom measurements do not address.

In conclusion, we have demonstrated that it is feasible to measure GABA+ levels in the upper brainstem using MEGA-PRESS. Understanding alterations in upper brainstem neurotransmitters will provide insight into pathological dysfunction in neurodegenerative disorders.

DATA AVAILABILITY STATEMENT

All datasets generated for this study are included in the article/supplementary material.

ETHICS STATEMENT

The studies involving human participants were reviewed and approved by the Ethics Committee of Shandong Medical Imaging Research Institute. The patients/participants provided their written informed consent to participate in this study. Written informed consent was obtained from each participant for the publication of any potentially identifiable images or data included in this article.

AUTHOR CONTRIBUTIONS

YS and TG contributed conception and design of the study. YS and TG organized the database. YS performed the statistical analysis. YS wrote the first draft of the manuscript. RE and GW revised the manuscript. All authors contributed to the article and approved the submitted version. The corresponding author GW takes primary responsibility for communication with the journal and editorial office during the submission process, throughout peer review, and during publication. The corresponding author GW is also responsible for ensuring that the submission adheres to all journal requirements including, but not exclusive to, details of authorship, study ethics and ethics approval, clinical trial registration documents and conflict of interest declaration. The corresponding author GW should also be available post-publication to respond to any queries or critiques.

FUNDING

This study applies tools developed under NIH grants R01 EB016089 and P41 EB015909; RAEE also receives salary support from these grants. This project was also funded by National Natural Science Foundation of China(81671668;81371534), Major research project of Shandong province(2016ZDJS07A16). Wang G also receives salary support from these grants.

REFERENCES

1. Mullins PG, McGonigle DJ, O'Gorman RL, Puts NAJ, Vidyasagar R, Evans CJ, et al. Current practice in the use of MEGA-PRESS spectroscopy for the detection of GABA. *Neuroimage* (2014) 86:43–52. doi: 10.1016/j.neuroimage.2012.12.004
2. Lee KJ, Shim I, Sung JH, Hong JT, Kim IS, Cho CB. Striatal Glutamate and GABA after High Frequency Subthalamic Stimulation in Parkinsonian Rat. *J Korean Neurosurg Soc* (2017) 60(2):138–45. doi: 10.3340/jkns.2016.0202.020
3. Elmaki EEA, Gong T, Nkonika DM, Wang GB. Examining alterations in GABA concentrations in the basal ganglia of patients with Parkinson's disease using MEGA-PRESS MRS. *Jpn J Of Radiol* (2018) 36(3):194–9. doi: 10.1007/s11604-017-0714-z
4. Gao F, Edden RA, Li M, Puts NA, Wang G, Liu C, et al. Edited magnetic resonance spectroscopy detects an age-related decline in brain GABA levels. *Neuroimage* (2013) 78:75–82. doi: 10.1016/j.neuroimage.2013.04.012
5. Bai X, Harris AD, Gong T, Puts NAJ, Wang G, Schar M, et al. Voxel Placement Precision for GABA-Edited Magnetic Resonance Spectroscopy. *Open J Radiol* (2017) 7(1):35–44. doi: 10.4236/ojrad.2017.71004
6. Harris AD, Puts NAJ, Barker PB, Edden RAE. Spectral-Editing Measurements of GABA in the Human Brain with and without Macromolecule Suppression. *Magn Reson In Med* (2015) 74(6):1523–9. doi: 10.1002/mrm.25549
7. Shungu DC, Mao XL, Gonzales R, Soones TN, Dyke JP, van der Veen JW, et al. Brain -aminobutyric acid (GABA) detection in vivo with the J-editing H-1 MRS technique: a comprehensive methodological evaluation of sensitivity enhancement, macromolecule contamination and test-retest reliability. *NMR Biomed* (2016) 29(7):932–42. doi: 10.1002/nbm.3539
8. Greenhouse I, Noah S, Maddock RJ, Ivry RB. Individual differences in GABA content are reliable but are not uniform across the human cortex. *Neuroimage* (2016) 139:1–7. doi: 10.1016/j.neuroimage.2016.06.007
9. Bai X, Edden RA, Gao F, Wang G, Wu L, Zhao B, et al. Decreased gamma-aminobutyric acid levels in the parietal region of patients with Alzheimer's disease. *J Magn Reson Imaging* (2015) 41(5):1326–31. doi: 10.1002/jmri.24665
10. Chiang GC, Mao X, Kang G, Chang E, Pandya S, Vallabhajosula S, et al. Relationships among Cortical Glutathione Levels, Brain Amyloidosis, and Memory in Healthy Older Adults Investigated In Vivo with H-1-MRS and Pittsburgh Compound-B PET. *Am J Of Neuroradiol* (2017) 38(6):1130–7. doi: 10.3174/ajnr.A5143
11. Cao GM, Edden RAE, Gao F, Li H, Gong T, Chen WB, et al. Reduced GABA levels correlate with cognitive impairment in patients with relapsing-remitting multiple sclerosis. *Eur Radiol* (2018) 28(3):1140–8. doi: 10.1007/s00330-017-5064-9
12. Cawley N, Solanky BS, Muhlert N, Tur C, Edden RAE, Wheeler-Kingshott CAM, et al. Reduced gamma-aminobutyric acid concentration is associated with physical disability in progressive multiple sclerosis. *Brain* (2015) 138:2584–95. doi: 10.1093/brain/awv209
13. Puts NA, Wodka EL, Tommerdahl M, Mostofsky SH, Edden RA. Impaired tactile processing in children with autism spectrum disorder. *J Neurophysiol* (2014) 111(9):1803–11. doi: 10.1152/jn.00890.2013
14. de la Fuente-Sandoval C, Reyes-Madrigal F, Mao X, Leon-Ortiz P, Rodriguez-Mayoral O, Jung-Cook H, et al. Prefrontal and Striatal Gamma-Aminobutyric Acid Levels and the Effect of Antipsychotic Treatment in First-Episode Psychosis Patients. *Biol Psychiatry* (2018) 83(6):475–83. doi: 10.1016/j.biopsych.2017.09.028
15. Freed RD, Hollenhorst CN, Weiduschat N, Mao X, Kang G, Shungu DC, et al. A pilot study of cortical glutathione in youth with depression. *Psychiatry Res Neuroimaging* (2017) 270:54–60. doi: 10.1016/j.pscychresns.2017.10.001
16. Maddock RJ, Caton MD, Ragland JD. Estimating glutamate and Glx from GABA-optimized MEGA-PRESS: Off-resonance but not difference spectra values correspond to PRESS values. *Psychiatry Res Neuroimaging* (2018) 279:22–30. doi: 10.1016/j.pscychresns.2018.07.003

17. Brodski C, Blaess S, Partanen J, Prakash N. Crosstalk of Intercellular Signaling Pathways in the Generation of Midbrain Dopaminergic Neurons In Vivo and from Stem Cells. *J Dev Biol* (2019) 7(1):3. doi: 10.3390/jdb7010003
18. Macey PM, Sarma MK, Prasad JP, Ogren JA, Aysola R, Harper RM, et al. Obstructive Sleep Apnea Is Associated with Altered Midbrain Chemical Concentrations. *Neuroscience* (2017) 363:76–86. doi: 10.1016/j.neuroscience.2017.09.001
19. Snyder AZ, Perlmutter JS, Hacker CD. Reply: Levodopa increases functional connectivity in the cerebellum and brainstem in Parkinson's disease. *Brain* (2013) 136(7):e235. doi: 10.1093/brain/awt016
20. Grinberg LT, Rueb U, Alho AT, Heinsen H. Brainstem pathology and non-motor symptoms in PD. *J Neurol Sci* (2010) 289(1-2):81–8. doi: 10.1016/j.jns.2009.08.021
21. Grinberg LT, Rueb U, Heinsen H. Brainstem: neglected locus in neurodegenerative diseases. *Front Neurol* (2011) 2:42. doi: 10.3389/fneur.2011.00042
22. Emir UE, Tuite PJ, Oz G. Elevated pontine and putamenal GABA levels in mild-moderate Parkinson disease detected by 7 tesla proton MRS. *PloS One* (2012) 7(1):e30918. doi: 10.1371/journal.pone.0030918
23. Du G, Liu T, Lewis MM, Kong L, Wang Y, Connor J, et al. Quantitative susceptibility mapping of the midbrain in Parkinson's disease. *Mov Disord* (2016) 31(3):317–24. doi: 10.1002/mds.26417
24. Zarow C, Lyness SA, Mortimer JA, Chui HC. Neuronal loss is greater in the locus coeruleus than nucleus basalis and substantia nigra in Alzheimer and Parkinson diseases. *Arch Neurol* (2003) 60(3):337–41. doi: 10.1001/archneur.60.3.337
25. Braak H, Rub U, Del Tredici K. Cognitive decline correlates with neuropathological stage in Parkinson's disease. *J Neurol Sci* (2006) 248(1-2):255–8. doi: 10.1016/j.jns.2006.05.011
26. Liu B, Yang H, Gao F, Wang Q, Zhao B, Gong T, et al. Investigation of brain GABA plus in primary hypothyroidism using edited proton MR spectroscopy. *Clin Endocrinol* (2017) 86(2):256–62. doi: 10.1111/cen.13177
27. Gao F, Wang G, Ma W, Ren F, Li M, Dong Y, et al. Decreased auditory GABA+ concentrations in presbycusis demonstrated by edited magnetic resonance spectroscopy. *Neuroimage* (2015) 106:311–6. doi: 10.1016/j.neuroimage.2014.11.023
28. Oeltzschner G, Snoussi K, Puts NA, Mikkelsen M, Harris AD, Pradhan S, et al. Effects of eddy currents on selective spectral editing experiments at 3T. *J Magn Reson Imaging* (2018) 47(3):673–81. doi: 10.1002/jmri.25813
29. Evans CJ, McGonigle DJ, Edden RAE. Diurnal Stability of gamma-aminobutyric Acid Concentration in Visual and Sensorimotor Cortex. *J Magn Reson Imaging* (2010) 31(1):204–9. doi: 10.1002/jmri.21996
30. Michou E, Williams S, Vidyasagar R, Downey D, Mistry S, Edden RA, et al. fMRI and MRS measures of neuroplasticity in the pharyngeal motor cortex. *Neuroimage* (2015) 117:1–10. doi: 10.1016/j.neuroimage.2015.05.007
31. Mikkelsen M, Barker PB, Bhattacharyya PK, Brix MK, Buur PF, Cecil KM, et al. Big GABA: Edited MR spectroscopy at 24 research sites. *Neuroimage* (2017) 159:32–45. doi: 10.1016/j.neuroimage.2017.07.021
32. Harris AD, Puts NA, Edden RA. Tissue correction for GABA-edited MRS: Considerations of voxel composition, tissue segmentation, and tissue relaxations. *J Magn Reson Imaging* (2015) 42(5):1431–40. doi: 10.1002/jmri.24903
33. Myers JFM, Evans CJ, Kalk NJ, Edden RAE, Lingford-Hughes AR. Measurement of GABA Using J-Difference Edited H-1-MRS Following Modulation of Synaptic GABA Concentration with Tiagabine. *Synapse* (2014) 68(8):355–62. doi: 10.1002/syn.21747
34. Edden RA, Puts NA, Harris AD, Barker PB, Evans CJ. Gannet: A batch-processing tool for the quantitative analysis of gamma-aminobutyric acid-edited MR spectroscopy spectra. *J Magn Reson Imaging* (2014) 40(6):1445–52. doi: 10.1002/jmri.24478
35. Mikkelsen M, Rimbault DL, Barker PB, Bhattacharyya PK, Brix MK, Buur PF, et al. Big GABA II: Water-referenced edited MR spectroscopy at 25 research sites. *Neuroimage* (2019) 191:537–48. doi: 10.1016/j.neuroimage.2019.02.059
36. Wenneberg C, Nordentoft M, Rostrup E, Glenthoj LB, Bojesen KB, Fagerlund B, et al. Cerebral Glutamate and Gamma-Aminobutyric Acid Levels in Individuals at Ultra-high Risk for Psychosis and the Association With Clinical Symptoms and Cognition. *Biol Psychiatry Cognit Neurosci Neuroimaging* (2020) 5(6):569–79. doi: 10.1016/j.bpsc.2019.12.005
37. Kurcyus K, Annac E, Hanning NM, Harris AD, Oeltzschner G, Edden R, et al. Opposite Dynamics of GABA and Glutamate Levels in the Occipital Cortex during Visual Processing. *J Neurosci* (2018) 38(46):9967–76. doi: 10.1523/JNEUROSCI.1214-18.2018
38. Kakkar C, Kakkar S, Saggar K, Goraya JS, Ahluwalia A, Arora A. Paediatric brainstem: A comprehensive review of pathologies on MR imaging. *Insights Imaging* (2016) 7(4):505–22. doi: 10.1007/s13244-016-0496-3
39. Bjorklund A, Dunnett SB. Dopamine neuron systems in the brain: an update. *Trends Neurosci* (2007) 30(5):194–202. doi: 10.1016/j.tins.2007.03.006
40. Lai TH, Fuh JL, Lirng JF, Lin CP, Wang SJ. Brainstem 1H-MR spectroscopy in episodic and chronic migraine. *J Headache Pain* (2012) 13(8):645–51. doi: 10.1007/s10194-012-0491-0
41. Fan X, Qu F, Wang JJ, Du X, Liu WC. Decreased gamma-aminobutyric acid levels in the brainstem in patients with possible sleep bruxism: A pilot study. *J Oral Rehabil* (2017) 44(12):934–40. doi: 10.1111/joor.12572
42. Porges EC, Woods AJ, Edden RA, Puts NA, Harris AD, Chen H, et al. Frontal Gamma-Aminobutyric Acid Concentrations Are Associated With Cognitive Performance in Older Adults. *Biol Psychiatry Cognit Neurosci Neuroimaging* (2017) 2(1):38–44. doi: 10.1016/j.bpsc.2016.06.004
43. Porges EC, Woods AJ, Lamb DG, Williamson JB, Cohen RA, Edden RAE, et al. Impact of tissue correction strategy on GABA-edited MRS findings. *Neuroimage* (2017) 162:249–56. doi: 10.1016/j.neuroimage.2017.08.073
44. Pauwels L, Maes C, Hermans L, Swinnen SP. Motor inhibition efficiency in healthy aging: the role of gamma-aminobutyric acid. *Neural Regener Res* (2019) 14(5):741–4. doi: 10.4103/1673-5374.249216
45. Garbade SF, Boy N, Heringer J, Kolker S, Harting I. Age-Related Changes and Reference Values of Bicaudate Ratio and Sagittal Brainstem Diameters on MRI. *Neuropediatrics* (2018) 49(4):269–75. doi: 10.1055/s-0038-1660475
46. Luft AR, Skalej M, Schulz JB, Welte D, Kolb R, Burk K, et al. Patterns of age-related shrinkage in cerebellum and brainstem observed in vivo using three-dimensional MRI volumetry. *Cereb Cortex* (1999) 9(7):712–21. doi: 10.1093/cercor/9.7.712
47. O'Gorman RL, Michels L, Edden RA, Murdoch JB, Martin E. In vivo detection of GABA and glutamate with MEGA-PRESS: reproducibility and gender effects. *J Magn Reson Imaging* (2011) 33(5):1262–7. doi: 10.1002/jmri.22520
48. Aufhaus E, Weber-Fahr W, Sack M, Tunc-Skarka N, Oberthuer G, Hoerst M, et al. Absence of changes in GABA concentrations with age and gender in the human anterior cingulate cortex: a MEGA-PRESS study with symmetric editing pulse frequencies for macromolecule suppression. *Magn Reson Med* (2013) 69(2):317–20. doi: 10.1002/mrm.24257
49. Panman JL, To YY, van der Ende EL, Poos JM, Jiskoot LC, Meeter LHH, et al. Bias Introduced by Multiple Head Coils in MRI Research: An 8 Channel and 32 Channel Coil Comparison. *Front Neurosci* (2019) 13:729. doi: 10.3389/fnins.2019.00729
50. Lin Y, Chen Z, Zhong J. Signal-to-noise ratio enhancement of intermolecular double-quantum coherence MR spectroscopy in inhomogeneous fields with phased array coils on a 3 Tesla whole-body scanner. *J Magn Reson Imaging* (2011) 33(3):698–703. doi: 10.1002/jmri.22434
51. Henry ME, Lauriat TL, Shanahan M, Renshaw PF, Jensen JE. Accuracy and stability of measuring GABA, glutamate, and glutamine by proton magnetic resonance spectroscopy: A phantom study at 4 Tesla. *J Of Magn Reson* (2011) 208(2):210–8. doi: 10.1016/j.jmr.2010.11.003

Conflict of Interest: The authors declare that the research was conducted in the absence of any commercial or financial relationships that could be construed as a potential conflict of interest.

frontiers in Psychiatry

ORIGINAL RESEARCH
published: 11 September 2020
doi: 10.3389/fpsyt.2020.549749

Unaltered Brain GABA Concentrations and Resting fMRI Activity in Functional Dyspepsia With and Without Comorbid Depression

Arthur D. P. Mak[1], Yuen Man Ho[1], Owen N. W. Leung[1], Idy Wing Yi Chou[1], Rashid Lui[2], Sunny Wong[2], David K. W. Yeung[3], Winnie C. W. Chu[3], Richard Edden[4,5], Sandra Chan[1], Linda Lam[1] and Justin Wu[2]*

[1] Department of Psychiatry, Faculty of Medicine, The Chinese University of Hong Kong, Hong Kong, Hong Kong, [2] Institute of Digestive Disease, Department of Medicine and Therapeutics, Faculty of Medicine, The Chinese University of Hong Kong, Hong Kong, Hong Kong, [3] Department of Imaging and Interventional Radiology, Faculty of Medicine, The Chinese University of Hong Kong, Hong Kong, Hong Kong, [4] Russell H. Morgan Department of Radiology and Radiological Science, The Johns Hopkins University School of Medicine, Baltimore, MD, United States, [5] F.M. Kirby Research Center for Functional Brain Imaging, Kennedy Krieger Institute, Baltimore, MD, United States

OPEN ACCESS

Edited by:
Zafiris J. Daskalakis, University of Toronto, Canada

Reviewed by:
Gianluca Serafini, San Martino Hospital (IRCCS), Italy
Kiyotaka Nemoto, University of Tsukuba, Japan

***Correspondence:**
Arthur D. P. Mak
arthurdpmak@cuhk.edu.hk

Specialty section:
This article was submitted to Neuroimaging and Stimulation, a section of the journal Frontiers in Psychiatry

Received: *07 April 2020*
Accepted: *24 August 2020*
Published: *11 September 2020*

Citation:
Mak ADP, Ho YM, Leung ONW, Chou IWY, Lui R, Wong S, Yeung DKW, Chu WCW, Edden R, Chan S, Lam L and Wu J (2020) Unaltered Brain GABA Concentrations and Resting fMRI Activity in Functional Dyspepsia With and Without Comorbid Depression. Front. Psychiatry 11:549749. doi: 10.3389/fpsyt.2020.549749

Background: GABA-deficit characterizes depression (MDD), which is highly comorbid with Functional Dyspepsia (FD). We examined brain GABA concentrations and resting activities in post-prandial distress subtype FD (FD-PDS) patients with and without MDD.

Methods: 24 female age/education-matched FD-PDS with comorbid MDD (FD-PDS-MDD), non-depressed FD-PDS, and healthy controls each were compared on GABA concentrations, resting fMRI (fALFF) in bilateral pregenual anterior cingulate (pgACC), left dorsolateral prefrontal cortex (DLPFC), insula, and somatosensory cortex (SSC).

Results: FD-PDS-MDD patients had mild though elevated depressive symptoms. FD-PDS patients had generally mild dyspeptic symptoms. No significant between-group differences in GABA or fALFF were found. No significant correlations were found between GABA and depressive/dyspeptic symptoms after Bonferroni correction. In patients, GABA correlated positively with left insula fALFF ($r = 0.38$, Bonferroni-corrected $p = .03$).

Conclusion: We did not find altered GABA concentrations or brain resting activity in FD-PDS or its MDD comorbidity. The neurochemical link between MDD and FD remains elusive.

Keywords: major depressive disorder, functional dyspepsia, GABA, magnetic resonance spectroscopy, resting fMRI

INTRODUCTION

Functional dyspepsia (FD) is a common and chronic functional gastrointestinal disorder characterized by symptoms attributed to gastroduodenal origin in the absence of any organic, systemic, or metabolic disease likely to explain the symptoms (1).

Substantial evidence exists for gut-brain directed etiological mechanisms in FD, such as infection, inflammatory mechanisms, and altered gut microbiota. On the other hand, associations

of FD with personality traits, serotonin polymorphism and experience of childhood adversity provide some evidence for the brain-gut basis to FD (2). In particular, the significantly increased risk of comorbid Major Depressive Disorder (MDD) in community FD samples (3–5), bidirectional chronological relationship in the respective onsets of FD and MDD in community subjects (6), and response of non-depressed FD subjects to serotonin-modulating antidepressant drugs (7, 8) suggested substantial pathophysiological overlap between FD and MDD. In addition, both MDD and FD have been associated with trait characteristics of neuroticism (9, 10) and alexithymia. Alexithymia has even been shown to contribute to both somatization, depressive and anxiety symptoms, as well as suicide risk (11, 12). MDD has also been associated with trait-alterations in sensory processing patterns unique to the individual (13) that is akin to the experience-based alterations in salience computation of visceral signals in functional gastrointestinal disorders (14, 15). Examining neural mechanisms underlying the rich linkages in the FD-MDD comorbidity should help understand the brain-gut mechanisms that determine symptomatology and treatment response.

Visceral, cognitive and emotional processing occurs in cortical glutamatergic networks, including somatosensory cortex (SSC) [Sensorimotor Network (SMN) (15)] that relays visceral sensory input to the Salience Network (SN-insula) which integrates affective and interoceptive information (16) and send control signals to the (i) the Default Mode Network [DMN: midline structures including perigenual anterior cingulate cortex (pgACC)] (16) and (ii) engages the Executive Network [EN: Dorsal-lateral prefrontal cortex (DLPFC)]. These glutamatergic networks are modulated by inhibitory GABA-ergic interneurons (16), in turn innervated by serotonergic neurons at pgACC, VMPFC, and raphe nuclei (17). Dysfunction in these affective networks may lead to impaired gating of somatosensory signals (2, 16), contributing to somatosensory amplification (11, 14) in FD and MDD (18).

In MDD, inhibition of GABA-ergic neurons by dysfunctional serotonergic neurons at the pgACC may reduce GABA (19, 20), in turn disinhibiting glutamatergic neurons and resulting in DMN hyperactivity (21–23). This altered pgACC GABA/glutamate balance may underlie increased self-focus in MDD and has been suggested to be the neurochemical substrate of antidepressant action (24). MDD is also associated with resting-state hypoactivity in the EN (DLPFC) (22, 25) while in the insula, depressive affect is associated with reduced GABA concentration and insula hypoactivity in processing self-related information (26).

In FD-PDS, the predominant FD subtype where psychiatric comorbidity is the commonest, resting-state positron-emission tomography (PET) (27) and functional MRI (28) showed increased SN, DMN, thalamus, and precuneus resting activity, as well as lowered SMN and SN activation threshold to gastric distension and failure of pain-related pgACC activation (29). These correlated positively with dyspeptic (27), anxiety, and depressive symptoms (29), suggesting abnormal mood-related processing of somatic signals in the SMN, SN, and DMN (29–31). In our earlier magnetic resonance spectroscopy (MRS) study, we found significant increase in SSC glutamate levels in FD that correlated with anxiety and dyspeptic symptom severity but were independent of depressive severity (32). The short-TE PRESS sequence used for resolving glutamate peaks from glutamine (TR/TE = 3,000/24ms) did not yield accurate measurements of GABA. In fact, there have been no studies on GABA transmission in FD. As such, it is unknown whether FD-PDS would be similar to MDD in GABA-deficit-driven SN and DMN abnormal activities.

In the present investigation, we used MEGAPRESS (33) to examine GABA concentrations in major nodes of the SN, SMN, DMN, and EN in matched FD-PDS patient groups differentiated by the presence of MDD, to clarify the pathophysiological abnormalities peculiar to FD and depressive comorbidity. To reduce demand on sample size and owing to evidence showing gender effects in neural activities in the brain (34), as well as the female predominance in MDD and FD (32), we decided to perform the study on female subjects only. We hypothesized that altered GABA concentrations in representative regions in the DMN, SN, EN, and SMN would be found amid subjects with FD-PDS with and without comorbid MDD as compared to healthy controls, with those with comorbid MDD showing a greater deficit than their counterparts.

MATERIALS AND METHODS

Participants and Recruitment

Twenty-six FD-PDS with comorbid MDD (FD-PDS-MDD) and 28 FD-PDS without comorbid MDD were consecutively recruited at a specialist gastrointestinal clinic. Inclusion criteria were as follows: (i) currently satisfying ROME III criteria for FD-PDS as assessed by a gastroenterologist (1), (ii) normal oesophago-gastroduodenoscopy results within 2 years from recruitment, (iii) for FD-PDS-MDD group only, comorbid Major Depressive Disorder (MDD) as meeting DSM-IV-TR criteria for MDD, and (iv) right-handed. Exclusion criteria included having other functional gastrointestinal disorders (irritable bowel syndrome or history of symptoms of acid regurgitation, heartburn or those with abdominal pain as the predominant symptom), consuming drugs that may affect gastrointestinal motility (neuroleptic drugs, non-steroidal anti-inflammatory drugs, aspirin and steroids) within 2 weeks prior to scan, chronic or severe medical conditions, intellectual disability, organic brain syndromes, having other mental disorders including anxiety disorders, psychosis, bipolar disorder, substance abuse, or dependence and presence of any metallic devices or materials in the body that are contraindicated for magnetic resonance imaging.

Thirty age-sex-education matched healthy controls (HC) were recruited *via* hospital posters and online advertisements, after a baseline assessment screening against the same exclusion criteria described above, along with any personal history of gastrointestinal complaints and personal or family history of any mental disorders.

Ten subjects with excessively noisy MRS spectra were excluded from analyses, resulting in a final sample consisting of 24 subjects per arm.

All eligible participants provided valid written informed consent. All experimental protocols were approved by the New Territories East Cluster-Chinese University of Hong Kong Clinical Research Ethics Committee and all procedures were performed in accordance with the approved guidelines and regulations.

Sociodemographic and Symptomatic Assessments

Socio-demographic data including age, marital status, employment status, monthly family income, and educational background were obtained using a questionnaire. Diagnoses of MDD and other mental disorders stated within the exclusion criteria were obtained by trained clinician interviewers using the Chinese-Bilingual version of the Structured Clinical Interview for DSM IV-TR Mental Disorders-I (35). Current dyspeptic symptoms and other gastrointestinal disorder symptoms were enquired with a structured Rome III symptom assessment questionnaire. Dyspeptic symptom severity was measured with the dyspepsia items from FGI-Checklist, a validated 20-item structured questionnaire assessing common upper and lower gastrointestinal symptoms (36), each self-rated on a scale of 0 to 3. A global dyspeptic symptom severity score was generated by averaging the scores for the items included. Current depressive and anxiety symptoms were evaluated with the commonly-used interviewer-administered scales of MADRS (37) and HAM-A (38), respectively. MADRS consists of 10 items rated on a 0 to 6 continuum that evaluate core symptoms of depression, with a total score of 7–19 denoting mild depression, 20–34 for moderate depression, and >34 for severe depression. HAM-A consists of 14 items on psychic and somatic aspects of anxiety, each rated from 0 (not present) to 4 (severe), with a total score of <17 denoting mild severity, 18–24 for mild to moderate, and 25–30 for moderate to severe. Interoceptive awareness was measured using the Body Perception Questionnaire, a 122-item self-report instrument consisting of subscales on body awareness, stress response, autonomic nervous system reactivity, stress style, and health history, respectively (39). General severity of somatic symptoms was measured using a Chinese version of the 15-item Patient Health Questionnaire (PHQ-15) which has been validated in the local community, showing satisfactory reliability and validity (40). General health-related quality of life was measured by a validated Chinese version of the Short-form-36 health survey (SF-36) (41). Current medication history was enquired and checked with hospital records. The Three-subtest Short Form of the Wechsler Adult Intelligence Scale-III (42) was conducted on all participants at baseline to control for confounding effects of intelligence on scan results.

Imaging

All imaging protocols were performed using a 3 Tesla MRI scanner (Achieva TX series, Philips Healthcare, Best, Netherlands).

Anatomical MRI

High resolution structural images were acquired using an eight-channel receive-only head coil using a sagittal 3D T1-weighted sequence (TR/TE: 7.4/3.4 ms; field of view: 250,250 mm, 285 contiguous slices, 0.6-mm (RL) thickness, reconstruction matrix: 240,240, flip angle 8°). T1-weighted images were segmented into gray matter (GM), white matter and cerebrospinal fluid (CSF) maps using SPM12 (43). GM volume of each MRS volume-of-interest (see below) was extracted using FSL (44).

Magnetic Resonance Spectroscopy

Anatomical MRI images were used to guide positioning of MRS volumes-of-interest in bilateral pregenual anterior cingulate cortex (pgACC), left insula, left SSC, and left dorsolateral prefrontal cortex (DLPFC). The bilateral pgACC voxels (30 mm × 30 mm × 30 mm) were positioned bordering the lower edge of the genu of the corpus callosum and with its posterior limits just touching the anterior border of the genu of the corpus callosum (**Figure 1A**) (45). The left insula voxels (25 mm × 40 mm × 25 mm) were aligned along the edge of the insula cortex in an anterior-posterior direction with the anterior edge of the volume-of-interest aligned to the anterior limit of the insula (**Figure 1B**) (26). The left SSC (30 mm × 30 mm × 30 mm) was placed on the post-central gyrus (Brodmann areas 1, 2, and 3) (**Figure 1C**) (46). The left DLPFC (30 mm × 30 mm × 30 mm) was placed in the left inferior frontal gyrus between the inferior frontal sulcus and horizontal ramus (**Figure 1D**) (47, 48).

Signal reception for H-MRS were achieved using the same eight-channel received-only head coil under the following parameters: TE, 68 ms; TR, 2,000 ms; 400 transients of 4,096 data points acquired in 12 min; 14-ms Gaussian editing pulses to be applied either to the GABA spins (at 1.9 ppm) or symmetrically about the water peak (7.5 ppm) in an interleaved manner. A further eight transients were acquired, without water suppression, as an internal concentration reference.

GABA concentrations in the 4 volumes-of-interest were gauged as GABA signal intensities relative to water, as derived from GABA-edited MEGA-PRESS MRS spectra using Gannet v3.0 (33). GABA signal was scaled to account for the fraction of cerebrospinal fluid (CSF) within the voxel, and the water signal was scaled to account for the different water content in CSF, gray, and white matter. A concentration measurement in institutional units is derived from the ratio of the GABA and water signals by further adjusting for the editing efficiency and the T1 and T2 relaxation times of water and GABA. The overall fit errors, represented by the standard deviation of the fitting residuals relative to the GABA and water fitting peaks, converged to mean values of 6.5%, 5.1%, 5.3%, and 4.1% for left DLPFC, left insula, pgACC, and left SSC, respectively.

Functional MRI - fALFF

Subjects were instructed to have their eyes closed for 6 min and hold still without falling asleep. Resting fMRI data was collected with a single-shot echo-planar sequence sensitive to BOLD contrast (TR, 2,050 ms; TE, 25 ms; flip angle, 90°; slab

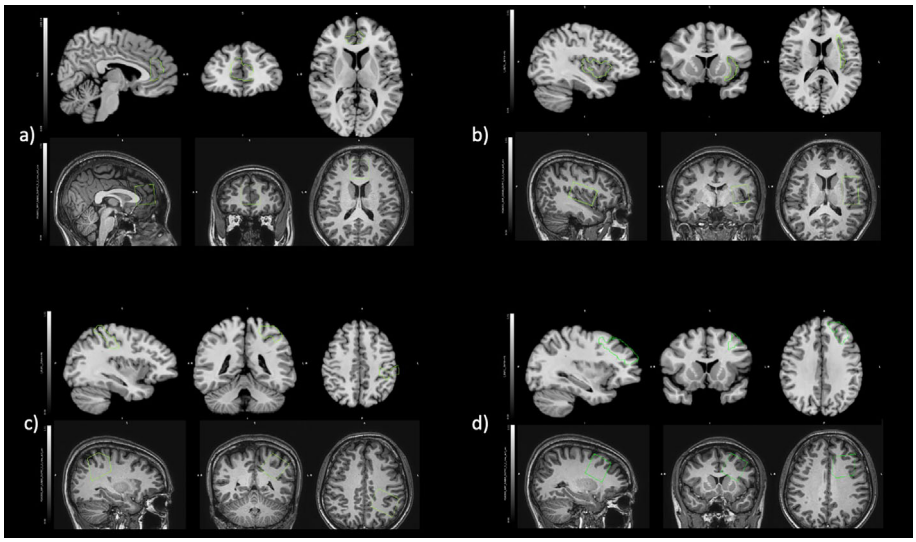

FIGURE 1 | Positioning of regions of interest in fALFF (Top) and MRS (Bottom) for **(A)** bilateral pregenual anterior cingulate cortex, **(B)** left insula, **(C)** left somatosensory cortex, and **(D)** left dorsolateral prefrontal cortex.

thickness, 150 mm; field of view, 205' 205 mm; image matrix, 6,464; parallel imaging acceleration factor of 2) to acquire 150 dynamic scans under each condition. BOLD images acquired had a nominal in-plane resolution of 3.23.2 mm and a temporal resolution of 2 s per dynamic scan.

The first three volumes were removed to eliminate the effects of start-up transients. Resting-state imaging data were preprocessed using AFNI (Analysis of Functional Neuro-Images) (49). Preprocessing steps included slice-timing correction, alignment between the structural image and the third functional volume, estimation of motion correction parameters (three translational and three rotational components) that co-register each functional volume to a reference volume with the lowest motion, and warping structural image to the Talaraich space. Fractional amplitude of low frequency fluctuations (fALFF) were derived from the rsfMRI data using AFNI's 3dRSFC program (50, 51). First, each voxel time series was converted into the frequency domain (0–0.25 Hz) using a fast Fourier transform without band-pass filtering and the square root of each frequency of the power spectrum was calculated. Second, each voxel time-series was band-pass filtered (0.01–0.10 Hz) before converting to the power spectrum and the sum amplitude of this low frequency domain was calculated. Finally, the ratio between the sum amplitude of the low frequency domain and the full frequency domain was extracted for each voxel. Also, mean fALFF was calculated for each volume-of-interest.

Statistical Analysis

Baseline demographic characteristics were compared between the three arms using chi-square and one-way ANOVAs as appropriate.

Mean GABA concentrations were compared between the three groups using generalized estimating equations, ANCOVA, and a t-test where healthy controls were compared against a combined patient group (FD with comorbid MDD + pure FD). Generalized estimating equation analyses were all adjusted for age, IQ, and same-region GM volume, whereas ANCOVA and t-test included any of these covariates only when correlation with GABA concentration was presented.

Pearson correlation was used to identify relationships between GABA concentrations of each region with dyspeptic severity (FGISQ), introspective awareness (BDQ), depressive severity (MADRS), anxiety severity (HAMA), somatization (PHQ15), health-related quality of life (SF36), and same region fALFF. For each VOI, the mean fALFF was extracted and its correlation with same-region GABA concentrations was examined by Pearson correlation, corrected for age, IQ and same-region GM volume, or any combination therefor, whichever correlated with GABA concentration. All correlation analyses were performed across the whole sample, for each patient group individually, and for a combined patient group (FD-PDS and FD-PDS-MDD).

Between group mean difference of fALFF was assessed using voxel-wise permutation analysis, corrected for the effect of age, IQ and same-region GM volume.

IBM SPSS Statistics v23 for Windows was used for all statistical analyses. Results of $p < 0.05$ were considered significant. All tests were two-tailed. To account for multiple comparisons in four ROIs, Bonferroni correction was applied to all statistical analysis involving GABA and fALFF.

RESULTS

Demographics

Twenty-four female subjects were recruited in each group: 1. FD-PDS patients with comorbid MDD (FD-PDS-MDD), 2. FD-PDS

patients without MDD (FD-PDS), and 3. healthy controls (HC). 10 subjects with noisy MRS spectra were excluded (see *Materials and Methods*). All subjects were female and had a mean age of 42.44 and on average 11.86 years of education. Over half of the sample were married and had full-time employment. No significant differences were found in age, education, marital status, and employment status between the 3 groups (**Table 1**).

Clinical

FD-PDS-MDD patients had a mean Montgomery–Åsberg Depression Rating Scale (MADRS) and Hamilton Anxiety Rating Scale (HAMA) scores of 18.01 (SD 6.08) and 15.38 (SD 7.1), which were within the mild range (37, 38). These were significantly greater than the FD-PDS group (ps <.001) and HC (ps < .001) (**Table 1**).

Patients had generally mild dyspeptic symptoms. On a composite score of current dyspeptic symptom derived by summing self-rated scores on four dyspeptic symptoms (36) (epigastric pain, epigastric burning, postprandial fullness, early satiety), FD-PDS patients with and without MDD comorbid showed significantly elevated dyspeptic symptoms compared to HC ($p < 0.001$), while no significant differences were found between FD-PDS and comorbid FD-PDS-MDD patients (**Table 1**).

Group Difference in GABA Concentration and fALFF

Figure 2 shows the GABA concentration in different VOIs in the three groups. No significant differences were found between the three groups in GABA concentrations in any of the voxels of interest, using AN(C)OVA (**Table 2**), generalized estimating equation (**Table 2**), or in the T-test comparing HC against a combined patient group (**Table 3**).

No significant difference was found in fALFF among the three groups in any of the four regions examined (5,000 permutations, adjusted for age, IQ, and same-region GM volumes) (**Table 4**).

Correlations Between GABA Concentration and Clinical Measurements

Negative correlations of left insula GABA with dyspeptic symptom severity for FD-PDS-MSS (r = −0.49, corrected p = 0.06) and across all patients (r = −0.35, corrected p = 0.06) became insignificant after correction for multiple comparison (**Table 5**). The negative correlation between bilateral pgACC GABA and anxiety symptoms also rendered insignificant after Bonferroni's correction (r = −0.29, p = 0.19) (**Table 5**).

No correlations between GABA and health-related quality of life, somatization and introspective awareness were found.

Correlations Between GABA Concentration and fALFF

In the combined patient group (FD-PDS and FD-PDS-MDD), left insula GABA correlated with same-region fALFF (r = 0.38, corrected p = 0.03) (**Table 6**).

There were no significant GABA-fALFF correlations in any regions within each patient group or across all subjects.

TABLE 1 | Demographics.

	FD-PDS-MDD (n = 24)	FD-PDS (n = 24)	HC (n = 24)	Chi-square	F/W	p	Cohen's d: FD-PDS-MDD vs. FD-PDS	Cohen's d: FD-PDS-MDD vs. HC	Cohen's d: FD-PDS vs. HC	Hedges' g: All patients vs. HC
Sociodemographic										
Age, years (SD)	41.92 (10.88)	42.75 (11.96)	42.67 (12.13)	–	0.04	0.96	–	–	–	–
Education, years (SD)	11.78 (2.63)	11.75 (2.25)	12.04 (2.33)	–	0.11	0.9	–	–	–	–
Marital status, n (%)				9.46	–	0.49	–	–	–	–
Single	7 (30.4)	8 (33.3)	10 (41.7)	–	–	–	–	–	–	–
Married	11 (47.8)	14 (58.3)	13 (54.2)	–	–	–	–	–	–	–
Separated/widowed	4 (17.3)	2 (8.3)	1 (4.2)	–	–	–	–	–	–	–
Others	2 (8.3)	0 (0.0)	0 (0.0)	–	–	–	–	–	–	–
Occupation status, n (%)[a]				3.04	–	0.8	–	–	–	–
Employed	17 (70.8)	16 (66.7)	20 (83.3)	–	–	–	–	–	–	–
Student	3 (12.5)	3 (12.5)	2 (8.3)	–	–	–	–	–	–	–
Homemaker	3 (12.5)	5 (20.8)	2 (8.3)	–	–	–	–	–	–	–
Missing data	1 (4.2)	0 (0.0)	0 (0.0)	–	–	–	–	–	–	–
Affective Symptoms[a]										
Depression—MADRS	18.08 (6.08)	1.71 (2.14)	0.67 (1.24)	–	93.21	<.001***	3.59***	3.97***	0.60*	1.19***
Anxiety—HAMA	15.38 (7.10)	5.29 (4.79)	2.17 (2.30)	–	38.44	<.001***	1.67***	2.50***	0.83**	1.24***
Somatization—PHQ-15	12.52 (3.96)	7.54 (2.64)	2.96 (2.81)	–	46.67	<.001***	1.48***	2.78***	1.68***	1.86***
Dyspeptic Symptoms – FGI-Checklist[a]										
Symptom severity[b]	4.48 (2.13)	3.42 (1.44)	0.50 (.88)	–	57.62	<.001***	0.58	2.44***	2.44***	2.13***

[a]*Equal variances are not assumed.*

[b]*Composite score from summing self-rated severity of four symptoms – epigastric pain, epigastric burning, postprandial fullness, early satiation, each rated on a four-point scale of 0 to 3, i.e., 0 (none), 1 (mild), 2 (moderate), and 3 (severe).*

*$p < 0.05$, **$p < 0.01$, ***$p < 0.001$.

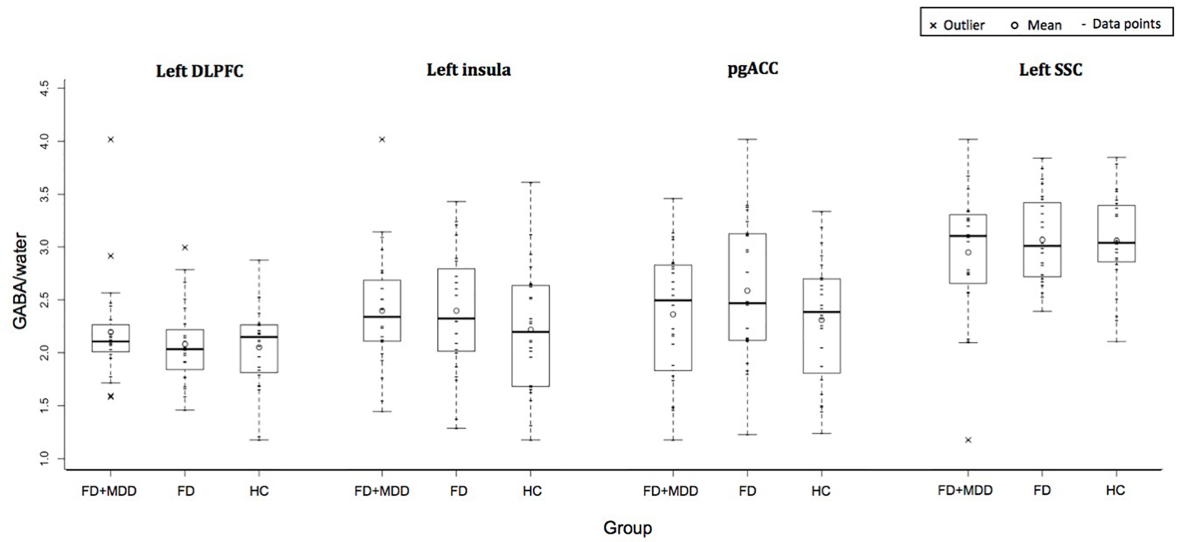

FIGURE 2 | Group difference in GABA/water in four regions of interest: left dorsolateral prefrontal cortex, left insula, bilateral pregenual anterior cingulate cortex, and left somatosensory cortex.

TABLE 2 | Group difference of GABA/water.

	AN(C)OVA									
	FD-PDS-MDD		FD-PDS		HC		AN(C)OVA[a]			
	(*n* = 24)		(*n* = 24)		(*n* = 24)					
ROI	**mean**	**SD**	**mean**	**SD**	**Mean**	**SD**	**F**	**df**	**p**	**Bonferroni-corrected p**
Left Dorsolateral Prefrontal Cortex[b]	2.2	0.49	2.08	0.38	2.05	0.39	1.7	2, 1, 68	0.19	0.76
Left Insula	2.53	0.22	2.53	0.23	2.46	0.24	0.8	2, 69	0.46	>0.99
Bilateral Pregenual Anterior Cingulate	2.3	0.23	2.38	0.25	2.28	0.22	1.3	2, 69	0.28	>0.99
Left Somatosensory Cortex	2.28	0.33	2.34	0.22	2.33	0.23	0.4	2, 69	0.67	>0.99

		Generalized Estimating Equation[c]				
ROI	**Group**	**β**	**Z**	**p**	**Bonferroni-corrected p**	**95% CI**
Left DLPFC	FD-PDS-MDD					
	FD-PDS	-0.16	-1.26	0.21	0.84	0.85 (0.67-1.09)
	HC	-0.21	-1.63	0.1	0.4	0.81 (0.63-1.04)
Left Insula	FD-PDS-MDD					
	FD-PDS	0.002	0.03	0.98	>0.99	1 (0.89-1.13)
	HC	-0.07	-1.02	0.31	>0.99	0.94 (0.82-1.06)
pgACC	FD-PDS-MDD					
	FD-PDS	0.1	1.41	0.16	0.64	1.1 (0.96-1.27)
	HC	0.003	0.04	0.97	>0.99	1 (0.88-1.14)
Left SSC	FD-PDS-MDD					
	FD-PDS	0.08	1.03	0.3	>0.99	1.09 (0.93-1.28)
	HC	0.1	1.1	0.27	>0.99	1.1 (0.93-1.31)

[a]*Levene's test confirmed equal variances across groups.*
[b]*Covariate: IQ.*
[c]*Adjusted for age, gray matter volume in same-region MRS ROI and IQ.*

DISCUSSION

This is the first study reporting on GABA concentrations in the major somatic-cognitive-affective network in patients with functional gastrointestinal disorders. We failed to find any evidence for altered GABA concentrations in representative regions in the DMN, SN, EN, and SMN in these age/education-matched group of female subjects with FD-PDS with or without comorbid FD-PDS, and healthy subjects. As such, the neurochemical link between FD-PDS and MDD remains elusive.

TABLE 3 | Group difference of GABA/water between healthy controls and combined patient group tested with t-test (n = 72).

ROI	All patients (n = 48)		HC (n = 24)		t-test[a]			
	mean	SD	mean	SD	t	df	p	Bonferroni-corrected p
Left Dorsolateral Prefrontal Cortex	2.14	0.44	2.05	0.39	-0.8	70	0.2	0.8
Left Insula	2.53	0.22	2.46	0.24	-1.3	70	0.11	0.44
Bilateral Pregenual Anterior Cingulate	2.34	0.24	2.28	0.22	-1	70	0.15	0.6
Left Somatosensory Cortex	2.31	0.28	2.33	0.23	0.4	70	0.35	>0.99

[a]*No significant correlation present in GABA/water of individual ROI against age, same-region gray matter volume and IQ.*

TABLE 4 | Group difference of fALFF from voxel-wise permutation analysis.

ROI	ANCOVA[a]			Talaraich coordinates		
	p[b]	Bonferroni-corrected p	F[b]	x	y	z
Left DLPFC	0.707	>0.99	67.076	29	53	34
Left insula	0.738	>0.99	16.02	37	26	25
pgACC	0.543	>0.99	36.084	26	47	22
Left SSC	0.353	>0.99	87.685	40	23	37

[a]*Corrected for the effect of age, IQ and same-region GM volume.*
[b]*Minimum p and maximum F across all voxels in the corresponding ROI.*

TABLE 5 | Correlations between GABA/water and clinical measures.

MRS ROI	Measure	All subjects (n = 72)			Combined patient group (n = 48)			FD-PDS-MDD (n = 24)			FD-PDS (n = 24)		
		r	p	Bonferroni-corrected p	r	p	Bonferroni-corrected p	r	p	Bonferroni-corrected p	r	p	Bonferroni-corrected p
Left Insula	FGISQ	–0.05	0.66	>0.99	–0.35	0.01	0.06	–0.49	0.01	0.06	–0.23	0.28	>0.99
Bilateral Pregenual Anterior Cingulate	HAMA	–0.11	0.35	>0.99	–0.29	0.05	0.19	–0.34	0.10	0.40	–0.09	0.66	>0.99

MRS ROIs tested: left dorsolateral prefrontal cortex, left insula, bilateral pregenual anterior cingulate, left somatosensory cortex.
Clinical measures tested: FGISQ, Functional Gastrointestinal Standard Questionnaire; BPQ, Body Perception Questionnaire; MADRS, Montgomery–Åsberg Depression Rating Scale; HAMA, Hamilton Anxiety Rating Scale; PHQ15, Patient Health Questionnaire-15; SF36, 36-item Short Form Survey.

TABLE 6 | Correlations between GABA/water and same-region fALFF.

Group	n	MRS ROI	Pearson's Correlation		
			p	Bonferroni-corrected p	r
All Subjects	72	Left Dorsolateral Prefrontal Cortex	0.92	>0.99	0.01
	72	Left Insula	0.02	0.09	0.27
	72	Bilateral Pregenual Anterior Cingulate	0.47	>0.99	0.09
	72	Left Somatosensory Cortex	0.27	>0.99	–0.13
FD-PDS-MDD	24	Left Dorsolateral Prefrontal Cortex	0.89	>0.99	0.03
	24	Left Insula	0.06	0.24	0.39
	24	Bilateral Pregenual Anterior Cingulate	0.37	>0.99	0.19
	24	Left Somatosensory Cortex	0.33	>0.99	–0.21
FD-PDS	24	Left Dorsolateral Prefrontal Cortex	0.99	>0.99	0.003
	24	Left Insula	0.08	0.32	0.37
	24	Bilateral Pregenual Anterior Cingulate	0.95	>0.99	–0.01
	24	Left Somatosensory Cortex	0.03	0.10	–0.45
Patient	48	Left Dorsolateral Prefrontal Cortex	0.97	>0.99	0.006
	48	Left Insula	0.009	0.03	0.38*
	48	Bilateral Pregenual Anterior Cingulate	0.42	>0.99	–0.12
	48	Left Somatosensory Cortex	0.07	0.26	–0.27

**Bonferroni-corrected p < 0.05.*

In measuring GABA concentrations, we used MEGAPRESS which is the standard tool in resolving GABA and with which significant differences had been detected in the DLFPC, pgACC, insula, and somatosensory cortices in (52) patients with various psychiatric conditions using comparable parameters (53–56). We only included subjects with good spectral quality into the analysis; therefore, poor spectral quality, which would have ensued from poor voxel placement, was unlikely to explain the unequivocal findings.

This could be a case of type-II error, although sample size calculation based on previous depression study (GABA = 0.89 (sd = 0.11) in MDD, 1.0 (sd = 0.11) in controls, Cohen's d = 1.0) showed that 17 subjects were already sufficient to achieve a power of 0.8 with type I error = 0.05 (19). However, the dyspeptic subjects had largely mild dyspeptic severity and for the comorbid MDD group, all met DSM criteria for MDD but also with mild-to-moderate severity of depressive symptoms. While, in lieu of precedence, no comparison can be made with GABA concentrations in other studies on FD, our comorbid FD-MDD did not show changes in GABA in SN (26), DMN (19, 20), and EN (22, 25) reported in previous studies on depressed patients.

Although we used rigorous recruitment assessment for DSM-IV-TR MDD, and Rome III FD-PDS, with negative upper endoscopy results in all recruited dyspeptic subjects to minimize recruitment error, by excluding subjects on centrally-acting drugs we might have recruited subjects with milder symptoms, which may not represent the full spectrum of clinical severity we usually see in our patients. GABA deficit may be obvious only in more clinically severe patients. In order to elucidate the role of GABA in the FD/MDD comorbidity, it is likely that a much larger sample size would be required.

We found, only in depressed dyspeptic subjects, subsignificant negative correlation of GABA concentration in left insula with dyspeptic symptoms. This would require examination in a larger sample to ascertain if SN GABA deficit actually contributed to somatic symptoms, as previous studies on depression suggested (22). However, the weakly positive correlation between GABA concentration with fALFF contradicted the possibility of GABA deficit driving these symptoms by reduction of its inhibitory drive (23, 57). Further examination in larger, well-defined clinical samples would help test against the possibility of spurious associations linked to multiple testing and small sample sizes.

Even more difficult to explain were the unequivocal findings in ALFF from resting state fMRI in all of the regions of interest. This contradicted with two previous reports (27, 28) showing significant increase in SN and DMN resting activity in FD. It is unclear if the difference was attributed to the sample sizes in the dyspeptic comparison arms (40 in Zeng et al., 49 in Liu et al., both from the same group of investigators). Nevertheless, earlier PET-CT studies were not in agreement on resting state findings. One research group in Sichuan reported increased resting activity in pgACC, insula, SSC, and thalamus in FD-PDS patients, positively correlating with dyspeptic symptom severity (27), while the Leuven group reported reduced somatosensory, insula, and cingulate resting glucose metabolism (29). Notwithstanding the fine rigor in these experiments, reports on resting state fMRI changes in FD have remained sparse. Worryingly, after the publication of a number of highly influential studies earlier in the past decade, few if any further neuroimaging studies on FD have been published in the recent few years.

If we accept the validity of our results, their conflict with existing reports may be reconcilable with the complex gut/brain origins of FD and the vast heterogeneity of its pathophysiology across different patients. This may not be entirely surprising if randomized controlled trials of central serotonergic agents have so far reported conflicting results (7, 58, 59). Replication of the previously reported resting state activity findings on larger, cross-national samples including patients of different sociodemographic characteristics and clinical profiles and subsequently, meta-analytic examination will be warranted.

Apart from sample size and potential recruitment bias as mentioned above, our investigation also suffered from a few limitations. Firstly, we did not include a group of MDD-only subjects with no FD and low on somatic symptom scores. Given that somatic symptoms are common in MDD and are even considered a marker of depressive severity (60–63), it would be hard to presume that MDD-only patients without somatic symptoms such as dyspepsia would have more abnormal brain GABA and resting state activity findings. Secondly, we only examined resting-state activity but did not examine brain activations to gastric stimuli. Although significant correlation of anterior cingulate resting activity with regional GABA concentration has been demonstrated (57), GABA was linked to altered task-dependent insula activation in an interoceptive awareness paradigm (26). It should be of interest to examine the link of GABA with task-dependent activation in FD and MDD (29). Thirdly, owing to time constraints, we only included voxels on the left side of the brain (apart from pgACC which was bilateral) considering the vast literature reporting left EN underactivity in major depression (64), but considering the bilateral involvement of prefrontal resting activity reported in FD (27), including right-sided DLPFC, insula and somatosensory voxels may reveal different GABA-resting activity interactions in the FD-MDD comorbidity. Lastly, the present study was planned for comparison of regional GABA concentration and their respective correlation with resting-state activity measure (fALFF). A larger sample size, would be preferred for examination of the correlation of regional GABA concentration with functional connectivity measures in the various different networks owing to the increased number of comparisons involved (57).

In summary, we were unable to identify significant GABA alterations or any contingent changes in resting brain activity in FD-PDS nor could we identify any impact of the FD-depressive comorbidity on neural activity and brain GABA concentrations in the major affective-cognitive-somatosensory networks. FD is a complex and heterogeneous disease of the brain-gut axis (2) with a link to depression—from etiology to treatment—that is fascinating and intriguing. It is possible that the main cortical

neurochemical disturbance in FD is glutamatergic (32). A study with larger sample size to delineate the stimulus-dependent activity/glutamate-GABA interactions in the anterior cingulate and bilateral brain networks on patients of a more representative spectrum of clinical severity is clearly indicated. Until then, the foundations for FD to hold claim as a brain-gut disorder will remain uncertain.

DATA AVAILABILITY STATEMENT

The datasets involved in the study are available from the corresponding author upon reasonable request.

ETHICS STATEMENT

The studies involving human participants were reviewed and approved by New Territories East Cluster- Chinese University of Hong Kong Clinical Research Ethics Committee. The patients/participants provided their written informed consent to participate in this study.

AUTHOR CONTRIBUTIONS

AM: study concept and design, study supervision, analysis and interpretation of data, and drafting of manuscript. JH: data analysis, recruitment and behavioral data collection. OL: manuscript drafting. IC: image data processing and analysis. RL: recruitment, medical assessment, and endoscopic evaluation. SW: recruitment, medical assessment, and endoscopic evaluation. DY: image acquisition, technical support. WC: image acquisition, data processing, protocol design and advice on analysis. RE: design of MRS acquisition and voxel placement, image acquisition, data processing, and initial analysis. SC: study conception and design. LL: study conception and design. JW: study concept and design, critical revision of the manuscript for important intellectual content, and study supervision.

FUNDING

This research was supported by the Research Grants Council of Hong Kong (Reference: 14100815). This study applies tools developed under NIH R01 EB016089 and P41 EB015909; RAEE also receives salary support from these grants.

REFERENCES

1. Tack J, Talley NJ, Camilleri M, Holtmann G, Hu P, Malagelada JR, et al. Functional gastroduodenal disorders. *Gastroenterology* (2006) 130(5):1466–79. doi: 10.1053/j.gastro.2005.11.059
2. Van Oudenhove L, Aziz Q. The role of psychosocial factors and psychiatric disorders in functional dyspepsia. *Nat Rev Gastroenterol Hepatol* (2013) 10 (3):158–67. doi: 10.1038/nrgastro.2013.10
3. Mak AD, Wu JC, Chan Y, Chan FK, Sung JJ, Lee S. Dyspepsia is strongly associated with major depression and generalised anxiety disorder - a community study. *Aliment Pharmacol Ther* (2012) 36(8):800–10. doi: 10.1111/apt.12036
4. Aro P, Talley NJ, Ronkainen J, Storskrubb T, Vieth M, Johansson SE, et al. Anxiety is associated with uninvestigated and functional dyspepsia (Rome III criteria) in a Swedish population-based study. *Gastroenterology* (2009) 137 (1):94–100. doi: 10.1053/j.gastro.2009.03.039
5. Castillo EJ, Camilleri M, Locke GR, Burton DD, Stephens DA, Geno DM, et al. A community-based, controlled study of the epidemiology and pathophysiology of dyspepsia. *Clin Gastroenterol Hepatol* (2004) 2(11):985–96. doi: 10.1016/S1542-3565(04)00454-9
6. Koloski NA, Jones M, Kalantar J, Weltman M, Zaguirre J, Talley NJ. The brain-gut pathway in functional gastrointestinal disorders is bidirectional: a 12-year prospective population-based study. *Gut* (2012) 61(9):1284–90. doi: 10.1136/gutjnl-2011-300474
7. Tack J, Ly HG, Carbone F, Vanheel H, Vanuytsel T, Holvoet L, et al. Efficacy of Mirtazapine in Patients With Functional Dyspepsia and Weight Loss. *Clin Gastroenterol Hepatol* (2016) 14(3):385–92.e4. doi: 10.1016/j.cgh.2015.09.043
8. van Kerkhoven LA, van Rossum LG, van Oijen MG, Witteman EM, Jansen JB, Laheij RJ, et al. Anxiety, depression and psychotropic medication use in patients with persistent upper and lower gastrointestinal symptoms. *Aliment Pharmacol Ther* (2005) 21(8):1001–6. doi: 10.1111/j.1365-2036.2005.02435.x
9. Chioqueta AP, Stiles TC. Personality traits and the development of depression, hopelessness, and suicide ideation. *Pers Individ Dif* (2005) 38:1283–91. doi: 10.1016/j.paid.2004.08.010
10. Filipoviæ BF, Randjelovic T, Ille T, Markovic O, Milovanović B, Kovacevic N, et al. Anxiety, personality traits and quality of life in functional dyspepsia suffering patients. *Eur J Intern Med* (2013) 24:83–6. doi: 10.1016/j.ejim.2012.06.017
11. Jones MP, Schettler A, Olden K, Crowell MD. Alexithymia and somatosensory amplification in functional dyspepsia. *Psychosomatics* (2004) 45(6):508–16. doi: 10.1176/appi.psy.45.6.508
12. De Berardis D, Fornaro M, Orsolini L, Valchera A, Carano A, Vellante F, et al. Alexithymia and Suicide Risk in Psychiatric Disorders: A Mini-Review. *Front Psychiatry* (2017) 8:148. doi: 10.3389/fpsyt.2017.00148
13. Engel-Yeger B, Muzio C, Rinosi G, Salano P, Geoffroy PA, Pompili M, et al. Extreme sensory processing patterns and their relation with clinical conditions among individuals with major affective disorders. *Psychiatry Res* (2016) 236:112–8. doi: 10.1016/j.psychres.2015.12.022
14. Jones MP, Coppens E, Vos R, Holvoet L, Luyten P, Tack J, et al. A multidimensional model of psychobiological interactions in functional dyspepsia: a structural equation modelling approach. *Gut* (2013) 62 (11):1573–80. doi: 10.1136/gutjnl-2012-302634
15. Mayer EA, Labus JS, Tillisch K, Cole SW, Baldi P. Towards a systems view of IBS. *Nat Rev Gastroenterol Hepatol* (2015) 12(10):592–605. doi: 10.1038/nrgastro.2015.121
16. Menon V. Large-scale brain networks and psychopathology: a unifying triple network model. *Trends Cognit Sci* (2011) 15(10):483–506. doi: 10.1016/j.tics.2011.08.003
17. Morgane PJ, Galler JR, Mokler DJ. A review of systems and networks of the limbic forebrain/limbic midbrain. *Prog Neurobiol* (2005) 75(2):143–60. doi: 10.1016/j.pneurobio.2005.01.001
18. Northoff G, Wiebking C, Feinberg T, Panksepp J. The 'resting-state hypothesis' of major depressive disorder-a translational subcortical-cortical framework for a system disorder. *Neurosci Biobehav Rev* (2011) 35(9):1929–45. doi: 10.1016/j.neubiorev.2010.12.007
19. Hasler G, van der Veen JW, Tumonis T, Meyers N, Shen J, Drevets WC. Reduced prefrontal glutamate/glutamine and gamma-aminobutyric acid levels in major depression determined using proton magnetic resonance spectroscopy. *Arch Gen Psychiatry* (2007) 64(2):193–200. doi: 10.1001/archpsyc.64.2.193
20. Bhagwagar Z, Wylezinska M, Jezzard P, Evans J, Boorman E, MM P, et al. Low GABA concentrations in occipital cortex and anterior cingulate cortex in medication-free, recovered depressed patients. *Int J Neuropsychopharmacol* (2008) 11(2):255–60. doi: 10.1017/S1461145707007924
21. Price JL, Drevets WC. Neural circuits underlying the pathophysiology of mood disorders. *Trends Cognit Sci* (2012) 16(1):61–71. doi: 10.1016/j.tics.2011.12.011

22. Hasler G, Northoff G. Discovering imaging endophenotypes for major depression. *Mol Psychiatry* (2011) 16(6):604–19. doi: 10.1038/mp.2011.23
23. Northoff G, Sibille E. Why are cortical GABA neurons relevant to internal focus in depression? A cross-level model linking cellular, biochemical and neural network findings. *Mol Psychiatry* (2014) 19(9):966–77. doi: 10.1038/mp.2014.68
24. Sanacora G, Mason GF, Rothman DL, Krystal JH. Increased occipital cortex GABA concentrations in depressed patients after therapy with selective serotonin reuptake inhibitors. *Am J Psychiatry* (2002) 159(4):663–5. doi: 10.1176/appi.ajp.159.4.663
25. Fitzgerald PB, Sritharan A, Daskalakis ZJ, de Castella AR, Kulkarni J, Egan G. A functional magnetic resonance imaging study of the effects of low frequency right prefrontal transcranial magnetic stimulation in depression. *J Clin Psychopharmacol* (2007) 27(5):488–92. doi: 10.1097/jcp.0b013e318151521c
26. Wiebking C, Duncan NW, Tiret B, Hayes DJ, Marjanska M, Doyon J, et al. GABA in the insula - a predictor of the neural response to interoceptive awareness. *Neuroimage* (2014) 86:10–8. doi: 10.1016/j.neuroimage.2013.04.042
27. Zeng F, Qin W, Liang F, Liu J, Tang Y, Liu X, et al. Abnormal resting brain activity in patients with functional dyspepsia is related to symptom severity. *Gastroenterology* (2011) 141(2):499–506. doi: 10.1053/j.gastro.2011.05.003
28. Liu P, Zeng F, Zhou G, Wang J, Wen H, von Deneen KM, et al. Alterations of the default mode network in functional dyspepsia patients: a resting-state fmri study. *Neurogastroenterol Motil* (2013) 25(6):e382–8. doi: 10.1111/nmo.12131
29. Van Oudenhove L, Vandenberghe J, Dupont P, Geeraerts B, Vos R, Dirix S, et al. Abnormal regional brain activity during rest and (anticipated) gastric distension in functional dyspepsia and the role of anxiety: a H(2)(15)O-PET study. *Am J Gastroenterol* (2010) 105(4):913–24. doi: 10.1038/ajg.2010.39
30. Van Oudenhove L, Dupont P, Vandenberghe J, Geeraerts B, van Laere K, Bormans G, et al. The role of somatosensory cortical regions in the processing of painful gastric fundic distension: an update of brain imaging findings. *Neurogastroenterol Motil* (2008) 20(5):479–87. doi: 10.1111/j.1365-2982.2007.01045.x
31. Vandenberghe J, Dupont P, Van Oudenhove L, Bormans G, Demyttenaere K, Fischler B, et al. Regional cerebral blood flow during gastric balloon distention in functional dyspepsia. *Gastroenterology* (2007) 132(5):1684–93. doi: 10.1053/j.gastro.2007.03.037
32. Mak ADP, Northoff G, Yeung DKW, Chu WCW, Hui SCN, Cheung C, et al. Increased Glutamate in Somatosensory Cortex in Functional Dyspepsia. *Sci Rep* (2017) 7(1):3926. doi: 10.1038/s41598-017-04405-1
33. Edden RAE, Puts NAJ, Harris AD, Barker PB, Evans CJ. Gannet: A batch-processing tool for the quantitative analysis of gamma-aminobutyric acid–edited MR spectroscopy spectra. *J Magn Reson Imaging* (2014) 40:1445–52. doi: 10.1002/jmri.24478
34. Hong JY, Kilpatrick LA, Labus JS, Gupta A, Katibian D, Ashe-McNalley C, et al. Sex and disease-related alterations of anterior insula functional connectivity in chronic abdominal pain. *J Neurosci* (2014) 34(43):14252–9. doi: 10.1523/JNEUROSCI.1683-14.2014
35. So E, Kam I, Leung CM, Chung D, Liu Z, Fong S. The Chinese- bilingual SCID-I/P Project: stage 1 — reliability for mood disorders and schizophrenia. *Hong Kong J Psychiatry* (2003) 13:7–18.
36. Chan Y, Cheong PK, Fang FF, Cheung CKY, Lan LL, Wing KKY, et al. A symptom severity questionnaire for patients suffering from functional gastrointestinal disorder: FGI-Checklist. *J Gastroenterol Hepatol* (2019) 35:1130–5. doi: 10.1111/jgh.14937
37. Montgomery SA, Asberg M. A new depression scale designed to be sensitive to change. *Br J Psychiatry* (1979) 134:382–9. doi: 10.1192/bjp.134.4.382
38. Hamilton M. The assessment of anxiety states by rating. *Br J Med Psychol* (1959) 32(1):50–5. doi: 10.1111/j.2044-8341.1959.tb00467.x
39. Porges SW. *Body Perception Questionnaire: Laboratory of Developmental Assessment*. Maryland: University of Marryland (1993).
40. Lee S, Ma YL, Tsang A. Psychometric properties of the Chinese 15-item patient health questionnaire in the general population of Hong Kong. *J Psychosom Res* (2011) 71(2):69–73. doi: 10.1016/j.jpsychores.2011.01.016
41. Lam CL, Tse EY, Gandek B, Fong DY. The SF-36 summary scales were valid, reliable, and equivalent in a Chinese population. *J Clin Epidemiol* (2005) 58(8):815–22. doi: 10.1016/j.jclinepi.2004.12.008
42. Chan ELS, Chen EYH, Chan RCK. Three-subtest Short Form of the Wechsler Adult Intelligence Scale-III for Patients with Psychotic Disorders: a Preliminary Report. *Hong Kong J Psychiatry* (2005) 15:39–42.
43. The Wellcome Centre for Human Neuroimaging. *Statistical Parametric Mapping*. Elsevier Inc (2004). Available at: https://www.fil.ion.ucl.ac.uk/spm/.
44. Smith SM, Jenkinson M, Woolrich MW, Bechmann CF, Behrens TEJ, Johansen-Berg H, et al. Advances in functional and structural MR image analysis and implementation as FSL. *Neuroimage* (2004) 23:208–19. doi: 10.1016/j.neuroimage.2004.07.051
45. Duncan NW, Enzi B, Wiebking C, Northoff G. Involvement of glutamate in rest-stimulus interaction between perigenual and supragenual anterior cingulate cortex: a combined fMRI-MRS study. *Hum Brain Mapp* (2011) 32(12):2172–82. doi: 10.1002/hbm.21179
46. Sharma NK, McCarson K, Van Dillen L, Lentz A, Khan T, Cirstea CM. Primary somatosensory cortex in chronic low back pain - a H-MRS study. *J Pain Res* (2011) 4:143–50. doi: 10.2147/JPR.S19297
47. Boy F, Evans CJ, Edden RAE, Lawrence AD, Singh KD, Husain M, et al. Dorsolateral Prefrontal γ-Aminobutyric Acid in Men Predicts Individual Differences in Rash Impulsivity. *Biol Psychiatry* (2011) 70(9):866–72. doi: 10.1016/j.biopsych.2011.05.030
48. Harris AD, Puts NAJ, Anderson BA, Yantis S, Pekar JJ, Barker PB, et al. Multi-Regional Investigation of the Relationship between Functional MRI Blood Oxygenation Level Dependent (BOLD) Activation and GABA Concentration. *PloS One* (2015) 10(2):e0117531. doi: 10.1371/journal.pone.0117531
49. Cox RW. AFNI: Software for Analysis and Visualization of Functional Magnetic Resonance Neuroimages. *Comput BioMed Res* (1996) 29:162–73. doi: 10.1006/cbmr.1996.0014
50. Zou QH, Zhu CZ, Yang Y, Zuo X, Long X, Cao Q, et al. An improved approach to detection of amplitude of low-frequency fluctuation (ALFF) for resting-state fMRI: Fractional ALFF. *J Neurosci Methods* (2008) 172:137–41. doi: 10.1016/j.jneumeth.2008.04.012
51. Taylor PA, Saad ZS. FATCAT: (an efficient) functional and tractographic connectivity analysis toolbox. *Brain Connect* (2013) 3:523–35. doi: 10.1089/brain.2013.0154
52. Wodka EL, Puts NA, Mahone EM, Edden RA, Tommerdahl M, Mostofsky SH. The Role of Attention in Somatosensory Processing: A Multi-trait, Multi-method Analysis. *J Autism Dev Disord* (2016) 46(10):3232–41. doi: 10.1007/s10803-016-2866-6
53. Edden RAE, Crocetti D, Zhu H, Gilbert DL, Mostofsky SH. Reduced GABA Concentration in Attention-Deficit/Hyperactivity Disorder. *Arch Gen Psychiatry* (2012) 69(7):750–3. doi: 10.1001/archgenpsychiatry.2011.2280
54. Li Y, Zhang CC, Kathrin W, Zhang Y, He N, Jin H, et al. Investigation of anterior cingulate cortex gamma-aminobutyric acid and glutamate-glutamine levels in obsessive-compulsive disorder using magnetic resonance spectroscopy. *BMC Psychiatry* (2019) 19(1):164. doi: 10.1186/s12888-019-2160-1
55. Flores-Ramos M, Alcauter S, López-Titla M, Bernal-Santamaría N, Calva-Coraza E, Edden RAE. Testosterone is related to GABA+ levels in the posterior-cingulate in unmedicated depressed women during reproductive life. *J Affect Disord* (2019) 242:143–9. doi: 10.1016/j.jad.2018.08.033
56. Puts NAJ, Heba S, Harris AD, Evans CJ, McGonigle DJ, Tegenthoff M, et al. GABA Levels in Left and Right Sensorimotor Cortex Correlate across Individuals. *Biomedicines* (2018) 6(3):1–9. doi: 10.3390/biomedicines6030080
57. Levar N, Van Doesum TJ, Denys D, Van Wingen GA. Anterior cingulate GABA and glutamate concentrations are associated with resting-state network connectivity. *Sci Rep* (2019) 9(1):2116–. doi: 10.1038/s41598-018-38078-1
58. Talley NJ, Locke GR, Saito YA, Almazar AE, Bouras EP, Howden CW, et al. Effect of Amitriptyline and Escitalopram on Functional Dyspepsia: A Multicenter, Randomized Controlled Study. *Gastroenterology* (2015) 149(2):340–9.e2. doi: 10.1053/j.gastro.2015.04.020
59. Cheong PK, Ford AC, Cheung CKY, Ching JYL, Chan Y, Sung JJY, et al. Low-dose imipramine for refractory functional dyspepsia: a randomised, double-blind, placebo-controlled trial. *Lancet Gastroenterol Hepatol* (2018) 3(12):837–44. doi: 10.1016/S2468-1253(18)30303-0
60. Katon W, Lin EH, Kroenke K. The association of depression and anxiety with medical symptom burden in patients with chronic medical illness. *Gen Hosp Psychiatry* (2007) 29(2):147–55. doi: 10.1016/j.genhosppsych.2006.11.005

61. Kroenke K. Symptoms are sufficient: refining our concept of somatization. *Adv Mind Body Med* (2001) 17(4):244–9; discussion 70-6. doi: 10.1054/ambm.2000.0241
62. Lowe B, Spitzer RL, Williams JB, Mussell M, Schellberg D, Kroenke K. Depression, anxiety and somatization in primary care: syndrome overlap and functional impairment. *Gen Hosp Psychiatry* (2008) 30(3):191–9. doi: 10.1016/j.genhosppsych.2008.01.001
63. Kroenke K, Jackson JL, Chamberlin J. Depressive and anxiety disorders in patients presenting with physical complaints: clinical predictors and outcome. *Am J Med* (1997) 103(5):339–47. doi: 10.1016/S0002-9343(97)00241-6
64. Grimm S, Beck J, Schuepbach D, Hell D, Boesiger P, Bermpohl F, et al. Imbalance between left and right dorsolateral prefrontal cortex in major depression is linked to negative emotional judgment: an fMRI study in severe major depressive disorder. *Biol Psychiatry* (2008) 63(4):369–76. doi: 10.1016/j.biopsych.2007.05.033

Conflict of Interest: The authors declare that the research was conducted in the absence of any commercial or financial relationships that could be construed as a potential conflict of interest.

frontiers in Psychiatry

ORIGINAL RESEARCH
published: 17 February 2021
doi: 10.3389/fpsyt.2021.643564

Glutamate- and GABA-Modulated Connectivity in Auditory Hallucinations—A Combined Resting State fMRI and MR Spectroscopy Study

Sarah Weber[1,2,3]*, *Helene Hjelmervik*[1,2,3], *Alexander R. Craven*[1,4], *Erik Johnsen*[2,5], *Rune A. Kroken*[2,5], *Else-Marie Løberg*[2,6,7], *Lars Ersland*[1,4], *Kristiina Kompus*[1,2,8] and *Kenneth Hugdahl*[1,2,9]

[1] Department of Biological and Medical Psychology, University of Bergen, Bergen, Norway, [2] Division of Psychiatry and NORMENT Centre of Excellence, Haukeland University Hospital, Bergen, Norway, [3] School of Health Sciences, Kristiania University College, Bergen, Norway, [4] Department of Clinical Engineering, Haukeland University Hospital, Bergen, Norway, [5] Department of Clinical Medicine, University of Bergen, Bergen, Norway, [6] Department of Addiction Medicine, Haukeland University Hospital, Bergen, Norway, [7] Department of Clinical Psychology, University of Bergen, Bergen, Norway, [8] Institute of Psychology, University of Tartu, Tartu, Estonia, [9] Department of Radiology, Haukeland University Hospital, Bergen, Norway

OPEN ACCESS

Edited by:
Maria Concepcion Garcia Otaduy, University of São Paulo, Brazil

Reviewed by:
Saskia Sophie Steinmann, University Medical Center Hamburg-Eppendorf, Germany
Andrea Federspiel, University of Bern, Switzerland

***Correspondence:**
Sarah Weber
sarah.weber@kristiania.no

Specialty section:
This article was submitted to Neuroimaging and Stimulation, a section of the journal Frontiers in Psychiatry

Received: *18 December 2020*
Accepted: *26 January 2021*
Published: *17 February 2021*

Citation:
Weber S, Hjelmervik H, Craven AR, Johnsen E, Kroken RA, Løberg E-M, Ersland L, Kompus K and Hugdahl K (2021) Glutamate- and GABA-Modulated Connectivity in Auditory Hallucinations—A Combined Resting State fMRI and MR Spectroscopy Study. Front. Psychiatry 12:643564. doi: 10.3389/fpsyt.2021.643564

Background: Auditory verbal hallucinations (AVH) have been linked to aberrant interhemispheric connectivity between the left and the right superior temporal gyrus (STG), labeled the interhemispheric miscommunication theory. The present study investigated if interhemispheric miscommunication is modulated at the neurochemical level by glutamate (Glu) and gamma-aminobutyric acid (GABA) concentrations in temporal and prefrontal lobe areas, as proposed by the theory.

Methods: We combined resting-state fMRI connectivity with MR spectroscopy (MRS) in a sample of 81 psychosis patients, comparing patients with high hallucination severity (high-AVH) and low hallucination severity (low-AVH) groups. Glu and GABA concentrations were acquired from the left STG and the anterior cingulate cortex (ACC), an area of cognitive control that has been proposed to modulate STG functioning in AVH.

Results: Functional connectivity showed significant interaction effects between AVH Group and ACC-recorded Glu and GABA metabolites. Follow-up tests showed that there was a significant positive association for Glu concentration and interhemispheric STG connectivity in the high-AVH group, while there was a significant negative association for GABA concentration and interhemispheric STG connectivity in the low-AVH group.

Conclusion: The results show neurochemical modulation of STG interhemispheric connectivity, as predicted by the interhemispheric miscommunication hypothesis. Furthermore, the findings are in line with an excitatory/inhibitory imbalance model for AVH. By combining different neuroimaging modalities, the current results provide a more comprehensive insight into the neural correlates of AVH.

Keywords: schizophrenia, psychosis, neurochemistry, neurotransmitters, functional connectivity, neuroimaging

INTRODUCTION

Auditory verbal hallucinations (AVH) have been associated with aberrant functioning of the left superior temporal gyrus (STG), a brain area associated with auditory processing and speech perception (1–3). Concurrent evidence from diffusion-tensor imaging (DTI), functional magnetic resonance imaging (fMRI) and electrophysiology (EEG) shows in particular abnormal connectivity between the left STG and its right-hemispheric homolog in patients with AVH [e.g., (4–7)]. Findings of hyper-connectivity are thought to reflect an overactive positive feedback-loop where the left and the right STG continuously activate each other, causing abnormalities of auditory processing (8, 9). Recently, these findings have been summarized in the interhemispheric miscommunication theory of AVH (10). The theory also proposes neurochemical modulation of interhemispheric STG connectivity by glutamate (Glu) and gamma-aminobutyric acid (GABA), the brain's main excitatory and inhibitory neurotransmitters, respectively. Glu and GABA concentrations are altered in schizophrenia patients compared to healthy control subjects (11, 12). In addition, altered Glu concentrations have specifically been associated with AVH (13–15). Glu and GABA have also been linked to AVH in studies using ketamine, which blocks Glu binding to GABAergic neurons. Administration of ketamine exacerbates psychotic symptoms such as hallucinations in schizophrenia patients (16, 17) and induces schizophrenia-like symptoms in healthy subjects (16, 18–20). Interestingly, ketamine-induced AVH have also been found to be related to increased interhemispheric STG gamma-band connectivity (20), which arises from synchronous firing of GABAergic neurons (21). Together, these findings suggest that Glu- and GABA-modulated interhemispheric STG connectivity plays a role in the occurrence of AVH (10). The interhemispheric miscommunication theory proposes that Glu and GABA in the left STG and prefrontal brain regions might be of particular importance, based on reports of AVH-related altered Glu concentrations in those regions (13, 15). Furthermore, the prefrontal cortex is an area of cognitive control which is central to the interplay between different brain regions, and has previously been suggested to modulate left STG functioning in AVH (22).

The current study investigated the relationship between left STG connectivity and Glu and GABA concentrations in a sample of psychosis patients, with a focus on how this relationship might differ between patients with high hallucination severity (high-AVH) and patients with low hallucination severity (low-AVH). Glu and GABA were measured with hydrogen magnetic resonance spectroscopy (^{1}H-MRS). Regions of interest for Glu and GABA measurements were the left STG in the temporal lobe and the anterior cingulate cortex (ACC) in the frontal lobe (10, 14, 22). Glu and GABA were hypothesized to modulate interhemispheric STG functional connectivity, as predicted by the interhemispheric miscommunication theory (10). More specifically, we predicted increased Glu concentrations to be associated with increased connectivity, while we predicted increased GABA concentrations to be associated with decreased connectivity, based on the respective excitatory and inhibitory action of these transmitters. Since AVH have previously been associated with an increase in interhemispheric STG connectivity (4, 5, 20), excitatory effects should be more pronounced in high-AVH patients, whereas inhibitory effects should be more pronounced in low-AVH patients.

TABLE 1 | Demographic and clinical data for the patient sample.

Age		30.92 (11.56)
Gender (m/f)		58/23
Duration of illness		3.63 (6.31)
PANSS scores		
	Total	62.28 (17.65)
	Positive	15.24 (5.52)
	Negative	14.91 (5.16)
	General	32.13 (9.73)
Medication		
	DDD antipsychotics	1.05 (0.59)
	Antidepressants	10
	Mood stabilizers	3
	Opioids	1
	Benzodiazepines	13
	Anticholinergic	4
	ADHD	1

Mean values (and SD) are given. For additional medications, the number of patients per respective group is indicated. PANSS, Positive and Negative Syndrome Scale; DDD, Defined Daily Dose of antipsychotic medication.

METHODS

Subjects

Data were collected from 81 patients with a psychosis diagnosis, predominantly with a schizophrenia spectrum disorder according to the ICD-10 diagnostic manual (F20-F29: Schizophrenia, schizotypal and delusional disorders) (23). Ten of the patients fulfilled the criterion of hallucination proneness and psychosis but were diagnosed with drug-induced psychotic disorder ($n = 7$) or mood disorders with psychotic symptoms ($n = 3$). The majority of patients used antipsychotic medication, of which all used second-generation antipsychotics, with some patients in addition using first-generation antipsychotics (see **Table 1** for details). There were no significant differences between high-AVH and low-AVH patients with respect to duration of illness ($p = 0.689$) or defined daily dose (DDD) of antipsychotic medication ($p = 0.818$). Further information on sample characteristics can be found in **Table 1**. All subjects gave written informed consent to take part in the study prior to participation.

Clinical Data Acquisition

Clinical data were acquired at the Psychiatric Clinic at the Haukeland University Hospital in Bergen, Norway. The study

Abbreviations: ACC, anterior cingulate cortex; AVH, auditory verbal hallucinations; DDD, defined daily dose; DTI, diffusion tensor imagining; EEG, electroencephalography; fMRI, functional magnetic resonance imaging; GABA, gamma-aminobutyric acid; Glu, glutamate; MRS, magnetic resonance spectroscopy; NMDA, N-methyl-D-aspartate; PANSS, Positive and Negative Syndrome Scale; STG, superior temporal gyrus.

was approved by the Regional Committee for Medical Research Ethics in Western Norway (REK Vest) (REK # 2010/3387) and conducted according to the Declaration of Helsinki. Severity of AVH was assessed with the P3 item of the Positive and Negative Syndrome Scale [PANSS, (24)]. All PANSS raters were trained and certified, and satisfactory inter-rater reliability was documented. Although the PANSS P3 item does not explicitly differentiate between different sensory modalities of hallucinations, auditory hallucinations are by far the most common type of hallucination in psychotic patients (25), typically in the form of hearing voices (26). Furthermore, AVH are also the main focus during the PANSS P3 interview (27). Therefore, the PANSS P3 is a good indicator of AVH.

MR Data Acquisition

MR data were acquired on a 3T GE Signa HDx MR scanner in the Haukeland University Hospital in Bergen. In the course of the study, the MR scanner was upgraded to Discovery MR750 and the head coil was changed from 8-channel to 32-channel. The scanner/head coil version was included as a regressor of no interest in all statistical analyses. fMRI resting-state data were collected during a 5.3-min eyes-closed scanning session. There were 160 volumes acquisitions, each with 30 slices containing a 0.5 mm gap between slices (voxel size 1.72 × 1.72 × 3 mm) with the following parameters: repetition time (TR)/echo time (TE)/flip angle (FA)/field of view (FOV) 2,000 ms/30 ms/90°/220 mm. In addition, a structural T1-weighted image was acquired using a 3D SPGR sequence (7.42 min) with the following parameters: TR/TE/FA/FOV 7.78 ms/2.94 ms/14°/256 mm (post-upgrade: 6.9 ms/3.0 ms/12°/256 mm), isotropic voxel size of 1 mm^3.

^{1}H-MRS-spectra were obtained from the left STG (voxel size 24 × 40 × 30 mm; **Figure 1A**) and from the ACC (voxel size 40 × 40 × 25 mm; **Figure 1B**) by using a single-voxel point-resolved spectroscopy (PRESS) sequence (TE/TR = 35 ms/1,500 ms, 128 repetitions, ∼ 4 min), followed by a Mescher-Garwood PRESS (MEGA PRESS) sequence (TE/TR = 68 ms/1,500 ms, 128/192 repetitions pre/post-upgrade with edit pulse at 1.9/7.5 ppm, ∼12 min). Unsuppressed water reference spectra (eight repetitions) were acquired automatically after the water-suppressed metabolite spectra. Due to a change in the scanning protocol during the course of the study, only a subsample of patients ($n = 42$) completed the ACC-scan, whereas all patients completed the left STG-scan.

Data Preprocessing

Functional MRI Data

Data were pre-processed in the SPM12 software package (https://www.fil.ion.ucl.ac.uk/spm/). This included realignment of functional volumes for head motion correction, coregistration of the T1 structural image to the mean functional image, normalization of functional data into the MNI (Montreal Neurological Institute) standardized space, and smoothing with a Gaussian kernel of 6 mm FWHM. Data then went through a default denoising procedure implemented in the CONN toolbox (version v.17.f http://www.nitrc.org/projects/conn) where motion realignment parameters (including their first derivatives), as well as time courses from white matter and cerebrospinal fluid were regressed out. Lastly, a band-pass filter of 0.008–0.09 Hz was applied to the data.

MR Spectroscopy Data

PRESS and MEGA-PRESS data were processed with the LCModel analysis software, version 6.3-IJ. For details of the processing procedure and quality control of the spectra see (14). Glx (the composite signal of Glu and Gln) and GABA+ (GABA including an unknown macromolecule contribution) levels were used for further analyses. Glx is commonly used as an indicator of Glu concentration levels, since it is a more robust measure than Glu and Gln alone, which can be difficult to separate at 3T. Therefore, the term Glx will hereafter be used when referring to specific results, whereas Glu will be used when discussing general neurochemical mechanisms in a theoretical context. After quality-control, the following number of valid data sets remained: left STG Glx/left STG GABA/ACC Glx/ACC GABA = 81/76/42/41.

Data Analysis

Seed-based functional connectivity analyses were conducted using the CONN toolbox (https://web.conn-toolbox.org/). A seed region of interest was defined and created for the left STG which covered the MRS voxel location (i.e., voxels that were covered by the left STG MRS voxel in 80% of subjects, transformed into standard space, see **Figure 1A**). In order to investigate relationships of Glx- and GABA-concentrations with BOLD functional connectivity data, MRS data were included as regressors in seed-to-voxel analyses, together with age, gender and scanner version, which were defined as regressors of no interest. Furthermore, all analyses were repeated with daily defined dose (DDD) of antipsychotic medication as an additional regressor, since antipsychotic medication can affect N-methyl-D-aspartate receptor (NMDA-receptor) functioning and might therefore also affect the Glx and GABA measurements (36,37). However, all results remained substantially unchanged when adding the medication regressor to the analyses. Two groups of patients were compared: patients with high hallucination severity (high-AVH; $n = 38$; PANSS P3 score of ≥3) and patients with low hallucination severity (low-AVH; $n = 43$; P3 score of <3). For the connectivity analyses, a cluster correction procedure was applied with an initial threshold of $p < 0.001$ uncorrected at the single-voxel level and $p < 0.05$ at the cluster-level, FDR-corrected for multiple comparisons. For analyses that did not yield significant results at the pre-set threshold level, the threshold was lowered in order to further explore statistically weaker results.

RESULTS

Functional Connectivity and Glx and GABA in the Left STG

Glx in the Left STG

There was a significant difference between the high-AVH and the low-AVH group for the relationship between Glx and left

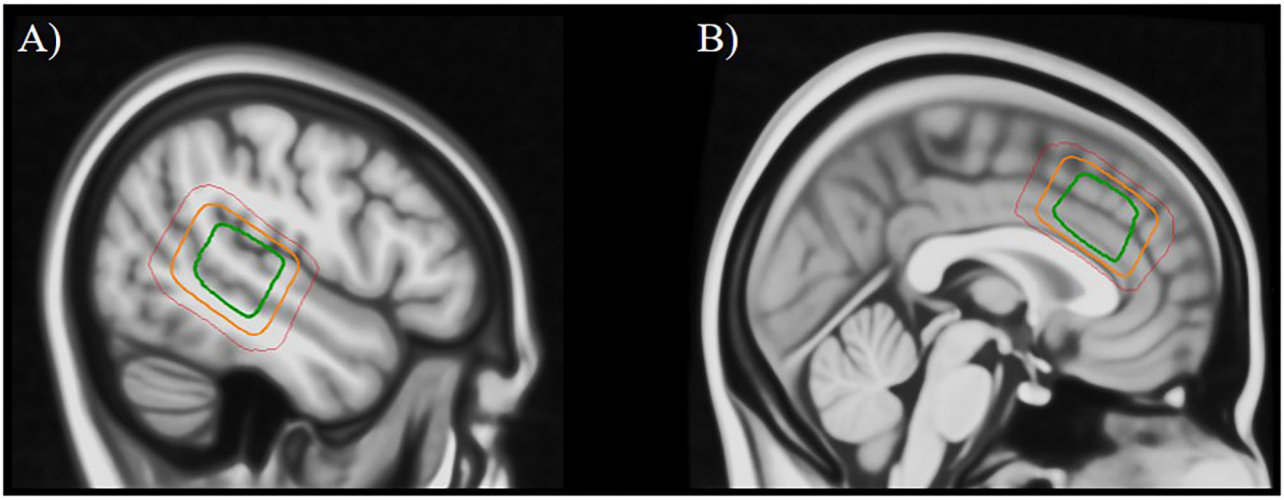

FIGURE 1 | Placement of the MRS voxel in the left superior temporal gyrus **(A)** and the anterior cingulate cortex **(B)**. The three squares indicate the areas that were covered by the individually placed MRS voxels in 95% of subjects (green), 50% of subjects (orange), and 5% of subjects (red).

STG connectivity with several clusters, primarily bilaterally in the postcentral gyrus and in occipital areas. Investigating Glx effects separately per group showed a negative correlation between Glx and left STG connectivity with the thalamus for the high-AVH group. For the low-AVH group, there was a negative correlation between Glx and connectivity between left STG and left postcentral gyrus. There was no overlap of areas with a significant group difference and those with within-group effects. The results are shown in **Table 2** and **Figure 2**.

GABA in the Left STG

There were no significant group differences between the high-AVH and the low-AVH group for the relationship between left STG GABA and left STG connectivity. Furthermore, left STG GABA did not show any significant correlations with left STG connectivity within either of the two groups separately, even when lowering the statistical threshold to voxel-level $p < 0.01$, cluster $p > 0.05$.

Functional Connectivity and Glx and GABA in the ACC

Glx in the ACC

There was a significant Group by Glx interaction, with ACC Glx levels having a significantly stronger effect on left STG connectivity with bilateral STG/MTG and frontal orbital cortex in the high-AVH group compared to the low-AVH group. Within the high-AVH group, there was a positive correlation between Glx and left STG connectivity with left and right STG/MTG, when lowering the voxel-level threshold to voxel-level $p < 0.01$. These STG/MTG clusters overlapped with the areas found significant in the between-group analysis. The results are shown in **Table 3** and **Figures 3A**, **4**. For the low-AVH group, there was no significant relationship between Glx and left STG connectivity, irrespective of the statistical thresholding level.

GABA in the ACC

There was a significant Group by GABA interaction, with ACC GABA levels having a stronger effect on left STG connectivity with right STG/MTG in the low-AVH group compared to the high-AVH group. Within the low-AVH group, there was a significant negative correlation between GABA and left STG connectivity with an overlapping right STG/MTG cluster. For the high-AVH group, there was no significant relationship between GABA and STG connectivity. The results are displayed in **Table 4** and **Figures 3B, 5**.

DISCUSSION

The current study investigated how functional connectivity of the left STG is related to Glx and GABA concentrations in temporal and frontal brain regions and how this relationship is associated with AVH. As hypothesized, Glx and GABA concentration levels in the ACC showed relationships with interhemispheric STG connectivity that were in opposite directions for patients with high vs. low AVH severity. In contrast, Glx and GABA in the left STG did not show any relationships with interhemispheric STG connectivity.

ACC-Measured Glx and GABA Relationships With Functional Connectivity

The modulation of interhemispheric STG connectivity by Glx and GABA and the AVH-related group differences in this modulation are in line with the interhemispheric miscommunication theory of AVH (10). ACC *Glx* levels were *positively* related to interhemispheric STG connectivity, but only in the high-AVH group. In contrast, ACC *GABA* levels were *negatively* related to interhemispheric STG connectivity, but only in the low-AVH group. The dissociation between Glx and GABA effects is particularly interesting given that

TABLE 2 | Relationships between Glx concentration in left STG and left STG functional connectivity.

	Brain area	Coordinates			Cluster size	Beta	Voxel-level *p*	Cluster *p*
High-AVH – low-AVH								
	Postcentral gyrus	56	−14	56	83	0.05	< 0.001	0.011
	Postcentral gyrus	−15	−43	77	51	0.04	< 0.001	0.034
	Lingual gyrus	23	−54	−1	77	0.04	< 0.001	0.011
	Lateral/temporo-occipital gyrus	49	−62	2	67	0.05	< 0.001	0.015
Effects within the high-AVH group								
(*n* = 38)	Thalamus	4	−26	14	52	−0.03	< 0.001	0.046
Effects within the low-AVH group								
(*n* = 43)	Postcentral gyrus	−41	−29	59	77	−0.03	< 0.001	0.023

The listed clusters showed a group difference in the relationship between Glx and connectivity (high-AVH – low-AVH) or a relationship between Glx and connectivity within one of the groups (effects within high-AVH group and effects within low-AVH group, respectively). Coordinates are given in MNI space. Brain areas are derived from the FSL Harvard-Oxford atlas in Conn. Cluster size is given as the number of voxels.

FIGURE 2 | Group comparison of high-AVH patients (*n* = 38) and low-AVH patients (*n* = 43). Glx in left STG had a significantly stronger effect on left STG connectivity with the areas shown in red for high-AVH vs. low-AVH.

TABLE 3 | Relationships between Glx concentration in ACC and left STG functional connectivity.

	Brain area	Coordinates			Cluster size	Beta	Voxel-level *p*	Cluster *p*
High-AVH – low-AVH								
	STG/MTG	−66	−5	2	54	0.11	< 0.001	0.027
	STG/MTG	64	3	−4	66	0.09	< 0.001	0.021
	Frontal orbital	16	19	−19	49	0.08	< 0.001	0.028
Effects within the high-AVH group								
(*n* = 21)	STG/MTG	−65	−5	−1	256	0.08	< 0.01	0.004
	STG/MTG	63	0	−13	141	0.08	< 0.01	0.044
	hippocampus/amygdala	20	−16	−19	157	0.05	< 0.01	0.035
	Cerebellum	6	−67	−25	244	−0.02	< 0.01	0.004
Effects within the low-AVH group								
(*n* = 21)	–		–		–	–	–	–

The listed clusters showed a group difference in the relationship between Glx and connectivity (high-AVH – low-AVH) or a relationship between Glx and connectivity within one of the groups (effects within high-AVH group and effects within low-AVH group, respectively). Coordinates are given in MNI space. Brain areas are derived from the FSL Harvard-Oxford atlas in Conn. Cluster size is given as the number of voxels.

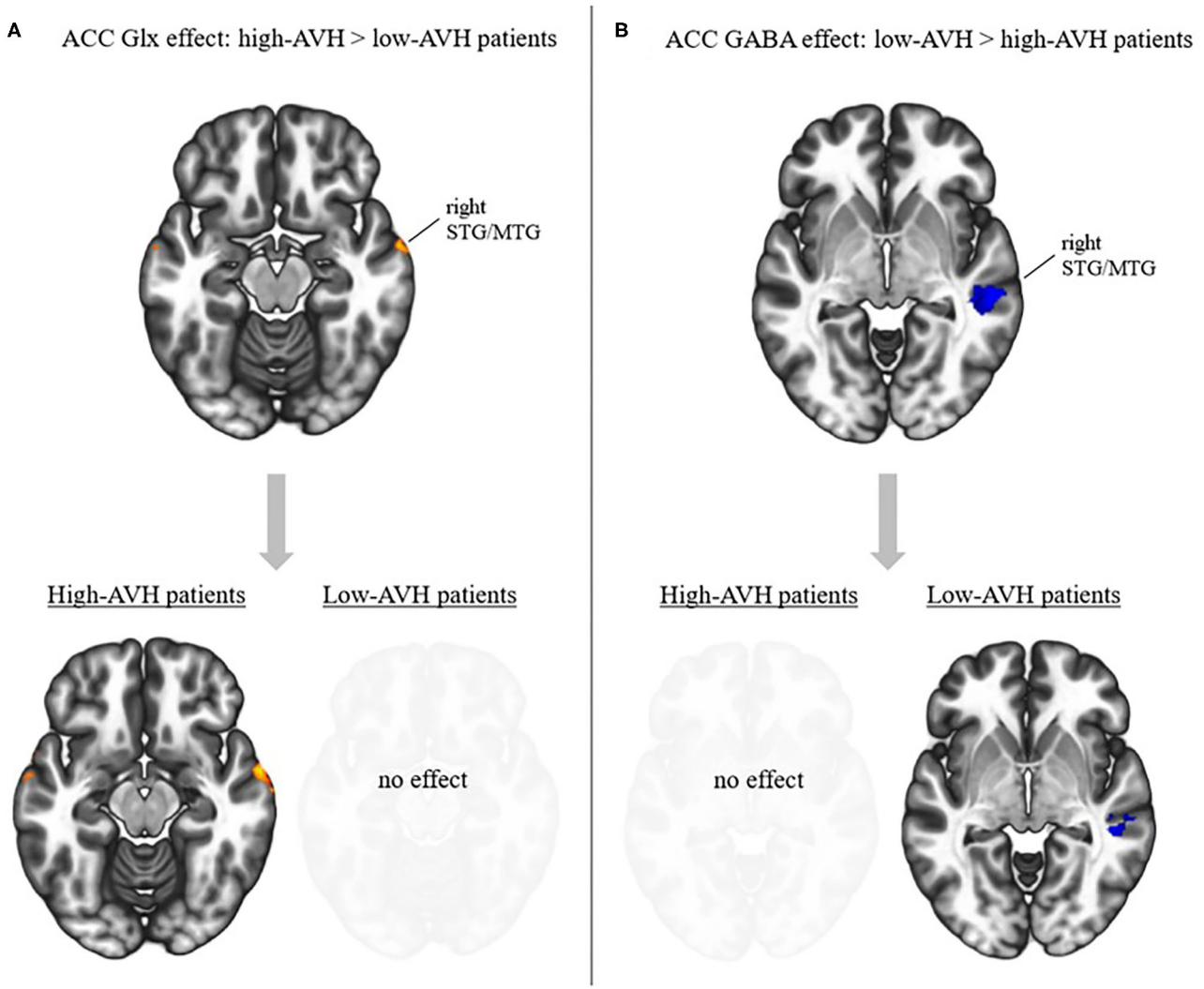

FIGURE 3 | Effects of ACC Glx and GABA on left STG connectivity in relation to AVH. **(A)** Top: Interaction effect between Glx and AVH group: Glx has a stronger effect in high-AVH ($n = 21$) than in low-AVH patients ($n = 21$) on left STG connectivity with the areas shown in red. Bottom: *post-hoc* tests for within-group effects of Glx on connectivity. Higher Glx is associated with increased connectivity between left STG and areas shown in red. **(B)** Top: Interaction effect between GABA and AVH group: GABA has a stronger effect in low-AVH ($n = 20$) than in high-AVH patients ($n = 21$) on left STG connectivity with the areas shown in blue. Bottom: *post-hoc* tests for within-group effects of GABA on connectivity. Higher GABA is associated with decreased connectivity between left STG and areas shown in blue. Slices were taken from MNI coordinates $z = -15$ for Glx effects and $z = -4$ for GABA effects.

the two neurotransmitters are linked, with Glu (the dominant component in Glx measurements) binding to NMDA-receptors on GABAergic neurons as a trigger for the release of GABA. In a previous paper (14), Glx concentrations in the ACC were elevated in low-AVH patients compared to high-AVH patients, and even compared to healthy controls, in a sample that is largely overlapping with that of the current study. This finding was confirmed for the current study's sample. Elevated Glx levels might reflect a compensation mechanism in low-AVH patients to counter schizophrenia-related NMDA-receptor hypofunctioning (13, 28), with elevated Glx concentrations increasing the probability of binding. Such a compensation mechanism might result in sufficient Glu amounts to bind to GABAergic neurons in order to allow for the release of GABA. This would explain the GABA effect on interhemispheric STG connectivity in the low-AVH patients. In contrast, in high-AVH patients, the reduced levels of Glx may prevent a sufficient amount of Glu binding to GABAergic cells, which could explain the absence of a significant GABA effect on connectivity in the high-AVH group. This lack of inhibitory GABA effect to balance the excitatory Glu effect found in the high-AVH group might lead to an increase in interhemispheric STG connectivity in high-AVH patients compared to low-AVH patients, as predicted by the interhemispheric miscommunication theory of AVH (10).

Thus, the current results suggest that it is the interplay between Glu and GABA – i.e., between excitatory and

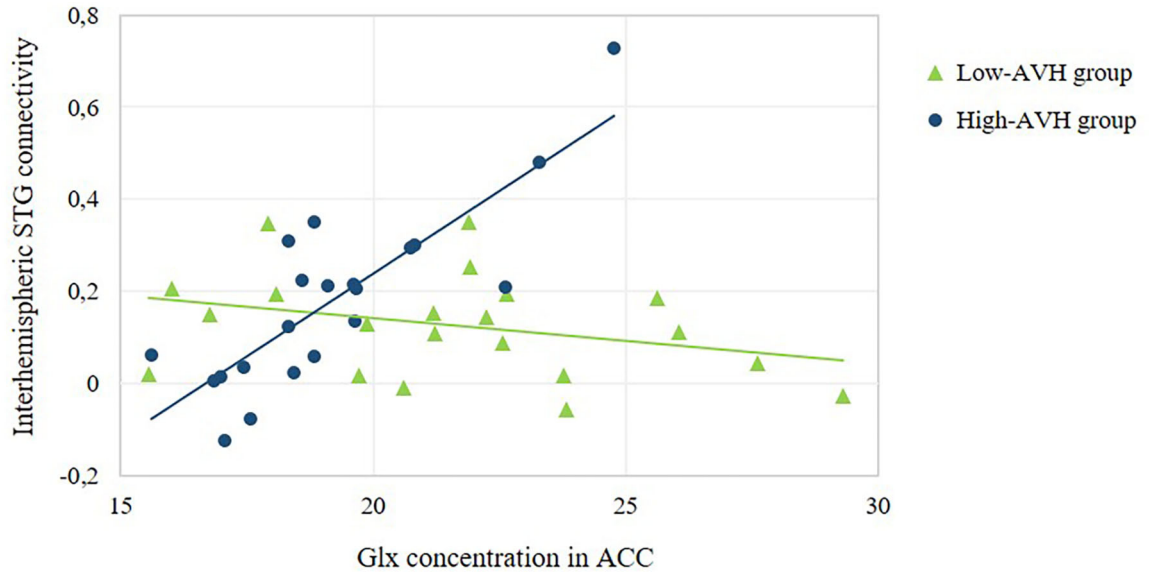

FIGURE 4 | Relationship between ACC Glx concentration and the strength of interhemispheric STG connectivity. The scatterplot offers a numerical depiction of the effect shown in the bottom row of **Figure 3A** with functional connectivity values extracted from the significant cluster in the right STG/MTG. For low-AVH patients, there was no significant relationship between ACC Glx and left STG connectivity with that cluster, $p = 0.160$. For high-AVH patients, there was a significant positive relationship, $r = 0.83$, $p = 0.000$.

TABLE 4 | Relationships between GABA concentration in ACC and left STG functional connectivity.

	Brain area	Coordinates			Cluster size	Beta	Voxel-level *p*	Cluster *p*
High-AVH – low-AVH								
	STG/MTG	57	−28	−4	147	0.31	< 0.005	0.027
Effects within the high-AVH group								
(*n* = 21)	–		–		–	–	–	–
Effects within the low-AVH group								
(*n* = 20)	STG/MTG	47	−33	−4	88	−0.22	< 0.001	0.005
	Medial superior frontal gyrus	4	51	44	58	−0.25	< 0.001	0.030

The listed clusters showed a group difference in the relationship between Glx and connectivity (high-AVH – low-AVH) or a relationship between Glx and connectivity within one of the groups (effects within high-AVH group and effects within low-AVH group, respectively). Coordinates are given in MNI space. Brain areas are derived from the FSL Harvard-Oxford atlas in Conn. Cluster size is given as the number of voxels.

inhibitory effects – that modulates functional connectivity in AVH, and dysfunction in one system may go together with dysfunction in the other system (15). An excitatory/inhibitory imbalance has previously been suggested as a key factor in AVH (14, 29, 30). The current study suggests that one of the mechanisms underlying the relationship between this imbalance and AVH might be altered interhemispheric STG connectivity.

Left STG-Measured Glx and GABA Relationships With Functional Connectivity

Contrary to our hypothesis, Glx and GABA concentrations in the left STG did not have any AVH-dependent effects on interhemispheric STG connectivity. There were Glx effects on left STG connectivity with occipital and postcentral areas and the thalamus, all of which have been associated with hallucinations (3, 31, 32). However, these findings are difficult to interpret and should be taken with caution, given the lack of overlap of any group differences with within-group effects.

Limitations of the Study and Directions for Future Research

When interpreting the results of the current study, it should be borne in mind that, for some of the analyses, the sample sizes were relatively small. This may have reduced statistical power and could be the reason that some analyses failed to survive conservative statistical thresholding. These findings should be taken with caution and should be replicated. The fact that the current results were corrected for potential effects of age, gender and medication, should enhance the generalizability to different samples. It is interesting to note that accounting for exposure to antipsychotic medication did not change the results

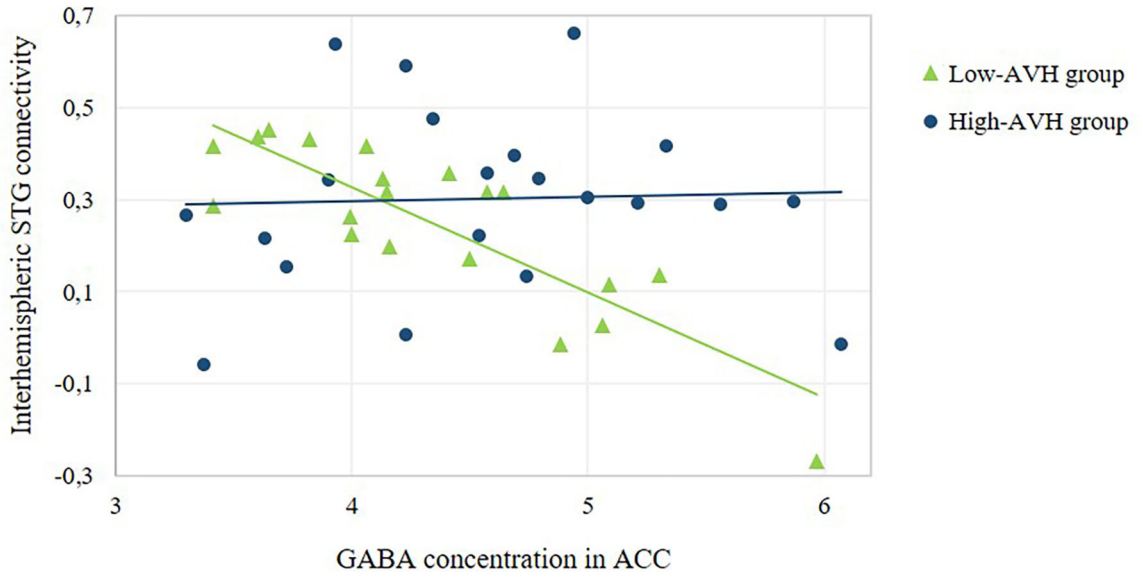

FIGURE 5 | Relationship between ACC GABA concentration and the strength of interhemispheric STG connectivity. The scatterplot offers a numerical depiction of the effect shown in the bottom row of **Figure 3B** with functional connectivity values extracted from the significant cluster in the right STG/MTG. For high-AVH patients, there was no significant relationship between ACC GABA and left STG connectivity with that cluster, $p = 0.867$. For low-AVH patients, there was a significant negative relationship, $r = -0.84$, $p = 0.000$.

compared to a model where medication was not accounted for. This suggests that antipsychotics did not significantly modulate the relationship between Glx or GABA and left STG connectivity. However, future studies with a pre/post design with fMRI assessment before and after antipsychotic drug exposure might provide more insight into effects of antipsychotics on neurotransmitter concentrations and relationships with functional connectivity.

The current findings on the modulation of interhemispheric STG connectivity by ACC Glx and GABA showed high inner consistency in the sense that group differences were reflected in differential within-group effects in the same brain areas, which strengthens the confidence in these results. The fact that only Glx and GABA in the ACC but not in the left STG showed the expected effects on interhemispheric connectivity is noteworthy and emphasizes the modulatory role of the ACC in AVH. Based on findings of impaired cognitive control in patients with AVH during an auditory task (33) as well as abnormal connectivity between the ACC and the STG (2), it has been suggested that AVH arise from impaired top-down control of prefrontal areas over bottom-up processes in auditory areas (2, 22, 29). The exact role of Glx and GABA in the left STG for brain functioning in AVH remains less clear but could potentially be more strongly related to brain activity, rather than connectivity, given the activation of the left STG during AVH (3, 32, 34).

Conclusion

Given the rich evidence for AVH-related alterations on the level of brain structure, brain functioning and neurochemistry when studied in isolation, any explanation of AVH will ultimately have to integrate these separate effects at the different levels of explanation (35, 36). The interhemispheric miscommunication theory provides a promising model for such an endeavor since it is based on robust evidence from different levels of explanation, incorporating behavioral, structural and functional abnormalities in interhemispheric STG connectivity. The current study provides an investigation of this model and shows how it is linked to other existing hypotheses about AVH, such as impaired prefrontal top-down control (22) and excitatory/inhibitory imbalances (30). Thereby, the study shows an example of how a combination of different neuroimaging modalities can lead to a more comprehensive understanding of AVH, with possible implications for the development of new therapeutic interventions.

DATA AVAILABILITY STATEMENT

The raw data supporting the conclusions of this article will be made available by the authors, without undue reservation, to any qualified researcher.

ETHICS STATEMENT

The studies involving human participants were reviewed and approved by Regional Committee for Medical Research Ethics in Western Norway (REK Vest # 2010/3387). The patients/participants provided their written informed consent to participate in this study.

DISCLOSURE

The authors AC, LE, and KH own shares in the NordicNeuroLab inc. company, which produces some of the add-on equipment used during data acquisition.

AUTHOR CONTRIBUTIONS

SW contributed data analysis and interpretation of the data and wrote the first draft of the manuscript. HH contributed to interpretation of the data and wrote parts of the manuscript. AC contributed processing of MRS data. EJ contributed conception and design of the study. RK and E-ML contributed to the data collection. KK organized the database. KH contributed conception and design of the study and interpretation of the data. All authors contributed to manuscript revision.

FUNDING

The present research was funded from a Western Norway Regional Health Authority grant #912045 to KH and grants from the Norwegian Research Council (RCN) #213727, and the Western Norway Regional Health Authority #911820 and #911679 to EJ. The funding sources did not have any role in the conduct or reporting of the work.

ACKNOWLEDGMENTS

The authors would like to thank the MR-technicians and patients who made the study possible.

REFERENCES

1. Alderson-Day B, McCarthy-Jones S, Fernyhough C. Hearing voices in the resting brain: a review of intrinsic functional connectivity research on auditory verbal hallucinations. *Neurosci Biobehav Rev*. (2015) 55:78–87. doi: 10.1016/J.NEUBIOREV.2015.04.016
2. Curčić-Blake B, Ford JM, Hubl D, Orlov ND, Sommer IE, Waters F, et al. Interaction of language, auditory and memory brain networks in auditory verbal hallucinations. *Prog Neurobiol*. (2017) 148:1–20. doi: 10.1016/J.PNEUROBIO.2016.11.002
3. Kompus K, Westerhausen R, Hugdahl K. The "paradoxical" engagement of the primary auditory cortex in patients with auditory verbal hallucinations: a meta-analysis of functional neuroimaging studies. *Neuropsychologia*. (2011) 49:3361–9. doi: 10.1016/J.NEUROPSYCHOLOGIA.2011.08.010
4. Gavrilescu M, Rossell S, Stuart GW, Shea TL, Innes-Brown H, Henshall K, et al. Reduced connectivity of the auditory cortex in patients with auditory hallucinations: a resting state functional magnetic resonance imaging study. *Psychol Med*. (2010) 40:1149–58. doi: 10.1017/S0033291709991632
5. Mulert C, Kirsch V, Pascual-Marqui R, McCarley RW, Spencer KM. Long-range synchrony of gamma oscillations and auditory hallucination symptoms in schizophrenia. *Int J Psychophysiol*. (2011) 79:55–63. doi: 10.1016/J.IJPSYCHO.2010.08.004
6. Mulert C, Kirsch V, Whitford TJ, Alvarado J, Pelavin P, McCarley RW, et al. Hearing voices: A role of interhemispheric auditory connectivity? *World J Biol Psychiatry*. (2012) 13:153–8. doi: 10.3109/15622975.2011.570789
7. Wigand M, Kubicki M, Clemm von Hohenberg C, Leicht G, Karch S, Eckbo R, et al. Auditory verbal hallucinations and the interhemispheric auditory pathway in chronic schizophrenia. *World J Biol Psychiatry*. (2015) 16:31–44. doi: 10.3109/15622975.2014.948063
8. Diesch E, Schummer V, Kramer M, Rupp A. Structural changes of the corpus callosum in tinnitus. *Front Syst Neurosci*. (2012) 6:17. doi: 10.3389/fnsys.2012.00017
9. Steinmann S, Leicht G, Mulert C. Interhemispheric auditory connectivity: structure and function related to auditory verbal hallucinations. *Front Hum Neurosci*. (2014) 8:55. doi: 10.3389/fnhum.2014.00055
10. Steinmann S, Leicht G, Mulert C. The interhemispheric miscommunication theory of auditory verbal hallucinations in schizophrenia. *Int J Psychophysiol*. (2019) 145:93–90. doi: 10.1016/J.IJPSYCHO.2019.02.002
11. Egerton A, Modinos G, Ferrera D, McGuire P. Neuroimaging studies of GABA in schizophrenia: a systematic review with meta-analysis. *Transl Psychiatry*. (2017) 7:e1147. doi: 10.1038/tp.2017.124
12. Merritt K, Egerton A, Kempton MJ, Taylor MJ, McGuire PK. Nature of glutamate alterations in schizophrenia. *JAMA Psychiatry*. (2016) 73:665. doi: 10.1001/jamapsychiatry.2016.0442
13. Curčić-Blake B, Bais L, Sibeijn-Kuiper A, Pijnenborg HM, Knegtering H, Liemburg E, et al. Glutamate in dorsolateral prefrontal cortex and auditory verbal hallucinations in patients with schizophrenia: A 1H MRS study. *Prog Neuro-Psychopharmacol Biol Psychiatry*. (2017) 78:132–9. doi: 10.1016/J.PNPBP.2017.05.020
14. Hjelmervik H, Craven AR, Sinceviciute I, Johnsen E, Kompus K, Bless JJ, et al. Intra-regional Glu-GABA vs inter-regional glu-glu imbalance: a 1H-MRS study of the neurochemistry of auditory verbal hallucinations in schizophrenia. *Schizophr Bull*. (2019) 46:633–42. doi: 10.1093/schbul/sbz099
15. Hugdahl K, Craven AR, Nygård M, Løberg E-M, Berle JØ, Johnsen E, et al. Glutamate as a mediating transmitter for auditory hallucinations in schizophrenia: a 1H MRS study. *Schizophr Res*. (2015) 161:252–60. doi: 10.1016/J.SCHRES.2014.11.015
16. Lahti AC, Weiler MA, Tamara Michaelidis B, Parwani A, Tamminga CA. Effects of ketamine in normal and schizophrenic volunteers. *Neuropsychopharmacology*. (2001) 25:455–67. doi: 10.1016/S0893-133X(01)00243-3
17. Malhotra AK, Pinals A, Adler M, Elman I, Clifton A, Pickar D, et al. Ketamine-induced exacerbation of psychotic symptoms and cognitive impairment in neuroleptic-free schizophrenics. *Neuropsychopharmacology*. (1997) 17:141–50. doi: 10.1016/S0893-133X(97)00036-5
18. Adler CM, Malhotra AK, Elman I, Goldberg T, Egan M, Pickar D, et al. Comparison of ketamine-induced thought disorder in healthy volunteers and thought disorder in schizophrenia. *Am J Psychiatry*. (1999) 156:1646–9. doi: 10.1176/ajp.156.10.1646
19. Krystal JH, Karper LP, Seibyl JP, Freeman GK, Delaney R, Bremner JD, et al. Subanesthetic effects of the noncompetitive NMDA antagonist, ketamine, in humans. *Arch Gen Psychiatry*. (1994) 51:199. doi: 10.1001/archpsyc.1994.03950030035004
20. Thiebes S, Steinmann S, Curic S, Polomac N, Andreou C, Eichler I-C, et al. Alterations in interhemispheric gamma-band connectivity are related to the emergence of auditory verbal hallucinations in healthy subjects during NMDA-receptor blockade. *Neuropsychopharmacology*. (2018) 43:1608–15. doi: 10.1038/s41386-018-0014-z
21. Steinmann S, Leicht G, Andreou C, Polomac N, Mulert C. Auditory verbal hallucinations related to altered long-range synchrony of gamma-band oscillations. *Sci Rep*. (2017) 7:8401. doi: 10.1038/s41598-017-09253-7
22. Hugdahl K. Hearing voices: auditory hallucinations as failure of top-down control of bottom-up perceptual processes. *Scand J Psychol*. (2009) 50:553–60. doi: 10.1111/j.1467-9450.2009.00775.x
23. World Health Organization. *The ICD-10 Classification of Mental and Behavioural Disorders*. World Health Organization (1992). Available online at: https://www.who.int/classifications/icd/en/bluebook.pdf
24. Kay SR, Fiszbein A, Opler LA. The Positive and Negative Syndrome Scale (PANSS) for schizophrenia. *Schizophr Bull*. (1987) 13:261–76. doi: 10.1093/schbul/13.2.261
25. McCarthy-Jones S, Smailes D, Corvin A, Gill M, Morris DW, Dinan TG, et al. Occurrence and co-occurrence of hallucinations by modality in schizophrenia-spectrum disorders. *Psychiatry Res*. (2017) 252:154–60. doi: 10.1016/J.PSYCHRES.2017.01.102

26. Nayani TH, David AS. The auditory hallucination: a phenomenological survey. *Psychol Med*. (1996) 26:177–89. doi: 10.1017/S003329170003381X
27. Opler LA, Kay SR, Lindenmayer JP, Fiszbein A. *Structured Clinical Interview: The Positive and Negative Syndrome Scale (SCI-PANSS)*. North Tonawanda, NY: Multi-Health Systems Inc. (1999).
28. Poels EMP, Kegeles LS, Kantrowitz JT, Slifstein M, Javitt DC, Lieberman JA, et al. Imaging glutamate in schizophrenia: review of findings and implications for drug discovery. *Mol Psychiatry*. (2014) 19:20–9. doi: 10.1038/mp.2013.136
29. Hugdahl K. Auditory hallucinations: a review of the ERC "VOICE" project. *World J Psychiatry*. (2015) 5:193. doi: 10.5498/WJP.V5.I2.193
30. Jardri R, Hugdahl K, Hughes M, Brunelin J, Waters F, Alderson-Day B, et al. Are hallucinations due to an imbalance between excitatory and inhibitory influences on the brain? *Schizophr Bull*. (2016) 42:1124–34. doi: 10.1093/schbul/sbw075
31. Kuhn S, Gallinat J. Quantitative meta-analysis on state and trait aspects of auditory verbal hallucinations in schizophrenia. *Schizophr Bull*. (2012) 38:779–86. doi: 10.1093/schbul/sbq152
32. Zmigrod L, Garrison JR, Carr J, Simons JS. The neural mechanisms of hallucinations: a quantitative meta-analysis of neuroimaging studies. *Neurosci Biobehav Rev*. (2016) 69:113–23. doi: 10.1016/J.NEUBIOREV.2016.05.037
33. Hugdahl K, Nygård M, Falkenberg LE, Kompus K, Westerhausen R, Kroken R, et al. Failure of attention focus and cognitive control in schizophrenia patients with auditory verbal hallucinations: evidence from dichotic listening. *Schizophr Res*. (2013) 147:301–9. doi: 10.1016/j.schres.2013.04.005
34. Jardri R, Pouchet A, Pins D, Thomas P. Cortical activations during auditory verbal hallucinations in schizophrenia: a coordinate-based meta-analysis. *Am J Psychiatry*. (2011) 168:73–81. doi: 10.1176/appi.ajp.2010.09101522
35. Calhoun VD, Sui J. Multimodal fusion of brain imaging data: a key to finding the missing link(s) in complex mental illness. *Biol Psychiatry Cogn Neurosci Neuroimaging*. (2016) 1:230–44. doi: 10.1016/J.BPSC.2015.12.005
36. Hugdahl K, Sommer IE. Auditory verbal hallucinations in schizophrenia from a levels of explanation perspective. *Schizophr Bull*. (2018) 44:234–41. doi: 10.1093/schbul/sbx142

Conflict of Interest: The authors declare that the research was conducted in the absence of any commercial or financial relationships that could be construed as a potential conflict of interest.

frontiers in Psychiatry

REVIEW
published: 23 February 2021
doi: 10.3389/fpsyt.2021.640977

Elevated Brain Glutamate Levels in Bipolar Disorder and Pyruvate Carboxylase-Mediated Anaplerosis

Jun Shen and Jyoti Singh Tomar*

Section on Magnetic Resonance Spectroscopy, Molecular Imaging Branch, National Institute of Mental Health Intramural Research Program, National Institutes of Health, Bethesda, MD, United States

In vivo ^{1}H magnetic resonance spectroscopy studies have found elevated brain glutamate or glutamate + glutamine levels in bipolar disorder with surprisingly high reproducibility. We propose that the elevated glutamate levels in bipolar disorder can be explained by increased pyruvate carboxylase-mediated anaplerosis in brain. Multiple independent lines of evidence supporting increased pyruvate carboxylase-mediated anaplerosis as a common mechanism underlying glutamatergic hyperactivity in bipolar disorder and the positive association between bipolar disorder and obesity are also described.

Keywords: glutamate, magnetic resonance spectroscopy, pyruvate carboxylase, bipolar disorder, obesity

OPEN ACCESS

Edited by:
Marcio Gerhardt Soeiro-de-Souza, University of São Paulo, Brazil

Reviewed by:
João M. N. Duarte, Lund University, Sweden
Sumeet Sharma, Emory University, United States

****Correspondence:***
Jun Shen
shenj@intra.nimh.nih.gov

Specialty section:
This article was submitted to Molecular Psychiatry, a section of the journal Frontiers in Psychiatry

Received: *12 December 2020*
Accepted: *19 January 2021*
Published: *23 February 2021*

Citation:
Shen J and Tomar JS (2021) Elevated Brain Glutamate Levels in Bipolar Disorder and Pyruvate Carboxylase-Mediated Anaplerosis. Front. Psychiatry 12:640977. doi: 10.3389/fpsyt.2021.640977

INTRODUCTION

The etiologic and disease mechanisms of bipolar disorder remain poorly understood. A growing body of evidence indicates a central role of mitochondrial dysfunction in the pathophysiology of bipolar disorder. Post-mortem brain studies have revealed abnormal size, structure and distribution of mitochondria as well as a pronounced and extensive decrease in nuclear gene expression governing oxidative phosphorylation in bipolar disorder (1–3). These post-mortem results are consistent with *in vivo* findings of elevated cerebrospinal fluid pyruvate and lactate levels (4, 5), decreased adenosine triphosphate production and a significant shift from oxidative phosphorylation to glycolysis in brain in bipolar disorder accompanied by elevated brain lactate levels and lowered intracellular pH as reported by *in vivo* ^{31}P and ^{1}H magnetic resonance spectroscopy (MRS) studies (6–10). Paradoxically, despite the impaired mitochondrial function and oxidative metabolism in bipolar disorder *in vivo* ^{1}H MRS studies have also reported a highly reproducible pattern of elevated total glutamate or glutamate + glutamine levels (11) (glutamate + glutamine is dominated by glutamate in MRS spectra).

Pyruvate carboxylase is a mitochondrial enzyme. It catalyzes the thermodynamically irreversible carboxylation of pyruvate to oxaloacetate which is a tricarboxylic acid (TCA) cycle intermediate used for various biosynthetic pathways depending on the tissues. The biotin-dependent pyruvate carboxylase employs pyruvate and the polar molecule bicarbonate instead of CO_2 as its substrates:

$$\text{pyruvate} + HCO_3^- + \text{adenosine triphosphate} \rightarrow \text{oxaloacetate} + \text{adenosine diphosphate} + \text{inorganic phosphate}$$

Pyruvate carboxylase-mediated anaplerosis is at the metabolic crossroad of carbohydrate and lipid metabolism, playing a key role in gluconeogenesis, lipogenesis, and glutamate homeostasis

(see **Figure 1**). In brain, released neurotransmitter glutamate is replenished by the glutamate-glutamine neurotransmitter cycle and *de novo* glutamate synthesis via pyruvate carboxylase-mediated anaplerosis in astrocytes (12–21). In this work we propose that the elevated brain glutamate levels in bipolar disorder observed by ^{1}H MRS with very high consistency can be explained by an increase in pyruvate carboxylase-mediated anaplerosis. Evidence supporting increased pyruvate carboxylase-mediated anaplerosis as a common mechanism underlying glutamatergic hyperactivity in bipolar disorder and the positive association between bipolar disorder and obesity is also discussed. The pyruvate carboxylase-mediated anaplerotic pathway may represent future therapeutic targets for bipolar disorder.

BRAIN PYRUVATE CARBOXYLATION IN BIPOLAR DISORDER

Pyruvate Carboxylase-Mediated Anaplerosis Is Essential for Maintaining Glutamate Homeostasis

Presynaptic release of neurotransmitter glutamate is accompanied by its rapid uptake into astrocytes to maintain an extremely low extracellular glutamate level. The released neuronal glutamate is replenished predominantly by astrocytic glutamine supplied by the glutamate-glutamine neurotransmitter cycle and *de novo* glutamate synthesis (22–24). Abundant evidence shows that neurons lack the anaplerotic enzyme pyruvate carboxylase required for *de novo* synthesis of TCA cycle intermediates (19, 21, 25). Through pyruvate carboxylase-mediated anaplerosis in astrocytes pyruvate and bicarbonate enter the TCA cycle to replenish carbon skeletons lost via glutamine efflux. The subsequently formed TCA cycle intermediate α-ketoglutarate is converted to glutamate by transamination via aspartate aminotransferase or reductive amination via glutamate dehydrogenase. Glutamate can be subsequently converted to glutamine by glutamine synthetase (15), an enzyme exclusively expressed in astrocytes (26). Numerous *in vivo* ^{13}C MRS studies have established that the glutamate-glutamine neurotransmitter cycle between astrocytes and neurons is a major metabolic flux in brain (12, 13, 16, 20, 23). In the meanwhile, glutamine efflux from the brain is highly significant (27). Many studies have demonstrated that *de novo* synthesis of glutamate is a significant metabolic pathway essential for maintaining glutamate/glutamine homeostasis in the central nervous system (16, 18).

Glutamate and Glutamatergic Hyperactivity in Bipolar Disorder

Glutamate is the major excitatory neurotransmitter in the central nervous system. Although the pathophysiology of bipolar disorder is still poorly understood, growing evidence suggests that glutamatergic abnormalities play a key role in the pathogenesis and treatment of bipolar disorder. For example, many rodent studies have demonstrated that mood stabilizers modulate glutamatergic receptors while manipulation of glutamatergic receptors causes significant changes in mood-associated behaviors (28, 29). Post-mortem studies of bipolar disorder have also produced evidence of excitotoxicity in the frontal cortex (30), altered glutamatergic function on both presynaptic and post-synaptic sides, and abnormal excitatory synaptic connections (31, 32). In keeping with the preclinical and post-mortem findings of glutamatergic hyperactivity in bipolar disorder an *in vivo* transcranial magnetic stimulation study has reported impaired cortical inhibition in bipolar disorder (33).

High glutamate + glutamine levels were shown to correlate with cognitive impairment in many brain disorders associated with glutamatergic abnormalities (34). The increased glutamate availability suggests activity-dependent vesicular glutamate release of larger quantal size because vesicle glutamate filling levels are dependent on the concentration of cytoplasmic glutamate to be packaged into synaptic vesicles (35). As excessive glutamate activates ionotropic receptors in extra-synaptic sites and causes neurotoxicity by calcium influx and generation of free radicals including nitric oxide, the sustained elevation of glutamate levels therefore may be a significant part of the pathogenesis of the widespread glutamatergic abnormalities in bipolar disorder (36).

Elevated Glutamate Levels in Bipolar Disorder Can Be Explained by Increased Pyruvate Carboxylase-Mediated Anaplerosis in Brain

Despite the highly reproducible evidence of elevated brain glutamate levels in bipolar disorder from numerous *in vivo* MRS studies, to the best of our knowledge, a connection between the MRS results and pyruvate carboxylase-mediated anaplerosis has not been made in the literature. However, several drugs used in the treatment of bipolar disorder have important links to pyruvate carboxylase. For example, carbamazepine has long been a therapeutic option for bipolar disorder. It has been used in the treatment of bipolar disorder in both acute mania and maintenance therapy. In rats chronically administered dietary carbamazepine the abundance and activity of biotinylated pyruvate carboxylase were significantly reduced in both liver and brain (37, 38). The potential connection between the efficacy of carbamazepine in bipolar disorder treatment and its effect on pyruvate carboxylase has yet to be investigated.

The important role of the mitochondrial enzyme pyruvate carboxylase in brain function is also well-recognized clinically. Pyruvate carboxylase deficiency, a rare autosomal recessive inborn error of metabolism, is characterized by impairment of lactate metabolism and gluconeogenesis, producing severe lactic acidosis accompanied by compromised psychomotor development and intellectual disability (39). Certain drugs used in the treatment of bipolar disorder improve cerebral metabolism. For example, lithium was demonstrated to enhance oxidative phosphorylation in post-mortem human brain tissue (40) and quetiapine reduced lactate in rapid cycling manic bipolar patients (41).

Despite numerous variations across the studies (e.g., patient selection, disease state, medication history, and ^{1}H MRS

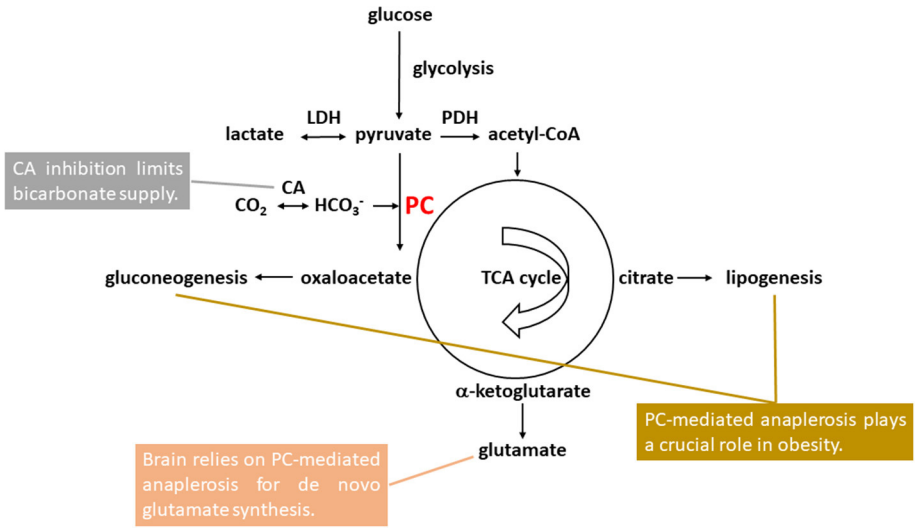

FIGURE 1 | Pyruvate carboxylase (PC)-mediated anaplerosis in bipolar disorder and comorbid obesity. Glucose first undergoes glycolysis with pyruvate as the end product. Pyruvate is in rapid exchange with lactate catalyzed by lactate hydrogenase (LDH). Brain pyruvate and lactate levels were found to be elevated in bipolar disorder. Pyruvate enters mitochondria either for oxidation to acetyl-CoA catalyzed by pyruvate dehydrogenase (PDH) or carboxylation to oxaloacetate catalyzed by PC. PC uses bicarbonate as its substrate instead of CO_2. Carbonic anhydrase (CA) inhibition limits bicarbonate supply to PC. For *de novo* glutamate synthesis in astrocytes, oxaloacetate formed by pyruvate carboxylation condenses with acetyl-CoA and is converted to citrate and subsequently to α-ketoglutarate as part of the tricarboxylic acid (TCA) cycle. α-ketoglutarate can be further converted into glutamate, which was found to be elevated bipolar disorder. Formation of oxaloacetate from pyruvate via PC represents the first committed step of gluconeogenesis which primarily takes place in liver and, to a lesser extent, the cortex of kidneys. For lipogenesis, citrate synthesized via pyruvate carboxylation and subsequent condensation with acetyl-CoA in mitochondria is exported to the cytosol to supply acetyl-CoA for *de novo* fatty acid synthesis. Both fatty acid and triglyceride synthesis take place mainly in liver and adipose tissue.

methodologies) *in vivo* ^{1}H MRS studies of bipolar disorder have found elevated glutamate or glutamate + glutamine with surprisingly high consistency (8, 11, 36, 42–45). Consistent, mood phase-independent elevation in glutamate levels in the frontal brain areas was measured in adult bipolar disorder patients by many ^{1}H MRS studies (43) while treatment of bipolar disorder patients by lithium and valproate resulted in glutamate + glutamine reduction (45). A meta-analysis (11) of the ^{1}H MRS measurement of glutamate + glutamine found elevated glutamate + glutamine levels in bipolar patients when compared with healthy controls with an effect size of 0.72 and a 95% confidence interval of 0.17–1.27 ($p = 0.01$) for the pooled studies that reported glutamate + glutamine in all area of the brain (nine studies with 162 bipolar disorder patients and 165 healthy controls). Analyses of medicated and non-medicated bipolar disorder patients found that the effect size for glutamate level increase in non-medicated patients was much higher (1.91; $p = 0.03$) than in medicated patients (0.31; $p = 0.03$), consistent with that medications decreased brain glutamate. Increased serum α-ketoglutarate and glutamate and increased glutamate in post-mortem brain tissue samples obtained from bipolar disorder individuals have also been reported (46–49). For instance, plasma glutamate levels in patients with bipolar mania ($n = 20$) were significantly higher in both mania phase ($46 \pm 19\,\mu M$, $p = 0.03$) and remission ($57 \pm 27\,\mu M$, $p = 0.04$) than matched controls ($36 \pm 9\,\mu M$, $n = 20$) (46). After correcting for post-mortem changes the level of glutamate at the time of death measured from post-mortem frontal cortex samples (Brodmann area 6) of bipolar disorder patients (15.33 ± 5.72 nmol/mg tissue, $n = 15$) was found to be significantly higher than in the normal control samples (10.68 ± 2.59 nmol/mg tissue, $n = 15$, $p = 0.013$) (47). In contrast, only a few studies have reported no change in glutamate + glutamine or reduced glutamate + glutamine in brain areas studied (36).

It is well-known in the neurochemical literature that brain relies on pyruvate carboxylase-mediated anaplerosis for *de novo* glutamate synthesis (15–21). Because of the unique role of pyruvate carboxylase in brain glutamate formation the highly consistent findings of elevated glutamate or glutamate + glutamine levels in bipolar disorder observed by *in vivo* ^{1}H MRS, serum and post-mortem studies can be readily explained by increased pyruvate carboxylase-mediated anaplerosis in brain of patients with bipolar disorders. This explanation is also supported by the significant comorbidity between bipolar disorder and obesity as described in section Glutamate, Bipolar Disorder, and Comorbid Obesity.

Elevated Glutamate Levels in Bipolar Disorder Is Consistent With a Chronic Mismatch Between Glucose Utilization and Oxidative Metabolism

A large body of evidence has consistently demonstrated that there is a significant mismatch or uncoupling between glucose utilization and oxidative metabolism in stimulated brain accompanying increased glutamatergic activities (50). Similar mismatches have also been observed in brain after vigorous physical exercise (51). Many functional ^{1}H MRS studies have reported transient elevation of glutamate or glutamate + glutamine levels in activated brain tissue in

response to stimuli or tasks (52). In preclinical studies, increased glutamatergic activities were found to cause an increase in pyruvate carboxylation, resulting in enlarged glutamate and glutamine pools (17). These results suggest that enhanced glutamatergic activity increases *de novo* synthesis of glutamate from glucose (17). It should be noted that literature evidence for a transient increase in glutamate levels following a functional task or stimulus is not conclusive (52). Recent *in vivo* ^{13}C MRS studies of anesthetized rodents found that acute stimulation did not increase pyruvate carboxylase-mediated anaplerotic flux rate in brain (53, 54).

The molar ratio of the arterio-venous difference of oxygen to glucose + ½ lactate is commonly referred to as the oxygen-to-carbohydrate index. The oxygen-to-carbohydrate index is reduced when more glucose and lactate are taken up into the brain than are oxidized to CO_2. As lactate accumulation can only account for a portion of the large decrease in oxygen-to-carbohydrate index accompanying the mismatch between stimulation of glucose utilization and oxidative metabolism, it has been proposed that increased *de novo* glutamate synthesis via pyruvate carboxylase-mediated anaplerosis contributes to the large decrease in oxygen-to-carbohydrate index when glucose utilization outpaces oxidative metabolism during stimulation of brain activity (17, 51).

^{31}P and ^{1}H MRS studies have found reduced oxidative phosphorylation and elevated lactate and glutamate + glutamine levels in brain in bipolar disorder, indicating impaired oxidative metabolism (7–10, 36, 42, 43). In contrast, positron emission tomography (PET) studies using [^{18}F]fluorodeoxyglucose have reported small or no differences between healthy controls and bipolar disorder patients in glucose utilization rate in the prefrontal cortex or brain as a whole (55–58). There is no consensus in the directionality of the reported differences by the PET studies (55–58). Considering the variations across the PET studies, the lack of consensus in the direction of the changes suggests that the overall abnormalities in cerebral glucose utilization in bipolar disorder are likely very small. The ^{31}P and ^{1}H MRS and PET results, taken together, indicate that there is a considerable mismatch between oxidative metabolism and glucose utilization in brain in bipolar disorder. Therefore, the elevated glutamate + glutamine levels are consistent with mitochondrial dysfunction and a chronic mismatch between glucose utilization and oxidative metabolism in bipolar disorder accompanied by incomplete carbohydrate oxidation and increased pyruvate carboxylase-mediated anaplerosis.

GLUTAMATE, BIPOLAR DISORDER, AND COMORBID OBESITY

Glutamate Levels and Body Mass Index in Bipolar Disorder

Bipolar disorder and obesity are positively associated (59–62) with cardiovascular disease as the most common cause of death in bipolar disorder patients (63). Bipolar disorder patients are two-thirds more likely to be obese than the age-, race-, and sex-adjusted general population (60). A study of the association between body weight and bipolar illness in drug-naïve patients reported that ∼41% of untreated patients with bipolar disorder were overweight or obese (59). Obese bipolar disorder patients also have a more severe mood illness than normal weight patients (61). The underlying causes of the effects of obesity on bipolar disorder are still being investigated (61, 64). Recent neuroimaging studies reported that structural and neurochemical abnormalities in brain characteristic of bipolar disorder were more prominent with higher body mass index (65, 66). In particular, the increase in bilateral hippocampal glutamate + glutamine in patients with first-episode mania measured by ^{1}H MRS was found to be more pronounced with higher body mass index (67). In comparison, the correlation between glutamate + glutamine and body mass index in healthy individuals was insignificant (67).

Obesity Is Associated With Increased Pyruvate Carboxylase-Mediated Anaplerosis

Pyruvate carboxylase plays a crucial role in lipogenesis and gluconeogenesis in mammals. It converts pyruvate and bicarbonate into oxaloacetate for further conversion into citrate which is then exported from mitochondria and cleaved in cytosol to supply precursors for *de novo* fatty acid synthesis [(68); **Figure 1**]. The activity of pyruvate carboxylase is dramatically increased during adipocyte differentiation. Over expression of pyruvate carboxylase is associated with obesity and type 2 diabetes (69). Of the four gluconeogenic enzymes (phosphoenolpyruvate carboxykinase, fructose-1,6-bisphosphatase, glucose-6-phosphatase, and pyruvate carboxylase) pyruvate carboxylase reaction is the first committed step and likely rate-limiting in gluconeogenesis (70). The pyruvate carboxylase reaction provides oxaloacetate for subsequent conversion into phosphoenolpyruvate by phosphoenolpyruvate carboxykinase and regulates hepatic glucose production. In humans, increased hepatic pyruvate carboxylase expression was closely correlated with plasma glycemia, indicating that hepatic pyruvate carboxylase is a key determinant of gluconeogenesis in liver (71). Animal studies have demonstrated that increased pyruvate carboxylase flux is an important pathway responsible for increased hepatic glucose production in diabetes development (72). Furthermore, selective inhibition of pyruvate carboxylase expression in liver and adipose tissue significantly reduced adiposity, plasma lipid levels and hepatic steatosis (71). A recent *in vivo* ^{1}H and ^{13}C MRS study of a mouse model of high-fat diet consumption has also found significantly elevated glutamate and glutamate + glutamine levels as well as increased pyruvate carboxylase-mediated anaplerotic flux rate in the hypothalamus of treated animals (73). Taken together, the above evidence demonstrates that increased pyruvate carboxylase-mediated anaplerosis is a metabolic hallmark of obesity.

Carbonic Anhydrase Inhibition in Bipolar Disorder and Obesity

Catalysis by carbonic anhydrase is necessary to speed up the reversible hydration of CO_2 for a variety of biological processes. In the central nervous system carbonic anhydrase

inhibition enhances inhibitory neurotransmission. Many anticonvulsants are strong carbonic anhydrase inhibitors. Adjunctive acetazolamide, a sulfonamide carbonic anhydrase inhibitor, improved prophylactic efficacy in 44% of the treatment-resistant bipolar disorder patients (74). One of the common adverse effects of acetazolamide is weight loss. Adjunctive topiramate and zonisamide have been used in the treatment of bipolar disorder. They are also strong carbonic anhydrase inhibitors and caused persistent weight loss in obese patients (75–79). Of the three anticonvulsants, the efficacy of topiramate in the treatment of bipolar disorder has been demonstrated by many studies (77). Topiramate also caused substantial weight loss in patients with bipolar disorders in those studies (77).

Inhibition of carbonic anhydrase limits the access of CO_2-fixing enzymes pyruvate carboxylase and acetyl-CoA carboxylase to bicarbonate and decreases pyruvate carboxylase-mediated anaplerosis in peripheral tissues (**Figure 1**). It has been demonstrated that carbonic anhydrase activity is required for optimal activity of hepatic pyruvate carboxylase in *de novo* synthesis of both fatty acids and non-saponifiable lipids (80). Carbonic anhydrase inhibitors are known to inhibit *de novo* lipogenesis and gluconeogenesis in liver (81, 82). In cultured adipocytes inhibition of carbonic anhydrase by sulfonamides also significantly decreased lipogenesis (83).

Carbonic anhydrase in brain is predominantly expressed in glial and choroid cells (84–88). The much lesser carbonic anhydrase expression in neurons facilitates rapid removal of CO_2, which is generated by the highly active neuronal oxidative metabolism, from neurons by free diffusion. This distinct distribution of intracellular carbonic anhydrase in brain leads to the conversion of CO_2 into bicarbonate primarily in astrocytes, rendering astrocytes as sinks of CO_2 (89). In cultured astrocytes inhibition of carbonic anhydrase caused a large reduction in pyruvate carboxylase-mediated CO_2 fixation by limiting the supply of bicarbonate to pyruvate carboxylase, resulting in reduced TCA cycle intermediate levels and reduced glutamate production (90). Since in the central nervous system astrocytes are the predominant site for both CO_2 hydration catalyzed by carbonic anhydrase and pyruvate carboxylation catalyzed by pyruvate carboxylase (**Figure 1**), limitation of *de novo* synthesis of glutamate by carbonic anhydrase inhibition may play a significant role in the antiepileptic properties and mood stabilization effects of anticonvulsants that are also carbonic anhydrase inhibitors. Therefore, both mechanistic and clinical studies of carbonic anhydrase inhibition support the proposed connections among bipolar disorder, obesity and pyruvate carboxylase-mediated anaplerosis.

Pyruvate Carboxylase-Mediated Anaplerosis Is a Potential Therapeutic Target for Bipolar Disorder and Comorbid Obesity

A single pyruvate carboxylase isoform is expressed in humans and found in mitochondria only (91). Pyruvate carboxylase expression is regulated by complex mechanisms and many exogenous and endogenous modulators (80, 91). Many modulators of pyruvate carboxylase pass the blood brain barrier (80) therefore may affect pyruvate carboxylase activities in both peripheral tissues and the brain. Obesity and diabetes are associated with increased pyruvate carboxylase expression in liver and adipose tissue (69). In contrast, insulin inhibits pyruvate carboxylase expression in liver (80). In the central nervous system increased pyruvate supply was found to augment pyruvate carboxylase-mediated anaplerotic flux and glutamate production in astrocytes (15).

Previous studies have shown that pharmacological inhibition of pyruvate carboxylase by phenylacetic acid markedly reduced hepatic gluconeogenesis in rats (92). The effects of pyruvate carboxylase on glucose and lipid metabolism in several rodent models were measured using a specific antisense oligonucleotide to selectively decrease pyruvate carboxylase expression in liver and adipose tissue (71). The specific antisense oligonucleotide approach significantly reduced plasma glucose concentrations and endogenous glucose production. In a high-fat-diet rat model, pyruvate carboxylase antisense oligonucleotide reduced adiposity, plasma lipid levels, and hepatic steatosis (71). It has been suggested that pyruvate carboxylase is a potential therapeutic target for several diseases associated with obesity (71, 92). As the experimental findings discussed here indicate that elevated pyruvate carboxylation may be a significant part of the pathogenesis of glutamatergic hyperactivity and comorbid obesity in bipolar disorder, designing inhibitors of pyruvate carboxylase to pharmacologically modulate pyruvate carboxylase-mediated anaplerosis may be a useful new treatment strategy for bipolar disorder and comorbid obesity.

CONCLUSIONS

Increased pyruvate carboxylase-mediated anaplerosis can readily explain the elevated glutamate or glutamate + glutamine levels in brain in bipolar disorder observed by *in vivo* ^{1}H MRS. Multiple independent lines of evidence suggest that increased pyruvate carboxylase-mediated anaplerosis is a common mechanism underlying glutamatergic hyperactivity and the significant positive association between bipolar disorder and obesity. As the increased prevalence of obesity in bipolar disorder is associated with illness severity and poor treatment outcomes development of preventive and treatment strategies targeting pyruvate carboxylase-mediated anaplerosis may be warranted.

AUTHOR CONTRIBUTIONS

JS performed literature analysis and proposed the hypothesis. JT performed literature search. JS and JT wrote the paper. Both authors reviewed the manuscript and agreed on its final version.

FUNDING

This work was supported by the Intramural Research Program of National Institute of Mental Health, NIH (ZIA MH002803).

REFERENCES

1. Cataldo AM, McPhie DL, Lange NT, Punzell S, Elmiligy S, Ye NZ, et al. Abnormalities in mitochondrial structure in cells from patients with bipolar disorder. *Am J Pathol.* (2010) 177:575–85. doi: 10.2353/ajpath.2010.081068
2. Konradi C, Eaton M, MacDonald ML, Walsh J, Benes FM, Stephan Heckers S. Molecular evidence for mitochondrial dysfunction in bipolar disorder. *Arch Gen Psychiatry.* (2004) 61:301–8. doi: 10.1001/archpsyc.61.3.300
3. Mertens J, Wang QW, Kim Y, Yu DX, Pham S, Yang B, et al. Differential responses to lithium in hyperexcitable neurons from patients with bipolar disorder. *Nature.* (2015) 527:95–9. doi: 10.1038/nature15526
4. Regenold WT, Phatak P, Marano CM, Sassan A, Conley RR, Kling MA. Elevated cerebrospinal fluid lactate concentrations in patients with bipolar disorder and schizophrenia: implications for the mitochondrial dysfunction hypothesis. *Biol Psychiatry.* (2009) 65:489–94. doi: 10.1016/j.biopsych.2008.11.010
5. Yoshimi N, Futamura T, Bergen SE, Iwayama Y, Ishima T, Sellgren C, et al. Cerebrospinal fluid metabolomics identifies a key role of isocitrate dehydrogenase in bipolar disorder: evidence in support of mitochondrial dysfunction hypothesis. *Mol Psychiatry.* (2016) 21:1504–10. doi: 10.1038/mp.2015.217
6. Kato T, Kato N. Mitochondrial dysfunction in bipolar disorder. *Bipolar Disord.* (2000) 2:180–90. doi: 10.1034/j.1399-5618.2000.020305.x
7. Dager SR, Friedman SD, Parow A, Demopulos C, Stoll AL, Lyoo IK, et al. Brain metabolic alterations in medication-free patients with bipolar disorder. *Arch Gen Psychiatry.* (2004) 61:450–8. doi: 10.1001/archpsyc.61.5.450
8. Stork C, Renshaw PF. Mitochondrial dysfunction in bipolar disorder: evidence from magnetic resonance spectroscopy research. *Mol Psychiatry.* (2005) 10:900–19. doi: 10.1038/sj.mp.4001711
9. Frey BN, Stanley JA, Nery FG, Serap Monkul E, Nicoletti MA, Chen HH, et al. Abnormal cellular energy and phospholipid metabolism in the left dorsolateral prefrontal cortex of medication-free individuals with bipolar disorder: an *in vivo* 1H MRS study. *Bipolar Disord.* (2007) 9:119–27. doi: 10.1111/j.1399-5618.2007.00454.x
10. Chu WJ, DelBello MP, Jarvis KB, Norris MM, Kim M-J, Weber W, et al. Magnetic resonance spectroscopy imaging of lactate in patients with bipolar disorder. *Psychiatry Res.* (2013) 213:230–4. doi: 10.1016/j.pscychresns.2013.03.004
11. Gigante AD, Bond DJ, Lafer B, Lam RW, Young LT, Yatham LN. Brain glutamate levels measured by magnetic resonance spectroscopy in patients with bipolar disorder: a meta-analysis. *Bipolar Disord.* (2012) 14:478–87. doi: 10.1111/j.1399-5618.2012.01033.x
12. Sibson NR, Dhankhar A, Mason GF, Behar KL, Rothman DL, Shulman RG. *In vivo* ^{13}C NMR measurements of cerebral glutamine synthesis as evidence for glutamate-glutamine cycling. *Proc Natl Acad Sci USA.* (1997) 94:2699–704. doi: 10.1073/pnas.94.6.2699
13. Rothman DL, de Graaf RA, Hyder F, Mason GF, Behar KL, De Feyter HM. *In vivo* ^{13}C and ^{1}H-[^{13}C] MRS studies of neuroenergetics and neurotransmitter cycling, applications to neurological and psychiatric disease and brain cancer. *NMR Biomed.* (2019) 32:e4172. *doi: 10.1002/nbm.4172*
14. Pardo B, Contreras L, Satrustegui J. *De novo* synthesis of glial glutamate and glutamine in young mice requires aspartate provided by the neuronal mitochondrial aspartate-glutamate carrier aralar/AGC1. *Front Endocrinol.* (2013) 4:149. doi: 10.3389/fendo.2013.00149
15. Gamberino WC, Berkich DA, Lynch CJ, Xu B, LaNoue KF. Role of pyruvate carboxylase in facilitation of synthesis of glutamate and glutamine in cultured astrocytes. *J Neurochem.* (1997) 69:2312–25. doi: 10.1046/j.1471-4159.1997.69062312.x
16. Sibson NR, Mason GF, Shen J, Cline GW, Herskovits AZ, Wall JE, et al. *In vivo* (13)C NMR measurement of neurotransmitter glutamate cycling, anaplerosis and TCA cycle flux in rat brain during [2-13C]glucose infusion. *J Neurochem.* (2001) 76:975–89. doi: 10.1046/j.1471-4159.2001.00074.x
17. Hertz L. Intercellular metabolic compartmentation in the brain: past, present and future. *Neurochem Int.* (2004) 45:285–96. doi: 10.1016/j.neuint.2003.08.016
18. Lapidot A, Gopher A. Cerebral metabolic compartmentation. Estimation of glucose flux via pyruvate carboxylase/pyruvate dehydrogenase by ^{13}C NMR isotopomer analysis of D-[U-^{13}C]glucose metabolites. *J Biol Chem.* (1994) 269:27198–208. doi: 10.1016/S0021-9258(18)46969-4
19. Shank RP, Bennett GS, Freytag SO, Campbell GL. Pyruvate carboxylase: an astrocyte-specific enzyme implicated in the replenishment of amino acid neurotransmitter pools. *Brain Res.* (1985) 329:364–7. doi: 10.1016/0006-8993(85)90552-9
20. Shen J. Modeling the glutamate-glutamine neurotransmitter cycle. *Front Neuroenergetics.* (2013) 5:1. doi: 10.3389/fnene.2013.00001
21. Waagepetersen HS, Qu H, Schousboe A, Sonnewald U. Elucidation of the quantitative significance of pyruvate carboxylation in cultured cerebellar neurons and astrocytes. *J Neurosci Res.* (2001) 66:763–70. doi: 10.1002/jnr.10061
22. Hertz L. Functional interactions between neurons and astrocytes I. Turnover and metabolism of putative amino acid transmitters. *Prog Neurobiol.* (1979) 13:277–323. doi: 10.1016/0301-0082(79)90018-2
23. Rothman DL, Sibson NR, Hyder F, Shen J, Behar KL, Shulman RG. *In vivo* nuclear magnetic resonance spectroscopy studies of the relationship between the glutamate-glutamine neurotransmitter cycle and functional neuroenergetics. *Philos Trans R Soc Lond B.* (1999) 354:1165–77. doi: 10.1098/rstb.1999.0472
24. Shen J. ^{13}C MRS studies of alterations in glutamate neurotransmission. *Biol Psychiatry.* (2006) 59:883–7. doi: 10.1016/j.biopsych.2005.07.042
25. Cesar M, Hamprecht B. Immunocytochemical examination of neural rat and mouse primary cultures using monoclonal antibodies raised against pyruvate carboxylase. *J Neurochem.* (1995) 64:2312–8. doi: 10.1046/j.1471-4159.1995.64052312.x
26. Martinez-Hernandez A, Bell KP, Norenberg MD. Glutamine synthetase: glial localization in brain. *Science.* (1977) 195:1356–8. doi: 10.1126/science.14400
27. Grill V, Bjorkman O, Gutniak M, Lindqvist M. Brain uptake and release of amino acids in nondiabetic and insulin-dependent diabetic subjects: important role of glutamine release for nitrogen balance. *Metabolism.* (1992) 41:28–32. doi: 10.1016/0026-0495(92)90186-E
28. Lapidus KA, Soleimani L, Murrough JW. Novel glutamatergic drugs for the treatment of mood disorders. *Neuropsychiatr Dis Treat.* (2013) 9:1101–12. doi: 10.2147/NDT.S36689
29. Du J, Wei Y, Liu L, Wang Y, Khairova R, Blumenthal R, et al. A kinesin signaling complex mediates the ability of GSK-3beta to affect mood-associated behaviors. *Proc Natl Acad Sci USA.* (2010) 107:11573–8. doi: 10.1073/pnas.0913138107
30. Rao JS, Harry GJ, Rapoport SI, Kim HW. Increased excitotoxicity and neuroinflammatory markers in postmortem frontal cortex from bipolar disorder patients. *Mol Psychiatry.* (2009) 15:384–92. doi: 10.1038/mp.2009.47
31. Eastwood SL, Harrison PJ. Markers of glutamate synaptic transmission and plasticity are increased in the anterior cingulate cortex in bipolar disorder. *Biol Psychiatry.* (2010) 67:1010–6. doi: 10.1016/j.biopsych.2009.12.004
32. Jun C, Choi Y, Lim SM, Bae S, Hong YS, Kim JE, et al. Disturbance of the glutamatergic system in mood disorders. *Exp. Neurobiol.* (2014) 23:28–35. doi: 10.5607/en.2014.23.1.28
33. Levinson AJ, Young LT, Fitzgerald PB, Daskalakis ZJ. Cortical inhibitory dysfunction in bipolar disorder: a study using transcranial magnetic stimulation. *J Clin Psychopharmacol.* (2007) 27:493–7. doi: 10.1097/jcp.0b013e31814ce524
34. Fayed N, Andres E, Viguera L, Modrego PJ, Garcia-Campayo J. Higher glutamate+glutamine and reduction of N-acetylaspartate in posterior cingulate according to age range in patients with cognitive impairment and/or pain. *Acad Radiol.* (2014) 21:1211–7. doi: 10.1016/j.acra.2014.04.009
35. Pietrancosta N, Djibo M, Daumas S, El Mestikawy S, Erickson JD. Molecular, structural, functional, and pharmacological sites for vesicular glutamate transporter regulation. *Mol. Neurobiol.* (2020) 30:1–25. doi: 10.1007/s12035-020-01912-7
36. Yüksel C, Öngür D. Magnetic resonance spectroscopy studies of glutamate-related abnormalities in mood disorders. *Biol Psychiatry.* (2010) 68:785–94. doi: 10.1016/j.biopsych.2010.06.016
37. Rathman SC, Eisenschenk S, McMahon RJ. The abundance and function of biotin-dependent enzymes are reduced in rats chronically administered carbamazepine. *J Nutr.* (2002) 132:3405–10. doi: 10.1093/jn/132.11.3405
38. Rathman SC, Gregory JF, McMahon RJ. Pharmacological biotin supplementation maintains biotin status and function in rats

administered dietary carbamazepine. *J Nutr.* (2003) 133:2857–62. doi: 10.1093/jn/133.9.2857
39. Marin-Valencia I, Roe CR, Pascual JM. Pyruvate carboxylase deficiency: mechanisms, mimics and anaplerosis. *Mol Genet Metab.* (2010) 101:9–17. doi: 10.1016/j.ymgme.2010.05.004
40. Maurer IC, Schippel P, Volz HP. Lithium-induced enhancement of mitochondrial oxidative phosphorylation in human brain tissue. *Bipolar Disord.* (2009) 11:515–22. doi: 10.1111/j.1399-5618.2009.00729.x
41. Kim DJ, Lyoo IK, Yoon SJ, Choi T, Lee B, Kim JE, et al. Clinical response of quetiapine in rapid cycling manic bipolar patients and lactate level changes in proton magnetic resonance spectroscopy. *Prog Neuropsychopharmacol Biol Psychiatry.* (2007) 31:1182–8. doi: 10.1016/j.pnpbp.2007.04.009
42. Ehrlich A, Schubert F, Pehrs C, Gallinat J. Alterations of cerebral glutamate in the euthymic state of patients with bipolar disorder. *Psychiatry Res.* (2015) 233:73–80. doi: 10.1016/j.pscychresns.2015.05.010
43. Chitty KM, Lagopoulos J, Lee RS, Hickie IB, Hermens DF. A systematic review and meta-analysis of proton magnetic resonance spectroscopy and mismatch negativity in bipolar disorder. *Eur Neuropsychopharmacol.* (2013) 23:1348–63. doi: 10.1016/j.euroneuro.2013.07.007
44. Kim Y, Santos R, Gage FH, Marchetto MC. Molecular mechanisms of bipolar disorder: progress made and future challenges. *Front Cell Neurosci.* (2017) 11:30. doi: 10.3389/fncel.2017.00030
45. Friedman S, Dager S, Parow A, Hirashima F, Demopulos C, Stoll AL, et al. Lithium and valproic acid treatment effects on brain chemistry in bipolar disorder. *Biol Psychiatry.* (2004) 56:340–48. doi: 10.1016/j.biopsych.2004.06.012
46. Hoekstra R, Fekkes D, Loonen A, Pepplinkhuizen L, Tuinier S, Verhoeven W. Bipolar mania and plasma amino acids: increased levels of glycine. *Eur Neuropsychopharmacol.* (2006) 16:71–7. doi: 10.1016/j.euroneuro.2005.06.003
47. Hashimoto K, Sawa A, Iyo M. Increased levels of glutamate in brains from patients with mood disorders. *Biol Psychiatry.* (2007) 62:1310–6. doi: 10.1016/j.biopsych.2007.03.017
48. Lan MJ, McLoughlin GA, Griffin JL, Tsang TM, Huang JTJ, Yuan P, et al. Metabonomic analysis identifies molecular changes associated with the pathophysiology and drug treatment of bipolar disorder. *Mol. Psychiatry.* (2009) 14:269–79. doi: 10.1038/sj.mp.4002130
49. Yoshimi N, Futamura T, Kakumoto K, Salehi AM, Sellgren CM, HolménLarsson J, et al. Blood metabolomics analysis identifies abnormalities in the citric acid cycle, urea cycle and amino acid metabolism in bipolar disorder. *BBA Clin.* (2016) 5:151–8. doi: 10.1016/j.bbacli.2016.03.008
50. Fox PT, Raichle ME. Focal physiological uncoupling of cerebral blood flow and oxidative metabolism during somatosensory stimulation in human subjects. *Proc Natl Acad Sci USA.* (1986) 83:1140–4. doi: 10.1073/pnas.83.4.1140
51. Maddock RJ, Casazza GA, Buonocore MH, Tanase C. Vigorous exercise increases brain lactate and Glx (glutamate + glutamine): a dynamic 1H-MRS study. *NeuroImage.* (2011) 57:1324–30. doi: 10.1016/j.neuroimage.2011.05.048
52. Duncan NW, Wiebking C, Northoff G. Associations of regional GABA and glutamate with intrinsic and extrinsic neural activity in humans—a review of multimodal imaging studies. *Neurosci Biobehav Rev.* (2014) 47:36–52. doi: 10.1016/j.neubiorev.2014.07.016
53. Sonnay S, Duarte JMN, Just N, Gruetter R. Compartmentalised energy metabolism supporting glutamatergic neurotransmission in response to increased activity in the rat cerebral cortex: A ^{13}C MRS study *in vivo* at 14.1 T. *J Cereb Blood Flow Metab.* (2016) 6:928–40. doi: 10.1177/0271678X16629482
54. Sonnay S, Poirot J, Just N, Clerc AC, Gruetter R. Astrocytic and neuronal oxidative metabolism are coupled to the rate of glutamate–glutamine cycle in the tree shrew visual cortex. *Glia.* (2018) 66:477–91. doi: 10.1002/glia.23259
55. Ketter TA, George MS, Kimbrell TA, Benson BE, Post RM. Functional brain imaging, limbic function, and affective disorders. *Neuroscientist.* (1996) 2:55–65. doi: 10.1177/107385849600200113
56. Ketter TA, Kimbrell TA, George MS, Dunn RT, Speer AM, Benson BE, et al. Effects of mood and subtype on cerebral glucose metabolism in treatment-resistant bipolar disorder. *Biol Psychiatry.* (2001) 49:97–109. doi: 10.1016/S0006-3223(00)00975-6
57. Soares JC, Mann JJ. The functional neuroanatomy of mood disorders. *J Psychiatr Res.* (1997) 31:393–432. doi: 10.1016/S0022-3956(97)00016-2
58. Baxter LR Jr, Schwartz JM, Phelps ME, Mazziotta JC, Guze BH, Selin CE, et al. Ruction of prefrontal cortex glucose metabolism common to three types of depression. *Arch Gen Psychiatry.* (1989) 46:243–50. doi: 10.1001/archpsyc.1989.01810030049007
59. Maina G, Salvi V, Vitalucci A, D'Ambrosio *V*, Bogetto F. Prevalence and correlates of overweight in drug-naive patients with bipolar disorder. *J Affect Disord.* (2008) 110:149–55. doi: 10.1016/j.jad.2007.12.233
60. Goldstein BI, Liu SM, Zivkovic N, Schaffer A, Chien LC, Blanco C. The burden of obesity among adults with bipolar disorder in the United States. *Bipolar Disord.* (2011) 13:387–95. doi: 10.1111/j.1399-5618.2011.00932.x
61. McElroy SL, Keck PE Jr. Obesity in bipolar disorder: an overview. *Curr Psychiatry Rep.* (2012) 14:650–8. doi: 10.1007/s11920-012-0313-8
62. Zhao Z, Okusaga OO, Quevedo J, Soares JC, Teixeira AL. The potential association between obesity and bipolar disorder: a meta-analysis. *J Affect Disord.* (2016) 202:120–3. doi: 10.1016/j.jad.2016.05.059
63. Weiner M, Warren L, Fiedorowicz JG. Cardiovascular morbidity and mortality in bipolar disorder. *Ann Clin Psychiatry.* (2011) 23:40–7.
64. Taylor VH, McIntyre RS, Remington G, Levitan RD, Stonehocker B, Sharma AM. Beyond pharmacotherapy: understanding the links between obesity and chronic mental illness. *Can J Psychiatry.* (2012) 57:5–12. doi: 10.1177/070674371205700103
65. Kuswanto CN, Sum MY, Yang GL, Nowinski WL, McIntyre RS, Sim K. Increased body mass index makes an impact on brain white-matter integrity in adults with remitted first-episode mania. *Psychol Med.* (2014) 44:533–41. doi: 10.1017/S0033291713000858
66. Bond DJ, da Silveira LE, MacMillan EL, Torres IJ, Lang DJ, Su W, et al. Diagnosis and body mass index effects on hippocampal volumes and neurochemistry in bipolar disorder. *Transl Psychiatry.* (2017) 7:e1071. doi: 10.1038/tp.2017.42
67. Bond DJ, da Silveira LE, MacMillan EL, Torres IJ, Lang DJ, Su W, et al. Relationship between body mass index and hippocampal glutamate/glutamine in bipolar disorder. *Br J Psychiatry.* (2016) 208:146–52. doi: 10.1192/bjp.bp.115.163360
68. Mackall JC, Lane MD. Role of pyruvate carboxylase in fatty acid synthesis: alterations during preadipocyte differentiation. *Biochem Biophys Res Commun.* (1977) 79:720–5. doi: 10.1016/0006-291X(77)91171-8
69. Lynch CJ, McCall KM, Billingsley ML, Bohlen LM, Hreniuk SP, Martin LF, et al. Pyruvate carboxylase in genetic obesity. *Am J Physiol.* (1992) 262:E608–18. doi: 10.1152/ajpendo.1992.262.5.E608
70. Attwood PA, Keech DB. Pyruvate carboxylase. *Curr Top Cell Regul.* (1984) 23:1–55. doi: 10.1016/B978-0-12-152823-2.50005-2
71. Kumashiro N, Beddow SA, Vatner DF, Majumdar SK, Cantley JL, Guebre-Egziabher F, et al. Targeting pyruvate carboxylase reduces gluconeogenesis and adiposity and improves insulin resistance. *Diabetes.* (2013) 62:2183–94. doi: 10.2337/db12-1311
72. Lee P, Leong W, Tan T, Lim M, Han W, Radda GK. *In vivo* hyperpolarized carbon-13 magnetic resonance spectroscopy reveals increased pyruvate carboxylase flux in an insulin-resistant mouse model. *Hepatol.* (2013) 57:515–24. doi: 10.1002/hep.26028
73. Lizarbre B, Cherix A, Duarte JMN, Cardinaux JR, Gruetter R. High-fat diet consumption alters energy metabolism in the mouse hypothalamus. *Intl J Obesity.* (2019) 43:1295–304. doi: 10.1038/s41366-018-0224-9
74. Hayes SG. Acetazolamide in bipolar affective disorders. *Ann Clin Psychiatry.* (1994) 6:91–8. doi: 10.3109/10401239409148987
75. McElroy SL, Suppes T, Keck PE Jr., Frye MA, Denicoff KD, Altshuler LL, et al. Open-label adjunctive topiramate in the treatment of bipolar disorders. *Biol Psychiatry.* (2000) 47:1025–33. doi: 10.1016/S0006-3223(99)00316-9
76. Gadde KM, Kopping MF, Wagner HR, Yonish GM, Allison DB, Bray GA. Zonisamide for weight reduction in obese adults a 1-year randomized controlled trial. *Arch Intern Med.* (2012) 172:1557–64. doi: 10.1001/2013.jamainternmed.99
77. Grootens KP, Meijer A, Hartong EG, Doornbos B, Bakker PR, Al Hadithy A, et al. Weight changes associated with antiepileptic mood stabilizers in the treatment of bipolar disorder. *Eur J Clin Pharmacol.* (2018) 74:1485–9. doi: 10.1007/s00228-018-2517-2
78. Gupta S, Masand PS, Frank BL, Lockwood KL, Keller PL. Topiramate in bipolar and schizoaffective disorders: weight loss and efficacy, *Prim Care Companion J. Clin. Psychiatry.* (2000) 2:96–100. doi: 10.4088/PCC.v02n0304

79. Dodgson SJ, Shank RP, Maryanoff BE. Topiramate as an inhibitor of carbonic anhydrase isoenzymes. *Epilepsia.* (2000) 41(Suppl. 1):S35–9. doi: 10.1111/j.1528-1157.2000.tb02169.x
80. Jitrapakdee S, St Maurice M, Rayment I, Cleland, Wallace WW, Attwood JC, et al. Structure, mechanism and regulation of pyruvate carboxylase. *Biochem J.* (2008) 413:369–87. doi: 10.1042/BJ20080709
81. Dodgson SJ, Forster RE. Inhibition of CA V decreases glucose synthesis from pyruvate. *Arch Biochem Biophys.* (1986) 251:198–204. doi: 10.1016/0003-9861(86)90066-4
82. Lynch CJ, Fox H, Hazcn SA, Stanley BA, Dodgson SJ, LaNouc KF. The role of hepatic carbonic anhydrase in de novo lipogenesis. *Biochem J.* (1995) 310:197–202. doi: 10.1042/bj3100197
83. Hazen SA, Waheed A, Sly WS, LaNoue KF, Lynch CJ. Differentiation-dependent expression of CA V and the role of carbonic anhydrase isozymes in pyruvate carboxylation in adipocytes. *FASEB J.* (1996) 10:481–90. doi: 10.1096/fasebj.10.4.8647347
84. Giacobini E. A cytochemical study of the localization of carbonic anhydrase in the nervous system. *J Neurochem.* (1962) 9:169–77. doi: 10.1111/j.1471-4159.1962.tb11859.x
85. Sapirstein VS, Strocchi P, Gilbert JM. Properties and function of brain carbonic anhydrase. *Ann NY Acad Sci.* (1984) 429:481–93. doi: 10.1111/j.1749-6632.1984.tb12375.x
86. Kumpulainen T. Immunohistochemical localization of human carbonic anhydrase isozymes. *Ann NY Acad Sci.* (1984) 429:359–67. doi: 10.1111/j.1749-6632.1984.tb12360.x
87. Cammer W. Immunostaining of carbamoylphosphate synthase II and fatty acid synthase in glial cells in rat, mouse, and hamster brains suggests roles for carbonic anhydrase in biosynthetic processes. *Neurosci Lett.* (1991) 129:247–50. doi: 10.1016/0304-3940(91)90472-6
88. Agnati LF, Tinner B, Staines WA, Vaananen K, Fuxe K. On the cellular localization and distribution of carbonic anhydrase II immunoreactivity in the rat brain. *Brain Res.* (1995) 676:10–24. doi: 10.1016/0006-8993(95)00026-M
89. Deitmer JW. Strategies for metabolic exchange between glial cells and neurons. *Respir Physiol.* (2001) 129:71– 81. doi: 10.1016/S0034-5687(01)00283-3
90. Hazen SA, Waheed A, Sly WS, LaNoue KF, Lynch CJ. Effect of carbonic anhydrase inhibition and acetoacetate on anaplerotic pyruvate carboxylase activity in cultured rat astrocytes. *Dev Neurosci.* (1997) 19:162–71. doi: 10.1159/000111202
91. Gray LR, Tompkins SC, Taylor EB. Regulation of pyruvate metabolism and human disease. *Cell Mol Life Sci.* (2014) 71:2577–604. doi: 10.1007/s00018-013-1539-2
92. Bahl JJ, Matsuda M, DeFronzo RA, Bressler R. *In vitro* and *in vivo* suppression of gluconeogenesis by inhibition of pyruvate carboxylase. *Biochem Pharmacol.* (1997) 53:67–74. doi: 10.1016/S0006-2952(96)00660-0

Conflict of Interest: The authors declare that the research was conducted in the absence of any commercial or financial relationships that could be construed as a potential conflict of interest.

frontiers in Psychiatry

SYSTEMATIC REVIEW
published: 08 March 2021
doi: 10.3389/fpsyt.2021.644315

GABA, Glutamate and Neural Activity: A Systematic Review With Meta-Analysis of Multimodal ^{1}H-MRS-fMRI Studies

Amanda Kiemes[1], Cathy Davies[1], Matthew J. Kempton[1,2], Paulina B. Lukow[1], Carly Bennallick[2], James M. Stone[3] and Gemma Modinos[1,2,4]*

[1] Psychosis Studies Department, Institute of Psychiatry, Psychology and Neuroscience, King's College London, London, United Kingdom, [2] Department of Neuroimaging, Institute of Psychiatry, Psychology and Neuroscience, King's College London, London, United Kingdom, [3] Brighton and Sussex Medical School, University of Sussex & University of Brighton, Brighton, United Kingdom, [4] Medical Research Centre Centre for Neurodevelopmental Disorders, King's College London, London, United Kingdom

OPEN ACCESS

Edited by:
Richard Edden, Johns Hopkins University, United States

Reviewed by:
Yoshihiko Matsumoto, Yamagata University, Japan
Maria Grazia Morgese, University of Foggia, Italy

***Correspondence:**
Amanda Kiemes
amanda.s.kiemes@kcl.ac.uk

Specialty section:
This article was submitted to Molecular Psychiatry, a section of the journal Frontiers in Psychiatry

Received: *20 December 2020*
Accepted: *15 February 2021*
Published: *08 March 2021*

Citation:
Kiemes A, Davies C, Kempton MJ, Lukow PB, Bennallick C, Stone JM and Modinos G (2021) GABA, Glutamate and Neural Activity: A Systematic Review With Meta-Analysis of Multimodal ^{1}H-MRS-fMRI Studies. Front. Psychiatry 12:644315. doi: 10.3389/fpsyt.2021.644315

Multimodal neuroimaging studies combining proton magnetic resonance spectroscopy (^{1}H-MRS) to quantify GABA and/or glutamate concentrations and functional magnetic resonance imaging (fMRI) to measure brain activity non-invasively have advanced understanding of how neurochemistry and neurophysiology may be related at a macroscopic level. The present study aimed to perform a systematic review and meta-analysis of available studies examining the relationship between ^{1}H-MRS glutamate and/or GABA levels and task-related fMRI signal in the healthy brain. Ovid (Medline, Embase, and PsycINFO) and Pubmed databases were systematically searched to identify articles published until December 2019. The primary outcome of interest was the association between resting levels of glutamate or GABA and task-related fMRI. Fifty-five papers were identified for inclusion in the systematic review. A further 22 studies were entered into four separate meta-analyses. These meta-analyses found evidence of significant negative associations between local GABA levels and (a) fMRI activation to visual tasks in the occipital lobe, and (b) activation to emotion processing in the medial prefrontal cortex (mPFC)/anterior cingulate cortex (ACC). However, there was no significant association between mPFC/ACC glutamate levels and fMRI activation to cognitive control tasks or to emotional processing, with the relationship to emotion processing related neural activity narrowly missing significance. Moreover, our systematic review also found converging evidence of negative associations between GABA levels and local brain activity, and positive associations between glutamate levels and distal brain activity, outside of the ^{1}H-MRS sampling region. Albeit less consistently, additional relationships between GABA levels and distal brain activity and between glutamate levels and local brain activity were found. It remains unclear if the absence of effects for other brain regions and other cognitive-emotional domains reflects study heterogeneity or potential confounding effects of age, sex, or other unknown factors. Advances in

^{1}H-MRS methodology as well as in the integration of ^{1}H-MRS readouts with other imaging modalities for indexing neural activity hold great potential to reveal key aspects of the pathophysiology of mental health disorders involving aberrant interactions between neurochemistry and neurophysiology such as schizophrenia.

Keywords: glutamate, GABA, magnetic resonance spectroscopy, fMRI, multimodal neuroimaging

INTRODUCTION

Excitation-inhibition balance plays a major role in determining neural activity (1). At a microscopic level, the influence of the brain's major excitatory and inhibitory neurotransmitters [glutamate and γ-aminobutyric acid (GABA)], on neural activity has been studied in detail [see Isaacson and Scanziani (1), Lauritzen et al. (2)]. At a macroscopic level, this investigation has been achieved through the development and optimisation of neuroimaging techniques enabling quantification of GABA and glutamate concentrations via proton magnetic resonance spectroscopy (^{1}H-MRS), and of neural activation via measurement of blood oxygen level dependent (BOLD) signal with functional magnetic resonance imaging (fMRI). BOLD signal has been linked to local field potentials of dendritic origins, implying the signal is likely to reflect incoming input (3), thereby being closely linked to, and affected by, neurotransmission. However, the relationship between neurotransmitter levels and task-related neural activity remains unclear.

A previous narrative review by Duncan et al. (4) sought to address this question with a comprehensive overview of studies using imaging techniques such as magnetoencephalography, electroencephalography, fMRI, positron emission tomography and ^{1}H-MRS, as well as behavioural measures as proxies for neural activity and pharmaceutical manipulations of neurotransmitter levels. The authors reported that GABA levels were related to reduced positive BOLD response or reduced negative BOLD response (NBR) within the same brain region, while glutamate levels were more commonly related to inter-regional neural responses. The number of publications using multimodal fMRI and ^{1}H-MRS techniques has more than doubled since this review was published, and studies using this type of multimodal combination are expected to keep increasing in the future due to the ease of collecting both types of data within a single scanning session. More recent reports outside of the previous review include studies on regions of interest that had previously been examined too infrequently to permit meta-analysis, providing important insights into the nature of neurochemistry-neurophysiology associations in a variety of brain regions and task domains.

The present study aims to address these issues by conducting a systematic review and meta-analysis of ^{1}H-MRS and task-based fMRI studies in the healthy brain. We then meta-analyse homogeneous studies based on the location of ^{1}H-MRS voxel placement and fMRI paradigm. Finally, we discuss the findings in light of abnormalities in these relationships in psychiatric populations, such as schizophrenia patients, and their potential implications on brain processes in psychiatric disorders.

METHODS

Systematic searches were performed on Pubmed and Ovid (Medline, Embase and PsycINFO) databases from database inception to 4 December 2019. Search strategies for the individual databases included the terms "functional magnetic resonance imaging" AND "magnetic resonance spectroscopy" AND ("GABA" OR "glutamate") (for full search syntax see **Supplementary Table 1**). We included studies that used ^{1}H-MRS to measure GABA, glutamate or Glx (combined glutamate and glutamine) metabolite levels to test associations with task-related fMRI activation. Eligible study designs included observational studies, cohort studies, case-control studies, cross-sectional studies, or experimental studies (for full eligibility criteria see **Supplementary Table 2**). The population of interest were healthy human participants, or healthy human control groups from case-control studies. Interventional studies were excluded, unless those studies conducted and reported the outcome of interest analysis with baseline measures. Studies assessing only changes in metabolite levels before, during and after a task together with BOLD activation were not included as they do not investigate the relationship between resting-state neurotransmitter levels and neural activity modulated by stimuli. Two reviewers (AK and CB) independently screened search result titles and abstracts of papers for eligibility according to the inclusion and exclusion criteria. All potentially eligible studies were screened full-text for inclusion. Reference lists of eligible studies were hand-searched for further relevant articles.

Two independent reviewers (AK and PBL) extracted data using a standardised template datasheet. The primary outcomes extracted were the metabolite type, ^{1}H-MRS metabolite sampling region, fMRI task paradigm, neural activation region, and relationship between metabolite and neural activity. Studies investigating the relationship between ^{1}H-MRS GABA or glutamate and task-related BOLD signal performed analyses in one or both of two different ways: by including metabolite levels as a covariate in a regression, or by extracting the percentage of BOLD signal change (%SC) from a region of interest (ROI) and using correlation analysis with the metabolite levels. Both types of analysis methods were included in this review. Regressions either covered the whole-brain or a predetermined ROI such as the ^{1}H-MRS voxel, an anatomical ROI or a mask derived from an activation cluster. Correlation analyses used %SC extracted from sources such as the peak voxel within or mean activation across an activated cluster, an anatomically defined ROI, or the ^{1}H-MRS voxel. Additional extracted data for the systematic review included the statistical significance of the relationship, covariates tested in the analysis, sample size, age and sex characteristics of

the sample, scanner strength, ^{1}H-MRS sequence, and reference metabolite. In cases where no statistical significance value was reported for the relationship itself and only Pearson's *r* correlation coefficients were reported [e.g., (5)], *p*-values were calculated through conversion of r values to test statistic *t* with the formula

$$t = \frac{r}{\sqrt{((1 - r^2)/(df))}}$$

The *p*-value was then derived using the sampling distribution of Student's *t*. This calculation of the *p*-value was used to ascertain the significance of the correlation coefficient.

Some studies verified their main findings (^{1}H-MRS x fMRI response) in the following ways: (1) substituting the metabolite levels from their primary region of interest with those from a different, control sampling region; (2) substituting the fMRI response from their primary task paradigm with that from a control task; (3) substituting the fMRI response from their primary region of interest with that from a control region during the same task. Such control analyses may be found in **Supplementary Tables 7, 8**. A formal quality assessment was not conducted due to a lack of standard quality assessment for such types of studies. Imaging and study design parameters were, however, collected (**Supplementary Tables 3–6, 9**). Review findings [see **Figure 1** for PRISMA flowchart (6)] are presented according to the brain region from which metabolite levels were sampled.

Meta-Analysis

Studies were further subdivided by ^{1}H-MRS voxel location, task domain and fMRI activation foci. For quantitative analysis, *r* correlation coefficients, *t*-values, *z*-values and sample sizes were compiled. Although the recommended minimum number of studies for meta-analysis is two, this does not apply to random-effect models (7), which the MetaNSUE method employs (8). Additionally, given the likelihood of a non-statistically significant unreported effect, the minimum number of comparable studies was set at a more conservative number of ≥4. Meta-analysis was conducted using the MetaNSUE package for R (8), where r correlation coefficients were converted into effect sizes for a meta-analytic pooled effect size. This tool was used due to its ability to impute results for unreported correlation coefficients, which can often be the case when correlations are non-significant. Authors were contacted for unreported *r* correlation coefficients. However, in the case of unreported *r* correlation coefficients, the number of imputations was kept at the package's default of 500 imputations per study.

In instances where studies reported both *t*- and *z*-values of significantly correlated clusters from a regression analysis, *t*- and *z*-values were converted into *r* correlation coefficients as follows:

1. *Z*-score to *p*-value calculation: $P(Z \leq z) = \int_{-\infty}^{z} \frac{1}{\sqrt{2\pi}} e^{\frac{-u^2}{2}} du$
2. *P*-value to student *t*-value: using Microsoft Excel's TINV function
3. *T*-value to *r* correlation coefficient conversion: $r = \sqrt{t^2/(t^2 + df)}$

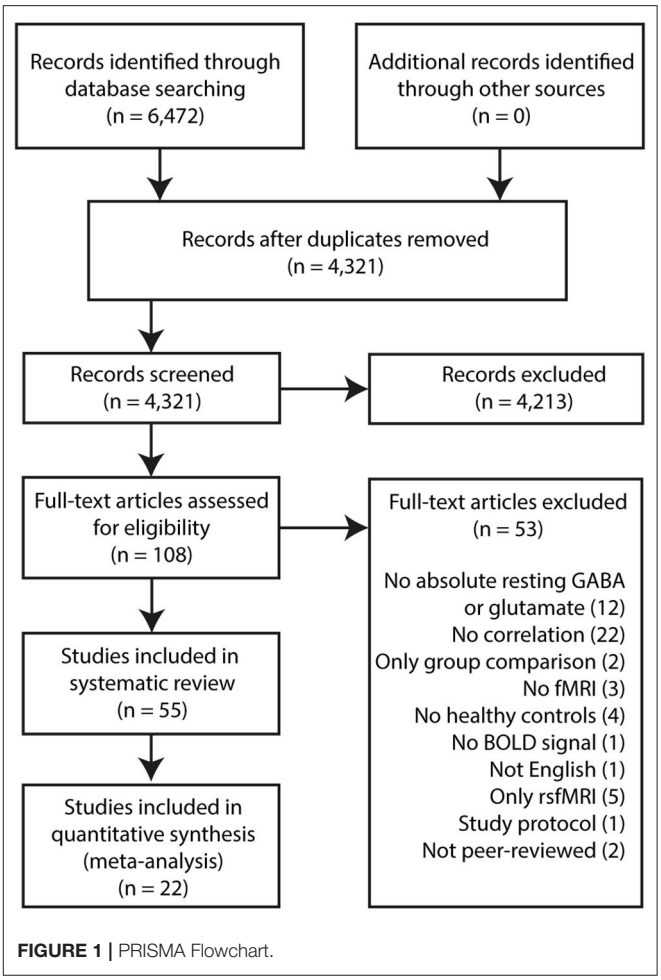

FIGURE 1 | PRISMA Flowchart.

Significance was determined using two-tailed 95% confidence intervals. Further sensitivity analyses are detailed in the **Supplementary Material**.

RESULTS

Systematic Review of Associations With GABA and Glutamate Concentrations

Occipital Cortex

^{1}H-MRS studies sampling GABA levels from the occipital lobe have been largely homogeneous (**Table 1**): using visual fMRI tasks and focusing only on co-localised neural activity. The first few studies in this domain found negative associations between occipital lobe GABA levels and local BOLD response to visual stimuli (9–12, 14). Muthukumaraswamy et al. (11) not only found a negative association to BOLD response amplitude, but also a positive correlation with BOLD response width. However, this relationship to response amplitude was not replicated in subsequent studies (13, 15, 16, 18). Harris et al. (15) investigated this relationship empirically, and combined their result with prior studies in a meta-analysis, where they found no evidence

TABLE 1 | Occipital lobe ^{1}H-MRS studies.

Authors	*n* Male % Age M(SD)	System Sequence	Reference	fMRI task/stimuli	Relationship	Covariates
GABA						
Medial occipital cortex/Visual cortex						
Muthukumaraswamy et al. (9)	12 100 34.8	3T MEGA-PRESS	/Wt	Stationary visual grating	Visual stimuli (–) GABA	–
Donahue et al. (10)	12 50 30 (4)	3T MEGA-PRESS	/Cr	Flashing checkerboard	Visual stimuli (–) GABA+	–
Muthukumaraswamy et al. (11)	14 100 24.2 (2.4)	3T MEGA-PRESS	/Wt	Stationary visual grating	Visual stimuli (–) GABA	–
Violante et al. (12)	26 38.5 13.1 (2.9)	3T MEGA-PRESS	/Cr	Stationary visual grating	Visual stimuli (–) GABA	–
Bridge et al. (13)	13 0 30 (6)	3T SPECIAL	/tCr	Visual stimuli (diffuse light/flickering checkerboard)	Visual stimuli (#) GABA	–
Bednarík et al. (14)	12 46.7 33 (13)	7T Semi-LASER	/Wt	Flickering checkerboard	Visual stimuli (–) GABA	–
Harris et al. (15)	18 38.9 27.8 (4.0)	3T MEGA-PRESS	/Wt, /Cr	Stationary visual grating	Visual stimuli (#) GABA+	–
Duncan et al. (16)	31 0.65 23.0 (3.1)	3T MEGA-PRESS	/Wt	Stationary visual grating	Visual stimuli (#) GABA-	–
Wijtenburg et al. (17)	18 50 36.2 (16)	3T MEGA-PRESS	/Wt	Visual plasticity task	Visual plasticity (+) GABA- Baseline visual stimuli (–) GABA-	age
Costigan et al. (18)	40 30 22.1 (2.1)	3T MEGA-PRESS	/Wt	Odd-one-out task	Scene viewing (#) GABA	–
Schallmo et al. (19)	22 12 24 (3.6)	3T MEGA-PRESS	/Wt	Visual spatial suppression task	Visual spatial suppression (#) GABA+	–
Lateral occipital cortex/visual motion complex						
Schallmo et al. (19)	22 12 24 (3.6)	3T MEGA-PRESS	/Wt	Visual spatial suppression task	Visual spatial suppression (#) GABA+	–
Glutamate						
Medial occipital lobe/Visual cortex						
Muthukumaraswamy et al. (9)	12 100 34.8	3T MEGA-PRESS	/Wt	Stationary visual grating	Visual stimuli (#) Glx	–
Violante et al. (12)	26 38.5 13.1 (2.9)	3T MEGA-PRESS	/Cr	Moving visual grating	Visual stimuli (#) Glx	–
Bridge et al. (13)	13 0 30 (6)	3T SPECIAL	/tCr	Visual stimuli (light/flickering checkerboard)	Visual stimuli (#) Glu	–
Bednarík et al. (14)	12 46.7 33 (13)	7T Semi-LASER	/Wt	Flickering checkerboard	Visual stimuli (#) Glu	–
Ip et al. (20)	13 50 28.7 (5.6)	7T Semi-Laser	/Wt	Flickering checkerboard	Visual stimuli (#) Glu	–

(Continued)

TABLE 1 | Continued

Authors	*n* Male % Age M(SD)	System Sequence	Reference	fMRI task/stimuli	Relationship	Covariates
Wijtenburg et al. (17)	18 50 36.2 (16)	PR-STEAM		Visual plasticity task	Visual plasticity (+) Glu	Age
Schallmo et al. (21)	22 40.9 24 (3.7)	MEGA-PRESS	/Wt	Visual spatial suppression task	Visual spatial suppression (#) Glx	–
Lateral occipital cortex/visual motion complex						
Schallmo et al. (21)	22 40.9 24 (3.7)	MEGA-PRESS	/Wt	Visual spatial suppression task	Visual spatial suppression (+) Glx	–

Wt, Water; Cr, Creatine; (+) positive association; (#) no association; (–) negative association; GABA+, GABA+macromolecules; Glx, Glutamate + Glutamine.

for a significant association between the two measures. More recently, Duncan et al. (16) attempted to address this issue using improved methodology. A MEGA-PRESS sequence that was adapted to suppress macromolecule signal was used so that both GABA+ and GABA– were measured from the occipital lobe. Although their empirical study found no significant relationship, Duncan et al. (16) added their results to the five studies meta-analysed in Harris et al. (15)—using the same Hunter-Schmidt method employed by the *metafor* R package—and found evidence in favour of a negative relationship between GABA and BOLD, regardless of macromolecule suppression.

Neural activity in the occipital lobe was also studied in different contexts beyond simple visual perception. Wijtenburg (17) found a positive correlation between GABA and neural activation difference before and after a high frequency visual stimulus, an effect thought to reflect visual plasticity. In agreement with other studies, when only baseline visual stimulation-related activation was used, a negative correlation was found with GABA levels. However, results for this analysis were not published and only mentioned in the discussion. Schallmo et al. (19) used a spatial suppression paradigm where participants had to indicate the direction of moving gratings with varying contrasts. No correlations between GABA levels in the early visual cortex and the more laterally located visual motion complex and neural response in the same regions were found.

Glutamate levels repeatedly did not show a relationship to co-localised neural activity in studies of the occipital lobe (9, 12–14, 20, 21). Some of these studies utilised the same sequence to measure GABA and glutamate levels simultaneously (9, 12–14, 21). Two studies reporting a relationship with GABA levels found no association between neural activity and co-localised Glx (9, 12). Wijtenburg et al. (17) found a relationship between glutamate levels and an activation contrast comparing neural response before and after a high frequency visual stimulus. This relationship was also a positive one, similar to what had been observed with GABA levels. However, in this case, the association between glutamate levels and activity related to baseline visual stimuli was not reported. Finally, within the visual motion complex glutamate levels were positively correlated with neural response during motion perception in a spatial suppression paradigm (21).

Sensorimotor Cortex

Studies sampling metabolite levels in the sensorimotor cortex and adjacent areas (**Table 2**) mostly utilised a simple paradigm, in this case some form of finger-tapping task. In multiple studies, no significant associations were found between sensorimotor cortex GABA levels and local neural activity (15, 22–24). Using the same finger-tapping task, Draper et al. (24) also found no correlation between GABA levels in a supplementary motor area and BOLD %SC. Only one study (25), using a visually cued reaction time task, indicated a negative relationship between BOLD and GABA concentrations in the sensorimotor cortex. This same study was the only one to look at neural activity with glutamate levels in the sensorimotor cortex area and found no correlated activation clusters in a whole-brain regression.

Anterior Cingulate Cortex/Medial Prefrontal Cortex

GABA Concentrations in the Anterior Cingulate Cortex/Medial Prefrontal Cortex

Due to the involvement of the anterior cingulate cortex (ACC) and medial prefrontal cortex (mPFC) in different processes such as emotion, attention and cognition (26), various task contexts have been used (**Table 3**). Many studies investigated NBR within this region, due to the close coupling between the ACC/mPFC and the default mode network (DMN). Four studies investigating GABA levels in the mPFC/ACC region found a positive relationship with regional NBR, i.e., a negative relationship with neural activity (27, 30, 31, 35). Northoff et al. (35) found that during conditions that produced little NBR compared to rest, this negative relationship between GABA levels and neural activity was not apparent. In agreement with these findings, using facial expressions Stan et al. (29) observed that mPFC GABA+ concentration was negatively correlated with subgenual ACC (sgACC) fMRI response to sadness. However, neural activity during other emotion categories—happy, fear, or anger—was not correlated with GABA+ concentrations. When using an emotion processing task, Levar et al. (32) only found a negative correlation with GABA+ levels when contrasting

TABLE 2 | Sensorimotor cortex ^{1}H-MRS studies.

Authors	*n* Male % Age M(SD)	System Sequence	Reference	fMRI task/stimuli	Relationship	Covariates
GABA						
Sensorimotor cortex						
Bhattacharyya et al. (22) Bhattacharyya et al. (23)	9 11.1 38.3 (14.1)	3T MEGA-PRESS	Absolute	Bilateral finger tapping	Finger tapping (#) GABA	–
Draper et al. (24)	14 92.86 15.8 (3.2)	7T STEAM	/NAA	Finger-thumb opposition task	Finger tapping (#) GABA	–
Harris et al. (15)	18 38.9 27.8 (4.0)	3T MEGA-PRESS	/Wt, /Cr	Finger tapping	Finger tapping (#) GABA+	–
Stagg et al. (25)	12 50 23	3T MEGA-PRESS	/NAA	Visually cued reaction time task	Movement performance (–) GABA	–
Supplementary motor area						
Draper et al. (24)	14 92.86 15.8 (3.2)	7T STEAM	/NAA	Finger-thumb opposition task	Finger tapping (#) GABA	–
Glutamate						
Primary motor cortex						
Stagg et al. (25)	12 50 23	3T MEGA-PRESS	/NAA	Visually cued reaction time task	Motor performance (#) Glx	–

Wt, Water; Cr, Creatine; NAA, N-acetylaspartate; (+) positive association; (#) no association; (–) negative association; GABA+, GABA + macromolecule; Glx, glutamate + glutamine.

neural activity during negative emotional stimuli with response to positive emotional stimuli. Other studies failed to find negative correlations between regional GABA concentrations and neural activity, or positive relationships with NBR, during cognitive control tasks (34, 36), a verbal working memory task (5), a reward-guided decision-making task (28), and a fear conditioning, extinction, and extinction retrieval task (33).

Correlations between GABA levels and distal neural activity were also found in some of these studies (32–34). Neural activity related to fear recovery in the amygdala was positively correlated with dACC GABA levels, while neural activity related to late phases of fear extinction in the right amygdala, cerebellum, middle cingulate gyrus, and right insula were negatively correlated with GABA (33). Levar et al. (32), using non-facial picture stimuli, found that dACC GABA concentrations correlated positively with activity in the left amygdala during positive emotion, negative emotion, all emotion and positive over negative emotion. Right amygdala activity related to positive emotion was also positively correlated with dACC GABA levels. Activity of the right superior frontal gyrus during negative pictures was negatively correlated with GABA levels. BOLD signal related to all picture conditions was positively correlated with GABA levels in the left and right hippocampi. ACC GABA concentrations were negatively associated with cognitive control-related BOLD signal in two clusters. The first was localised mainly to the left parietal cortex, spanning the postcentral gyrus, inferior parietal lobe, supramarginal gyrus, angular gyrus, and the middle occipital lobe. The second cluster was found mainly in the left dlPFC, including regions within the middle frontal lobe, inferior frontal lobe, precentral gyrus, superior temporal lobe, rolandic operculum, and postcentral gyrus.

Glutamate Concentrations in the Anterior Cingulate Cortex/Medial Prefrontal Cortex

Twenty-one studies sampled glutamate levels within the mPFC/ACC regions and investigated its relationship to neural activity within the same region as well as in other brain regions. Of those, 15 studies did not find an association between mPFC/ACC glutamate levels and local activation. These studies used a variety of tasks encompassing: emotion (31, 32), cognitive control (34, 37–40), working memory (5, 27), reward (28, 41), intero- and exteroceptive awareness (30), aversion (42), and a verbal fluency task (43). Nonetheless, other studies did find relation between glutamate concentration and regional neural activity. Stan et al. (29) found mPFC glutamate levels were correlated with pregenual ACC (pgACC) response to anger, but not with regional activity during viewing of other emotional categories. Using an empathy task, Duncan et al. (44) sought to investigate the relationship between pgACC glutamate levels and neural activity in the task-activated supragenual ACC, as well as between supragenual ACC glutamate with pgACC activity. A whole-brain regression with pgACC Glx levels showed a relationship to empathy-related BOLD in the supragenual ACC (a cluster overlapping with the supragenual ACC ^{1}H-MRS voxel). supragenual ACC Glx levels, however, were not associated with pgACC activation during the empathy task. ACC glutamate

TABLE 3 | Medial prefrontal cortex/anterior cingulate cortex ^{1}H-MRS GABA studies.

Authors	n Male % Age M(SD)	System Sequence	Reference	fMRI task/stimuli	Relationship	Covariates
Medial prefrontal cortex/pregenual anterior cingulate cortex						
Chen et al. (27)	19 31.6 24 (2)	3T MEGA-PRESS	/Wt	Working memory task (Sternberg item recognition paradigm)	High cognitive load NBR (+) GABA Low cognitive load NBR (#) GABA	Sex, co-localised Glu
Jocham et al. (28)	25 H 100 –	3T MEGA-PRESS	/Cr	Reward-guided decision-making task	Value difference BOLD signal (+) GABA Raw BOLD signal (#) GABA	–
Stan et al. (29)	16 50 22.42 (2.9)	3T MEGA-PRESS	/Cr	Implicit emotion processing and regulation task	Subgenual, pregenual, dorsal ACC: happy/fear/anger (#) GABA+ subgenual ACC: Sad (–) GABA+	–
Wiebking et al. (30)	9H 55.6 21.11 (2.9)	3T MEGA-PRESS	/NAA	Intero- & exteroceptive awareness paradigm	Interoceptive awareness NBR (#) GABA Exteroceptive awareness NBR (+) GABA	GM
Witt et al. (5)	20 40 17.4 (2.6)	3T MEGA-PRESS	/Wt	Verbal working memory task	Encoding NBR (#) GABA+ Recognition NBR (#) GABA+	–
Walter et al. (31)	24 25 34.6	3T 2D-JPRESS	/Cr	Emotional stimulation paradigm	Emotional stimulation NBR (+) GABA	Age
Dorsal anterior cingulate cortex						
Levar et al. (32)	70 100 21.8 (3.2)	3T MEGA-PRESS	/Cr	Fear conditioning and extinction task + extinction retrieval	Fear retrieval (#) GABA+ R amygdala: Fear retrieval (+) GABA+ R amygdala, cerebellum, middle cingulate gyrus, R insula: Late fear extinction (–) GABA+ Fear extinction retrieval (#) GABA+	–
Levar et al. (33)	68 100 21.7 (3.2)	3T MEGA-PRESS	/Cr	Emotion processing task	Hippocampus, cerebellum, R fusiform gyrus: all stimuli (+) GABA+ L amygdala: emotion > neutral (+) GABA+ Amygdala, L PCu, L middle occipital gyrus: positive > neutral (+) GABA+ L amygdala: negative > neutral (+) GABA+ R superior frontal gyrus: negative > neutral (–) GABA+ dACC, superior frontal gyrus, R MCC: negative > positive (–) GABA+	–
Overbeek et al. (34)	21 76.2 23.5 (4.5)	7T STEAM	/Wt	Stroop task	L postcentral gyrus, L inferior parietal lobe, L supramarginal gyrus, L angular gyrus, L middle occipital lobe, L middle frontal lobe, L inferior frontal lobe, L precentral gyrus, L superior temporal lobe, L rolandic operculum, L postcentral gyrus: cognitive control (–) GABA	Glu, Gln, WM

(Continued)

TABLE 3 | Continued

Authors	n Male % Age M(SD)	System Sequence	Reference	fMRI task/stimuli	Relationship	Covariates
Anterior cingulate cortex						
Northoff et al. (35)	12 33.3 33.8	3T JD-PRESS	/Cr	Emotion processing task	All pictures NBR (+) GABA Picture judgement NBR (+) GABA Picture viewing NBR (#) GABA	Glx, GSH
Wang et al. (36)	25 0 27.5 (6.6)	3T MEGA-PRESS		Cognitive control hybrid task	Fronto-striatal regions: cognitive control (#) GABA	–

Wt, Water; Cr, Creatine; NAA, N-acetylaspartic acid; NBR, negative BOLD response; (+) positive association; (#) no association; (–) negative association; GABA+, GABA + macromolecule; Glx, glutamate+glutamine; GSH, glutathione; PCu, Precuneus; dACC, dorsal anterior cingulate cortex; MCC, middle cingulate cortex; WM, white mater volume fraction within ^{1}H-MRS voxel; GM, grey mater volume fraction within ^{1}H-MRS voxel; /, OR. Neural activity is co-localised with the ^{1}H-MRS sampling region unless otherwise specified in the relationship column [i.e., Region: task related activity (+/#–) GABA/Glu/Glx].

levels were also studied in conjunction to neural activity during a salience processing task using emotional and erotic pictures (45). Activation in the sgACC related to unexpectedness of emotional pictures displayed a negative correlation with glutamate. Dissecting this association, the authors found that a positive relationship between glutamate and expected emotional picture viewing drove this finding. In a separate study, Cadena et al. (46) scanned a control group twice with a 6-week interval (46). ACC Glx levels were positively correlated with ACC activation during cognitive control at the baseline scan, a relationship that was not observed at the second scanning session 6 weeks later. Enzi et al. (47) sampled Glx concentrations from the pgACC, where they found a partial positive correlation to NBR during anticipation of reward and of no outcome. Through further investigation, the authors found that Glx concentrations were correlated to the rest condition and hypothesised that this relationship was largely driving the relationship between glutamate levels and deactivation during reward anticipation.

In terms of associations between glutamate levels and neural activity outside of the ^{1}H-MRS region, three studies reported positive correlations with neural activity outside of the ACC/mPFC. Duncan et al. (42) found mPFC glutamate levels were correlated positively with sensorimotor cortex and left insula activation during the anticipation of aversion. In a different study, Duncan et al. (44) showed, through whole-brain regression with Glx levels in the pgACC, a significant correlation with empathy-related activation in the left precuneus, bilateral amygdala and putamen, right superior frontal gyrus and right supramarginal gyrus. Cadena et al. (46) observed a correlation with cognitive control-related activation within the insula, hippocampus, inferior parietal lobule and precuneus. Notably, the findings in the bilateral insula and left inferior parietal lobule were replicated in the sample 6 weeks later. Interestingly, one study observed different correlations depending on task load. Falkenberg et al. (39) found three activation clusters where there was a significant interaction between glutamate levels and the parameters of a cognitive control task: five auditory intensity difference conditions and the instruction of which ear to pay attention to. *Post-hoc* tests showed that in individuals with lower levels of glutamate, neural response was higher during high cognitive control conditions, i.e., when attention was directed towards the less salient stimulus, whereas in individuals with high levels of glutamate, neural activity was higher during low cognitive control conditions. Four studies found negative correlations between glutamate or Glx levels and neural activity outside of the ACC/mPFC. Overbeek et al. (34) observed ACC glutamate levels were positively associated with NBR in a cluster spanning from the PCC and precuneus to the occipital cortex and cerebellum. Von During et al. (45) also found that ACC glutamate levels were positively associated with NBR in the PCC, with higher glutamate predicting higher deactivation of this area in response to a variety of stimuli. Neural activity in a variety of other regions were also negatively correlated with ACC glutamate levels in this study (see **Table 4**). One study investigated ACC glutamate levels with cognitive control-related activation within the striatum only, to which a negative relationship was found in a composite group of ADHD patients, unaffected siblings and healthy controls (48). Similarly, Gleich et al. (41) found a negative relationship with ventral striatum activation in adolescents but not in adults.

Dorsolateral Prefrontal Cortex

All studies sampling GABA or glutamate levels from the dorsolateral prefrontal cortex (dlPFC) used a working memory fMRI task (**Table 5**). Only one study, comparing children and adolescents with sport-related injuries not involving the head and with no history of concussion, to a group of concussed individuals, found a significant positive correlation between dlPFC GABA levels and local activation (50). Two studies did not find a relationship (15, 27). Similarly, three studies that investigated glutamate levels also found no relationships to regional neural activity (27, 51, 52).

Temporal Lobe

Within studies of the temporal lobe (**Table 6**), the auditory cortex, anterior temporal lobe and hippocampus were sampled

TABLE 4 | Medial prefrontal cortex/anterior cingulate cortex ^{1}H-MRS glutamate studies.

Authors	*n* Male % Age M(SD)	System Sequence	Reference	fMRI task/stimuli	Relationship	Covariates
Medial prefrontal cortex/rostral anterior cingulate cortex						
Brennan et al. (40)	28 46.4 32.4 (12.1)	3T 2D-JPRESS	/Cr	Emotional Stroop task	Cognitive control (#) Glu	Age, sex
Chen et al. (27)	19 31.6 24 (2)	3T Semi-LASER	/Wt	Working memory task (Sternberg item recognition paradigm)	Working memory (#) Glu	Sex, co-localised GABA
Duncan et al. (44)	13 30.8 31.6 (–)	3T PRESS	/Cr	Empathy task	supragenual ACC/MCC, L precuneus, amygdala/putamen, R superior temporal gyrus, R supramarginal gyrus: empathy (+) Glx	–
Duncan et al. (42)	12 50 23 (3.5)	3T MEGA-PRESS	/NAA	Aversion Task	Sensorimotor cortex, L posterior supramarginal gyrus, L Insula/operculum: anticipation of certain aversion (+^) Glu Anticipation of certain aversion (#) Glx Anticipation of uncertain aversion (#) Glu/Glx	-
Enzi et al. (47)	19 52.6 29.6 (–)	3T PRESS	/Cr	Modified monetary incentive delay task	Fixation (+) Glx Reward anticipation (#) Glx Punishment anticipation (#) Glx No outcome (#) Glx Fixation > Reward anticipation (+) Glx Fixation > Punishment anticipation (#) Glx Fixation > No outcome (+) Glx	Age
Jocham et al. (28)	25 100 –	3T MEGA-PRESS	/Cr	Reward-guided decision-making task	Value difference BOLD signal (+) Glu Raw BOLD signal (#) Glu	–
Naaijen et al. (48)	32 68.7 22 (3.8), 21 (4.9), 20.7 (2.5)	3T PRESS	/Cr	Stroop task	Striatum: cognitive control (–) Glu	–
Stan et al. (29)	18 50 22.79 (3.04)	3T PRESS	/Cr	Implicit emotion processing and regulation task	Happy/sad/fear (#) pre-task Glu Anger (+) pre-task Glu	Age
					Happy/fear/anger/sad (#) post-task Glu	Co-localised GABA+
Walter et al. (31)	24 25 34.6	3T 2D-JPRESS	/Cr	Emotional stimulation paradigm	Emotional stimulation NBR (#) Glu	Age
Wiebking et al. (30)	18 50 17.4 (2.6)	3T MEGA-PRESS	/NAA	Intero- & exteroceptive awareness paradigm	Interoceptive/exteroceptive awareness NBR (#) Glx	GM
Witt et al. (5)	20 40 17.7 (2.6)	3T MEGA-PRESS	/Wt	Verbal working memory task	Encoding/recognition (#) Glx	–
Dorsal anterior cingulate cortex						
Cadena et al. (46)	20 70 33.0 (9.3)	3T PRESS	/Cr	Stroop task (baseline)	Insula, R ACC: cognitive control (+) Glx Hippocampus, inferior parietal, precuneus: cognitive control (+) Glx	–

(Continued)

TABLE 4 | Continued

Authors	*n* Male % Age M(SD)	System Sequence	Reference	fMRI task/stimuli	Relationship	Covariates
	19			Stroop task (6 weeks later)	Insula: cognitive control (+) Glx L inferior parietal: cognitive control (+) Glx	–
Duncan et al. (44)	13 30.8 31.6 (–)	3T PRESS	/Cr	Empathy task	Empathy (#) Glx	–
Levar et al. (33)	68 100 21.7 (3.2)	3T MEGA-PRESS	/Cr	Emotion processing task	All stimuli/positive>neutral/negative>neutral/negative>positive//emotion>neutral (#) Glx	–
Overbeek et al. (34)	21 76.2 23.5 (4.5)	7T STEAM	/Wt	Stroop task	PCu, calcarine sulcus, cuneus, lingual gyrus, middle cingulum, posterior cingulum, cerebellum: cognitive control (–) Glu	GABA, Gln, WM
Reid et al. (38)	18 61.1 36.8 (12.0)	3T PRESS	/Cr	Stroop task	Cognitive control (#) Glx	–
Von During et al. (45)	27 65 29.8 (7.8)	7T STEAM	/Cr	Salience processing	R PCC/PCu, R occipital, cerebellum: all picture viewing (–) Glu PCC: erotic picture viewing/unexpected emotional picture viewing (–) Glu Emotional picture viewing (#) Glu R vStr, sgACC: expected emotional picture viewing (+) Glu	Age, sex, GM
Yücel et al. (37)	24 54.2 29.6 (6.5)	3T PRESS	Absolute	Multi-source interference task	Cognitive control (#) Glx	
Anterior cingulate cortex						
Falkenberg et al. (39)	40 50 m 25.0 (3.6), f 26.0 (4.0)	3T PRESS	/Cr	Dichotic listening task	ACC: cognitive control (#) Glu Basal ganglia, R orbitofrontal cortex, L inferior parietal lobe: high cognitive control (–) Glu Basal ganglia, R orbitofrontal cortex, L inferior parietal lobe: low cognitive control (+) Glu	
Fusar-Poli et al. (43)	17 58.8 25.5 (3.6)	3T PRESS		Verbal fluency task	Verbal fluency (#) Glu	–
Gleich et al. (41)	26 adults 46.2 26.1 (4.4)	3T PRESS		Virtual slot machine	vStr,ACC: win>loss (#) Glu	–
	28 adolescents 53.6 14.4 (0.6)	3T PRESS		Virtual slot machine	vStr: win>loss (–) Glu ACC: win>loss (#) Glu	–
Modinos et al. (49)	21 low schizotypy 57.1 27.0 (5.6)	3T PRESS	/Wt	Emotional viewing task	Emotional viewing (#) Glu	–

(Continued)

TABLE 4 | Continued

Authors	*n* Male % Age M(SD)	System Sequence	Reference	fMRI task/stimuli	Relationship	Covariates
Northoff et al. (35)	12 33.3 33.8	3T 2D-JPRESS	/Cr	Emotion processing task	Emotion processing (#) Glx	–

Wt, Water; Cr, Creatine; NAA, N-acetylaspartic acid; NBR, negative BOLD response; ACC, anterior cingulate cortex; MCC, middle cingulate cortex; vStr, ventral striatum; PCu, precuneus; PCC, posterior cingulate cortex; sgACC, subgenual ACC; Glx, glutamate+glutamine; WM, white mater volume fraction within ^{1}H-MRS voxel; GM, grey mater volume fraction within ^{1}H-MRS voxel; ^, uncorrected finding; (+) positive association; (#) no association; (–) negative association; /= OR. Neural activity is co-localised with the ^{1}H-MRS sampling region unless otherwise specified in the relationship column [i.e., Region: task related activity (+/#/–) GABA/Glu/Glx].

TABLE 5 | Dorsolateral prefrontal cortex ^{1}H-MRS studies.

Authors	n Male % Age M(SD)	System Sequence	Reference	fMRI task/stimuli	Relationship	Covariates
GABA						
Harris et al. (15)	18 38.9 27.8 (4.0)	3T MEGA-PRESS	/Wt, /Cr	Working memory task (n-back task)	Working memory (#) GABA+	–
Friedman et al. (50)	10 50 15.2 (1.2)	3T MEGA-PRESS	/tCr	Working memory task (1-back task)	Working memory (+) GABA	–
Chen et al. (27)	19 31.6 24 (2)	3T MEGA-PRESS	/Wt	Working memory task (Sternberg item recognition paradigm)	Working memory (#) GABA	Sex, co-localised Glu
Glutamate						
Moon and Joeng (51)	18 61.1 30.7 (7.5)	3T PRESS	/Cr	Working memory task with face distractors	Working memory (#) Glx	
Chen et al. (27)	19 31.6 24 (2)	3T Semi-LASER	/Wt	Working memory task (Sternberg item recognition paradigm)	Working memory (#) Glu	Sex, co-localised GABA
Kaminski et al. (52)	35 H 82.9 34.3 (8.5)	3T PRESS	/Wt	Working memory task (n-back task)	Working memory (#) Glu	age

Wt, water; Cr, creatine; tCr, creatine+phosphocreatine; Glx, glutamate+glutamine.

for metabolites and fMRI tasks were largely based on the respective functions of the ^{1}H-MRS sampling regions. Two studies found a negative relationship between GABA levels and local activation during thought retrieval and though suppression (54) and during semantic processing (53). However, Harris et al. (15) found no relationship between fMRI activity in the auditory cortex and local GABA levels.

Unlike GABA, hippocampal glutamate levels were not found to be correlated with local activity in several studies (43, 55, 56). Glutamate levels were, however, positively correlated to neural activity outside of the hippocampus: parahippocampus (55), inferior frontal gyrus (56) and ventral striatum (57).

Insula

Three studies (30, 58, 59) measured relationships between metabolites and neural activity in this region (**Table 7**). Lipp et al. (58) reported a negative association between GABA concentration and insula neural activity only to animal picture stimuli, while pictures of other categories did not elicit such association. Interestingly, another study (30) identified a positive correlation between GABA levels and neural response to interoceptive awareness. Insula GABA levels were additionally correlated to distal neural activity: positively to activation in the amgydala and ventral striatum (58), and negatively to activation in the medial cingulate cortex and supplementary motor area (59). Meanwhile, glutamate levels did not correlate with neural activity in the insular cortex (30, 59).

Posterior Cingulate Cortex/Precuneus

Two studies investigated both GABA and glutamate levels within the posterior cingulate cortex (PCC)/precuneus (PCu) region (18, 60) (**Table 8**) that typically deactivate during some cognitive tasks but activate putatively during processing of scenes to support autobiographical memory and imagined events (61). Deactivation of the PCC/PCu region as well as the entire DMN

TABLE 6 | Temporal lobe ^{1}H-MRS studies.

Authors	*n* Male % Age M(SD)	System Sequence	Reference	fMRI task/stimuli	Relationship	Covariates
GABA						
Auditory cortex						
Harris et al. (15)	18 38.9 27.8 (4.0)	3T MEGA-PRESS	/Wt, /Cr	Auditory white noise	Auditory stimuli (#) GABA+	–
Anterior temporal lobe						
Jung et al. (53)	20 35 23 (4)	3T MEGA-PRESS	/NAA	Semantic association task	Semantic association (–) GABA	GM
Hippocampus						
Schmitz et al. (54)	30 23.3 24.7 (4.3)	3T 2D-JPRESS	/Cr	Thought suppression task (Think/No think task)	Think (–) GABA No-Think (–) GABA	Sex, GM, co-localised Glu, dlPFC GABA, functional control signal
Glutamate						
Anterior temporal lobe						
Jung et al. (53)	20 35 23 (4)	3T MEGA-PRESS	/NAA	Semantic association task	Semantic association (#) Glx	GM
Hippocampus						
Fusar-Poli et al. (43)	17 58.8 25.5 (3.6)	3T PRESS		Verbal fluency task	Verbal fluency (#) Glu	–
Valli et al. (55)	14 42.9 25.62 (3.7)	3T PRESS	/Wt	Episodic memory task	Parahippocampus: Memory encoding (+) Glu	–
Hutcheson et al. (56)	28 60.7 35.6 (11.1)	3T PRESS	/Cr	Episodic memory task	Encoding/Retrieval (#) Glx IFG: retrieval (+) Glx	–
Bossong et al. (57)	19 52.6 25.8 (5.6)	3T PRESS		Monetary incentive delay task	vStr: Reward anticipation (+) Glx	–

Wt, water; Cr, creatine; GABA+, GABA+macromolecules; NAA, N-acetylaspartic acid; GM, grey matter volume fraction within ^{1}H-MRS voxel; dlPFC, dorsolateral prefrontal cortex; IFG, inferior frontal gyrus; vStr, ventral striatum; /, OR. Neural activity is co-localised with the ^{1}H-MRS sampling region unless otherwise specified in the relationship column (i.e. Region: task related activity (+/#/–) GABA/Glu/Glx).

(including the mPFC, PCC/PCu, and bilateral parahippocampus) during a working memory task were investigated separately in relation to glutamate and GABA concentrations (60). Regression models showed that as glutamate increased NBR decreased (i.e., weaker deactivation). Conversely, GABA levels were positively correlated with NBR for all but the lowest cognitive load (1-back condition), i.e., as GABA levels increased, deactivation increased, in both the model with PCC/PCu deactivation and DMN deactivation as dependent variable. In contrast, when using a perceptual discrimination task, Costigan et al. (18) found no association between PCC/PCu activation and local Glx and GABA+ levels.

Other Regions

A few studies have sampled GABA and glutamate levels from less frequently inspected regions combined with neural activity (**Table 9**). Harris et al. (15) found no relationship between activation related to eye saccades and GABA levels in the frontal eye field. Two studies sampled glutamate from the thalamus, both using a verbal fluency task. Fusar-Poli et al. (43) found no significant effects, while Allen et al. (64) found significant correlations with activation in the right superior frontal gyrus/sulcus and the right cingulate sulcus. Two studies found a positive correlation between Glx levels and local activity in two different brain regions: the substantia nigra (63) and the dorsal striatum (62).

Meta-Analysis of Associations With GABA Concentrations

Within the studies sampling GABA, two groups of more than four studies emerged: occipital lobe GABA levels in combination with a visual task, and ACC GABA levels in

TABLE 7 | Insula ^{1}H-MRS studies.

Authors	n Male % Age M(SD)	System Sequence	Reference	fMRI task/stimuli	Relationship	Covariates
GABA						
Wiebking et al. (30)	15 66.7 23.13 (4.58)	3T MEGA-PRESS	/NAA	Intero- & exteroceptive awareness paradigm	Interoceptive awareness (+) GABA Exteroceptive awareness (#) GABA	GM
Lipp et al. (58)	29 0	3T MEGA-PRESS	/Wt	Fear inducing paradigm	Whole brain: negative>neutral (#) GABA+ L amygdala, insula, vStr, frontal cortex: spiders>animals (+) GABA+ Neutral/negative/spiders (#) GABA+ Animals (–) GABA+	–
Cleve et al. (59)	27 100 24.9 (3.0)	3T MEGA-PRESS	/tCr	Pain stimulation	Pain perception (#) GABA+ MCC/SMA: pain perception (–) GABA+	–
Glutamate						
Wiebking et al. (30)	15 66.7 23.13 (4.58)	3T MEGA-PRESS	/NAA	Intero- & exteroceptive awareness paradigm	Interoceptive awareness (#) Glu/Glx Exteroceptive awareness (#) Glu/Glx	GM
Cleve et al. (59)	27 100 24.9 (3.0)	3T MEGA-PRESS	/tCr	Pain stimulation	Pain perception (#) Glx	–

Wt, water; NAA, N-acetylaspartic acid; tCr, creatine+phosphocreatine; GM, grey matter volume within ^{1}H-MRS voxel; vStr, ventral Striatum; MCC, middle cingulate cortex; SMA, supplementary motor area; /, OR. Neural activity is co-localised with the ^{1}H-MRS sampling region unless otherwise specified in the relationship column (i.e. Region: task related activity (+/#/–) GABA/Glu/Glx).

combination with emotion processing tasks. For illustration of the voxel positions of each study per meta-analysis see **Figures 2**, **3**.

For the relationship between GABA levels and BOLD within the occipital lobe, the systematic search for articles identified nine eligible studies for quantitative analysis (9–16, 18). The results of the meta-analysis demonstrated a significant relationship between GABA and BOLD in the occipital lobe ($r = -0.45$ [-0.63, -0.22], $p = 0.002$, $I^2 = 47.06\%$) (**Figure 2**).

Another four studies investigated ACC GABA in relation to local response to emotion tasks (29, 31, 32, 35). Correlation coefficients were available for three of these, while Levar et al. (32) used a regression with ACC GABA levels as a covariate. The latter found a negatively correlated cluster in the dorsal ACC for negative vs. positive emotion, however, this result was not used for the main meta-analysis for which comparable contrasts were selected only (specific or all emotion vs. baseline). The main meta-analysis of this relationship yielded a significant negative relationship between ACC GABA and regional emotion-related neural activity ($r = 0.53$ [-0.79, -0.11], $p = 0.02$, $I^2 = 34.04\%$) (**Figure 3**).

Meta-Analysis of Associations With Glutamate Concentrations

Two meta-analyses were performed. One combined glutamate levels in the ACC and local activation during cognitive control tasks. The other combined glutamate levels in the ACC and local activation during emotional tasks. For illustration of the voxel positions of each study per meta-analysis see **Figures 4**, **5**.

Six studies (34, 37–40, 46) were included in the meta-analysis of the relationship between ACC glutamate levels and local activation during cognitive control. These were a mixture of studies using correlation and regression analysis. When regression analysis had been performed on the whole-brain level and no significant correlation with the ACC was found, this was entered into the meta-analysis as a non-significant result to avoid bias. The meta-analysis did not find support for a relationship between ACC glutamate levels and neural activity during cognitive control [$r = 0.19$ (-0.24, 0.56), $p = 0.39$, $I^2 = 71.62$] (**Figure 4**).

For the meta-analysis investigating the relationship between ACC glutamate levels and local activation during emotion processing, seven studies were included (29, 31, 32, 35, 44, 45, 49). As with the previous meta-analysis on cognitive control, studies

TABLE 8 | Posterior cingulate cortex/precuneus ^{1}H-MRS studies.

Authors	*n* Male % Age M(SD)	System Sequence	Reference	fMRI task/stimuli	Relationship	Covariates
GABA						
Hu et al. (60)	24 58.3 34.4 (8.6)	3T MEGA-PRESS	/Wt	Working memory task (n-back)	Low cognitive load NBR (#) GABA+ Mid/high cognitive load NBR (+) GABA+ DMN: low cognitive load NBR (#) GABA+ DMN: mid/high cognitive load NBR (+) GABA+	Age, GM, co-localised Glu
Costigan et al. (18)	40 30 22.1 (2.1)	3T MEGA-PRESS	/Wt	Odd-one-out task	Scene discrimination (#) GABA+	–
Glutamate						
Hu et al. (60)	24 58.3 34.4 (8.6)	3T MEGA-PRESS	/Wt	Working memory task (n-back)	All cognitive loads NBR (–) Glu DMN: low/mid cognitive load NBR (–) Glu DMN: high cognitive load NBR (#) Glu	Age, GM, co-localised GABA
Costigan et al. (18)	40 30 22.1 (2.1)	3T MEGA-PRESS	/Wt	Odd-one-out task	Scene discrimination (#) Glx	–

Wt, water; GM, grey matter volume within ^{1}H-MRS voxel; Glx, glutamate+glutamine; NBR, negative BOLD response; DMN, default mode network; /, OR. Neural activity is co-localised with the ^{1}H-MRS sampling region unless otherwise specified in the relationship column (i.e. Region: task related activity (+/#/–) GABA/Glu/Glx).

TABLE 9 | Remaining ^{1}H-MRS studies.

Authors	*n* Male % Age M(SD)	System Sequence	Reference	fMRI task/stimuli	Relationship	Covariates
GABA						
Frontal eye field						
Harris et al. (15)	18 38.9 27.8 (4.0)	3T MEGA-PRESS	/Wt, /Cr	Eye saccades	Saccades (#) GABA+	–
Glutamate						
Thalamus						
Allen et al. (2015)	27 66.7 24.4 (4.6)	3T PRESS		Verbal fluency task	R superior frontal gyrus/sulcus, R cingulate sulcus: verbal fluency (+) Glx	–
Fusar-Poli et al. (43)	17 58.8 25.5 (3.6)	3T PRESS		Verbal fluency task	Verbal fluency (#) Glu	–
Dorsal striatum						
Lorenz et al. (62)	32 59.4 47.3 (19.3)	3T PRESS	/Wt	Modified stop signal task	L caudate nucleus: response inhibition (+) Glx	–
Substantia nigra						
White et al. (63)	19 57.9 36.5 (12.1)	3T PRESS	/Cr	Monetary reward decision task	vStr/NAc: prediction error (#) Glx substantia nigra: prediction error (+) Glx	–

Wt, water; /, OR; GABA+, GABA+macromolecules; Glx, glutamate+glutamaine; vStr, ventral striatum; NAc, nucleus accumbens. Neural activity is co-localised with the ^{1}H-MRS sampling region unless otherwise specified in the relationship column (i.e. Region: task related activity (+/#/–) GABA/Glu/Glx).

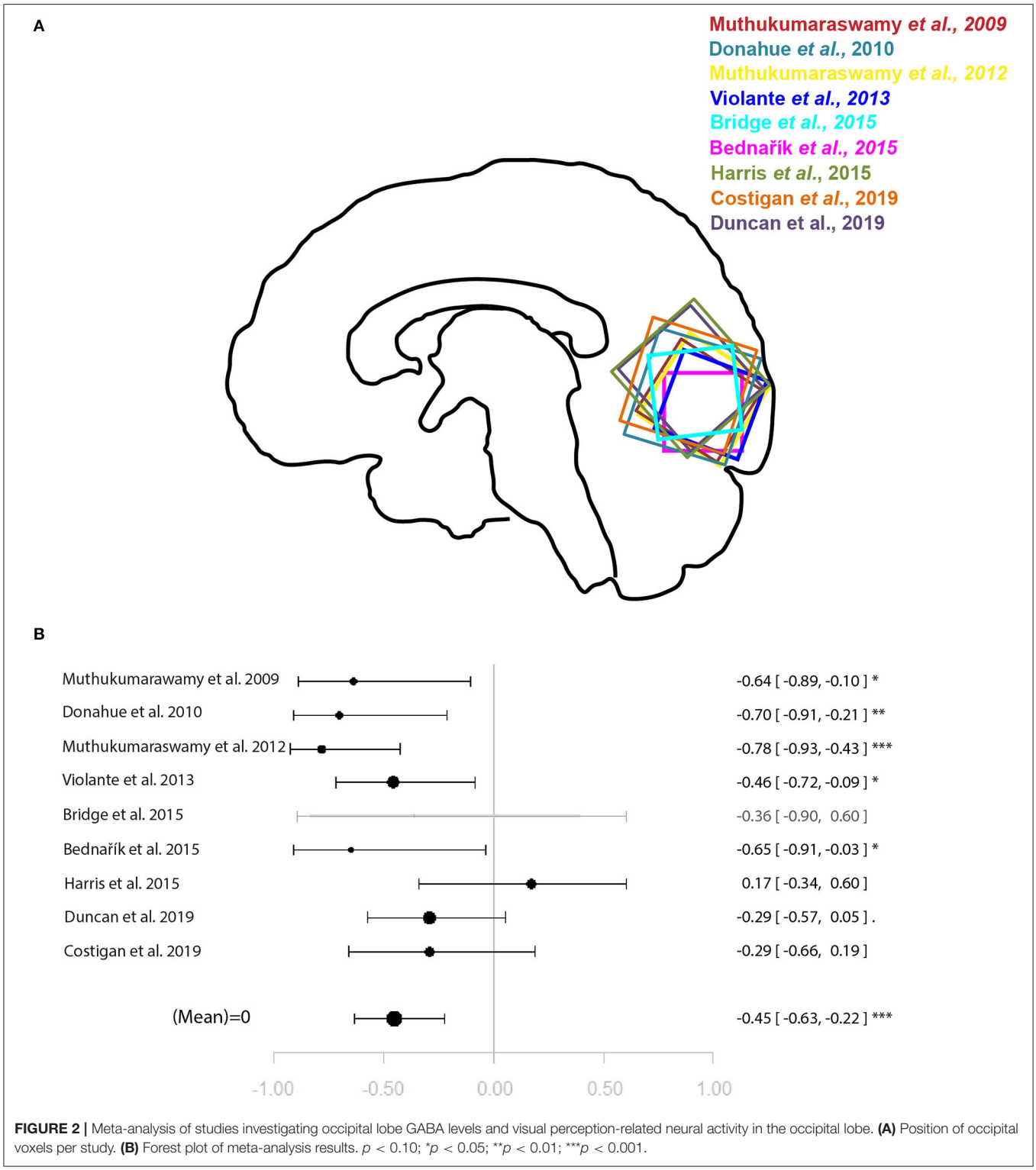

FIGURE 2 | Meta-analysis of studies investigating occipital lobe GABA levels and visual perception-related neural activity in the occipital lobe. **(A)** Position of occipital voxels per study. **(B)** Forest plot of meta-analysis results. $p < 0.10$; *$p < 0.05$; **$p < 0.01$; ***$p < 0.001$.

utilised a mixture of correlation and regression analyses. This analysis marginally missed significance for a positive relationship between ACC glutamate levels and regional emotion related neural activity [$r = 0.41$ (−0.04, 0.72), $p = 0.07$, $I^2 = 79.69\%$] (**Figure 5**).

DISCUSSION

The main finding of this meta-analysis was that GABA levels were negatively correlated with co-localised neural activity within the ACC during emotion processing and within the occipital

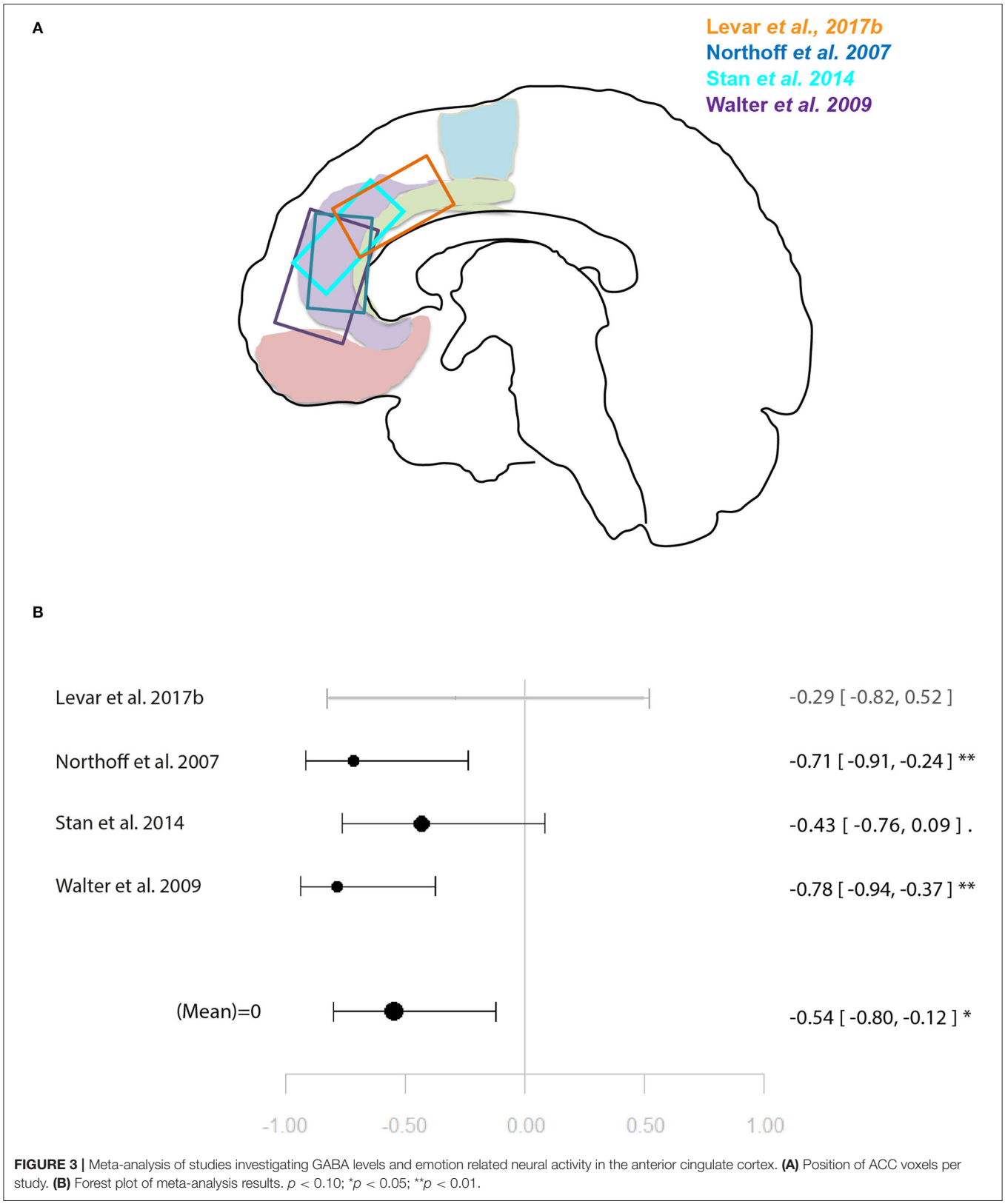

FIGURE 3 | Meta-analysis of studies investigating GABA levels and emotion related neural activity in the anterior cingulate cortex. **(A)** Position of ACC voxels per study. **(B)** Forest plot of meta-analysis results. $p < 0.10$; *$p < 0.05$; **$p < 0.01$.

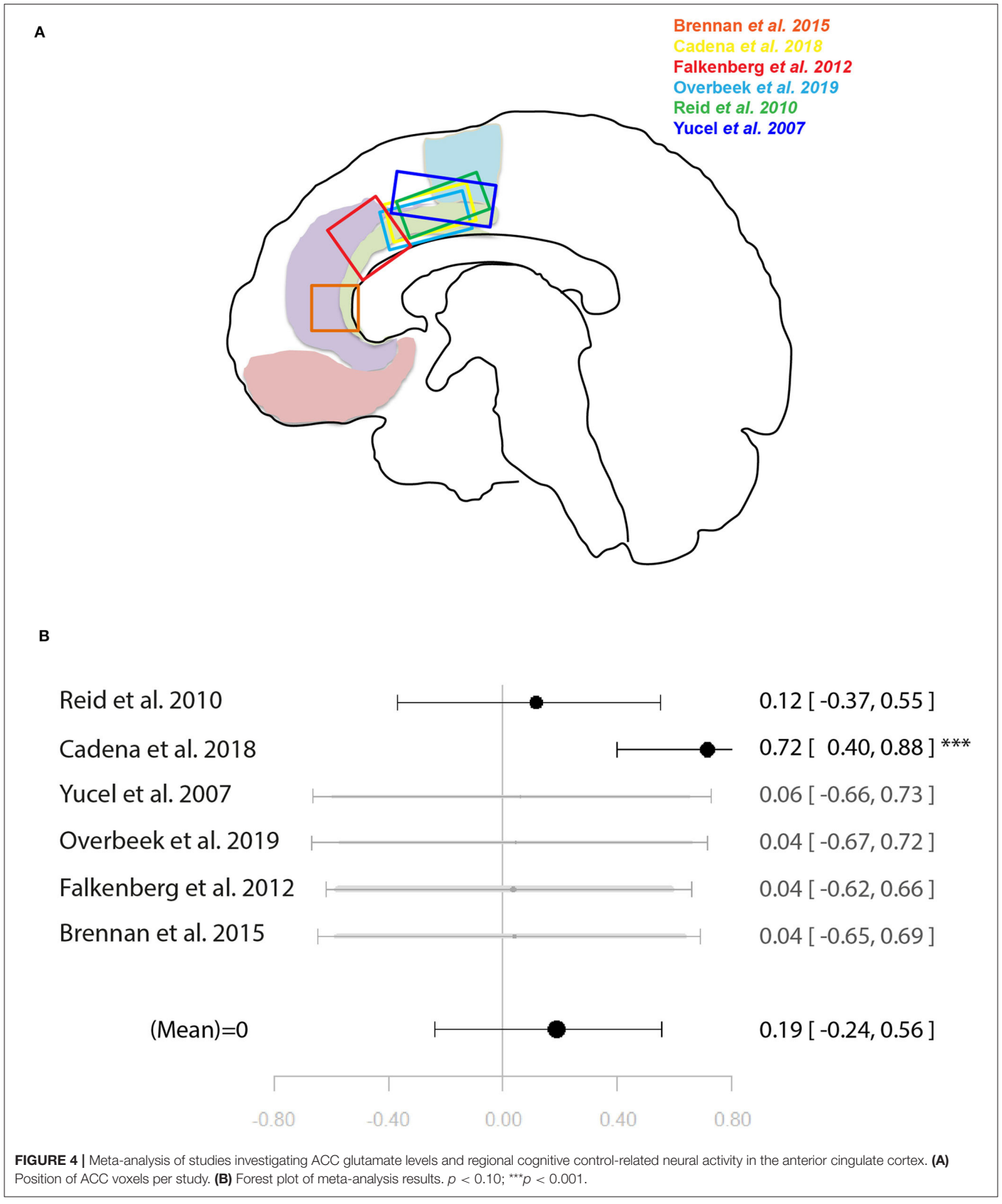

FIGURE 4 | Meta-analysis of studies investigating ACC glutamate levels and regional cognitive control-related neural activity in the anterior cingulate cortex. **(A)** Position of ACC voxels per study. **(B)** Forest plot of meta-analysis results. $p < 0.10$; ***$p < 0.001$.

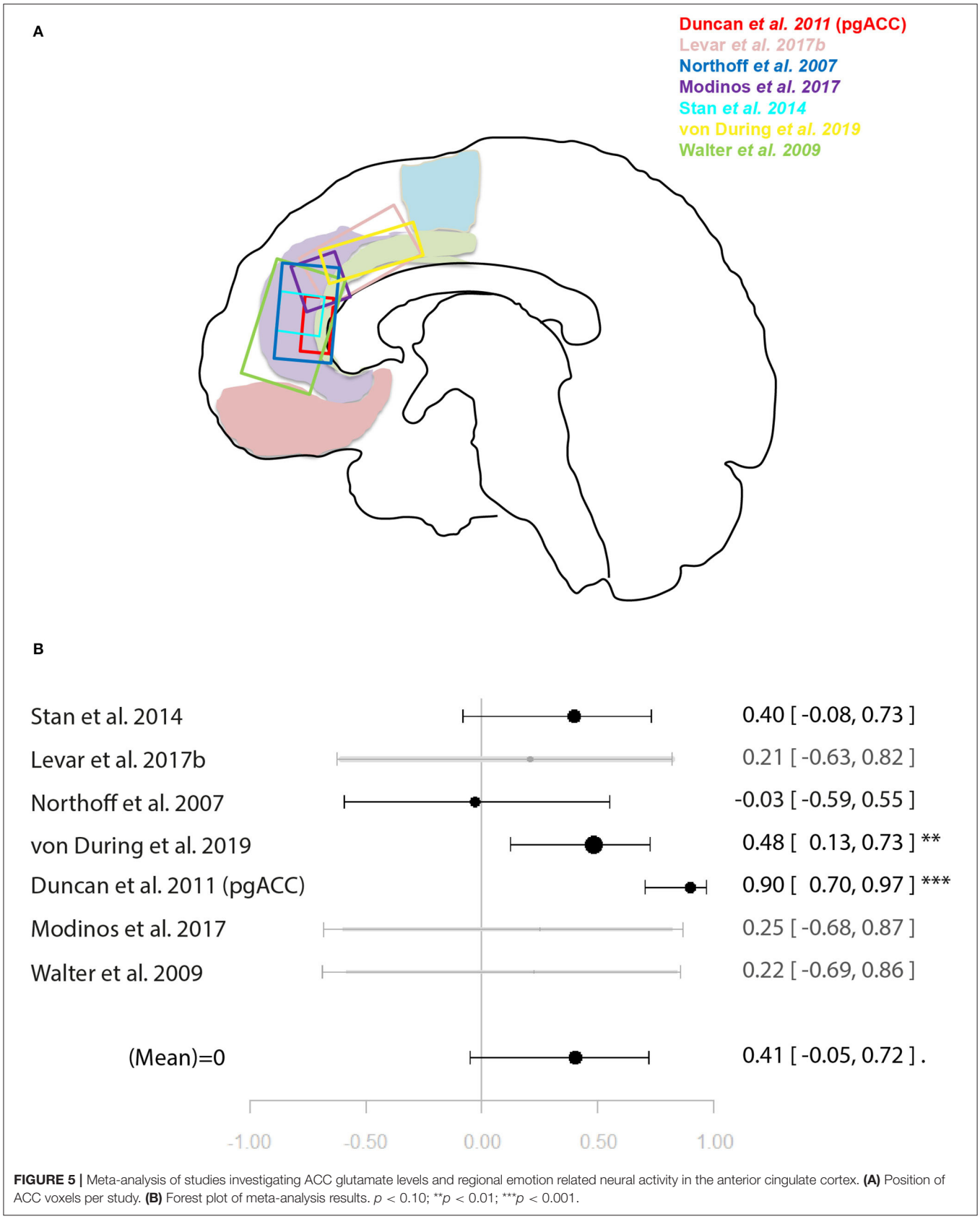

FIGURE 5 | Meta-analysis of studies investigating ACC glutamate levels and regional emotion related neural activity in the anterior cingulate cortex. **(A)** Position of ACC voxels per study. **(B)** Forest plot of meta-analysis results. $p < 0.10$; $^{**}p < 0.01$; $^{***}p < 0.001$.

lobe during visual stimulation. Further meta-analyses showed that glutamate levels within the ACC were not correlated with co-localised neural activity during either cognitive control or emotion processing, however, the latter meta-analysis narrowly missed significance. These findings were further supported by a systematic review of all fMRI-^{1}H-MRS association studies to date, where increasing resting GABA levels were repeatedly associated with either weaker neural activation or stronger neural deactivation. On the other hand, glutamate levels were largely not correlated with intra-regional neural activity, although a handful of studies did find a positive correlation. An additional finding was that glutamate concentrations were largely positively correlated with regions outside of the ^{1}H-MRS sampling area; however, negative inter-regional associations were also identified in multiple studies. GABA concentrations were less likely to be associated with regions outside of the ^{1}H-MRS sampling area with only a few studies providing evidence of a positive or negative relationship with inter-regional neural activation depending on the metabolite sampling region and the neural activation region.

These findings support and extend prior reported trends. Previously, in a narrative review Duncan et al. (4) highlighted that GABA tended to be negatively correlated with regional neural activity in the visual, auditory, sensorimotor and anterior cingulate cortices, while glutamate was positively correlated with neural activity in regions outside of the sampling region of the metabolite. In the present study, by using a systematic rather than narrative review method and capitalising on the large increase in available studies specifically using ^{1}H-MRS and fMRI, a more region-dependent relationship between these specific measures emerged. The negative relationship between GABA levels and regional neural activation was confirmed within the occipital cortex, ACC/mPFC, temporal lobe, and PCC. However, regions such as the sensorimotor cortex, auditory cortex and dorsolateral prefrontal cortex either did not exhibit this relationship clearly or in a few studies the relationship was in the opposite direction (30, 50). A negative relationship between GABA levels and regional neural activation appears intuitive: increased inhibition as measured through resting state ^{1}H-MRS would be associated with decreased net activation of a region through regulation of resting excitatory activity (4, 65). Prior work in animals found that pharmacological manipulation increasing endogenous GABA concentrations produced lower positive BOLD signal changes (66). In the context of NBR, previous work in rats found hyperpolarisation of neurons through neuronal inhibition to correspond to a decrease in blood oxygenation (67). Findings of a positive relationship between GABA levels and neural activity may be a result of more complex neural processes that require suppression of neural response to irrelevant stimuli to promote concurrent activation to target stimuli (68). A relationship between GABA levels and neural activity in distal regions had not previously been identified in the literature (4). While initial studies suggested that the relationship between GABA levels and neural activity was limited to the same region (4, 68), a handful of recent studies reported both negative and positive relationships with activation outside of the ^{1}H-MRS voxel (32–34, 58–60). Negative relationships with inter-regional neural activity may be the result of local inhibition of excitatory projections that regulate activity in other regions (32–34).

In terms of glutamate, a few studies observed a positive relationship between glutamate and local neural activity in the ACC and PCC (29, 44, 46, 60). Additionally, both positive and negative relationships with distal neural activity were found. These findings add to the simplified positive relationship with inter-regional neural activity reported in Duncan et al. (4). A negative relationship between BOLD activity in DMN regions, such as the PCC/PCu, were speculated to be due to higher ACC glutamate levels supporting facilitation of salience processing, thus resulting in stronger deactivation of DMN regions (39, 45). However, this relationship seems to be region-dependant as glutamate levels measured within the DMN, specifically the PCC, were positively related with DMN neural activation, where higher glutamate levels predicted lower local deactivation (60). The positive relationship between glutamate levels and intra-regional neural activity may stem from an excitatory drive stimulating neural activation within the same region through recurring feedback (46, 69). However, the relationship between glutamate levels and intra-regional neural activity may be difficult to replicate: one study failed to replicate a positive correlation between ACC glutamate and ACC neural activity at a 6-week follow-up scan within the same cohort (46). In fact, Enzi et al. (47) suggested resting glutamate levels may be more closely related to resting-state activation, thus being less intimately linked with task-related activity. As previously observed by Duncan et al. (4), glutamate levels were positively associated with neural activity outside of the sampling regions for glutamate. The long-range projections of glutamatergic neurons (70) are thought to influence neural activity in distal regions, thus giving rise to this relationship. However, a number of studies have shown that these projections may not simply reflect positive relationships with neural activity, but may also indicate that glutamate levels can negatively predict neural activity inter-regionally.

The ACC has been commonly investigated across studies, for which effects have been inconsistent. The discrepancies in ^{1}H-MRS x fMRI relationships may arise from functional segregation within the ACC (71), its involvement in different behaviours (72), and that it hosts both task-positive and task-negative subdivisions (e.g., pgACC and supragenual ACC). The ability of ^{1}H-MRS to discriminate between ACC subregions is still limited due to the ^{1}H-MRS voxel size, especially in the case of GABA. This may be improved by the use of high-field MRI scanners that will allow for smaller voxel sizes (73). An additional consideration is that relationships between metabolite levels and neural activity may also be task-specific. Studies that used an active control task, rather than a low-level baseline condition such as a fixation cross [e.g., (44, 53, 54)], indicate that baseline metabolite levels are not simply correlated with any type of neural response. When neural response was confirmed for both the task of interest and the control task, different relationships between GABA levels and neural response were found indicating that metabolite levels may not be simply associated with all types of neural activity within a region (54).

Despite some incongruent findings, a pattern of neurochemical-neurofunctional relationships has emerged, which give valuable insight into psychiatric disorders where this relationship is aberrant. Measurement of metabolite levels at rest with ^{1}H-MRS is thought to reflect individual differences in number of glutamatergic and GABAergic neurons, number of glutamatergic and GABAergic synapses, and glutamate and GABA turnover (68). It is conceivable, then, that abnormalities in metabolite levels would be reflected in differential neurochemical-neurofunctional relationships. In psychiatric disorders such as schizophrenia, case-control studies have suggested an aberrant relationship between ACC glutamate and local neural activity (46) and in regions receiving inputs from the ACC, such as the insula and DMN (34, 46, 74). Differences were found in the relationship between hippocampal Glx and inferior frontal gyrus activation, with medicated schizophrenia patients showing a less robust relationship (56) potentially reflecting differential coupling between the two regions (75). Activation related to prediction error within the substantia nigra was not correlated with regional glutamate levels in schizophrenia patients, which was interpreted as a glutamatergic dysfunction leading to abnormal prediction error coding (38). Furthermore, a relationship between glutamate and working memory activation, both within the dlPFC, was found in unmedicated schizophrenia patients where no such relationship existed in healthy controls—potentially due to compensatory action to glutamatergic insensitivity (52). Given the known and increasingly well-characterised abnormalities in glutamatergic and GABAergic function associated with this psychiatric disorder (76, 77) and the close relationship between metabolites and neurofunction, abnormalities in brain function should arise. The neurochemical-neurofunctional relationship has been investigated less frequently in other psychiatric disorders such as obsessive-compulsive disorder and major depressive disorder. While this line of investigation showed no differences in the relationship in patients with obsessive compulsive disorder (40, 51), patients with major depressive disorder showed stronger coupling between glutamate levels and NBR compared with healthy controls (31). Walter et al. (31) concluded that reduced resting state activity was driven by glutamatergic metabolism in patients with major depressive disorder. Differences in ^{1}H-MRS x fMRI relationships may be the result of variations in neurochemistry, differential abnormal functions regionally and inter-regionally, as well as structural abnormalities. Despite the correlational nature of all the studies identified here, understanding healthy relationships between metabolite and neural activity allows some insight into compensatory action within mental illness and can provide potential pharmaceutical targets for intervention. Targeting GABAergic or glutamatergic neurotransmission may be a promising avenue to treating symptoms of schizophrenia (78) and major depressive disorder (79).

Considerations on the Choice of Analytical Approaches

The studies included in this review used two main types of methods to derive relationships. Harris et al. (15) demonstrated that when using the correlational technique with %SC, the source of sampling for %SC could have a large effect on the observed relationship. Harris et al. (15) tested five different BOLD activation sources: peak within the ^{1}H-MRS voxel, mean across the ^{1}H-MRS voxel, mean across significant activation, peak within anatomical ROI and mean across anatomical ROI. From the peak within ^{1}H-MRS voxel to the mean across significant activation, there was a maximum change in effect size of $r = 0.47$, although it should be noted that these individual correlation coefficients were not statistically significant due to Bonferroni correction. Despite these potential sources of variation, the vast majority of articles cited in our systematic review that used the correlational technique with %SC only tested the relationship between metabolites and neural activation with one source of %SC, which may cause inconsistencies in findings.

Effects of Potential Confounders

Previously published studies controlled for potential confounds in diverse ways. Commonly used covariates were age, voxel tissue composition and sex. Age may have region-specific effects on levels of glutamate (80) and of GABA (81) and thus should be consistently controlled for. Our systematic review was not restricted to a certain age limit and instead attempted to collect data on all age ranges and noted whether studies controlled for age. Similarly, a potentially confounding effect of sex on metabolite levels was not consistently considered in individual studies, although sex has previously been identified to alter levels of glutamate (82) and GABA (83).

A further issue refers to the use of other regions as specificity control (4). In order to confirm that a significant association is not a global effect, metabolite analyses should be conducted both for the main region of interest as well as for a control region. Similarly, to ensure relationships can be specific to the experimental task, researchers should also evaluate the relationship between metabolite levels and a control, unrelated task. However, time constraints and participant fatigue during scanning may not enable such control measures in all studies.

Future Directions

Although it is tempting to suggest that future studies using the correlational approach should test various sources of %SC [e.g., (15)], the multiple testing corrections needed would require strong relationship effects between metabolite and BOLD signal. However, the present systematic review and meta-analyses seem to suggest such effect sizes are moderate at best for the metabolite glutamate. An alternative suggestion would be to consistently utilise %SC derived from the peak voxel within the ^{1}H-MRS voxel as many studies have done, with deviations from a standard source of %SC needing to be specifically addressed and justified.

Other future suggestions for studies of this kind are to include age and sex as confounding covariates more consistently. Similarly, task and region specificity controls should be included wherever possible. One reason for the lack of substantial conclusions to be made from the above listed studies is the heterogeneity of ^{1}H-MRS locations, BOLD %SC sampling locations and region coverage within regression studies. Replication studies would allow more insight into studies that used emotional, working memory, reward and motor tasks. Additionally, combination with additional modalities such as

arterial spin labelling as a different measure of brain function may help parse out the less consistent relationships seen here. Future studies should also aim to investigate the ^{1}H-MRS x fMRI relationship in further psychiatric disorders that feature glutamatergic or GABAergic abnormalities, such as autism spectrum disorder (ASD). Abnormalities in excitation-inhibition balance are well-known and characterised in individuals in ASD (84, 85), where reduced neural activity in corticostriatal circuits have been proposed (86, 87) to be linked to the reduction of striatal glutamate (85). However, further investigation of these hypotheses and the nature of the neurochemical-neurofunctional relationship in ASD is required. Finally, capitalising on the findings presented here, future studies in psychiatric populations such as schizophrenia patients may modulate metabolite levels such as glutamate to test whether neurofunction can be modulated as a result.

CONCLUSIONS

The significant expansion of studies combining multi-modal ^{1}H-MRS and fMRI in recent years has enabled more detailed examination of the interactions between neurochemistry and neurophysiology in the healthy brain. These studies have shown robust negative correlations between GABA levels and local activation in regions such as the occipital cortex and ACC, and positive correlations between glutamate levels and activation in distal regions. These findings have implications for our understanding of pathophysiology of psychiatric disorders such as schizophrenia, a field in which studies combining ^{1}H-MRS and fMRI are burgeoning in recent years. In this context, findings from multimodal studies may provide key insights into the neurobiology of schizophrenia not only by informing how the interplay between neurochemistry and neurophysiology may be altered prior and across disease stages, but also by their translational potential to elucidate whether pharmacological modulation of glutamate and/or GABA may be a new target for addressing abnormal neurophysiology in this psychiatric disorder.

DATA AVAILABILITY STATEMENT

The original contributions presented in the study are included in the article/**Supplementary Material**, further inquiries can be directed to the corresponding author/s.

AUTHOR CONTRIBUTIONS

GM, AK, and MJK: concept and design. CB and AK: systematic search. PBL and AK: data extraction. AK: statistical analysis and drafting of the manuscript. MJK and AK: statistical support. CD, JMS, PBL, GM, and AK: critical revisions of the manuscript. CD, JMS, and GM: supervision. All authors contributed to the article and approved the submitted version.

FUNDING

This study was supported by a Sir Henry Dale Fellowship, jointly funded by the Wellcome Trust and the Royal Society to Dr. Gemma Modinos (202397/Z/16/Z).

ACKNOWLEDGMENTS

The authors would like to thank Dr. Alice Egerton for kindly providing templates for our figures.

SUPPLEMENTARY MATERIAL

The Supplementary Material for this article can be found online at: https://www.frontiersin.org/articles/10.3389/fpsyt.2021.644315/full#supplementary-material

REFERENCES

1. Isaacson JS, Scanziani M. How inhibition shapes cortical activity. *Neuron.* (2011) 72:231–43. doi: 10.1016/j.neuron.2011.09.027
2. Lauritzen M, Mathiesen C, Schaefer K, Thomsen KJ. Neuronal inhibition and excitation, and the dichotomic control of brain hemodynamic and oxygen responses. *Neuroimage.* (2012) 62:1040–50. doi: 10.1016/j.neuroimage.2012.01.040
3. Logothetis NK. The underpinnings of the BOLD functional magnetic resonance imaging signal. *J Neurosci.* (2003) 23:3963–71. doi: 10.1523/JNEUROSCI.23-10-03963.2003
4. Duncan NW, Wiebking C, Northoff G. Associations of regional GABA and glutamate with intrinsic and extrinsic neural activity in humans—a review of multimodal imaging studies. *Neurosci Biobehav Rev.* (2014) 47:36–52. doi: 10.1016/j.neubiorev.2014.07.016
5. Witt ST, Drissi NM, Tapper S, Wretman A, Szakacs A, Hallbook T, et al. Evidence for cognitive resource imbalance in adolescents with narcolepsy. *Brain Imaging Behav.* (2018) 12:411–24. doi: 10.1007/s11682-017-9706-y
6. Moher D, Liberati A, Tetzlaff J, Altman DG, The PRISMA Group. preferred reporting items for systematic reviews and meta-analyses: the PRISMA statement. *PLoS Med.* (2009) 6:e1000097. doi: 10.1371/journal.pmed1000097
7. Borenstein M, Hedges LV, Higgins JP, Rothstein HR. *Introduction to Meta-Analysis*. Chichester: John Wiley & Sons (2011).
8. Albajes-Eizagirre A, Solanes A, Radua J. Meta-analysis of non-statistically significant unreported effects. *Stat Methods Med Res.* (2019) 28:3741–54. doi: 10.1177/0962280218811349
9. Muthukumaraswamy SD, Edden RA, Jones DK, Swettenham JB, Singh KD. Resting GABA concentration predicts peak gamma frequency and fMRI amplitude in response to visual stimulation in humans. *Proc Natl Acad Sci USA.* (2009) 106:8356–61. doi: 10.1073/pnas.0900728106
10. Donahue MJ, Near J, Blicher JU, Jezzard, P. Baseline GABA concentration and fMRI response. *NeuroImage.* (2010) 53:392–8. doi: 10.1016/j.neuroimage.2010.07.017
11. Muthukumaraswamy SD, Edden RAE, Wise RG, Singh KD. Individual variability in the shape and amplitude of the BOLD-HRF correlates with endogenous GABAergic inhibition. *Hum Brain Mapping.* (2012) 33:455–65. doi: 10.1002/hbm.21223
12. Violante IR, Ribeiro MJ, Edden RA, Guimaraes P, Bernardino I, Rebola J, et al. GABA deficit in the visual cortex of patients with neurofibromatosis type 1: genotype-phenotype correlations and functional impact. *Brain.* (2013) 136:918–25. doi: 10.1093/brain/aws368

13. Bridge H, Stagg CJ, Near J, Lau C-i, Zisner A, Cader MZ. Altered neurochemical coupling in the occipital cortex in migraine with visual aura. *Cephalalgia*. (2015) 35:1025–30. doi: 10.1177/0333102414566860
14. Bednarík P, Tkáč I, Giove F, DiNuzzo M, Deelchand DK, Emir UE, et al. Neurochemical and BOLD responses during neuronal activation measured in the human visual cortex at 7 tesla. *J Cerebral Blood Flow Metabolism*. (2015) 35:601–10. doi: 10.1038/jcbfm.2014.233
15. Harris AD, Puts NA, Anderson BA, Yantis S, Pekar JJ, Barker PB, Edden RAE. Multi-regional investigation of the relationship between functional MRI blood oxygenation level dependent (BOLD) activation and GABA concentration. *PLoS ONE*. (2015) 10:e0117531. doi: 10.1371/journal.pone.0117531
16. Duncan NW, Zhang J, Northoff G, Weng X. Investigating GABA concentrations measured with macromolecule suppressed and unsuppressed MEGA-PRESS MR spectroscopy and their relationship with BOLD responses in the occipital cortex. *J Magnet Resonance Imag*. (2019) 50:1285–94. doi: 10.1002/jmri.26706
17. Wijtenburg SA, West J, Korenic SA, Kuhney F, Gaston FE, Chen H, et al. Glutamatergic metabolites are associated with visual plasticity in humans. *Neurosci Let*. (2017) 644:30–6. doi: 10.1016/j.neulet.2017.02.020
18. Costigan AG, Umla-Runge K, Evans C, Hodgetts CJ, Lawrence AD, Graham KS. Neurochemical correlates of scene processing in the precuneus/posterior cingulate cortex: a multimodal fMRI and 1H-MRS study. *Hum Brain Map*. (2019) 40:2884–98. doi: 10.1002/hbm.24566
19. Schallmo MP, Kale AM, Millin R, Flevaris AV, Brkanac Z, Edden RA, Bernier RA, Murray SO. Suppression and facilitation of human neural responses. *eLife*. (2018) 7:29. doi: 10.7554/eLife.30334
20. Ip IB, Berrington A, Hess AT, Parker AJ, Emir UE, Bridge H. Combined fMRI-MRS acquires simultaneous glutamate and BOLD-fMRI signals in the human brain. *NeuroImage*. (2017) 155:113–9. doi: 10.1016/j.neuroimage.2017.04.030
21. Schallmo MP, Millin R, Kale AM, Kolodny T, Edden RA, Bernier RA, et al. Glutamatergic facilitation of neural responses in MT enhances motion perception in humans. *NeuroImage*. (2019) 184:925–31. doi: 10.1016/j.neuroimage.2018.10.001
22. Bhattacharyya PK, Phillips MD, Stone LA, Bermel RA, Lowe MJ. Sensorimotor cortex gamma-aminobutyric acid concentration correlates with impaired performance in patients with MS. *AJNR Am J Neuroradiol*. (2013) 34:1733–9. doi: 10.3174/ajnr.A3483
23. Bhattacharyya PK, Phillips MD, Stone LA, Lowe MJ. Activation volume vs BOLD signal change as measures of fMRI activation - Its impact on GABA - fMRI activation correlation. *Magn Reson Imaging*. (2017) 42:123–9. doi: 10.1016/j.mri.2017.06.009
24. Draper A, Stephenson MC, Jackson GM, Pepes S, Morgan PS, Morris PG, Jackson SR. Increased GABA contributes to enhanced control over motor excitability in Tourette syndrome. *Curr Biol*. (2014) 24:2343–7. doi: 10.1016/j.cub.2014.08.038
25. Stagg CJ, Bachtiar V, Johansen-Berg H. The role of GABA in human motor learning. *Curr Biol*. (2011) 21:480–4. doi: 10.1016/j.cub.2011.01.069
26. Torta DM, Cauda F. Different functions in the cingulate cortex, a meta-analytic connectivity modeling study. *NeuroImage*. (2011) 56:2157–72. doi: 10.1016/j.neuroimage.2011.03.066
27. Chen X, Fan X, Hu Y, Zuo C, Whitfield-Gabrieli S, Holt D, et al. Regional GABA concentrations modulate inter-network resting-state functional connectivity. *Cereb Cortex*. (2019) 29:1607–18. doi: 10.1093/cercor/bhy059
28. Jocham G, Hunt LT, Near J, Behrens TE. A mechanism for value-guided choice based on the excitation-inhibition balance in prefrontal cortex. *Nat Neurosci*. (2012) 15:960–1. doi: 10.1038/nn.3140
29. Stan AD, Schirda CV, Bertocci MA, Bebko GM, Kronhaus DM, Aslam HA, et al. Glutamate and GABA contributions to medial prefrontal cortical activity to emotion: implications for mood disorders. *Psychiatry Res*. (2014) 223:253–60. doi: 10.1016/j.pscychresns.2014.05.016
30. Wiebking C, Duncan NW, Tiret B, Hayes DJ, Marjanska M, Doyon J, et al. GABA in the insula - a predictor of the neural response to interoceptive awareness. *NeuroImage*. (2014) 86:10–8. doi: 10.1016/j.neuroimage.2013.04.042
31. Walter M, Henning A, Grimm S, Schulte RF, Beck J, Dydak U, et al. The relationship between aberrant neuronal activation in the pregenual anterior cingulate, altered glutamatergic metabolism, and anhedonia in major depression. *Arch GenPsychiatry*. (2009) 66:478–86. doi: 10.1001/archgenpsychiatry.2009.39
32. Levar N, van Leeuwen JM, Denys D, van Wingen GA. Divergent influences of anterior cingulate cortex GABA concentrations on the emotion circuitry. *NeuroImage*. (2017) 158:136–44. doi: 10.1016/j.neuroimage.2017.06.055
33. Levar N, van Leeuwen JMC, Puts NAJ, Denys D, Van Wingen GA. GABA concentrations in the anterior cingulate cortex are associated with fear network function and fear recovery in humans. *Front Hum Neurosci*. (2017) 11:202. doi: 10.3389/fnhum.2017.00202
34. Overbeek G, Gawne TJ, Reid MA, Salibi N, Kraguljac NV, White DM, et al. Relationship between cortical excitation and inhibition and task-induced activation and deactivation: a combined magnetic resonance spectroscopy and functional magnetic resonance imaging study at 7T in first-episode psychosis. *Biol Psychiatry*. (2019) 4:121–30. doi: 10.1016/j.bpsc.2018.10.002
35. Northoff G, Walter M, Schulte RF, Beck J, Dydak U, Henning A, et al. GABA concentrations in the human anterior cingulate cortex predict negative BOLD responses in fMRI. *Nat Neurosci*. (2007) 10:1515–7. doi: 10.1038/nn2001
36. Wang GY, van Eijk J, Demirakca T, Sack M, Krause-Utz A, Cackowski S, et al. ACC GABA levels are associated with functional activation and connectivity in the fronto-striatal network during interference inhibition in patients with borderline personality disorder. *NeuroImage*. (2017) 147:164–74. doi: 10.1016/j.neuroimage.2016.12.013
37. Yücel M, Lubman DI, Harrison BJ, Fornito A, Allen NB, Wellard RM, et al. A combined spectroscopic and functional MRI investigation of the dorsal anterior cingulate region in opiate addiction. *Mol Psychiatry*. (2007) 12:691–702. doi: 10.1038/sj.mp.4001955
38. Reid MA, Stoeckel LE, White DM, Avsar KB, Bolding MS, Akella NS, et al. Assessments of function and biochemistry of the anterior cingulate cortex in schizophrenia. *Biol Psychiatry*. (2010) 68:625–33. doi: 10.1016/j.biopsych.2010.04.013
39. Falkenberg LE, Westerhausen R, Specht K, Hugdahl K. Resting-state glutamate level in the anterior cingulate predicts blood-oxygen level-dependent response to cognitive control. *Proc Natl Acad Sci USA*. (2012) 109:5069–73. doi: 10.1073/pnas.1115628109
40. Brennan BP, Tkachenko O, Schwab ZJ, Juelich RJ, Ryan EM, Athey AJ, et al. An examination of rostral anterior cingulate cortex function and neurochemistry in obsessive-compulsive disorder. *Neuropsychopharmacology*. (2015) 40:1866–76. doi: 10.1038/npp.2015.36
41. Gleich T, Lorenz RC, Pöhland L, Raufelder D, Deserno L, Beck A, et al. Frontal glutamate and reward processing in adolescence and adulthood. *Brain Struct Funct*. (2015) 220:3087–99. doi: 10.1007/s00429-014-0844-3
42. Duncan NW, Hayes DJ, Wiebking C, Tiret B, Pietruska K, Chen DQ, et al. Negative childhood experiences alter a prefrontal-insular-motor cortical network in healthy adults: a preliminary multimodal rsfMRI-fMRI-MRS-dMRI study. *Hum Brain Mapp*. (2015) 36:4622–37. doi: 10.1002/hbm.22941
43. Fusar-Poli P, Stone JM, Broome MR, Valli I, Mechelli A, McLean MA, et al. Thalamic glutamate levels as a predictor of cortical response during executive functioning in subjects at high risk for psychosis. *Arch Gen Psychiatry*. (2011) 68:881–90. doi: 10.1001/archgenpsychiatry.2011.46
44. Duncan NW, Enzi B, Wiebking C, Northoff, G. Involvement of glutamate in rest-stimulus interaction between perigenual and supragenual anterior cingulate cortex: a combined fMRI-MRS study. *Hum Brain Mapp*. (2011) 32:2172–82. doi: 10.1002/hbm.21179
45. von Düring F, Ristow I, Li M, Denzel D, Colic L, Demenescu LR, et al. Glutamate in salience network predicts BOLD response in default mode network during salience processing. *Front Behav Neurosci*. (2019) 13:2172–82. doi: 10.3389/fnbeh.2019.00232
46. Cadena EJ, White DM, Kraguljac NV, Reid MA, Maximo JO, Nelson EA, et al. A longitudinal multimodal neuroimaging study to examine relationships between resting state glutamate and task related BOLD response in schizophrenia. *Front Psychiatry*. (2018) 9:632. doi: 10.3389/fpsyt.2018.00632
47. Enzi B, Duncan NW, Kaufmann J, Tempelmann C, Wiebking C, Northoff G. Glutamate modulates resting state activity in the perigenual anterior cingulate cortex - a combined fMRI-MRS study. *Neuroscience*. (2012) 227:102–9. doi: 10.1016/j.neuroscience.2012.09.039
48. Naaijen J, Lythgoe DJ, Zwiers MP, Hartman CA, Hoekstra PJ, Buitelaar JK, et al. Anterior cingulate cortex glutamate and its association with striatal

functioning during cognitive control. *Eur Neuropsychopharmacol.* (2018) 28:381–91. doi: 10.1016/j.euroneuro.2018.01.002
49. Modinos G, McLaughlin A, Egerton A, McMullen K, Kumari V, Barker GJ, et al. Corticolimbic hyper-response to emotion and glutamatergic function in people with high schizotypy: a multimodal fMRI-MRS study. *Transl Psychiatry Psychiatry.* (2017) 7:e1083. doi: 10.1038/tp.2017.53
50. Friedman SD, Poliakov AV, Budech C, Shaw DWW, Breiger D, Jinguji T, et al. GABA alterations in pediatric sport concussion. *Neurology.* (2017) 89:2151–6. doi: 10.1212/WNL.0000000000004666
51. Moon CM, Jeong GW. Associations of neurofunctional, morphometric and metabolic abnormalities with clinical symptom severity and recognition deficit in obsessive-compulsive disorder. *J Affect Disord.* (2018) 227:603–12. doi: 10.1016/j.jad.2017.11.059
52. Kaminski J, Gleich T, Fukuda Y, Katthagen T, Gallinat J, Heinz A, et al. Association of cortical glutamate and working memory activation in patients with schizophrenia: a multimodal proton magnetic resonance spectroscopy and functional magnetic resonance imaging study. *Biol Psychiatry.* (2020) 87:225–33. doi: 10.1016/j.biopsych.2019.07.011
53. Jung J, Williams SR, Sanaei Nezhad F, Lambon Ralph MA. GABA concentrations in the anterior temporal lobe predict human semantic processing. *Sci Rep.* (2017) 7:15748. doi: 10.1038/s41598-017-15981-7
54. Schmitz TW, Correia MM, Ferreira CS, Prescot AP, Anderson MC. Hippocampal GABA enables inhibitory control over unwanted thoughts. *Nat Commun.* (2017) 8:1311. doi: 10.1038/s41467-017-00956-z
55. Valli I, Stone J, Mechelli A, Bhattacharyya S, Raffin M, Allen P, et al. Altered medial temporal activation related to local glutamate levels in subjects with prodromal signs of psychosis. *Biol Psychiatry.* (2011) 69:97–9. doi: 10.1016/j.biopsych.2010.08.033
56. Hutcheson NL, Reid MA, White DM, Kraguljac NV, Avsar KB, Bolding MS, et al. Multimodal analysis of the hippocampus in schizophrenia using proton magnetic resonance spectroscopy and functional magnetic resonance imaging. *Schizophr Res.* (2012) 140:136–42. doi: 10.1016/j.schres.2012.06.039
57. Bossong MG, Wilson R, Appiah-Kusi E, McGuire P, Bhattacharyya S. Human striatal response to reward anticipation linked to hippocampal glutamate levels. *Int J Neuropsychopharmacol.* (2018) 21:623–30. doi: 10.1093/ijnp/pyy011
58. Lipp I, Evans CJ, Lewis C, Murphy K, Wise RG, Caseras X. The relationship between fearfulness, GABA+, and fear-related BOLD responses in the insula. *PLoS ONE.* (2015) 10:e0120101. doi: 10.1371/journal.pone.0120101
59. Cleve M, Gussew A, Wagner G, Bär KJ, Reichenbach JR. Assessment of intra- and inter-regional interrelations between GABA+, Glx and BOLD during pain perception in the human brain – a combined 1H fMRS and fMRI study. *Neuroscience.* (2017) 365:125–36. doi: 10.1016/j.neuroscience.2017.09.037
60. Hu Y, Chen X, Gu H, Yang Y. Resting-state glutamate and GABA concentrations predict task-induced deactivation in the default mode network. *J Neurosci.* (2013) 33:18566–73. doi: 10.1523/JNEUROSCI.1973-13.2013
61. Robin J, Buchsbaum BR, Moscovitch M. The primacy of spatial context in the neural representation of events. *J Neurosci.* (2018) 2018:1638–17. doi: 10.1523/JNEUROSCI.1638-17.2018
62. Lorenz RC, Gleich T, Buchert R, Schlagenhauf F, Kühn S, Gallinat J. Interactions between glutamate, dopamine, and the neuronal signature of response inhibition in the human striatum. *Hum Brain Mapp.* (2015) 36:4031–40. doi: 10.1002/hbm.22895
63. White DM, Kraguljac NV, Reid MA, Lahti AC. Contribution of substantia nigra glutamate to prediction error signals in schizophrenia: a combined magnetic resonance spectroscopy/functional imaging study. *NPJ Schizophr.* (2015) 1:14001. doi: 10.1038/npjschz.2014.1
64. Allen P, Chaddock CA, Egerton A, Howes OD, Barker G, Bonoldi I, et al. Functional outcome in people at high risk for psychosis predicted by thalamic glutamate levels and prefronto-striatal activation. *Schizophr Bull.* (2015) 41:429–39. doi: 10.1093/schbul/sbu115
65. Hyder F, Fulbright RK, Shulman RG, Rothman DL. Glutamatergic function in the resting awake human brain is supported by uniformly high oxidative energy. *J Cerebral Blood Flow Metab.* (2013) 33:339–47. doi: 10.1038/jcbfm.2012.207
66. Chen Z, Silva AC, Yang J, Shen J. Elevated endogenous GABA level correlates with decreased fMRI signals in the rat brain during acute inhibition of GABA transaminase. *J Neurosci Res.* (2005) 79:383–91. doi: 10.1002/jnr.20364
67. Devor A, Tian P, Nishimura N, Teng IC, Hillman EMC, Narayanan SN, et al. Suppressed neuronal activity and concurrent arteriolar vasoconstriction may explain negative blood oxygenation level-dependent signal. *J Neurosci.* (2007) 27:4452–9. doi: 10.1523/JNEUROSCI.0134-07.2007
68. Sumner P, Edden RA, Bompas A, Evans CJ, Singh KD. More GABA, less distraction: a neurochemical predictor of motor decision speed. *Nat Neurosci.* (2010) 13:825–7. doi: 10.1038/nn.2559
69. Logothetis NK. What we can do and what we cannot do with fMRI. *Nature.* (2008) 453:869–78. doi: 10.1038/nature06976
70. Rockland KS. Elements of cortical architecture. In: *Extrastriate Cortex in Primates.* Boston, MA: Springer (1997). p. 243-93. doi: 10.1007/978-1-4757-9625-4_6
71. Stevens FL, Hurley RA, Taber KH. Anterior cingulate cortex: unique role in cognition and emotion. *J Neuropsychiatry Clin Neurosci.* (2011) 23:121–5. doi: 10.1176/jnp.23.2.jnp121
72. Devinsky O, Morrell MJ, Vogt BA. Contributions of anterior cingulate cortex to behavior. *Brain.* (1995) 118:279–306. doi: 10.1093/brain/118.1.279
73. Fleysher R, Fleysher L, Liu S, Gonen O. On the voxel size and magnetic field strength dependence of spectral resolution in magnetic resonance spectroscopy. *Magn Reson Imaging.* (2009) 27:222–32. doi: 10.1016/j.mri.2008.06.009
74. Falkenberg LE, Westerhausen R, Craven AR, Johnsen E, Kroken RA, Loerg EM, et al. Impact of glutamate levels on neuronal response and cognitive abilities in schizophrenia. *NeuroImage Clin.* (2014) 4:576–84. doi: 10.1016/j.nicl.2014.03.014
75. Gallinat J, Kunz D, Senkowski D, Kienast T, Seifert F, Schubert F, et al. Hippocampal glutamate concentration predicts cerebral theta oscillations during cognitive processing. *Psychopharmacology.* (2006) 187:103–11. doi: 10.1007/s00213-006-0397-0
76. Merritt K, Egerton A, Kempton MJ, Taylor MJ, McGuire PK. Nature of glutamate alterations in schizophrenia: a meta-analysis of proton magnetic resonance spectroscopy studies. *JAMA Psychiatry.* (2016) 73:665–74. doi: 10.1001/jamapsychiatry.2016.0442
77. Hashimoto T, Volk DW, Eggan SM, Mirnics K, Pierri JN, Sun Z, et al. Gene expression deficits in a subclass of GABA neurons in the prefrontal cortex of subjects with schizophrenia. *J Neurosci.* (2003) 23:6315–26. doi: 10.1523/JNEUROSCI.23-15-06315.2003
78. Yang AC, Tsai SJ. New targets for schizophrenia treatment beyond the dopamine hypothesis. *Int J Mol Sci.* (2017) 18:1689. doi: 10.3390/ijms18081689
79. Sanacora G, Zarate CA, Krystal JH, Manji HK. Targeting the glutamatergic system to develop novel, improved therapeutics for mood disorders. *Nat Rev Drug Discov.* (2008) 7:426–37. doi: 10.1038/nrd2462
80. Chang L, Jiang CS, Ernst T. Effects of age and sex on brain glutamate and other metabolites. *Magnetic Resonance Imaging.* (2009) 27:142–5. doi: 10.1016/j.mri.2008.06.002
81. Gao F, Edden RAE, Li M, Puts NAJ, Wang G, Liu C, et al. Edited magnetic resonance spectroscopy detects an age-related decline in brain GABA levels. *NeuroImage.* (2013) 78:75–82. doi: 10.1016/j.neuroimage.2013.04.012
82. Sailasuta N, Ernst T, Chang L. Regional variations and the effects of age and gender on glutamate concentrations in the human brain. *Magnetic Resonance Imaging.* (2008) 26:667–75. doi: 10.1016/j.mri.2007.06.007
83. O'Gorman RL, Michels L, Edden RA, Murdoch JB, Martin E. *In vivo* detection of GABA and glutamate with MEGA-PRESS: reproducibility and gender effects. *J Magnetic Resonance Imaging.* (2011) 33:1262–7. doi: 10.1002/jmri.22520
84. Canitano R, Pallagrosi M. Autism spectrum disorders and schizophrenia spectrum disorders: excitation/inhibition imbalance and developmental trajectories. *Front Psychiatry.* (2017) 8:69. doi: 10.3389/fpsyt.2017.00069

85. Horder J, Petrinovic MM, Mendez MA, Bruns A, Takumi T, Spooren W, et al. Glutamate and GABA in autism spectrum disorder—a translational magnetic resonance spectroscopy study in man and rodent models. *Translational Psychiatry.* (2018) 8:106. doi: 10.1038/s41398-018-0155-1
86. Delmonte S, Balsters JH, McGrath J, Fitzgerald J, Brennan S, Fagan AJ, et al. Social and monetary reward processing in autism spectrum disorders. *Mol Autism.* (2012) 3:1–13. doi: 10.1186/2040-2392-3-7
87. Kohls G, Schulte-Rüther M, Nehrkorn B, Müller K, Fink GR, Kamp-Becker I, et al. Reward system dysfunction in autism spectrum disorders. *Social Cognitive Affective Neurosci.* (2013) 8:565–72. doi: 10.1093/scan/nss033

Conflict of Interest: The authors declare that the research was conducted in the absence of any commercial or financial relationships that could be construed as a potential conflict of interest.

frontiers in Human Neuroscience

ORIGINAL RESEARCH
published: 24 March 2021
doi: 10.3389/fnhum.2021.644079

Simultaneous Measurement of the BOLD Effect and Metabolic Changes in Response to Visual Stimulation Using the MEGA-PRESS Sequence at 3 T

Gerard Eric Dwyer[1,2*], *Alexander R. Craven*[1,2,3], *Justyna Bereśniewicz*[1,2], *Katarzyna Kazimierczak*[1,4], *Lars Ersland*[1,2,3], *Kenneth Hugdahl*[1,5,6] *and Renate Grüner*[2,4,5,7]

[1] *Department of Biological and Medical Psychology, University of Bergen, Bergen, Norway,* [2] *NORMENT Centre of Excellence, Haukeland University Hospital, Bergen, Norway,* [3] *Department of Clinical Engineering, Haukeland University Hospital, Bergen, Norway,* [4] *Mohn Medical Imaging and Visualization Centre, Haukeland University Hospital, University of Bergen, Bergen, Norway,* [5] *Department of Radiology, Haukeland University Hospital, Bergen, Norway,* [6] *Division of Psychiatry, Haukeland University Hospital, Bergen, Norway,* [7] *Department of Physics and Technology, University of Bergen, Bergen, Norway*

OPEN ACCESS

Edited by:
Maria Concepcion Garcia Otaduy, University of São Paulo, Brazil

Reviewed by:
Adam Steel, Dartmouth College, United States
Hironaka Igarashi, Niigata University, Japan

***Correspondence:**
Gerard Eric Dwyer
gerard.dwyer@uib.no

Specialty section:
This article was submitted to Brain Imaging and Stimulation, a section of the journal Frontiers in Human Neuroscience

Received: *19 December 2020*
Accepted: *26 February 2021*
Published: *24 March 2021*

Citation:
Dwyer GE, Craven AR, Bereśniewicz J, Kazimierczak K, Ersland L, Hugdahl K and Grüner R (2021) Simultaneous Measurement of the BOLD Effect and Metabolic Changes in Response to Visual Stimulation Using the MEGA-PRESS Sequence at 3 T. Front. Hum. Neurosci. 15:644079. doi: 10.3389/fnhum.2021.644079

The blood oxygen level dependent (BOLD) effect that provides the contrast in functional magnetic resonance imaging (fMRI) has been demonstrated to affect the linewidth of spectral peaks as measured with magnetic resonance spectroscopy (MRS) and through this, may be used as an indirect measure of cerebral blood flow related to neural activity. By acquiring MR-spectra interleaved with frames without water suppression, it may be possible to image the BOLD effect and associated metabolic changes simultaneously through changes in the linewidth of the unsuppressed water peak. The purpose of this study was to implement this approach with the MEGA-PRESS sequence, widely considered to be the standard sequence for quantitative measurement of GABA at field strengths of 3 T and lower, to observe how changes in both glutamate (measured as Glx) and GABA levels may relate to changes due to the BOLD effect. MR-spectra and fMRI were acquired from the occipital cortex (OCC) of 20 healthy participants whilst undergoing intrascanner visual stimulation in the form of a red and black radial checkerboard, alternating at 8 Hz, in 90 s blocks comprising 30 s of visual stimulation followed by 60 s of rest. Results show very strong agreement between the changes in the linewidth of the unsuppressed water signal and the canonical haemodynamic response function as well as a strong, negative, but not statistically significant, correlation with the Glx signal as measured from the OFF spectra in MEGA-PRESS pairs. Findings from this experiment suggest that the unsuppressed water signal provides a reliable measure of the BOLD effect and that correlations with associated changes in GABA and Glx levels may also be measured. However, discrepancies between metabolite levels as measured from the difference and OFF spectra raise questions regarding the reliability of the respective methods.

Keywords: functional, spectroscopy, MRS, GABA, glutamate

INTRODUCTION

Performing magnetic resonance spectroscopy (MRS) in a time-resolved or functional manner makes it an ideal complement to functional magnetic resonance imaging (fMRI) in that it has the potential to allow patterns of neural activity to be related to associated biochemical events. Due to their roles as the principal excitatory and inhibitory neurotransmitters in the human brain, functional MRS studies have largely focused on dynamic changes in glutamate, or a composite signal of glutamate and glutamine denoted "Glx," and γ-aminobutyric acid (GABA) levels. To date, functional spectroscopy paradigms have been used to measure increases in glutamate and lactate in the occipital cortex (OCC) in response to visual stimulation (Mangia et al., 2006, 2007; Lin et al., 2012; Schaller et al., 2013; Bednarík et al., 2015; Mekle et al., 2017; Boillat et al., 2019), changes in glutamate in the anterior cingulate cortex (ACC) and insula in response to pain (Mullins et al., 2005; Gussew et al., 2010; Gutzeit et al., 2011; Cleve et al., 2017) as well as dynamic changes in GABA in the sensorimotor cortex in response to learning (Floyer-Lea et al., 2006) and in the dorsolateral prefrontal cortex (DLPFC) under a working memory task (Michels et al., 2012).

Activity within a neural circuit may be characterized in terms of the balance of excitatory and inhibitory inputs to the circuit, commonly referred to as the excitation-inhibition balance (Denève and Machens, 2016; Jardri et al., 2016). As Isaacson and Scanziani (2011) illustrate, inhibition plays a critical role in shaping spontaneous and sensory-evoked cortical activity, placing a particular importance on the ability to quantify GABA in understanding the relationship between neural activity and the excitation-inhibition balance. Furthermore, where glutamate serves a myriad of functions in addition to its role as a neurotransmitter, including its roles in energy metabolism, protein synthesis and as a precursor to GABA (Agarwal and Renshaw, 2012; Mangia et al., 2012), in the brain GABA is almost exclusively a neurotransmitter, suggesting that changes in GABA levels as measured with MRS are likely to be more closely related to changes in the excitation-inhibition balance and synaptic transmission.

As challenging as it may be to investigate relationships between neural activity and glutamate or Glx, investigating relationships with GABA are further complicated by factors such as the relatively low biological concentration of GABA and significant spectral overlap with other more abundant metabolites. At lower field strengths (i.e., $\leq$3 T) many spectroscopy sequences may not sufficiently resolve GABA signals for accurate quantification (Gussew et al., 2010; Siniatchkin et al., 2012; Apšvalka et al., 2015). The MEGA-PRESS (MEscher-GArwood Point RESolved Spectroscopy) sequence (Mescher et al., 1998), widely considered to be the standard for performing MRS of GABA at field strengths of 3 T or less (Mullins et al., 2014), may facilitate accurate quantification of GABA, but requires the acquisition of two interleaved spectral datasets: one with a frequency selective editing pulse ("ON" spectrum) and one without ("OFF" spectrum) to create a difference spectrum, effectively reducing temporal resolution and complicating its implementation for functional paradigms.

Despite the usefulness of functional MRS, many implementations give no indication of neural activity or how it relates to changes in measured metabolite levels. Similarly, the blood oxygen level dependent (BOLD) effect that provides the contrast used in BOLD-fMRI provides a measure of changes in cerebral blood flow, which infers neural activity, but says little about its nature. However, the BOLD effect also induces a decrease in R_2^* rate, i.e., the inverse of T_2^*, resulting in a decrease in linewidth and increase in height of spectral peaks (Just, 2020). Previous studies have utilized this phenomenon as an indirect measurement of the BOLD effect through changes in the linewidth of an unsuppressed water signal (Hennig et al., 1994; Frahm et al., 1996; Zhu and Chen, 2001). By interleaving spectral frames with and without water suppression, Apšvalka et al. (2015) demonstrated that it may be possible to exploit this effect to perform functional measurement of both the BOLD effect and related changes in Glx levels simultaneously.

The purpose of this study was to implement this approach with a GABA specific MEGA-PRESS sequence at 3 T, effectively permitting simultaneous functional imaging of the BOLD effect and changes in both Glx and GABA levels with the linewidth of the unsuppressed water signal as an indirect measure of the BOLD effect. MR-spectra were acquired from the occipital cortex (OCC) in response to visual stimulation in the form of a red-black radial checkerboard, alternating at a frequency of 8 Hz, a stimulation paradigm previously demonstrated to induce a measurable positive BOLD response (Kwong et al., 1992; Ogawa et al., 1992) and metabolic changes in the OCC (Mangia et al., 2006, 2007; Ip et al., 2017; Boillat et al., 2019). Previous studies suggest that visual stimulation will induce a measurable increase in Glx levels (Mangia et al., 2006, 2007; Ip et al., 2017; Boillat et al., 2019) and a possible decrease in GABA levels (Lin et al., 2012; Bednarík et al., 2015; Mekle et al., 2017). Assessment of activity through BOLD related linewidth changes predicts a significant difference in the linewidth of the unsuppressed water signal between spectra acquired during stimulation and at rest.

MATERIALS AND METHODS

This study was conducted under regional review board approved protocols (REK-Vest, REK case number 2016/1629) with written informed consent from all participants.

Participants

The participant group for this study comprised 20 healthy individuals (mean age: 29 years, range: 20–40 years, 11 male). Based on self-report, participants were free from psychiatric and neurological conditions, and not currently using any psychoactive/psychotropic substances.

MR-Imaging and Spectroscopy

All imaging and spectroscopy was performed on a 3 T GE 750 Discovery Scanner from GE Healthcare (General Electric, Milwaukee, United States of America) using a standard 8-channel head coil from Invivo (Invivo corp., Gainsville, Florida, United States of America).

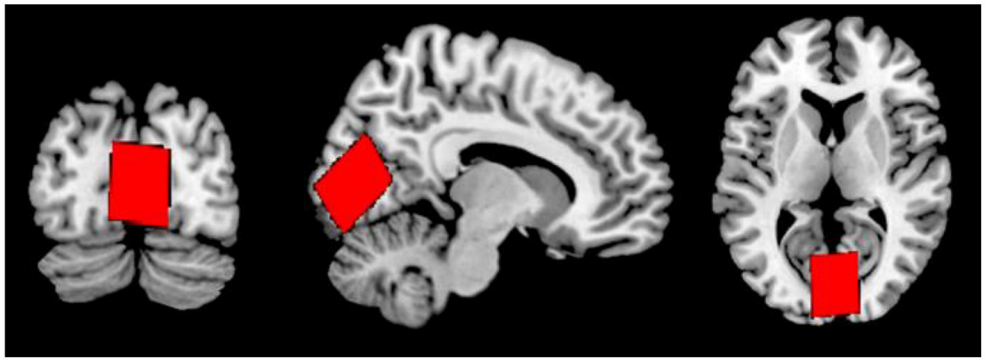

FIGURE 1 | Voxel placement in the midline OCC in coronal (left), sagittal (middle), and axial (right) views.

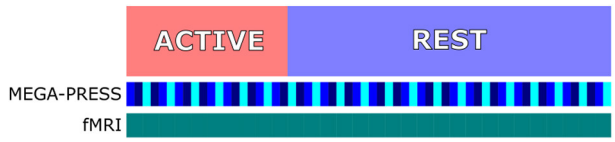

FIGURE 2 | Experimental design showing one 90 s round of a 30 s active block (red) and 60 s rest block (blue). MEGA-PRESS spectra acquired with water suppression and editing pulse ("ON," blue), with water suppression and without editing pulse ("OFF," dark blue), and without water suppression or editing pulse ("REF" light blue). fMRI volumes acquired continuously with one volume acquired every 3 s (green).

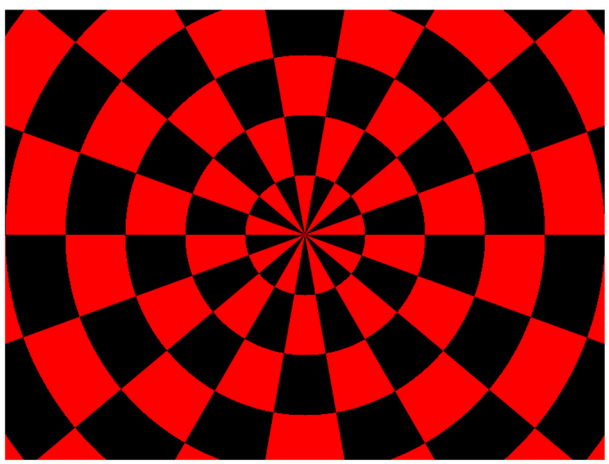

FIGURE 3 | Radial red and black checkerboard used for visual stimulation.

Following a 3-plane localiser sequence (2D Spin Echo, TE = 80 ms, FOV = 240 mm, slice thickness = 8 mm, slice spacing = 15 mm) structural anatomical imaging was performed using a 3D T1 weighted fast spoiled gradient sequence (number of slices = 192, slice thickness = 1.0 mm, repetition time (TR) = 7.8 ms, echo time (TE) = 2.95 ms, field of view = 260 × 260 mm^2, flip angle = 14 degrees, matrix = 256 × 256). These structural images were used to position a 31 × 26 × 24 mm^3 voxel in the midline occipital cortex, across the longitudinal fissure and angled parallel to the parieto-occipital sulcus (**Figure 1**).

Spectroscopy was performed using a GABA-specific MEGA-PRESS sequence (Mescher et al., 1998) (TE/TR = 68/1500 ms, editing pulses at 1.9 and 7.5 ppm) consisting of 600 spectral frames for a total acquisition time of 15 min and 30 s with an additional 16 frames acquired without water suppression to be used for scaling in quantitative metabolite estimates. Shimming, RF calibration and frequency adjustment were performed using an automated pre-scan prior to each spectral acquisition, providing a measure of the linewidth of the unsuppressed water signal that would be used in assessment of spectral quality. Spectra were acquired in groups of six spectral frames, first with water suppression and the MEGA-editing refocusing pulse ("ON"), secondly with water suppression and without the editing pulse ("OFF"), and thirdly without the editing pulse and without water suppression ("REF"), then with the ON and OFF spectra acquired in reverse order before the next reference frame (i.e., ON—OFF—REF—OFF—ON—REF repeated, **Figure 2**).

Following spectroscopy, BOLD-fMRI was performed using an echo-planar imaging (EPI) sequence (TR = 3000 ms, TE = 30 ms, image matrix = 96 × 96, FOV = 220 mm, flip angle = 90°, slice thickness = 3.0 mm, slice spacing 0.5 mm) with the same visual stimulation parameters, also for a total of 15 min and 30 s. In order to minimize the effects of thermal frequency drift on spectra, fMRI data were acquired after MRS for all participants.

Visual stimulation was delivered to participants through a set of MR-compatible binocular video goggles (NordicNeurolab Inc., Bergen, Norway) as an alternating, red-black, radial checkerboard (**Figure 3**) flickering at 8 Hz. Stimulation was delivered in blocks of 30 s followed by 1 min of a white fixation cross on black background, repeated for 8 blocks, with 2 min of fixation cross presented before the first and after the final stimulus presentation.

Spectral Analysis

Following zero and first order phase correction, coil combination and frequency alignment, ON and OFF pairs were combined to produce MEGA-PRESS difference spectra providing quantitative

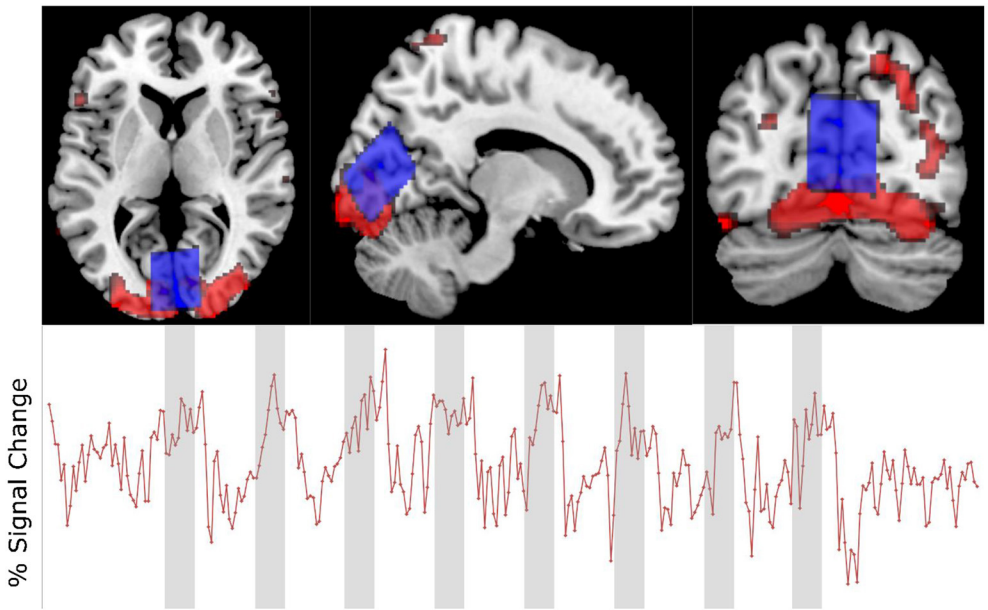

FIGURE 4 | Upper: Voxel placement (blue) and activation map (red) in one participant. Lower: fMRI time course of same participant showing % signal change.

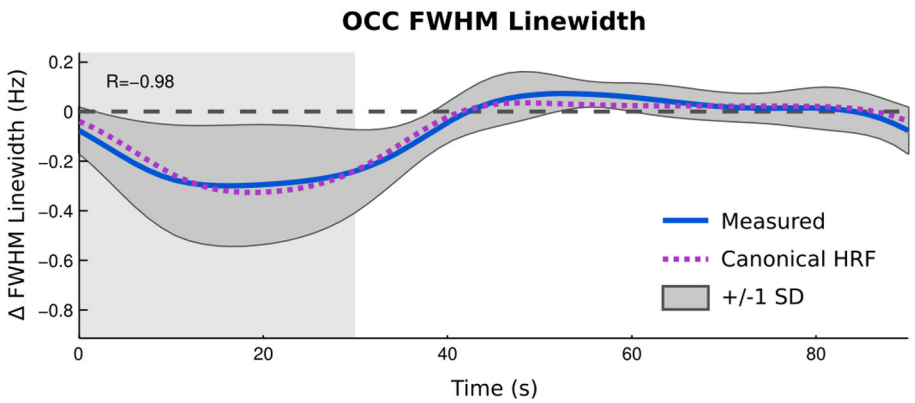

FIGURE 5 | Time resolved analysis of changes in FWHM of unsuppressed water signal compared to predicted BOLD response between active blocks (gray background) and rest (white background). Zero line indicates average linewidth during rest blocks.

estimates of Glx, GABA, and NAA. MEGA-PRESS OFF spectra were used to provide quantitative estimates of Glx, NAA, Creatine, Choline, lactate and glucose, equivalent to a PRESS sequence with TE = 68 ms. For each participant, four spectra were produced, a difference and OFF spectrum containing all frames acquired during visual stimulation blocks, referred to as the "Active" condition, and a difference and OFF spectrum containing all frames acquired as the white fixation cross was present, referred to as the "Rest" condition (**Figure 2**).

Quantitative spectral analysis was performed with LCModel (version 6.3-1J) (Provencher, 1993, 2001) using a simulated basis set (Dydak et al., 2011) with Kaiser coupling constants (Kaiser et al., 2008) to provide quantitative estimates of Glx, GABA and *N*-acetyl aspartate (NAA) from the MEGA-PRESS difference spectra, and from the OFF spectra in the MEGA-PRESS pairs: Glx (Glx OFF), NAA (NAA OFF), creatine (Cr OFF), choline (Cho OFF), lactate (Lac OFF), and glucose (Glc OFF).

It is important to note that when performing MEGA-edited GABA spectroscopy, co-edited macromolecule resonances contaminate the GABA signal. Thus, when referring to GABA as measured with a MEGA-PRESS sequence in this study, this refers to both GABA and the co-edited macromolecule (Edden et al., 2012).

Unsuppressed Water Signal Analysis

In order to investigate how changes in the linewidth of the unsuppressed water signal relate to the haemodynamic response function (HRF), and how they may be used as a proxy measure of neural activity in the same manner as BOLD-fMRI, a response curve was constructed as a time course of the response for each

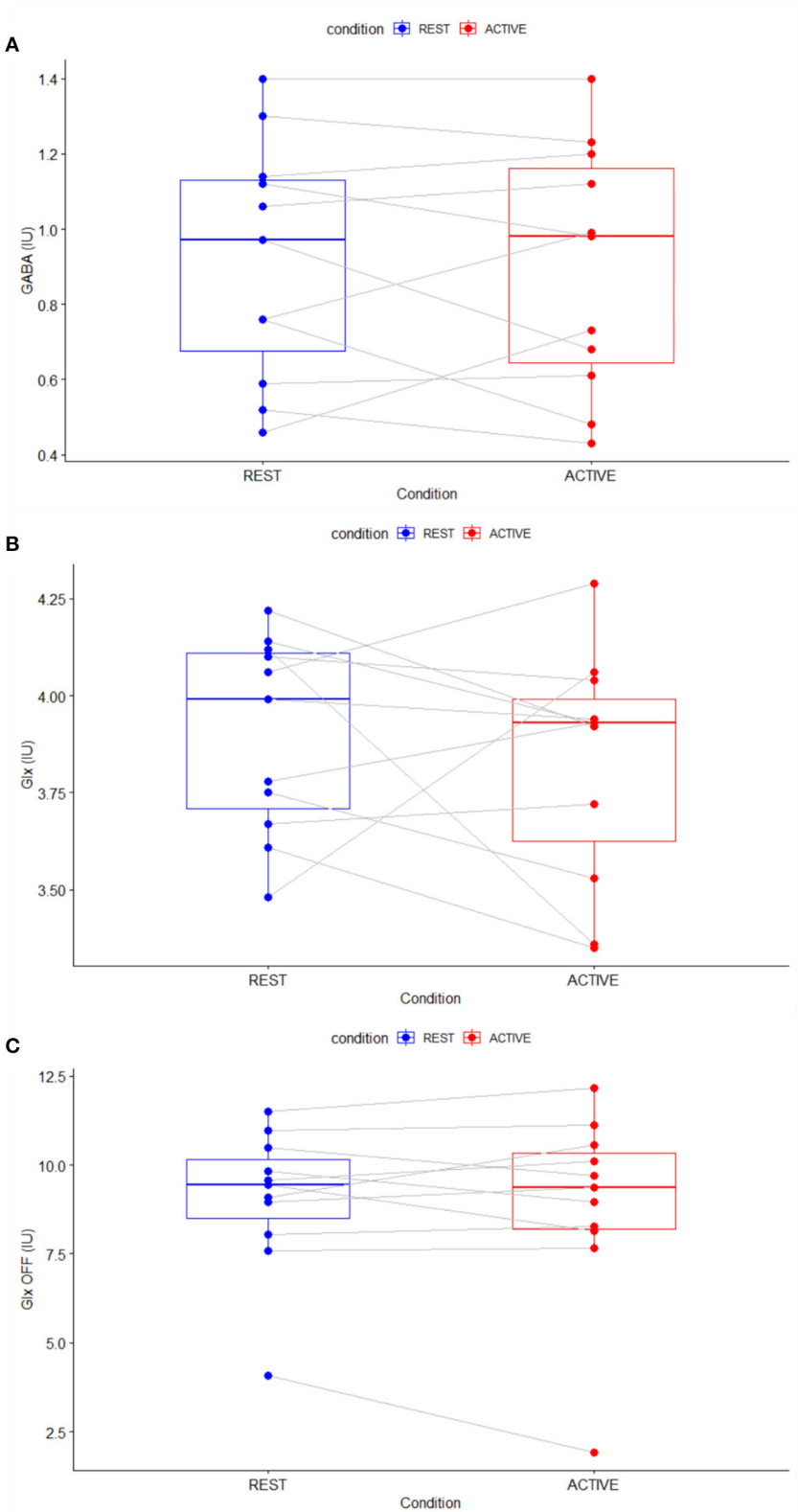

FIGURE 6 | Parallel difference plots showing difference in metabolite levels between rest (blue) and active (red) conditions for GABA **(A)**, Glx **(B)**, and Glx measured from the OFF spectra **(C)**.

TABLE 1 | Metabolite estimates and Cramér-Rao lower bounds (%SD) for the active and rest conditions (*Mean, SD*) with results of repeated-measures *t*-tests.

Metabolite	Active (IU)	Active %SD	Rest (IU)	Rest %SD	Mean of the difference	*t*	*p*
GABA	0.89 (0.33)	18.27 (11.64)	0.92 (0.32)	18.18 (14.87)	−0.02	−0.39	0.71
Glx	3.82 (0.30)	8.36 (2.50)	3.90 (0.25)	7.45 (3.17)	−0.08	−0.75	0.47
NAA	6.03 (0.60)	1.64 (0.50)	6.23 (0.78)	1.36 (0.50)	−0.20	−1.43	0.18
Glx OFF	8.91 (2.68)	11.18 (11.91)	9.05 (2.02)	8.91 (4.46)	−0.14	−0.46	0.65
NAA OFF	14.22 (4.16)	2.00 (2.05)	14.14 (4.18)	1.91 (2.07)	0.08	0.77	0.45
Cr	9.08 (0.93)	4.71 (0.90)	8.98 (0.74)	4.67 (0.74)	0.09	1.22	0.25
Cho	1.53 (0.23)	1.84 (6.11)	1.51 (0.20)	0.45 (1.51)	0.02	0.92	0.38
Lac	0.67 (0.71)	304.64 (446.44)	0.31 (0.33)	282.00 (365.40)	0.36	1.53	0.16
Glc	2.79 (0.51)	19.45 (4.03)	2.66 (0.92)	22.00 (8.10)	0.13	0.76	0.46

TABLE 2 | Correlation matrix for differences between active and rest for linewidth of the unsuppressed water signal (H_2O) and measured metabolites.

	Correlation (Pearson's r)									
	H_2O	**GABA**	**Glx**	**NAA**	**Glx OFF**	**NAA OFF**	**Cr**	**Cho**	**Lac**	**Glc**
H_2O	1.00									
GABA	0.40	1.00								
Glx	0.14	−0.25	1.00							
NAA	−0.06	−0.60	0.76	1.00						
Glx OFF	−0.66	−0.56	0.29	0.37	1.00					
NAA OFF	0.15	0.39	−0.23	−0.19	−0.38	1.00				
Cr	0.51	−0.25	−0.19	−0.04	−0.27	0.18	1.00			
Cho	0.53	−0.15	−0.33	−0.05	−0.37	0.02	0.86	1.00		
Lac	−0.08	0.01	−0.17	−0.07	0.33	−0.04	0.05	0.22	1.00	
Glc	0.08	0.66	0.10	−0.18	−0.28	0.06	−0.48	−0.22	0.23	1.00
	***p*-values (lower) and FDR-adjusted *p*-values (upper)**									
H_2O		0.83	0.93	0.95	0.31	0.93	0.62	0.62	0.95	0.95
GABA	0.22		0.91	0.48	0.54	0.83	0.91	0.93	0.99	0.31
Glx	0.68	0.46		0.15	0.91	0.91	0.91	0.91	0.91	0.95
NAA	0.87	0.05	0.01		0.83	0.91	0.95	0.95	0.95	0.91
Glx OFF	0.03	0.07	0.38	0.26		0.83	0.91	0.83	0.91	0.91
NAA OFF	0.67	0.24	0.49	0.58	0.25		0.91	0.97	0.95	0.95
Cr	0.11	0.46	0.58	0.90	0.42	0.59		0.03	0.95	0.67
Cho	0.10	0.65	0.33	0.89	0.26	0.95	0.00		0.91	0.91
Lac	0.82	0.99	0.61	0.84	0.33	0.91	0.89	0.51		0.91
Glc	0.81	0.03	0.78	0.60	0.41	0.87	0.13	0.52	0.51	

stimulation block for each subject based on a method previously used by Brix et al. (2017) for investigating reproducibility of GABA measurements.

Linewidth was measured as the full-width at half-maximum (FWHM) in Hz. The time course was constructed using a Gaussian-weighted combination of between 60 and 100 time points of the FWHM of the unsuppressed water signal to produce a curve reflecting the change in FWHM of the unsuppressed water signal over the course of each 90 s stimulation block, including both active and rest periods.

Correlation was performed between the time courses for unsuppressed water FWHM and the task model convolved with a canonical haemodynamic response function (HRF) from the Statistical Parametrical Mapping software toolkit version 12 (SPM12, http://www.fil.ion.ucl.ac.uk/spm/).

fMRI Analysis

Prior to analysis, all fMRI volumes acquired using the EPI sequence were converted from DICOM to NIfTI format using the dcm2nii program (http://people.cas.sc.edu/rorden/mricron/dcm2nii.html). Pre-processing of the converted images was performed using the Matlab/SPM based toolbox CONN (Whitfield-Gabrieli and Nieto-Castanon, 2012). Volumes were realigned to the first volume in each set and unwarped to correct for subject motion (Friston et al., 1995) then spatially normalized to an EPI template based on the Montreal Neurological Institute

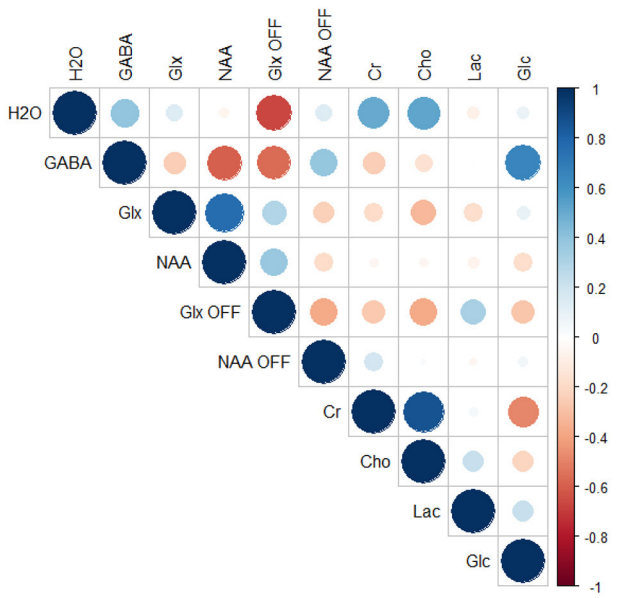

FIGURE 7 | Correlation plot depicting differences in linewidth of unsuppressed water signal (H_2O) and all measured metabolites.

(MNI) standard reference brain (Evans et al., 1992). Images were finally smoothed through spatial convolution with a 5 mm Gaussian kernel.

Following pre-processing, beta values (i.e., parameter estimates in the general linear model) were extracted from a region of interest defined by a mask based on the placement of the spectroscopy voxel for each participant, using an in-house script drawing on the tools for NIfTI and ANALYZE image toolbox (https://se.mathworks.com/matlabcentral/fileexchange/8797-tools-for-nifti-and-analyze-image).

Statistical Analyses

All statistical analyses were performed using R (R Development Core Team, 2020). Repeated measures *t*-tests were performed comparing the measured linewidth of the unsuppressed water signal (i.e., the measured difference, not subject to convolution with the HRF) and LCModel estimates for each of the measured metabolites between the rest and active conditions for each participant.

In order to investigate how changes in metabolite levels may relate both to one another and to changes in the local BOLD response, particularly with respect to the excitation/inhibition balance and Glx and GABA levels within the region (Isaacson and Scanziani, 2011), a correlation analysis was performed on the differences in all measured metabolite levels and the difference in unsuppressed water signal linewidth changes as measured (i.e., not subject to convolution with the HRF) between the active and rest blocks. Given the multiple comparisons performed as part of the correlation matrix, *p*-values for the correlation analysis were adjusted for using the false discovery rate (FDR) method (Benjamini and Hochberg, 1995; Benjamini and Yekutieli, 2001) as part of the p.adjust function in the R base package. Significance was tested at $\alpha = 0.05$, results were considered statistically significant if the FDR adjusted *p*-value was <0.05.

RESULTS

Due to poor quality data or withdrawal before fMRI data could be acquired, four participants were excluded from fMRI analyses. The resulting participant group for the fMRI analysis component comprised 16 individuals (mean age: 29 years, range: 20–40 years, 10 male).

The fMRI data showed that the visual stimulation paradigm used elicited a positive BOLD response within the region of interest (**Figure 4**) with a mean difference in intensity between the active and rest blocks that was statistically significant [$t(15) = 6.62$, $p < 0.001$].

Figure 5 depicts the changes in the FWHM of the unsuppressed water signal reconstructed as a time-resolved curve. Linewidth changes in the unsuppressed water signal showed a very strong correlation between the group average of time courses for unsuppressed water FWHM and the task model convolved with a canonical haemodynamic response function (HRF) and the predicted haemodynamic response ($r = -0.98$, $p < 0.001$) with a mean change in FWHM between the active and rest blocks of 1.2%.

Prior to statistical analysis, spectral quality was assessed based on FWHM of the unsuppressed water peak measured during the automated prescan and Cramér-Rao lower bounds (%SD) for quantitative estimates provided by LCModel. Spectra with a prescan FWHM >12 Hz and %SD for GABA, Glx or Glx OFF great than or equal to 50 were excluded from further analyses. The resulting participant group for the MRS analysis comprised 11 individuals (mean age: 30 years, range: 21–40, seven male).

Repeated measures *t*-tests revealed no significant difference between the active and rest conditions for the linewidth of the unsuppressed water signal as it was measured [$t(10) = 0.09$, $p = 0.92$]. There were also no significant changes in GABA [$t(10) = -0.39$, $p = 0.71$] or Glx levels whether measured from the difference spectra [$t(10) = -0.75$, $p = 0.47$] or the OFF spectra [$t(10) = -0.46$, $p = 0.66$] (**Figure 6**). Differences were found in NAA levels as measured from the difference spectrum [$t(10) = -1.43$, $p = 0.18$] but did not reach statistical significance at the $\alpha = 0.05$ level. Full results from the repeated measures *t*-tests are presented in **Table 1**.

Correlation analysis of the differences between the active and rest blocks revealed a moderate negative correlation between the change in the measured water peak linewidth and the change in Glx as measured from the OFF spectra ($r = -0.66$, $p = 0.03$, FDR adjusted $p = 0.31$) but not from the difference spectra ($r = 0.14$, $p = 0.67$, FDR adjusted $p = 0.93$). Correlations were also observed between GABA levels as measured from the difference spectra and NAA ($r = -0.60$, $p = 0.05$, FDR adjusted $p = 0.48$) and glucose ($r = 0.66$, $p = 0.03$, FDR adjusted $p = 0.31$), and a moderate negative correlation was observed between GABA and Glx as measured from the OFF spectra ($r = -0.56$, $p = 0.07$, FDR adjusted $p = 0.54$). However, none of these correlations were statistically significant when accounting for

multiple comparisons. Full results from the correlation analysis are provided in **Table 2** and depicted graphically in a correlation plot in **Figure 7**.

DISCUSSION

The purpose of this study was to determine whether a MEGA-PRESS sequence, modified to include spectral frames without water suppression, could be used to perform simultaneous measurement of the BOLD effect and associated metabolic changes. This implementation is based on one previously used by Apšvalka et al. (2015) with a PRESS sequence (TE/TR = 105/1500 ms) for simultaneous measurement of the BOLD effect and glutamate dynamics in response to a repetition suppression paradigm. The advantage to this implementation with a MEGA-PRESS sequence is the ability to measure both GABA and glutamate (as Glx) dynamics at a field strength of 3 T. The results show that the unsuppressed water signal provides a reliable measure of the BOLD effect, and the experimental design and analysis methods used allow differences in the water signal linewidth and differences in metabolite levels to be assessed in terms of how they correlated with one another. However, this study also illustrates a number of problems regarding the use of spectral editing methods in functional spectroscopy paradigms.

One of the issues adversely affecting this this study was the amount of data that had to be excluded from analysis as part of the MRS component. Though 20 participants were scanned, nine were excluded from final analyses, mostly due to large errors surrounding metabolite estimates. Though small, this number is comparable to other, similar studies employing fMRS paradigms (e.g., $N = 13$ (Apšvalka et al., 2015), $N = 13$ (Kupers et al., 2009), $N = 12$ (Mullins et al., 2005). A power analysis conducted with G*power (Faul et al., 2009) found that the correlation analysis component of this study had sufficient power to detect a medium to strong effect (for $d > 0.6$, $1–\beta = 0.74$, $\alpha = 0.05$). However, for changes in Glx and GABA in the OCC in response to visual stimulation, the effect may be much smaller.

According to both the fMRI acquisition and the changes in the FWHM of the unsuppressed water signal, the visual stimulation paradigm used in this experiment was able to elicit a BOLD effect in the area of interest (**Figure 4**). The agreement between the changes in FWHM over the course of a 90 s experimental block and the modeled response show that the unsuppressed water signal provides a reliable measure of the BOLD effect (**Figure 5**), echoing the findings of Frahm et al. (1996) and Hennig et al. (1994) who, in the early days of fMRI suggested that it could be a useful alternative on systems where appropriate imaging sequences could not be implemented.

Despite this, measuring changes in spectral linewidth offers little advantage over conventional BOLD-fMRI in measuring haemodynamic responses. The advantage to this method was the ability to measure both the BOLD response and associated metabolic changes. The repeated measures *t*-tests revealed no significant changes between the rest and active conditions, and while the correlation analysis similarly revealed no statistically significant correlations when adjusted for multiple comparisons, a number of the finds warrant further discussion.

The observed correlation between the change in water signal linewidth and Glx OFF is consistent with many of the common findings from both fMRS and combined fMRI/MRS studies that glutamate or Glx levels correlate positively with a positive BOLD signal or a task/stimulus positive condition (Mullins et al., 2005; Mangia et al., 2007; Gussew et al., 2010; Lin et al., 2012; Apšvalka et al., 2015; Bednařík et al., 2015; Cleve et al., 2015; Ip et al., 2017). It is worth bearing in mind that the linewidth of the water signal is expected to decrease as a result of the BOLD effect, hence the negative correlation. What is interesting, however, is that the correlation was only observed in the Glx signal as measured from the MEGA-PRESS OFF spectrum, and not from the difference spectrum.

Although previous studies have found the MEGA-PRESS sequence to be comparable to standard short echo time PRESS sequences for quantitative estimates of the Glx signal (Henry et al., 2011), the presence of such a strong, positive correlation between Glx measured from the OFF spectra but not from the difference spectra raises questions regarding both the accuracy and sensitivity of the two approaches to quantifying Glx when using the MEGA-PRESS sequence. Maddock et al. (2018) compared the two measurements of the Glx signal, i.e., from the difference and OFF spectra from a MEGA-PRESS sequence (TE/TR = 68/1500 ms), with the Glx signal from a glutamate optimized PRESS sequence (TE/TR = 80/1500 ms) and found that in healthy participants, Glx measured from the OFF spectra correlated much more strongly ($r \geq 0.88$) than the difference spectra ($r \leq 0.36$) with the PRESS measurements. This discrepancy suggests that difference spectra may not be as sensitive to dynamic changes in metabolite levels as unedited spectra, but as there is no alternative measure for GABA in the OFF-spectra, there is insufficient evidence to determine how it applies to GABA in this study. It is possible that the reduced amount of spectral information available in the difference spectrum makes it less sensitive to dynamic changes.

In addition to being considered the optimal method for quantitative measures of GABA at field strengths of 3 T and lower, the findings of Mullins (2018) suggest that another benefit to measuring GABA with the MEGA-PRESS sequence, particularly in a functional capacity, may be the ability to distinguish synaptic GABA from vesicular GABA. Due to restrictions on their ability to tumble and move when packaged in synaptic vesicles, vesicular neurotransmitters may have a shorter T_2 time than neurotransmitters in the cytosol or synapse. Using short echo time sequences (i.e., ≤15 ms) such as those frequently used with STEAM sequences and similar at 7 T, the measurement of neurotransmitters such as glutamate and GABA include contributions from both the vesicular and synaptic compartments, whereas with a longer echo time sequence, vesicular neurotransmitter signals may have dephased to the extent that they no longer contribute significantly to the measured signal. Thus, measurements performed with longer echo time sequences may more accurately reflect changes related to GABAergic synaptic transmission.

Though not statistically significant when adjusted for multiple comparisons, it is worth noting that a negative correlation was observed between Glx OFF and GABA ($r = -0.56$, $p = 0.07$, FDR adjusted $p = 0.54$). This observation is also consistent with previous studies finding that GABA levels correlate negatively with BOLD or a task/stimulus positive condition (Lin et al., 2012; Bednarík et al., 2015; Cleve et al., 2015; Chen et al., 2017; Just and Sonnay, 2017; Mekle et al., 2017) but further suggest a relationship between glutamate and GABA within neural circuits. GABA levels did not show a statistically significant correlation with the FWHM of the water signal, though the differences between Glx signals from the difference and OFF spectra suggest that in a similar fashion, the difference spectrum lacks sufficient spectral information to detect changes with sensitivity comparable to the OFF spectra. Options for measuring GABA in a functional manner at 3 T without spectral editing do exist, such as the STEAM sequence (TE = 20 ms) as used by Kupers et al. (2009) and SPECIAL sequence (TE = 8.5 ms) used by Kühn et al. (2016), both of which were able to measure large, significant changes in GABA in the ACC. In light of the issues raised by this study, they may provide a promising alternative for functional imaging of the BOLD effect and metabolic changes and their use warrants further investigation. However, as stated previously, short echo time sequences may include contributions from vesicular, cytosolic and synaptic GABA, making them less sensitive to compartmental changes in GABA.

The visual stimulation paradigm used in this study was chosen as previous studies have shown it to unambiguously produce a positive BOLD response in the visual cortex, a part of the brain ideal for fMRS experiments as it typically allows placement of a large voxel away from areas of air, bone or fluid that typically contribute to spectral artifacts, and it is typically associated with an increase in glutamate or Glx levels (Mangia et al., 2007; Bednarík et al., 2015; Ip et al., 2017), and decrease in GABA levels (Lin et al., 2012; Mekle et al., 2017). In this study, the MRS voxel was placed in the midline occipital cortex, crossing the longitudinal fissure. It was believed that placing a large voxel in this location would help increase signal-to-noise ratio, and improve spectral quality, however, as can be seen in **Figure 4**, the positive BOLD signal from an individual participant does not fill the entire voxel. As Just (2020) states, one of the critical issues in determining BOLD responses is positioning of the voxel with respect to the activated area. It is possible that blind placement of the voxel lead to some participants having less positive BOLD signal generated in the MRS voxel. Future studies may benefit from voxel placement guided by fMRI. This was not performed in the present study because it was believed that performing fMRI before MRS could adversely affect the MRS component due to thermal frequency drift.

Taken together, the absence of any statistically significant differences according to the repeated measures *t*-tests suggest that it is possible that no consistent changes were observed between the active and rest conditions due to differences in the amount of activity within the spectroscopy voxel across participants. However, the correlation analysis suggests that for those participants in which there was a haemodynamic response within the spectroscopy voxel that was able to elicit a measurable change in the linewidth of the unsuppressed water peak, there were corresponding metabolic changes. However, this represents only a portion of an already limited sample, and lacks statistical power for reliable conclusions to be drawn.

The main difference between the present study and others in which a change in either Glx or GABA was measured in response to a similar visual stimulation paradigm is firstly that the majority of these studies were conducted using 7 T scanners, and secondly that, with the exception of Ip et al. (2017), participants viewed stimulation in blocks of at least 5 min. The theory behind the shorter, 30 s blocks used in this experiment was that it would be possible to disentangle metabolic changes related to synaptic transmission from changes related to shifts in energy metabolism and possibly the effects of long term potentiation that may be seen with longer stimulation blocks. The absence of any significant measured change in Glx levels between the active and rest blocks in this study suggests that the more consistently measured changes in glutamate or Glx levels measured in other studies represent changes in energy metabolism, but make it difficult to evaluate the performance of the modified MEGA-PRESS technique. It is possible that a longer stimulation block may have elicited a more significant response in the measured Glx levels, however, visual stimulation may not be the optimal form of stimulation for inducing a large, measurable change in neurotransmitter levels.

Mullins (2018) illustrates that with regard to changes in glutamate or Glx in fMRS studies, larger changes were observed in event-related paradigms 13.429% (±3.59) compared to block designs 4.749% (±1.45%) and of those stimuli that elicited a metabolic response, visual stimuli elicited the smallest response, with a mean glutamate increase of 2.318% (±1.227%) with painful stimuli eliciting the largest change 14.458% (±3.736%). This observation holds for fMRS studies into GABA changes as well, with studies using some form of pain stimulus recording ∼15% changes in GABA in the anterior cingulate cortex (ACC) (Kupers et al., 2009; Cleve et al., 2017) compared to a ∼5% change measured with visual stimulation in the OCC (Mekle et al., 2017). Kühn et al. (2016), in a study measuring changes in the ACC in response to an interference task, namely the Stroop task, measured an 18% increase in GABA in the ACC between the pre-task and task windows. It is possible that the changes in both glutamate and GABA related to synaptic transmission are transient, and that these short-lived changes are diluted when averaging over the entire block. Unfortunately there were too few stimulation blocks per participant for the data to be analyzed as an event-related design. Future studies in evaluating fMRS methods for detecting changes in GABA levels may benefit from implementing event-related or hybrid event-related/block designs where possible.

Finally, one of the fundamental problems facing functional spectroscopy is that of how to disentangle the BOLD effect on spectral linewidth from its consequences on quantitative spectral analysis. It has been established that the BOLD effect affects all peaks in an MR-spectra, not just the unsuppressed water signal, and that this may lead to an overestimation in metabolite levels in quantitative analyses (Zhu and Chen, 2001; Mangia et al., 2006; Bednarík et al., 2015; Ip et al., 2017) and should be corrected

for. Creatine is noted for being particularly stable under normal physiological conditions, so much so that metabolite levels are often reported as a ratio relative to creatine (Stagg and Rothman, 2014), a practice that has attracted some criticism as creatine has been shown to be affected in some pathologies as well as being susceptible to the influence of sex hormones (Hjelmervik et al., 2018). Apšvalka et al. (2015) and Mullins et al. (2005) suggest that because no statistically significant change in the concentration of creatine, nor total NAA or choline, was measured in their study, the significant differences in glutamate measured represent a genuine change rather than a generalized effect. Bednaríkˇ et al. (2015) and Ip et al. (2017), under the assumption that levels of total creatine should remain stable across changes in neural activity, used the change in the FWHM of the creatine signal between active and rest conditions as a correction factor for the other measured metabolites. Similarly, Mangia et al. (2007) used the difference between spectra acquired during rest and stimulation to calculate a line-broadening correction function to be applied to spectra acquired during the stimulation conditions.

Many of the suggested correction factors for BOLD interference, however, are applied generally and do not account for how the BOLD effect may affect different metabolite signals to different degrees. Zhu and Chen (2001) show the larger, singlet peaks typically found in an MR-spectrum, such as those from creatine, choline and NAA, to be more susceptible to BOLD interference than the smaller multiplets from GABA and Glx. Given the absence of significant correlation between the difference in creatine and choline levels and the change in BOLD signal, there is insufficient evidence to conclude that the BOLD effect has significantly interfered with quantitative analyses. The experimental results are presented as they were measured with the caveat that no correction has been applied and that while significant interference from the BOLD effect appears unlikely it cannot be ruled out entirely.

In conclusion, the modified MEGA-PRESS sequence presented here provides a reliable measure of the BOLD effect through linewidth changes in the unsuppressed water peak, but whether it may also be used to measure associated metabolic changes remains inconclusive. Future studies may benefit from the use of event-related or hybrid block/event-related designs were possible, and the use of sequences that do not rely on spectral editing may be advantageous in light of the increased spectral information and sensitivity they may provide.

DATA AVAILABILITY STATEMENT

The raw data supporting the conclusions of this article will be made available by the authors, without undue reservation.

ETHICS STATEMENT

The studies involving human participants were reviewed and approved by The Regional Committees for Medical and Health Research Ethics for Western Norway (REK-Vest, REK case number 2016/1629). The patients/participants provided their written informed consent to participate in this study.

AUTHOR CONTRIBUTIONS

GD, AC, KH, and RG were involved in the conception and design of the study. AC and LE were involved in programming pulse sequences. GD and AC planned and performed data acquisition with assistance from LE. AC performed spectral analyses. JB and KK performed fMRI analyses. GD conducted statistical analyses and wrote the manuscript with the assistance of KH and RG with critical feedback from all contributing authors. All authors contributed to the article and approved the submitted version.

FUNDING

This research was funded by grants from the European Research Council (ERC) Advance Grants (#693124) to KH.

REFERENCES

Agarwal, N., and Renshaw, P. F. (2012). Proton MR spectroscopy–detectable major neurotransmitters of the brain: biology and possible clinical applications. *Am. J. Neuroradiol.* 33, 595–602. doi: 10.3174/ajnr.A2587

Apšvalka, D., Gadie, A., Clemence, M., and Mullins, P. G. (2015). Event-related dynamics of glutamate and BOLD effects measured using functional magnetic resonance spectroscopy (fMRS) at 3T in a repetition suppression paradigm. *NeuroImage* 118, 292–300. doi: 10.1016/j.neuroimage.2015.06.015

Bednaríkˇ, P., Tkáč, I., Giove, F., DiNuzzo, M., Deelchand, D. K., Emir, U. E., et al. (2015). Neurochemical and BOLD responses during neuronal activation measured in the human visual cortex at 7 Tesla. *J. Cereb. Blood Flow Metab.* 35, 601–610. doi: 10.1038/jcbfm.2014.233

Benjamini, Y., and Hochberg, Y. (1995). Controlling the false discovery rate: a practical and powerful approach to multiple testing. *J. R. Stat. Soc. Ser. B Methodol.* 57, 289–300. doi: 10.1111/j.2517-6161.1995.tb02031.x

Benjamini, Y., and Yekutieli, D. (2001). The control of the false discovery rate in multiple testing under dependency. *Ann. Stat.* 29, 1165–1188. doi: 10.1214/aos/1013699998

Boillat, Y., Xin, L., van der Zwaag, W., and Gruetter, R. (2019). Metabolite concentration changes associated with positive and negative BOLD responses in the human visual cortex: a functional MRS study at 7 Tesla. *J. Cereb. Blood Flow Metab.* 40, 488–500. doi: 10.1177/0271678X19831022

Brix, M. K., Ersland, L., Hugdahl, K., Dwyer, G. E., Grüner, R., Noeske, R., et al. (2017). Within- and between-session reproducibility of GABA measurements with MR spectroscopy. *J. Magn. Reson. Imaging* 46, 421–430. doi: 10.1002/jmri.25588

Chen, C., Sigurdsson, H. P., Pépés, S. E., Auer, D. P., Morris, P. G., Morgan, P. S., et al. (2017). Activation induced changes in GABA: functional MRS at 7T with MEGA-sLASER. *NeuroImage* 156, 207–213. doi: 10.1016/j.neuroimage.2017.05.044

Cleve, M., Gussew, A., and Reichenbach, J. R. (2015). *In vivo* detection of acute pain-induced changes of GABA+ and Glx in the human brain by using functional 1 H MEGA-PRESS MR spectroscopy. *Neuroimage* 105, 67–75. doi: 10.1016/j.neuroimage.2014.10.042

Cleve, M., Gussew, A., Wagner, G., Bär, K.-J., and Reichenbach, J. R. (2017). Assessment of intra- and inter-regional interrelations between GABA+, Glx and BOLD during pain perception in the human brain—a combined 1H fMRS and fMRI study. *Neuroscience* 365, 125–136. doi: 10.1016/j.neuroscience.2017.09.037

Denève, S., and Machens, C. K. (2016). Efficient codes and balanced networks. *Nat. Neurosci.* 19, 375–382. doi: 10.1038/nn.4243

Dydak, U., Jiang, Y.-M., Long, L.-L., Zhu, H., Chen, J., Li, W.-M., et al. (2011). *In vivo* measurement of brain GABA concentrations by magnetic resonance spectroscopy in smelters occupationally exposed to manganese. *Environ. Health Perspect.* 119, 219–224. doi: 10.1289/ehp.1002192

Edden, R. A. E., Puts, N. A. J., and Barker, P. B. (2012). Macromolecule-suppressed GABA-edited magnetic resonance spectroscopy at 3T. *Magn. Reson. Med.* 68, 657–661. doi: 10.1002/mrm.24391

Evans, A. C., Marrett, S., Neelin, P., Collins, L., Worsley, K., Dai, W., et al. (1992). Anatomical mapping of functional activation in stereotactic coordinate space. *NeuroImage* 1, 43–53. doi: 10.1016/1053-8119(92)90006-9

Faul, F., Erdfelder, E., Buchner, A., and Lang, A.-G. (2009). Statistical power analyses using G*Power 3.1: tests for correlation and regression analyses. *Behav. Res. Methods* 41, 1149–1160. doi: 10.3758/BRM.41.4.1149

Floyer-Lea, A., Wylezinska, M., Kincses, T., and Matthews, P. M. (2006). Rapid modulation of GABA concentration in human sensorimotor cortex during motor learning. *J. Neurophysiol.* 95, 1639–1644. doi: 10.1152/jn.00346.2005

Frahm, J., Krüger, G., Merboldt, K.-D., and Kleinschmidt, A. (1996). Dynamic uncoupling and recoupling of perfusion and oxidative metabolism during focal brain activation in man. *Magn. Reson. Med.* 35, 143–148. doi: 10.1002/mrm.1910350202

Friston, K. J., Holmes, A. P., Poline, J. B., Grasby, P. J., Williams, S. C. R., Frackowiak, R. S. J., et al. (1995). Analysis of fMRI time-series revisited. *NeuroImage* 2, 45–53. doi: 10.1006/nimg.1995.1007

Gussew, A., Rzanny, R., Erdtel, M., Scholle, H. C., Kaiser, W. A., Mentzel, H. J., et al. (2010). Time-resolved functional 1 H MR spectroscopic detection of glutamate concentration changes in the brain during acute heat pain stimulation. *Neuroimage* 49, 1895–1902. doi: 10.1016/j.neuroimage.2009.09.007

Gutzeit, A., Meier, D., Meier, M. L., von Weymarn, C., Ettlin, D. A., Graf, N., et al. (2011). Insula-specific responses induced by dental pain. *Proton Magn. Reson. Spectrosc. Study* 21, 807–815. doi: 10.1007/s00330-010-1971-8

Hennig, J., Emst, T., Speck, O., Deuschl, G., and Feifel, E. (1994). Detection of brain activation using oxygenation sensitive functional spectroscopy. *Magn. Reson. Med.* 31, 85–90. doi: 10.1002/mrm.1910310115

Henry, M. E., Lauriat, T. L., Shanahan, M., Renshaw, P. F., and Jensen, J. E. (2011). Accuracy and stability of measuring GABA, glutamate, and glutamine by proton magnetic resonance spectroscopy: a phantom study at 4 Tesla. *J. Magn. Reson.* 208, 210–218. doi: 10.1016/j.jmr.2010.11.003

Hjelmervik, H., Hausmann, M., Craven, A. R., Hirnstein, M., Hugdahl, K., and Specht, K. (2018). Sex- and sex hormone-related variations in energy-metabolic frontal brain asymmetries: a magnetic resonance spectroscopy study. *Neuroimage* 172, 817–825. doi: 10.1016/j.neuroimage.2018.01.043

Ip, I. B., Berrington, A., Hess, A. T., Parker, A. J., Emir, U. E., and Bridge, H. (2017). Combined fMRI-MRS acquires simultaneous glutamate and BOLD-fMRI signals in the human brain. *Neuroimage* 155, 113–119. doi: 10.1016/j.neuroimage.2017.04.030

Isaacson, J. S., and Scanziani, M. (2011). How inhibition shapes cortical activity. *Neuron* 72, 231–243. doi: 10.1016/j.neuron.2011.09.027

Jardri, R., Hugdahl, K., Hughes, M., Brunelin, J., Waters, F., Alderson-Day, B., et al. (2016). Are hallucinations due to an imbalance between excitatory and inhibitory influences on the brain? *Schizophr. Bull.* 42, 1124–1134. doi: 10.1093/schbul/sbw075

Just, N. (2020). Proton functional magnetic resonance spectroscopy in rodents. *NMR Biomed*. e4254. doi: 10.1002/nbm.4254

Just, N., and Sonnay, S. (2017). Investigating the role of glutamate and GABA in the modulation of transthalamic activity: a combined fMRI-fMRS study. *Front. Physiol.* 8:30. doi: 10.3389/fphys.2017.00030

Kaiser, L. G., Young, K., Meyerhoff, D. J., Mueller, S. G., and Matson, G. B. (2008). A detailed analysis of localized J-difference GABA editing: theoretical and experimental study at 4 T. *NMR Biomed.* 21, 22–32. doi: 10.1002/nbm.1150

Kühn, S., Schubert, F., Mekle, R., Wenger, E., Ittermann, B., Lindenberger, U., et al. (2016). Neurotransmitter changes during interference task in anterior cingulate cortex: evidence from fMRI-guided functional MRS at 3 T. *Brain Struct. Funct.* 221, 2541–2551. doi: 10.1007/s00429-015-1057-0

Kupers, R., Danielsen, E. R., Kehlet, H., Christensen, R., and Thomsen, C. (2009). Painful tonic heat stimulation induces GABA accumulation in the prefrontal cortex in man. *Pain* 142, 89–93. doi: 10.1016/j.pain.2008.12.008

Kwong, K. K., Belliveau, J. W., Chesler, D. A., Goldberg, I. E., Weisskoff, R. M., Poncelet, B. P., et al. (1992). Dynamic magnetic resonance imaging of human brain activity during primary sensory stimulation. *Proc. Natl. Acad. Sci.U.S.A.* 89, 5675–5679. doi: 10.1073/pnas.89.12.5675

Lin, Y., Stephenson, M. C., Xin, L., Napolitano, A., and Morris, P. G. (2012). Investigating the metabolic changes due to visual stimulation using functional proton magnetic resonance spectroscopy at 7 T. *J. Cereb. Blood Flow Metab.* 32, 1484–1495. doi: 10.1038/jcbfm.2012.33

Maddock, R. J., Caton, M. D., and Ragland, J. D. (2018). Estimating glutamate and Glx from GABA-optimized MEGA-PRESS: Off-resonance but not difference spectra values correspond to PRESS values. *Psychiatry Res. Neuroimaging* 279, 22–30. doi: 10.1016/j.pscychresns.2018.07.003

Mangia, S., Giove, F., and DiNuzzo, M. (2012). Metabolic pathways and activity-dependent modulation of glutamate concentration in the human brain. *Neurochem. Res.* 37, 2554–2561. doi: 10.1007/s11064-012-0848-4

Mangia, S., Tkáč, I., Gruetter, R., Van De Moortele, P.-F., Giove, F., Maraviglia, B., et al. (2006). Sensitivity of single-voxel 1H-MRS in investigating the metabolism of the activated human visual cortex at 7 T. *Magn. Reson. Imaging* 24, 343–348. doi: 10.1016/j.mri.2005.12.023

Mangia, S., Tkáč, I., Gruetter, R., Van de Moortele, P.-F., Maraviglia, B., and Ugurbil, K. (2007). Sustained neuronal activation raises oxidative metabolism to a new steady-state level: evidence from 1H NMR spectroscopy in the human visual cortex. *J. Cereb. Blood Flow Metab.* 27, 1055–1063. doi: 10.1038/sj.jcbfm.9600401

Mekle, R., Kühn, S., Pfeiffer, H., Aydin, S., Schubert, F., and Ittermann, B. (2017). Detection of metabolite changes in response to a varying visual stimulation paradigm using short-TE 1H MRS at 7 T. *NMR Biomed.* 30:e3672. doi: 10.1002/nbm.3672

Mescher, M., Merkle, H., Kirsch, J., Garwood, M., and Gruetter, R. (1998). Simultaneous *in vivo* spectral editing and water suppression. *NMR Biomed.* 11, 266–272.

Michels, L., Martin, E., Klaver, P., Edden, R., Zelaya, F., Lythgoe, D. J., et al. (2012). Frontal GABA levels change during working memory. *PLoS ONE* 7:e31933. doi: 10.1371/journal.pone.0031933

Mullins, P. G. (2018). Towards a theory of functional magnetic resonance spectroscopy (fMRS): a meta-analysis and discussion of using MRS to measure changes in neurotransmitters in real time. *Scand. J. Psychol.* 59, 91–103. doi: 10.1111/sjop.12411

Mullins, P. G., McGonigle, D. J., O'Gorman, R. L., Puts, N. A., Vidyasagar, R., Evans, C. J., et al. (2014). Current practice in the use of MEGA-PRESS spectroscopy for the detection of GABA. *Neuroimage* 86, 43–52. doi: 10.1016/j.neuroimage.2012.12.004

Mullins, P. G., Rowland, L. M., Jung, R. E., and Sibbitt, W. L. (2005). A novel technique to study the brain's response to pain: proton magnetic resonance spectroscopy. *NeuroImage* 26, 642–646. doi: 10.1016/j.neuroimage.2005.02.001

Ogawa, S., Tank, D. W., Menon, R., Ellermann, J. M., Kim, S. G., Merkle, H., et al. (1992). Intrinsic signal changes accompanying sensory stimulation: functional brain mapping with magnetic resonance imaging. *Proc. Natl. Acad. Sci. U.S.A.* 89, 5951–5955. doi: 10.1073/pnas.89.13.5951

Provencher, S. W. (1993). Estimation of metabolite concentrations from localized *in vivo* proton NMR spectra. *Magn. Reson. Med.* 30, 672–679. doi: 10.1002/mrm.1910300604

Provencher, S. W. (2001). Automatic quantitation of localized *in vivo* 1H spectra with LCModel. *NMR Biomed.* 14, 260–264. doi: 10.1002/nbm.698

R Development Core Team (2020). *R: A Language and Environment for Statistical Computing*. Vienna: R Foundation for Statistical Computing. Available online at: https://www.R-project.org/ (accessed December 11, 2020).

Schaller, B., Mekle, R., Xin, L., Kunz, N., and Gruetter, R. (2013). Net increase of lactate and glutamate concentration in activated human visual cortex detected with magnetic resonance spectroscopy at 7 tesla. *J. Neurosci. Res.* 91, 1076–1083. doi: 10.1002/jnr.23194

Siniatchkin, M., Sendacki, M., Moeller, F., Wolff, S., Jansen, O., Siebner, H., et al. (2012). Abnormal changes of synaptic excitability in migraine with aura. *Cereb. Cortex* 22, 2207–2216. doi: 10.1093/cercor/bhr248

Stagg, C., and Rothman, D. (2014). *Magnetic Resonance Spectroscopy: Tools for Neuroscience Research and Emerging Clinical Applications*. San Diego, CA: Academic Press.

Whitfield-Gabrieli, S., and Nieto-Castanon, A. (2012). Conn: a functional connectivity toolbox for correlated and anticorrelated brain networks. *Brain Connect.* 2, 125–141. doi: 10.1089/brain.2012.0073

Zhu, X. H., and Chen, W. (2001). Observed BOLD effects on cerebral metabolite resonances in human visual cortex during visual stimulation: a functional (1)H MRS study at 4 T. *Magn. Reson. Med.* 46, 841–847. doi: 10.1002/mrm.1267

Conflict of Interest: AC, LE, KH, and RG have shares in the company NordicNeuroLab A/S which produces add-on equipment for MRI examinations that were used in this study.

The remaining authors declare that the research was conducted in the absence of any commercial or financial relationships that could be construed as a potential conflict of interest.

frontiers in Psychiatry

ORIGINAL RESEARCH
published: 01 April 2021
doi: 10.3389/fpsyt.2021.644271

Multimodal Neuroimaging Study of Visual Plasticity in Schizophrenia

S. Andrea Wijtenburg, Jeffrey West, Stephanie A. Korenic, Franchesca Kuhney, Frank E. Gaston, Hongji Chen and Laura M. Rowland*

Maryland Psychiatric Research Center, Department of Psychiatry, University of Maryland School of Medicine, Baltimore, MD, United States

Schizophrenia is a severe mental illness with visual learning and memory deficits, and reduced long term potentiation (LTP) may underlie these impairments. Recent human fMRI and EEG studies have assessed visual plasticity that was induced with high frequency visual stimulation, which is thought to mimic an LTP-like phenomenon. This study investigated the differences in visual plasticity in participants with schizophrenia and healthy controls. An fMRI visual plasticity paradigm was implemented, and proton magnetic resonance spectroscopy data were acquired to determine whether baseline resting levels of glutamatergic and GABA metabolites were related to visual plasticity response. Adults with schizophrenia did not demonstrate visual plasticity after family-wise error correction; whereas, the healthy control group did. There was a significant regional difference in visual plasticity in the left visual cortical area V2 when assessing group differences, and baseline GABA levels were associated with this specific ROI in the SZ group only. Overall, this study suggests that visual plasticity is altered in schizophrenia and related to basal GABA levels.

Keywords: visual plasticity, schizophrenia, fMRI, GABA, glutamate, healthy adults, magnetic resonance spectroscopy

OPEN ACCESS

Edited by:
Maria Concepcion Garcia Otaduy, University of São Paulo, Brazil

Reviewed by:
Carol A. Tamminga, University of Texas Southwestern Medical Center, United States
Chao Xu, University of Oklahoma Health Sciences Center, United States

****Correspondence:***
S. Andrea Wijtenburg
awijtenburg@som.umaryland.edu

Specialty section:
This article was submitted to Molecular Psychiatry, a section of the journal Frontiers in Psychiatry

Received: *20 December 2020*
Accepted: *08 March 2021*
Published: *01 April 2021*

Citation:
Wijtenburg SA, West J, Korenic SA, Kuhney F, Gaston FE, Chen H and Rowland LM (2021) Multimodal Neuroimaging Study of Visual Plasticity in Schizophrenia. Front. Psychiatry 12:644271. doi: 10.3389/fpsyt.2021.644271

INTRODUCTION

Schizophrenia (SZ) is a severe psychiatric illness with well-documented visual learning and processing deficits (1–3), which may be due to alterations in long-term potentiation (LTP). LTP is a basic cellular plasticity mechanism underlying learning and memory, and it has been previously studied in a variety of regions including the hippocampus and visual cortex using high frequency electrical or visual stimulation, respectively (4–7). Clapp et al. adapted a visual plasticity paradigm that employed low and high frequency stimulation known to induce LTP-like changes in rodents and successfully tested the paradigm in healthy adults using EEG and fMRI. In these studies, increased visual evoked potentials (8) or increased fMRI BOLD activation (9) were observed following high frequency stimulation, which was similar to previous animal studies. A similar visual plasticity paradigm has been used in several other studies in healthy adults and shown elevations in visual evoked potentials or fMRI BOLD activation post-high frequency stimulation (10, 11) as well as a variable response in fMRI BOLD activation post-high frequency stimulation (12).

Several studies have utilized visual paradigms to assess visual plasticity in adults with SZ vs. healthy controls using EEG. Cavus et al. demonstrated impaired visual cortical plasticity in adults with SZ compared to healthy controls as evidenced by a lack of persistent visual evoked potentials in the visual cortex post-high frequency stimulation (13). In a study where participants were given D-cycloserine or placebo, exploratory analyses by Forsyth et al. (14) showed impaired visual evoked

potentials post-high frequency stimulation in adults with SZ who received placebo compared to healthy controls who received placebo. The visual plasticity response in the SZ group did not change with administration of 100 mg of D-cycloserine. D'Souza et al. reported an LTP-like enhancement with a dose of a glycine transporter-1 (∼75% occupancy) in adults with SZ (15). Another study by Wynn et al. demonstrated a plasticity effect (visual evoked potential post-high frequency stimulation) in both healthy controls and adults with SZ; however, the groups were not significantly different (16). In other visual paradigms that employed monocular deprivation or sensory adaption, adults with SZ have significantly reduced visual evoked potential amplitudes compared to controls (17, 18). Thus, in the literature to date, there appears to be mixed results regarding whether visual plasticity is impaired in SZ.

Glutamate, the primary excitatory neurotransmitter in the human brain, is significantly involved in LTP such that it modulates NMDA receptors, which triggers a cascade of events leading to a long-lasting increase in signal transmission between neurons (4, 19). Currently, in humans, the only non-invasive methodology to quantify glutamatergic metabolites *in vivo* is proton magnetic resonance spectroscopy. This technique has been used to show altered levels of glutamatergic metabolites in several different brain regions in adults with SZ (20). In addition to glutamate, magnetic resonance spectroscopy can be used to measure glutamine, of which 80% is derived from glutamate involved in neurotransmission, and GABA, the primary inhibitory transmitter in the human brain and modulator of LTP *in vivo* (21). Gaining a better understanding of basal glutamate, glutamine, and GABA levels and the relationship to visual plasticity may provide insight into the mixed visual plasticity results in SZ and in the future, serve as a potential pharmacological treatment target.

The first aim of this study was to test the hypothesis that visual plasticity is reduced in SZ using fMRI. A second aim was to use a multimodal approach to determine whether baseline resting levels of occipital cortex glutamatergic metabolites and GABA as measured using magnetic resonance spectroscopy were related to visual plasticity response as assessed using fMRI. Given that glutamatergic function is altered in SZ and a previous study by our group in healthy controls showed that glutamine was related to visual plasticity (11), we hypothesized that the relationship between glutamine to visual plasticity would be weaker in adults with SZ compared to healthy controls. We expected the magnitude of the relationship between glutamate and visual plasticity as well as GABA and visual plasticity to be smaller in adults with SZ compared to healthy controls.

MATERIALS AND METHODS

All research was conducted at the University of Maryland Center for Brain Imaging Research (CBIR) at the Maryland Psychiatric Research Center. This study was approved by the University of Maryland Baltimore Institutional Review Board, and all participants (both SZ and healthy controls) provided written, informed consent prior to study initiation. Adults with SZ were evaluated for capacity to consent to ensure that each participant fully understood the study procedures. The healthy control data was previously reported in (11).

TABLE 1 | Participant characteristics, mean (standard deviation).

	Schizophrenia	Healthy controls	*p*-value
Gender (M/F)	10/7	9/9	0.6
Age (years)	41.5 (15)	36.2 (16)	0.32
Education (years)	13.7 (2.3)	14.6 (1.6)	0.22
Illness duration (years)	20.4 (14)	N/A	
Smoker (Yes/No)	3/14	2/16	0.58
Psychiatric ratings			
BPRS (total)	39.7 (15.0)	N/A	
BPRS (positive)	8.9 (6.0)	N/A	
BPRS (negative)	7.1 (2.0)	N/A	
BNSS	17.5 (10.1)	N/A	
Antipsychotics'			
1st Generation	1	N/A	
2nd Generation	11	N/A	
Both	3	N/A	
None	2	N/A	
Cognitive measures			
HVLT	22.1 (6.3)	26.8 (3.6)	0.01*
BVMT	17.1 (9.1)	25.6 (5.1)	0.02*
UPSA	92.0 (11.5)	100.8 (9.6)	0.023*

$p < 0.05$, '– number of participants taking these medications, BNSS, Brief Negative Symptom Scale; BPRS, Brief Psychiatric Rating Scale; BVMT, Brief Visuospatial Memory Task; HVLT, Hopkins Verbal Learning Task; UPSA, UCSD Performance Based Skills Assessment.

Participant Characteristics

Seventeen adults with SZ and 18 healthy controls participated in the study. Participant demographics are described in **Table 1**. Adults with SZ were characterized and evaluated with the Structured Clinical Interview for DSM-IV (SCID), the Brief Psychiatric Rating Scale (BPRS) (22), and the Brief Negative Symptom Scale (BNSS) (23). For both groups, inclusion criteria for the study were: (1) no contraindication for magnetic resonance imaging scanning, (2) no current or past neurological condition, head trauma, or focal findings on an magnetic resonance imaging, or (3) no substance abuse in the past 6 months or lifetime dependence excluding nicotine. The healthy control group had no current or past psychiatric, neurological, or major medical disorders or substance abuse/dependence. Functional capacity was assessed using the UCSD Performance Based Skills Assessment (UPSA-2) (24). From the MATRICS Consensus Cognitive Battery (MCCB), verbal and visuo-spatial learning were assessed using the Hopkins Verbal Learning Task—Revised (HVLT) and the Brief Visuospatial Memory Task—Revised (BVMT) (25, 26).

Neuroimaging

A Siemens TIM Trio 3T MR system with a 32-channel phased array head coil was utilized for this study. The imaging protocol

consisted of axial T_1-weighted MP-RAGE images used for both magnetic resonance spectroscopy voxel and echo planar imaging placement, spectroscopy data acquisition, and finally fMRI.

MRS methods were previously described (11). Briefly, the magnetic resonance spectroscopy voxel was placed along the midline in the occipital cortex (**Figure 1**) in both groups. Participants were asked to rest but remain awake. To detect glutamate and glutamine, spectra were acquired with phase rotation STEAM (PR-STEAM) (27–30): TR/TM/TE = 2,000/10/6.5-ms, VOI ~ 3.0 × 4.0 × 2.0-cm^3, NEX = 128, and water reference NEX = 16. Data were post-processed offline using in-house MATLAB code and then quantified in LCModel (6.3-0I). For GABA detection, a macromolecule–suppressed MEGA-PRESS sequence was utilized (31): TR/TE = 2,000/68 ms, VOI ~ 3.0 × 4.0 × 2.0-cm^3, NEX = 256 (128 ON and 128 OFF), and water reference NEX = 16, and data were quantified in Gannet 2.0. In-house MATLAB code based on Gasparovic et al. (32) was used to calculate metabolite levels using water as a reference as well as correct for the proportion of the gray matter (GM), white matter (WM), and cerebrospinal fluid (CSF) within each spectroscopic voxel and relaxation effects. More details regarding quantification are outlined here (33). All metabolite levels are reported in institutional units. See **Figure 1** for representative voxel placement and spectra.

fMRI methods were previously described (11). In brief, E-Prime 2.0 (Psychology Software Tools, Inc., Sharpsburg, PA, USA) was used to display the visual stimulus: a centrally located flashing checkerboard, based on based on previous studies (5, 8, 10, 12, 13) and similar to Cavus et al. (13) and Lahr et al. (12). The task involved two low frequency (0.9 Hz) stimulation runs, one high frequency (9 Hz) stimulation to induce visual plasticity, 2 min of rest, and two runs of low frequency stimulation. During the low frequency stimulation and high frequency stimulation, participants were asked to fixate on a centrally located crosshair except during the 2-min rest period where eyes were closed. During the low frequency stimulation blocks, echo-planar imaging data were acquired TR = 2,100 ms, TE = 27 ms, FOV = 220 × 220 mm, matrix size = 128 × 128, Number of slices = 39,143 measurements, voxel size = 1.7 × 1.7 × 4.0 mm). Echo planar imaging data were analyzed using MATLAB (R2013a) (The Mathworks Inc., Natick, Massachusetts) and Statistical Parametric Mapping (SPM) 8.0 (Wellcome Trust Center for Neuroimaging, Department of Cognitive Neurology, Institute of Neurology, London: http://www.fil.ion.ucl.ac.uk/spm).

First and second level models were previously described (11). Briefly, first level models were performed for each group, and second level modeling involved the following contrasts: (post-high frequency stimulation "on"—"off") minus (pre-high frequency stimulation "on"—"off"). Second level analysis for both healthy controls and adults with SZ tested for visual plasticity *via* a one sample *t*-test, appropriate for within subject designs. A mask of the spectroscopic voxel was applied to restrict the analyses to only the magnetic resonance spectroscopy region.

Statistical Analyses

Using SPSS 23.0 (IBM SPSS Statistics, Armonk, NY, USA), group differences were assessed among the demographic variables *via* chi-square or *t*-test as appropriate with significance set to $p < 0.05$. Normality assessments conducted *via* the Shapiro-Wilk-test

TABLE 2 | Magnetic resonance spectroscopy metabolite means (standard deviation).

Metabolites (I.U.)	Schizophrenia	Healthy controls	*p*-value
Glutamate (Glu)	7.4 (1.3)	6.6 (0.7)	0.021*
Glutamine (Gln)	2.2 (0.6)	1.8 (0.4)	0.016*
GABA	0.87 (0.2)	0.95 (0.2)	0.22
Linewidth (LW)[a]	0.046 (0.02)	0.042 (0.01)	0.55
Signal-to-Noise Ratio (SNR)[a]	73 (18)	76 (16)	0.67

*$p < 0.05$, 1 Glu and 1 Gln were excluded, 3 GABA datasets were excluded.
[a]LW and SNR as computed by LCModel.
I.U., institutional units.

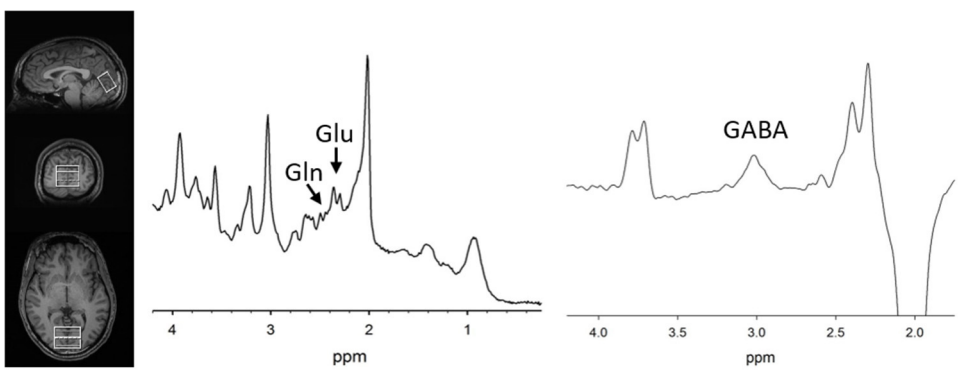

FIGURE 1 | (Left) T1-weighted images showing voxel placement along the midline in the occipital cortex. Representative PR-STEAM spectrum (center) and MEGA-PRESS spectrum (right) from the same participant showing excellent quality data. tCr, total creatine; Glu, glutamate; Gln, glutamine; GABA, γ-aminobutyric acid.

revealed that the data were normally distributed. For the three metabolites of interest, *t*-tests with significance set at $p < 0.05$ were performed to examine differences between the two groups. Similarly, *t*-tests with significance set at $p < 0.05$ were also computed for magnetic resonance spectroscopy quality factors such as linewidth (LW), signal-to-noise ratio (SNR), and metabolite Cramer Rao Lower Bounds (CRLBs) or GABA fit errors to examine whether data were of similar quality between groups.

Visual plasticity within group differences were considered significant with a threshold set to $p < 0.05$ FWE-corrected. For between group visual plasticity differences, small volume correction with a region of interest diameter of 4 mm was applied to examine differences in visual plasticity between adults with SZ and healthy controls with significance threshold set to $p < 0.05$, Family Wise Error (FWE)-corrected.

To examine the relationship between visual plasticity and metabolites, correlations were computed using SPSS 27.0 (IBM SPSS Statistics, Armonk, NY, USA) between region of interest values extracted from significant activations using MarsBar (5) with 4 mm radius and the three metabolite levels ($p = 0.05/3$). In the SZ group, exploratory analyses were conducted to determine whether cognition function or symptom ratings related to visual plasticity.

RESULTS

Demographics

The two groups were well-matched in terms of gender, age, education, and smoking (p's > 0.05, **Table 1**). There were significant differences in terms of Hopkins Verbal Learning Test ($p = 0.01$), Brief Visuospatial Memory Test ($p = 0.02$), and UPSA-2 ($p = 0.023$) such that the SZ group performed worse on measures of memory and functional capacity compared to the healthy control group.

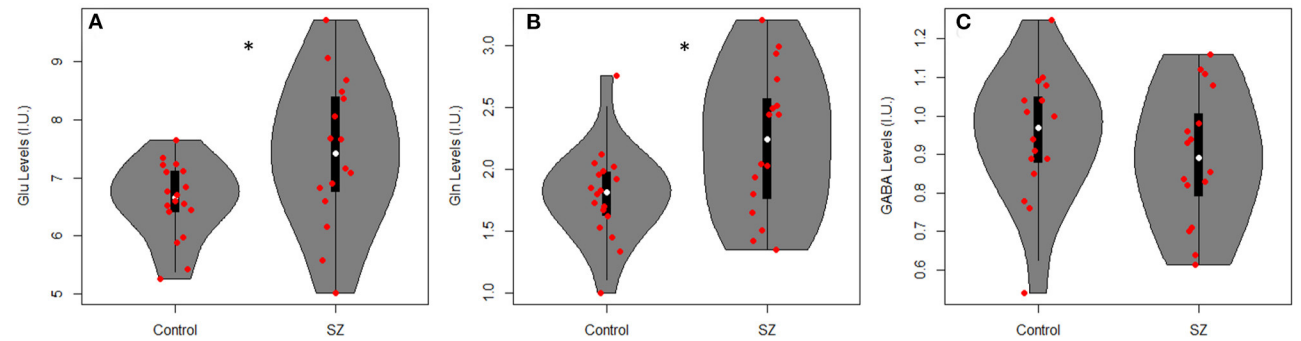

FIGURE 2 | Violin plots with individual data points overlayed in red showing metabolite levels in institutional units (I.U.) for **(A)** glutamate (Glu), **(B)** glutamine (Gln), and **(C)** GABA in adults with SZ and healthy controls (Controls). There were significant differences between groups for Glu ($p = 0.021$) and Gln levels ($p = 0.016$) such that Glu and Gln were higher in SZ vs. healthy controls. *$p < 0.05$.

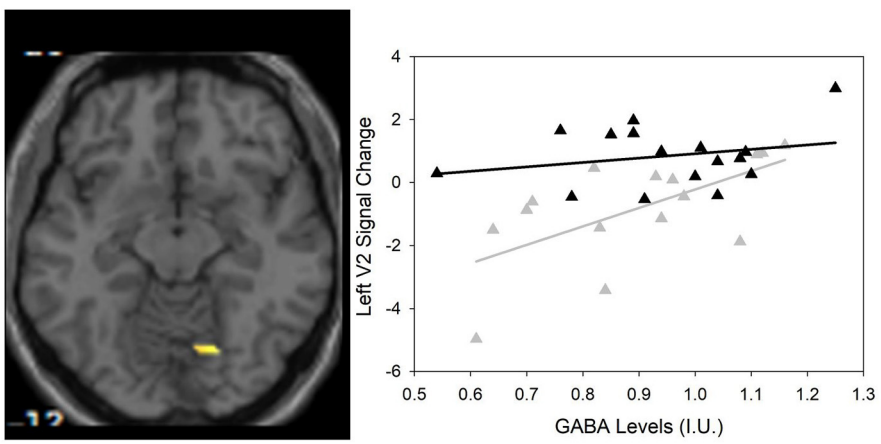

FIGURE 3 | (Left) Group differences in visual activation within the magnetic resonance spectroscopy voxel between healthy controls and SZ using small volume correction that survived Family Wise Error (FWE)-correction ($p < 0.05$). One region of interest emerges at −12, −82, 26 (scale is from 1.5 to 4) in the left V2 visual cortical area. (Right) Scatter plot showing the significant relationship between GABA and visual plasticity response ($r = 0.622$, $p = 0.013$) in the left V2 region of interest in SZ only (▲) compared to HC (▲).

TABLE 3 | Correlations between left V2 region of interest (ROI) and metabolites in SZ.

	r	*p*-value
Left V2 ROI and Glutamate	0.18	0.51
Left V2 ROI and Glutamine	0.23	0.42
Left V2 ROI and GABA	0.62	0.013*

*$p < 0.05/3$.

MRS

Table 2 summarizes mean metabolite levels and quality factors. One PR-STEAM dataset was not acquired, and three GABA datasets were excluded due to fit error > 15%. All glutamate and glutamine CRLBs from both healthy controls and SZ were <20 or 30%, respectively. Overall, data were of excellent quality in both groups, and there were no significant differences between groups for linewidth, signal-to-noise ratio, glutamate CRLB, glutamine CRLB, or GABA fit error (p's > 0.05). There were significant differences between healthy controls and SZ for glutamate ($p = 0.021$) and glutamine levels ($p = 0.016$) such that glutamate and glutamine levels were higher in SZ compared to healthy controls as shown in **Figure 2**. There were no differences in GABA levels between groups ($p = 0.22$).

fMRI

For the healthy control group, visual plasticity was observed in dorsal V2 and V3 and positively related to glutamine with details reported elsewhere (11). There were no significant regions of interest showing visual plasticity in the SZ group that survived FWE-correction. The opposite contrast of pre-high frequency stimulation vs. post-high frequency stimulation yielded no significant regions in both healthy controls and SZ.

Between group differences in visual plasticity were observed in left V2 with region of interest at −12, −82, 26 ($p = 0.003$ FWE-corrected, $T = 3.72$) such that healthy controls had greater visual plasticity compared to SZ (**Figure 3**).

Regression Analyses

As previously described by Wijtenburg et al. (11), higher glutamine was related to greater visual plasticity in healthy controls. In SZ, there were no significant regions of interest that demonstrated visual plasticity therefore the relationships between glutamine, glutamate, or GABA with visual plasticity were not assessed. However, the left V2 region of interest from the group difference analysis was significantly correlated with GABA in the SZ group ($r = 0.622$, $p = 0.013$) with significance set to $p = 0.05/3$ for the 3 metabolites of interest (**Table 3**). Higher levels of GABA were associated with greater visual plasticity response in the left V2 region of interest in SZ.

Correlations With Cognitive Function and Symptom Ratings

Since visual plasticity was not observed in any regions of interest in adults with SZ, there were no relationships to be explored between cognitive function and symptom ratings. Using the left V2 region of interest from the group difference analysis, there were no significant relationships between the left V2 region of interest and cognitive function with $p = 0.05/3$ (for three cognitive function variables). Further, there was a relationship between visual plasticity in the left V2 region of interest and Brief Negative Symptom Scale score ($r = -0.510$, $p = 0.044$) that did not survive correction for multiple comparisons.

DISCUSSION

This study reports for the first time impaired visual plasticity, assessed with fMRI, in adults with SZ compared to healthy controls. While no significant visual plasticity regions of interest survived FWE correction in SZ, group difference analyses revealed a significant visual plasticity region of interest in the left V2. This visual plasticity response region of interest was positively related to GABA levels in SZ. As a whole, these add to the body of evidence implicating altered LTP-like phenomena in SZ.

The study results add to the growing body of literature surrounding impaired visual plasticity in SZ. The majority of EEG studies examining visual plasticity in SZ and healthy controls utilized a flashing checkerboard during the high frequency stimulation component of the protocol (8, 13, 14). Similarly, the two studies that showed visual plasticity in healthy controls also used the same paradigm as part of a fMRI task (9, 11). In contrast, a recent paper by Wynn et al. reported comparable visual plasticity in both healthy control and SZ groups using EEG (16). There were two major differences between the Wynn et al. study and this study that may account for the different study findings: the high frequency stimulus and the time when low frequency stimulation was sampled post-high frequency stimulation. Wynn et al. used a set of vertical or horizontal gratings and recorded post-high frequency stimulation visual evoked potentials 30 min after the high frequency stimulation. Thus, the differences in high frequency stimulus and sampling intervals could account for the differing results.

One question is whether there was a blunted or complete lack of visual plasticity in the SZ group compared to healthy controls. From the double subtraction analysis, examination of the subject level data in the SZ group revealed that 12 of the 17 subjects did show visual plasticity in visual cortical area V3; however, the finding was significant at $p < 0.01$ uncorrected. Upon further inspection, there was a difference between participants that had a visual plasticity response and participants that did not have a visual plasticity response on the negative symptom subscale of the Brief Psychiatric Rating Scale ($p = 0.042$) such that participants with a visual plasticity response had greater negative symptom severity than those that did not have a plasticity response. There were no other differences between participants that had a visual plasticity response and participants that did not have a visual plasticity on measures

of cognitive function, symptom ratings, or chlorpromazine equivalents (all p's > 0.05). The varied amount of visual plasticity in the patient group reflects the heterogeneity of the illness.

While there were no relationships between the glutamatergic metabolites with visual plasticity in SZ, there were significantly higher levels of glutamate and glutamine in SZ compared to healthy controls in the occipital cortex. Three previous studies in the occipital cortex region over a range of illness durations have not found any glutamate to creatine ratio or glutamate+glutamine to creatine ratio differences (34–36). Our data are the first to show an elevation in these metabolites in the SZ group compared to the healthy control group. This may be due to the fact that our sequence is specifically optimized for glutamatergic metabolite detection; whereas the three previous studies used a spectral editing technique that cannot separate glutamate from glutamine. In terms of GABA in the occipital cortex region, previous study findings are mixed when comparing healthy controls and SZ in that lower GABA to creatine ratio in a SZ group was found in mixed illness duration SZ group (34) to no differences in first episode SZ (35) or chronic group when removing those on anticonvulsants (36). This study also found no significant GABA differences between healthy controls and SZ. Our previous work in healthy controls suggested that optimal basal levels of Glu and Gln are necessary for plasticity and in particular, higher Gln was related to greater visual plasticity response (11). Despite higher levels of glutamate and glutamine, there was no significant visual plasticity in SZ that survived FWE-correction. However, there was one region of interest that was significant at $p < 0.01$ uncorrected, but there were no significant correlations between the visual plasticity region of interest in SZ and any of the three metabolites (p's > 0.5). Further, there were no significant differences in glutamate, glutamine, or GABA levels between adults with SZ that had visual plasticity and those that did not.

The mechanism underlying the relationship between higher levels of GABA associated with higher visual plasticity in the left V2 in SZ implies that inhibition plays a role in plasticity mechanisms consistent with non-human animal work (37–39). In a previous study using less stringent multiple correction criteria for the region of interest analyses, a similar positive relationship between visual plasticity and GABA levels was observed in healthy controls (11). Here, a similar relationship observed in SZ suggests GABAergic inhibition may influence excitation necessary for visual plasticity and lower GABA levels consistent with alterations in the GABAergic system are documented in the SZ literature (40–42). Examining a rough estimate of excitation/inhibition balance in the occipital cortex (GABA/Glu and GABA/Gln) revealed a trend level difference in GABA/Gln such that GABA/Gln was lower in SZ compared to healthy controls (see **Supplementary Material**). Further, both ratios were related at trend level (see **Supplementary Material**) to higher visual plasticity response in SZ only and not in healthy controls. Given the highly complex nature of excitation/inhibition balance (43, 44), these exploratory findings plus the main findings of the manuscript must be interpreted with caution given the small sample size. More studies are needed to thoroughly investigate the inhibition/excitation as it relates to visual plasticity in SZ.

There are several limitations to this study. Glutamate and GABA levels measured *via* magnetic resonance spectroscopy are a reflection of multiple pools involved in neurotransmission and other mechanisms (e.g., protein synthesis, glutathione formation, etc.). All but one of our SZ participants were taking antipsychotic medications at the time of the study, and the exact effects of these medications on visual plasticity remains unknown. A limitation of the study was that visual attention was not assessed during the fMRI portion of scan. While participants were reminded before each run to stare at the crosshair in the middle of the screen, future studies may benefit from incorporating a means of ensuring attention such as a button to a specific stimulus similar to (13, 16). Another limitation of the study was that *post-hoc* power calculations revealed that the significant findings were underpowered (61–75%) compared to the standard of 80%. Significant results in this study should be interpreted with caution as further studies are needed with a larger sample size to definitively answer whether visual plasticity is different in SZ and whether baseline metabolite levels in the occipital cortex are related to visual plasticity in SZ. A final limitation is that the adults with SZ are in the chronic phase of the illness, and these study findings may not translate to first episode SZ or those at clinical high risk for psychosis. Future studies are needed to assess visual plasticity response across the illness course.

Thus, this fMRI study tested a visual stimulation paradigm in SZ, and the results further supports several previous EEG studies that show adults with SZ have reduced response to high frequency visual stimulation. The results also show that unlike in healthy controls, glutamatergic levels did not predict plasticity activations in SZ. Future studies may utilize pharmacological or brain stimulation (e.g., TMS) interventions that modulate the glutamatergic or GABAergic systems and potentially improve visual plasticity response.

DATA AVAILABILITY STATEMENT

The datasets generated in this article are not readily available because anonymized data sharing was not included in the consent form for the study. Requests to access the datasets should be directed to S. Andrea Wijtenburg, awijtenburg@som.umaryland.edu.

ETHICS STATEMENT

The studies involving human participants were reviewed and approved by University of Maryland Institutional Review Board. The patients/participants provided

their written informed consent to participate in this study.

AUTHOR CONTRIBUTIONS

LR designed the study. SK collected the data. FK, JW, FG, and HC analyzed the data. LR and SW interpreted the results. SW wrote the manuscript. All authors contributed to the article and approved the submitted version.

FUNDING

This work was supported by the National Institutes of Health: R01MH094520 and P50MH103222.

SUPPLEMENTARY MATERIAL

The Supplementary Material for this article can be found online at: https://www.frontiersin.org/articles/10.3389/fpsyt.2021.644271/full#supplementary-material

REFERENCES

1. Butler PD, Javitt DC. Early-stage visual processing deficits in schizophrenia. *Curr Opin Psychiatry*. (2005) 18:151–7. doi: 10.1097/00001504-200503000-00008
2. Grimes KM, Zanjani A, Zakzanis KK. Memory impairment and the mediating role of task difficulty in patients with schizophrenia. *Psychiatry Clin Neurosci*. (2017) 71:600–11. doi: 10.1111/pcn.12520
3. Green MF. Cognitive impairment and functional outcome in schizophrenia and bipolar disorder. *J Clin Psychiatry*. (2006) 67(Suppl. 9):3–8; discussion 36–42. doi: 10.4088/JCP.1006e12
4. Malenka RC, Bear MF. LTP and LTD: an embarrassment of riches. *Neuron*. (2004) 44:5–21. doi: 10.1016/j.neuron.2004.09.012
5. Teyler TJ, Hamm JP, Clapp WC, Johnson BW, Corballis MC, Kirk IJ. Long-term potentiation of human visual evoked responses. *Eur J Neurosci*. (2005) 21:2045–50. doi: 10.1111/j.1460-9568.2005.04007.x
6. Bliss TV, Lomo T. Long-lasting potentiation of synaptic transmission in the dentate area of the anaesthetized rabbit following stimulation of the perforant path. *J Physiol*. (1973) 232:331–56. doi: 10.1113/jphysiol.1973.sp010273
7. Meunier CN, Chameau P, Fossier PM. Modulation of synaptic plasticity in the cortex needs to understand all the players. *Front Synaptic Neurosci*. (2017) 9:2. doi: 10.3389/fnsyn.2017.00002
8. Clapp WC, Kirk IJ, Hamm JP, Shepherd D, Teyler TJ. Induction of LTP in the human auditory cortex by sensory stimulation. *Eur J Neurosci*. (2005) 22:1135–40. doi: 10.1111/j.1460-9568.2005.04293.x
9. Clapp WC, Zaehle T, Lutz K, Marcar VL, Kirk IJ, Hamm JP, et al. Effects of long-term potentiation in the human visual cortex: a functional magnetic resonance imaging study. *Neuroreport*. (2005) 16:1977–80. doi: 10.1097/00001756-200512190-00001
10. Porto FH, Fox AM, Tusch ES, Sorond F, Mohammed AH, Daffner KR. *In vivo* evidence for neuroplasticity in older adults. *Brain Res Bull*. (2015) 114:56–61. doi: 10.1016/j.brainresbull.2015.03.004
11. Wijtenburg SA, West J, Korenic SA, Kuhney F, Gaston FE, Chen H, et al. Glutamatergic metabolites are associated with visual plasticity in humans. *Neurosci Lett*. (2017) 644:30–6. doi: 10.1016/j.neulet.2017.02.020
12. Lahr J, Peter J, Bach M, Mader I, Nissen C, Normann C, et al. Heterogeneity of stimulus-specific response modification-an fMRI study on neuroplasticity. *Front Hum Neurosci*. (2014) 8:695. doi: 10.3389/fnhum.2014.00695
13. Cavus I, Reinhart RM, Roach BJ, Gueorguieva R, Teyler TJ, Clapp WC, et al. Impaired visual cortical plasticity in schizophrenia. *Biol Psychiatry*. (2012) 71:512–20. doi: 10.1016/j.biopsych.2012.01.013
14. Forsyth JK, Bachman P, Mathalon DH, Roach BJ, Ye E, Asarnow RF. Effects of augmenting N-methyl-D-aspartate receptor signaling on working memory and experience-dependent plasticity in schizophrenia: an exploratory study using acute d-cycloserine. *Schizophr Bull*. (2017) 43:1123–33. doi: 10.1093/schbul/sbw193
15. D'Souza DC, Carson RE, Driesen N, Johannesen J, Ranganathan M, Krystal JH, et al. Dose-related target occupancy and effects on circuitry, behavior, and neuroplasticity of the glycine transporter-1 inhibitor PF-03463275 in healthy and schizophrenia subjects. *Biol Psychiatry*. (2018) 84:413–21. doi: 10.1016/j.biopsych.2017.12.019
16. Wynn JK, Roach BJ, McCleery A, Marder SR, Mathalon DH, Green MF. Evaluating visual neuroplasticity with EEG in schizophrenia outpatients. *Schizophr Res*. (2019) 212:40–6. doi: 10.1016/j.schres.2019.08.015
17. Foxe JJ, Yeap S, Leavitt VM. Brief monocular deprivation as an assay of short-term visual sensory plasticity in schizophrenia—"the binocular effect". *Front Psychiatry*. (2013) 4:164. doi: 10.3389/fpsyt.2013.00164
18. Andrade GN, Butler JS, Peters GA, Molholm S, Foxe JJ. Atypical visual and somatosensory adaptation in schizophrenia-spectrum disorders. *Transl Psychiatry*. (2016) 6:e804. doi: 10.1038/tp.2016.63
19. Goncalves-Ribeiro J, Pina CC, Sebastiao AM, Vaz SH. Glutamate transporters in hippocampal LTD/LTP: not just prevention of excitotoxicity. *Front Cell Neurosci*. (2019) 13:357. doi: 10.3389/fncel.2019.00357
20. Wijtenburg SA, Yang S, Fischer BA, Rowland LM. *In vivo* assessment of neurotransmitters and modulators with magnetic resonance spectroscopy: application to schizophrenia. *Neurosci Biobehav Rev*. (2015) 51:276–95. doi: 10.1016/j.neubiorev.2015.01.007
21. Arima-Yoshida F, Watabe AM, Manabe T. The mechanisms of the strong inhibitory modulation of long-term potentiation in the rat dentate gyrus. *Eur J Neurosci*. (2011) 33:1637–46. doi: 10.1111/j.1460-9568.2011.07657.x
22. Overall JE, Gorham DR. The brief psychiatric rating scale. *Psychol Rep*. (1962) 10:799–812. doi: 10.2466/pr0.1962.10.3.799
23. Kirkpatrick B, Strauss GP, Nguyen L, Fischer BA, Daniel DG, Cienfuegos A, et al. The brief negative symptom scale: psychometric properties. *Schizophr Bull*. (2011) 37:300–5. doi: 10.1093/schbul/sbq059
24. Patterson TL, Goldman S, McKibbin CL, Hughs T, Jeste DV. UCSD performance-based skills assessment: development of a new measure of everyday functioning for severely mentally ill adults. *Schizophr Bull*. (2001) 27:235–45. doi: 10.1093/oxfordjournals.schbul.a006870
25. Nuechterlein KH, Green MF, Kern RS, Baade LE, Barch DM, Cohen JD, et al. The MATRICS consensus cognitive battery, part 1: test selection, reliability, and validity. *Am J Psychiatry*. (2008) 165:203–13. doi: 10.1176/appi.ajp.2007.07010042
26. Kern RS, Nuechterlein KH, Green MF, Baade LE, Fenton WS, Gold JM, et al. The MATRICS consensus cognitive battery, part 2: co-norming and standardization. *Am J Psychiatry*. (2008) 165:214–20. doi: 10.1176/appi.ajp.2007.07010043
27. Wijtenburg SA, Knight-Scott J. Very short echo time improves the precision of glutamate detection at 3T in 1H magnetic resonance spectroscopy. *J Magn Reson Imaging*. (2011) 34:645–52. doi: 10.1002/jmri.22638
28. Wijtenburg SA, Gaston FE, Spieker EA, Korenic SA, Kochunov P, Hong LE, et al. Reproducibility of phase rotation STEAM at 3T: Focus on glutathione. *Magn Reson Med*. (2014) 72:603–9. doi: 10.1002/mrm.24959
29. Bustillo JR, Rediske N, Jones T, Rowland LM, Abbott C, Wijtenburg SA. Reproducibility of phase rotation stimulated echo acquisition mode at 3T in schizophrenia: emphasis on glutamine. *Magn Reson Med*. (2016) 75:498–502. doi: 10.1002/mrm.25638
30. Wijtenburg SA, Near J, Korenic SA, Gaston FE, Chen H, Mikkelsen M, et al. Comparing the reproducibility of commonly used magnetic resonance spectroscopy techniques to quantify cerebral glutathione. *J Magn Reson Imaging*. (2019) 49:176–83. doi: 10.1002/jmri.26046

31. Rowland LM, Krause BW, Wijtenburg SA, McMahon RP, Chiappelli J, Nugent KL, et al. Medial frontal GABA is lower in older schizophrenia: a MEGA-PRESS with macromolecule suppression study. *Mol Psychiatry*. (2016) 21:198–204. doi: 10.1038/mp.2015.34
32. Gasparovic C, Song T, Devier D, Bockholt HJ, Caprihan A, Mullins PG, et al. Use of tissue water as a concentration reference for proton spectroscopic imaging. Magn Reson Med. (2006) 55:1219–26. doi: 10.1002/mrm.20901
33. Wijtenburg SA, Wright SN, Korenic SA, Gaston FE, Ndubuizu N, Chiappelli J, et al. Altered glutamate and regional cerebral blood flow levels in schizophrenia: a (1)H-MRS and pCASL study. *Neuropsychopharmacology*. (2017) 42:562–71. doi: 10.1038/npp.2016.172
34. Yoon JH, Maddock RJ, Rokem A, Silver MA, Minzenberg MJ, Ragland JD, et al. GABA concentration is reduced in visual cortex in schizophrenia and correlates with orientation-specific surround suppression. *J Neurosci*. (2010) 30:3777–81. doi: 10.1523/JNEUROSCI.6158-09.2010
35. Goto N, Yoshimura R, Kakeda S, Nishimura J, Moriya J, Hayashi K, et al. Six-month treatment with atypical antipsychotic drugs decreased frontal-lobe levels of glutamate plus glutamine in early-stage first-episode schizophrenia. *Neuropsychiatr Dis Treat*. (2012) 8:119–22. doi: 10.2147/NDT.S25582
36. Ongur D, Prescot AP, McCarthy J, Cohen BM, Renshaw PF. Elevated gamma-aminobutyric acid levels in chronic schizophrenia. *Biol Psychiatry*. (2010) 68:667–70. doi: 10.1016/j.biopsych.2010.05.016
37. Staff NP, Spruston N. Intracellular correlate of EPSP-spike potentiation in CA1 pyramidal neurons is controlled by GABAergic modulation. *Hippocampus*. (2003) 13:801–5. doi: 10.1002/hipo.10129
38. Grover LM, Yan C. Blockade of GABAA receptors facilitates induction of NMDA receptor-independent long-term potentiation. *J Neurophysiol*. (1999) 81:2814–22. doi: 10.1152/jn.1999.81.6.2814
39. Wigstrom H, Gustafsson B. Facilitated induction of hippocampal long-lasting potentiation during blockade of inhibition. *Nature*. (1983) 301:603–4. doi: 10.1038/301603a0
40. Taylor SF, Tso IF. GABA abnormalities in schizophrenia: a methodological review of *in vivo* studies. *Schizophr Res*. (2015) 167:84–90. doi: 10.1016/j.schres.2014.10.011
41. Gonzalez-Burgos G, Fish KN, Lewis DA. GABA neuron alterations, cortical circuit dysfunction and cognitive deficits in schizophrenia. *Neural Plast*. (2011) 2011:723184. doi: 10.1155/2011/723184
42. de Jonge JC, Vinkers CH, Hulshoff Pol HE, Marsman A. GABAergic mechanisms in schizophrenia: linking postmortem and *in vivo* studies. *Front Psychiatry*. (2017) 8:118. doi: 10.3389/fpsyt.2017.00118
43. Kehrer C, Maziashvili N, Dugladze T, Gloveli T. Altered excitatory-inhibitory balance in the NMDA-hypofunction model of schizophrenia. *Front Mol Neurosci*. (2008) 1:6. doi: 10.3389/neuro.02.006.2008
44. Foss-Feig JH, Adkinson BD, Ji JL, Yang G, Srihari VH, McPartland JC, et al. Searching for cross-diagnostic convergence: neural mechanisms governing excitation and inhibition balance in schizophrenia and autism spectrum disorders. *Biol Psychiatry*. (2017) 81:848–61. doi: 10.1016/j.biopsych.2017.03.005

Conflict of Interest: The authors declare that the research was conducted in the absence of any commercial or financial relationships that could be construed as a potential conflict of interest.

frontiers in Psychiatry

ORIGINAL RESEARCH
published: 15 April 2021
doi: 10.3389/fpsyt.2021.642976

Higher Levels of Pro-inflammatory Cytokines Are Associated With Higher Levels of Glutamate in the Anterior Cingulate Cortex in Depressed Adolescents

Tiffany C. Ho[1], Giana I. Teresi[2], Jillian R. Segarra[2], Amar Ojha[3], Johanna C. Walker[2], Meng Gu[4], Daniel M. Spielman[4], Matthew D. Sacchet[5], Fei Jiang[6], Yael Rosenberg-Hasson[7], Holden Maecker[7] and Ian H. Gotlib[2]*

[1] Department of Psychiatry and Weill Institute for Neurosciences, University of California, San Francisco, San Francisco, CA, United States, [2] Department of Psychology, Stanford University, Stanford, CA, United States, [3] Center for Neuroscience, University of Pittsburgh, Pittsburgh, PA, United States, [4] Department of Radiology, Stanford University, Stanford, CA, United States, [5] Center for Depression, Anxiety, and Stress Research, McLean Hospital and Harvard Medical School, Belmont, MA, United States, [6] Department of Epidemiology and Biostatistics, University of California, San Francisco, San Francisco, CA, United States, [7] Department of Microbiology and Immunology, Stanford University, Stanford, CA, United States

OPEN ACCESS

Edited by:
Marcio Gerhardt Soeiro-de-Souza, University of São Paulo, Brazil

Reviewed by:
Gabriele Ende, University of Heidelberg, Germany
Sophie E. Holmes, Yale University, United States

***Correspondence:**
Tiffany C. Ho
tiffany.ho@ucsf.edu

Specialty section:
This article was submitted to Molecular Psychiatry, a section of the journal Frontiers in Psychiatry

Received: *18 December 2020*
Accepted: *26 February 2021*
Published: *15 April 2021*

Citation:
Ho TC, Teresi GI, Segarra JR, Ojha A, Walker JC, Gu M, Spielman DM, Sacchet MD, Jiang F, Rosenberg-Hasson Y, Maecker H and Gotlib IH (2021) Higher Levels of Pro-inflammatory Cytokines Are Associated With Higher Levels of Glutamate in the Anterior Cingulate Cortex in Depressed Adolescents. Front. Psychiatry 12:642976. doi: 10.3389/fpsyt.2021.642976

Animal models of stress and related conditions, including depression, have shown that elevated peripheral levels of inflammatory cytokines have downstream consequences on glutamate (Glu) in the brain. Although studies in human adults with depression have reported evidence of higher inflammation but lower Glu in the anterior cingulate cortex (ACC), the extent to which peripheral inflammation contributes to glutamatergic abnormalities in adolescents with depression is not well-understood. It is also unclear whether antioxidants, such as ascorbate (Asc), may buffer against the effects of inflammation on Glu metabolism. Fifty-five depressed adolescents were recruited in the present cross-sectional study and provided blood samples, from which we assayed pro-inflammatory cytokines, and underwent a short-TE proton magnetic spectroscopy scan at 3T, from which we estimated Glu and Asc in the dorsal ACC. In the 31 adolescents with usable cytokine and Glu data, we found that IL-6 was significantly positively associated with dorsal ACC Glu ($\beta = 0.466 \pm 0.199$, $p = 0.029$). Of the 16 participants who had usable Asc data, we found that at higher levels of dorsal ACC Asc, there was a negative association between IL-6 and Glu (interaction effect: $\beta = -0.906 \pm 0.433$, $p = 0.034$). Importantly, these results remained significant when controlling for age, gender, percentage of gray matter in the dorsal ACC voxel, BMI, and medication (antidepressant and anti-inflammatory) usage. While preliminary, our results underscore the importance of examining both immune and neural contributors to depression and highlight the potential role of anti-inflammatory compounds in mitigating the adverse effects of

inflammation (e.g., glutamatergic neuroexcitotoxicity). Future studies that experimentally manipulate levels of inflammation, and of ascorbate, and that characterize these effects on cortical glutamate concentrations and subsequent behavior in animals and in humans are needed.

Keywords: glutamate, depression, magnetic resonance spectroscopy, interleukin-6, ascorbate

INTRODUCTION

Depression is an impairing and prevalent disorder that commonly emerges during adolescence (1, 2). While there is growing evidence that elevated inflammation, measured by peripheral levels of pro-inflammatory cytokines and proteins, are implicated in the development and maintenance of depression in adults [(3, 4); for reviews see also (5, 6)], the role of these immune markers in adolescent depression is unclear [although see (7, 8) for recent research in non-depressed adolescents]. It is well recognized both that life stress is one of the most potent risk factors for depression during adolescence (9–11), and that the effects of stress on the immune and nervous systems are critical in understanding the onset and persistence of depression. Extensive research has shown that psychosocial stressors activate the immune system by initiating a cascade of inflammatory responses, including increased production of pro-inflammatory cytokines in the peripheral nervous system (12). Importantly, peripheral cytokines can cross and alter the permeability of the blood-brain barrier (13) and influence processes that affect glutamate metabolism through a variety of mechanisms, including, but not limited to, increased production of quinolinic acid-which binds to glutamatergic NMDAreceptors and provokes release of glutamate into the synapse-and the impediment of astrocyte reuptake of glutamate (5, 12, 14, 15). Indeed, preclinical data indicate that inflammatory cytokines stimulate glutamate release that, over time, leads to cell apoptosis and to damage to oligodendrocytes (16, 17). Thus, glutamatergic excitotoxicity may be one mechanism by which inflammatory cytokines effect depression-related changes both in the brain and in behavior (18).

Consistent with this framework, investigators have conducted studies in adults of translocator protein 18 kDA (TSPO)-positron emission topography (PET) binding that index microglial activation by measuring TSPO expression; these researchers report higher TSPO binding in the ACC in patients with depression compared to healthy controls (19, 20). Neuroinflammation and mediators of the immune response (e.g., microglia) in the central nervous system cannot be measured non-invasively; however, technologies such as proton magnetic resonance spectroscopy (MRS) can be used to measure non-invasively the downstream effects of peripheral cytokines on levels of neurotransmitters, including glutamate. Studies using MRS to examine depression-related alterations in glutamate have primarily focused on the anterior cingulate cortex [ACC; for reviews and meta-analyses, see (21, 22)], a large brain region with distinct subdivisions (23). While these recent reviews report that the published literature thus far has identified *lower* glutamate in the ACC in depressed individuals compared to healthy controls, these patterns have been equivocal in the nine MRS studies conducted with depressed adolescents. Prior studies have focused primarily on adults with depression, in which measures of glutamate are often confounded by medication usage, chronicity of illness, and age-related effects on overall brain development (e.g., thinner gray matter) that likely complicate the nature of how, and the extent to which, inflammation affects glutamate in the context of MDD. Importantly, with the exception of one study (24), all MRS studies of depressed adolescents conducted to date have each recruited fewer than 17 depressed adolescents (22), and many have acquired spectral data on MR scanners at 1.5 Tesla (22), which have poorer signal-to-noise ratios and more limited resolution for resolving spectral resonances than do scanners at 3 Tesla.

The present study was designed to examine the role of glutamatergic abnormalities in adolescent depression by testing associations between peripheral levels of inflammation, indexed by pro-inflammatory cytokines, and levels of Glu in the dorsal ACC (dACC) in clinically depressed adolescents scanned at 3 Tesla. Our focus on the dACC is motivated in part by previous studies that have identified functional and structural abnormalities in this division of the ACC in depressed vs. non-depressed adolescents. From a neurodevelopmental perspective, the dACC has been shown to be a key region in which there are dramatic changes in connectivity with limbic and cortical regions that underlie affective processing and cognitive control during adolescence (25, 26). Thus, it is likely that insults in the form of psychosocial stress and psychiatric disease have a profound impact on dACC development and, subsequently, on psychosocial skills associated with adaptive emotion regulation (23, 27). Indeed, our group has reported that depressed adolescents exhibit lower dACC network connectivity than do psychiatrically healthy controls and, further, that dACC network connectivity is associated with an earlier age of depression onset (28). Together, these results suggest that the dACC is a critically important region to examine in understanding the neurobiological substrates of adolescent depression.

An exploratory aim of the study was to examine the role of antioxidants in a model of inflammatory contributions to glutamatergic metabolism in adolescent depression. Basic researchers have begun to report that antioxidants, such as ascorbate (Asc, also known as Vitamin C), buffer against the neurotoxic effects of excessive glutamate in neurons, and may serve a neuroprotective role against glutamatergic excitotoxicity (29–32). These findings, however, have yet to be replicated in humans.

To address these gaps, we recruited 55 clinically depressed adolescents who underwent short-TE MRS scans that permitted modeling of Glu and Asc resonances at 3 Tesla, and who provided blood samples from which we assayed inflammatory cytokines. We tested whether peripheral levels of inflammation were positively associated with glutamate concentrations in the dorsal ACC, and explored whether levels of ascorbate in the dACC moderated the associations between peripheral levels of inflammation and dACC glutamate.

METHODS AND MATERIALS

Participants

Fifty-five adolescents between the ages of 13 and 18 years were recruited from the San Francisco Bay Area community as part of a longitudinal study examining neurobiological mechanisms underlying adolescent stress and depression (18). We interviewed participants and their caregiver at an initial session to assess study eligibility (see below) using the Kiddie Schedule for Affective Disorders and Schizophrenia–Present and Lifetime [K-SADS-PL; (33, 34)], the Children's Depressive Rating Scale–Revised [CDRS-R; (35)], and the Family Interview for Genetics Studies [FIGS; (36)]. Eligible participants were invited to complete additional questionnaires, and to complete an MRI scan and provide blood samples at a subsequent session held ∼2 weeks after the initial baseline session (interval: 10.85 ± 6.08 days). Inclusion criteria for potentially depressed adolescents included being 13–18 years of age, being fluent in English, and having a depressive disorder (Major Depressive Disorder, Dysthymia, or Depressive Disorder Not Otherwise Specified) based on a combination of the K-SADS-PL and CDRS-R (i.e., *t*-scores ≥55 or raw scores ≥30) for those who did not meet full criteria for MDD or Dysthymia in the K-SADS-PL screening, provided that the participant also endorsed at least 2 symptoms of MDD or Dysthymia in the K-SADS-PL screening [see (18) for more details]. Exclusion criteria included meeting lifetime or current criteria for Mania, Psychosis, or Alcohol Dependence (based on DSM-IV) or Moderate Substance Use Disorder with substance-specific threshold for withdrawal (based on DSM-V), premenarchal status (for females), history of concussion within the past 6 weeks or history of any concussion with loss of consciousness, contraindications for MRI scanning (e.g., braces, metal implants, or claustrophobia), and any serious neurological or intellectual disorders that could interfere with the ability to complete study components. The study was approved by the Institutional Review Boards (IRBs) at Stanford University and the University of California, San Francisco. All participants and their legal guardian(s) gave written assent and informed consent, respectively, in accordance with the Declaration of Helsinki, and were compensated for their participation.

Depression Symptom Severity

Trained research assistants administered the CDRS-R to participants and their parents/legal guardians as a measure of depression symptom severity. The CDRS-R is a clinician-rated scale composed of 17 questions; both participants and caregivers were administered the first 14 questions to assess depressive symptomology, while the last 3 questions were rated based on the interviewer's observation of the adolescent participant to assess non-verbal characteristics of depression including depressed affect, listless speech, and hypoactivity. Interviewers integrated responses from both parent and child interviews to produce summary items ratings, which were then summed to attain a total summary score for each participant. All item ratings were discussed by a subset of the co-authors to ensure consistency across interviewers to maximize reliability and validity. The CDRS-R is the most widely used rating scale in clinical research trials for assessing the severity of depression and change in depressive symptoms in children and adolescents with depression. While there are no thresholds for distinguishing mild, moderate, and severe levels of depression beyond the cutoff score of 30 that is used to determine depression and the score of ≤28 that is used to determine remission, there is evidence that scores of 35–40 indicate mild depression (37). In our full sample, 37 participants (67.3%) met the clinical cutoff score of 40 on the CDRS-R, 15 participants (27.3%) scored 35–40, 2 participants (3.6%) scored 28–35, and 1 participant (1.8%) had a score <28. In our final analytic sample with usable ACC Glu and cytokine data, 20 participants (64.5%) had scores higher than 40 and 11 participants (35.5%) scored 35–40; no participants had scores <35.

Pro-inflammatory Cytokines

Peripheral levels of pro-inflammatory cytokines were assayed from dried blood spot (DBS) samples. Blood samples were collected using mini contact-activated lancets (BD 366594 Microtainer, BD Biosciences, San Jose, CA) that were used to prick the participant's finger from their non-dominant hand after running their hand under hot water for 2 min. Blood spots were collected on 1.3 cm filter paper cards (Whatman #903, GE Healthcare, Piscataway, NJ) with ∼150–250 μL amount of blood per spot; spots were then dried overnight at room temperature before being transferred to Ziplock bags with a desiccant for storage in a −20°C freezer. Sample extraction and Luminex analysis was performed by the Human Immune Monitoring Center at Stanford University. Samples were extracted and diluted 3-fold in the Luminex assay buffer prior to being run on a 62-plex Procarta plex assay (Thermo Fisher, Santa Clara, CA) on the Luminex FlexMap 3D. Custom Assay Chex control beads were added to all wells (Radix Biosolutions, Georgetown, Texas). Data were analyzed using MasterPlex software (Hitachi Software Engineering America Ltd., MiraiBio Group). Both median fluorescence intensity (MFI) and calculated concentration values (in pg/mL) were estimated for each analyte. Based on prior work demonstrating advantages of using MFI over concentration values for low abundant analytes from multiplex assays (38), we conducted all analyses using median fluorescence intensity (MFI) values (log-transformed). To correct for non-specific binding, we employed ordinary non-linear least squares (ONLS) regression by regressing cytokine values (log MFI) on CHEX4 values; the resulting residualized scores were thus used in subsequent statistical analyses (39). To minimize multiple comparisons, we focused our analyses on the pro-inflammatory cytokines IL-1β,

IL-6, TNF-α, as these cytokines have been previously linked with depression (4, 7, 8, 40–43) and have been shown to be assayed reliably from DBS (44, 45). Of the 55 participants, 1 participant did not return after their initial assessment, and 1 did not feel comfortable providing a blood sample. Of the 53 participants who provided blood samples, 6 had samples that were collected and assayed differently (for the purposes of piloting protocols), and 9 did not provide sufficient blood volume for the assay.

MR Scanning Acquisition

All MRI scans were acquired at the Stanford Center for Cognitive and Neurobiological Imaging (CNI) with a 3T GE Discovery MR750 (General Electric Healthcare, Milwaukee, WI, USA) and Nova 32-channel head coil (Nova Medical, Wilmington, MA, USA). Participants completed a T1-weighted anatomical scan based on the GE BRAVO IR-prep, fast spoiled gradient (SPGR) sequence: TR/TE/TI = 8.2/3.2/600 ms; flip angle = 12°; 156 axial slices; FOV = 256 mm; matrix = 256 mm × 256 mm, voxel resolution = 1 × 1 × 1 mm^3; total scan time = 3 min 40 s. Participants also completed proton MRS scans based on a modification of the GE Healthcare PRESS product sequence, PROBE-p™. Two features were added to the product PROBE-p™ sequence for improved localization: (1) 16 step phase cycling (EXORCYCLE on the two refocusing RF pulses) and (2) application of a sensitive point echo planar (EP) waveform during acquisition to further eliminate out-of-slice artifact in the logical z direction (46–48). The bandwidth of the CHESS RF water-suppression pulses was reduced from 150 to 75 Hz to avoid suppression of the ascorbate peak at 4.1 ppm. We performed single voxel spectroscopy using this sequence with TE/TR = 35/2,000 ms, 128 averages, total scan time = 5 min 4 s on the graphically prescribed region of the dACC based on the 3D T1-weighted anatomical images using anatomical landmarks (all prescriptions confirmed by TCH).

MR Spectral Processing

Concentrations of Glu, Asc, and other metabolites in the dACC were quantified and expressed as ratios to total creatine (i.e., creatine and phosphocreatine) levels using LCModel (49), which models *in vivo* spectrum as a linear combination of basis *in vitro* spectra from individual metabolites. Experimental Asc basis spectrum was acquired using the same sequence as for the *in vivo* studies from a custom built 50 mM Asc spherical phantom with pH of 7.2 at 37°C in an otherwise synthetic basis set to improve accuracy, due to the complexity of the Asc resonances and their dependence on temperature. Previous studies have indicated that Asc can be reliably measured from the human brain at 3 Tesla (50); independent data from our group also indicate that Asc at physiological concentrations can be reliably estimated from LCModel using this method at 3 Tesla with a mean Cramer-Rao Lower Bound (CRLB) of 16% in cortical gray matter (51). We used CRLB, a measure of the reliability of the fit, with a quality criterion set at ≤35% for each individual metabolite. All T1-weighted MR images were run through FreeSurfer 6.0 [(52); http://surfer.nmr.mgh.harvard.edu/fswiki/recon-all] to perform tissue segmentation and to estimate percentage of gray matter, white matter, and cerebrospinal fluid in the dACC voxel. For all statistical analyses involving Glu or Asc, we included percentage of gray matter in the prescribed dACC voxel as a covariate (see below). See **Figure 1** for exemplary spectra from a representative subject. Of the 55 participants, 1 participant did not return after their initial assessment and 2 did not feel comfortable completing the MR scan. Of the 52 participants who completed the MRS scans, 44 provided usable data for Glu and 19 for Asc, based on CRLB criteria.

Statistical Approach

All analyses were conducted in R (version 3.5.3; R Core Team). All associations between main variables of interest were tested using Pearson's correlations. We conducted multiple linear regressions to test whether baseline levels of pro-inflammatory cytokines were associated with concentrations of Glu in the dACC and whether levels of Asc in the dACC moderated any of these associations. To probe significant interaction effects, we applied the Johnson-Neyman procedure for continuous predictors using *sim_slopes* in R. In all statistical models, we covaried for age, gender (male, female, non-binary), psychotropic medication use (coded as a dichotomous variable), percentage of gray matter in the dACC voxel, Body Mass Index (BMI), and anti-inflammatory medication usage (coded as a dichotomous variable). We selected these covariates based on previous work identifying potential influences of these factors on both peripheral cytokine levels and MRS-based estimates of neurometabolites. To estimate standardized coefficient weights (β), all predictor and response variables were z-scored.

Code Availability

Scripts for conducting functional clustering and statistical analyses can be found at: https://github.com/tiffanycheingho/TIGER/.

RESULTS

Demographic and Clinical Characteristics

Demographic and clinical characteristics of participants at baseline are presented in **Table 1**. Of the 55 participants enrolled in the study, 11 did not provide usable Glu data, 36 did not provide usable Asc data, and 17 did not provide usable blood data. We compared the 16 participants who were not missing any data on any measure to the 39 participants who were missing data on at least one measure of interest on baseline demographic and clinical characteristics. None of the effect sizes of the differences were statistically significant (all $ps > 0.081$) and all were small or negligible, with the exception of highest level of parental education, which had a large effect size [Cramer's $\phi = 0.586$, $\chi^2_{(5,\ 50)} = 17.193, p < 0.01$].

Descriptive statistics of the main variables of interest are presented in **Table 2**. A correlation matrix of the primary predictors and outcomes of interest, covariates, and clinical characteristics is presented in **Figure 2**. As expected, the inflammatory cytokines of interest were all highly intercorrelated (all $rs > 0.67$, all $ps < 0.0001$). IL-6 was positively correlated with Glu in the dACC ($r = 0.41$, $p = 0.02$), and both IL-6 and

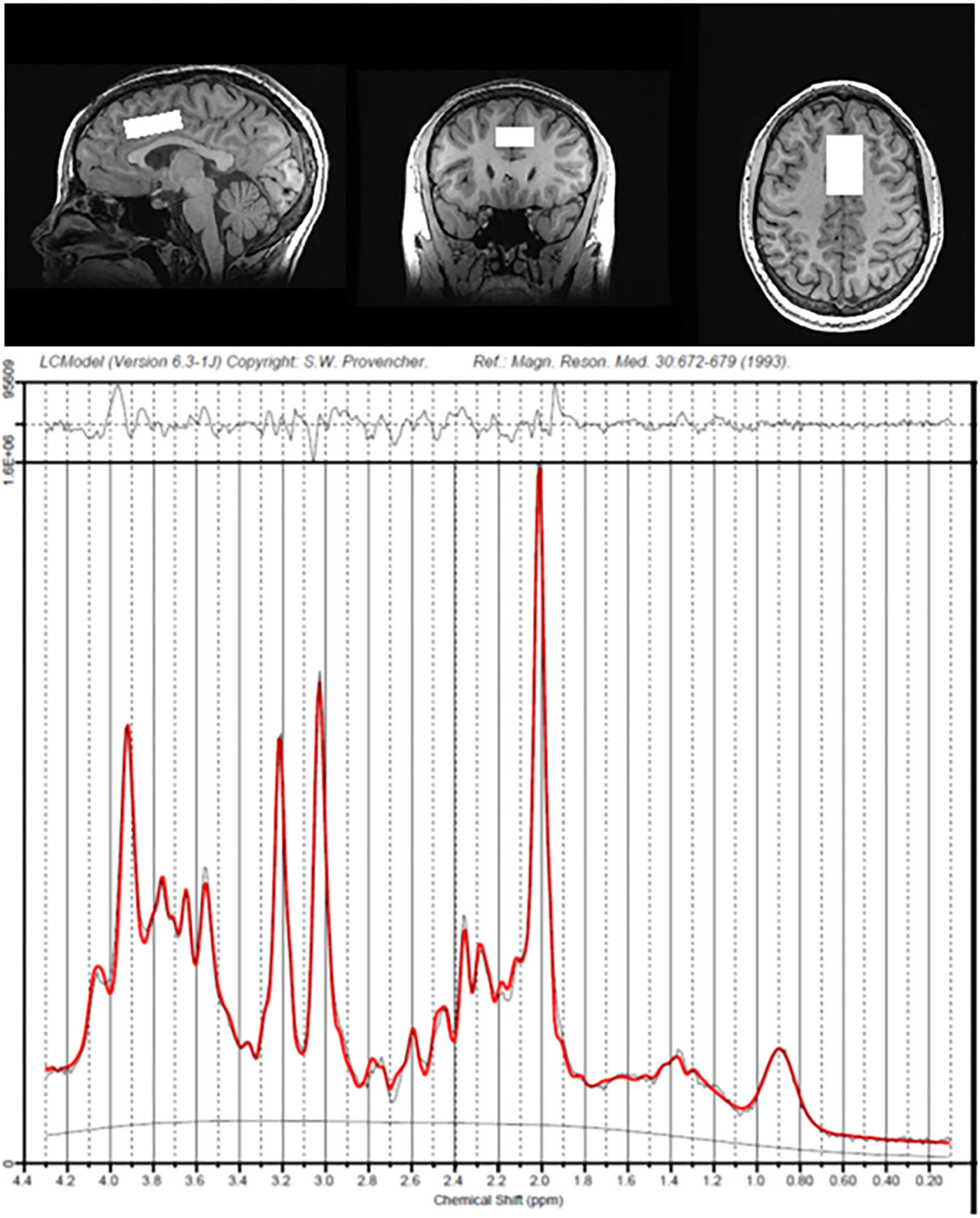

FIGURE 1 | Voxel placement of dorsal anterior cingulate cortex and spectra data from a representative participant.

TABLE 1 | Descriptive statistics of participant demographic and clinical characteristics.

Variable	Descriptive statistics
Age at V1 (years)	16.25 ± 1.32 (13.65 – 18.37)
Time between V1 and V2 (Days)	10.85 ± 6.08 (1 – 29) [1]
Sex (Female/Male)	65.45% (36)/34.55% (19)
Gender	
Male	34.55% (19)
Female	60.00% (33)
Non-binary/Other	5.45% (3)
Sexual orientation[a]	
Straight/Heterosexual	49.09% (27)
Gay/Lesbian	3.64% (2)
Bisexual	27.27% (15)
Other	5.45% (3)
Prefer not to say/Missing	14.55% (8)
Body Mass Index (BMI)	23.39 ± 5.63 (16.59 – 38.51) [2]
CDRS-R total	48.22 ± 12.12 (26 – 81)
Age of current depressive episode onset	13.65 ± 2.4 (4 – 17)
Number of depressive episodes	1.73 ± 1.04 (1 – 5)
Current psychotropic medication	**47.27% (26)**
Antidepressant	34.55% (19)
Antipsychotic	5.45% (3)
Stimulant	10.91% (6)
Benzodiazepine	1.82% (1)
Other[b]	12.73% (7)
Concurrent therapy	27.27% (15)
Therapy[c]	49.09% (27)
Anti-inflammatory medication[d]	12.73% (7)
Ethnicity	
Hispanic/Latinx	16.36% (9)
Not Hispanic/Latinx	83.64% (46)
Race	
White	47.27% (26)
Black/African American	3.64% (2)
American Indian/Alaska Native	3.64% (2)
Asian	18.18% (10)
Native Hawaiian/Pacific Islander	0% (0)
Multiracial	21.82% (12)
Other	5.45% (3)
Highest parental education	
Less than a high school diploma	0% (0)
High school graduate or equivalent (e.g., GED)	1.82% (1)
Some college (no degree)	9.09% (5)
Associate's degree (e.g., AA, AS)	3.64% (2)
Bachelor's degree (e.g., BA, BS)	27.27% (15)
Master's degree (e.g., MA, MS, MEd)	34.55% (19)
Doctoral or Professional degree (e.g., MD, DDS, DVM, Ph.D., EdD)	14.55% (8)
Unknown/Missing	9.09% (5)
Annual household income	
<$20,000	5.45% (3)
$20,000–$34,999	0% (0)
$35,000–$49,999	1.82% (1)
$50,000–$74,999	7.27% (4)
$75,000–$99,999	5.45% (3)
Over $100,000	69.09% (38)
Unknown/Missing	10.91% (6)
Comorbidity	**Lifetime reports**
Anxiety disorders[e]	43.64% (24)
Obsessive compulsive disorder	3.64% (2)
Eating disorders[f]	5.45% (3)
Disruptive, impulse control, and conduct disorders[g]	3.64% (2)
Post-traumatic stress disorder	20.00% (11)
Attention deficit hyperactivity disorder	23.64% (13)
Other[h]	1.82% (1)
Unknown/Missing	14.55% (8)

All continuous values are reported as mean ± SD (min – max). Numbers in brackets [ ] indicate the number of missing or unusable responses. Categorical variables are reported as percentage (count). Lifetime comorbidities (includes past and current reports integrated across parent and child interviews) are reported as percentage (count). CDRS-R, Children's Depression Rating Scale-Revised.

[a]Other sexual orientations indicated by participants, with ( ) indicating count, include pansexual (1), queer (1), and demi-sexual (1).

[b]Other medications taken by participants, with ( ) indicating count, include Gabapentin (1), Trazodone (4), Prazosin (1), Buspar (1), Dextromethorphan (1), and Cannabidiol (1).

[c]Therapy indicates the percentage (count) of participants who reported attending therapy sessions for their depression in the 2 months prior to their first visit.

[d]Anti-inflammatory medication includes any anti-histaminergic, antibiotic, or steroid medications participants reported taking at the time of their session. In the subsample that provided a usable blood sample (n = 38), 7.89% (3) participants reported use of anti-inflammatory medication.

[e]Anxiety disorders reported with counts across participants: Panic Disorder (4), Social Phobia (11), Simple Phobia (5), Agoraphobia (2), Generalized Anxiety Disorder (16).

[f]Eating Disorders: Anorexia Nervosa (2), Bulimia Nervosa (0), Eating Disorder Not Otherwise Specified (2).

[g]Disruptive, Impulse Control, and Conduct Disorders: Oppositional Defiant Disorder (1), Conduct Disorder (1).

[h]Other Disorders: Disruptive Mood Dysregulation Disorder (1), Austism Spectrum Disorder (1).

TNF-α were negatively correlated with Asc in the dACC (both $rs < -0.54$, both $ps < 0.03$). Finally, age of study assessment was associated with age of onset for current depressive episode ($r = 0.46, p < 0.001$).

TABLE 2 | Descriptive statistics for main variables of interest.

Variable	Descriptive statistics
Glu/Cr + PCr	1.40 ± 0.17 (1.10 – 2.25) [11]
Asc/Cr + PCr	0.24 ± 0.05 (0.17 – 0.32) [36]
Gray Matter Percentage dACC Voxel (%)	0.56 ± 0.06 (0.35 – 0.68) [11]
IL-6 (log)	4.57 ± 0.13 (4.3 – 4.86) [17]
TNF-α (log)	4.83 ± 0.17 (4.51 – 5.13) [17]
IL-1β (log)	4.02 ± 0.17 (3.64 – 4.45) [17]

All values are reported as mean ± SD (min – max). Numbers in brackets [ ] indicate the number of missing or unusable responses.

Higher Levels of IL-6 Are Associated With Higher Concentrations of Glutamate in the Dorsal Anterior Cingulate Cortex

Thirty-one participants provided both usable cytokine and Glu data. Levels of IL-6 were significantly positively associated with concentrations of dACC Glu ($\beta = 0.466 \pm 0.199$, $t_{22} = 2.339$, $p = 0.029$, $\Delta R^2 = 0.199$). Levels of IL-1β and TNF-α were not significantly associated with concentrations of Glu in the dorsal ACC (all ps > 0.288). See **Figure 3** for more details.

One participant who exhibited abnormally high levels of Glu in the dACC was a statistical outlier despite having adequate CRLB for estimates of Glu. Although winsorizing the outlier data (based on a median-unbiased estimator interpolated from the sample without strict distribution assumptions, see *quantile* in R) did not change the significance of the association between IL-6 and dACC Glu ($p < 0.05$), removal of the outlier changed the statistical significance ($p = 0.235$). The associations between IL-1β and TNF-α with dACC Glu remained non-significant regardless of the treatment of the outlier (all ps > 0.397 when winsorizing, all ps > 0.764 when removing the statistical outlier).

Exploring the Moderating Role of Ascorbate in the Dorsal Anterior Cingulate Cortex on the Association Between IL-6 and Glutamate in the Dorsal Anterior Cingulate Cortex

Sixteen participants provided usable cytokine, Glu, and Asc data. Higher levels of Asc in the dorsal ACC moderated the associations between levels of IL-6 and Glu in the dorsal ACC, even after accounting for age, gender, BMI, percentage of gray matter in the voxel, and antidepressant and anti-inflammatory medication usage (interaction effect: $\beta = -0.906 \pm 0.433$, $t_6 = -2.74$, $p = 0.034$, $\Delta R^2 = 0.557$). We used the Johnson-Neyman procedure to compute the values of dACC Asc where the linear correlation between IL-6 and dACC Glu was statistically significant. We found that whereas Asc levels lower than 0.16 were associated with a significantly positive correlation between IL-6 and Glu, Asc levels higher than 0.32 were associated with a significantly negative correlation between IL-6 and Glu; Asc values between 0.16 and 0.32 were not associated with significant correlations between IL-6 and Glu. See **Figure 4** for more details.

DISCUSSION

The present study was designed to examine, in depressed adolescents, associations between peripheral levels of inflammation, as indexed by pro-inflammatory cytokines, and concentrations of glutamate (Glu) in the dorsal anterior cingulate cortex (dACC), a region that has been implicated in adolescent depression in a range of structural and functional MRI studies but that has been relatively neglected in studies using MRS. We found that levels of IL-6, but not of IL-1β or TNF-α, were positively associated with concentrations of Glu in the dACC. In an exploratory analysis, we also found that higher concentrations of Asc in the dACC moderated the association between IL-6 and concentrations of Glu in the dACC, such that these markers were negatively correlated at higher levels of Asc only.

Our primary finding that higher levels of inflammatory cytokines, specifically IL-6, are associated with higher concentrations of glutamate in the dACC significantly advances our understanding of glutamatergic abnormalities in adolescent depression, particularly given the sparse and conflicting research in this area. First, our results are consistent with animal models demonstrating the role of inflammatory cytokines in contributing to glutamatergic excitotoxicity (12, 18); they appear to be inconsistent, however, with findings from MRS studies indicating lower concentrations of Glu in the ACC of depressed adults (22). One explanation for this discrepancy involves the specific region examined in this study. We focused on the dorsal division of the ACC based on findings of previous studies that abnormalities in this region may be a neurodevelopmentally sensitive marker of adolescent depression (28), in contrast to the rostral (pregenual) or medial ACC (22). Studies focused on the rostral and medial ACC in depressed adolescents, however, have found evidence of higher Glx (sum of glutamate and glutamine, a precursor to glutamate and GABA) in depressed adolescents with suicidal ideation than in healthy controls (53), as well as reductions in the ratio of glutamine to glutamate (Gln/Glu) in response to treatment-related symptom improvement (54). Although these studies examined Glx and Gln/Glu rather than solely Glu, their data are nonetheless consistent with our findings that higher levels of Glu may contribute to depressive symptomatology. Thus, a second explanation of the discrepancy between our findings and those of previous studies is that higher levels of Glu in the ACC may characterize depression that occurs at earlier developmental stages, when the consequences of chronically high levels of glutamate on brain structure (e.g., cell apoptosis, cortical thinning, etc.) have not yet had as large an impact. Future research with larger samples that include both adolescents and adults and that image the distinct portions of the ACC are needed to test these hypotheses more explicitly and to determine whether higher Glu in the ACC is an adolescent-specific indicator of depression.

Our finding that the positive association IL-6 and Glu in the dACC was found only at lower levels of Asc is broadly consistent with basic science work showing that Asc prevents excitotoxic damage to cells by inhibiting the binding of Glu to NMDA receptors and by limiting the effects of oxidative

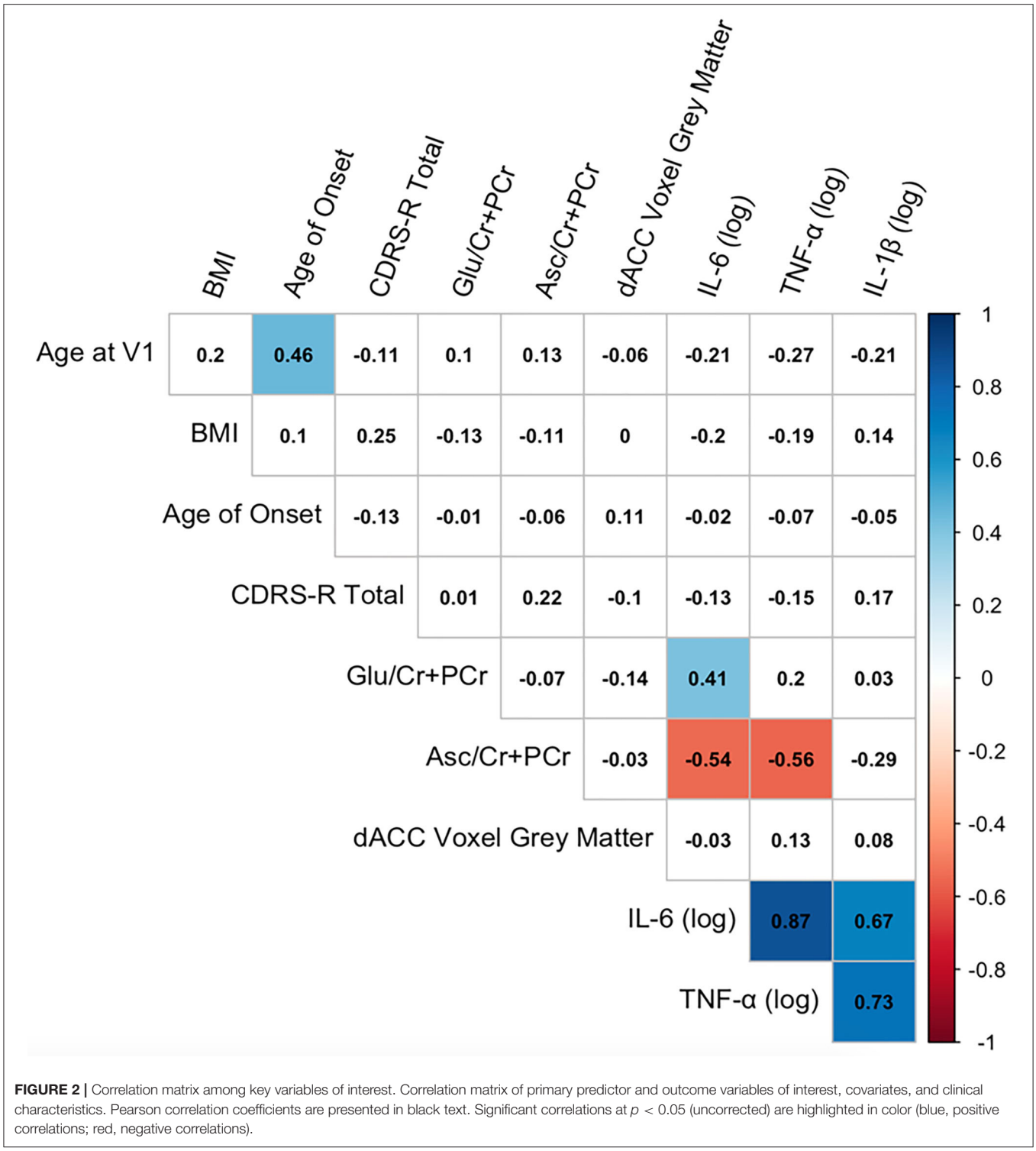

FIGURE 2 | Correlation matrix among key variables of interest. Correlation matrix of primary predictor and outcome variables of interest, covariates, and clinical characteristics. Pearson correlation coefficients are presented in black text. Significant correlations at $p < 0.05$ (uncorrected) are highlighted in color (blue, positive correlations; red, negative correlations).

stress markers, including quercetin (29–32). Other studies have also shown that Asc is pharmacologically effective against glutamate-induced phosphorylation of AMPK, a mechanism of neuronal cell death (55). While preliminary, these results highlight the potential role of antioxidants in mitigating the downstream effects of inflammation on the brain, including glutamate metabolism. Indeed, several studies have reported that ascorbic acid supplements produce an antidepressant (and not anxiolytic, suggesting specificity) effect [for a review, see (56)]. The low toxicity and high tolerance of Asc may make

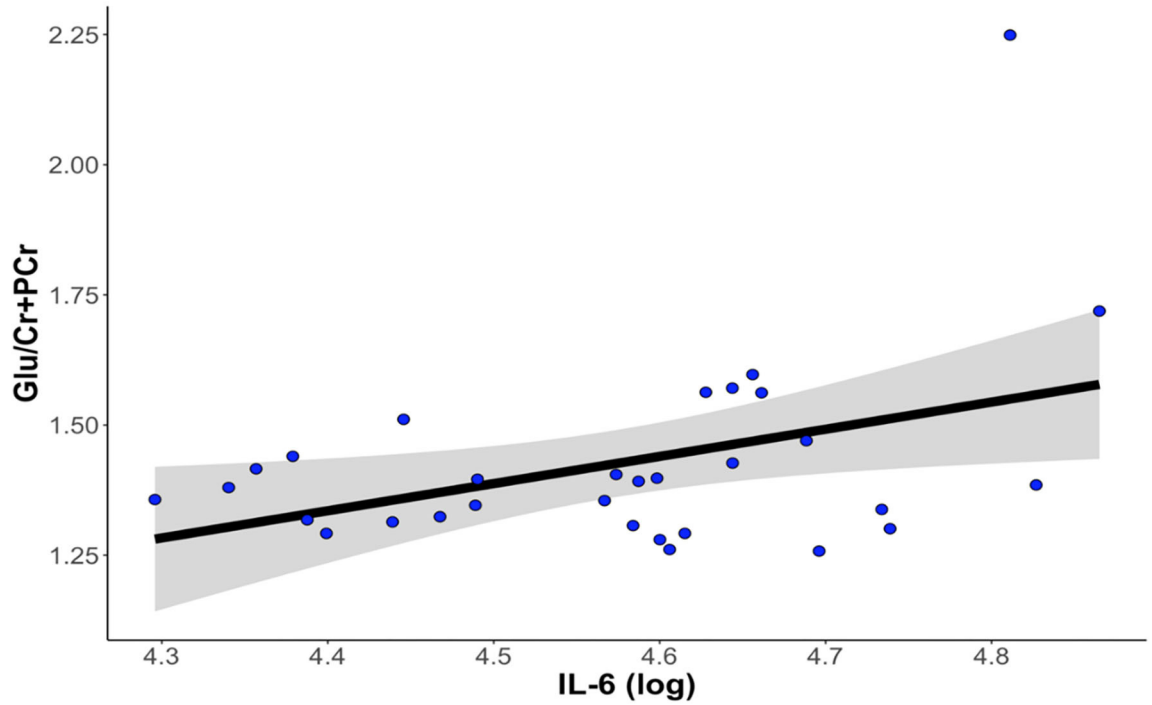

FIGURE 3 | Higher levels of IL-6 at baseline are associated with higher levels of Glu in the dorsal anterior cingulate cortex. The correlation between IL-6 and dACC Glu remained statistically significant after controlling for age, gender, percentage of gray matter volume in the dACC voxel, antidepressant medication usage, and anti-inflammatory medication usage. dACC, dorsal anterior cingulate cortex; Glu, glutamate; IL-6, interleukin-6.

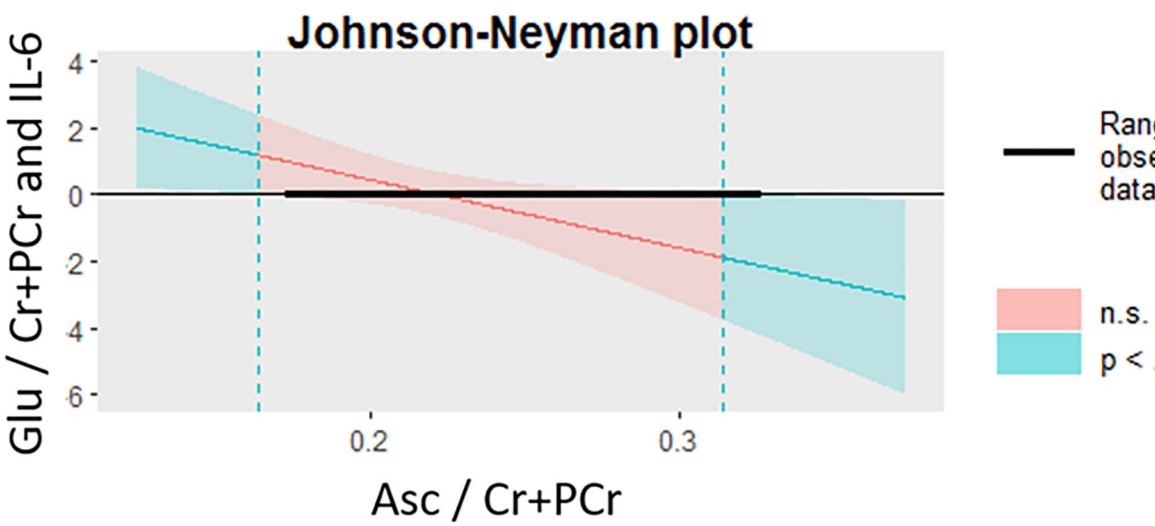

FIGURE 4 | Levels of Asc in the dACC moderate the association between IL-6 and glutamate in the dACC. The Johnson-Neyman procedure was used to probe the interaction effect of dACC Asc and IL-6 on dACC Glu. At lower levels of Asc (<0.16, indicated by dotted teal line, left), the correlation between IL-6 and Glu was significantly positive ($p < 0.05$) whereas at higher levels of Asc (>0.32, indicated by dotted teal line, right), the correlation between IL-6 and Glu was significantly negative ($p < 0.05$). Asc, ascorbate; dACC, dorsal anterior cingulate cortex; Glu, glutamate; IL-6, interleukin-6.

Asc a possible adjuvant to first-line antidepressant treatments. An important direction of future research will be to test the extent to which anti-inflammatory strategies—including pharmacological agents, psychosocial therapies targeting stress reduction, or lifestyle and behavioral changes (e.g., changes in sleep, exercise, and/or diet)—affect levels of Asc in the

brain and whether they help to reduce or prevent depression in adolescents.

Although the effect size of the association between IL-1β as well as TNF-α and Glu in the dACC was in the same direction as that of IL-6 and Glu, it is notable that we detected effects that were specific to IL-6. IL-1β, IL-6, and TNF-α are similar in their role in mediating immune responses; all three are released into circulation by innate immune cells to act on organs throughout the body [e.g., signaling the release of acute phase reactants such as C-reactive protein; (57)]. All three have also been shown to alter glutamate production (58, 59); in particular, TNF-α, has been strongly linked with glutamate-mediated oxidative stress and impairment of glutamate reuptake from astrocytes (59). Importantly, however, *in vivo* studies conducted with rodents have found that chronic stress paradigms that upregulate levels of IL-6 do so in the absence of increases in IL-1b and, further, that administration of IL-6 specifically produces depressive-like phenotypes in rodents (60). *In vivo* studies in human adolescents who are not clinically depressed have also showed that IL-6 predicts subsequent changes in depressive symptoms, although the extent of these effects appears to be conditional on other factors, including sex, stressful life events, and time or, possibly, developmental stage (7, 61). Our findings are consistent with much of the emerging human research in adults (12, 14, 15), by showing that in depressed adolescents higher levels of IL-6 specifically are associated with higher levels of glutamate. Nevertheless, it is critical that future studies with larger sample sizes replicate our findings and reconcile important differences between humans and animals in neuroimmune systems in order to facilitate forward and backward translation.

There are several limitations of our investigation that warrant additional discussion and that should be addressed in future research. First, our sample size was relatively small with a high degree of psychiatric comorbidity and medication use (including agents with some anti-inflammatory effects); it is important to note, however, that our study is one of the largest MRS studies to date conducted with depressed adolescents and the first to focus on the dACC (22), and also includes a sample that is representative of the type of patients who often present at clinics. Second, we did not exclude participants on the basis of medication history or usage. While we included both antidepressant and anti-inflammatory medications as statistical covariates in all of our analyses, it is possible that the effects of these medications nevertheless influenced our results. Bearing in mind issues concerning the generalizability of the findings (for example, many depressed adolescents seek treatment and are medicated), it will be important for future studies to consider recruiting unmedicated adolescents with depression. Third, we did not assess healthy control participants in our study. Future research will benefit from including psychiatrically healthy adolescents to clarify the extent to which the associations we observed are specific to adolescents who are depressed. Fourth, the reliability of Asc at 3 Tesla was significantly worse than the reliability of Glu; the advent of ultra-field MR imaging (e.g., 7 Tesla) may prove to be especially fruitful in improving detection and quantification of Asc. Finally, our study was a naturalistic observational study, which precluded our ability to make causal interpretations of the associations among IL-6, Glu, Asc, and depressive symptoms. Studies are needed that experimentally manipulate levels of inflammation, and of ascorbate, and that characterize these effects on cortical glutamate concentrations and subsequent behavior in samples of both depressed and non-depressed adolescents.

Despite these limitations, this study is important in establishing the associations among peripheral levels of inflammation and concentrations of glutamate and ascorbate in the dACC in humans with depression. In a cohort of depressed adolescents, we found that higher levels of IL-6 were associated with higher concentrations of Glu in the dACC and, further, that higher concentrations of Asc in the dACC moderated this effect, such that the positive association between IL-6 and Glu in the dACC was present only at lower levels of Asc. Although preliminary, our results underscore the importance of examining both immune and neural contributors to depression in adolescence and highlight the potential role of anti-inflammatory compounds in mitigating the adverse effects of inflammation (e.g., glutamatergic neuroexcitotoxicity) in depressed adolescents.

DATA AVAILABILITY STATEMENT

The datasets used and analyzed during the current study will be made available by the corresponding author upon reasonable request.

ETHICS STATEMENT

The studies involving human participants were reviewed and approved by Institution Review Board at Stanford University. Written informed consent to participate in this study was provided by the participants' legal guardian/next of kin.

AUTHOR CONTRIBUTIONS

TH designed the research. GT, JS, AO, and JW helped perform research. TH, GT, JS, AO, and YR-H analyzed the data. MG, DS, MS, FJ, YR-H, and HM provided additional analytic tools to assist with data analysis. TH and IG obtained funding support. All authors contributed to the writing of the manuscript.

FUNDING

This research was supported by the National Institutes of Health (K01MH117442 to TH, R37MH101495 to IG), the Klingenstein Third Generation Foundation (Child and Adolescent Depression Fellow Award to TH), the Stanford Maternal Child and Health Institute (Early Career Award and K Support Award to TH), the Stanford Center for Cognitive and Neurobiological Imaging Center (Seed Grant to TH), and the Ray and Dagmar Dolby Family Fund (to TH). The funding agencies played no role in the design and conduct of the study; collection, management, analysis, and interpretation of the data; and preparation, review, or approval of the manuscript.

ACKNOWLEDGMENTS

We thank Anna Cichocki, Miranda Edwards, Holly Pham, Michelle Sanabria, Lucinda Sisk, Alexess Sosa, and Rachel Weisenburger for assistance with data collection and organization. Finally, we thank the participants and their families for contributing to this study.

REFERENCES

1. World Health Organization. *Depression and Other Common Mental Disorders: Global Health Estimates*. World Health Organization (2017).
2. Breslau J, Gilman SE, Stein BD, Ruder T, Gmelin T, Miller E. Sex differences in recent first-onset depression in an epidemiological sample of adolescents. *Transl Psychiatry*. (2017) 7:e1139. doi: 10.1038/tp.2017.105
3. Huang M, Su S, Goldberg J, Miller AH, Levantsevych OM, Shallenberger L, et al. Longitudinal association of inflammation with depressive symptoms: a 7-year cross-lagged twin difference study. *Brain Behav Immun*. (2019) 75:200–7. doi: 10.1016/j.bbi.2018.10.007
4. Mac Giollabhui N, Ng TH, Ellman LM, Alloy LB. The longitudinal associations of inflammatory biomarkers and depression revisited: systematic review, meta-analysis, and meta-regression. *Mol Psychiatry*. (2020). doi: 10.1038/s41380-020-00867-4. [Epub ahead of print].
5. Miller AH, Raison CL. The role of inflammation in depression: from evolutionary imperative to modern treatment target. *Nat Rev Immunol*. (2016) 16:22. doi: 10.1038/nri.2015.5
6. Dooley LN, Kuhlman KR, Robles TF, Eisenberger NI, Craske MG, Bower JE. The role of inflammation in core features of depression: Insights from paradigms using exogenously-induced inflammation. *Neurosci Biobehav Rev*. (2018) 94:219–37. doi: 10.1016/j.neubiorev.2018.09.006
7. Moriarity DP, Mac Giollabhui N, Ellman LM, Klugman J, Coe CL, Abramson LY, et al. Inflammatory proteins predict change in depressive symptoms in male and female adolescents. *Clin Psychol Sci*. (2019) 7:754–67. doi: 10.1177/2167702619826586
8. Moriarity DP, Kautz MM, Mac Giollabhui N, Klugman J, Coe CL, Ellman LM, et al. Bidirectional associations between inflammatory biomarkers and depressive symptoms in adolescents: potential causal relationships. *Clin Psychol Sci*. (2020) 8:690–703. doi: 10.1177/2167702620917458
9. Hammen C. Adolescent depression: stressful interpersonal contexts and risk for recurrence. *Curr Direct Psychol Sci*. (2009) 18:200–4. doi: 10.1111/j.1467-8721.2009.01636.x
10. LeMoult J, Humphreys KL, Tracy A, Hoffmeister JA, Ip E, Gotlib IH. Meta-analysis: exposure to early life stress and risk for depression in childhood and adolescence. *J Am Acad Child Adolesc Psychiatry*. (2019) 59:842–55. doi: 10.1016/j.jaac.2019.10.011
11. Patton GC, Coffey C, Posterino M, Carlin JB, Bowes G. Life events and early onset depression: cause or consequence? *Psychol Med*. (2003) 33:1203–10. doi: 10.1017/S0033291703008626
12. Miller RJ, Jung H, Bhangoo SK, White FA. Cytokine and chemokine regulation of sensory neuron function. *Handb Exp Pharmacol*. (2009) 417–49. doi: 10.1007/978-3-540-79090-7_12
13. Banks WA. Characteristics of compounds that cross the blood-brain barrier. *BMC Neurol*. (2009) 9(Suppl. 1):S3. doi: 10.1186/1471-2377-9-S1-S3
14. Haroon E, Miller AH, Sanacora G. Inflammation, glutamate, and glia: a trio of trouble in mood disorders. *Neuropsychopharmacology*. (2017) 42:193–215. doi: 10.1038/npp.2016.199
15. Haroon E, Miller AH. Inflammation effects on brain glutamate in depression: mechanistic considerations and treatment implications. *Curr Top Behav Neurosci*. (2017) 31:173–98. doi: 10.1007/7854_2016_40
16. Káradóttir R, Attwell D. Neurotransmitter receptors in the life and death of oligodendrocytes. *Neuroscience*. (2007) 145:1426–38. doi: 10.1016/j.neuroscience.2006.08.070
17. Matute C. Glutamate and ATP signalling in white matter pathology. *J Anat*. (2011) 219:53–64. doi: 10.1111/j.1469-7580.2010.01339.x
18. Walker JC, Teresi GI, Weisenburger RL, Segarra JR, Ojha A, Kulla A, et al. Study protocol for teen inflammation glutamate emotion research (TIGER). *Front Hum Neurosci*. (2020) 14:414. doi: 10.3389/fnhum.2020.585512
19. Richards EM, Zanotti-Fregonara P, Fujita M, Newman L, Farmer C, Ballard ED, et al. PET radioligand binding to translocator protein (TSPO) is increased in unmedicated depressed subjects. *EJNMMI Res*. (2018) 8:57. doi: 10.1186/s13550-018-0401-9
20. Setiawan E, Attwells S, Wilson AA, Mizrahi R, Rusjan PM, Miler L, et al. Association of translocator protein total distribution volume with duration of untreated major depressive disorder: a cross-sectional study. *Lancet Psychiatry*. (2018) 5:339–47. doi: 10.1016/S2215-0366(18)30048-8
21. Luykx JJ, Laban KG, van den Heuvel MP, Boks MP, Mandl RC, Kahn RS, et al. Region and state specific glutamate downregulation in major depressive disorder: a meta-analysis of (1)H-MRS findings. *Neurosci Biobehav Rev*. (2012) 36:198–205. doi: 10.1016/j.neubiorev.2011.05.014
22. Moriguchi S, Takamiya A, Noda Y, Horita N, Wada M, Tsugawa S, et al. Glutamatergic neurometabolite levels in major depressive disorder: a systematic review and meta-analysis of proton magnetic resonance spectroscopy studies. *Mol Psychiatry*. (2019) 24:952–64. doi: 10.1038/s41380-018-0252-9
23. Stevens FL, Hurley RA, Taber KH. Anterior cingulate cortex: unique role in cognition and emotion. *J Neuropsychiatry Clin Neurosci*. (2011) 23:121–5. doi: 10.1176/jnp.23.2.jnp121
24. Gabbay V, Mao X, Klein RG, et al. Anterior cingulate cortexγ-aminobutyric acid in depressed adolescents: relationship to anhedonia. *Arch Gen Psychiatry*. (2012) 69:139–49. doi: 10.1001/archgenpsychiatry.2011.131
25. Fair DA, Dosenbach NU, Church JA, Cohen AL, Brahmbhatt S, Miezin FM, et al. Development of distinct control networks through segregation and integration. *Proc Natl Acad Sci USA*. (2007) 104:13507–12. doi: 10.1073/pnas.0705843104
26. Power JD, Fair DA, Schlaggar BL, Petersen SE. The development of human functional brain networks. *Neuron*. (2010) 67:735–48. doi: 10.1016/j.neuron.2010.08.017
27. Lichenstein SD, Verstynen T, Forbes EE. Adolescent brain development and depression: a case for the importance of connectivity of the anterior cingulate cortex. *Neurosci Biobehav Rev*. (2016) 70:271–87. doi: 10.1016/j.neubiorev.2016.07.024
28. Ho TC, Sacchet MD, Connolly CG, Margulies DS, Tymofiyeva O, Paulus MP, et al. Inflexible functional connectivity of the dorsal anterior cingulate cortex in adolescent major depressive disorder. *Neuropsychopharmacology*. (2017) 42:2434–45. doi: 10.1038/npp.2017.103
29. Ballaz S, Morales I, Rodríguez M, Obeso JA. Ascorbate prevents cell death from prolonged exposure to glutamate in an *in vitro* model of human dopaminergic neurons. *J Neurosci Res*. (2013) 91:1609–17. doi: 10.1002/jnr.23276
30. Majewska MD, Bell JA. Ascorbic acid protects neurons from injury induced by glutamate and NMDA. *Neuroreport*. (1990) 1:194–6. doi: 10.1097/00001756-199011000-00004
31. Sandstrom MI, Rebec GV. Extracellular ascorbate modulates glutamate dynamics: role of behavioral activation. *BMC Neurosci*. (2007) 8:1–6. doi: 10.1186/1471-2202-8-32
32. Kocot J, Luchowska-Kocot D, Kiełczykowska M, Musik I, Kurzepa J. Does vitamin C influence neurodegenerative diseases and psychiatric disorders? *Nutrients*. (2017) 9:659. doi: 10.3390/nu9070659
33. Kaufman J, Birmaher B, Brent D, Rao U, Flynn C, Moreci P, et al. Schedule for affective disorders and schizophrenia for school-age children-present and lifetime version (K-SADS-PL): initial reliability and validity data. *J Am Acad Child Adolesc Psychiatry*. (1997) 36:980–8. doi: 10.1097/00004583-199707000-00021
34. Kaufman J, Birmaher B, Brent DA, Ryan ND, Rao U. K-SADS-PL. *J Am Acad Child Adolesc Psychiatry*. (2000) 39:1208. doi: 10.1097/00004583-200010000-00002

35. Poznanski EO, Grossman JA, Buchsbaum Y, Banegas M, Freeman L, Gibbons R. Preliminary studies of the reliability and validity of the children's depression rating scale. *J Am Acad Child Psychiatry*. (1984) 23:191–7. doi: 10.1097/00004583-198403000-00011
36. Maxwell ME. *Family Interview for Genetic Studies (FIGS): A Manual for FIGS*. Bethesda, MD: Clinical Neurogenetics Branch, Intramural Research Program, National Institute of Mental Health (1992).
37. Mayes TL, Bernstein IH, Haley CL, Kennard BD, Emslie GJ. Psychometric properties of the children's depression rating scale-revised in adolescents. *J Child Adolesc Psychopharmacol*. (2010) 20:513–6. doi: 10.1089/cap.2010.0063
38. Breen EJ, Tan W, Khan A. The statistical value of raw fluorescence signal in luminex xMAP based multiplex immunoassays. *Sci Rep*. (2016) 6:26996. doi: 10.1038/srep26996
39. Maecker HT, Rosenberg-Hasson Y, Kolstad KD, Steen VD, Chung LS. A novel utility to correct for plate/batch/lot and nonspecific binding artifacts in luminex data. *J Immunol.* (2020) 204:3425–33. doi: 10.4049/jimmunol.2000017
40. Howren MB, Lamkin DM, Suls J. Associations of depression with c-reactive protein, IL-1, and IL-6: a meta-analysis. *Psychosomat Med*. (2009) 71:171–86. doi: 10.1097/PSY.0b013e3181907c1b
41. Liu Y, Ho RCM, Mak A. Interleukin (IL)-6, tumour necrosis factor alpha (TNF-α) and soluble interleukin-2 receptors (sIL-2R) are elevated in patients with major depressive disorder: a meta-analysis and meta-regression. *J Affect Dis.* (2012) 139:230–9. doi: 10.1016/j.jad.2011.08.003
42. Raison CL, Rutherford RE, Woolwine BJ, Shuo C, Schettler P, Drake DF, et al. A randomized controlled trial of the tumor necrosis factor antagonist infliximab for treatment-resistant depression: The role of baseline inflammatory biomarkers. *Archiv Gen Psychiatry*. (2013) 70:31–41. doi: 10.1001/2013.jamapsychiatry.4
43. Valkanova V, Ebmeier KP, Allan CL. CRP, IL-6 and depression: a systematic review and meta-analysis of longitudinal studies. *J Affect Dis.* (2013) 150:736–44. doi: 10.1016/j.jad.2013.06.004
44. Miller EM, Mcdade TW. A highly sensitive immunoassay for interleukin-6 in dried blood spots. *Am J Hum Biol.* (2012) 24:863–5. doi: 10.1002/ajhb.22324
45. Skogstrand K, Thysen AH, Jørgensen CS, Rasmussen EM, Andersen ÅB, Lillebaek T, et al. Antigen-induced cytokine and chemokine release test for tuberculosis infection using adsorption of stimulated whole blood on filter paper and multiplex analysis. *Scand J Clin Lab Invest.* (2012) 72:204–11. doi: 10.3109/00365513.2011.649014
46. Bodenhausen G, Freeman R, Turner DL. Suppression of artifacts in two-dimensional J spectroscopy. *J Magnet Res.* (1977) 27:511–4. doi: 10.1016/0022-2364(77)90016-6
47. Gu M, Hurd R, Noeske R, Baltusis L, Hancock R, Sacchet MD, et al. GABA editing with macromolecule suppression using an improved MEGA-SPECIAL sequence. *Magnet Res Med.* (2018) 79:41–7. doi: 10.1002/mrm.26691
48. Webb PG, Sailasuta N, Kohler SJ, Raidy T, Moats RA, Hurd R. Automated single-voxel proton MRS: technical development and multisite verification. *Magnet Res Med.* (1994) 31:365–73. doi: 10.1002/mrm.1910310404
49. Provencher SW. Automatic quantitation of localized *in vivo* 1H spectra with LCModel. *NMR Biomed.* (2001) 14:260–4. doi: 10.1002/nbm.698
50. Shih Y, Buchert M, Chung HW, Jurgen H, Von Elverfeldt D. Vitamin C estimation with standard 1H spectroscopy using a clinical 3T MR system: detectability and reliability within the human brain. *J Magnet Res Imaging.* (2008) 28:351–8. doi: 10.1002/jmri.21466
51. Gu M, Hurd RE, Spielman DM. *Quantification of Glutathione and Asocrbate in the human Brain Using Short-TE PRESS*. International Society of Magnetic Resonance in Medication (2019). Available online at: https://index.mirasmart.com/ISMRM2019/PDFfiles/2230.html (accessed February 01, 2021).
52. Fischl B, Salat DH, Busa E, Albert M, Dieterich M, Haselgrove C, et al. Whole brain segmentation: automated labeling of neuroanatomical structures in the human brain. *Neuron.* (2002) 33:341–55. doi: 10.1016/S0896-6273(02)00569-X
53. Lewis CP, Port JD, Blacker CJ, Sonme AI, Seewoo BJ, Leffler JM, et al. Altered anterior cingulate glutamatergic metabolism in depressed adolescents with current suicidal ideation. *Transl Psychiatry*. (2020). 10, 1–12. doi: 10.1038/s41398-020-0792-z
54. Croarkin PE, Nakonezny PA, Wall CA, Murphy LL, Sampson SM, Frye MA, et al. Transcranial magnetic stimulation potentiates glutamatergic neurotransmission in depressed adolescents. *Psychiatr Res Neuroimaging.* (2016) 247:25–33. doi: 10.1016/j.pscychresns.2015.11.005
55. Shah SA, Yoon GH, Kim HO, Kim MO. Vitamin C neuroprotection against dose-dependent glutamate-induced neurodegeneration in the postnatal brain. *Neurochem Res.* (2015) 40:875–84. doi: 10.1007/s11064-015-1540-2
56. Moritz B, Schmitz AE, Rodrigues ALS, Dafre AL, Cunha MP. The role of vitamin C in stress-related disorders. *J Nutr Biochem.* (2020) 85(Suppl. 1):108459. doi: 10.1016/j.jnutbio.2020.108459
57. Cray C, Zaias J, Altman NH. Acute phase response in animals: a review. *Comp Med*. (2009) 59:517–2.
58. Nelson TE, Ur CL, Gruol DL. Chronic interleukin-6 exposure alters electrophysiological properties and calcium signaling in developing cerebellar purkinje neurons in culture. *J Neurophysiol*. (2002) 88:475–86. doi: 10.1152/jn.2002.88.1.475
59. Liao SL, Chen CJ. Differential effects of cytokines and redox potential on glutamate uptake in rat cortical glial cultures. *Neurosci Lett.* (2001) 299:113–6. doi: 10.1016/S0304-3940(01)01499-9
60. Rizzo SS, Neal SJ, Hughes ZA, Beyna M, Rosenzweig-Lipson S, Moss SJ, et al. Evidence for sustained elevation of IL-6 in the CNS as a key contributor of depressive-like phenotypes. *Transl Psychiatry*. (2012) 2:e199. doi: 10.1038/tp.2012.120
61. Kautz MM, Coe CL, McArthur BA, Mac Giollabhui N, Ellman LM, Abramson LY, et al. Longitudinal changes of inflammatory biomarkers moderate the relationship between recent stressful life events and prospective symptoms of depression in a diverse sample of urban adolescents. *Brain Behav Immun.* (2020) 86:43–52. doi: 10.1016/j.bbi.2019.02.029

Conflict of Interest: The authors declare that the research was conducted in the absence of any commercial or financial relationships that could be construed as a potential conflict of interest.

frontiers in Psychiatry

REVIEW
published: 27 April 2021
doi: 10.3389/fpsyt.2021.637863

Glutamate and GABA Homeostasis and Neurometabolism in Major Depressive Disorder

Ajay Sarawagi[1,2], *Narayan Datt Soni*[1] *and Anant Bahadur Patel*[1,2]*

[1] *NMR Microimaging and Spectroscopy, CSIR-Centre for Cellular and Molecular Biology, Hyderabad, India,* [2] *Academy of Scientific and Innovative Research, Ghaziabad, India*

Major depressive disorder (MDD) is a leading cause of distress, disability, and suicides. As per the latest WHO report, MDD affects more than 260 million people worldwide. Despite decades of research, the underlying etiology of depression is not fully understood. Glutamate and γ-aminobutyric acid (GABA) are the major excitatory and inhibitory neurotransmitters, respectively, in the matured central nervous system. Imbalance in the levels of these neurotransmitters has been implicated in different neurological and psychiatric disorders including MDD. ^{1}H nuclear magnetic resonance (NMR) spectroscopy is a powerful non-invasive method to study neurometabolites homeostasis *in vivo*. Additionally, ^{13}C-NMR spectroscopy together with an intravenous administration of non-radioactive ^{13}C-labeled glucose or acetate provides a measure of neural functions. In this review, we provide an overview of NMR-based measurements of glutamate and GABA homeostasis, neurometabolic activity, and neurotransmitter cycling in MDD. Finally, we highlight the impact of recent advancements in treatment strategies against a depressive disorder that target glutamate and GABA pathways in the brain.

Keywords: antidepressant, brain, ^{13}C-NMR spectroscopy, glutamine, ketamine, neurocircuitry, neurometabolism, neurotransmitter

OPEN ACCESS

Edited by:
Richard Edden,
Johns Hopkins University,
United States

Reviewed by:
Richard E. Harris,
University of Michigan, United States
Nicolaas Puts,
Johns Hopkins University,
United States

***Correspondence:**
Anant Bahadur Patel
abpatel@ccmb.res.in

Specialty section:
This article was submitted to Molecular Psychiatry, a section of the journal Frontiers in Psychiatry

Received: *04 December 2020*
Accepted: *09 March 2021*
Published: *27 April 2021*

Citation:
Sarawagi A, Soni ND and Patel AB (2021) Glutamate and GABA Homeostasis and Neurometabolism in Major Depressive Disorder. Front. Psychiatry 12:637863. doi: 10.3389/fpsyt.2021.637863

INTRODUCTION

Major depressive disorder (MDD) is a neuropsychiatric condition, characterized by low mood, loss of interest in pleasurable activities, and suicidal ideation. It affects ∼5% of the population worldwide (1). As per the WHO report (2020), around 0.8 million people commit suicide every year, and more than 90% of these had a psychiatric diagnosis (2, 3). MDD is one of the major contributors to chronic disease burden over the world population, and imparts a high socioeconomic impact (4). Despite several decades of research, there are no robust physiological and molecular markers for psychiatric disorders. Therefore, diagnosis of these disorders is achieved mostly by questionnaire-based psychiatric evaluation. The diagnostic criteria for psychiatric disorders have been evolving continuously. The diagnostic standards and specifiers of MDD as per the latest edition of the Diagnostic and Statistical Manual of Mental Disorders (DSM-5, 2013)

BOX 1 | Symptoms of MDD: as per diagnostic and statistical manual of mental disorder (DSM-V) at least five of the following symptoms must be present during entire 2-week period (5).

- Consistently feeling sad, empty, and hopeless
- Markedly diminished interest in pleasurable activities
- Significant weight loss or weight gain
- Increased or decreased appetite
- Insomnia or hypersomnia
- Fatigue or loss of energy
- Feeling of worthlessness, feeling excessive, or inappropriate guilt
- Diminished ability to think or concentrate, or indecisiveness
- Recurrent thoughts of death and suicidal ideation without a specific plan
- Psychomotor agitation or retardation

These symptoms cause clinically significant distress or impairment in social, occupational, or other important areas of functioning. Moreover, the episode is not attributable to the physiological effects of a substance or another medical condition.

are described in **Box 1** (5). Very often, the symptoms of different neuropsychiatric disorders overlap with each other and interfere in precise diagnosis. Hence, there is a need for extensive research on the identification of biomarkers for the development of novel diagnostic strategies for MDD. Depression is a highly variable disorder with multiple risk factors and causes that vary at the individual level. Certain environmental factors such as prematernal stress, childhood abuse, physical and sexual abuse, continuous failures, substance abuse, sadness and severe trauma increase the risk of depression (6, 7). Depression has been often seen to be associated with various neurodegenerative disorders (8) such as Parkinson's disease, Alzheimer's disease, amyotrophic lateral sclerosis, and systemic diseases like diabetes (9) and cancer (10).

Despite enormous efforts made by the global psychiatric research community, the molecular mechanism of MDD is not yet very clear. Several neuroimaging and postmortem studies have shown a loss of neuronal and glial population in the cingulate cortex, prefrontal cortex (PFC) (11) and hippocampus (12, 13) of depressed subjects (**Figure 1**) (14, 15). Various genetic factors (16), epigenetic changes (17) and endocrine pathways (18) are believed to be involved in the pathophysiology of the disorder. The elevated activity of the hypothalamic–pituitary–adrenal (HPA) axis is at the heart of the neurobiological presumptions of depression (19). Higher activity of HPA axis increases levels of glucocorticoids in blood, plasma and cerebrospinal fluid (CSF), which are greatly associated with stress. Additionally, environmental factors and stress influence neuronal function epigenetically. These factors alter gene expression by histone acetylation or DNA methylation (20).

The role of epigenetics in depression is supported by studies reporting antidepressive effects of histone deacetylase inhibitors in rodent models of depression (20, 21). Additionally, a large number of studies have reported a reduced level of brain-derived neurotrophic factor (BDNF) in the hippocampus (HPC) and PFC of depressed subjects (22). BDNF is crucial for the activity-dependent formation and maintenance of synapses by regulating the activity of the mTORC1 complex. Activation of mTORC1 pathways promotes *de novo* synthesis of various synaptic proteins, including GluA1, α-amino-3-hydroxy-5-methyl-4-isoxazolepropionic acid (AMPA) receptor subunits and postsynaptic density protein 95 (PSD95) (23). Interventions with different antidepressants have shown increased expression of BDNF in PFC of the rodent brain (24, 25).

Neurotransmitters are the chemical messengers present in presynaptic nerve terminals and are released into the synaptic cleft in response to the action potential (26). These neurotransmitters bind to specific receptors present on the postsynaptic membrane, and thus facilitate the transmission of the action potential across the synapse (26). Neurotransmitters are broadly classified into amino acids, peptides, and monoamines depending on their chemical properties. Amino acid neurotransmitters include glutamate, γ-aminobutyric acid (GABA), aspartate and glycine, which are abundant in the central nervous system (CNS). Substance P, cholecystokinin, opioids and neuropeptide Y belong to the peptide neurotransmitter category (27). In the monoamine category, several neurotransmitters including serotonin, dopamine, norepinephrine and epinephrine are well-studied, and are shown to be involved in various neuropsychiatric disorders (28, 29). Functionally, glutamate, aspartate, dopamine, epinephrine and norepinephrine are considered as excitatory neurotransmitters, while GABA, glycine and serotonin are the major inhibitory neurotransmitters in the matured mammalian CNS (30).

^{1}H magnetic resonance spectroscopy (MRS) has emerged as a powerful non-invasive method for the measurement of levels of neurometabolites including glutamate and GABA in the brain (31). In addition, ^{13}C-MRS in conjunction with administration of ^{13}C-labeled respiratory substrates (glucose and acetate) allows analysis of the cell-specific metabolic activity in animals as well as in the human brain. This provides a non-invasive measurement of the cerebral metabolic rate of glucose oxidation, ATP production and neurotransmitter cycling (32, 33).

Neurocircuitry of Reward and Emotions

Depression is characterized by a deficit in various aspects of reward, which is defined as responses toward positive emotional stimuli such as food, sex and social interaction (34).

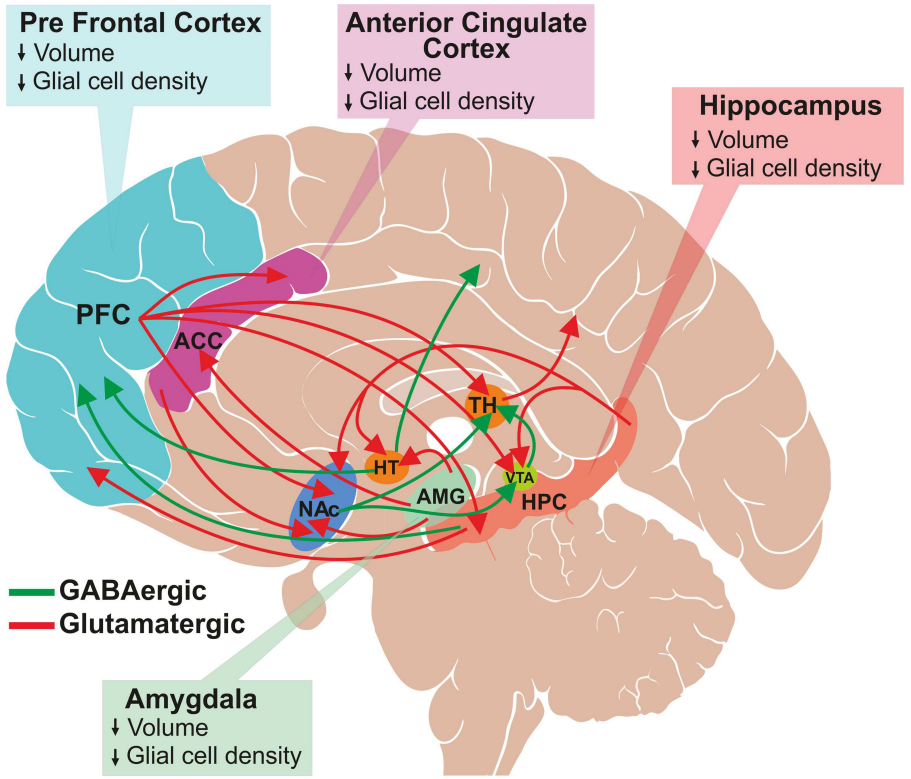

FIGURE 1 | Schematic of glutamatergic and GABAergic projections involved in mood regulation and reward pathway. A subset of several known interconnections among different brain regions are shown. Major glutamatergic projections (red color) arise from the frontal cortex to the anterior cingulate cortex (ACC), thalamus (TH), ventral tegmental area (VTA), hippocampus (HPC) and nucleus accumbens (NAc). Additionally, glutamatergic neurons originate from hippocampus, and innervate into hypothalamus (HT), VTA, NAc and PFC and from amygdala to HT, ACC and NAc. The GABAergic projections (green color) are widely distributed throughout the brain. The major projections that are relevant to this review are from HT to the occipital and parietal cortex, HPC to PFC, and NAc to the thalamus and VTA. The structural changes observed in the brain regions of depressed subjects are shown in the respective boxes.

Several brain regions such as prefrontal cortex (PFC), nucleus accumbens (NAc), ventral tegmental area (VTA), hippocampus (HPC) and amygdala are interconnected with each other via dopaminergic, serotonergic, glutamatergic and GABAergic neurons, which comprise the reward circuit (35, 36). The reward circuitry mainly includes dopaminergic projection from VTA to NAc, PFC, hippocampus, amygdala, as well as other brain regions. Additionally, glutamatergic and GABAergic projections interconnect these regions very densely (**Figure 1**). The cortical glutamate connections can be divided broadly into five major arcs that include PFC to the brainstem, PFC to the striatum and NAc, cerebral cortex to the thalamus, intracortical glutamate projections, and from the thalamus to the cerebral cortex (37, 38). Moreover, glutamatergic connections are found in subcortical regions: hippocampus to VTA, hypothalamus, NAc and PFC; and amygdala to NAc, hypothalamus and ACC. GABAergic neurons also make dense connections between brain regions that include projections from the striatum to substantia nigra (SN) and brainstem; thalamus to SN; HPC to occipital and parietal cortex; HPC to thalamus and striatum; NAc to VTA and thalamus; and VTA to PFC and NAc (**Figure 1**) (37, 39). The brain reward regions have been linked with specific behavioral functions, e.g., PFC for decision making and intelligence, HPC for emotional management, amygdala as the fear center, and NAc-VTA for motivation, pleasure and reward. These brain regions have broader functions in the management of emotional and cognitive behavior. Various imaging and postmortem studies have shown reduced volume and atrophy in these brain regions of depressed subjects and animal models of depression (11–15).

Neurometabolites Homeostasis in Healthy Brain

Neurometabolites homeostasis plays a very important role in brain function, and has been shown to be affected in animal models and human subjects of various neuropsychiatric disorders including MDD (40, 41). Several small molecules including N-acetyl-aspartate (NAA) (∼9 μmol/g), alanine (∼1 μmol/g), aspartate (∼1.2 μmol/g), choline (∼1.5 μmol/g), creatine (∼7 μmol/g), GABA (∼1.5 μmol/g), glutamate (∼10 μmol/g), glutamine (∼2.5 μmol/g), glycine (∼1 μmol/g), myo-inositol (∼6 μmol/g) and taurine (∼1.2 μmol/g) contribute to major fraction of neurometabolites pool in healthy brain (42).

In addition to precursors for different metabolites, these molecules play various critical functions that include signal

transduction, osmoregulation, cell growth and protein synthesis (42). Glutamate released into synaptic cleft increases the membrane potential of postsynaptic neurons, making them more likely to lead to an action potential. Moreover, it plays a critical role in long-term potentiation (43), synaptic plasticity (44), learning and memory (45), and various cognitive functions (46). Likewise, GABA, the major inhibitory neurotransmitter in the matured CNS, inhibits the propagation of action potential (47). Several studies have revealed the involvement of GABA in learning and memory (48–50), aggressive–defensive behavior, and impulsivity (51, 52). NAA is localized mostly in neurons, and is known to be a marker of neuronal viability and health. It acts as a precursor for NAAG, the storage form of aspartate, and serves a variety of other functions (53). Myo-inositol, mostly localized in astroglia, acts as an osmolite, plays an essential role in cell growth, and is believed to be a marker of the glial population (42). Moreover, it is considered an inflammatory marker in CNS (42). Nearly 20 vital metabolites, which include the above-mentioned molecules, can be detected and quantified *in vivo* by different MR spectroscopic approaches in human (54) and animal brains (55) (**Figure 2**). The most commonly used NMR methods for detection and quantification of brain metabolites are described in the subsequent section.

Glutamate and GABA Energy Metabolism in Brain

The human brain accounts for 2% of the body weight, but it contributes to 20% of the total energy consumed, indicating the overwhelming energy demand of the brain (56, 57). In a matured brain, this energy requirement is majorly fulfilled by the oxidation of glucose. Most of the energy harvested in the brain is utilized for the processes associated with glutamatergic and GABAergic neurotransmission (57). The glutamate released from glutamatergic neurons into the synaptic cleft is taken up by astrocytes and converted to glutamine by glutamine synthetase. Glutamine is transported back to neurons, hydrolyzed to glutamate, and repackaged into vesicles for the next release. This process is referred as glutamate–glutamine neurotransmitter cycling (58). Similarly, substrate cycle involving GABA and glutamine (GABA–glutamine) occurs between GABAergic neurons and astrocytes (58). In this cycle, the released GABA into the synapse is taken up majorly by astrocytes, wherein it is metabolized to succinate by GABA-transaminase, and enters into the TCA cycle and ultimately converted to glutamine. The glutamine thus formed is further transported to GABAergic neurons and converted to GABA by the successive action of glutaminase and glutamate decarboxylase (59, 60). The rates of neuronal glucose oxidation and neurotransmitter cycling have been monitored by a tracer approach, wherein ^{13}C-labeled glucose is administered intravenously, and labeling of brain amino acids is measured *in vivo* by ^{13}C-NMR spectroscopy (61). The metabolism of [1,6-$^{13}C_2$]glucose via glycolysis followed by TCA cycle labels Glu_{C4} in glutamatergic and GABAergic neurons (**Figure 3**). In GABAergic neurons, Glu_{C4} is decarboxylated to $GABA_{C2}$ by glutamate decarboxylase (GAD). Gln_{C4} gets labeled from Glu_{C4} and $GABA_{C2}$ through glutamate–glutamine and GABA-glutamine neurotransmitter cycling, respectively. Further metabolism of Glu_{C4} and $GABA_{C2}$ in the corresponding TCA cycle labels $Asp_{C2/C3}$, $Glu_{C2/C3}$, and $GABA_{C3/C4}$. The kinetics of label incorporation in different amino acids is analyzed to determine the rate of glucose oxidation in the glutamatergic, GABAergic neurons, and rate of neurotransmitter cycling (59). Energy budget estimates for the cost of signaling based on anatomic and physiological data in the cerebral cortex indicated that most of the signaling energy is utilized on postsynaptic glutamate receptors, followed by action potentials and resting potentials. In the cerebellar cortex, glutamatergic neurons use 75%, while

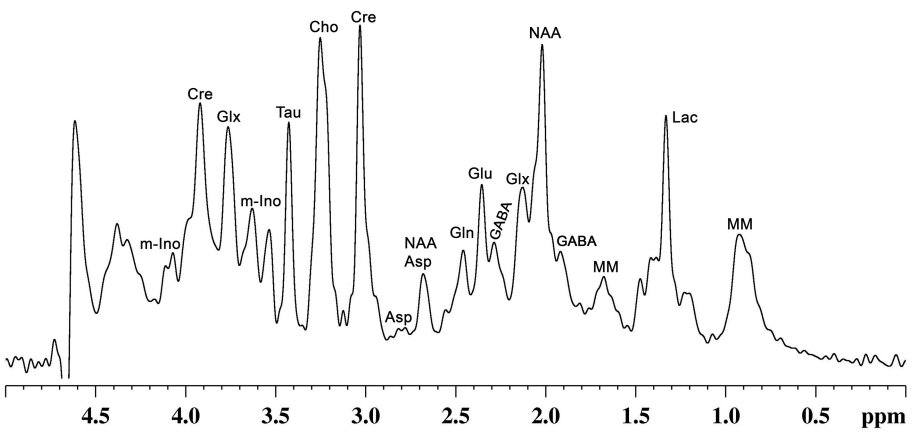

FIGURE 2 | A representative localized *in vivo* ^{1}H-NMR spectrum from mouse cerebral cortex. NMR spectrum was recorded using, a vertical wide bore magnet interfaced with 600 MHz MR spectrometer. ^{1}H-MR spectroscopy was carried out using STEAM method in conjunction with outer volume suppression (OVS) and water suppression (VAPOR) from a voxel (4.0 × 1.2 × 2.5 mm^3) with TE/TR = 4/4,000 ms with 512 averaging: Peak labels are Asp, aspartate; Cho, choline; Cr, creatine; GABA, γ-aminobutyric acid; Gln, glutamine; Glu, glutamate; Glx, glutamate + glutamine; Lac, lactate; m-Ino, myo-inositol; MM, macromolecule; NAA, N-acetyl aspartate; Tau, taurine.

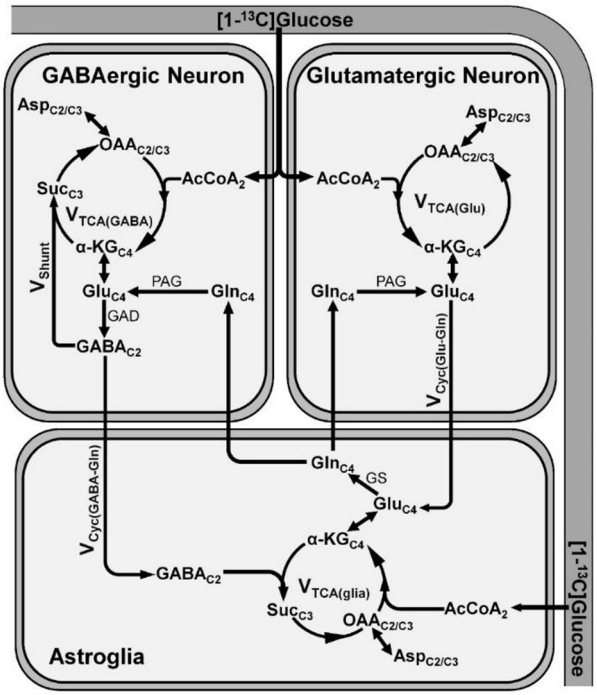

FIGURE 3 | A schematic of three compartment metabolic model showing ^{13}C labeling of amino acids from [1-^{13}C]glucose. Metabolism of [1-^{13}C]glucose via glutamatergic and GABAergic TCA cycle labels Glu_{C4}. In GABAergic neurons, Glu_{C4} is further decarboxylated to $GABA_{C2}$ by glutamate decarboxylase (GAD). The labeling of Gln_{C4} occurs by release and uptake of Glu_{C4} and $GABA_{C2}$ in astrocytes followed by transamination by glutamine synthetase (GS). Further metabolism of Glu_{C4} and $GABA_{C2}$ transfers the label into $Asp_{C2/C3}$. α-KG_{C4}, α-ketoglutarate-C4; $AcCoA_2$, acetyl co-enzymeA-C2; $Asp_{C2/C3}$, aspartate-C2/C3; $GABA_{C2}$, γ-aminobutyric acid-C2; Glu_{C4}, glutamate-C4; GAD, glutamate decarboxylase; Gln_{C4}, glutamine-C4; GS, glutamine synthetase; $OAA_{C2/C3}$, oxaloacetate-C2/C3; PAG, phosphate activated glutaminase; Suc_{C3}, succinate-C3; $V_{cyc(GABA-Gln)}$, GABA–glutamine cycling flux; $V_{cyc(Glu-Gln)}$, glutamate–glutamine cycling flux; V_{shunt}, flux of GABA shunt; $V_{TCA(glia)}$, astroglial TCA cycle flux; $V_{TCA(GABA)}$, GABAergic TCA cycle flux; $V_{TCA(Glu)}$, glutamatergic TCA cycle flux.

GABAergic neurons use 25% of the signaling energy (57). Hence, an estimate of the energy expenditure of the glutamatergic and GABAergic neurons using ^{13}C-MRS approach directly reflects their functional status.

HYPOTHESIS

The most prevalent hypothesis of depression posits that depletion in monoamine neurotransmitters level is the underlying cause of the disease (62, 63). Recent studies in animal models and human subjects have suggested an association of glutamatergic and GABAergic systems with the pathophysiology of depression (64–66). Reduced expression of receptor subunits, imbalances in their levels, decreased glutamatergic and GABAergic neurotransmission, and altered energy metabolism are known to play a critical role in the progression of depression (64, 65).

Glutamatergic Hypothesis of Depression

Glutamatergic neurons constitute approximately 80% of the synapses in the neocortex (67). Glutamate is released at synapses throughout the brain, and exerts changes in postsynaptic excitability and neuroplasticity (68). It activates various downstream pathways of nuclear genes by binding to a variety of membrane-bound receptors present on the postsynaptic membrane, which regulate secondary messenger systems. α-Amino-3-hydroxy-5-methyl-4-isoxazolepropionic acid ($AMPA_R$), N-methyl-D-aspartate ($NMDA_R$), and kainate are the fast-acting ionotropic receptors that get activated by glutamate binding (69). Glutamate also binds to G-protein-coupled receptors, known as metabotropic glutamate receptors, which mediate various cellular processes and slow-acting changes through secondary messengers such as cyclic adenosine monophosphate (cAMP), cyclic guanosine monophosphate (cGMP) and phosphatidylinositol (69). AMPA and kainate receptors help in the conduction of action potential primarily through the flux of Na^+ ions, while $NMDA_R$ is distinguished by its more permeability to Ca^{2+} ions. NMDA receptor signaling promotes various responses such as excitation, neurotrophic function, and can even activate cell death pathways. Abnormal activity of NMDA receptor imparts harmful effects on neurons (69). Overexcitation of $NMDA_R$ by excessive glutamate release or impaired synaptic clearance leads to the death of neurons by excitotoxicity (70).

A large number of clinical as well as animal studies have reported impairment in the glutamatergic system in various limbic and cortical areas of the brain of depressed subjects (71, 72). Additionally, postmortem histopathology (73) and a number of ^1H-MRS studies (74, 75) have shed light on the association of the aberrant glutamate system with maladaptive changes in the structure and function of excitatory circuitry. Several studies have reported decreased expression of NMDA (73, 76, 77) and AMPA receptor subunits (77, 78) in PFC of depressed individuals. Reduced expression of NMDA receptor subunits has also been seen in the postmortem brains of suicide victims (73, 79). Moreover, the decreased availability of metabotropic receptor mGluR5 in PFC, cingulate cortex, thalamus, hippocampus, and other cortical regions has been reported in depressed individuals (80, 81). Additionally, loss of glutamatergic neurons in the orbitofrontal cortex is associated with the pathophysiology of depression (82). These shreds of evidence suggest the involvement of glutamatergic system with the pathophysiology of MDD.

GABAergic Hypothesis of Depression

Glutamate acts as the precursor for GABA, the predominant inhibitory neurotransmitter in the matured brain (83). GABAergic neurons contribute to one-third of total synapses in the CNS and help in shaping the neural network dynamics (84). These inhibitory neurons are known to play a pivotal role in physiological processes that are often affected in psychiatric disorders such as neural plasticity, sensory processing, stress reactivity, memory formation, and attention (84, 85). GABA binds to two different classes of receptors, the fast-acting ligand gated or ionotropic receptor $GABA_A$ and $GABA_B$. Activation

of $GABA_A$ receptor leads to an influx of chloride ions, which inhibits the propagation of action potential. However, activation of $GABA_B$ receptors stimulates K^+ channel opening, which helps in achieving a hyperpolarized state that leads to reduced transmission of action potential (86, 87).

GABAergic interneurons are identified by their expression of specific receptors for somatostatin (SST), parvalbumin (PV), and 5-HT3a. SST and PV interneurons make up to 30 and 40%, respectively, of the total GABAergic neuronal pool (88). Postmortem studies of depressed subjects have shown a reduced level of SST and PV interneurons in PFC as well as in other cortical areas (89). Additionally, a decrease in the level of SST messenger RNA (mRNA) has been reported in several brain regions, including dorsolateral PFC (90, 91), ACC (92) and amygdala (93) in depression (47). Moreover, multiple studies have reported reduced expression of GAD67 and GABA transporters in the brain of MDD subjects (90, 93, 94). In addition, genetically modified animals with deletion of specific GABA receptor subunits show depressive phenotypes (95, 96). Furthermore, treatment with various antidepressants (97), electroconvulsive therapy (ECT) (98) and cognitive behavioral therapy (74) tends to restore GABA level in depressed subjects (47). These multiple evidence suggest that impairment in GABAergic transmission plays a significant role in the pathophysiology of depression (99).

IN VIVO ^{1}H-MR SPECTROSCOPY

Proton (^{1}H) is the most abundant and sensitive NMR active nucleus, and is an integral part of every neurometabolite. Due to the presence of different functional groups, ^{1}H belonging to different molecules or attached to different carbon atoms within the same molecule experiences variation in the electronic environment. This results in differences in ^{1}H frequencies, which is commonly known as chemical shift. This parameter is used for the distinction of metabolites by ^{1}H-MR spectroscopy without administering any chemical agent.

The neurochemical profile provides valuable information when measured from a well-defined region/volume of the brain. This is measured using localized *in vivo* MR spectroscopy. The localization methods in MR spectroscopy are generally based on magnetic field gradients and radiofrequency pulses. A three dimensional voxel is selected by application of band selective radiofrequency (RF) pulses together with magnetic field gradient along X-, Y- and Z-axes. The most commonly used MR localization methods are described below.

Image Selected *in vivo* Spectroscopy

This approach employs three frequency selective inversion pulses followed by non-selective excitation of the entire sample in the presence of three orthogonal magnetic field gradients. Image selected *in vivo* spectroscopy (ISIS) achieves complete 3D localization of voxel in eight scans (100).

Point-Resolved Spectroscopy (PRESS)

This is referred as a double spin-echo localization method, wherein a 90° radiofrequency pulse is followed by two 180° pulses together with magnetic field gradients along three orthogonal axes (101). This produces signals exclusively from the desired volume of interest. Due to complete refocusing of the magnetization, the signal-to-noise ratio (SNR) is relatively higher in point-resolved spectroscopy (PRESS).

Stimulated Echo Acquisition Mode (STEAM)

It is a single scan localization technique, which involves application of three 90° radiofrequency pulses together with magnetic field gradients along three orthogonal axes. Due to selection of stimulated echo using three slice-selective 90° radiofrequency pulses, stimulated echo acquisition mode (STEAM) provides signals from metabolites at a very short echo time (∼5 ms) (102). Furthermore, as all the three pulses are 90° in STEAM, the amount of energy absorbed per mass of tissue is lower in this sequence as compared with PRESS. However, as STEAM focuses only 50% of the magnetization, the SNR of NMR signal in STEAM is 50% of that obtained in PRESS approach.

A combination of these localization methods together with outer volume suppression (103) provides better quality localization, especially when the voxel is relatively small to the entire excited volume. Furthermore, *in vivo* measurements of metabolites whose concentration is in the range of 1–30 μmol/g often encounter huge water signals (55,555 μmol/g), hence requires effective suppression of water for quantification. Various NMR characteristics like relaxation time, scalar coupling, chemical shift and diffusion have been exploited to develop several effective approaches for water suppression. Chemical shift selective (CHESS) (104) and variable pulse powers and optimized relaxation delay (VAPOR) (105) are commonly used approaches for water suppression during *in vivo* ^{1}H-MR spectroscopy.

^{13}C-MR Spectroscopy

^{1}H-MRS provides static information for metabolites from a given brain region. In contrast, ^{13}C-MRS is very useful in monitoring the flow of labels from ^{13}C-labeled substrates to different neurotransmitters such as GABA, glutamate and aspartate, similar to that is used in the tracer approach to evaluate the functional status of tissues and organs (**Figure 4**). The kinetics of ^{13}C labeling of brain amino acids from ^{13}C-labeled precursors (glucose/acetate) is useful to estimate the rates of synthesis and catabolism, and thus offer a measurement of neuroenergetics in a given brain region. ^{13}C-NMR spectroscopy in the brain has been exploited extensively to understand brain energy metabolism in healthy and different neurological disorders (61).

NEUROMETABOLITES HOMEOSTASIS AND METABOLISM IN DEPRESSION

As mentioned earlier, the maintenance of neurometabolites homeostasis is critical for the proper functioning of a healthy brain. The changes in the levels of glutamate, GABA, and NAA are often reported under MDD. These are described in details in the following sections.

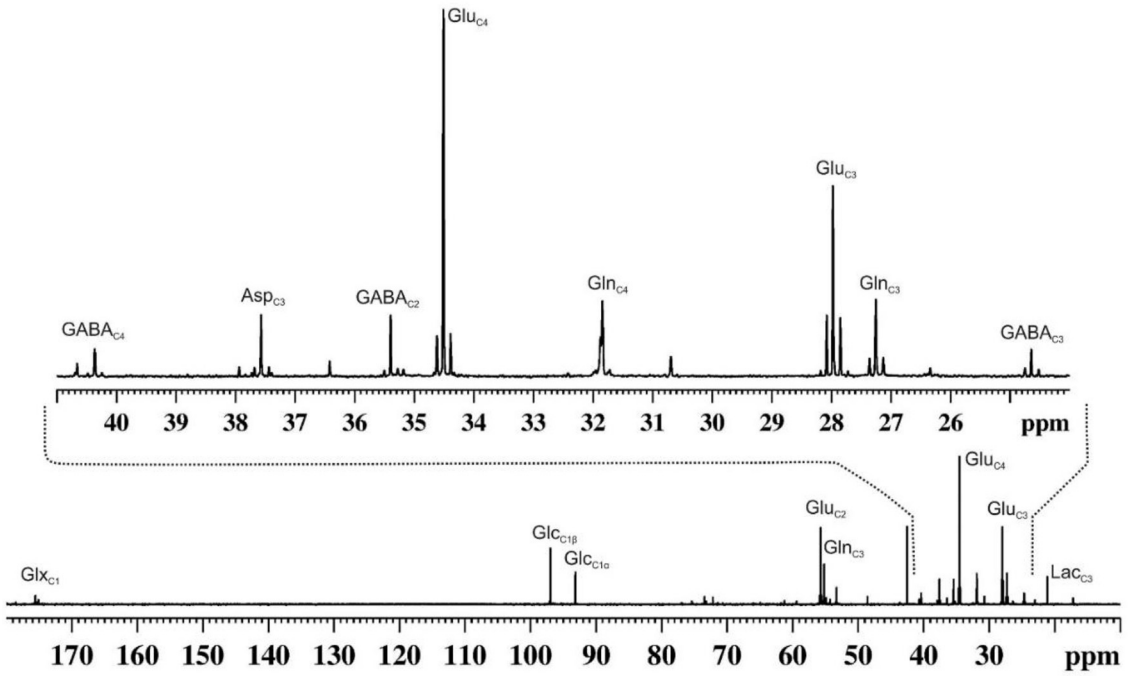

FIGURE 4 | A representative ^{13}C NMR spectrum of cortical extract of mouse brain showing labeling of various amino acids from [1,6-$^{13}C_2$]glucose. Urethane anesthetized mouse was infused with [1,6-$^{13}C_2$]glucose for 90 min. Brain metabolites were extracted from the cerebral cortex, and ^{13}C NMR spectrum of the extract was recorded at 150 MHz NMR spectrometer using power gate decoupling. The spectrum shown in the upper panel is the expansion from 24 to 41 ppm. Asp_{C3}, aspartate-C3; $GABA_{C2}$, γ-aminobutyric acid-C2; $GABA_{C3}$, γ-aminobutyric acid-C3; $GABA_{C4}$, γ-aminobutyric acid-C4; Glu_{C2}, glutamate-C2; Glu_{C3}, glutamate-C3; Glu_{C4}, glutamate-C4; Gln_{C2}, glutamine-C2; Gln_{C3}, glutamine-C3; Gln_{C4}, glutamine-C4; Glx_{C1}, (glutamate + glutamine)-C1; $Glc_{C1\beta}$, β-D-glucose-C1; $Glc_{C1\alpha}$, α-D-glucose-C; Lac_{C3}, lactate-C3.

Glutamate Homeostasis Under Depression

The ^{1}H-MRS method has been used extensively for the assessment of glutamate and other metabolite levels in the brain of depressed subjects and rodent models of depression (**Table 1**). Reduced level of glutamate has been reported in PFC of mice in different models of depression such as chronic unpredictable mild stress (CUMS) (66), chronic social defeat stress (CSDS) (112, 116), and chronic forced swim stress (CFSS) (122). The decreased glutamate level in PFC has also been reported during the first episode of depression (107, 114). The progress of depression plays a crucial role in abnormalities in glutamate, e.g., chronic or remitted–recurrent MDD subjects showed further reduction in glutamate level in PFC as compared with the first episode depressed subjects (119). Antidepressive medication aids in the restoration of neurometabolite homeostasis to normal level. The unmedicated subjects exhibited lower levels of glutamate plus glutamine (Glx) in the dorsomedial/dorsal anterolateral prefrontal and ventromedial prefrontal cortex as compared with the medicated ones (71). However, there are few inconsistencies in the level of glutamate in depression, as some reports have shown increased glutamate in PFC of the postpartum depressed female subjects (117) and animal model of depression (125).

Glutamate level was reported to be decreased together with myo-inositol (a glial marker) and NAA in ACC of depressed subjects (120, 126). Reduced levels of Glx and glutamine have also been reported in the hippocampus of unipolar MDD subjects (121). In accordance with these findings, a reduction in the levels of Glu and NAA have been reported in the hippocampus of chronic mild stress (CMS) (118) and CFSS mouse models of depression (122). In a very recent study, levels of glutamate and glutamine have been reported to be reduced in the sensorimotor cortex of the chronic restraint stressed (CRS) rat model of depression. However, several studies have shown an increase in the level of glutamate in ACC of depressed subjects (106, 111), hippocampus of MDD subjects with alcoholic tendencies (115), and CSDS model of depression in mice.

A meta-analysis of ^{1}H-MRS studies involving depressed subjects has revealed a decrease in levels of glutamate and glutamine primarily in ACC including the reduced level of Glx in other brain regions (127). Additionally, a very recent meta-analysis involving a greater number of participants concluded that lower levels of glutamatergic metabolites (glutamate and glutamine) in the medial frontal cortex are linked with the etiology of MDD (128). The reduced level of glutamate in MDD may be due to a lower supply of precursor glutamine by glutamate–glutamine, impaired glucose metabolism, and altered glial activity (64). The impaired functionality of glial cells in depression could lead to a reduction in synaptic glutamate uptake, which may result in elevated extracellular

TABLE 1 | Brain glutamate homeostasis in depression.

S. No.	Diagnosis/model	Brain region	Species	Technique	Quality index	Glu	Glx	NAA	References
1.	MDD	dACC	Human (H 25, D 51)	MEGAPRESS, 4T	CRI < 19%	↓	–	–	Benson et al. (106)
2.	MDD	vmPFC	Human (H 63, D 31)	PRESS, 3T	CRLB < 30%	↓	↓	–	Draganov et al. 2020 (107)
3.	MDD	RFL	Human (H 32, D 32)	EPSI, 3T	CRLB < 25%	NS	–	↓	Kahl et al. (108)
4.	Depression (CRS)	SSC	Rat (H 8, D 33)	PRESS, 9.4T	CRLB < 15%, NR > 9.5	↓	↓	–	Seewo et al. (109)
5.	Depression (CRS)	NAc	Mice (H 14, D 14)	SPECIAL, 14.1T	CRLB < 20%	↓	–	↓	Cherix et al. (110)
6	BID EU	ACC	Humans (H 80, D 128)	PRESS, 3T	CRLB < 20%, SNR > 10	↑	↑	NS	Soeiro-de-SouZa et al. (111)
7.	Depression (CSDS)	PFC	Mice (H 24, D 25)	*Ex vivo*, ^{1}H-[^{13}C]-NMR, 14T	–	↓	–	↓	Mishra et al. (112)
8.	MDD	rdPFC	Human (H 33, D 25)	SPECIAL	CRLB < 20%	NS	↓	↓	Jollant et al. (113)
9.	MDD	PFC	Human (H 27, D 22)	PRESS, 3T	CRLB < 10%	↓	↓	–	Shirayama et al. (114)
10.	MDD	HPC	Human (H 38, D 63)	PRESS, 3T	CRLB < 20%	↑	–	–	Hermens et al. (115)
11.	Depression (CSDS)	PFC	Mice (H 15, D 30)	*Ex vivo*, ^{1}H-[^{13}C]-NMR, 14T	–	↓	–	↓	Veeraiah et al. (116)
12.	PPD	mPFC	Humans (H 12, D 12)	STEAM, 3T	CRLB < 20%	↑	NS	NS	McEwen et al. (117)
13.	Depression (CMS)	PFC & HPC	Rat (H 10, D 10)	PRESS, 7T	CRLB < 20%	↓	↓	↓	Hemanth Kumar et al. (118)
14.	MDD	vmPFC	Humans (H 15, D 45)	PRESS, 3T	CRLB < 30%	↓	–	↓	Portella et al. (119)
15.	MDD	ACC	Humans (H 26, D 23)	PRESS, 3T	CRLB < 20%, SNR > 15	↓	NS	↓	Järnum et al. (120)
16.	MDD	HPC	Humans (H 10, D 18)	PRESS, 3T	–	–	↓	–	Block et al. (121)
17.	Depression (CFSS)	PFC	Mice (H 12, D 12)	*Ex vivo*, ^{1}H NMR, 11.7T	–	↓	↓	NS	Li et al. (122)
		HPC				↓	NS	↓	
18.	MDD	dm/da PFC	Humans (H 20, D 20)	PRESS based J editing, 3T	–	–	↓	NS	Hasler et al. (71)
19.	MDD	Subcortical nuclei	Humans (H 21, D 20)	PRESS, 1.5T	–	↓	↓	–	Ajilore et al. (123)
20.	MDD	OCC	Humans (H 38, D 33)	ISIS, J-editing, 2.1T	–	↑	–	–	Sanacora et al. (72)
21.	MDD	ACC	Humans (H 18, D 19)	PRESS, 1.5T	–	↓	↓	NS	Auer et al. (124)

ACC, anterior cingulate cortex; BID EU, euthymic bipolar I disorder; CFS, chronic forced swim stress; CRS, chronic restraint stress; CUMS, chronic unpredictable mild stress; CSDS, chronic social defeat stress; CRI, Cramer–Rao index; CRLB, Cramer–Rao lower bound; dACC, dorsal anterior cingulate cortex; dm/daPFC, dorsomedial/dorsal anterolateral PFC; EPSI, echo planar spectroscopic imaging; EAP, experimental autoimmune prostitis; HPC, hippocampus; ISIS, image selected in vivo spectroscopy; LD, light deprivation; MDD, major depressive disorder; mPFC, medial prefrontal cortex; MEGA-PRESS, Meshcher–Garwood point-resolved spectroscopy; NAc, nucleus accumbens; NS, no significant change; OCC, occipital cortex; PFC, prefrontal cortex; PPD, postpartum depression; PRESS, point-resolved spectroscopy; rdPFC, right dorsal PFC; RFL, right frontal lobe; SNR, signal-to-noise ratio; SPECIAL, spin echo full intensity acquired localized sequence; SSC, sensorimotor cortex; STEAM, stimulated echo acquisition mode; TRD, treatment resistant depression; UDR, unipolar depression; vmPFC, ventromedial prefrontal region; ↓ depicts decrease, ↑ represents increase. The numbers in the parenthesis under species represent the number of healthy (H) and depressed (D) subject.

glutamate level that ultimately accelerates neuronal death by glutamate excitotoxicity (129). In fact, reduced expression of excitatory amino acid transporter (EAAT2) and glutamate synthetase (GS) transcripts, which are localized in glia, have been reported in CSDS mouse model of depression (116, 130). These studies support the hypo-glutamatergic hypothesis of depression and suggest that modulation of the glutamatergic system for remission of depression.

GABA Homeostasis Under Depression

GABAergic system is involved in most psychiatric disorders including major depressive disorder (131), schizophrenia (132), bipolar disorder (133) and autism (134). Several approaches including epigenetics, postmortem studies, and measurement of GABA level in cerebrospinal fluid and plasma have been used to unravel the role of the GABA system in the pathophysiology of psychiatric disorders (131). Lower GABA levels in plasma (135) and cerebrospinal fluid (136) have been reported in depressed subjects. A summary of ^{1}H MRS-based measure of GABA level in the depressed subjects as well as in animal models of depression is presented in **Table 2**. Several studies have shown a lower level of GABA in MDD subjects as compared with healthy controls (131, 154). These include lower GABA concentration in OCC (72, 75, 144), dorsomedial/dorsal anterolateral PFC (71) and ACC of depressed subjects (137, 139, 142, 143, 155). Moreover, a very recent report has shown reduced GABA level in ventromedial PFC (107) of depressed subjects. Additionally, reduced level of GABA has been reported in PFC of chronic stress model of depression in rodents (112, 118). Hence, lower GABA level is often considered as one of the most promising endophenotypes of MDD (156).

TABLE 2 | Brain GABA homeostasis in depression.

S. No.	Diagnosis/model	Brain region	Species	Technique	Quality index	GABA	NAA	References
1.	MDD	vmPFC	Human (H 63, D 31)	PRESS, 3T	CRLB < 30%	↑	–	Draganov et al. (107)
2.	MDD	Striatum	Human (H 16, D 20)	J-edited MEGAPRESS, 3T	–	↑	–	Bradley et al. (137)
		ACC				↓	–	
3.	CUMS	HPC	Rat (H 12, D 12)	PRESS, 9.4T	CRLB < 10%	↑	NS	Sekar et al. (138)
4.	MDD	ACC	Human (H 36, D 44)	J-edited, 3T	–	↓	–	Gabbay et al. (139)
5.	MDD	ACC	Human (H 26, D 33)	J-edited, 3T	–	↓	–	Abdallah et al. (140)
6.	MDD	ACC	Humans (H 21, D 20)	J-edited, 3T	–	↓	–	Gabbay et al. (141)
7.	CMS	PFC and HPC	Rat (H 10, D 10)	PRESS, 7T	CRLB < 20%	↓	↓	Hemanth Kumar et al. (118)
8.	MDD	ACC and OCC	Humans (H 24, D 33)	J-edited, 3T	–	↓	–	Price et al. (142)
9.	MDD	pgACC	Humans (H 24, D 19)	2D-JPRESS, 3T	CRLB < 20%	NS	NS	Walter et al. (143)
10.	MDD-R	OCC and ACC	Humans (H 11, D 12)	MEGA-PRESS, 3T	CRLB < 20%	↓	NS	Bhagwagar et al. (144)
11.	MDD	dm/da PFC	Humans (H 20, D 20)	PRESS based J editing, 3T	–	↓	NS	Hasler et al. (71)
12.	PPD	OCC	Humans (H 14, D 9)	J-editing, 2.1T	–	↓	–	Epperson et al. (145)
13.	MDD	OCC	Humans (H 38, D 33)	J-editing, 2.1T	–	↓	–	Sanacora et al. (72)
14.	MDD	OCC	Humans (H 18, D 14)	J-editing, 2.1T	–	↓	–	Sanacora et al. (75)

ACC, anterior cingulate cortex; CMS, chronic mild stress; CUMS, chronic unpredictable mild stress; CRLB, Cramer–Rao lower bound; dm/daPFC, dorsomedial/dorsal anterolateral PFC; HPC, hippocampus; MDD, major depressive disorder; MDD-R, recovered depression; MEGA-PRESS, Meshcher–Garwood point-resolved spectroscopy; NS, no significant change; OCC, occipital cortex; pgACC, pregenual anterior cingulate cortex; PFC, prefrontal cortex; PPD, postpartum depression; PRESS, point-resolved spectroscopy; SNR, signal-to-noise ratio; vmPFC, ventromedial prefrontal region; ↓ depicts decrease, ↑ represents increase. The numbers in the parenthesis under species represent the number of healthy (H) and depressed (D) subject.

In contrast to glutamate, whose level is independent of the mood of depressed subjects, the GABA level is state dependent, as its concentration in remitted MDD subjects is similar to healthy controls (40). It has been observed that unmedicated patients had reduced level of GABA in the dorsomedial/dorsal anterolateral PFC as compared with medicated subjects. Additionally, longitudinal ^{1}H-MRS studies in MDD subjects have shown restoration of GABA level after electroconvulsive therapy (98), cognitive behavioral therapy (74), treatment with ketamine (150), and selective serotonin reuptake inhibitors (SSRIs) (97). Moreover, ^{1}H-MRS measurements have shown lower OCC GABA level in treatment-resistant depressed subjects as compared with non-resistant depressed subjects and healthy volunteers (142, 157).

N-Acetyl Aspartate Homeostasis Under Depression

NAA is the strongest signal in ^{1}H-MRS, and is exclusively localized in neurons. Although the physiological role of NAA in neural function is unclear, it is typically associated with neuronal integrity and mitochondrial health (158). Reduced level of NAA is reported in different brain regions of depressed subjects, including PFC (112, 113), ACC (120, 126), right frontal and parietal lobe (108), and in the hippocampus (122, 159) (**Tables 1**, **2**). A lower level of NAA has also been seen in the hippocampus (122), nucleus accumbens (110) and PFC (112, 116) of rodent models of depression. Reduced levels of NAA along with glutamate suggest decrease in viability of glutamatergic neurons in depression.

Glutamate and GABA Energy Metabolism in Depression

Positron emission tomography (PET) (160, 161) and ^{13}C-MRS are widely used techniques for evaluating brain energy metabolism (162) in humans and rodents. Neurometabolic activities have been investigated using ^{13}C-MRS with an administration of ^{13}C-labeled substrates (59, 61). As ^{13}C-MRS can distinguish labeling of different carbon positions of glutamate, glutamine, GABA and aspartate, it is possible to measure TCA cycle fluxes separately for glutamatergic neurons, GABAergic neurons and astrocytes by appropriate modeling of the ^{13}C turnover of neurometabolites (60, 163). Early ^{13}C-MRS studies from Shulman et al. have led the foundation of quantitative measurement of rates of neuronal glucose oxidation and neurotransmitter cycling (164, 165). The ^{13}C-NMR measurements together with the infusion of ^{13}C-labeled substrates in mice (60), rats (163) and human (166) have shown that neuronal mitochondrial TCA cycle in the cerebral

cortex contributes ∼70–85% of the total energy produced and the remaining (∼15–30%) by astroglia. The GABAergic mitochondrial TCA cycle contributes to ∼20% of total neuronal TCA cycle in rats (59) and mice cerebral cortex (60). Most of the neuronal energy is used to support the processes associated with glutamate signaling such as postsynaptic glutamate receptors (50%) and action potential (20%) in the cerebral cortex (56, 57). Most importantly, ^{13}C-NMR measurements have shown that rates of oxidative glucose metabolism in neurons and neurotransmitter cycling are stoichiometrically (1:1) coupled (165, 167), indicating that energy requirement for cycling of each glutamate molecule is powered by complete oxidation of one molecule of glucose in neurons (168, 169).

There is limited information about brain mitochondrial energetics in depressed subjects. A recent ^{13}C-MRS study performed by the Yale Psychiatric group has reported a ∼25% reduction in the mitochondrial energy production in glutamatergic neurons in the occipital cortex of depressed subjects (64). However, there was no change in the GABA synthesis rate and glutamate–glutamine neurotransmitter cycling flux. Using CSDS mouse model of depression, we have reported a reduction in the rate of glucose oxidation in glutamatergic and GABAergic neurons in PFC of C57BL6 mice (116). Additionally, glutamate–glutamine cycling was reduced in mice exhibiting depression-like phenotype (112). Moreover, a very recent measurement has revealed decreased glutamatergic (40%) and GABAergic (20%) neurometabolic activity in PFC of CUMS model of depression (66). These alterations were reflected in a large reduction in the rate of neuronal ATP synthesis. Additionally, excitatory and inhibitory synaptic transmissions were reduced by ∼40% in these mice. The reduced synaptic transmission in CUMS mice was corroborated by decreased labeling of GABA-C2, Glu-C4, and Gln-C4 from [2-^{13}C]acetate (66).

Effect of Antidepressants on the Glutamatergic and GABAergic Systems

Antidepressants are categorized into different classes: selective serotonin reuptake inhibitors, serotonin–norepinephrine reuptake inhibitors, and selective norepinephrine reuptake inhibitors, which increase the level of synaptic monoamine neurotransmitters by blocking their reuptake in neurons. The antidepressants belonging to the monoamine oxidase inhibitors category increase tissue levels of monoamines by suppressing the activity of corresponding oxidases. These molecules increase synaptic plasticity, activate neurogenesis in the adult hippocampus, and enhance the expression of neurotrophic factors (170, 171). However, despite the increase in brain monoamine level with few doses of conventional antidepressants, the desired outcomes are usually achieved only after several weeks to months of continuous administration (172). Moreover, a significant fraction of subjects, commonly referred to as treatment-resistant, do not respond to these antidepressants despite the use of various therapeutic strategies (173).

Interestingly, a single subanesthetic dose of ketamine, a non-competitive NMDA channel blocker, produces rapid antidepressant actions within hours of administration, and the effects last for several days (150, 174) (**Table 3**). Although, the precise mechanism of ketamine action is elusive, various studies have reported that acute intervention with a low dose of ketamine increases glutamate efflux in PFC of mice and rats (112, 175, 176). These studies led to hypothesize that partial antagonism of NMDA receptor by a subanesthetic dose of ketamine may

TABLE 3 | Impact of ketamine on neurometabolites homeostasis in depression.

S. No.	Species	Brain region	Sample size	Dose	Technique	Quality index	Glu	Glx	GABA	References
1.	Human (MDD)	pgACC	HP: 12, HK: 11 DP: 16, DK: 18	0.5 mg/kg (iv) for 40 min	PRESS, 7T	SNR > 150	NS	–	–	Evans et al. (146)
2.	Human (HV)	ACC	HP: 16, HK: 31	0.23 mg/kg (iv) in 1 h	PRESS, 3T	–	–	↑	–	Javitt et al. (147)
3.	Humans (HV)	pgACC	HP: 14, HK: 12	0.5 mg/kg (iv) for 40 min	STEAM, 7T	CRLB < 20%	↓	–	–	Li M. et al. (148)
4.	Human (HV)	HPC	HP: 12, HK: 15	0.27 mg/kg (iv)	PRESS, 3T	CRLB < 20%	–	↑	–	Kraguljac et al. (149)
5.	Human (MDD)	mPFC	DK: 11	0.5 mg/kg (iv) for 40 min	J-editing, 3T	–	–	↑	↑	Milak et al. (150)
6.	Rats (Social isolation)	ACC	HP: 8, HK: 8	25 mg/kg (ip)	PRESS, 7T	CRLB < 25%	NS	–	↓	Napolitano et al. (151)
7.	Rat (CUS)	ACC	HP: 5, HK: 6 DP: 6, DK: 7	40 mg/kg (ip)	*Ex vivo* CPMG, 11.7T	CRLB < 20%	NS	NS	↓	Perrine et al. (152)
8.	Rat (H)	PFC	HP: 12, HK: 12	30 mg/kg (sc) for 6 days	PRESS, 4.7T	CRLB < 30%	↑	–	–	Kim et al. (153)

ACC, anterior cingulate cortex; CPMG, Car–Purcell–Meiboom–Gill; CRLB, Cramer–Rao lower bound; CUS, chronic unpredictable stress; DK, depressed subject with ketamine; DP, depressed subject with placebo; HK, healthy subject with ketamine; HP, healthy subject with placebo; HPC, hippocampus; HV, Healthy volunteer; ip, intraperitoneal; iv, intravenous; MDD, major depressive disorder; NS, no significant change; PFC, prefrontal cortex; pgACC, pregenual anterior cingulate cortex; PRESS, point-resolved spectroscopy; SNR, signal-to-noise ratio; sc, subcutaneous; STEAM, stimulated echo acquisition mode; ↓ depicts decrease, ↑ represents increase.

induce antidepressive effects by increasing neurotransmission and neurometabolism in PFC (175). Moreover, the antidepressive effects of ketamine could be related to the selective impact on GABAergic interneurons. Ketamine blocks the NMDA receptors of GABA interneurons, thus suppresses their ability to inhibit pyramidal neurons, thereby induces cortical excitation (11, 177).

A very recent pilot study has evaluated the impact of intravenous ketamine administration on neurotransmitter levels in the medial prefrontal cortex (mPFC) of MDD subjects (150). GABA/water and Glx/water peaked ∼38% above baseline within 30 min of ketamine infusion (150) (**Table 3**). However, the majority of the studies reported insignificant changes in GABA and glutamate levels following ketamine treatment (178, 179). As mentioned above, the antidepressant effects of ketamine could be related to its impact on neurotransmitter cycling, oxidative energy metabolism, and neuronal–astroglial coupling. Very recently, we have shown that the subanesthetic dose of ketamine (10 mg/kg, intraperitoneal) increases ^{13}C labeling of glutamate, GABA and glutamine from glucose and acetate in PFC of CSDS mice. These findings indicate that ketamine normalizes the neurometabolic activity of glutamatergic and GABAergic neurons along with astrocytes in depression (112, 175). Moreover, recent studies with ketamine in MDD subjects indicated an increase in the rate of glutamate–glutamine neurotransmitter cycling without any change in oxidative energy production in neurons (180, 181).

OUTLOOK

The homeostasis of tissue glutamate and GABA plays important role in neural activity. The GABAergic neurons are known to control the dopaminergic reward circuitry in the VTA (182, 183). Alteration in the GABAergic neurotransmission with defective $GABA_A$ receptor subunits (94, 95, 184) and GAD67 (90, 93) have been reported in depressed subjects. Moreover, modulation of GABAergic activity in mice using genetic and optogenetic approaches leads to anhedonia and neophobia, which are characteristics of depressive disorder (185, 186). The reduced regulatory inhibition on principal neurons may lead to the excessive release of excitatory neurotransmitters in the synapse. The elevated glutamate level in the synaptic cleft stimulates prolonged and excessive activation of NMDA receptors (187). This increased neural activity ultimately leads to atrophy of glutamatergic neurons by excitotoxicity. A homeostatic reduction in glutamate receptors and functional impairment of glutamatergic synapses in the hippocampus and medial prefrontal cortex have been reported in γ2-subunit of $GABA_A$ receptor knockout mice, which exhibit a modest defect in GABAergic transmission (188).

^{1}H-MRS measures combined intracellular and extracellular glutamate and GABA pool in neurons and glia. The intracellular neurotransmitter pool dominates excessively with the extracellular (2,000–5,000:1) (189). Therefore, ^{1}H-MRS measured changes in the levels of glutamate and GABA may not reflect the abnormalities in synaptic concentration and *vice versa*. Hence, the findings of ^{1}H-MRS studies should be interpreted with great caution. ^{1}H- and ^{13}C-NMR measurements have revealed several vital information about depression. Limited measurements based on ^{13}C-NMR spectroscopy together with administration of ^{13}C precursor have suggested a reduced rate of glucose oxidation, neuronal and astroglial metabolic activity, and altered neurotransmitter trafficking in the prefrontal cortex in depression. However, there are some inconsistencies in the literature, which may be attributed to differences in the disease severity, age, gender, comorbidity, the investigated brain regions, the status and duration of medications in subjects. Hence, there is a further need for comprehensive large-scale collaborative analysis about neurotransmitter homeostasis and their energetics to better understand the etiology of depression similar to that proposed by the ENIGMA consortium for genetic and neuroimaging data.

AUTHOR CONTRIBUTIONS

AS: literature survey, preparation of figure, manuscript writing, and editing. NS: preparation of figure, manuscript writing, and editing. AP: conception of the idea, preparation of figures, manuscript writing and editing, supervised and directed the overall project. All authors contributed to the article and approved the submitted version.

FUNDING

This work was supported by the Council for Scientific and Industrial Research, Government of India (Health Care Theme FBR/MLP0150). AS thanks the Department of Biotechnology for the award of Junior Research fellowship.

ACKNOWLEDGMENTS

We would like to thank Mr. Kamal Saba for his help with graphical works.

REFERENCES

1. Bromet E, Andrade LH, Hwang I, Sampson NA, Alonso J, de Girolamo G, et al. Cross-national epidemiology of DSM-IV major depressive episode. *BMC Med.* (2011) 9:90. doi: 10.1186/1741-7015-9-90
2. Mullins N, Bigdeli TB, Borglum AD, Coleman JRI, Demontis D, Mehta D, et al. GWAS of suicide attempt in psychiatric disorders and association with major depression polygenic risk scores. *Am J Psychiatry.* (2019) 176:651–60. doi: 10.1176/appi.ajp.2019.18080957
3. Qin P. The impact of psychiatric illness on suicide: differences by diagnosis of disorders and by sex and age of subjects. *J Psychiatr Res.* (2011) 45:1445–52. doi: 10.1016/j.jpsychires.2011.06.002
4. GBD 2016 Disease and Injury Incidence and Prevalence Collaborators. Global, regional, and national incidence, prevalence, and years lived with disability for 328 diseases and injuries for 195 countries, 1990-2016: a systematic analysis for the Global Burden of Disease Study 2016. *Lancet.* (2017) 390:1211–59. doi: 10.1016/S0140-6736(17)32154-2

5. American Psychiatric Pub. *Diagnostic and Statistical Manual of Mental Disorders (DSM-5®)*. Washington, DC: American Psychiatric Pub (2013).
6. Kessler RC. The effects of stressful life events on depression. *Annu Rev Psychol.* (1997) 48:191–214. doi: 10.1146/annurev.psych.48.1.191
7. Schlossberg K, Massler A, Zalsman G. Environmental risk factors for psychopathology. *Isr J Psychiatry Relat Sci.* (2010) 47:139–43.
8. Galts CPC, Bettio LEB, Jewett DC, Yang CC, Brocardo PS, Rodrigues ALS, et al. Depression in neurodegenerative diseases: common mechanisms and current treatment options. *Neurosci Biobehav Rev.* (2019) 102:56–84. doi: 10.1016/j.neubiorev.2019.04.002
9. Semenkovich K, Brown ME, Svrakic DM, Lustman PJ. Depression in type 2 diabetes mellitus: prevalence, impact, and treatment. *Drugs.* (2015) 75:577–87. doi: 10.1007/s40265-015-0347-4
10. Szelei A, Dome P. Cancer and depression: a concise review. *Orv Hetil.* (2020) 161:908–16. doi: 10.1556/650.2020.31759
11. Duman RS, Aghajanian GK, Sanacora G, Krystal JH. Synaptic plasticity and depression: new insights from stress and rapid-acting antidepressants. *Nat Med.* (2016) 22:238–49. doi: 10.1038/nm.4050
12. Elbejjani M, Fuhrer R, Abrahamowicz M, Mazoyer B, Crivello F, Tzourio C, et al. Depression, depressive symptoms, and rate of hippocampal atrophy in a longitudinal cohort of older men and women. *Psychol Med.* (2015) 45:1931–44. doi: 10.1017/S0033291714003055
13. Kim K, Shin JH, Myung W, Fava M, Mischoulon D, Papakostas GI, et al. Deformities of the globus pallidus are associated with severity of suicidal ideation and impulsivity in patients with major depressive disorder. *Sci Rep.* (2019) 9:7462. doi: 10.1038/s41598-019-43882-4
14. Kempton MJ, Salvador Z, Munafo MR, Geddes JR, Simmons A, Frangou S, et al. Structural neuroimaging studies in major depressive disorder. Meta-analysis and comparison with bipolar disorder. *Arch Gen Psychiatry.* (2011) 68:675–90. doi: 10.1001/archgenpsychiatry.2011.60
15. Schmaal L, Pozzi E, T CH, van Velzen LS, Veer IM, Opel N, et al. ENIGMA MDD: seven years of global neuroimaging studies of major depression through worldwide data sharing. *Transl Psychiatry.* (2020) 10:172. doi: 10.1038/s41398-020-0842-6
16. Howard DM, Adams MJ, Clarke TK, Hafferty JD, Gibson J, Shirali M, et al. Genome-wide meta-analysis of depression identifies 102 independent variants and highlights the importance of the prefrontal brain regions. *Nat Neurosci.* (2019) 22:343–52. doi: 10.1038/s41593-018-0326-7
17. Park C, Rosenblat JD, Brietzke E, Pan Z, Lee Y, Cao B, et al. Stress, epigenetics and depression: a systematic review. *Neurosci Biobehav Rev.* (2019) 102:139–52. doi: 10.1016/j.neubiorev.2019.04.010
18. Juruena MF, Bocharova M, Agustini B, Young AH. Atypical depression and non-atypical depression: is HPA axis function a biomarker? A systematic review. *J Affect Disord.* (2018) 233:45–67. doi: 10.1016/j.jad.2017.09.052
19. Pariante CM, Lightman SL. The HPA axis in major depression: classical theories and new developments. *Trends Neurosci.* (2008) 31:464–8. doi: 10.1016/j.tins.2008.06.006
20. Nestler EJ. Epigenetic mechanisms of depression. *JAMA Psychiatry.* (2014) 71:454–6. doi: 10.1001/jamapsychiatry.2013.4291
21. Menke A, Binder EB. Epigenetic alterations in depression and antidepressant treatment. *Dialogues Clin Neurosci.* (2014) 16:395–404. doi: 10.31887/DCNS.2014.16.3/amenke
22. Mondal AC, Fatima M. Direct and indirect evidences of BDNF and NGF as key modulators in depression: role of antidepressants treatment. *Int J Neurosci.* (2019) 129:283–96. doi: 10.1080/00207454.2018.1527328
23. Jernigan CS, Goswami DB, Austin MC, Iyo AH, Chandran A, Stockmeier CA, et al. The mTOR signaling pathway in the prefrontal cortex is compromised in major depressive disorder. *Prog Neuropsychopharmacol Biol Psychiatry.* (2011) 35:1774–9. doi: 10.1016/j.pnpbp.2011.05.010
24. Li N, He X, Qi X, Zhang Y, He S. The mood stabilizer lamotrigine produces antidepressant behavioral effects in rats: role of brain-derived neurotrophic factor. *J Psychopharmacol.* (2010) 24:1772–8. doi: 10.1177/0269881109359102
25. Voleti B, Navarria A, Liu RJ, Banasr M, Li N, Terwilliger R, et al. Scopolamine rapidly increases mammalian target of rapamycin complex 1 signaling, synaptogenesis, and antidepressant behavioral responses. *Biol Psychiatry.* (2013) 74:742–9. doi: 10.1016/j.biopsych.2013.04.025
26. Sourkes TL. Chapter 54: the discovery of neurotransmitters, and applications to neurology. *Handb Clin Neurol.* (2010) 95:869–83. doi: 10.1016/S0072-9752(08)02154-4
27. Snyder SH, Innis RB. Peptide neurotransmitters. *Annu Rev Biochem.* (1979) 48:755–82. doi: 10.1146/annurev.bi.48.070179.003543
28. Conio B, Martino M, Magioncalda P, Escelsior A, Inglese M, Amore M, et al. Opposite effects of dopamine and serotonin on resting-state networks: review and implications for psychiatric disorders. *Mol Psychiatry.* (2020) 25:82–93. doi: 10.1038/s41380-019-0406-4
29. Hamon M, Blier P. Monoamine neurocircuitry in depression and strategies for new treatments. *Prog Neuropsychopharmacol Biol Psychiatry.* (2013) 45:54–63. doi: 10.1016/j.pnpbp.2013.04.009
30. Hyman SE. Neurotransmitters. *Curr Biol.* (2005) 15:R154–8. doi: 10.1016/j.cub.2005.02.037
31. Bertholdo D, Watcharakorn A, Castillo M. Brain proton magnetic resonance spectroscopy: introduction and overview. *Neuroimaging Clin N Am.* (2013) 23:359–80. doi: 10.1016/j.nic.2012.10.002
32. Rodrigues TB, Valette J, Bouzier-Sore AK. (13)C NMR spectroscopy applications to brain energy metabolism. *Front Neuroenergetics.* (2013) 5:9. doi: 10.3389/fnene.2013.00009
33. Rothman DL, de Graaf RA, Hyder F, Mason GF, Behar KL, De Feyter HM. In vivo (13) C and (1) H-[(13) C] MRS studies of neuroenergetics and neurotransmitter cycling, applications to neurological and psychiatric disease and brain cancer. *NMR Biomed.* (2019) 32:e4172. doi: 10.1002/nbm.4172
34. Russo SJ, Nestler EJ. The brain reward circuitry in mood disorders. *Nat Rev Neurosci.* (2013) 14:609–25. doi: 10.1038/nrn3381
35. Hoflich A, Michenthaler P, Kasper S, Lanzenberger R. Circuit mechanisms of reward, anhedonia, and depression. *Int J Neuropsychopharmacol.* (2019) 22:105–18. doi: 10.1093/ijnp/pyy081
36. Nestler EJ, Carlezon WA, Jr. The mesolimbic dopamine reward circuit in depression. *Biol Psychiatry.* (2006) 59:1151–9. doi: 10.1016/j.biopsych.2005.09.018
37. Barth C, Villringer A, Sacher J. Sex hormones affect neurotransmitters and shape the adult female brain during hormonal transition periods. *Front Neurosci.* (2015) 9:37. doi: 10.3389/fnins.2015.00037
38. Schwartz TL, Sachdeva S, Stahl SM. Glutamate neurocircuitry: theoretical underpinnings in schizophrenia. *Front Pharmacol.* (2012) 3:195. doi: 10.3389/fphar.2012.00195
39. Fields HL, Hjelmstad GO, Margolis EB, Nicola SM. Ventral tegmental area neurons in learned appetitive behavior and positive reinforcement. *Annu Rev Neurosci.* (2007) 30:289–316. doi: 10.1146/annurev.neuro.30.051606.094341
40. Schur RR, Draisma LW, Wijnen JP, Boks MP, Koevoets MG, Joels M, et al. Brain GABA levels across psychiatric disorders: a systematic literature review and meta-analysis of (1) H-MRS studies. *Hum Brain Mapp.* (2016) 37:3337–52. doi: 10.1002/hbm.23244
41. Wenneberg C, Glenthoj BY, Hjorthoj C, Buchardt Zingenberg FJ, Glenthoj LB, Rostrup E, et al. Cerebral glutamate and GABA levels in high-risk of psychosis states: a focused review and meta-analysis of (1)H-MRS studies. *Schizophr Res.* (2020) 215:38–48. doi: 10.1016/j.schres.2019.10.050
42. Govindaraju V, Young K, Maudsley AA. Proton NMR chemical shifts and coupling constants for brain metabolites. *NMR Biomed.* (2000) 13:129–53. doi: 10.1002/1099-1492(200005)13:3<129::AID-NBM619>3.0.CO;2-V
43. Miyamoto E. Molecular mechanism of neuronal plasticity: induction and maintenance of long-term potentiation in the hippocampus. *J Pharmacol Sci.* (2006) 100:433–42. doi: 10.1254/jphs.CPJ06007X
44. Barnes JR, Mukherjee B, Rogers BC, Nafar F, Gosse M, Parsons MP. The relationship between glutamate dynamics and activity-dependent synaptic plasticity. *J Neurosci.* (2020) 40:2793–807. doi: 10.1523/JNEUROSCI.1655-19.2020
45. Balschun D, Wetzel W. Inhibition of mGluR5 blocks hippocampal LTP in vivo and spatial learning in rats. *Pharmacol Biochem Behav.* (2002) 73:375–80. doi: 10.1016/S0091-3057(02)00847-X
46. Peng S, Zhang Y, Zhang J, Wang H, Ren B. Glutamate receptors and signal transduction in learning and memory. *Mol Biol Rep.* (2011) 38:453–60. doi: 10.1007/s11033-010-0128-9

47. Fogaca MV, Duman RS. Cortical GABAergic dysfunction in stress and depression: new insights for therapeutic interventions. *Front Cell Neurosci.* (2019) 13:87. doi: 10.3389/fncel.2019.00087
48. Heaney CF, Kinney JW. Role of GABA(B) receptors in learning and memory and neurological disorders. *Neurosci Biobehav Rev.* (2016) 63:1–28. doi: 10.1016/j.neubiorev.2016.01.007
49. Kolasinski J, Hinson EL, Divanbeighi Zand AP, Rizov A, Emir UE, Stagg CJ. The dynamics of cortical GABA in human motor learning. *J Physiol.* (2019) 597:271–82. doi: 10.1113/JP276626
50. Sampaio-Baptista C, Filippini N, Stagg CJ, Near J, Scholz J, Johansen-Berg H. Changes in functional connectivity and GABA levels with long-term motor learning. *Neuroimage.* (2015) 106:15–20. doi: 10.1016/j.neuroimage.2014.11.032
51. Ende G, Cackowski S, Van Eijk J, Sack M, Demirakca T, Kleindienst N, et al. Impulsivity and aggression in female BPD and ADHD patients: association with ACC glutamate and GABA concentrations. *Neuropsychopharmacology.* (2016) 41:410–8. doi: 10.1038/npp.2015.153
52. Jager A, Amiri H, Bielczyk N, van Heukelum S, Heerschap A, Aschrafi A, et al. Cortical control of aggression: GABA signalling in the anterior cingulate cortex. *Eur Neuropsychopharmacol.* (2020) 30:5–16. doi: 10.1016/j.euroneuro.2017.12.007
53. Baslow MH. N-acetylaspartate in the vertebrate brain: metabolism and function. *Neurochem Res.* (2003) 28:941–53. doi: 10.1023/A:1023250721185
54. Tkac I, Oz G, Adriany G, Ugurbil K, Gruetter R. In vivo 1H NMR spectroscopy of the human brain at high magnetic fields: metabolite quantification at 4T vs. 7T. *Magn Reson Med.* (2009) 62:868–79. doi: 10.1002/mrm.22086
55. Pfeuffer J, Tkac I, Provencher SW, Gruetter R. Toward an in vivo neurochemical profile: quantification of 18 metabolites in short-echo-time (1)H NMR spectra of the rat brain. *J Magn Reson.* (1999) 141:104–20. doi: 10.1006/jmre.1999.1895
56. Attwell D, Laughlin SB. An energy budget for signaling in the grey matter of the brain. *J Cereb Blood Flow Metab.* (2001) 21:1133–45. doi: 10.1097/00004647-200110000-00001
57. Howarth C, Gleeson P, Attwell D. Updated energy budgets for neural computation in the neocortex and cerebellum. *J Cereb Blood Flow Metab.* (2012) 32:1222–32. doi: 10.1038/jcbfm.2012.35
58. Bak LK, Schousboe A, Waagepetersen HS. The glutamate/GABA-glutamine cycle: aspects of transport, neurotransmitter homeostasis and ammonia transfer. *J Neurochem.* (2006) 98:641–53. doi: 10.1111/j.1471-4159.2006.03913.x
59. Patel AB, de Graaf RA, Mason GF, Rothman DL, Shulman RG, Behar KL. The contribution of GABA to glutamate/glutamine cycling and energy metabolism in the rat cortex in vivo. *Proc Natl Acad Sci USA.* (2005) 102:5588–93. doi: 10.1073/pnas.0501703102
60. Tiwari V, Ambadipudi S, Patel AB. Glutamatergic and GABAergic TCA cycle and neurotransmitter cycling fluxes in different regions of mouse brain. *J Cereb Blood Flow Metab.* (2013) 33:1523–31. doi: 10.1038/jcbfm.2013.114
61. Gruetter R, Adriany G, Choi IY, Henry PG, Lei H, Oz G. Localized in vivo 13C NMR spectroscopy of the brain. *NMR Biomed.* (2003) 16:313–38. doi: 10.1002/nbm.841
62. Harmer CJ, Duman RS, Cowen PJ. How do antidepressants work? New perspectives for refining future treatment approaches. *Lancet Psychiatry.* (2017) 4:409–18. doi: 10.1016/S2215-0366(17)30015-9
63. Perez-Caballero L, Torres-Sanchez S, Romero-Lopez-Alberca C, Gonzalez-Saiz F, Mico JA, Berrocoso E. Monoaminergic system and depression. *Cell Tissue Res.* (2019) 377:107–13. doi: 10.1007/s00441-018-2978-8
64. Abdallah CG, Jiang L, De Feyter HM, Fasula M, Krystal JH, Rothman DL, et al. Glutamate metabolism in major depressive disorder. *Am J Psychiatry.* (2014) 171:1320–7. doi: 10.1176/appi.ajp.2014.14010067
65. Duman RS, Sanacora G, Krystal JH. Altered connectivity in depression: GABA and glutamate neurotransmitter deficits and reversal by novel treatments. *Neuron.* (2019) 102:75–90. doi: 10.1016/j.neuron.2019.03.013
66. Mishra PK, Adusumilli M, Deolal P, Mason GF, Kumar A, Patel AB. Impaired neuronal and astroglial metabolic activity in chronic unpredictable mild stress model of depression: reversal of behavioral and metabolic deficit with lanicemine. *Neurochem Int.* (2020) 137:104750. doi: 10.1016/j.neuint.2020.104750
67. Douglas RJ, Martin KA. Mapping the matrix: the ways of neocortex. *Neuron.* (2007) 56:226–38. doi: 10.1016/j.neuron.2007.10.017
68. Ohgi Y, Futamura T, Hashimoto K. Glutamate signaling in synaptogenesis and NMDA receptors as potential therapeutic targets for psychiatric disorders. *Curr Mol Med.* (2015) 15:206–21. doi: 10.2174/1566524015666150330143008
69. Kew JN, Kemp JA. Ionotropic and metabotropic glutamate receptor structure and pharmacology. *Psychopharmacology.* (2005) 179:4–29. doi: 10.1007/s00213-005-2200-z
70. Hardingham GE, Bading H. Synaptic versus extrasynaptic NMDA receptor signalling: implications for neurodegenerative disorders. *Nat Rev Neurosci.* (2010) 11:682–96. doi: 10.1038/nrn2911
71. Hasler G, van der Veen JW, Tumonis T, Meyers N, Shen J, Drevets WC. Reduced prefrontal glutamate/glutamine and gamma-aminobutyric acid levels in major depression determined using proton magnetic resonance spectroscopy. *Arch Gen Psychiatry.* (2007) 64:193–200. doi: 10.1001/archpsyc.64.2.193
72. Sanacora G, Gueorguieva R, Epperson CN, Wu YT, Appel M, Rothman DL, et al. Subtype-specific alterations of gamma-aminobutyric acid and glutamate in patients with major depression. *Arch Gen Psychiatry.* (2004) 61:705–13. doi: 10.1001/archpsyc.61.7.705
73. Feyissa AM, Chandran A, Stockmeier CA, Karolewicz B. Reduced levels of NR2A and NR2B subunits of NMDA receptor and PSD-95 in the prefrontal cortex in major depression. *Prog Neuropsychopharmacol Biol Psychiatry.* (2009) 33:70–5. doi: 10.1016/j.pnpbp.2008.10.005
74. Sanacora G, Fenton LR, Fasula MK, Rothman DL, Levin Y, Krystal JH, et al. Cortical gamma-aminobutyric acid concentrations in depressed patients receiving cognitive behavioral therapy. *Biol Psychiatry.* (2006) 59:284–6. doi: 10.1016/j.biopsych.2005.07.015
75. Sanacora G, Mason GF, Rothman DL, Behar KL, Hyder F, Petroff OA, et al. Reduced cortical gamma-aminobutyric acid levels in depressed patients determined by proton magnetic resonance spectroscopy. *Arch Gen Psychiatry.* (1999) 56:1043–7. doi: 10.1001/archpsyc.56.11.1043
76. Shatillo A, Salo RA, Giniatullin R, Grohn OH. Involvement of NMDA receptor subtypes in cortical spreading depression in rats assessed by fMRI. *Neuropharmacology.* (2015) 93:164–70. doi: 10.1016/j.neuropharm.2015.01.028
77. Treccani G, Gaarn du Jardin K, Wegener G, Muller HK. Differential expression of postsynaptic NMDA and AMPA receptor subunits in the hippocampus and prefrontal cortex of the flinders sensitive line rat model of depression. *Synapse.* (2016) 70:471–4. doi: 10.1002/syn.21918
78. Yuen EY, Wei J, Liu W, Zhong P, Li X, Yan Z. Repeated stress causes cognitive impairment by suppressing glutamate receptor expression and function in prefrontal cortex. *Neuron.* (2012) 73:962–77. doi: 10.1016/j.neuron.2011.12.033
79. Gray AL, Hyde TM, Deep-Soboslay A, Kleinman JE, Sodhi MS. Sex differences in glutamate receptor gene expression in major depression and suicide. *Mol Psychiatry.* (2015) 20:1057–68. doi: 10.1038/mp.2015.91
80. Esterlis I, DellaGioia N, Pietrzak RH, Matuskey D, Nabulsi N, Abdallah CG, et al. Ketamine-induced reduction in mGluR5 availability is associated with an antidepressant response: an [(11)C]ABP688 and PET imaging study in depression. *Mol Psychiatry.* (2018) 23:824–32. doi: 10.1038/mp.2017.58
81. Shin S, Kwon O, Kang JI, Kwon S, Oh S, Choi J, et al. mGluR5 in the nucleus accumbens is critical for promoting resilience to chronic stress. *Nat Neurosci.* (2015) 18:1017–24. doi: 10.1038/nn.4028
82. Rajkowska G, Miguel-Hidalgo JJ, Dubey P, Stockmeier CA, Krishnan KR. Prominent reduction in pyramidal neurons density in the orbitofrontal cortex of elderly depressed patients. *Biol Psychiatry.* (2005) 58:297–306. doi: 10.1016/j.biopsych.2005.04.013
83. Patel AB, Rothman DL, Cline GW, Behar KL. Glutamine is the major precursor for GABA synthesis in rat neocortex in vivo following acute GABA-transaminase inhibition. *Brain Res.* (2001) 919:207–20. doi: 10.1016/S0006-8993(01)03015-3
84. Mohler H. Molecular regulation of cognitive functions and developmental plasticity: impact of GABAA receptors. *J Neurochem.* (2007) 102:1–12. doi: 10.1111/j.1471-4159.2007.04454.x

85. Mody I, Pearce RA. Diversity of inhibitory neurotransmission through GABA(A) receptors. *Trends Neurosci.* (2004) 27:569–75. doi: 10.1016/j.tins.2004.07.002
86. Jewett BE, Sharma S. Physiology, GABA. StatPearls. Treasure Island (FL)2020.
87. Mederos S, Perea G. GABAergic-astrocyte signaling: a refinement of inhibitory brain networks. *Glia.* (2019) 67:1842–51. doi: 10.1002/glia.23644
88. Fee C, Banasr M, Sibille E. Somatostatin-positive gamma-aminobutyric acid interneuron deficits in depression: cortical microcircuit and therapeutic perspectives. *Biol Psychiatry.* (2017) 82:549–59. doi: 10.1016/j.biopsych.2017.05.024
89. Rajkowska G, O'Dwyer G, Teleki Z, Stockmeier CA, Miguel-Hidalgo JJ. GABAergic neurons immunoreactive for calcium binding proteins are reduced in the prefrontal cortex in major depression. *Neuropsychopharmacology.* (2007) 32:471–82. doi: 10.1038/sj.npp.1301234
90. Banasr M, Lepack A, Fee C, Duric V, Maldonado-Aviles J, DiLeone R, et al. Characterization of GABAergic marker expression in the chronic unpredictable stress model of depression. *Chronic Stress.* (2017) 1:2470547017720459. doi: 10.1177/2470547017720459
91. Sibille E, Morris HM, Kota RS, Lewis DA. GABA-related transcripts in the dorsolateral prefrontal cortex in mood disorders. *Int J Neuropsychopharmacol.* (2011) 14:721–34. doi: 10.1017/S1461145710001616
92. Tripp A, Kota RS, Lewis DA, Sibille E. Reduced somatostatin in subgenual anterior cingulate cortex in major depression. *Neurobiol Dis.* (2011) 42:116–24. doi: 10.1016/j.nbd.2011.01.014
93. Guilloux JP, Douillard-Guilloux G, Kota R, Wang X, Gardier AM, Martinowich K, et al. Molecular evidence for BDNF- and GABA-related dysfunctions in the amygdala of female subjects with major depression. *Mol Psychiatry.* (2012) 17:1130–42. doi: 10.1038/mp.2011.113
94. Klempan TA, Sequeira A, Canetti L, Lalovic A, Ernst C, ffrench-Mullen J, et al. Altered expression of genes involved in ATP biosynthesis and GABAergic neurotransmission in the ventral prefrontal cortex of suicides with and without major depression. *Mol Psychiatry.* (2009) 14:175–89. doi: 10.1038/sj.mp.4002110
95. Choudary PV, Molnar M, Evans SJ, Tomita H, Li JZ, Vawter MP, et al. Altered cortical glutamatergic and GABAergic signal transmission with glial involvement in depression. *Proc Natl Acad Sci USA.* (2005) 102:15653–8. doi: 10.1073/pnas.0507901102
96. Shen Q, Lal R, Luellen BA, Earnheart JC, Andrews AM, Luscher B. gamma-Aminobutyric acid-type A receptor deficits cause hypothalamic-pituitary-adrenal axis hyperactivity and antidepressant drug sensitivity reminiscent of melancholic forms of depression. *Biol Psychiatry.* (2010) 68:512–20. doi: 10.1016/j.biopsych.2010.04.024
97. Sanacora G, Mason GF, Rothman DL, Krystal JH. Increased occipital cortex GABA concentrations in depressed patients after therapy with selective serotonin reuptake inhibitors. *Am J Psychiatry.* (2002) 159:663–5. doi: 10.1176/appi.ajp.159.4.663
98. Sanacora G, Mason GF, Rothman DL, Hyder F, Ciarcia JJ, Ostroff RB, et al. Increased cortical GABA concentrations in depressed patients receiving ECT. *Am J Psychiatry.* (2003) 160:577–9. doi: 10.1176/appi.ajp.160.3.577
99. Mohler H. The GABA system in anxiety and depression and its therapeutic potential. *Neuropharmacology.* (2012) 62:42–53. doi: 10.1016/j.neuropharm.2011.08.040
100. Ordidge RJ, Connelly A, Lohman JA. Image-selected in vivo spectroscopy (ISIS). A new technique for spatially selective NMR spectroscopy. *J Magnet Reson.* (1986) 66:283–94. doi: 10.1016/0022-2364(86)90031-4
101. Bottomley PA. Spatial localization in NMR spectroscopy in vivo. *Ann N Y Acad Sci.* (1987) 508:333–48. doi: 10.1111/j.1749-6632.1987.tb32915.x
102. Frahm J, Bruhn H, Gyngell ML, Merboldt KD, Hanicke W, Sauter R. Localized high-resolution proton NMR spectroscopy using stimulated echoes: initial applications to human brain in vivo. *Magn Reson Med.* (1989) 9:79–93. doi: 10.1002/mrm.1910090110
103. Duyn JH, Gillen J, Sobering G, van Zijl PC, Moonen CT. Multisection proton MR spectroscopic imaging of the brain. *Radiology.* (1993) 188:277–82. doi: 10.1148/radiology.188.1.8511313
104. Haase A, Frahm J, Hanicke W, Matthaei D. 1H NMR chemical shift selective (CHESS) imaging. *Phys Med Biol.* (1985) 30:341–4. doi: 10.1088/0031-9155/30/4/008
105. Tkac I, Starcuk Z, Choi IY, Gruetter R. *In vivo* 1H NMR spectroscopy of rat brain at 1 ms echo time. *Magn Reson Med.* (1999) 41:649–56. doi: 10.1002/(SICI)1522-2594(199904)41:4<649::AID-MRM2>3.0.CO;2-G
106. Benson KL, Bottary R, Schoerning L, Baer L, Gonenc A, Eric Jensen J, et al. (1)H MRS measurement of cortical GABA and glutamate in primary insomnia and major depressive disorder: relationship to sleep quality and depression severity. *J Affect Disord.* (2020) 274:624–31. doi: 10.1016/j.jad.2020.05.026
107. Draganov M, Vives-Gilabert Y, de Diego-Adelino J, Vicent-Gil M, Puigdemont D, Portella MJ. Glutamatergic and GABA-ergic abnormalities in First-episode depression. A 1-year follow-up 1H-MR spectroscopic study. *J Affect Disord.* (2020) 266:572–7. doi: 10.1016/j.jad.2020.01.138
108. Kahl KG, Atalay S, Maudsley AA, Sheriff S, Cummings A, Frieling H, et al. Altered neurometabolism in major depressive disorder: a whole brain (1)H-magnetic resonance spectroscopic imaging study at 3T. *Prog Neuropsychopharmacol Biol Psychiatry.* (2020) 101:109916. doi: 10.1016/j.pnpbp.2020.109916
109. Seewoo BJ, Hennessy LA, Feindel KW, Etherington SJ, Croarkin PE, Rodger J. Validation of chronic restraint stress model in young adult rats for the study of depression using longitudinal multimodal MR imaging. *eNeuro.* (2020) 7:1–22. doi: 10.1523/ENEURO.0113-20.2020
110. Cherix A, Larrieu T, Grosse J, Rodrigues J, McEwen B, Nasca C, et al. Metabolic signature in nucleus accumbens for anti-depressant-like effects of acetyl-L-carnitine. *Elife.* (2020) 9:e50631. doi: 10.7554/eLife.50631
111. Soeiro-de-Souza MG, Otaduy MCG, Machado-Vieira R, Moreno RA, Nery FG, Leite C, et al. Anterior cingulate cortex glutamatergic metabolites and mood stabilizers in euthymic bipolar i disorder patients: a proton magnetic resonance spectroscopy study. *Biol Psychiatry Cogn Neurosci Neuroimaging.* (2018) 3:985–91. doi: 10.1016/j.bpsc.2018.02.007
112. Mishra PK, Kumar A, Behar KL, Patel AB. Subanesthetic ketamine reverses neuronal and astroglial metabolic activity deficits in a social defeat model of depression. *J Neurochem.* (2018) 146:722–34. doi: 10.1111/jnc.14544
113. Jollant F, Near J, Turecki G, Richard-Devantoy S. Spectroscopy markers of suicidal risk and mental pain in depressed patients. *Prog Neuropsychopharmacol Biol Psychiatry.* (2016) 73:64–71. doi: 10.1016/j.pnpbp.2016.10.005
114. Shirayama Y, Takahashi M, Osone F, Hara A, Okubo T. Myo-inositol, glutamate, and glutamine in the prefrontal cortex, hippocampus, and amygdala in major depression. *Biol Psychiatry Cogn Neurosci Neuroimaging.* (2017) 2:196–204. doi: 10.1016/j.bpsc.2016.11.006
115. Hermens DF, Chitty KM, Lee RS, Tickell A, Haber PS, Naismith SL, et al. Hippocampal glutamate is increased and associated with risky drinking in young adults with major depression. *J Affect Disord.* (2015) 186:95–8. doi: 10.1016/j.jad.2015.07.009
116. Veeraiah P, Noronha JM, Maitra S, Bagga P, Khandelwal N, Chakravarty S, et al. Dysfunctional glutamatergic and gamma-aminobutyric acidergic activities in prefrontal cortex of mice in social defeat model of depression. *Biol Psychiatry.* (2014) 76:231–8. doi: 10.1016/j.biopsych.2013.09.024
117. McEwen AM, Burgess DT, Hanstock CC, Seres P, Khalili P, Newman SC, et al. Increased glutamate levels in the medial prefrontal cortex in patients with postpartum depression. *Neuropsychopharmacology.* (2012) 37:2428–35. doi: 10.1038/npp.2012.101
118. Hemanth Kumar BS, Mishra SK, Rana P, Singh S, Khushu S. Neurodegenerative evidences during early onset of depression in CMS rats as detected by proton magnetic resonance spectroscopy at 7 T. *Behav Brain Res.* (2012) 232:53–9. doi: 10.1016/j.bbr.2012.03.011
119. Portella MJ, de Diego-Adelino J, Gomez-Anson B, Morgan-Ferrando R, Vives Y, Puigdemont D, et al. Ventromedial prefrontal spectroscopic abnormalities over the course of depression: a comparison among first episode, remitted recurrent and chronic patients. *J Psychiatr Res.* (2011) 45:427–34. doi: 10.1016/j.jpsychires.2010.08.010
120. Jarnum H, Eskildsen SF, Steffensen EG, Lundbye-Christensen S, Simonsen CW, Thomsen IS, et al. Longitudinal MRI study of cortical thickness, perfusion, and metabolite levels in major depressive disorder. *Acta Psychiatr Scand.* (2011) 124:435–46. doi: 10.1111/j.1600-0447.2011.01766.x
121. Block W, Traber F, von Widdern O, Metten M, Schild H, Maier W, et al. Proton MR spectroscopy of the hippocampus at 3 T in patients with unipolar major depressive disorder: correlates and predictors

of treatment response. *Int J Neuropsychopharmacol.* (2009) 12:415–22. doi: 10.1017/S1461145708009516
122. Li CX, Wang Y, Gao H, Pan WJ, Xiang Y, Huang M, et al. Cerebral metabolic changes in a depression-like rat model of chronic forced swimming studied by ex vivo high resolution 1H magnetic resonance spectroscopy. *Neurochem Res.* (2008) 33:2342–9. doi: 10.1007/s11064-008-9739-0
123. Ajilore O, Haroon E, Kumaran S, Darwin C, Binesh N, Mintz J, et al. Measurement of brain metabolites in patients with type 2 diabetes and major depression using proton magnetic resonance spectroscopy. *Neuropsychopharmacology.* (2007) 32:1224–31. doi: 10.1038/sj.npp.1301248
124. Auer DP, Putz B, Kraft E, Lipinski B, Schill J, Holsboer F. Reduced glutamate in the anterior cingulate cortex in depression: an in vivo proton magnetic resonance spectroscopy study. *Biol Psychiatry.* (2000) 47:305–13. doi: 10.1016/S0006-3223(99)00159-6
125. Yoo CH, Song KH, Lim SI, Woo DC, Choe BY. Metabolic effects of light deprivation in the prefrontal cortex of rats with depression-like behavior: *in vivo* proton magnetic resonance spectroscopy at 7T. *Brain Res.* (2018) 1687:95–103. doi: 10.1016/j.brainres.2018.02.047
126. Lewis CP, Port JD, Blacker CJ, Sonmez AI, Seewoo BJ, Leffler JM, et al. Altered anterior cingulate glutamatergic metabolism in depressed adolescents with current suicidal ideation. *Transl Psychiatry.* (2020) 10:119. doi: 10.1038/s41398-020-0792-z
127. Luykx JJ, Laban KG, van den Heuvel MP, Boks MP, Mandl RC, Kahn RS, et al. Region and state specific glutamate downregulation in major depressive disorder: a meta-analysis of (1)H-MRS findings. *Neurosci Biobehav Rev.* (2012) 36:198–205. doi: 10.1016/j.neubiorev.2011.05.014
128. Moriguchi S, Takamiya A, Noda Y, Horita N, Wada M, Tsugawa S, et al. Glutamatergic neurometabolite levels in major depressive disorder: a systematic review and meta-analysis of proton magnetic resonance spectroscopy studies. *Mol Psychiatry.* (2019) 24:952–64. doi: 10.1038/s41380-018-0252-9
129. Rajkowska G, Miguel-Hidalgo JJ. Gliogenesis and glial pathology in depression. *CNS Neurol Disord Drug Targets.* (2007) 6:219–33. doi: 10.2174/187152707780619326
130. Zhu X, Ye G, Wang Z, Luo J, Hao X. Sub-anesthetic doses of ketamine exert antidepressant-like effects and upregulate the expression of glutamate transporters in the hippocampus of rats. *Neurosci Lett.* (2017) 639:132–7. doi: 10.1016/j.neulet.2016.12.070
131. Luscher B, Shen Q, Sahir N. The GABAergic deficit hypothesis of major depressive disorder. *Mol Psychiatry.* (2011) 16:383–406. doi: 10.1038/mp.2010.120
132. Gonzalez-Burgos G, Fish KN, Lewis DA. GABA neuron alterations, cortical circuit dysfunction and cognitive deficits in schizophrenia. *Neural Plast.* (2011) 2011:723184. doi: 10.1155/2011/723184
133. Brambilla P, Perez J, Barale F, Schettini G, Soares JC. GABAergic dysfunction in mood disorders. *Mol Psychiatry.* (2003) 8:721–37, 15. doi: 10.1038/sj.mp.4001362
134. Horder J, Petrinovic MM, Mendez MA, Bruns A, Takumi T, Spooren W, et al. Glutamate and GABA in autism spectrum disorder-a translational magnetic resonance spectroscopy study in man and rodent models. *Transl Psychiatry.* (2018) 8:106. doi: 10.1038/s41398-018-0155-1
135. Petty F, Kramer GL, Gullion CM, Rush AJ. Low plasma gamma-aminobutyric acid levels in male patients with depression. *Biol Psychiatry.* (1992) 32:354–63. doi: 10.1016/0006-3223(92)90039-3
136. Gold BI, Bowers MB Jr, Roth RH, Sweeney DW. GABA levels in CSF of patients with psychiatric disorders. *Am J Psychiatry.* (1980) 137:362–4. doi: 10.1176/ajp.137.3.362
137. Bradley KA, Alonso CM, Mehra LM, Xu J, Gabbay V. Elevated striatal gamma-aminobutyric acid in youth with major depressive disorder. *Prog Neuropsychopharmacol Biol Psychiatry.* (2018) 86:203–10. doi: 10.1016/j.pnpbp.2018.06.004
138. Sekar S, Grandjean J, Garnell JF, Willems R, Duytschaever H, Seramani S, et al. Neuro-metabolite profiles of rodent models of psychiatric dysfunctions characterised by MR spectroscopy. *Neuropharmacology.* (2019) 146:109–16. doi: 10.1016/j.neuropharm.2018.11.021
139. Gabbay V, Bradley KA, Mao X, Ostrover R, Kang G, Shungu DC. Anterior cingulate cortex gamma-aminobutyric acid deficits in youth with depression. *Transl Psychiatry.* (2017) 7:e1216. doi: 10.1038/tp.2017.187
140. Abdallah CG, Averill LA, Krystal JH. Ketamine as a promising prototype for a new generation of rapid-acting antidepressants. *Ann N Y Acad Sci.* (2015) 1344:66–77. doi: 10.1111/nyas.12718
141. Gabbay V, Mao X, Klein RG, Ely BA, Babb JS, Panzer AM, et al. Anterior cingulate cortex gamma-aminobutyric acid in depressed adolescents: relationship to anhedonia. *Arch Gen Psychiatry.* (2012) 69:139–49. doi: 10.1001/archgenpsychiatry.2011.131
142. Price RB, Shungu DC, Mao X, Nestadt P, Kelly C, Collins KA, et al. Amino acid neurotransmitters assessed by proton magnetic resonance spectroscopy: relationship to treatment resistance in major depressive disorder. *Biol Psychiatry.* (2009) 65:792–800. doi: 10.1016/j.biopsych.2008.10.025
143. Walter M, Henning A, Grimm S, Schulte RF, Beck J, Dydak U, et al. The relationship between aberrant neuronal activation in the pregenual anterior cingulate, altered glutamatergic metabolism, and anhedonia in major depression. *Arch Gen Psychiatry.* (2009) 66:478–86. doi: 10.1001/archgenpsychiatry.2009.39
144. Bhagwagar Z, Wylezinska M, Jezzard P, Evans J, Boorman E, P MM, et al. Low GABA concentrations in occipital cortex and anterior cingulate cortex in medication-free, recovered depressed patients. *Int J Neuropsychopharmacol.* (2008) 11:255–60. doi: 10.1017/S1461145707007924
145. Epperson CN, Gueorguieva R, Czarkowski KA, Stiklus S, Sellers E, Krystal JH, et al. Preliminary evidence of reduced occipital GABA concentrations in puerperal women: a 1H-MRS study. *Psychopharmacology.* (2006) 186:425–33. doi: 10.1007/s00213-006-0313-7
146. Evans JW, Lally N, An L, Li N, Nugent AC, Banerjee D, et al. 7T (1)H-MRS in major depressive disorder: a Ketamine Treatment Study. *Neuropsychopharmacology.* (2018) 43:1908–14. doi: 10.1038/s41386-018-0057-1
147. Javitt DC, Carter CS, Krystal JH, Kantrowitz JT, Girgis RR, Kegeles LS, et al. Utility of imaging-based biomarkers for glutamate-targeted drug development in psychotic disorders: a randomized clinical trial. *JAMA Psychiatry.* (2018) 75:11–9. doi: 10.1001/jamapsychiatry.2017.3572
148. Li M, Demenescu LR, Colic L, Metzger CD, Heinze HJ, Steiner J, et al. Temporal dynamics of antidepressant ketamine effects on glutamine cycling follow regional fingerprints of AMPA and NMDA receptor densities. *Neuropsychopharmacology.* (2017) 42:1201–9. doi: 10.1038/npp.2016.184
149. Kraguljac NV, Frolich MA, Tran S, White DM, Nichols N, Barton-McArdle A, et al. Ketamine modulates hippocampal neurochemistry and functional connectivity: a combined magnetic resonance spectroscopy and resting-state fMRI study in healthy volunteers. *Mol Psychiatry.* (2017) 22:562–9. doi: 10.1038/mp.2016.122
150. Milak MS, Proper CJ, Mulhern ST, Parter AL, Kegeles LS, Ogden RT, et al. A pilot in vivo proton magnetic resonance spectroscopy study of amino acid neurotransmitter response to ketamine treatment of major depressive disorder. *Mol Psychiatry.* (2016) 21:320–7. doi: 10.1038/mp.2015.83
151. Napolitano A, Shah K, Schubert MI, Porkess V, Fone KC, Auer DP. In vivo neurometabolic profiling to characterize the effects of social isolation and ketamine-induced NMDA antagonism: a rodent study at 7.0 T. *Schizophr Bull.* (2014) 40:566–74. doi: 10.1093/schbul/sbt067
152. Perrine SA, Ghoddoussi F, Michaels MS, Sheikh IS, McKelvey G, Galloway MP. Ketamine reverses stress-induced depression-like behavior and increased GABA levels in the anterior cingulate: an 11.7 T 1H-MRS study in rats. *Prog Neuropsychopharmacol Biol Psychiatry.* (2014) 51:9–15. doi: 10.1016/j.pnpbp.2013.11.003
153. Kim SY, Lee H, Kim HJ, Bang E, Lee SH, Lee DW, et al. In vivo and ex vivo evidence for ketamine-induced hyperglutamatergic activity in the cerebral cortex of the rat: potential relevance to schizophrenia. *NMR Biomed.* (2011) 24:1235–42. doi: 10.1002/nbm.1681
154. Kalueff AV, Nutt DJ. Role of GABA in anxiety and depression. *Depress Anxiety.* (2007) 24:495–517. doi: 10.1002/da.20262
155. Abdallah CG, Jackowski A, Sato JR, Mao X, Kang G, Cheema R, et al. Prefrontal cortical GABA abnormalities are associated with reduced hippocampal volume in major depressive disorder. *Eur Neuropsychopharmacol.* (2015) 25:1082–90. doi: 10.1016/j.euroneuro.2015.04.025
156. Hasler G, Northoff G. Discovering imaging endophenotypes for major depression. *Mol Psychiatry.* (2011) 16:604–19. doi: 10.1038/mp.2011.23

157. Levinson AJ, Fitzgerald PB, Favalli G, Blumberger DM, Daigle M, Daskalakis ZJ. Evidence of cortical inhibitory deficits in major depressive disorder. *Biol Psychiatry.* (2010) 67:458–64. doi: 10.1016/j.biopsych.2009.09.025
158. Paslakis G, Traber F, Roberz J, Block W, Jessen F. N-acetyl-aspartate (NAA) as a correlate of pharmacological treatment in psychiatric disorders: a systematic review. *Eur Neuropsychopharmacol.* (2014) 24:1659–75. doi: 10.1016/j.euroneuro.2014.06.004
159. de Diego-Adelino J, Portella MJ, Gomez-Anson B, Lopez-Moruelo O, Serra-Blasco M, Vives Y, et al. Hippocampal abnormalities of glutamate/glutamine, N-acetylaspartate and choline in patients with depression are related to past illness burden. *J Psychiatry Neurosci.* (2013) 38:107–16. doi: 10.1503/jpn.110185
160. Magistretti PJ, Allaman I. A cellular perspective on brain energy metabolism and functional imaging. *Neuron.* (2015) 86:883–901. doi: 10.1016/j.neuron.2015.03.035
161. Jones T, Rabiner EA, Company PETRA. The development, past achievements, and future directions of brain PET. *J Cereb Blood Flow Metab.* (2012) 32:1426–54. doi: 10.1038/jcbfm.2012.20
162. Rothman DL, De Feyter HM, de Graaf RA, Mason GF, Behar KL. 13C MRS studies of neuroenergetics and neurotransmitter cycling in humans. *NMR Biomed.* (2011) 24:943–57. doi: 10.1002/nbm.1772
163. Patel AB, de Graaf RA, Rothman DL, Behar KL, Mason GF. Evaluation of cerebral acetate transport and metabolic rates in the rat brain in vivo using 1H-[13C]-NMR. *J Cereb Blood Flow Metab.* (2010) 30:1200–13. doi: 10.1038/jcbfm.2010.2
164. Mason GF, Gruetter R, Rothman DL, Behar KL, Shulman RG, Novotny EJ. Simultaneous determination of the rates of the TCA cycle, glucose utilization, alpha-ketoglutarate/glutamate exchange, and glutamine synthesis in human brain by NMR. *J Cereb Blood Flow Metab.* (1995) 15:12–25. doi: 10.1038/jcbfm.1995.2
165. Sibson NR, Dhankhar A, Mason GF, Rothman DL, Behar KL, Shulman RG. Stoichiometric coupling of brain glucose metabolism and glutamatergic neuronal activity. *Proc Natl Acad Sci USA.* (1998) 95:316–21. doi: 10.1073/pnas.95.1.316
166. Rothman DL, Behar KL, Hyder F, Shulman RG. In vivo NMR studies of the glutamate neurotransmitter flux and neuroenergetics: implications for brain function. *Annu Rev Physiol.* (2003) 65:401–27. doi: 10.1146/annurev.physiol.65.092101.142131
167. Patel AB, de Graaf RA, Mason GF, Kanamatsu T, Rothman DL, Shulman RG, et al. Glutamatergic neurotransmission and neuronal glucose oxidation are coupled during intense neuronal activation. *J Cereb Blood Flow Metab.* (2004) 24:972–85. doi: 10.1097/01.WCB.0000126234.16188.71
168. Hyder F, Patel AB, Gjedde A, Rothman DL, Behar KL, Shulman RG. Neuronal-glial glucose oxidation and glutamatergic-GABAergic function. *J Cereb Blood Flow Metab.* (2006) 26:865–77. doi: 10.1038/sj.jcbfm.9600263
169. Magistretti PJ, Pellerin L, Rothman DL, Shulman RG. Energy on demand. *Science.* (1999) 283:496–7. doi: 10.1126/science.283.5401.496
170. Castren E, Hen R. Neuronal plasticity and antidepressant actions. *Trends Neurosci.* (2013) 36:259–67. doi: 10.1016/j.tins.2012.12.010
171. Krishnan V, Nestler EJ. Linking molecules to mood: new insight into the biology of depression. *Am J Psychiatry.* (2010) 167:1305–20. doi: 10.1176/appi.ajp.2009.10030434
172. Gaynes BN, Warden D, Trivedi MH, Wisniewski SR, Fava M, Rush AJ. What did STAR*D teach us? Results from a large-scale, practical, clinical trial for patients with depression. *Psychiatr Serv.* (2009) 60:1439–45. doi: 10.1176/ps.2009.60.11.1439
173. Mrazek DA, Hornberger JC, Altar CA, Degtiar I. A review of the clinical, economic, and societal burden of treatment-resistant depression: 1996-2013. *Psychiatr Serv.* (2014) 65:977–87. doi: 10.1176/appi.ps.201300059
174. Berman RM, Cappiello A, Anand A, Oren DA, Heninger GR, Charney DS, et al. Antidepressant effects of ketamine in depressed patients. *Biol Psychiatry.* (2000) 47:351–4. doi: 10.1016/S0006-3223(99)00230-9
175. Chowdhury GM, Behar KL, Cho W, Thomas MA, Rothman DL, Sanacora G. (1)H-[(1)(3)C]-nuclear magnetic resonance spectroscopy measures of ketamine's effect on amino acid neurotransmitter metabolism. *Biol Psychiatry.* (2012) 71:1022–5. doi: 10.1016/j.biopsych.2011.11.006
176. Moghaddam B, Adams B, Verma A, Daly D. Activation of glutamatergic neurotransmission by ketamine: a novel step in the pathway from NMDA receptor blockade to dopaminergic and cognitive disruptions associated with the prefrontal cortex. *J Neurosci.* (1997) 17:2921–7. doi: 10.1523/JNEUROSCI.17-08-02921.1997
177. Homayoun H, Moghaddam B. NMDA receptor hypofunction produces opposite effects on prefrontal cortex interneurons and pyramidal neurons. *J Neurosci.* (2007) 27:11496–500. doi: 10.1523/JNEUROSCI.2213-07.2007
178. Rowland LM, Bustillo JR, Mullins PG, Jung RE, Lenroot R, Landgraf E, et al. Effects of ketamine on anterior cingulate glutamate metabolism in healthy humans: a 4-T proton MRS study. *Am J Psychiatry.* (2005) 162:394–6. doi: 10.1176/appi.ajp.162.2.394
179. Valentine GW, Mason GF, Gomez R, Fasula M, Watzl J, Pittman B, et al. The antidepressant effect of ketamine is not associated with changes in occipital amino acid neurotransmitter content as measured by [(1)H]-MRS. *Psychiatry Res.* (2011) 191:122–7. doi: 10.1016/j.pscychresns.2010.10.009
180. Abdallah CG, De Feyter HM, Averill LA, Jiang L, Averill CL, Chowdhury GMI, et al. The effects of ketamine on prefrontal glutamate neurotransmission in healthy and depressed subjects. *Neuropsychopharmacology.* (2018) 43:2154–60. doi: 10.1038/s41386-018-0136-3
181. Pothula S, Kato T, Liu RJ, Wu M, Gerhard D, Shinohara R, et al. Cell-type specific modulation of NMDA receptors triggers antidepressant actions. *Mol Psychiatry.* (2020). doi: 10.1038/s41380-020-0796-3
182. Brown MT, Tan KR, O'Connor EC, Nikonenko I, Muller D, Luscher C. Ventral tegmental area GABA projections pause accumbal cholinergic interneurons to enhance associative learning. *Nature.* (2012) 492:452–6. doi: 10.1038/nature11657
183. Tan KR, Yvon C, Turiault M, Mirzabekov JJ, Doehner J, Labouebe G, et al. GABA neurons of the VTA drive conditioned place aversion. *Neuron.* (2012) 73:1173–83. doi: 10.1016/j.neuron.2012.02.015
184. Sequeira A, Mamdani F, Ernst C, Vawter MP, Bunney WE, Lebel V, et al. Global brain gene expression analysis links glutamatergic and GABAergic alterations to suicide and major depression. *PLoS ONE.* (2009) 4:e6585. doi: 10.1371/journal.pone.0006585
185. Kolata SM, Nakao K, Jeevakumar V, Farmer-Alroth EL, Fujita Y, Bartley AF, et al. Neuropsychiatric phenotypes produced by GABA reduction in mouse cortex and hippocampus. *Neuropsychopharmacology.* (2018) 43:1445–56. doi: 10.1038/npp.2017.296
186. Luscher B, Fuchs T. GABAergic control of depression-related brain states. *Adv Pharmacol.* (2015) 73:97–144. doi: 10.1016/bs.apha.2014.11.003
187. Ankarcrona M, Dypbukt JM, Bonfoco E, Zhivotovsky B, Orrenius S, Lipton SA, et al. Glutamate-induced neuronal death: a succession of necrosis or apoptosis depending on mitochondrial function. *Neuron.* (1995) 15:961–73. doi: 10.1016/0896-6273(95)90186-8
188. Ren Z, Pribiag H, Jefferson SJ, Shorey M, Fuchs T, Stellwagen D, et al. Bidirectional homeostatic regulation of a depression-related brain state by gamma-aminobutyric acidergic deficits and ketamine treatment. *Biol Psychiatry.* (2016) 80:457–68. doi: 10.1016/j.biopsych.2016.02.009
189. Lehmann A, Isacsson H, Hamberger A. Effects of in vivo administration of kainic acid on the extracellular amino acid pool in the rabbit hippocampus. *J Neurochem.* (1983) 40:1314–20. doi: 10.1111/j.1471-4159.1983.tb13572.x

Conflict of Interest: The authors declare that the research was conducted in the absence of any commercial or financial relationships that could be construed as a potential conflict of interest.

frontiers in Psychiatry

BRIEF RESEARCH REPORT
published: 11 May 2021
doi: 10.3389/fpsyt.2021.665402

Intermittent Theta-Burst Stimulation Transcranial Magnetic Stimulation Increases GABA in the Medial Prefrontal Cortex: A Preliminary Sham-Controlled Magnetic Resonance Spectroscopy Study in Acute Bipolar Depression

Chad Diederichs[1], *Marilena M. DeMayo*[1,2,3,4,5,6], *Jaeden Cole*[1,2,3], *Lakshmi N. Yatham*[7], *Ashley D. Harris*[2,4,5,6] *and Alexander McGirr*[1,2,3]*

[1] Department of Psychiatry, University of Calgary, Calgary, AB, Canada, [2] Hotchkiss Brain Institute, University of Calgary, Calgary, AB, Canada, [3] Mathison Centre for Mental Health Research and Education, Calgary, AB, Canada, [4] Department of Radiology, University of Calgary, Calgary, AB, Canada, [5] Child and Adolescent Imaging Research Program, University of Calgary, Calgary, AB, Canada, [6] Alberta Children's Hospital Research Institute, University of Calgary, Calgary, AB, Canada, [7] Department of Psychiatry, University of British Columbia, Vancouver, BC, Canada

OPEN ACCESS

Edited by:
Maria Concepcion Garcia Otaduy, University of São Paulo, Brazil

Reviewed by:
Paul Croarkin, Mayo Clinic, United States
Susanne Karch, Ludwig Maximilian University of Munich, Germany

***Correspondence:**
Alexander McGirr
alexander.mcgirr@ucalgary.ca

Specialty section:
This article was submitted to Neuroimaging and Stimulation, a section of the journal Frontiers in Psychiatry

Received: 08 February 2021
Accepted: 12 April 2021
Published: 11 May 2021

Citation:
Diederichs C, DeMayo MM, Cole J, Yatham LN, Harris AD and McGirr A (2021) Intermittent Theta-Burst Stimulation Transcranial Magnetic Stimulation Increases GABA in the Medial Prefrontal Cortex: A Preliminary Sham-Controlled Magnetic Resonance Spectroscopy Study in Acute Bipolar Depression. Front. Psychiatry 12:665402. doi: 10.3389/fpsyt.2021.665402

Background: Magnetic resonance spectroscopy (MRS) has been used to identify gamma-aminobutyric acid (GABA) alterations in mood disorders, particularly in the medial prefrontal cortex (mPFC) where decreased concentrations have been associated with anhedonia. In major depressive disorder (MDD), prior work suggests that repetitive transcranial magnetic stimulation (rTMS) increases mPFC GABA concentrations proportional to antidepressant response. To our knowledge, this has not been examined in acute bipolar depression.

Methods: As part of a multicentre 4-week randomized, double-blind, sham-controlled trial using intermittent theta-burst stimulation (iTBS) of the left dorsolateral prefrontal cortex (DLPFC) in individuals with acute bipolar depression, we quantified mPFC GABA and Glx (glutamate+glutamine) concentrations using a 3T MRS scan at baseline and after the intervention. Depressive symptoms were measured using the Montgomery-Asberg Depression Rating Scale (MADRS) and the Hamilton Depression Rating Scale-17 (HRDS-17), and anhedonia was measured using the Snaith-Hamilton Pleasure Scale (SHAPS).

Results: The trial was terminated for futility and magnetic resonance spectroscopy data was acquired for 18 participants. At baseline, there were no associations between GABA or Glx concentrations and anhedonia, however GABA was negative correlated with depressive symptom severity on the HRDS-17. Compared to the sham-iTBS group, participants receiving active-iTBS had a significant increase in mPFC GABA concentrations. This was unrelated to antidepressant outcomes or improvements in anhedonia.

Conclusion: Our data suggests that iTBS targeting the DLPFC is associated with physiological changes in the mPFC. In acute bipolar depression, our preliminary data suggests that mPFC GABA is dissociated from antidepressant iTBS treatment outcomes and anhedonia.

Keywords: repetitive transcranial magnetic stimulation, intermittent theta burst stimulation, bipolar disorder, bipolar depression, magnetic resonance spectroscopy, gamma-aminobutyric acid

INTRODUCTION

Bipolar disorder (BD) is a leading cause of global disability that is defined by episodes of mania or hypomania (1). Yet, patients with BD type I spend as much as 70% of the time of the symptomatic periods experiencing syndromic or sub-syndromic depressive symptoms, while this proportion is over 80% in patients with BD type II (2). There are currently only four treatments that have been approved by the US Food and Drug Administration for the treatment of acute bipolar depression, namely olanzapine and fluoxetine combination, quetiapine, lurasidone, and caripirazine, and limited alternatives for those who do not respond to or tolerate these treatments (3).

Non-invasive neurostimulation techniques, such as transcranial magnetic stimulation (TMS), are efficacious in the treatment of Major Depressive Disorder (MDD). Accordingly, they are often considered in acute bipolar depression, however the literature in BD is small (4, 5). Newer TMS protocols, such as intermittent theta-burst stimulation (iTBS), are efficacious in MDD (6, 7) but have not demonstrated efficacy in BD to date (8, 9). Given lack of efficacy in BD, this may provide an opportunity to dissociate physiological effects that are and are not treatment mechanisms.

A growing body of research highlights alterations in brain gamma-aminobutyric acid (GABA) and glutamate systems in mood disorders (10, 11). ^{1}H-MRS studies report decreases in cortical GABA in unipolar depression that correlate inversely with glutamate (12–15). Lower GABA levels have been repeatedly seen in the medial prefrontal cortex (mPFC) in depression, and this has been associated with anhedonia (16–18). Importantly, mPFC GABA levels increase with successful pharmacological treatment of MDD (19), as well as with repetitive transcranial magnetic stimulation (rTMS) treatment (20).

Several lines of evidence highlight the importance of the mPFC, and the anterior cingulate cortex more specifically, in the therapeutic effects of rTMS when the target is the dorsolateral prefrontal cortex (DLPFC). Indeed, a single treatment to the left DLPFC is associated with sustained changes in fMRI BOLD response and the GABA/Glx ratio in the anterior cingulate (21). Hyperactivity of the anterior cingulate predicts successful rTMS treatment (22), and clinical response to rTMS is associated with the degree of anticorrelated activity between the precise DLPFC target and the anterior cingulate cortex (23–25). In light of these findings, GABA concentrations in the medial prefrontal cortex (mPFC) may represent a physiological marker associated with large scale network changes in depression (26) that are amenable to rTMS.

To our knowledge, mPFC GABA concentrations during rTMS treatment in acute bipolar depression have not been measured. Therefore, in a randomized sham-controlled trial that examined the efficacy of iTBS in comparison to sham-iTBS (9), we used magnetic resonance spectroscopy (MRS) to assess mPFC GABA in the study patients. We hypothesized that mPFC GABA would be related to anhedonia, would increase with active-iTBS but not sham-iTBS, and that the change would be related to antidepressant response.

METHODS

We conducted a double-blind randomized controlled study in two Canadian centers (the University of British Columbia and University of Calgary) between October 2016 and March 2020. The study was registered with ClinicalTrials.gov (NCT02749006) and was approved by the clinical ethical review boards of the University of British Columbia and conjoint health ethical review board of the University of Calgary. The University of Calgary site, but not the University of British Columbia site, acquired GABA-edited MEGA-PRESS data in the mPFC.

The primary outcomes are described elsewhere (9). Briefly, the trial was terminated for futility after 37 participants were randomized due to the absence of an efficacy signal and overall low rates of clinical response (15.7% sham-iTBS vs. 16.6% active-iTBS). This low rate of clinical response was also observed after a 4-week open-label continuation for those that had not responded in the double-blind phase (23.8%).

Participants

Participants were recruited by referral or by online and community advertisements. Participants provided written informed consent. Eligibility criteria included: males and females 18–70 years of age with a primary diagnosis of Bipolar I Disorder or Bipolar II (BD1 or BD2), experiencing a major depressive episode with $\geq$15 on the 17-item Hamilton Depression Rating Scale (HRDS-17) (27), and having failed to achieve clinical response with CANMAT first-line recommended treatments (lithium, lamotrigine, quetiapine, lurasidone with or without concurrent lithium or valproate) for an acute major depressive episode (3). Participants were required to have been on a stable pharmacological regimen for 2 weeks prior to screening that had to include a mood stabilizer (lithium $>$0.6 mEq/L or valproate $>$350 mM/L), an atypical antipsychotic, or a combination of a mood stabilizer and an atypical antipsychotic. For participants with BD2 only, lamotrigine monotherapy was acceptable if the dose was $>$100 mg daily.

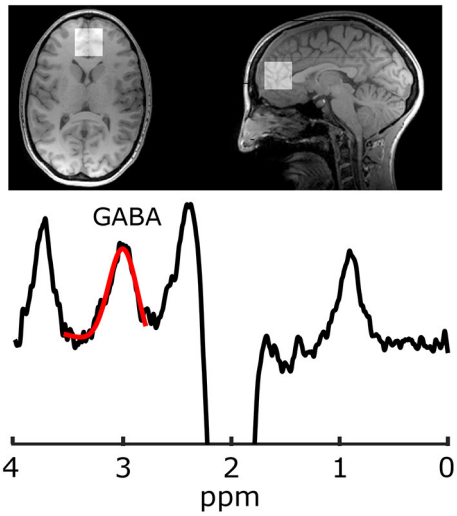

FIGURE 1 | Representative T1 weighted image with mPFC voxel placement and GABA-edited MEGAPRESS.

Exclusion criteria were acute suicidality; current psychosis; a substance use disorder within the last 3 months; seizures; a pacemaker or metallic implant; an unstable medical condition; previous TMS; current use of more than three antipsychotic agents; failed response to ECT in current episode; psychotherapy initiated within the last 3 months; a psychiatric condition other than BD that was deemed to be primary.

Treatment Protocol and Randomization

We generated three 1:1 randomization sequences for patients treated with (a) mood stabilizers, (b) atypical antipsychotics, or (c) a combination of mood stabilizer and antipsychotics to ensure that randomization was stratified according to current pharmacotherapy. Eligible patients were randomized with allocation concealment. Patients and clinical evaluators remained blind to their treatment condition. We utilized a MagPro X100 stimulator (MagVenture, Denmark), and a COOL-B70 or MCF-P-B70 placebo coil in conjunction with participant anatomical MRIs and neuronavigation (Visor2, ANT Neuro, the Netherlands). Resting motor threshold (rMT) was determined using electromyographic (EMG) electrodes placed over the first dorsal interosseous muscle, with threshold determined by the stimulus intensity required to elicit 5/10 EMG responses $>50\,\mu V$.

Patients were randomly allocated to either active or sham iTBS, consisting of a total of 600 pulses per session. Pulses were delivered as triplets at 50 Hz repeated at 5 Hz (2 on 8 s off) and at 120% rMT. These parameters reflect the stimulus parameters that have been shown to be non-inferior to gold standard high-frequency stimulation in a large single blind study (28). We targeted the participants' left DLPFC using neuronavigation (Visor 2, ANT Neuro) using the T1-weighted MRI acquired at baseline. For participants who could not tolerate the MRI, we used the BeamF3 method which was then registered to a template MRI to permit reliable targeting for the duration of the study (29).

Clinical Measures and Self-Reports

Participants were assessed by an independent evaluator (AM) blinded to treatment conditions. The diagnosis of BD was confirmed with the MINI International Neuropsychiatric Interview 7.0. Clinician rated instruments included the Hamilton Rating Depression Scale 17-item (HRDS-17), the Montgomery-Asberg Depression Rating Scale (MADRS) (30), the Young Mania Rating Scale (YMRS) (31), and the Clinical Global Impression (CGI) subscales for severity and improvement (32) at baseline, after 2 weeks, and after 4 weeks of double-blind treatment. Clinical response was defined as a reduction of 50% or more in MADRS score, and clinical remission was defined as a MADRS score of 12 or less. To measure anhedonia, participants completed the Snaith-Hamilton Pleasure Scale (SHAPS) (33) at baseline and at the conclusion of the double-blind phase.

GABA-MRS

Imaging was performed at 3 T (MR750, General Electric Healthcare, USA). Because the GABA peaks are overlapped by more abundant metabolite peaks, advanced spectroscopy methods are required for its accurate quantification; the most common being J-difference editing (34). For voxel localization and subsequent segmentation, first a T1-weighted acquisition was performed (TR/TE = 8.3/3.2 ms, 1mm isotropic voxels, aligned to the AC-PC line). Gamma-aminobutyric acid data were acquired from a $30 \times 30 \times 30$ mm^3 voxel in the mPFC using a GABA-edited MEGA-PRESS acquisition (TR/TE = 2 s/68 ms, 320 averages, 14 ms editing pulses alternating between 1.9 and 7.46 ppm every two averages, and eight unsuppressed averages for metabolite quantification). Voxels were then placed parallel to the AC-PC line anterior to the genu of the corpus callosum (**Figure 1**). Gamma-aminobutyric acid and the co-edited Glx (glutamate+glutamine) peak were analyzed in Gannet (35) including voxel localization and segmentation with SPM12, tissue correction for tissue specific T1 and T2 relaxation, and water visibilities (36, 37). Gamma-aminobutyric acid data also included tissue correction for concentration differences of GABA in white and gray matter, assuming the concentration of GABA in gray matter is twice that of white matter (38).

Data quality was visually assessed, which included assessing the GABA peak and resolution of subtraction artifact following spectral alignment, confirming the stability of water frequency (indicative of movement or scanner drift), confirming the quality of creatine alignment and fit of the spectrum and residuals. The included MEGA-PRESS acquisitions had a GABA fit error of 7.74 $\pm$ 3.28, full-width half-maximum of 22.03 $\pm$ 4.48 Hz, and signal to noise ratio of 11.97 $\pm$ 3.05.

Voxel Placement Consistency

The T1-weighted image from the follow-up session was registered to the baseline acquisition [FSL's FLIRT (39, 40)] and the transformation matrix for that registration was then applied to the follow-up voxel such that both voxels for each subject could be visualized in the same space to ensure voxel placement consistency. In addition to visual confirmation of voxel placement consistency across sessions, the dice coefficient

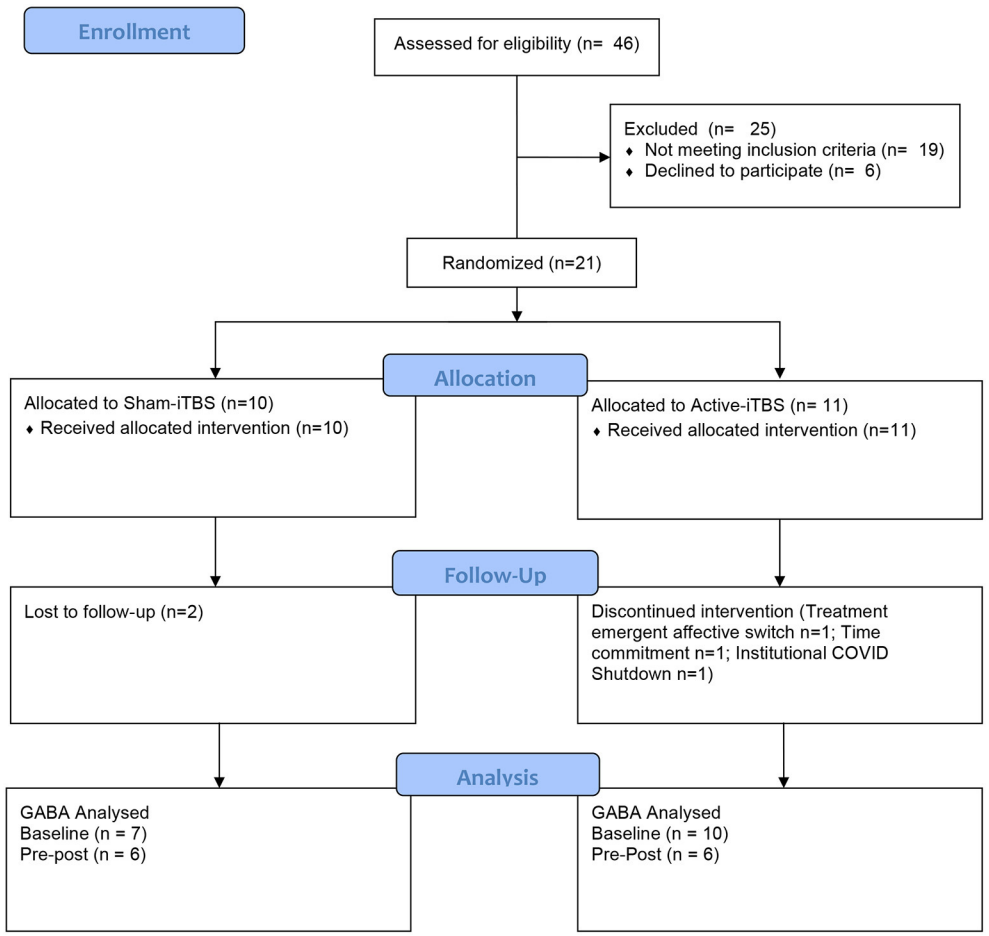

FIGURE 2 | CONSORT flow diagram.

of the voxel overlap was calculated. The average dice coefficient was 72% (standard deviation = 10%).

Statistical Analysis

Statistical analysis was performed in SPSS (IBM SPSS Statistics Version 26, IBM). Data normality was confirmed using the Shapiro-Wilk test and outliers were identified using Tukey's Fences (41). Cross-sectional analyses of continuous data were performed using Student's *t*-test or Mann Whitney U Test. Chi-square was used for dichotomized variables. One way ANOVA and linear regression was used to explore relationships between mPFC GABA and clinical characteristics. Change in mPFC GABA was quantified with repeated measures ANOVA. Two tailed significance was set at $\alpha < 0.05$.

RESULTS

The progress of participants through the University of Calgary site within this multisite study is described in the CONSORT flow diagram (**Figure 2**). Twenty-one participants were randomized between sham-iTBS ($n = 10$) and active iTBS-rTMS groups ($n = 11$). Three individuals did not tolerate the MRI, and therefore we acquired valid GABA data at baseline from 18 participants ($n = 7$ sham-iTBS and $n = 11$ active-iTBS). Sociodemographic and clinical characteristics were comparable between groups at baseline, and treatment outcomes also did not differ (**Table 1**).

mPFC GABA concentrations at baseline were skewed with one notable outlier >3 standard deviations from the mean. When this participant was removed, this data was normally distributed. There were no significant baseline differences in GABA levels between sham-iTBS and active-iTBS groups [$n = 7$ sham-iTBS 2.13 ± 0.36 mmol vs. $n = 10$ active-iTBS 1.96 ± 0.45 mmol $t_{(15)} = -0.84$, $p = 0.41$]. mPFC Glx concentrations were normally distributed and there was a trend toward higher Glx levels at baseline in the sham-iTBS group [$n = 7$ sham-iTBS 11.20 ± 2.53 mol/kg vs. $n = 10$ active-iTBS 9.41 ± 0.94 mmol $t_{(15)} = -2.06$, $p = 0.057$].

At baseline, there were no significant associations between GABA and SHAPS score [$F_{(1, 15)} = 0.07$, $p = 0.79$], medication regimen [$F_{(2, 16)} = 0.02$, $p = 0.97$], MADRS score [$F_{(1, 16)} = 2.41$, $p = 0.14$], or CGI-severity score [$F_{(1, 15)} = 1.53$, $p = 0.23$], however there was a significant association withHRDS-17 scores [**Figure 3A**; $F_{(1, 16)} = 5.18$, $p = 0.038$, Standardized $B = -0.50$]. mPFC Glx did not significantly correlate with any clinical characteristic ($p > 0.18$).

TABLE 1 | Sample characteristics and clinical outcomes.

	Sham-iTBS *n* (%) or M ± SD	Active-iTBS *n* (%) or M ± SD	Statistic	*p*
Age	42.20 ± 13.32	45.27 ± 14.52	$t(19) = 0.50$	0.62
Female sex	5 (50.0%)	5 (45.5%)	$\chi^2 = 0.04$	0.83
Education (years)	16.00 ± 2.16	16.64 ± 3.72	$t(19) = 0.47$	0.64
Diagnosis			$\chi^2 = 0.11$	0.73
BD1	2 (28.6%)	4 (36.4%)		
BD2	5 (71.4%)	7 (63.6%)		
Medication stratification			$\chi^2 = 0.06$	0.96
Mood stabilizer	4 (40.0%)	5 (45.5%)		
Atypical antipsychotic	1 (10.0%)	1 (9.1%)		
Mood stabilizer + atypical antipsychotic	5 (50.0%)	5 (45.5%)		
Baseline characteristics				
HRDS-17	20.50 ± 3.30	22.54 ± 3.88	$t(19) = 1.29$	0.21
MADRS	31.60 ± 3.89	32.90 ± 4.30	$t(19) = 0.72$	0.47
CGI-Severity	4.20 ± 0.42	4.70 ± 0.94	$t(19) = 1.52$	0.14
SHAPS	11.00 ± 3.09	10.30 ± 4.00	$t(18) = -0.43$	0.66
Treatment outcomes				
Percent MADRS improvement at 4 weeks	40.33 ± 34.93	24.69 ± 36.48	$t(15) = -0.90$	0.38
Clinical response	3 (33.3%)	1 (12.5%)	$\chi^2 = 1.02$	0.31
Clinical remission	3 (33.3%)	1 (12.5%)	$\chi^2 = 1.02$	0.31

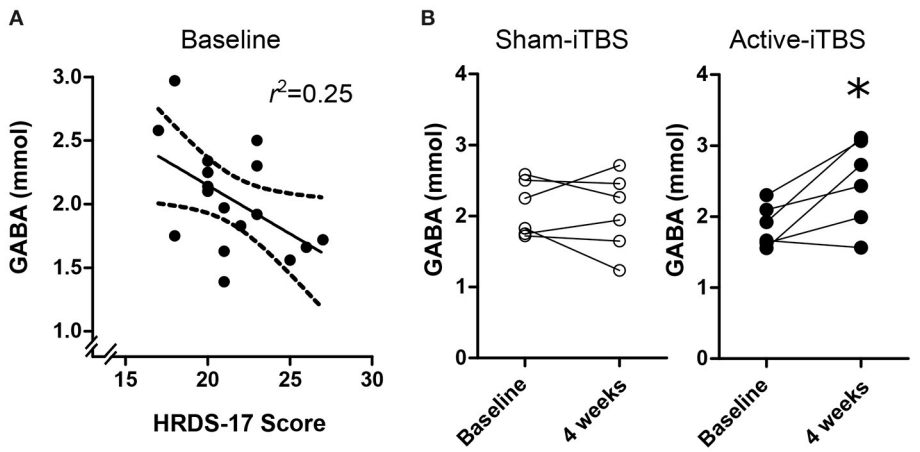

FIGURE 3 | (A) Baseline mPFC GABA concentrations were negative associated with HRDS-17 scores. **(B)** Active-iTBS, but not sham-iTBS, was associated with an increase in mPFC GABA concentrations after 4 weeks of treatment. *time interaction $p < 0.05$.

At the conclusion of double-blind treatment, paired pre-post MRS data were available for $n = 6$ sham-iTBS and $n = 6$ active-iTBS participants. We observed a significant increase in mPFC GABA in the active-iTBS group, but not the sham-iTBS group [**Figure 3B**; Time $F_{(1, 10)} = 4.65$, $p = 0.056$, Time * Group $F_{(1, 10)} = 6.99$, $p = 0.025$]. This significant effect persisted after controlling for percent change in MADRS scores [Time $F_{(1, 9)} = 0.69$, $p = 0.42$, Time * %MADRS $F_{(1, 9)} = 1.51$, $p = 0.24$, Time * Group $F_{(1, 9)} = 8.68$, $p = 0.016$]. We found no evidence for mPFC Glx time or treatment group effects [Time $F_{(1, 9)} = 0.00$, $p = 0.99$, Time * Group $F_{(1, 9)} = 0.00$, $p = 0.98$].

DISCUSSION

To our knowledge, this is the first study to use GABA-edited MRS to investigate mPFC metabolite changes during TMS therapy in acute bipolar depression. Though preliminary, our data suggests that iTBS results in increased GABA in the mPFC, consistent with previous data in MDD samples for the mPFC (20) and in the DLPFC (42). However, contrary to both of these rTMS studies, and others using pharmacological interventions (19), the GABA effect we observed was dissociated from antidepressant outcomes. We also failed to observe an association between mPFC GABA and anhedonia.

This data is interesting because it confirms a common physiological effect of DLPFC TMS stimulation in different pathologies. Yet, the lack of antidepressant effect in this subsample or in the larger multisite trial from which it is drawn highlights that not all physiological effects of therapeutic TMS are causally associated with improvement in depressive symptoms. Moreover, we did not observe associations between mPFC GABA and clinical features such as anhedonia, a replicated finding in MDD (18). While it is possible that the physiological effect we observe precedes symptomatic improvement, the 4 week open label extension of this trial for non-responders also had a low rate of clinical response (9).

Given the small sample and inference from a null finding, further research is required to determine whether our findings represent a physiological difference between acute bipolar depression and unipolar depression. It is possible that MRS quantified GABA in the mPFC is not as tightly linked to mood state in BD, given that previous studies in BD have not found differences compared to healthy controls in either depression (43) or euthymia (44, 45), and this has also been suggested in meta-analyses (46). Post-mortem staining for GABAergic subpopulations in the anterior cingulate cortex indicate heterogeneity between BD and MDD, however this is principally for calbindin positive neurons and appears layer specific and therefore cannot be resolved with MRS methods (47). Alternatively, concomitant medications indicated for acute and prophylactic treatment in BD may confound MRS GABA measures. Indeed, mood stabilizers modulate GABA (48–50) and lithium modulates Glx (51), and all but one participant was treated with these medications.

LIMITATIONS

Our preliminary data comes from a single site from a randomized controlled trial that was terminated for futility. As a result, the sample size is small, and the availability of paired pre-post MRS data is further reduced. As such, the magnitude of change seen in GABA concentrations in the active-iTBS group may be inflated due to to small sample size bias. Nevertheless, this increase is not observed in the sham-iTBS group, and therefore is likely to be a physiological effect of iTBS. Larger studies are required to more reliably determine the effect size, and independence from clinical improvements in acute bipolar depression. Participants in this trial were required to have stable dosing of an antimanic agent, which resulted in 20 of the 21 participants using medications known to influence GABA (48–50). While an unmedicated sample would resolve this limitation, it represents a safety concern as even with antimanic agents in this sample a treatment emergent affective switch occurred after a single active-iTBS treatment, and another participant experienced a treatment emergent affective switch within eight treatments after transitioning from sham-iTBS to open-label iTBS.

There is an inherent challenge in resolving GABA at 3 T due to its low concentration and overlapped, more abundant metabolites. The use of editing techniques, such as the MEGA-PRESS sequence used in this study, is preferable to the use of short-echo point resolved spectroscopy sequences for measuring GABA, particularly at 3 T (52–54). Nonetheless, there are some limitations and caveats worthy of discussion. Given the low signal and the J-difference editing approach used in MEGA-PRESS, a large voxel and many signal averages are required to obtain high signal-to-noise data for a reliable GABA measurements (53). The voxel used in the present study was 27 cm^3, placed in the mPFC. This large voxel limits the regional specificity of our results as it encompasses multiple functionally or anatomically distinct structures. Secondly, the measured GABA signal at 3 ppm includes a macromolecule contribution due to the limited specificity of the editing pulses applied at 1.9 ppm (55, 56). Macromolecules are typically considered functionally irrelevant, though the macromolecular signal is variable between subjects (53, 57). Finally, while frequency drift is known to affect efficiency of the editing pulses, the level of macromolecular signal contribution and can cause subtraction artifacts (58), the scanner used in this study is highly stable and no included data showed a frequency drift of >0.1 ppm.

CONCLUSION

Our sham-controlled data in acute bipolar depression suggests that iTBS targeting the DLPFC is associated with physiological changes in the mPFC. Unlike previous reports in MDD, in acute bipolar depression mPFC GABA concentrations appear to be dissociated from antidepressant treatment outcomes and anhedonia or have a much smaller effect. Future research is needed to better understand the clinical implications and network level changes associated with neural metabolites in acute bipolar depression.

DATA AVAILABILITY STATEMENT

The original contributions presented in the study are included in the article/supplementary material, further inquiries can be directed to the corresponding author/s.

ETHICS STATEMENT

The studies involving human participants were reviewed and approved by University of Calgary Conjoint Health Research Ethics Board. The patients/participants provided their written informed consent to participate in this study.

AUTHOR CONTRIBUTIONS

Study conception: AM, LY, and AH; Securing study funding: LY; Data collection: JC and AM; Data analyses: CD, MD, AH, and AM; Figure generation: AH and AM; Drafting manuscript: CD; Editing and approval of final manuscript: MD, JC, LY, AH, and AM. All authors contributed to the article and approved the submitted version.

FUNDING

This study was supported by the Campus Alberta Innovation Program Chair in Neurostimulation (AM) and through a philanthropic donation to Lakshmi Yatham through the University of British Columbia.

REFERENCES

1. Ferrari AJ, Stockings E, Khoo JP, Erskine HE, Degenhardt L, Vos T, et al. The prevalence and burden of bipolar disorder: findings from the Global Burden of Disease Study 2013. *Bipolar Disord.* (2016) 18:440–50. doi: 10.1111/bdi.12423
2. Forte A, Baldessarini RJ, Tondo L, Vázquez GH, Pompili M, Girardi P. Long-term morbidity in bipolar-I, bipolar-II, and unipolar major depressive disorders. *J Affect Disord.* (2015) 178:71–8. doi: 10.1016/j.jad.2015.02.011
3. Yatham LN, Kennedy SH, Parikh SV, Schaffer A, Bond DJ, Frey BN, et al. Canadian Network for Mood and Anxiety Treatments (CANMAT) and International Society for Bipolar Disorders (ISBD) 2018 guidelines for the management of patients with bipolar disorder. *Bipolar Disord.* (2018) 20:97–170. doi: 10.1111/bdi.12609
4. McGirr A, Karmani S, Arsappa R, Berlim MT, Thirthalli J, Muralidharan K, et al. Clinical efficacy and safety of repetitive transcranial magnetic stimulation in acute bipolar depression. *World Psychiatry.* (2016) 15:85–6. doi: 10.1002/wps.20300
5. Nguyen TD, Hieronymus F, Lorentzen R, McGirr A, Østergaard SD. The efficacy of repetitive transcranial magnetic stimulation (rTMS) for bipolar depression: a systematic review and meta-analysis. *J Affect Disord.* (2021) 279:250–5. doi: 10.1016/j.jad.2020.10.013
6. Berlim MT, McGirr A, Rodrigues Dos Santos N, Tremblay S, Martins R. Efficacy of theta burst stimulation (TBS) for major depression: an exploratory meta-analysis of randomized and sham-controlled trials. *J Psychiatr Res.* (2017) 90:102–9. doi: 10.1016/j.jpsychires.2017.02.015
7. Li C-T, Chen M-H, Juan C-H, Huang H-H, Chen L-F, Hsieh J-C, et al. Efficacy of prefrontal theta-burst stimulation in refractory depression: a randomized sham-controlled study. *Brain J Neurol.* (2014) 137:2088–98. doi: 10.1093/brain/awu109
8. Bulteau S, Beynel L, Marendaz C, Dall'Igna G, Peré M, Harquel S, et al. Twice-daily neuronavigated intermittent theta burst stimulation for bipolar depression: a randomized Sham-controlled pilot study. *Neurophysiol Clin Clin Neurophysiol.* (2019) 49:371–5. doi: 10.1016/j.neucli.2019.10.002
9. McGirr A, Vila-Rodriguez F, Cole J, Torres IJ, Arumugham SS, Keramatian K, et al. Efficacy of active vs Sham intermittent theta burst transcranial magnetic stimulation for patients with bipolar depression: a randomized clinical trial. *JAMA Netw Open.* (2021) 4:e210963. doi: 10.1001/jamanetworkopen.2021.0963
10. Duman RS, Sanacora G, Krystal JH. Altered connectivity in depression: GABA and glutamate neurotransmitter deficits and reversal by novel treatments. *Neuron.* (2019) 102:75–90. doi: 10.1016/j.neuron.2019.03.013
11. Schür RR, Draisma LWR, Wijnen JP, Boks MP, Koevoets MGJC, Joëls M, et al. Brain GABA levels across psychiatric disorders: a systematic literature review and meta-analysis of 1H-MRS studies. *Hum Brain Mapp.* (2016) 37:3337–52. doi: 10.1002/hbm.23244
12. Godfrey KEM, Gardner AC, Kwon S, Chea W, Muthukumaraswamy SD. Differences in excitatory and inhibitory neurotransmitter levels between depressed patients and healthy controls: a systematic review and meta-analysis. *J Psychiatr Res.* (2018) 105:33–44. doi: 10.1016/j.jpsychires.2018.08.015
13. Hasler G, van der Veen JW, Tumonis T, Meyers N, Shen J, Drevets WC. Reduced prefrontal glutamate/glutamine and γ-aminobutyric acid levels in major depression determined using proton magnetic resonance spectroscopy. *Arch Gen Psychiatry.* (2007) 64:193–200. doi: 10.1001/archpsyc.64.2.193
14. Krystal JH, Sanacora G, Blumberg H, Anand A, Charney DS, Marek G, et al. Glutamate and GABA systems as targets for novel antidepressant and mood-stabilizing treatments. *Mol Psychiatry.* (2002) 7:S71–80. doi: 10.1038/sj.mp.4001021
15. Price RB, Shungu DC, Mao X, Nestadt P, Kelly C, Collins KA, et al. Amino acid neurotransmitters assessed by proton magnetic resonance spectroscopy: relationship to treatment resistance in major depressive disorder. *Biol Psychiatry.* (2009) 65:792–800. doi: 10.1016/j.biopsych.2008.10.025
16. Colic L, von Düring F, Denzel D, Demenescu LR, Lord AR, Martens L, et al. Rostral anterior cingulate glutamine/glutamate disbalance in major depressive disorder depends on symptom severity. *Biol Psychiatry Cogn Neurosci Neuroimaging.* (2019) 4:1049–58. doi: 10.1016/j.bpsc.2019.04.003
17. Gabbay V, Bradley KA, Mao X, Ostrover R, Kang G, Shungu DC. Anterior cingulate cortex γ-aminobutyric acid deficits in youth with depression. *Transl Psychiatry.* (2017) 7:e1216. doi: 10.1038/tp.2017.187
18. Gabbay V, Mao X, Klein RG, Ely BA, Babb JS, Panzer AM, et al. Anterior cingulate cortex γ-aminobutyric acid in depressed adolescents: relationship to anhedonia. *Arch Gen Psychiatry.* (2012) 69:139–49. doi: 10.1001/archgenpsychiatry.2011.131
19. Brennan BP, Admon R, Perriello C, LaFlamme EM, Athey AJ, Pizzagalli DA, et al. Acute change in anterior cingulate cortex GABA, but not glutamine/glutamate, mediates antidepressant response to citalopram. *Psychiatry Res Neuroimaging.* (2017) 269:9–16. doi: 10.1016/j.pscychresns.2017.08.009
20. Dubin MJ, Mao X, Banerjee S, Goodman Z, Lapidus KAB, Kang G, et al. Elevated prefrontal cortex GABA in patients with major depressive disorder after TMS treatment measured with proton magnetic resonance spectroscopy. *J Psychiatry Neurosci.* (2016) 41:E37–45. doi: 10.1503/jpn.150223
21. Iwabuchi SJ, Raschke F, Auer DP, Liddle PF, Lankappa ST, Palaniyappan L. Targeted transcranial theta-burst stimulation alters fronto-insular network and prefrontal GABA. *NeuroImage.* (2017) 146:395–403. doi: 10.1016/j.neuroimage.2016.09.043
22. Hadas I, Sun Y, Lioumis P, Zomorrodi R, Jones B, Voineskos D, et al. Association of repetitive transcranial magnetic stimulation treatment with subgenual cingulate hyperactivity in patients with major depressive disorder: a secondary analysis of a randomized clinical trial. *JAMA Netw Open.* (2019) 2:e195578. doi: 10.1001/jamanetworkopen.2019.5578
23. Boes AD, Uitermarkt BD, Albazron FM, Lan MJ, Liston C, Pascual-Leone A, et al. Rostral anterior cingulate cortex is a structural correlate of repetitive TMS treatment response in depression. *Brain Stimulat.* (2018) 11:575–81. doi: 10.1016/j.brs.2018.01.029
24. Fox MD, Buckner RL, White MP, Greicius MD, Pascual-Leone A. Efficacy of transcranial magnetic stimulation targets for depression is related to intrinsic functional connectivity with the subgenual cingulate. *Biol Psychiatry.* (2012) 72:595–603. doi: 10.1016/j.biopsych.2012.04.028
25. Weigand A, Horn A, Caballero R, Cooke D, Stern AP, Taylor SF, et al. Prospective Validation that subgenual connectivity predicts antidepressant efficacy of transcranial magnetic stimulation sites. *Biol Psychiatry.* (2018) 84:28–37. doi: 10.1016/j.biopsych.2017.10.028
26. Northoff G, Walter M, Schulte RF, Beck J, Dydak U, Henning A, et al. GABA concentrations in the human anterior cingulate cortex predict negative BOLD responses in fMRI. *Nat Neurosci.* (2007) 10:1515–7. doi: 10.1038/nn2001
27. Hamilton M. A rating scale for depression. *J Neurol Neurosurg Psychiatry.* (1960) 23:56–62. doi: 10.1136/jnnp.23.1.56
28. Blumberger DM, Vila-Rodriguez F, Thorpe KE, Feffer K, Noda Y, Giacobbe P, et al. Effectiveness of theta burst versus high-frequency repetitive transcranial magnetic stimulation in patients with depression (THREE-D): a randomised non-inferiority trial. *Lancet Lond Engl.* (2018) 391:1683–92. doi: 10.1016/S0140-6736(18)30295-2
29. Beam W, Borckardt JJ, Reeves ST, George MS. An efficient and accurate new method for locating the F3 position for prefrontal TMS applications. *Brain Stimulat.* (2009) 2:50–4. doi: 10.1016/j.brs.2008.09.006
30. Montgomery SA, Asberg M. A new depression scale designed to be sensitive to change. *Br J Psychiatry J Ment Sci.* (1979) 134:382–9. doi: 10.1192/bjp.134.4.382
31. Young RC, Biggs JT, Ziegler VE, Meyer DA. A rating scale for mania: reliability, validity and sensitivity. *Br J Psychiatry.* (1978) 133:429–35. doi: 10.1192/bjp.133.5.429
32. Guy W. *ECDEU Assessment Manual for Psychopharmacology*. U.S. Department of Health, Education, and Welfare, Public Health Service, Alcohol, Drug Abuse, and Mental Health Administration, National Institute of Mental Health, Psychopharmacology Research Branch, Division of Extramural Research Programs (1976).
33. Snaith RP, Hamilton M, Morley S, Humayan A, Hargreaves D, Trigwell P. A scale for the assessment of hedonic tone the Snaith-Hamilton pleasure scale. *Br J Psychiatry J Ment Sci.* (1995) 167:99–03. doi: 10.1192/bjp.167.1.99
34. Harris AD, Saleh MG, Edden RAE. Edited 1 H magnetic resonance spectroscopy *in vivo*: methods and metabolites. *Magn Reson Med.* (2017) 77:1377–89. doi: 10.1002/mrm.26619

35. Edden RAE, Puts NAJ, Harris AD, Barker PB, Evans CJ. Gannet: a batch-processing tool for the quantitative analysis of gamma-aminobutyric acid–edited MR spectroscopy spectra. *J Magn Reson Imaging.* (2014) 40:1445–52. doi: 10.1002/jmri.24478
36. Gasparovic C, Song T, Devier D, Bockholt HJ, Caprihan A, Mullins PG, et al. Use of tissue water as a concentration reference for proton spectroscopic imaging. *Magn Reson Med.* (2006) 55:1219–26. doi: 10.1002/mrm.20901
37. Near J, Harris AD, Juchem C, Kreis R, Marjańska M, Öz G, et al. Preprocessing, analysis and quantification in single-voxel magnetic resonance spectroscopy: experts' consensus recommendations. *NMR Biomed.* (2020) 34:e4257. doi: 10.1002/nbm.4257
38. Harris AD, Puts NAJ, Edden RAE. Tissue correction for GABA-edited MRS: considerations of voxel composition, tissue segmentation, and tissue relaxations. *J Magn Reson Imaging.* (2015) 42:1431–40. doi: 10.1002/jmri.24903
39. Jenkinson M, Smith S. A global optimisation method for robust affine registration of brain images. *Med Image Anal.* (2001) 5:143–56. doi: 10.1016/s1361-8415(01)00036-6
40. Jenkinson M, Bannister P, Brady M, Smith S. Improved optimization for the robust and accurate linear registration and motion correction of brain images. *NeuroImage.* (2002) 17:825–41. doi: 10.1016/s1053-8119(02)91132-8
41. Tukey JW. *Exploratory Data Analysis*. Reading, MA: Addison-Wesley Pub. Co. (1977).
42. Levitt JG, Kalender G, O'Neill J, Diaz JP, Cook IA, Ginder N, et al. Dorsolateral prefrontal γ-aminobutyric acid in patients with treatment-resistant depression after transcranial magnetic stimulation measured with magnetic resonance spectroscopy. *J Psychiatry Neurosci.* (2019) 44:386–94. doi: 10.1503/jpn.180230
43. Soeiro-de-Souza MG, Henning A, Machado-Vieira R, Moreno RA, Pastorello BF, da Costa Leite C, et al. Anterior cingulate Glutamate–Glutamine cycle metabolites are altered in euthymic bipolar I disorder. *Eur Neuropsychopharmacol.* (2015) 25:2221–9. doi: 10.1016/j.euroneuro.2015.09.020
44. Huber RS, Kondo DG, Shi X-F, Prescot AP, Clark E, Renshaw PF, et al. Relationship of executive functioning deficits to N-acetyl aspartate (NAA) and gamma-aminobutyric acid (GABA) in youth with bipolar disorder. *J Affect Disord.* (2018) 225:71–8. doi: 10.1016/j.jad.2017.07.052
45. Prisciandaro JJ, Tolliver BK, Prescot AP, Brenner HM, Renshaw PF, Brown TR, et al. Unique prefrontal GABA and glutamate disturbances in co-occurring bipolar disorder and alcohol dependence. *Transl Psychiatry.* (2017) 7:e1163. doi: 10.1038/tp.2017.141
46. Scotti-Muzzi E, Umla-Runge K, Soeiro-de-Souza MG. Anterior cingulate cortex neurometabolites in bipolar disorder are influenced by mood state and medication: a meta-analysis of 1H-MRS studies. *Eur Neuropsychopharmacol.* (2021). doi: 10.1016/j.euroneuro.2021.01.096
47. Cotter D, Landau S, Beasley C, Stevenson R, Chana G, MacMillan L, et al. The density and spatial distribution of gabaergic neurons, labelled using calcium binding proteins, in the anterior cingulate cortex in major depressive disorder, bipolar disorder, and schizophrenia. *Biol Psychiatry.* (2002) 51:377–86. doi: 10.1016/S0006-3223(01)01243-4
48. Berrettini WH, Nurnberger JI, Hare T, Gershon ES, Post RM. Plasma and CSF GABA in affective illness. *Br J Psychiatry.* (1982) 141:483–7. doi: 10.1192/bjp.141.5.483
49. Löscher W. Anticonvulsant and biochemical effects of inhibitors of GABA aminotransferase and valproic acid during subchronic treatment in mice. *Biochem Pharmacol.* (1982) 31:837–42. doi: 10.1016/0006-2952(82)90471-3
50. Romeo B, Choucha W, Fossati P, Rotge JY. Meta-analysis of central and peripheral γ-aminobutyric acid levels in patients with unipolar and bipolar depression. *J Psychiatry Neurosci.* (2018) 43:58–66. doi: 10.1503/jpn.160228
51. Machado-Vieira R, Gattaz WF, Zanetti MV, De Sousa RT, Carvalho AF, Soeiro-de-Souza MG, et al. A longitudinal (6-week) 3T 1H-MRS study on the effects of lithium treatment on anterior cingulate cortex metabolites in bipolar depression. *Eur Neuropsychopharmacol.* (2015) 25:2311–7. doi: 10.1016/j.euroneuro.2015.08.023
52. Mescher M, Merkle H, Kirsch J, Garwood M, Gruetter R. Simultaneous *in vivo* spectral editing and water suppression. *NMR Biomed.* (1998) 11:266–72. doi: 10.1002/(sici)1099-1492(199810)11:6<266::aid-nbm530>3.0.co;2-j
53. Mullins PG, McGonigle DJ, O'Gorman RL, Puts NAJ, Vidyasagar R, Evans CJ, et al. Current practice in the use of MEGA-PRESS spectroscopy for the detection of GABA. *NeuroImage.* (2014) 86:43–52. doi: 10.1016/j.neuroimage.2012.12.004
54. Rothman DL, Petroff OA, Behar KL, Mattson RH. Localized 1H NMR measurements of gamma-aminobutyric acid in human brain *in vivo*. *Proc Natl Acad Sci U S A.* (1993) 90:5662–6. doi: 10.1073/pnas.90.12.5662
55. Henry PG, Dautry C, Hantraye P, Bloch G. Brain GABA editing without macromolecule contamination. *Magn Reson Med.* (2001) 45:517–20. doi: 10.1002/1522-2594(200103)45:3<517::aid-mrm1068>3.0.co;2-6
56. Behar KL, Rothman DL, Spencer DD, Petroff OA. Analysis of macromolecule resonances in 1H NMR spectra of human brain. *Magn Reson Med.* (1994) 32:294–302. doi: 10.1002/mrm.1910320304
57. Harris AD, Puts NAJ, Barker PB, Edden RAE. Spectral-editing measurements of GABA in the human brain with and without macromolecule suppression. *Magn Reson Med.* (2015) 74:1523–9. doi: 10.1002/mrm.25549
58. Harris AD, Glaubitz B, Near J, John Evans C, Puts NAJ, Schmidt-Wilcke T, et al. Impact of frequency drift on gamma-aminobutyric acid-edited MR spectroscopy. *Magn Reson Med.* (2014) 72:941–8. doi: 10.1002/mrm.25009

Conflict of Interest: The authors declare that the research was conducted in the absence of any commercial or financial relationships that could be construed as a potential conflict of interest.

frontiers in Psychiatry

ORIGINAL RESEARCH
published: 19 May 2021
doi: 10.3389/fpsyt.2021.656459

Metabolite Alterations in Adults With Schizophrenia, First Degree Relatives, and Healthy Controls: A Multi-Region 7T MRS Study

S. Andrea Wijtenburg[1], Min Wang[2‡], Stephanie A. Korenic[1], Shuo Chen[1], Peter B. Barker[2,3†] and Laura M. Rowland[1†]*

[1] Department of Psychiatry, Maryland Psychiatric Research Center, University of Maryland School of Medicine, Baltimore, MD, United States, [2] The Russell H. Morgan Department of Radiology and Radiological Science, Johns Hopkins University School of Medicine, Baltimore, MD, United States, [3] FM Kirby Research Center for Functional Brain Imaging, Kennedy Krieger Institute, Baltimore, MD, United States

Proton magnetic resonance spectroscopy (MRS) studies in schizophrenia have shown altered GABAergic, glutamatergic, and bioenergetic pathways, but if these abnormalities are brain region or illness-stage specific is largely unknown. MRS at 7T MR enables reliable quantification of multiple metabolites, including GABA, glutamate (Glu) and glutamine (Gln), from multiple brain regions within the time constraints of a clinical examination. In this study, GABA, Glu, Gln, the ratio Gln/Glu, and lactate (Lac) were quantified using 7T MRS in five brain regions in adults with schizophrenia (N = 40), first-degree relatives (N = 11), and healthy controls (N = 38). Metabolites were analyzed for differences between groups, as well as between subjects with schizophrenia with either short (<5 years, N = 19 or long (>5 years, N = 21) illness duration. For analyses between the three groups, there were significant glutamatergic and GABAergic differences observed in the anterior cingulate, centrum semiovale, and dorsolateral prefrontal cortex. There were also significant relationships between anterior cingulate cortex, centrum semiovale, and dorsolateral prefrontal cortex and cognitive measures. There were also significant glutamatergic, GABAergic, and lactate differences between subjects with long and short illness duration in the anterior cingulate, centrum semiovale, dorsolateral prefrontal cortex, and hippocampus. Finally, negative symptom severity ratings were significantly correlated with both anterior cingulate and centrum semiovale metabolite levels. In summary, 7T MRS shows multi-region differences in GABAergic and glutamatergic metabolites between subjects with schizophrenia, first-degree relatives and healthy controls, suggesting relatively diffuse involvement that evolves with illness duration. Unmedicated first-degree relatives share some of the same metabolic characteristics as patients with a diagnosis of schizophrenia, suggesting that these differences may reflect a genetic vulnerability and are not solely due to the effects of antipsychotic interventions.

Keywords: 7T MRS, schizophrenia, first degree relatives, brain, metabolism, glutamate, glutamine, GABA

OPEN ACCESS

Edited by:
Maria Concepcion Garcia Otaduy, University of São Paulo, Brazil

Reviewed by:
Gabriele Ende, University of Heidelberg, Germany
Katharine Thakkar, Michigan State University, United States
James Stone, University of Brighton, United Kingdom

****Correspondence:***
S. Andrea Wijtenburg
awijtenburg@som.umaryland.edu

† These authors share senior authorship

‡Present address:
Min Wang, Department of Biomedical Engineering, College of Biomedical Engineering and Instrument Science, Zhejiang University, Hangzhou, China

Specialty section:
This article was submitted to Neuroimaging and Stimulation, a section of the journal Frontiers in Psychiatry

Received: *20 January 2021*
Accepted: *06 April 2021*
Published: *19 May 2021*

Citation:
Wijtenburg SA, Wang M, Korenic SA, Chen S, Barker PB and Rowland LM (2021) Metabolite Alterations in Adults With Schizophrenia, First Degree Relatives, and Healthy Controls: A Multi-Region 7T MRS Study. Front. Psychiatry 12:656459. doi: 10.3389/fpsyt.2021.656459

INTRODUCTION

Recent proton magnetic resonance spectroscopy (MRS) studies in schizophrenia (SZ) have shown altered GABAergic (1–3), glutamatergic (4–7), and more recently, bioenergetic pathways (8) across multiple brain regions and illness durations. Often these studies quantify metabolites from one or two brain regions within a single session, and many have been performed at the standard field strength of 3T. An advantage of higher field strength magnets, such as 7T, is the increased signal to noise ratio (SNR) and improved spectral separation compared to lower field strengths (9–11). This can be used to acquire high quality MRS data in a shorter period of time, or alternatively to improve the measurement precision in similar periods of time. Several 7T MRS studies have reported good reproducibility in difficult to quantify metabolites like glutamate, glutamine, and GABA (12–14). Most previous 7T studies in schizophrenia have focused only on the anterior cingulate (7, 8, 15, 16) while others have expanded to acquisitions from two or three brain regions within a session (3, 17, 18). A recent study used 7T MRS to examine group differences in first episode patients (2 years or less illness duration) and healthy controls in five brain regions (19); however, there has not yet been a study that examined multiple brain regions thought to be involved in the pathophysiology of schizophrenia which also considers illness phase, or genetic risk for schizophrenia by investigating first-degree relatives (FDRs).

In this study, GABA, glutamate (Glu), glutamine (Gln), lactate, and the ratio of Gln/Glu were quantified from five brain regions [anterior cingulate cortex (ACC), dorsolateral prefrontal cortex (DLPFC), centrum semiovale (CSO), thalamus (Thal), and hippocampus (HP)] in each of the three groups: participants with schizophrenia (SZ), first-degree relatives (FDR), and healthy controls (HC). Glu and GABA, the primary excitatory and inhibitory neurotransmitters in the human brain, were included because animal and post-mortem studies have implicated them in the pathophysiology of SZ (20–22). Since 80% of glutamine is involved in glutamatergic neurotransmission (23), is quantifiable at 7T, and shown to be altered in previous SZ studies (24, 25), it was also included as a metabolite of interest. Total glutamate levels measured by MRS cannot differentiate glutamate involved in neurotransmission, GABA synthesis, protein synthesis, etc.; however, the ratio of Gln/Glu has been suggested as an index for glutamatergic neurotransmission (26, 27), so is also reported here. Lactate was included due to its integral role in energy metabolism, recent post-mortem SZ studies showing increased lactate in several brain regions including the DLPFC and hippocampus (28), and our prior work in a smaller sample size that showed elevated lactate levels in adults with SZ were related to reduced cognitive function and functional capacity (8). The five regions of interest (ACC, CSO, DLPFC, HP, and Thal) were chosen due to their implicated role in the pathophysiology of SZ in pre-clinical, post-mortem, and neuroimaging studies. The ACC and hippocampus have been extensively studied in SZ across the illness duration (19, 26, 29–34) so were included. Studies focused on the thalamus, a key node in many functional circuits, showed reduced thalamic volume in adults with SZ (35) and altered glutamatergic metabolites in clinical high risk for psychosis and chronic SZ participants (30, 36, 37). The CSO was included because it is a predominantly white matter region, and white matter is increasingly implicated as altered in SZ (38, 39). The DLPFC was included because reduced GAD67 mRNA expression, leading to reduce GABA synthesis in parvalbumin-expressing subpopulation of GABA neurons has been found in SZ and as noted above elevated Lac levels (20). First-degree relatives were chosen because they may share common, albeit sub-threshold psychopathology, traits as SZ patients. This group is genetically (40, 41), physiologically (42), cognitively (43, 44), and neurochemically (17, 45, 46) similar to adults with SZ, but without exposure to antipsychotic medications. In addition, within the SZ group, metabolite differences between short (<5 years illness duration) and long (>5 years illness duration) were examined as previous studies have suggested an aging effect in SZ (2, 4). Further, MRS studies of SZ suggest that Glu and Gln may change across the course of the illness with elevated glutamatergic metabolite levels being reported in clinical high risk for psychosis (30, 47) and first-episode (19, 48) populations. In contrast, lower glutamatergic metabolite levels have been reported in chronic SZ populations (31, 37). To our knowledge, this will be the first study to examine glutamatergic metabolites in multiple brain regions in SZ participants with short and long illness durations.

METHODS

This study was approved by the University of Maryland Baltimore and the Johns Hopkins University School of Medicine Institutional Review Boards, and all participants provided written informed consent prior to study enrollment. Forty adults with SZ [$N = 19$ with short illness duration (<5 years) and $N = 21$ with long illness duration (>5 years)], 38 healthy controls (HC), and 11 FDRs participated in this study. Some data from 29 HC and 27 SZ were previously reported (8). Participant demographics are shown in **Table 1**. The Brief Psychiatric Rating Scale (BPRS) (49) for assessment of positive symptoms and general psychopathology and the Brief Negative Symptom Scale (BNSS) (50) were administered to each participant with SZ. The BPRS evaluates the participant's positive symptoms such as suspiciousness, grandiosity, unusual thought content, and hallucinations. The BNSS contains specific subscales that evaluate the participant's negative symptoms such as anhedonia, asociality, avolition, blunted affect, and alogia. In addition, the Structured Clinical Interview for DSM-IV-TR (SCID), the UCSD Performance-Based Skills Assessment (UPSA) (51), Level of Functioning test (LOF) (52), and the MATRICS battery (53, 54) were administered to all participants. The UPSA assesses a participant's functional capacity in areas of household chores, communication, finance, transportation, and planning recreational activities. The LOF assesses the participant's physical functioning, personal care skills, interpersonal relationships, social acceptability, activities of community living, and work skills. The MATRICS battery evaluates the participant's processing speed, attention, verbal and non-verbal working memory, verbal learning, visual learning, reasoning, and social cognition. For all groups, inclusion criteria

TABLE 1 | Participant demographics.

	SZ	FDR	HC
Mean Age (years ± stdev)	34.2 ± 12.4	37.2 ± 12.7	30.5 ± 10.5
Gender (M/F)	23/17	2/9	19/19
Mean Education Level (years ± stdev)**	12.9 ± 1.6	14.5 ± 1.9	14.4 ± 1.8
Smoking Status (Yes/No)	11/29	1/10	8/30
Mean Illness Duration (years ± stdev)	12.4 ± 11.9	N/A	N/A
Cognitive Variables			
Matrics Composite Score (mean ± stdev)**	28.5 ± 14.0	46.5 ± 13.0	44.1 ± 8.9
UPSA Score (mean ± stdev)**	87.4 ± 19.5	101.5 ± 13.3	101.4 ± 9.5
LOF Score (mean ± stdev)**	23.2 ± 5.2	34.7 ± 2.0	33.6 ± 3.6
Symptom Ratings			
BPRS total score (mean ± stdev)	38.1 ± 8.1	N/A	N/A
BPRS positive score (mean ± stdev)	7.9 ± 3.6	N/A	N/A
BPRS negative score (mean ± stdev)	6.8 ± 2.3	N/A	N/A
BNSS score (mean ± stdev)	16.3 ± 10.5	N/A	N/A
Chlorpromazine Equivalents (mean ± stdev)	336.7 ± 329.0		

***statistically significant ($p < 0.05$), FDR, first degree relative; HC, healthy control; stdev, standard deviation; SZ, schizophrenia.*

were: (1) age range: 18–55 years old; (2) no lifetime substance dependence or abuse in the last 6 months; (3) no contraindication for 7T MRI scanning; (4) not pregnant or nursing; (5) no major medical or neurological illness. HC were included if he/she did not have psychiatric illness, while adults with SZ had a diagnosis of SZ or schizoaffective. FDRs have a first degree relative with SZ, but are not related to anyone in the SZ group. Also, FDRs did not have a DSM-IV psychosis diagnosis or current substance abuse or dependence. 10 out of 11 participants were not taking psychotropic medications.

Imaging Protocol

A 7T Philips Achieva scanner (Best, the Netherlands) equipped with a dual-transmit and 32-channel receive head coil (Nova Medical, Wilmington, MA) was used to scan each participant. Using an isotropic 0.8 mm T_1-weighted MPRAGE sequence for guidance, spectroscopic voxels were prescribed in ACC, left CSO, left DLFPC, left hippocampus, and bilateral thalamus (**Figure 1**). Voxel sizes were 12 ($3 \times 2 \times 2$) cm^3 in the ACC, 12 ($4 \times 2 \times 1.5$) cm^3 in the CSO, 10 ($2.5 \times 2 \times 2$) cm^3 in the DLPFC, ∼7.9 ($3.5 \times 1.5 \times 1.5$) cm^3 in the hippocampus, and 9 ($2 \times 3 \times 1.5$) cm^3 in the thalamus. Spectroscopic data were acquired using a STEAM sequence with TR/TM/TE = 3,000/33/14 ms, VAPOR (55) water suppression, and 128 excitations for all regions. A spectrum without water suppression (two excitations) was also acquired for phase and eddy current correction, and use as a quantitation reference (scan time 6 min 30 s per region for both suppressed and non-suppressed acquisitions). Prior to acquisition, shimming was applied up to 2nd order using a projection based method (56), and a localized power optimization performed (57) on the region of interest. High-resolution ($0.5 \times 0.5 \times 1.0$ mm) multi-slice coronal T_2-weighted images were also recorded.

Spectra were analyzed using the 'LCModel' software package version 6.3 (58). A basis set was created using the 'VESPA' program (59), and chemical shifts and coupling constants from (60) for the following metabolites: alanine (Ala), aspartate (Asp), creatine (Cr), γ-aminobutyric acid (GABA), glutamate (Glu), glutamine (Gln), glutathione (GSH), glycerophosphocholine (GPC), glycine (Gly), lactate (Lac), *myo*-inositol (mI), N-acetylaspartate (NAA), N-acetylaspartylglutamate (NAAG), phosphocholine (PCh), phosphocreatine (PCr), phosphorylethanolamine (PE), *scyllo*-inositol (sI), serine (Ser), and taurine (Tau). In the LCModel, a fit range of 0.6–4.0 ppm was used and the baseline spline control parameter ("dkntmn") set to 0.2 (58). All metabolites except lactate were corrected for the proportion of cerebrospinal fluid (CSF) within the MRS voxel, using $[X]_{corrected} = [X]/(1\text{-}f_{CSF})$ where [X] is the metabolite concentration [expressed in in institutional units (i.u.)] as output by LCModel, and f_{CSF} is the fraction of CSF within the voxel (8). f_{CSF}, as well as the fractions of the gray and white matter within the voxel, were calculated by segmentation of the anatomical T_1-weighted images using the "SPM12" program. Lactate was not corrected for the proportion of CSF because this metabolite can be quantified from the CSF using MRS (61, 62). No metabolite relaxation time corrections were performed.

Data were excluded from further analyses if the full-width half maximum (FWHM) > 0.1 ppm for all regions and SNR ≤ 10 for ACC, CSO, DLPFC or SNR ≤ 5 for hippocampus and thalamus (values reported by LCModel). There following datasets were excluded from further analyses: two from the AC (1 HC and 1 SZ), one from the CSO (1 FDR), two from DLPFC (2 SZ), 14 from the hippocampus (7 HC, 6 SZ, and 1 FDR), and none from the thalamus. Metabolites were included in statistical analyses if at least 75% of the possible datasets met the CRLB criteria listed of CRLBs ≤ 20% (Asp, Cr, GABA, Glu, GPC, GSH, mI, NAA, PCh, PCr, PE, sI, Tau, tCho, tNAA, tCr, Glx, mI+Gly) or CRLBs ≤ 30% (Ala, Gln, Gly, Lac, NAAG, Ser). In terms of the main metabolites of interest, Lac analyses were only conducted in the AC and CSO

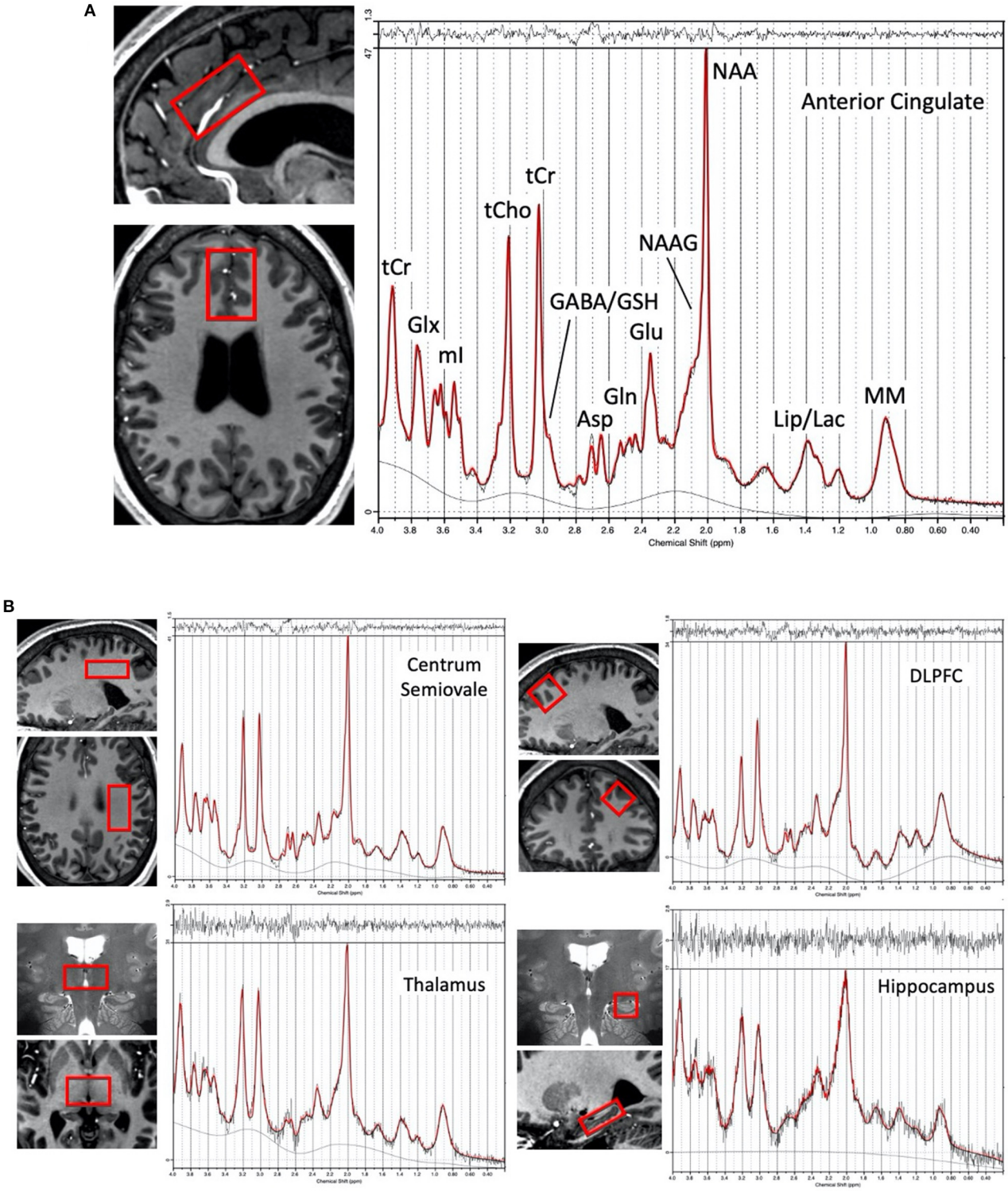

FIGURE 1 | (A) Representative voxel location chosen for the anterior cingulate cortex region in one subject (female, 28 yrs. old) and proton spectrum (LCModel output in red) with peak assignments indicated, **(B)** Representative voxel locations (overlaid in two planes on T_1 or T_2-weighted images) from the left centrum semiovale, left dorsolateral prefrontal cortex, bilateral thalamus, and left hippocampus with a corresponding representative spectrum from each region.

while GABA, Glu, Gln, and Gln/Glu analyses were conducted in all five regions.

Statistics

Due to non-normality, non-parametric tests (Kruskal-Wallis, Mann-Whitney or chi-square) were utilized to assess group differences between HC, SZ, and FDR for demographic variables, voxel composition, spectral quality, and metabolite levels. Based on the stated hypotheses, group differences were examined in each region for GABA, Glu, Gln, Gln/Glu, and Lac with significance set to $p < 0.05$. False discovery rate correction for multiple comparisons was performed for each metabolite across the five regions ($p < 0.05$). In addition, non-parametric tests (Mann-Whitney) were utilized to assess group metabolite level differences between patients with short (<5 years illness duration) or long (>5 years illness duration) illness durations. Similar to the three group analyses, group differences were assessed for GABA, Glu, Gln, Lac, and Gln/Glu ratio with significance set to $p < 0.05$, and false discovery rate correction for multiple comparisons was performed across the five regions ($p < 0.05$). To examine whether the differences between illness duration groups were a function of illness length or an age effect, non-parametric tests (Mann-Whitney) were conducted to assess metabolite differences between the short illness duration SZ group and an age-matched (within 1 year) subset of HC as well as non-parametric ANCOVAs with age as a covariate to assess metabolite differences between the short and long illness duration groups. Significance was set to $p < 0.05$.

For the three groups, Spearman's rho correlations were performed for cognitive and function variables (MATRICS total score, UPSA, and LOF) and MRS metabolite levels. Only metabolites that were significantly different between groups were used in the correlation analyses with significance set to $p < 0.05$. Within the SZ groups, Spearman's rho correlations were performed between symptom severity (BPRS total, BPRS positive, and BNSS) and metabolites that were statistically significant between groups with significance set to $p < 0.05$.

RESULTS

Participant Demographics

Participant demographics are given in **Table 1**. Adults with SZ, HC, and FDR did not differ in terms of age ($H = 298$, $p = 0.23$), gender ($X^2 = 3.9$, $p = 0.14$), and smoking status ($X^2 = 2.0$, $p = 0.37$). There was a significant difference in education level ($H = 11.25$, $p = 0.004$) such that adults with SZ had less years of formal education than HC. The FDR's education level was not significantly different from HC or SZ. Adults with SZ had lower total LOF score ($H = 57.1$, $p < 0.001$), MATRICS total score ($H = 25.5$, $p < 0.001$), and UPSA total score ($H = 13.33$, $p = 0.001$) compared to HC and FDR.

Group Differences in Metabolites

Means and standard deviations for the main metabolites for each group are summarized in **Figure 2** and **Supplementary Table 1**. The supplement (**Supplementary Table 2**) information regarding voxel GM, WM, and CSF percentage differences and quality metrics FWHM and SNR as reported by the LCModel for the three groups. Of the five regions investigated, the SNR was the highest in the ACC followed by the CSO, DLPFC, thalamus, and hippocampus. Similarly, the narrowest FWHM was measured from the ACC, followed by the CSO and DLPFC, then the thalamus and hippocampus. For completeness, mean, standard deviations, N, and statistical significance for other quantifiable metabolites e.g., NAA, mI, tCr, tCho, etc. that may be of interest are summarized in the supplement (**Supplementary Table 5**).

In the ACC, Glu levels were significantly different between groups ($H = 6.4$, $p = 0.04$) such that adults with SZ had lower Glu levels than HC and FDR.There were no significant group differences for GABA, Gln, Gln/Glu ratio, or Lac. After applying correction for multiple comparisons, there were no significant group differences for the other quantifiable metabolites (p's $= 0.168–0.933$).

In the CSO, GABA, Gln, and Gln/Glu ratio were significantly different between groups with ($H = 6.8$, $p = 0.034$, $H = 7.4$, $p = 0.025$, and $H = 9.2$, $p = 0.010$), respectively. Gln and Gln/Glu were significantly higher in the SZ group compared to the HC group. The FDR group's Gln and Gln/Glu levels fell in between the other two groups but were not significantly different. GABA levels were similar between SZ and HC but were significantly lower in the FDR group. After applying correction for multiple comparisons, there were no significant group differences for the other quantifiable metabolites (p's $= 0.05–0.98$).

In the DLPFC, hippocampus, and thalamus, there were no significant differences for GABA, Glu, Gln, and Gln/Glu ratio among the three groups. In addition, there were no other significant group differences for the remaining quantifiable metabolites.

Correlations Between Metabolites and Cognitive Measures

In the ACC, Glu was the only metabolite significantly different between groups. ACC Glu was strongly correlated to UPSA (rho $= 0.321$, $p = 0.004$) across groups (**Figure 3A**). Separating by diagnostic group revealed a trend correlation only in the SZ group (rho $= 0.329$, $p = 0.054$), and not in the HC ($p = 0.511$) or FDR ($p = 0.374$) groups. ACC Glu was also strongly correlated with LOF (rho $= 0.364$, $p = 0.001$) across groups and within the SZ group (rho $= 0.360$, $p = 0.024$) (**Figure 3B**). There were no significant correlations in HC ($p = 0.229$) or FDR ($p = 0.728$) groups. Finally, ACC Glu was also significantly correlated with MATRICS total score (rho $= 0.383$, $p < 0.001$) across groups, within the FDR group (rho $= 0.693$, $p = 0.026$), but not within the HC ($p = 0.132$) or SZ ($p = 0.524$) groups (**Figure 3C**). After correction for multiple comparisons, all three combined group correlations between Glu with UPSA, LOF, and MATRICS total score remained significant.

For the CSO, Gln and Gln/Glu were significantly correlated with LOF but not with other measures. Gln/Glu was correlated with LOF across groups (rho $= -0301$, $p = 0.005$) and within the SZ group (rho $= -0.362$, $p = 0.023$) but not HC ($p = 0.671$) or FDR ($p = 0.377$). Similarly, Gln was correlated

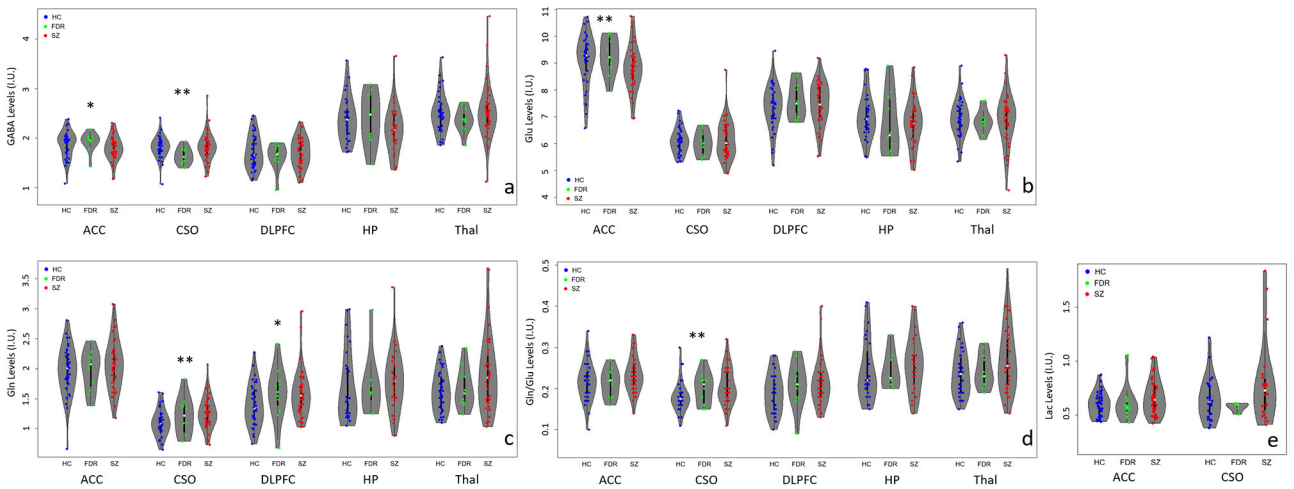

FIGURE 2 | Violin plots with individual data points highlighting metabolite differences between adults with SZ (●), first-degree relatives (●), and healthy controls (●) in the anterior cingulate cortex (ACC), left centrum semiovale (CSO), left dorsolateral prefrontal cortex (DLPFC), left hippocampus (HP), and bilateral thalamus (Thal). **(a)** GABA levels differed significantly between groups in the CSO (**$p < 0.05$) and at trend level (*$p < 0.1$) in the ACC. ACC GABA was significantly lower in the SZ compared to the HC and FDR groups. CSO GABA in the FDR group was trend level lower than the SZ or HC groups. **(b)** Glu levels differed significantly between groups in the ACC only such that adults with SZ had lower Glu levels than HC and FDR. **(c)** CSO Gln levels were significantly higher in the SZ group compared to HC and FDR while DLPFC Gln levels in the HC group was lower at trend level than the SZ and FDR groups. **(d)** CSO Gln/Glu ratio was significantly higher in the SZ group compared to the other two groups. **(e)** There were no significant Lac findings.

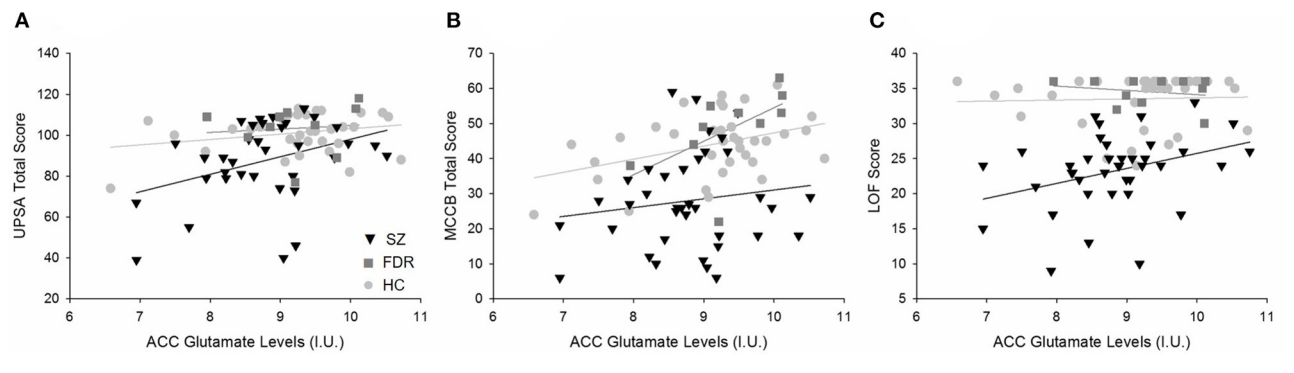

FIGURE 3 | Regression plots of the significant relationships between **(A)** ACC Glu levels and UPSA total scores, **(B)** ACC Glu and MATRICS total scores, and **(C)** ACC Glu levels and LOF scores. **(A)** Separating by diagnostic group revealed a trend level relationship in only the SZ group (H) and not the HC (●) or FDR (■). **(B)** ACC Glu levels were significantly correlated to MATRICS total score across diagnostic groups. Further analyses revealed a significant relationship in the FDR group only. **(C)** Similarly, ACC Glu levels were significantly correlated to LOF scores across diagnostic groups and in the SZ group. There were no significant relationships between HC and FDR. Similarly, ACC Glu levels were significantly correlated to MATRICS total score across diagnostic groups. Further analyses revealed a significant relationship in the FDR group only.

with LOF (rho = −0.229, $p = 0.036$) across groups, but did not remain significant at the diagnostic group level (p's = 0.076–0.96). GABA did not correlate with any measure. After correcting for multiple comparisons, none of these correlations remained significant.

Early vs. Later Illness Duration

Participant Demographics

Adults with SZ with shorter (<5 years) and longer (>5 years) illness durations differed significantly with age ($U = 21$, $p < 0.001$) such that the shorter illness duration group was younger than the longer illness duration group (**Table 2**). The two illness groups did not differ on education level ($p = 0.49$), gender ($p = 0.18$), smoking status ($p = 0.39$), and CPZ equivalents ($p = 0.73$). There were no significant group differences for LOF ($p = 0.18$), UPSA ($p = 0.07$) MATRICS total score ($p = 0.09$), BPRS total ($p = 0.71$), BPRS positive ($p = 0.16$), and BNSS ($p = 0.32$) scores.

Metabolite Differences Between Short vs. Long Illness Duration

Means and standard deviations for the main metabolite levels for the two groups are summarized in **Figure 4** and **Supplementary Table 3**, and the supplement contains

TABLE 2 | Participant demographics for short and long illness duration.

	Short	Long
Mean Age (years ± stdev)**	24.3 ± 3.9	43.1 ± 11.0
Gender (M/F)	13/6	10/11
Mean Education Level (years ± stdev)	13.1 ± 1.0	12.8 ± 2.0
Smoking Status (Yes/No)	4/19	7/21
Mean Illness Duration (years ± stdev)	2.7 ± 1.7	21.2 ± 10.3
Cognitive Variables		
Matrics Composite Score (mean ± stdev)	32.7 ± 13.4	24.6 ± 13.7
UPSA Score (mean ± stdev)	94.6 ± 13.2	80.7 ± 22.3
LOF Score (mean ± stdev)	24.7.2 ± 4.4	21.9 ± 5.7
Symptom Ratings		
BPRS total score (mean ± stdev)	37.2 ± 6.8	39.0 ± 9.2
BPRS positive score (mean ± stdev)	7.1 ± 3.3	8.6 ± 3.7
BPRS negative score (mean ± stdev)	6.7 ± 2.3	6.9 ± 2.3
BNSS score (mean ± stdev)	14.1 ± 9.2	18.2 ± 11.3
Chlorpromazine Equivalents (mean ± stdev)	290.9 ± 286.0	372.8 ± 362.8

***statistically significant ($p < 0.05$).*

information regarding the voxel GM, WM, and CSF percentage differences and quality metrics (FWHM and SNR as reported by LCModel) for the two groups (**Supplementary Table 2**). In addition, results from other quantifiable metabolites e.g., NAA, mI, tCr, tCho, etc. are summarized in the supplement (**Supplementary Table 6**).

In the ACC, there were significant group differences for Glu ($U = 286$, $p = 0.006$), but not for GABA, Gln, or Gln/Glu. Glu levels were higher in the early illness duration group vs. the later illness duration group. Lac levels between groups were trend level different ($U = 96$, $p = 0.06$) such that Lac levels were higher in the longer illness duration vs. the shorter illness duration group. After correcting for multiple comparisons for the other metabolites, Glx was also different between groups ($U = 284$, $p = 0.007$) such that higher Glx was observed in the short compared to the longer illness duration group. No other quantifiable metabolites were significantly different between groups.

In the CSO, Lac levels were significantly different between groups ($U = 13$, $p = 0.003$) such that the longer illness duration group had higher levels of Lac compared to the shorter illness duration group. However, the sample size for each group, particularly the short illness duration group, for the Lac analyses was much smaller than the sample size for the other metabolites so this finding should be interpreted with caution. There were no Gln, Glx, Gln/Glu, or GABA differences between groups. No other quantifiable metabolites were significantly different between groups.

In the DLPFC, there was a significant difference between groups for Glu ($U = 285$, $p = 0.002$) such that the short illness duration group had higher Glu levels than the long illness duration group. There were no significant group differences for Gln, Gln/Glu, or GABA. After correction for multiple comparisons for the other quantifiable metabolites, Glx ($U = 279$, $p = 0.003$) was the only metabolite with significant differences between groups. Glx was higher in the shorter illness duration group.

In the hippocampus, there here were no significant group differences for GABA, Glu, Gln, or Gln/Glu ratio. After correcting for multiple comparisons for the other quantifiable metabolites, there were no significant differences between groups.

In the thalamus, there were no significant group differences for GABA, Glu, Gln, or Gln/Glu ratio. After correcting for multiple comparisons for the other quantifiable metabolites, mI ($U = 96$, $p = 0.008$) and mI+Gly ($U = 92$, $p = 0.006$) were significantly different such that mI and mI+Gly were significantly higher in the long illness duration group vs. the short illness duration group.

Detailed results of the group difference analyses between age-matched short illness duration group and HC group are in the supplement (**Supplementary Text** and **Supplementary Table 7**). CSO Lac and ACC Glu were the only two metabolites that were different (significantly for Lac at $p = 0.037$ and trend level for Glu at $p = 0.083$) between the short illness duration and HC analyses. Detailed results regarding the illness duration group difference analysis that co-varied for age are in the **Supplementary Text**. Results from the non-parametric ANCOVA revealed no significant differences between the short and long illness duration groups for any metabolites after controlling for age; however, given the highly correlated nature of age and illness duration, these results should be interpreted with caution.

Correlations Between Metabolites and Clinical Measures

ACC Glu and Glx were significantly different between the three groups (SZ, FDR, HC) or the two patient groups and therefore waere included in correlation analysis. ACC Glu was trend level related to BNSS (rho $= -0.290$, $p = 0.072$), and not significantly related to BPRS total or BPRS positive symptom score. Separating by illness duration revealed a significant relationship between ACC Glu and BNSS (rho $= -0.445$, $p = 0.043$) for the long illness duration group only. ACC Glx was not significantly related to the symptom ratings in the SZ group as a whole (p's > 0.129) or when broken down by short or long illness duration groups (all p's > 0.146). None of the relationships presented survived multiple comparison correction.

For the CSO, Gln, Gln/Glu, GABA, and Lac were significantly different between the three groups (SZ, FDR, HC) or the two patient groups and therefore were included in the correlation analysis. Gln was significantly associated with BPRS total score (rho $= 0.363$, $p = 0.023$) across groups, and a similar relationship was present in the long (rho $= 0.433$, $p = 0.050$) both not short ($p = 0.335$) and illness duration groups. Gln/Glu was significantly associated with BNSS (rho $= 0.362$, $p = 0.023$) across groups, and a similar trend relationship was present in the short illness duration group (rho $= 0.468$, $p = 0.05$) but not the long ($p = 0.479$) illness duration group. The other metabolites were not significantly associated with any of the symptom ratings (all p's > 0.07). Similar to ACC, these correlations did not survive correction for multiple comparisons.

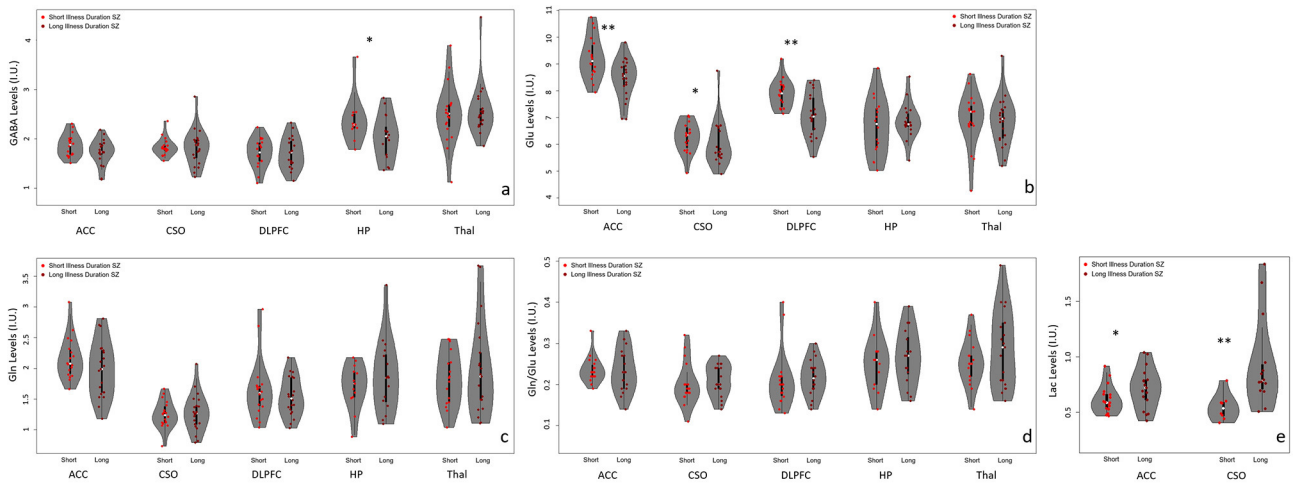

FIGURE 4 | Violin plots with individual data points summarizing the significant (**$p < 0.05$) and trend level (*$p < 0.1$) differences between adults with SZ with short (●) and long illness (●) durations in the anterior cingulate cortex (ACC), left centrum semiovale (CSO), left dorsolateral prefrontal cortex (DLPFC), left hippocampus (HP), and bilateral thalamus (Thal). **(a)** There was a trend level difference in GABA in the HP such that GABA was higher in the short illness duration group compared to the long illness duration group. **(b)** Glu levels were significantly higher in the short illness duration group vs. the long illness duration group in both the ACC and DLPFC. A similar relationship, but at trend level, was observed in the CSO. **(c,d)** There were no significant relationships between groups across all regions for Gln and Gln/Glu. **(e)** For Lac, there was a significant difference in the CSO such that the long illness duration group had higher Lac levels compared to the short illness duration group. A similar relationship was observed in the ACC but at trend level.

DLPFC Glu, and Glx, as well as thalamus mI and mI+Gly were significantly l different between the three groups (SZ, FDR, HC) or the two patient groups and therefore were included in the correlation analysis. There were no significant relationships between symptom rating and these metabolites for the SZ group as a whole (all p's > 0.095), but there was a relationship between thalamus mI+Gly and BPRS total symptoms in the long illness duration group only (rho $= 0.472$, $p = 0.031$). This did not survive correction for multiple comparisons.

DISCUSSION

This study examined metabolite differences in five brain regions in adults with SZ, HC, and FDR at 7T. It also compared metabolite differences in adults with SZ earlier in the illness (<5 years) compared to later in the illness (>5 years). The results add to the growing body of literature of glutamatergic and GABAergic differences in the ACC in SZ, and report 7T metabolite differences in the CSO, DLPFC, thalamus, and hippocampus, regions implicated in the pathophysiology of SZ. The ACC and the CSO emerged as key regions for metabolite differences that were related to psychopathology and function in SZ in this study. In terms of metabolic abnormalities, the longer illness group was more severely affected than the short illness group for all brain regions.

This study found lower ACC Glu and GABA in the SZ group and higher ACC lactate in the longer illness group, which are consistent with neuroimaging, post-mortem, and behavioral research implicating ACC abnormalities in SZ (7, 21, 29, 63–67). With respect to 7T MRS studies focused on ACC Glu, results have been mixed. Recent 7T MRS work by Posporelis et al. (16), Brandt et al. (15), Kumar et al. (18), and Taylor et al. (36) observed no differences in ACC Glu when comparing either recent onset SZ or chronic SZ with healthy controls. In contrast, Reid et al. (7) showed ACC Glu was lower in first episode patients (within 2 years of starting treatment) than in healthy controls in the dorsal ACC, and these results were similar to those by Wang et al. (19) showing lower Glu in the ACC in first episode patients (2 years from first psychotic symptoms) compared to healthy controls. The current results are similar to these studies in that lower ACC Glu was observed in the SZ group as a whole, and especially so in the longer illness duration group. ACC Glu levels may have functional relevance in schizophrenia, as lower levels were related to poorer functional capacity, functioning, and greater negative symptoms. These results suggest that ACC Glu may be impacted by illness chronicity and contribute to impaired function and negative symptom severity as indicated by findings in the longer illness group. It is not clear as to the cause of lower ACC Glu in schizophrenia since the MRS Glu signal provides a total tissue level and cannot differentiate between glutamate levels in specific cell types (i.e., neurons and glia), location (i.e., intracellular, extracellular, or synaptic), or function (i.e., neurotransmission, GABA synthesis, glutathione synthesis, and protein synthesis). It is possible that lower ACC Glu reflects reduced number or size of glutamatergic pyramidal neurons, consistent with previous research (68), reduced Glu synthesis, and/or impaired Glu-Gln neurotransmitter cycling (69). Interventions to increase ACC Glu levels, especially later in the illness, may reduce negative symptoms and enhance everyday function.

There was a trend for lower ACC GABA in SZ compared to HC which was related to lower level of function as a whole, and greater negative symptom severity in the longer illness group.

Three previous 7T MRS studies that did not report differences between SZ and HC (7, 15, 19) but differences in voxel placement, voxel size, acquisition parameters, and illness duration of the SZ group may contribute to this inconsistency. Lower GABA in SZ likely reflects reduced GABA synthesis, consistent with studies of lower GAD67 in SZ (70), resulting in reduced inhibition as suggested from studies of SZ (71).

Our previous paper showed higher ACC lactate in the SZ group compared to the HC group (8). Here, using an overlapping sample but larger N, we did not observe a significant group difference in the ACC when examining adults with SZ, HC, and FDR; however, ACC lactate levels were trend level higher in the longer illness group. This was consistent with the finding of higher CSO lactate in the longer illness group. In the longer illness group, higher ACC lactate was related to greater negative symptoms. Recent work has suggested that lactate may be altered in schizophrenia, potentially due to a bioenergtic or mitochondrial dysfunction (72, 73). The specificity of this relationship to the chronic phase of SZ (>5 years illness duration), in addition to a recent study that did not observe peripheral mitochondrial dysfunction in a clinical high risk for psychosis group (74), suggests that increased lactate may be a long-term consequence of impaired mitochondrial function. However, longitudinal studies are needed to assess the progression of brain lactate levels over the illness course. Further, while adults in both illness duration groups were predominantly treated with antipsychotics, long term antipsychotic medication exposure in rats does not result in increased frontal cortex lactate (72).

The CSO white matter region also revealed higher Gln/Glu ratio and Gln in SZ, which were related to poorer function across all groups, and greater negative symptom severity (Gln/Glu) and greater psychopathology (Gln) in the SZ group. In addition, CSO Glu was lower in the longer illness group and GABA lower in the FDR group. To our knowledge, there is one other study that has examined the CSO at 7T, and no differences in CSO Glu, Gln, or GABA were observed in first episode patients compared to controls (19). Since similar sequences, voxel placement, and voxel size were used, the significant Gln/Glu and Gln findings in this study may be attributed to the longer illness duration of the SZ group. These findings also lend further support to significant white matter alterations in SZ (39, 75) and the possibility that white matter alterations are related to abnormal glutamatergic function (38). Similar to the ACC, the reason for lower Glu or increased Gln/Glu and Gln in SZ is unclear. Abnormalities in the synthesis, degradation, or Glu-Gln cycling could be explanations. Also, specific neural cell types could be affected such as oligodendrocytes in white matter that play an important role in removing synaptic glutamate and the subsequent conversion to glutamine. It should also be noted that glutamine is synthesized in the brain from glutamate and ammonia; ammonia in blood crosses the blood-brain barrier, and if elevated (e.g., due to liver dysfunction or other factors) is known to drive brain glutamine synthesis (76). Blood ammonia levels were not measured in this study, so it is unknown if this is a significant factor or not in the subjects reported here.

There were no significant differences in metabolites across the three groups for the DLPFC, hippocampus, or thalamus. A trend for higher DLPFC Gln in both SZ and FDR compared to HC was found but this was not related to cognitive or functioning measures. Lower DLPFC Glu, lower hippocampal GABA, and higher thalamic mI were found in the longer compared to the shorter illness group. Only thalamus mI was related to a clinical measure, with greater thalamic mI related to more severe general psychopathology. One 7T MRS study of DLPFC did not find any group differences in first episode patients (19), which is in line with these results showing only a trend Gln difference and that lower Glu is likely associated again with illness duration. To our knowledge, there are no other studies examining the hippocampus at 7T in SZ. Finally, there were no group differences for the metabolites of interest in this study in bilateral thalamus, which was similar to another study (19). Another study at 7T that examined metabolite differences the left thalamus from an early illness SZ cohort and HC found higher Gln in the SZ group compared to the HC group (36). Our results showed higher Gln in the SZ group compared to the HC group for the thalamus, but the difference did not reach statistical significance ($p = 0.064$).

The FDR group was not distinguishable except for lower CSO GABA compared to HC and SZ and a similar trend as SZ for higher DLPFC Gln compared to HC. Since the FDR sample size is small, these analyses were restricted to non-parametric tests, and the results should be interpreted with caution. One prior study has compared patients with schizophrenia with both healthy siblings and unrelated control subjects using 7T MRS (17); that study found that reduced GABA in occipitalcortex was specific to the patient group only, but that glutamate was reduced in patients and relatives compared to healthy controls. These results suggest that glutamatergic metabolism may be altered both in patients with schizophrenia as well as those who may have genetic risk for schizophrenia.

There are a few limitations that are worth noting. First, the sample size for the FDR group was small compared to the SZ and HC groups. Second, the macromolecule background present in all short TE MRS studies was handled using the built-in capabilities of LCModel. While this methodology has been used previously and shown to be an effective means of handling the background, it remains unclear whether the proteins and lipids that make up the macromolecule spectrum are different in SZ or FDR. It should also be noted that spectral quality (including factors such as linewidth and SNR) vary depending on location within the human brain; this depends on both the size and location of the MRS voxel. For instance, it is well-known that structures such as the hippocampus are somewhat less favorable compared to more superior and/or posterior brain regions, both because of its small size and also proximity to intracranial air spaces that cause magnetic field inhomogeneity. Lower spectral quality implies more variance in the determination of metabolite concentration values, hence it may be more difficult to demonstrate statistically significant findings for regions with lower spectral quality; in the current study, quality metrics were lower for hippocampus and thalamus as compared to the other three, more superior, brain regions.

This study contributes to the building evidence of *in-vivo* glutamatergic and GABAergic abnormalities and relation to functional and clinical symptoms in schizophrenia. The results emphasize the potential worsening with illness chronicity and indicate the need for future studies focused on the chronic phase of the illness. The study also highlights the importance of lactate and potentially bioenergetic dysfunction in the pathophysiology of SZ, which are likely linked to abnormalities in glutamatergic and GABAergic systems and illness features.

DATA AVAILABILITY STATEMENT

Data are not readily available because anonymized data sharing was not in the consent form for this study. Requests to access the datasets should be directed to awijtenburg@som.umaryland.edu.

ETHICS STATEMENT

The studies involving human participants were reviewed and approved by University of Maryland Baltimore and Johns Hopkins University School of Medicine Institutional Review Boards. The patients/participants provided their written informed consent to participate in this study.

AUTHOR CONTRIBUTIONS

LR and PB had full access to all the data in the study and take responsibility for the integrity of the data and the accuracy of the data analysis, concept and design, obtained funding, and supervision. SW, LR, and PB: drafting of the manuscript. SC: statistical analysis. SW, MW, SK, LR, and PB: administrative, technical, or material support. All authors: acquisition, analysis, or interpretation of data, and critical revision of the manuscript for important intellectual content.

FUNDING

This work was supported by NIH R01MH096263.

SUPPLEMENTARY MATERIAL

The Supplementary Material for this article can be found online at: https://www.frontiersin.org/articles/10.3389/fpsyt.2021.656459/full#supplementary-material

REFERENCES

1. Egerton A, Modinos G, Ferrera D, McGuire P. Neuroimaging studies of GABA in schizophrenia: a systematic review with meta-analysis. *Transl Psychiatry*. (2017) 7:e1147. doi: 10.1038/tp.2017.124
2. Rowland LM, Krause BW, Wijtenburg SA, McMahon RP, Chiappelli J, Nugent KL, et al. Medial frontal GABA is lower in older schizophrenia: a MEGA-PRESS with macromolecule suppression study. *Mol Psychiatry*. (2016) 21:198–204. doi: 10.1038/mp.2015.34
3. Marsman A, Mandl RC, Klomp DW, Bohlken MM, Boer VO, Andreychenko A, et al. GABA and glutamate in schizophrenia: a 7 T (1)H-MRS study. *Neuroimage Clin*. (2014) 6:398–407. doi: 10.1016/j.nicl.2014.10.005
4. Marsman A, van den Heuvel MP, Klomp DW, Kahn RS, Luijten PR, Hulshoff Pol HE. Glutamate in schizophrenia: a focused review and meta-analysis of (1)H-MRS studies. *Schizophr Bull*. (2013) 39:120–9. doi: 10.1093/schbul/sbr069
5. Merritt K, Egerton A, Kempton MJ, Taylor MJ, McGuire PK. Nature of glutamate alterations in schizophrenia: a meta-analysis of proton magnetic resonance spectroscopy studies. *JAMA Psychiatry*. (2016) 73:665–74. doi: 10.1001/jamapsychiatry.2016.0442
6. Wijtenburg SA, Yang S, Fischer BA, Rowland LM. *In vivo* assessment of neurotransmitters and modulators with magnetic resonance spectroscopy: application to schizophrenia. *Neurosci Biobehav Rev*. (2015) 51:276–95. doi: 10.1016/j.neubiorev.2015.01.007
7. Reid MA, Salibi N, White DM, Gawne TJ, Denney TS, Lahti AC. 7T Proton magnetic resonance spectroscopy of the anterior cingulate cortex in first-episode schizophrenia. *Schizophr Bull*. (2019) 45:180–9. doi: 10.1093/schbul/sbx190
8. Rowland LM, Pradhan S, Korenic S, Wijtenburg SA, Hong LE, Edden RA, et al. Elevated brain lactate in schizophrenia: a 7 T magnetic resonance spectroscopy study. *Transl Psychiatry*. (2016) 6:e967. doi: 10.1038/tp.2016.239
9. Mekle R, Mlynarik V, Gambarota G, Hergt M, Krueger G, Gruetter R. MR spectroscopy of the human brain with enhanced signal intensity at ultrashort echo times on a clinical platform at 3T and 7T. *Magn Reson Med*. (2009) 61:1279–85. doi: 10.1002/mrm.21961
10. Tkac I, Oz G, Adriany G, Ugurbil K, Gruetter R. *In vivo* 1H NMR spectroscopy of the human brain at high magnetic fields: metabolite quantification at 4T vs. 7T. *Magn Reson Med*. (2009) 62:868–79. doi: 10.1002/mrm.22086
11. Pradhan S, Bonekamp S, Gillen JS, Rowland LM, Wijtenburg SA, Edden RA, et al. Comparison of single voxel brain MRS AT 3T and 7T using 32-channel head coils. *Magn Reson Imaging*. (2015) 33:1013–8. doi: 10.1016/j.mri.2015.06.003
12. Wijtenburg SA, Rowland LM, Edden RA, Barker PB. Reproducibility of brain spectroscopy at 7T using conventional localization and spectral editing techniques. *J Magn Reson Imaging*. (2013) 38:460–7. doi: 10.1002/jmri.23997
13. Wijtenburg SA, Rowland LM, Oeltzschner G, Barker PB, Workman CI, Smith GS. Reproducibility of brain MRS in older healthy adults at 7T. *NMR Biomed*. (2019) 32:e4040. doi: 10.1002/nbm.4040
14. Terpstra M, Cheong I, Lyu T, Deelchand DK, Emir UE, Bednarik P, et al. Test-retest reproducibility of neurochemical profiles with short-echo, single-voxel MR spectroscopy at 3T and 7T. *Magn Reson Med*. (2016) 76:1083–91. doi: 10.1002/mrm.26022
15. Brandt AS, Unschuld PG, Pradhan S, Lim IA, Churchill G, Harris AD, et al. Age-related changes in anterior cingulate cortex glutamate in schizophrenia: A (1)H MRS Study at 7 Tesla. *Schizophr Res*. (2016) 172:101–5. doi: 10.1016/j.schres.2016.02.017
16. Posporelis S, Coughlin JM, Marsman A, Pradhan S, Tanaka T, Wang H, et al. Decoupling of brain temperature and glutamate in recent onset of schizophrenia: a 7T proton magnetic resonance spectroscopy study. *Biol Psychiatry Cogn Neurosci Neuroimaging*. (2018) 3:248–54. doi: 10.1016/j.bpsc.2017.04.003
17. Thakkar KN, Rosler L, Wijnen JP, Boer VO, Klomp DW, Cahn W, et al. 7T Proton magnetic resonance spectroscopy of gamma-aminobutyric acid, glutamate, and glutamine reveals altered concentrations in patients with schizophrenia and healthy siblings. *Biol Psychiatry*. (2017) 81:525–35. doi: 10.1016/j.biopsych.2016.04.007
18. Kumar J, Liddle EB, Fernandes CC, Palaniyappan L, Hall EL, Robson SE, et al. Glutathione and glutamate in schizophrenia: a 7T MRS study. *Mol Psychiatry*. (2018) 25:873–82. doi: 10.1038/s41380-018-0104-7
19. Wang AM, Pradhan S, Coughlin JM, Trivedi A, DuBois SL, Crawford JL, et al. Assessing brain metabolism with 7-T proton magnetic resonance spectroscopy in patients with first-episode psychosis. *JAMA Psychiatry*. (2019) 76:314–23. doi: 10.1001/jamapsychiatry.2018.3637

20. Lewis DA, Hashimoto T, Volk DW. Cortical inhibitory neurons and schizophrenia. *Nat Rev Neurosci*. (2005) 6:312–24. doi: 10.1038/nrn1648
21. Zavitsanou K, Ward PB, Huang XF. Selective alterations in ionotropic glutamate receptors in the anterior cingulate cortex in schizophrenia. *Neuropsychopharmacology*. (2002) 27:826–33. doi: 10.1016/S0893-133X(02)00347-0
22. Benes FM, Berretta S. GABAergic interneurons: implications for understanding schizophrenia and bipolar disorder. *Neuropsychopharmacology*. (2001) 25:1–27. doi: 10.1016/S0893-133X(01)00225-1
23. Magistretti PJ, Pellerin L. Cellular mechanisms of brain energy metabolism and their relevance to functional brain imaging. *Philos Trans R Soc Lond B Biol Sci*. (1999) 354:1155–63. doi: 10.1098/rstb.1999.0471
24. Theberge J, Williamson KE, Aoyama N, Drost DJ, Manchanda R, Malla AK, et al. Longitudinal grey-matter and glutamatergic losses in first-episode schizophrenia. *Br J Psychiatry*. (2007) 191:325–34. doi: 10.1192/bjp.bp.106.033670
25. Aoyama N, Theberge J, Drost DJ, Manchanda R, Northcott S, Neufeld RW, et al. Grey matter and social functioning correlates of glutamatergic metabolite loss in schizophrenia. *Br J Psychiatry*. (2011) 198:448–56. doi: 10.1192/bjp.bp.110.079608
26. Bustillo JR, Rowland LM, Mullins P, Jung R, Chen H, Qualls C, et al. 1H-MRS at 4 tesla in minimally treated early schizophrenia. *Mol Psychiatry*. (2010) 15:629–36. doi: 10.1038/mp.2009.121
27. Shirayama Y, Obata T, Matsuzawa D, Nonaka H, Kanazawa Y, Yoshitome E, et al. Specific metabolites in the medial prefrontal cortex are associated with the neurocognitive deficits in schizophrenia: a preliminary study. *Neuroimage*. (2010) 49:2783–90. doi: 10.1016/j.neuroimage.2009.10.031
28. Pruett BS, Meador-Woodruff JH. Evidence for altered energy metabolism, increased lactate, and decreased pH in schizophrenia brain: a focused review and meta-analysis of human postmortem and magnetic resonance spectroscopy studies. *Schizophr Res*. (2020) 223:29–42. doi: 10.1016/j.schres.2020.09.003
29. Fornito A, Yucel M, Dean B, Wood SJ, Pantelis C. Anatomical abnormalities of the anterior cingulate cortex in schizophrenia: bridging the gap between neuroimaging and neuropathology. *Schizophr Bull*. (2009) 35:973–93. doi: 10.1093/schbul/sbn025
30. Stone JM, Day F, Tsagaraki H, Valli I, McLean MA, Lythgoe DJ, et al. Glutamate dysfunction in people with prodromal symptoms of psychosis: relationship to gray matter volume. *Biol Psychiatry*. (2009) 66:533–9. doi: 10.1016/j.biopsych.2009.05.006
31. Tayoshi S, Sumitani S, Taniguchi K, Shibuya-Tayoshi S, Numata S, Iga J, et al. Metabolite changes and gender differences in schizophrenia using 3-Tesla proton magnetic resonance spectroscopy (1H-MRS). *Schizophr Res*. (2009) 108:69–77. doi: 10.1016/j.schres.2008.11.014
32. Lieberman JA, Girgis RR, Brucato G, Moore H, Provenzano F, Kegeles L, et al. Hippocampal dysfunction in the pathophysiology of schizophrenia: a selective review and hypothesis for early detection and intervention. *Mol Psychiatry*. (2018) 23:1764–72. doi: 10.1038/mp.2017.249
33. Spieker EA, Astur RS, West JT, Griego JA, Rowland LM. Spatial memory deficits in a virtual reality eight-arm radial maze in schizophrenia. *Schizophr Res*. (2012) 135:84–9. doi: 10.1016/j.schres.2011.11.014
34. Beneyto M, Kristiansen LV, Oni-Orisan A, McCullumsmith RE, Meador-Woodruff JH. Abnormal glutamate receptor expression in the medial temporal lobe in schizophrenia and mood disorders. *Neuropsychopharmacology*. (2007) 32:1888–902. doi: 10.1038/sj.npp.1301312
35. Dorph-Petersen KA, Lewis DA. Postmortem structural studies of the thalamus in schizophrenia. *Schizophr Res*. (2017) 180:28–35. doi: 10.1016/j.schres.2016.08.007
36. Taylor R, Osuch EA, Schaefer B, Rajakumar N, Neufeld RW, Theberge J, et al. Neurometabolic abnormalities in schizophrenia and depression observed with magnetic resonance spectroscopy at 7 T. *BJPsych Open*. (2017) 3:6–11. doi: 10.1192/bjpo.bp.116.003756
37. Theberge J, Al-Semaan Y, Williamson PC, Menon RS, Neufeld RW, Rajakumar N, et al. Glutamate and glutamine in the anterior cingulate and thalamus of medicated patients with chronic schizophrenia and healthy comparison subjects measured with 4.0-T proton MRS. *Am J Psychiatry*. (2003) 160:2231–3. doi: 10.1176/appi.ajp.160.12.2231
38. Dias AM. The Integration of the glutamatergic and the white matter hypotheses of schizophrenia's etiology. *Curr Neuropharmacol*. (2012) 10:2–11. doi: 10.2174/157015912799362742
39. Kochunov P, Chiappelli J, Wright SN, Rowland LM, Patel B, Wijtenburg SA, et al. Multimodal white matter imaging to investigate reduced fractional anisotropy and its age-related decline in schizophrenia. *Psychiatry Res*. (2014) 223:148–56. doi: 10.1016/j.pscychresns.2014.05.004
40. Pulver AE, Mulle J, Nestadt G, Swartz KL, Blouin JL, Dombroski B, et al. Genetic heterogeneity in schizophrenia: stratification of genome scan data using co-segregating related phenotypes. *Mol Psychiatry*. (2000) 5:650–3. doi: 10.1038/sj.mp.4000814
41. Chiu YF, McGrath JA, Thornquist MH, Wolyniec PS, Nestadt G, Swartz KL, et al. Genetic heterogeneity in schizophrenia II: conditional analyses of affected schizophrenia sibling pairs provide evidence for an interaction between markers on chromosome 8p and 14q. *Mol Psychiatry*. (2002) 7:658–64. doi: 10.1038/sj.mp.4001045
42. Thaker GK, Avila M. Schizophrenia, V: risk markers. *Am J Psychiatry*. (2003) 160:1578. doi: 10.1176/appi.ajp.160.9.1578
43. Snitz BE, Macdonald AW, III, Carter CS. Cognitive deficits in unaffected first-degree relatives of schizophrenia patients: a meta-analytic review of putative endophenotypes. *Schizophr Bull*. (2006) 32:179–94. doi: 10.1093/schbul/sbi048
44. Harave VS, Shivakumar V, Kalmady SV, Narayanaswamy JC, Varambally S, Venkatasubramanian G. Neurocognitive impairments in unaffected first-degree relatives of schizophrenia. *Indian J Psychol Med*. (2017) 39:250–3. doi: 10.4103/0253-7176.207335
45. Lutkenhoff ES, van Erp TG, Thomas MA, Therman S, Manninen M, Huttunen MO, et al. Proton MRS in twin pairs discordant for schizophrenia. *Mol Psychiatry*. (2010) 15:308–18. doi: 10.1038/mp.2008.87
46. Tibbo P, Hanstock C, Valiakalayil A, Allen P. 3-T proton MRS investigation of glutamate and glutamine in adolescents at high genetic risk for schizophrenia. *Am J Psychiatry*. (2004) 161:1116–8. doi: 10.1176/appi.ajp.161.6.1116
47. de la Fuente-Sandoval C, Leon-Ortiz P, Azcarraga M, Favila R, Stephano S, Graff-Guerrero A. Striatal glutamate and the conversion to psychosis: a prospective 1H-MRS imaging study. *Int J Neuropsychopharmacol*. (2013) 16:471–5. doi: 10.1017/S1461145712000314
48. Theberge J, Bartha R, Drost DJ, Menon RS, Malla A, Takhar J, et al. Glutamate and glutamine measured with 4.0 T proton MRS in never-treated patients with schizophrenia and healthy volunteers. *Am J Psychiatry*. (2002) 159:1944–6. doi: 10.1176/appi.ajp.159.11.1944
49. Overall JE, Gorham DR. The brief psychiatric rating scale. *Psychol Rep*. (1962) 10:799–812. doi: 10.2466/pr0.1962.10.3.799
50. Kirkpatrick B, Strauss GP, Nguyen L, Fischer BA, Daniel DG, Cienfuegos A, et al. The brief negative symptom scale: psychometric properties. *Schizophr Bull*. (2011) 37:300–5. doi: 10.1093/schbul/sbq059
51. Patterson TL, Goldman S, McKibbin CL, Hughs T, Jeste DV. UCSD Performance-Based Skills Assessment: development of a new measure of everyday functioning for severely mentally ill adults. *Schizophr Bull*. (2001) 27:235–45. doi: 10.1093/oxfordjournals.schbul.a006870
52. Mucci A, Rucci P, Rocca P, Bucci P, Gibertoni D, Merlotti E, et al. The Specific Level of Functioning Scale: construct validity, internal consistency and factor structure in a large Italian sample of people with schizophrenia living in the community. *Schizophr Res*. (2014) 159:144–50. doi: 10.1016/j.schres.2014.07.044
53. Nuechterlein KH, Green MF, Kern RS, Baade LE, Barch DM, Cohen JD, et al. The MATRICS Consensus Cognitive Battery, part 1: test selection, reliability, and validity. *Am J Psychiatry*. (2008) 165:203–13. doi: 10.1176/appi.ajp.2007.07010042
54. Kern RS, Nuechterlein KH, Green MF, Baade LE, Fenton WS, Gold JM, et al. The MATRICS Consensus Cognitive Battery, part 2: co-norming and standardization. *Am J Psychiatry*. (2008) 165:214–20. doi: 10.1176/appi.ajp.2007.07010043
55. Tkac I, Starcuk Z, Choi IY, Gruetter R. *In vivo* 1H NMR spectroscopy of rat brain at 1 ms echo time. *Magn Reson Med*. (1999) 41:649–56
56. Gruetter R. Automatic, localized in vivo adjustment of all first- and second-order shim coils. *Magn Reson Med*. (1993) 29:804–11. doi: 10.1002/mrm.1910290613

57. Versluis MJ, Kan HE, van Buchem MA, Webb AG. Improved signal to noise in proton spectroscopy of the human calf muscle at 7 T using localized B1 calibration. *Magn Reson Med*. (2010) 63:207–11. doi: 10.1002/mrm.22195
58. Provencher SW. Estimation of metabolite concentrations from localized in vivo proton NMR spectra. *Magn Reson Med*. (1993) 30:672–9. doi: 10.1002/mrm.1910300604
59. Soher BJ, Young K, Bernstein A, Aygula Z, Maudsley AA. GAVA: spectral simulation for *in vivo* MRS applications. *J Magn Reson*. (2007) 185:291–9. doi: 10.1016/j.jmr.2007.01.005
60. Govindaraju V, Young K, Maudsley AA. Proton NMR chemical shifts and coupling constants for brain metabolites. *NMR Biomed*. (2000) 13:129–53. doi: 10.1002/1099-1492(200005)13:3<129::aid-nbm619>3.0.co;2-v
61. Murrough JW, Mao X, Collins KA, Kelly C, Andrade G, Nestadt P, et al. Increased ventricular lactate in chronic fatigue syndrome measured by 1H MRS imaging at 3.0 T. II: comparison with major depressive disorder. *NMR Biomed*. (2010) 23:643–50. doi: 10.1002/nbm.1512
62. Nagae-Poetscher LM, McMahon M, Braverman N, Lawrie WT Jr, Fatemi A, Degaonkar M, et al. Metabolites in ventricular cerebrospinal fluid detected by proton magnetic resonance spectroscopic imaging. *J Magn Reson Imaging*. (2004) 20:496–500. doi: 10.1002/jmri.20128
63. Kristiansen LV, Beneyto M, Haroutunian V, Meador-Woodruff JH. Changes in NMDA receptor subunits and interacting PSD proteins in dorsolateral prefrontal and anterior cingulate cortex indicate abnormal regional expression in schizophrenia. *Mol Psychiatry*. (2006) 11:737–47. doi: 10.1038/sj.mp.4001844
64. Wijtenburg SA, Wright SN, Korenic SA, Gaston FE, Ndubuizu N, Chiappelli J, et al. Altered glutamate and regional cerebral blood flow levels in schizophrenia: A (1)H-MRS and pCASL study. *Neuropsychopharmacology*. (2017) 42:562–71. doi: 10.1038/npp.2016.172
65. Baiano M, David A, Versace A, Churchill R, Balestrieri M, Brambilla P. Anterior cingulate volumes in schizophrenia: a systematic review and a meta-analysis of MRI studies. *Schizophr Res*. (2007) 93:1–12. doi: 10.1016/j.schres.2007.02.012
66. Quintana J, Wong T, Ortiz-Portillo E, Marder SR, Mazziotta JC. Anterior cingulate dysfunction during choice anticipation in schizophrenia. *Psychiatry Res*. (2004) 132:117–30. doi: 10.1016/j.pscychresns.2004.06.005
67. Kerns JG, Cohen JD, MacDonald AW, III, Johnson MK, Stenger VA, Aizenstein H, et al. Decreased conflict- and error-related activity in the anterior cingulate cortex in subjects with schizophrenia. *Am J Psychiatry*. (2005) 162:1833–9. doi: 10.1176/appi.ajp.162.10.1833
68. Lewis DA, Glantz LA, Pierri JN, Sweet RA. Altered cortical glutamate neurotransmission in schizophrenia: evidence from morphological studies of pyramidal neurons. *Ann N Y Acad Sci*. (2003) 1003:102–12. doi: 10.1196/annals.1300.007
69. Bustillo JR, Chen H, Jones T, Lemke N, Abbott C, Qualls C, et al. Increased glutamine in patients undergoing long-term treatment for schizophrenia: a proton magnetic resonance spectroscopy study at 3 T. *JAMA Psychiatry*. (2014) 71:265–72. doi: 10.1001/jamapsychiatry.2013.3939
70. de Jonge JC, Vinkers CH, Hulshoff Pol HE, Marsman A. GABAergic Mechanisms in schizophrenia: linking postmortem and *in vivo* studies. *Front Psychiatry*. (2017) 8:118. doi: 10.3389/fpsyt.2017.00118
71. Beech A, Powell T, McWilliam J, Claridge G. Evidence of reduced 'cognitive inhibition' in schizophrenia. *Br J Clin Psychol*. (1989) 28:109–16. doi: 10.1111/j.2044-8260.1989.tb00821.x
72. Sullivan CR, Mielnik CA, Funk A, O'Donovan SM, Bentea E, Pletnikov M, et al. Measurement of lactate levels in postmortem brain, iPSCs, and animal models of schizophrenia. *Sci Rep*. (2019) 9:5087. doi: 10.1038/s41598-019-41572-9
73. Fukushima T, Iizuka H, Yokota A, Suzuki T, Ohno C, Kono Y, et al. Quantitative analyses of schizophrenia-associated metabolites in serum: serum D-lactate levels are negatively correlated with gamma-glutamylcysteine in medicated schizophrenia patients. *PLoS ONE*. (2014) 9:e101652. doi: 10.1371/journal.pone.0101652
74. Da Silva T, Wu A, Laksono I, Prce I, Maheandiran M, Kiang M, et al. Mitochondrial function in individuals at clinical high risk for psychosis. *Sci Rep*. (2018) 8:6216. doi: 10.1038/s41598-018-24355-6
75. Wu CH, Hwang TJ, Chen YJ, Hsu YC, Lo YC, Liu CM, et al. Primary and secondary alterations of white matter connectivity in schizophrenia: a study on first-episode and chronic patients using whole-brain tractography-based analysis. *Schizophr Res*. (2015) 169:54–61. doi: 10.1016/j.schres.2015.09.023
76. Kreis R, Farrow N, Ross BD. Localized 1H NMR spectroscopy in patients with chronic hepatic encephalopathy. Analysis of changes in cerebral glutamine, choline and inositols. *NMR Biomed*. (1991) 4:109–16. doi: 10.1002/nbm.1940040214

Conflict of Interest: LR received consulting fees from Otsuka America Pharmaceutical, Inc for educational purposes only for the platform PsychU.

The remaining authors declare that the research was conducted in the absence of any commercial or financial relationships that could be construed as a potential conflict of interest.

frontiers in Psychiatry

ORIGINAL RESEARCH
published: 07 June 2021
doi: 10.3389/fpsyt.2021.660850

Increased Glutamate Plus Glutamine in the Right Middle Cingulate in Early Schizophrenia but Not in Bipolar Psychosis: A Whole Brain ^{1}H-MRS Study

Juan R. Bustillo[1], Elizabeth G. Mayer[1], Joel Upston[1,2], Thomas Jones[1], Crystal Garcia[1], Sulaiman Sheriff[3], Andrew Maudsley[3], Mauricio Tohen[1], Charles Gasparovic[4] and Rhoshel Lenroot[1]*

[1] Department of Psychiatry and Behavioral Sciences, University of New Mexico, Albuquerque, NM, United States, [2] Department of Mathematics and Statistics, University of New Mexico, Albuquerque, NM, United States, [3] Department of Radiology, University of Miami, Miami, FL, United States, [4] Mind Research Network, Albuquerque, NM, United States

Proton magnetic resonance spectroscopy (^{1}H-MRS) studies have examined glutamatergic abnormalities in schizophrenia and bipolar-I disorders, mostly in single voxels. Though the critical nodes remain unknown, schizophrenia and bipolar-I involve brain networks with broad abnormalities. To provide insight on the biochemical differences that may underlie these networks, the combined glutamine and glutamate signal (Glx) and other metabolites were examined in patients in early psychosis with whole brain ^{1}H-MRS imaging (^{1}H-MRSI). Data were acquired in young schizophrenia subjects ($N = 48$), bipolar-I subjects ($N = 21$) and healthy controls ($N = 51$). Group contrasts for Glx, as well as for N-acetyl aspartate, choline, myo-inositol and creatine, from all voxels that met spectral quality criteria were analyzed in standardized brain space, followed by cluster-corrected level alpha-value (CCLAV $\leq$ 0.05) analysis. Schizophrenia subjects had higher Glx in the right middle cingulate gyrus (19 voxels, CCLAV = 0.05) than bipolar-I subjects. Healthy controls had intermediate Glx values, though not significant. Schizophrenia subjects also had higher N-acetyl aspartate (three clusters, left occipital, left frontal, right frontal), choline (two clusters, left and right frontal) and myo-inositol (one cluster, left frontal) than bipolar-I, with healthy controls having intermediate values. These increases were likely accounted for by antipsychotic medication effects in the schizophrenia subgroup for N-acetyl aspartate and choline. Likewise, creatine was increased in two clusters in treated vs. antipsychotic-naïve schizophrenia, supporting a medication effect. Conversely, the increments in Glx in right cingulate were not driven by antipsychotic medication exposure. We conclude that increments in Glx in the cingulate may be critical to the pathophysiology of schizophrenia and are consistent with the NMDA hypo-function model. This model however may be more specific to schizophrenia than to psychosis in general. Postmortem and neuromodulation schizophrenia studies focusing on right cingulate, may provide critical mechanistic and therapeutic advancements, respectively.

Keywords: glutamate, choline, N-acetyl-aspartate, creatine, spectroscopy, psychosis, schizophrenia, bipolar

OPEN ACCESS

Edited by:
Marcio Gerhardt Soeiro-De-Souza, University of São Paulo, Brazil

Reviewed by:
Gabriele Ende, University of Heidelberg, Germany
Kim M. Cecil, Cincinnati Children's Hospital Medical Center, United States

****Correspondence:***
Juan R. Bustillo
jbustillo@salud.unm.edu

Specialty section:
This article was submitted to Neuroimaging and Stimulation, a section of the journal Frontiers in Psychiatry

Received: *29 January 2021*
Accepted: *19 April 2021*
Published: *07 June 2021*

Citation:
Bustillo JR, Mayer EG, Upston J, Jones T, Garcia C, Sheriff S, Maudsley A, Tohen M, Gasparovic C and Lenroot R (2021) Increased Glutamate Plus Glutamine in the Right Middle Cingulate in Early Schizophrenia but Not in Bipolar Psychosis: A Whole Brain ^{1}H-MRS Study. Front. Psychiatry 12:660850. doi: 10.3389/fpsyt.2021.660850

INTRODUCTION

The N-methyl-D-aspartate receptor (NMDAR) hypo-function model of psychosis originated from pharmacological studies documenting the emergence of positive and negative symptoms as well as cognitive deficits in healthy volunteers exposed acutely to the NMDAR blocker ketamine (1). Also, acute systemic NMDAR blockers in the awake rat lead to an increase in frontal extracellular glutamate (1). Consistent with these findings, a single ketamine infusion in healthy controls (HC) results in an increase in the combined glutamate and glutamine signal (Glx) (2) in medial frontal cortex, as measured with proton magnetic resonance spectroscopy (^{1}H-MRS). This paradoxical increase in glutamate release with NMDAR blockers has been postulated to result from higher sensitivity of NMDAR receptors in GABAergic interneurons than in pyramidal neurons, leading to disinhibition of pyramidal neurons (1).

Schizophrenia studies using single-voxel ^{1}H-MRS suggest glutamate increases in "basal ganglia" (3) though more recent studies at 7T in early antipsychotic-treated psychosis found prefrontal glutamate reductions (4, 5). Furthermore, never-treated schizophrenia patients had no glutamate differences relative to healthy control subjects in dorsal anterior cingulate (6), but increases have been documented in the dorsal striatum in this population (7). Like schizophrenia, bipolar-I is a chronic, neurodevelopmental disorder, often presents with psychotic symptoms, and is commonly treated with antipsychotic medications (8). Several ^{1}H-MRS studies have reported increased glutamatergic measures in bipolar-I (9) [but see (10)]. Hence, the literature on ^{1}H-MRS-measured glutamate in psychotic disorders is far from clear, with region of interest, medication status, chronicity and co-morbidity as possible confounders. To partially address some of these issues, a few direct comparisons between bipolar-I and schizophrenia have been implemented. Two of these used single-voxel ^{1}H-MRS and did not ascertain a history of psychosis in the bipolar-I sample (11, 12). Our previous study used single slice spectroscopic imaging and involved mainly chronic patients, all with history of psychosis (13). However, none of these three studies found glutamatergic differences between the two clinical groups.

Schizophrenia and bipolar-I are disorders that likely involve distributed brain networks and subtle global brain volume reductions (generally greater in schizophrenia than bipolar-I) have been repeatedly documented (14). Three-dimensional proton MR spectroscopic imaging (3D ^{1}H-MRSI) enables measurement in much larger brain regions, thereby reducing the bias of voxel selection intrinsic to single-voxel studies. Using 3D ^{1}H-MRSI with a short echo time (TE) and a voxel-wide approach, we recently reported reduced Glx in the left superior temporal gyrus (STG) in early schizophrenia vs. healthy control subjects as well as more widespread creatine increases in antipsychotic treated schizophrenia (15).

Here we report the use of the same imaging tool to compare Glx and other metabolites of interest in early schizophrenia vs. early bipolar-I disorder with psychotic features. Healthy control subjects (HC) were also examined to assist in interpretation. We include the schizophrenia (N = 36) and HC (N = 29) subjects' data previously reported plus an additional sample of schizophrenia, HC, and bipolar-I subjects. Consistent with our previous findings we expected Glx reductions in STG in schizophrenia (15) but not in bipolar-I. We also hypothesized higher creatine in antipsychotic-treated vs. antipsychotic-naïve schizophrenia (15).

METHODS AND MATERIALS

Subjects

Schizophrenia (Sz) and bipolar-I (BP-I) subjects were recruited from the University of New Mexico Hospitals (UNMH). Inclusion criteria were: (1) Schizophrenia, schizophreniform, schizoaffective or bipolar-I disorder with psychotic features made using the SCID-DSM-5; (2) Age between 16 and 40. Exclusion criteria were diagnosis of current substance use disorder (except for nicotine) or a neurological disorder. Healthy controls in the same age range were recruited from the community and excluded if they had: (1) any current DSM-5 disorder (SCID-DSM-5 Non-Patient-Version; except for nicotine use); (2) history of neurological disorder; or (3) first-degree relatives with any psychotic disorder. The UNMH Institutional Review Board approved the study and all subjects provided written informed consent and were reimbursed for their participation. Forty-eight Sz, 21 BP-I, and 51 HCs participated.

Clinical and Neuropsychological Assessments

Cognitive function was assessed in clinical and HC groups using the Measurement-and-Treatment-Research-to-Improve-Cognition-in-Schizophrenia (MATRICS) battery (11). Patients were assessed for psychopathology with the Positive-and Negative-Syndrome-Scale (16), the Young-Mania-Rating-Scale (17), and the Calgary-Depression-Scale (18). Patients were also evaluated for extra-pyramidal side-effects with the Abnormal-Involuntary-Movements-Scale (19), Simpson-Angus-Scale for Parkinsonism (20), and the Barnes-Akathisia-Scale (21). These assessments were completed within 1 week of the scan acquisition.

Magnetic Resonance Studies

Acquisition

Subjects underwent an MR study at 3T using a Siemens TIM Trio scanner as previously described (15). 3D ^{1}H-MRSI was acquired using an echo-planar-spectroscopic-imaging (EPSI) sequence with the following parameters: TE = 17.6 ms, TR = 1,551 ms, TR (H_2O) = 511 ms, non-selective lipid inversion nulling with TI = 198 ms, FOV = 280 × 280 × 180 mm, voxel size of 5.6 × 5.6 × 10 mm, echo train length of 1,000 points, bandwidth of 2,500 Hz, reduced k-space sampling (acceleration factor = 0.7), a nominal voxel volume of 0.313 cm^3 and acquisition time of 17 min (15). EPSI included a water reference measurement that was interleaved with the metabolite signal acquisition. The data processing pipeline has been fully described (15) and is briefly summarized below.

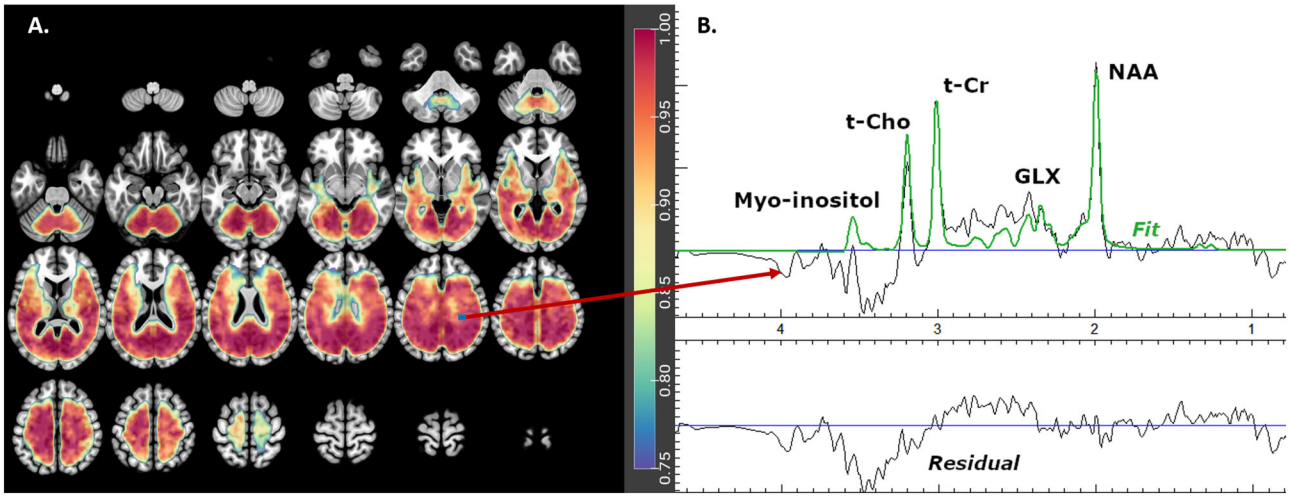

FIGURE 1 | Glx mask showing **(A)** axial brain slices with useful spectral coverage (color grading from blue- [0.75 coverage in each group] to red- [1.0 coverage in each group]) and **(B)** example of one fitted spectrum. Glx is glutamate plus glutamine, NAA is N-acetyl-aspartate compounds, t-Cho is choline, glycerol-phospho-choline, and phosphocholine and t-Cr is creatine plus phospho-creatine.

Reconstruction and Registration

EPSI reconstruction and analysis was carried out using the MIDAS package (22). Processing included corrections for B_0 shifts, generation of white-matter, gray-matter, and CSF tissue segmentation maps using FMRIB Software Library (FSL) FAST (https://fsl.fmrib.ox.ac.uk/fsl/fslwiki/), lipid k-space extrapolation and linear registration of the T_1-weighted MR images to the EPSI images. Metabolite maps were interpolated to 64 × 64 × 32 points (voxel size 4.375 × 4.375 × 5.625 mm). Following spatial smoothing the effective voxel volume was 1.55 cm^3. EPSI water reference measurement was spatially registered to the MPRAGE T_1-weighted image.

Spectral Fitting

The fitted metabolite values from the spectra were estimated using MIDAS and spectral analysis was carried out using the FITT2 program for: Glx, N-acetyl-aspartate compounds (NAA), total creatine (creatine and phosphocreatine, denoted t-Cr), total choline (choline, glycerol-phosphocholine, and phosphocholine, denoted t-Cho), and myo-inositol (**Figure 1**). Individual metabolite maps were normalized and corrected for any bias field variations using the signal from the water reference measurement corrected for tissue water density from literature values. These values were not corrected for relaxation rates and represent institutional units.

Warping and Quality Filtering

The metabolite maps were exported from MIDAS and warped using Statistical Parametric Mapping-8 (SPM8; https://www.fil.ion.ucl.ac.uk/spm/software/spm8/) to the Montreal Neurological Institute (MNI) space (http://brainmap.org/training/BrettTransform.html), keeping the interpolated voxel size, so that group analysis could be performed. Subsequently, to correct for partial volume effects, the metabolite maps values are divided by $1\text{-}f_{CSF}$ at the voxel level. For spectral quality, the metabolite maps were filtered according to three criteria: overall line widths = 2–12 Hz; specific spectral fits for each metabolite of Cramér–Rao lower bound (CRLB) = 1–20%; and $f_{CSF} \leq 0.3$ (these were labeled *best spectra*). Spectra that failed to meet these criteria were divided into two groups, *poor* and *intermediate* spectra. *Intermediate spectra* met the following criteria: linewidths >1 and less than or =16; CRLB = 1–99%; $f_{CSF} \leq 0.3$; and at least 18 of the 26 nearest neighboring voxels were *best spectra*. *Intermediate spectra* were considered to have some potential useful spectral information and hence their metabolite values were kept. All others were considered *poor spectra* and their metabolite values were discarded.

Metabolite Group Mask

These masks (one for each metabolite) included only the *best* and *intermediate spectra* voxels that were present in ≥ 75% of subjects in each diagnostic group (**Figure 1**). The masks were then smoothed using a spatially stationary Gaussian filter with a kernel width of 10mm in SPM12 to minimize potential spatial warping errors.

Imputation

Since up to 25% of subjects in each diagnostic group may not have a particular voxel value in the metabolite group mask after filtering out voxels according to the above quality criteria, the metabolite values for the *poor spectra* voxels were imputed using the diagnostic group (Sz, BP-I, HC) mean concentration for that voxel. This allowed us to preserve the maximum number of voxels possible for the analysis, without adding variability to the populations' metabolite concentrations. Imputations only

TABLE 1 | Demographic and clinical characteristics.

	Healthy controls (*N* = 51)	Schizophrenia (*N* = 48)	Bipolar-I (*N* = 21)
(Mean ± SD or %)			
Age (years)	23.7 ± 4.2	22.4 ± 3.9	22.2 ± 3.1
Gender (male/female)	57/43%	71/29%	57/43%
Race (Caucasian/Native/Other)	80/8/12%	85/4/11%	95/5/0%
SES[a]	4.1 ± 1.4*	6.2 ± 1.4	5.8 ± 1.3
Familial SES	3.6 ± 1.7	4.2 ± 1.8	3.7 ± 1.7
Vascular risk score[b]	0.02 ± 0.14	0.06 ± 0.2	0.19 ± 0.5
MATRICS-overall T score	48.2 ± 7.1*	31.50 ± 11.7	34.7 ± 11.9
Smoker (yes/no)	2/98%*	10/90%	19/81%
Alcohol (yes/no)	5/95%	12/86%	14/86%
Cannabis (yes/no)	0/100%*	52/48%	57/43%
Stimulant (yes/no)	0/100%	4/96%	5/95%
Opioid (yes/no)	0/100%	2/98%	10/90%
Phencyclidine (yes/no)	0/100%	4/96%	10/90%
Hallucinogens (yes/no)	0/100%	0/100%	0/100%
Sedative (yes/no)	0/100%	0/100%	0/100%
Inhalants (yes/no)	0/100%	0/100%	0/100%
Psychosis onset (years)	-	20.2 ± 4.4	21.1 ± 4.2
Positive symptoms	-	16.0 ± 5.0	14.5 ± 6.6
Negative symptoms	-	16.3 ± 5.2	12.6 ± 5.3^
Manic symptoms	-	2.2 ± 3.8	9.4 ± 11.1^
Depressive symptoms	-	2.8 ± 3.9	3.7 ± 3.5
Parkinsonism	-	8.1 ± 0.4	8.2 ± 0.9
Akathisia	-	0.5 ± 1.0	0.5 ± 1.6
Tardive dyskinesia	-	7.0 ± 0.0	7.0 ± 0.0
Antipsychotic use (yes/no)	-	62/38%	60/40%
Antipsychotic dose (mg)[c]	-	6.3 ± 7.0	4.7 ± 5.9%

[a]*SES is Socioeconomic Status.* [b]*Vascular risk score, 0–4 (score of 1 each for cardiac illness, hypertension, dyslipidemia and diabetes).* [c]*Antipsychotic dose, as olanzapine equivalents (25).*
Smoker refers to current use. Alcohol, cannabis, stimulant, opioid, phencyclidine, hallucinogens, sedative, inhalants, refer to past substance use disorder per SCID-5.
**p ≤ 0.05 for healthy controls vs. schizophrenia or bipolar-I.*
^*p ≤ 0.05 for schizophrenia vs. bipolar-I.*

accounted for an average of between 2 and 7% of the total spectra in each metabolite group mask.

Statistical Analyses

The principal analyses examined diagnostic group (Sz vs. BP-I) differences separately for each of the five metabolites of interest. Adjustments were made for age at a subject level and for gray matter proportion [GM/(GM+WM)] at the voxel level. These two factors have large effects on metabolite's variability (23). Analysis of Functional NeuroImages [AFNI's; (24)] *3dttest++*, *3dclust* and *3dClustSim* packages were used because they support both subject and voxel-level covariates (24). *3dClustSim* computed cluster-size thresholds using 10,000 simulated noise-only *t*-tests for a more accurate spatial autocorrelation function

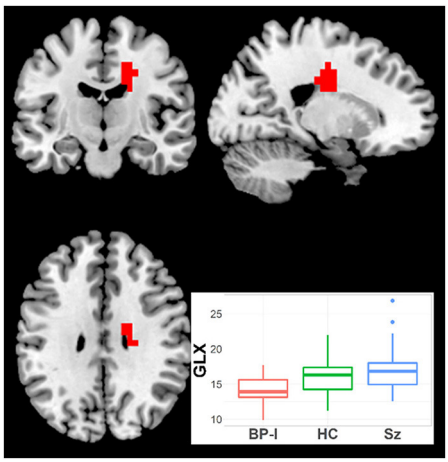

FIGURE 2 | Increased Glx in Schizophrenia (Sz) vs. Bipolar-I (BP) (healthy controls [HC] intermediate) in one cluster (19 voxels), CCLAV = 0.05, including the right cingulate gyrus (60.3%). Boxplot shows weighted-average Glx cluster concentrations in institutional units.

of the noise. It estimated the probability of false positive clusters and then corrected the voxel threshold to reduce the likelihood of false positive clusters. With *3dttest++*, voxel-wise Student t-tests were implemented for all voxels that fell within the supported quality group mask. The resulting maps were clustered using *3dclust* following three criteria: (1) each voxel differed between the groups with $p \leq 0.001$; (2) group differences for each voxel in the cluster were in the same direction; and (3) voxels had faces-touching. The corrected clustering thresholds from *ClustSim* were compared to the number of voxels clustered in *3dclust* to insure the cluster met a corrected cluster-level alpha-value (CCLAV) of ≤0.05. Lastly, Kendall's *Tau* (τ) tested correlations between the gray matter proportion-weighted average concentrations for clusters that differed between groups and clinical and cognitive assessments.

RESULTS

Demographic and Clinical Variables

Subjects were similarly aged, with no significant differences in gender, race, parental socioeconomic status (SES), cardiovascular risk, or history of substance use disorders, except for cannabis and current smoking (**Table 1**). Sz and BP-I had greater history of cannabis use disorder ($p < 0.001$) and current smoking ($p = 0.03$) as well as worse personal SES ($p < 0.001$) and MATRICS overall t-scores ($p < 0.001$) than HCs. The psychosis groups were similarly young (Sz age = 22.4, BP-I = 22.2) and early in the illness (Sz onset = 20.2, BP-I = 21.1). The two groups did not differ in any demographic measures, substance use history, positive or depressive symptoms, proportion of antipsychotic-naïve subjects or antipsychotic dose. Sz subjects had greater negative ($p = 0.009$) and lower manic symptoms ($p < 0.001$) than BP-I subjects.

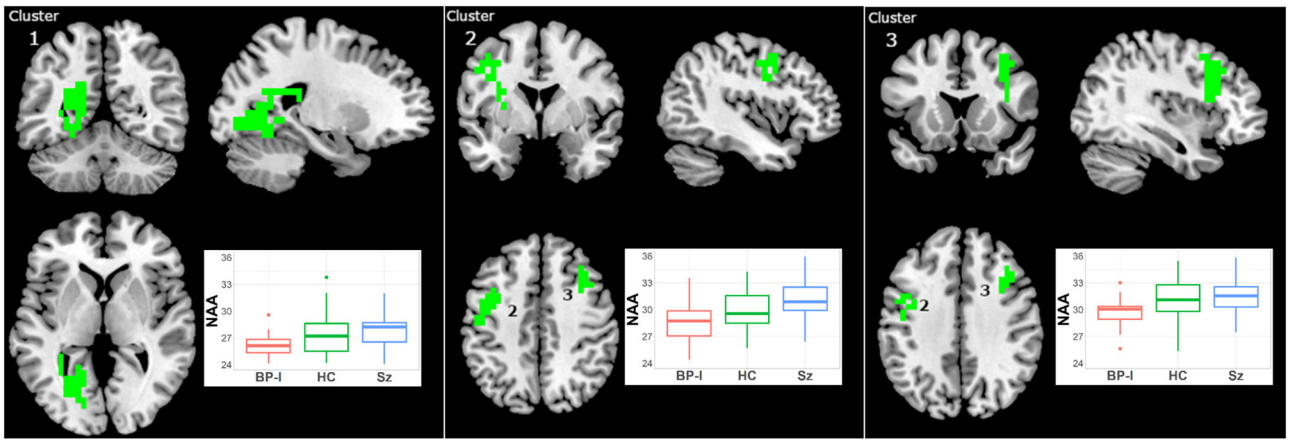

FIGURE 3 | Increased NAA in Schizophrenia (Sz) vs. Bipolar-I (BP) (healthy controls [HC] intermediate) in three clusters: (1) 114 voxels, CCLAV < 0.01, including the left lingual gyrus (29.9%) and left posterior cingulate (13.0%). (2) 61 voxels, CCLAV < 0.01, including the left precentral gyrus (34.7%%) and left middle frontal gyrus (22.1%). (3) 42 voxels, CCLAV = 0.05, including the right middle frontal gyrus (60.6%) and right precentral gyrus (10.2%). Boxplots shows weighted-average NAA cluster concentrations in institutional units.

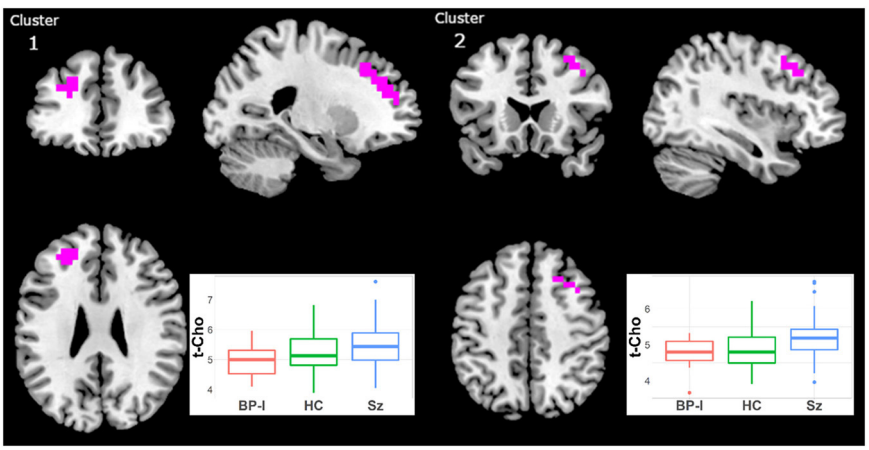

FIGURE 4 | Increased t-Cho in Schizophrenia (Sz) vs. Bipolar-I (BP) (healthy controls [HC] intermediate) in two clusters: (1) 40 voxels, CCLAV = 0.02, including the left superior frontal gyrus (47.3%) and left middle frontal gyrus (39.2%). (2) 29 voxels, CCLAV = 0.03, including the right middle frontal gyrus (47.3%) and the right superior frontal gyrus (14.6%). Boxplots shows weighted-average t-Cho cluster concentrations in institutional units.

Effect of Diagnosis: Sz vs. BP-I Group Differences in Neurometabolites

Glutamate ± Glutamine

One cluster (19 voxels) had higher Glx in Sz vs. BP-I's (CCLAV = 0.05; mainly in right middle cingulate gyrus (**Figure 2**, **Supplementary Table 1**). In this cluster, the HC group had values intermediate, but not significantly different from the clinical groups. Because BP-I subjects had slightly higher Glx CRLB than Sz (**Supplementary Table 3**), we co-varied for CRLB in the AFNI analysis. The significant Glx cluster (still Sz > BP-I) completely overlapped with the original 19 voxel cluster, but it increased in size to 44 voxels. Finally, within Sz, the antipsychotic-naïve subgroup tended to have higher Glx than the treated patients (though not significantly); this pattern was not present in the BP group (**Supplementary Figure 1**). The hypothesized left STG Glx reduction was not observed in Sz relative to BP-I or in Sz relative to HCs with CCLAV ≤ 0.05. When a more lenient statistical test focusing on the left STG cluster previously reported (15) was further explored, only 3/19 voxels had lower Glx ($p < 0.01$) in Sz vs. HC.

N-acetyl Aspartate

NAA was higher in Sz vs. BP-I in three clusters (**Figure 3**, **Supplementary Table 1**): (1) left occipital (114 voxels; CCLAV < 0.01); (2) left frontal (61 voxels; CCLAV ≤ 0.01); and (3) right frontal (42 voxels; CCLAV = 0.05). The HC group had values intermediate (not significant) to those of the clinical groups. Because in the first cluster BP-I subjects had slightly

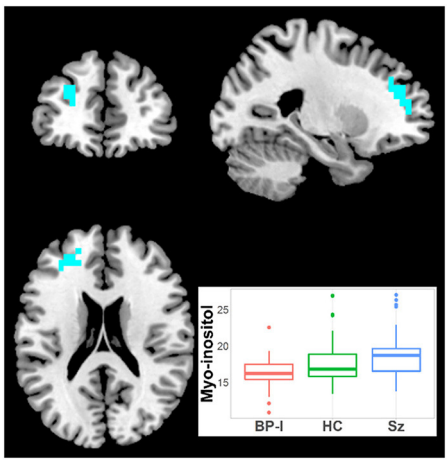

FIGURE 5 | Increased inositol in Schizophrenia (Sz) vs. Bipolar-I (BP) (healthy controls [HC] intermediate) in one cluster (19 voxels), CCLAV = 0.05, including the left superior frontal gyrus (65.7%) and the left middle frontal gyrus (23.1%). Boxplot shows weighted-average inositol cluster concentrations in institutional units.

higher NAA CRLB than Sz (**Supplementary Table 3**), we co-varied for CRLB. The significant NAA cluster 1 (still Sz > BP-I) completely overlapped with the original 114 voxel cluster, but it increased in size to 274 voxels. In all three clusters, for each of the Sz and the BP-I groups, the treated subjects had numerically higher NAA values than antipsychotic-naïve subjects (**Supplementary Figures 2a–c**).

Total Choline

t-Cho was higher in Sz than in BP-I subjects in two clusters (**Figure 4**, **Supplementary Table 1**): (1) left superior mid-frontal (40 voxels; CCLAV = 0.02); and (2) right superior mid-frontal (29 voxels; CCLAV = 0.03). The HC group had values intermediate (not significant), to those of the clinical groups. In both clusters, for each the Sz and the BP-I groups, the treated subjects had numerically higher t-Cho values than antipsychotic-naïve subjects (**Supplementary Figures 3a,b**).

Myo-Inositol

Myo-inositol was higher in Sz vs. BP-I subjects in one left superior frontal cluster (27 voxels; CCLAV = 0.03; **Figure 5**). The HCs had intermediate (not significant) metabolite values to those in Sz and BP-I. Amongst the BP-I group, medicated subjects tended to have numerically higher myo-inositol than naïve subjects (**Supplementary Figure 4**). Finally, there were no differences between Sz and BP-I in t-Cr.

Antipsychotic Medication Effects: Antipsychotic-Naïve vs. Treated Patients

Total-Creatine

Because we previously detected higher t-Cr in treated Sz relative to HC in three clusters (15) but not in antipsychotic-naïve Sz vs. HCs, we examined in our largest patient sample (i.e., Sz) the effect of antipsychotic medication. Hence, we compared the treated (N = 29) and naïve (N = 19) Sz subgroups. t-Cr was higher in two clusters in treated patients (**Figure 6**, **Supplementary Table 2**): (1) left Para hippocampal (34 voxels; CCLAV = 0.02); and (2) right occipital (27 voxels; CCLAV = 0.03). There were no significant differences between the naïve and treated BP-I subgroups, but the samples were small (N = 8 and N = 13, respectively).

Other Neurometabolites

Because the diagnostic group comparisons suggested effects of antipsychotic medication for Glx, NAA and t-Cho, we compared the Sz naïve and treated subgroups. For NAA there were increments in treated vs. naïve in one left middle frontal cluster (21 voxels; CCLAV = 0.05; **Figure 7**, **Supplementary Table 2**). There was higher t-Cho in treated vs. naïve groups in four clusters: (1) right cerebellar cluster (28 voxels; CCLAV = 0.02); (2) left middle frontal cluster (23 voxels; CCLAV = 0.03; (3) left insula cluster (18 voxels; CCLAV = 0.03; and (4) left Para hippocampal cluster (16 voxels; CCLAV = 0.04; **Figure 8**, **Supplementary Table 2**). There were no significant group differences for Glx. There were no significant differences between the naïve and treated BP-I subgroups.

Symptom and Cognitive Relationships

We examined the correlations between symptoms and cognition with the weighted-average neurochemical concentrations in the clusters that differed between Sz and BP-I (Glx, NAA, t-Cho or myo-inositol; see **Supplementary Figures 5–13**). Both t-Cho clusters correlated positively with negative symptom severity: (1) left superior mid-frontal (τ = 0.26, p = 0.002); and (2) right superior mid-frontal (τ = 0.26, p = 0.002). They also correlated negatively with the MATRICS overall t-score: (1) left superior mid-frontal (τ = −0.24, p = 0.01); and (2) right superior mid-frontal (τ = −0.24, p = 0.01). The one myo-inositol left superior frontal cluster positively correlated with negative symptoms (τ = 0.2, p = 0.02). Finally, the three NAA clusters correlated positively with negative symptom scores: (1) left occipital (τ = 0.23, p = 0.007); (2) left frontal (τ = 0.21, p = 0.01); and (3) right frontal (τ = 0.2, p = 0.01). The left frontal NAA cluster correlated negatively with MATRICS overall t-score (τ = −0.23, p = 0.01). There were no relationships with positive, manic or depressive symptoms.

DISCUSSION

To our knowledge this is the first study to compare Glx as well as the other more commonly measured neurometabolites in early schizophrenia and BP-I with psychotic features with a voxel-wise whole brain spectroscopic imaging approach. Several metabolites were higher in Sz subjects compared to BP-I subjects across various regions. Glx was higher in the right middle cingulate, NAA was higher in the left occipital and bilateral frontal areas of cortex, t-Cho was higher in bilateral frontal cortices and myo-inositol was higher in the left frontal regions. These differences were not due to demographic, clinical or spectral quality metrics (see **Supplementary Tables 3**, **4**). The HC

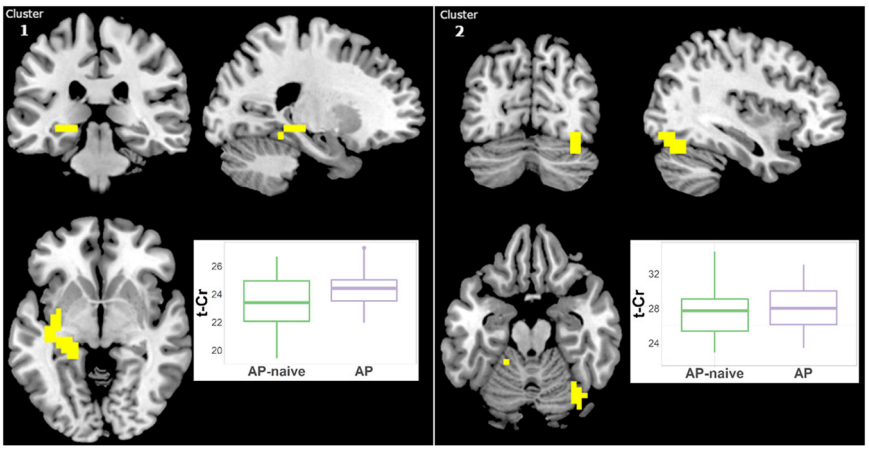

FIGURE 6 | Increased t-Cr in antipsychotic treated (AP) vs. antipsychotic naïve (AP-naive) Schizophrenia in two clusters: (1) 34 voxels (CCLAV = 0.02), including the left parahippocampal gyrus (25.0%) and left culmen (10.5%). (2) 27 voxels, CCLAV = 0.03, including the right declive (51.9%) and the right fusiform gyrus (16.5%). Boxplots show weighted-average t-Cr cluster concentrations in institutional units.

group had intermediate values of these metabolites (though not significantly different) relative to the clinical groups, supporting the view that the two early-psychosis groups may have opposite neurometabolic abnormalities: increases in Sz and reductions in BP-I. Additionally we demonstrated effects of antipsychotic treatment in t-Cr in the Sz group, as previously suggested (15). Likewise, the left frontal increases in NAA and t-Cho at least in part appear to be related to antipsychotic treatment. However, the elevated Glx in the right cingulate in Sz appears to be accounted for mainly by the antipsychotic-naïve subjects. Contrary to our hypothesis, Glx in Sz was not lower in the left STG relative to the other groups.

Three ^{1}H-MRS studies have directly compared chronically-ill Sz and BP-I subjects at magnetic fields >1.5T (3T and 4T). Two used single-voxel ^{1}H-MRS and also did not restrict their sample to BP-I with psychosis (11, 12). In a previous study we used single slice spectroscopic imaging and only included BP-I with history of psychosis (13). None of these three studies found significant glutamatergic differences between Sz and BP-I. Atagun et al. (11) did find higher t-Cr and inositol in the left STG in Sz vs. BP-I. We found some age-related differences with higher NAA and inositol in younger Sz (<40) as well as higher NAA in older Sz relative to older BP-I (13). These results are somewhat consistent with the higher NAA and myo-inositol in early Sz relative to BP-I in the current study.

Increased glutamate, glutamine, and Glx (glutamate + glutamine) in the "basal ganglia" has been reported in one schizophrenia meta-analysis (3). This is consistent with the NMDAR hypo-function pharmacological model of psychosis: acute ketamine induces increased extracellular frontal glutamate in rodents and of ^{1}H-MRS glutamatergic measures in healthy humans (1). Though concentrations of glutamate and glutamine measured with ^{1}H-MRS do not directly assesses synaptic glutamate turnover, it has been proposed that the acute increment in extracellular glutamate in rodents measured with micro-dialysis reflects synaptic function (1). In humans, the largest published ^{1}H-MRS ketamine challenge study reported increased Glx in anterior cingulate in a single-voxel (2). Hence, though less specific, Glx may be a more sensitive ^{1}H-MRS index for the paradoxical effect of higher glutamate observed in acute NMDAR inhibition by ketamine. In the present study, the one cluster with increased Glx in Sz involved a more posterior aspect of the right dorsal cingulate. We note, however, that with the whole-brain ^{1}H-MRSI approach we used, we may have been less able to detect group differences in the ventral and anterior cingulate, due to worse spectral quality in these regions (**Figure 1**). Likewise, the head of the caudate and the anterior thalamus, regions where glutamate increments have been described in antipsychotic-naïve schizophrenia (3), were mostly inaccessible with our approach.

The failure to confirm our previously reported Glx reduction in left STG in early Sz (15) was not due to differences in spectral quality between the original (CRLB = 7.58 ± 1.24) and the added Sz samples (CRLB = 7.07 ± 1.33). Also, the voxel coverage was the same in both groups (16 voxels over left STG). The two samples did differ in the number of antipsychotic-naïve Sz subjects: 57% in the original and 12% in the added samples (**Supplementary Table 5**). A histogram of z-scores of the examined voxels (**Supplementary Figure 14**) shows that the data from the current sample had a greater spread of Sz vs. HC differences, with the added subjects having z-scores around zero (i.e., no group effect). However, examination of the histogram z-scores did not support a greater effect in antipsychotic-naïve vs. HC than in treated Sz vs. HC (**Supplementary Figure 14**).

Results of previous spectroscopic studies examining glutamatergic metabolites are likely to have been affected or limited by antipsychotic medication, chronicity, and the brain region examined. More recent single-voxel studies at 7T in treated early schizophrenia have reported reduced

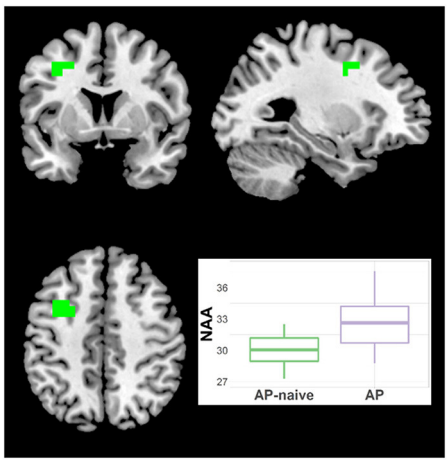

FIGURE 7 | Increased NAA in antipsychotic treated (AP) vs. antipsychotic naïve (AP-naive) Schizophrenia in one cluster: 21 voxels (CCLAV = 0.04), including the left middle frontal gyrus (61.5%%) and left precentral (15.7%). Boxplot shows weighted-average NAA cluster concentrations in institutional units.

glutamate in anterior cingulate (4, 5), suggesting an effect of antipsychotic medication. Consistently, antipsychotic-naïve schizophrenia patients had increased dorsal striatal glutamate, which normalized with prospective risperidone treatment (7). However, a recent study in antipsychotic-naïve schizophrenia failed to detect any differences in anterior cingulate glutamate (6). Furthermore, two 7T studies of the anterior cingulate in chronically-ill patients found glutamate reductions (26, 27). Hence, the inconsistencies in the results of glutamate studies in schizophrenia may be in part due to differences in stage of illness, medication effects and regions of interest with the single-voxel approach. Clearly, psychotic disorders involve multiple distributed brain networks (14) hence, examining glutamatergic measures with an unbiased voxel-wise approach offers advantages for future studies. Though antipsychotic medications may lower glutamate in some regions (7), glutamatergic dysfunction intrinsic to the illness is supported by the report of several glutamate-related risk-conferring genes in in the largest GWAS study in schizophrenia (28). Finally, in terms of diagnostic specificity our results suggest that glutamatergic abnormalities may differ fundamentally in bipolar-I and schizophrenia, with elevations in schizophrenia, consistent with a primary NMDAR hypofunction in GABA-ergic interneurons, and reductions in bipolar-I, suggestive of a different glutamatergic deficit, perhaps of NMDAR dysfunction in pyramidal neurons. However, the Glx differences were not related to symptom severity, like manic or negative symptoms, which suggests a trait effect of diagnosis.

Higher NAA, t-Cho and myo-inositol in Sz relative to BP-I were unexpected findings in the current study. The majority of the literature on schizophrenia reports lower NAA mainly in "basal ganglia" and frontal lobe (29). However, a recent meta-analysis of cross-sectional studies reported progressive, stage of illness-related NAA reductions: only in hippocampus in high-risk subjects; in frontal and thalamic regions in early schizophrenia; and more widespread reductions (frontal, hippocampal, temporal, thalamic and parietal regions) in chronically-ill patients (30). This is consistent with progressive brain volume reductions from multiple longitudinal MRI studies (31). In BP-I, lower NAA in "basal ganglia" has been reported (29). There is no consistent evidence of alterations in t-Cho or t-Cr in either disorder (29). The findings on myo-inositol have been more sparse, but lower concentrations in the medial frontal region was reported in a meta-analysis in schizophrenia (32). However, the great majority of the analyzed data came from single-voxel studies (29, 32). None of the studies included involved whole brain with voxel-wise analyses.

The literature on antipsychotic medication effects on ^{1}H-MRS measures was recently expanded by a meta-analysis of single-voxel longitudinal schizophrenia studies before and after treatment (33). Frontal Glx was found to be reduced and thalamic NAA increased by medication. In this meta-analysis no changes in inositol were found and t-Cho and t-Cr were not examined. However, one study reported increased medial temporal t-Cr and inositol in treated vs. anti-psychotic-naïve schizophrenia, suggesting a medication effect for these metabolites (34).

Antipsychotics clearly have acute metabolic effects with increased subcortical and reduced cortical metabolism (35, 36). In addition, these agents can induce striatal volume expansion in humans as well as cortical volume reductions as early as 12 weeks after treatment (37). In monkeys, antipsychotics induce global gray matter volume reductions (38) with a 14% glial reduction and 10% increase in neuronal density (39). Hence, because NAA is mainly found in neurons (40) [though also reported in immature oligodendrocytes (41)], it is possible that increased neuronal density causes a relative increase in NAA tissue concentration, which could account for the higher NAA findings in the treated early schizophrenia subgroup of the present study. The consistent more widespread NAA reductions reported later in the illness (30) suggest an effect of chronicity, perhaps related to loss of neuropil without gliosis as described in the postmortem literature (42).

We did confirm increased t-Cr in antipsychotic-treated vs. naïve Sz subgroups consistent with our previous report (15). The higher t-Cr with treatment suggests an effect on energy metabolism. A reduction in the forward rate constant of creatine kinase, the enzyme that converts creatine to phosphocreatine, was reported in antipsychotic-treated schizophrenia (43). Hence, the increase in t-Cr may represent an adaptation to the cortical metabolism-lowering effects of antipsychotics (35, 36), by increasing the total pool of creatine available for energetic transfer. Though alterations in t-Cho have not been consistently reported in single-voxel studies of schizophrenia (29), long-term exposure to antipsychotics in monkeys has been reported to result in increased frontal glial density (44) and reduced parietal glial density (39). Because the t-Cho signal represents cell membrane turnover (40), we speculate that the finding of higher t-Cho only in treated vs. naïve schizophrenia patients may

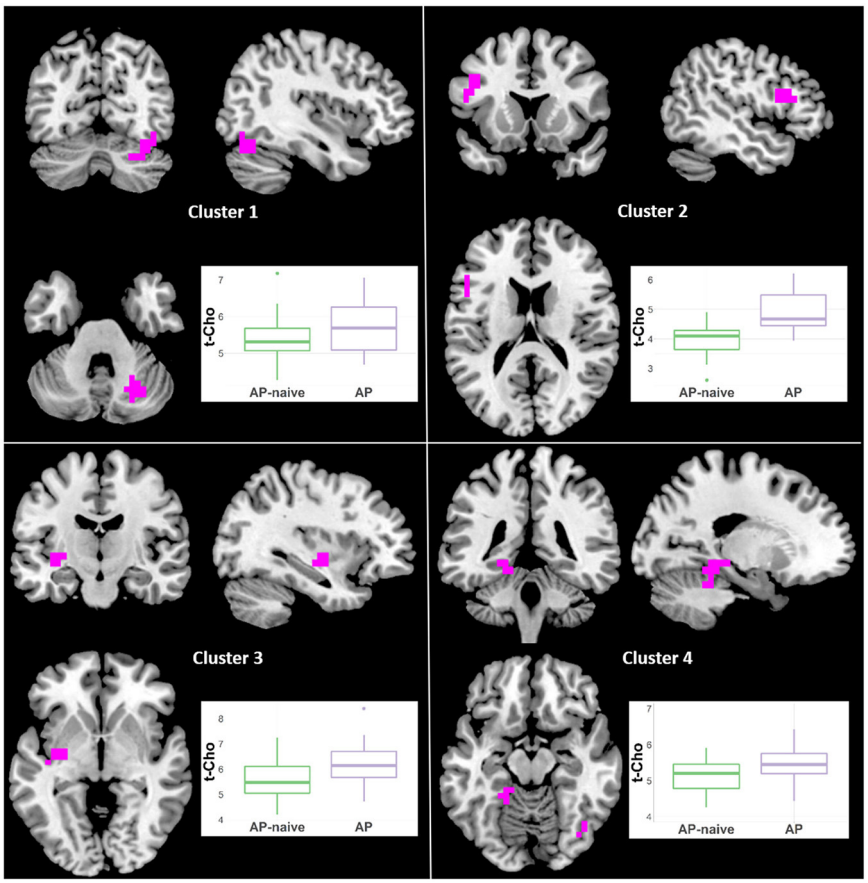

FIGURE 8 | Increased t-Cho in antipsychotic treated (AP) vs. antipsychotic naïve (AP-naive) Schizophrenia in four clusters: (1) 28 voxels; (CCLAV = 0.02), including the right declive (35.6%), right pyramis (19.6%), right tuber (16.3%), and right uvula (11%). (2) 23 voxels; (CCLAV = 0.03), including the left middle frontal gyrus (49.7%), and left inferior frontal gyrus (40%). (3) 18 voxels; (CCLAV = 0.03), including the left insula (21.7%), left claustrum (7.4%) and left lentiform nucleus (7.3%). (4) 16 voxels; (CCLAV = 0.04), including the left parahippocampal gyrus (46.9%), and the left culmen (38.4%).

suggest an adaptive glial response to antipsychotics in frontal cortex bilaterally.

The associations between some of the metabolite clusters that differed between Sz and BP-I and symptoms and cognition (for the whole clinical sample) were not predicted and do not survive multiple comparison correction. However, some intriguing patterns emerged. Mainly in bilateral frontal regions, higher t-Cho correlated with worse negative symptoms and more impaired cognition. Not surprisingly, negative symptoms and cognition were negatively correlated ($\tau = -0.38$, $p < 0.001$). This may suggest that increased frontal glial density (as reflected in higher t-Cho) may result in worsened negative symptoms and cognition in psychosis. However, the similar association between bilateral frontal NAA clusters and negative symptoms is harder to interpret as higher NAA is usually described as an index of improved neuronal viability (40).

This study has several strengths. 3D EPSI allowed examination of most of the brain, including numerous gray and white matter regions known to be affected in schizophrenia and bipolar-I (14). The use of AFNI permitted a voxel-wise approach with false-positive correction, as is standard with other neuroimaging modalities. AFNI also allowed introduction of co-variates at the voxel level, a critical issue in ^{1}H-MRS analyses since the partial volume tissue effects are substantial (23). However, some limitations should be acknowledged. First, the spectral resolution with the current sequence did not allow reliable discrimination of glutamate from glutamine, hence Glx results are presented. Second, though whole brain ^{1}H-MRSI was acquired, greater magnetic field inhomogeneity precluded examination of more ventral regions, such as orbitofrontal and inferior temporal areas. Third, our sample of 21 BP-I is small relative to the other two groups. Finally, as this was a case-control design, mechanistic interpretations are inherently limited.

In summary, this study of early psychosis using voxel-wise examination with 3D ^{1}H-MRSI revealed an increase in glutamate metabolism (Glx) in the right middle cingulate in

schizophrenia but not in bipolar-I. This increase did not appear to be related to antipsychotic treatment or due to other common confounders, such as substance use or chronicity. Also, the metabolite levels of the HC group, were intermediate between those of that Sz and BP-I groups. This suggests that Sz and BP-I may have abnormalities in metabolism that alter glutamate in opposite directions. In other regions explored in the current study, NAA, t-Cho, and myo-inositol were also higher in Sz. This differs in particular with the broad schizophrenia literature of reduced NAA in mainly chronically-ill schizophrenia populations examined with single voxels. However, in our sample medication status appears to account statistically for the higher NAA and t-Cho. Likewise, higher t-Cr appears clearly related to antipsychotic treatment. Replication of these findings would support mechanistic postmortem investigations and therapeutic neuromodulation studies of the right cingulate in schizophrenia.

DATA AVAILABILITY STATEMENT

The raw data supporting the conclusions of this article will be made available by the authors, without undue reservation.

ETHICS STATEMENT

The studies involving human participants were reviewed and approved by Human Research Programs Office, UNM Health Sciences Center. The patients/participants provided their written informed consent to participate in this study.

AUTHOR CONTRIBUTIONS

JB and RL were involved in the design, acquisition, analysis, interpretation of data for the work, drafting, and revising of the manuscript. EM, JU, TJ, and CGar were involved in the analysis, interpretation of data for the work, drafting, and revising of the manuscript. SS, AM, MT, and CGas were involved in the interpretation of data for the work, drafting, and revising of the manuscript. All authors contributed to the article and approved the submitted version.

FUNDING

This work was supported by NIMH R01MH084898 to JB and 1 P20 RR021938-01A1 and DHHS/NIH/NCRR 3 UL1 RR031977-02S2 to RL. The MIDAS software was supported by R01 EB016064 to AM.

ACKNOWLEDGMENTS

We are grateful to Nattida Payaknait and Nicholas Lemke, employees of the UNM Department of Psychiatry and to Diana South and Cathy Smith, MRN employees, for their contributions with data collection.

SUPPLEMENTARY MATERIAL

The Supplementary Material for this article can be found online at: https://www.frontiersin.org/articles/10.3389/fpsyt.2021.660850/full#supplementary-material

REFERENCES

1. Moghaddam B, Javitt D. From revolution to evolution: the glutamate hypothesis of schizophrenia and its implication for treatment. *Neuropsychopharmacology*. (2012) 37:4–15. doi: 10.1038/npp.2011.181
2. Javitt DC, Carter CS, Krystal JH, Kantrowitz JT, Girgis RR, Kegeles LS, et al. Utility of imaging-based biomarkers for glutamate-targeted drug development in psychotic disorders: a randomized clinical trial. *JAMA Psychiatry*. (2018) 75:11–9. doi: 10.1001/jamapsychiatry.2017.3572
3. Merritt K, Egerton A, Kempton MJ, Taylor MJ, McGuire PK. Nature of glutamate alterations in schizophrenia: a meta-analysis of proton magnetic resonance spectroscopy studies. *JAMA Psychiatry*. (2016) 73:665–74. doi: 10.1001/jamapsychiatry.2016.0442
4. Wang AM, Pradhan S, Coughlin JM, Trivedi A, DuBois SL, Crawford JL, et al. Assessing brain metabolism with 7-t proton magnetic resonance spectroscopy in patients with first-episode psychosis. *JAMA Psychiatry*. (2019) 76:314–23. doi: 10.1001/jamapsychiatry.2018.3637
5. Reid MA, Salibi N, White DM, Gawne TJ, Denney TS, Lahti AC. 7T proton magnetic resonance spectroscopy of the anterior cingulate cortex in first-episode schizophrenia. *Schizophr Bull*. (2019) 45:180–9. doi: 10.1093/schbul/sbx190
6. Li J, Ren H, He Y, Li Z, Ma X, Yuan L, et al. Anterior cingulate cortex glutamate levels are related to response to initial antipsychotic treatment in drug-naive first-episode Schizophrenia Patients. *Front Psychiatry*. (2020) 11:553269. doi: 10.3389/fpsyt.2020.553269
7. de la Fuente-Sandoval C, Leon-Ortiz P, Azcarraga M, Stephano S, Favila R, Diaz-Galvis L, et al. Glutamate levels in the associative striatum before and after 4 weeks of antipsychotic treatment in first-episode psychosis: a longitudinal proton magnetic resonance spectroscopy study. *JAMA Psychiatry*. (2013) 70:1057–66. doi: 10.1001/jamapsychiatry.2013.289
8. Birur B, Kraguljac NV, Shelton RC, Lahti AC. Brain structure, function, and neurochemistry in schizophrenia and bipolar disorder-a systematic review of the magnetic resonance neuroimaging literature. *NPJ Schizophrenia*. (2017) 3:15. doi: 10.1038/s41537-017-0013-9
9. Gigante AD, Bond DJ, Lafer B, Lam RW, Young LT, Yatham LN. Brain glutamate levels measured by magnetic resonance spectroscopy in patients with bipolar disorder: a meta-analysis. *Bipolar Disord*. (2012) 14:478–87. doi: 10.1111/j.1399-5618.2012.01033.x
10. Cao B, Stanley JA, Selvaraj S, Mwangi B, Passos IC, Zunta-Soares GB, et al. Evidence of altered membrane phospholipid metabolism in the anterior cingulate cortex and striatum of patients with bipolar disorder I: A multi-voxel (1)H MRS study. *J Psychiatr Res*. (2016) 81:48–55. doi: 10.1016/j.jpsychires.2016.06.006
11. Atagun MI, Sikoglu EM, Can SS, Karakas-Ugurlu G, Ulusoy-Kaymak S, Caykoylu A, et al. Investigation of Heschl's gyrus and planum temporale in patients with schizophrenia and bipolar disorder: a proton magnetic resonance spectroscopy study. *Schizophr Res*. (2015) 161:202–9. doi: 10.1016/j.schres.2014.11.012
12. Ongur D, Jensen JE, Prescot AP, Stork C, Lundy M, Cohen BM, et al. Abnormal glutamatergic neurotransmission and neuronal-glial interactions in acute mania. *Biol Psychiatry*. (2008) 64:718–26. doi: 10.1016/j.biopsych.2008.05.014
13. Bustillo JR, Jones T, Qualls C, Chavez L, Lin D, Lenroot RK, et al. Proton magnetic resonance spectroscopic imaging of gray and white matter in bipolar-I and schizophrenia. *J Affect Disord*. (2019) 246:745–53. doi: 10.1016/j.jad.2018.12.064

14. Thompson PM, Jahanshad N, Ching CRK, Salminen LE, Thomopoulos SI, Bright J, et al. ENIGMA and global neuroscience: a decade of large-scale studies of the brain in health and disease across more than 40 countries. *Transl Psychiatry.* (2020) 10:100. doi: 10.1016/j.biopsych.2020.02.167
15. Bustillo JR, Upston J, Mayer G, Jones T, Maudsley AA, Gasparovic C, et al. Glutamatergic hypo-function in the left superior and middle temporal gyri in early schizophrenia: a data-driven three-dimensional proton spectroscopic imaging study. *Neuropsychopharmacology.* (2020) 45:1851–9. doi: 10.1038/s41386-020-0707-y
16. Kay SR, Fiszbein A, Opler LA. The positive and negative syndrome scale (PANSS) for schizophrenia. *Schizophr Bull.* (1987) 13:261–76. doi: 10.1093/schbul/13.2.261
17. Young RC, Biggs JT, Ziegler VE, Meyer DA. A rating scale for mania: reliability, validity and sensitivity. *Br J Psychiatry.* (1978) 133:429–35. doi: 10.1192/bjp.133.5.429
18. Addington D AJ, Maticka-Tyndale E. Assessing depression in schizophrenia: the calgary depression scale. *Br J Psychiatry Suppl.* (1993) 1993:39–44. doi: 10.1192/S0007125000292581
19. Schooler NR, Kane JM. Research diagnoses for tardive dyskinesia. *Arch Gen Psychiatry.* (1982) 39:486–7. doi: 10.1001/archpsyc.1982.04290040080014
20. Simpson GM, Angus JW. A rating scale for extrapyramidal side effects. *Acta Psychiatr Scand Suppl.* (1970) 212:11–9. doi: 10.1111/j.1600-0447.1970.tb02066.x
21. Barnes TR. A rating scale for drug-induced akathisia. *Br J Psychiatry.* (1989) 154:672–6. doi: 10.1192/bjp.154.5.672
22. Maudsley AA, Darkazanli A, Alger JR, Hall LO, Schuff N, Studholme C, et al. Comprehensive processing, display and analysis for in vivo MR spectroscopic imaging. *NMR Biomed.* (2006) 19:492–503. doi: 10.1002/nbm.1025
23. Maudsley AA, Domenig C, Govind V, Darkazanli A, Studholme C, Arheart K, et al. Mapping of brain metabolite distributions by volumetric proton MR spectroscopic imaging (MRSI). *Magn Reson Med.* (2009) 61:548–59. doi: 10.1002/mrm.21875
24. Cox RW. AFNI: software for analysis and visualization of functional magnetic resonance neuroimages. *Comput Biomed Res.* (1996) 29:162–73. doi: 10.1006/cbmr.1996.0014
25. Gardner DM, Murphy AL, O'Donnell H, Centorrino F, Baldessarini RJ. International consensus study of antipsychotic dosing. *Am J Psychiatry.* (2010) 167:686–93. doi: 10.1176/appi.ajp.2009.09060802
26. Brandt AS, Unschuld PG, Pradhan S, Lim IA, Churchill G, Harris AD, et al. Age-related changes in anterior cingulate cortex glutamate in schizophrenia: A (1)H MRS Study at 7 Tesla. *Schizophr Res.* (2016) 172:101–5. doi: 10.1016/j.schres.2016.02.017
27. Kumar J, Liddle EB, Fernandes CC, Palaniyappan L, Hall EL, Robson SE, et al. Glutathione and glutamate in schizophrenia: a 7T MRS study. *Mol Psychiatry.* (2020) 25:873–82. doi: 10.1038/s41380-018-0104-7
28. Ripke S, Neale BM, Corvin A, Walters JTR, Farh KH, Holmans PA, et al. Biological insights from 108 schizophrenia-associated genetic loci. *Nature.* (2014) 511:421–+. doi: 10.1038/nature13595
29. Kraguljac NV, Reid M, White D, Jones R, den Hollander J, Lowman D, et al. Neurometabolites in schizophrenia and bipolar disorder - a systematic review and meta-analysis. *Psychiatry Res.* (2012) 203:111–25. doi: 10.1016/j.pscychresns.2012.02.003
30. Whitehurst TS, Osugo M, Townsend L, Shatalina E, Vava R, Onwordi EC, et al. Proton magnetic resonance spectroscopy of n-acetyl aspartate in chronic schizophrenia, first episode of psychosis and high-risk of psychosis: a systematic review and meta-analysis. *Neurosci Biobehav Rev.* (2020) 119:255–67. doi: 10.1016/j.neubiorev.2020.10.001
31. Olabi B, Ellison-Wright I, McIntosh AM, Wood SJ, Bullmore E, Lawrie SM. Are there progressive brain changes in schizophrenia? A meta-analysis of structural magnetic resonance imaging studies. *Biol Psychiatry.* (2011) 70:88–96. doi: 10.1016/j.biopsych.2011.01.032
32. Das TK, Dey A, Sabesan P, Javadzadeh A, Theberge J, Radua J, et al. Putative Astroglial Dysfunction in Schizophrenia: A Meta-Analysis of (1)H-MRS Studies of Medial Prefrontal Myo-Inositol. *Front Psychiatry.* (2018) 9:438. doi: 10.3389/fpsyt.2018.00438
33. Kubota M, Moriguchi S, Takahata K, Nakajima S, Horita N. Treatment effects on neurometabolite levels in schizophrenia: a systematic review and meta-analysis of proton magnetic resonance spectroscopy studies. *Schizophr Res.* (2020) 222:122–32. doi: 10.1016/j.schres.2020.03.069
34. Wood SJ, Berger GE, Wellard RM, Proffitt T, McConchie M, Velakoulis D, et al. A 1H-MRS investigation of the medial temporal lobe in antipsychotic-naive and early-treated first episode psychosis. *Schizophr Res.* (2008) 102:163–70. doi: 10.1016/j.schres.2008.03.012
35. Lahti AC, Holcomb HH, Weiler MA, Medoff DR, Tamminga CA. Functional effects of antipsychotic drugs: comparing clozapine with haloperidol. *Biol Psychiatry.* (2003) 53:601–8. doi: 10.1016/S0006-3223(02)01602-5
36. Lahti AC, Weiler MA, Medoff DR, Tamminga CA, Holcomb HH. Functional effects of single dose first- and second-generation antipsychotic administration in subjects with schizophrenia. *Psychiatry Res.* (2005) 139:19–30. doi: 10.1016/j.pscychresns.2005.02.006
37. Lieberman JA, Tollefson GD, Charles C, Zipursky R, Sharma T, Kahn RS, et al. Antipsychotic drug effects on brain morphology in first-episode psychosis. *Arch Gen Psychiatry.* (2005) 62:361–70. doi: 10.1001/archpsyc.62.4.361
38. Dorph-Petersen KA, Pierri JN, Perel JM, Sun Z, Sampson AR, Lewis DA. The influence of chronic exposure to antipsychotic medications on brain size before and after tissue fixation: a comparison of haloperidol and olanzapine in macaque monkeys. *Neuropsychopharmacology.* (2005) 30:1649–61. doi: 10.1038/sj.npp.1300710
39. Konopaske GT, Dorph-Petersen KA, Pierri JN, Wu Q, Sampson AR, Lewis DA. Effect of chronic exposure to antipsychotic medication on cell numbers in the parietal cortex of macaque monkeys. *Neuropsychopharmacology.* (2007) 32:1216–23. doi: 10.1038/sj.npp.1301233
40. Rae CD. A guide to the metabolic pathways and function of metabolites observed in human brain 1H magnetic resonance spectra. *Neurochem Res.* (2014) 39:1–36. doi: 10.1007/s11064-013-1199-5
41. Urenjak J, Williams SR, Gadian DG, Noble M. Specific expression of N-acetylaspartate in neurons, oligodendrocyte-type-2 astrocyte progenitors, and immature oligodendrocytes in vitro. *J Neurochem.* (1992) 59:55–61. doi: 10.1111/j.1471-4159.1992.tb08875.x
42. Harrison PJ. The neuropathology of schizophrenia. A critical review of the data and their interpretation. *Brain J Neurol.* (1999) 122 (Pt 4):593–624. doi: 10.1093/brain/122.4.593
43. Du F, Cooper AJ, Thida T, Sehovic S, Lukas SE, Cohen BM, et al. In vivo evidence for cerebral bioenergetic abnormalities in schizophrenia measured using 31P magnetization transfer spectroscopy. *JAMA Psychiatry.* (2014) 71:19–27. doi: 10.1001/jamapsychiatry.2013.2287
44. Selemon LD, Lidow MS, Goldman-Rakic PS. Increased volume and glial density in primate prefrontal cortex associated with chronic antipsychotic drug exposure. *Biol Psychiatry.* (1999) 46:161–72. doi: 10.1016/S0006-3223(99)00113-4

Conflict of Interest: The authors declare that the research was conducted in the absence of any commercial or financial relationships that could be construed as a potential conflict of interest.

frontiers in Psychiatry

ORIGINAL RESEARCH
published: 08 June 2021
doi: 10.3389/fpsyt.2021.668304

Lower Ventromedial Prefrontal Cortex Glutamate Levels in Patients With Obsessive–Compulsive Disorder

Marcelo C. Batistuzzo[1,2†], Bruna A. Sottili[3†], Roseli G. Shavitt[1], Antonio C. Lopes[1], Carolina Cappi[1], Maria Alice de Mathis[1], Bruno Pastorello[3], Juliana B. Diniz[1], Renata M. F. Silva[1], Euripedes C. Miguel[1], Marcelo Q. Hoexter[1,4] and Maria C. Otaduy[3]*

[1] Department & Institute of Psychiatry, University of São Paulo Medical School, São Paulo, Brazil, [2] Department of Methods and Techniques in Psychology, Pontifical Catholic University, São Paulo, Brazil, [3] Laboratory of Magnetic Resonance (LIM44), Department and Institute of Radiology, University of São Paulo (InRad-FMUSP), São Paulo, Brazil, [4] Laboratório Interdisciplinar de Neurociências Clínicas (LiNC), Universidade Federal de São Paulo (UNIFESP), São Paulo, Brazil

OPEN ACCESS

Edited by:
Lawrence Steven Kegeles, Columbia University, United States

Reviewed by:
Carolyn Rodriguez, Stanford University Medical Center, United States
Joseph O'Neill, University of California, Los Angeles, United States

***Correspondence:**
Marcelo C. Batistuzzo
marcelobatistuzzo@gmail.com

[†]These authors have contributed equally to this work

Specialty section:
This article was submitted to Neuroimaging and Stimulation, a section of the journal Frontiers in Psychiatry

Received: *16 February 2021*
Accepted: *23 April 2021*
Published: *08 June 2021*

Citation:
Batistuzzo MC, Sottili BA, Shavitt RG, Lopes AC, Cappi C, de Mathis MA, Pastorello B, Diniz JB, Silva RMF, Miguel EC, Hoexter MQ and Otaduy MC (2021) Lower Ventromedial Prefrontal Cortex Glutamate Levels in Patients With Obsessive–Compulsive Disorder. Front. Psychiatry 12:668304. doi: 10.3389/fpsyt.2021.668304

Background: Recent studies using magnetic resonance spectroscopy (^{1}H-MRS) indicate that patients with obsessive–compulsive disorder (OCD) present abnormal levels of glutamate (Glu) and gamma aminobutyric acid (GABA) in the frontal and striatal regions of the brain. These abnormalities could be related to the hyperactivation observed in cortico-striatal circuits of patients with OCD. However, most of the previous ^{1}H-MRS studies were not capable of differentiating the signal from metabolites that overlap in the spectrum, such as Glu and glutamine (Gln), and referred to the detected signal as the composite measure—Glx (sum of Glu and Gln). In this study, we used a two-dimensional JPRESS ^{1}H-MRS sequence that allows the discrimination of overlapping metabolites by observing the differences in J-coupling, leading to higher accuracy in the quantification of all metabolites. Our objective was to identify possible alterations in the neurometabolism of OCD, focusing on Glu and GABA, which are key neurotransmitters in the brain that could provide insights into the underlying neurochemistry of a putative excitatory/inhibitory imbalance. Secondary analysis was performed including metabolites such as Gln, creatine (Cr), N-acetylaspartate, glutathione, choline, lactate, and myo-inositol.

Methods: Fifty-nine patients with OCD and 42 healthy controls (HCs) underwent 3T ^{1}H-MRS in the ventromedial prefrontal cortex (vmPFC, 30 × 25 × 25 mm^3). Metabolites were quantified using ProFit (version 2.0) and Cr as a reference. Furthermore, Glu/GABA and Glu/Gln ratios were calculated. Generalized linear models (GLMs) were conducted using each metabolite as a dependent variable and age, sex, and gray matter fraction (fGM) as confounding factors. GLM analysis was also used to test for associations between clinical symptoms and neurometabolites.

Results: The GLM analysis indicated lower levels of Glu/Cr in patients with OCD ($z = 2.540$; $p = 0.011$). No other comparisons reached significant differences between groups for all the metabolites studied. No associations between metabolites and clinical symptoms were detected.

Conclusions: The decreased Glu/Cr concentrations in the vmPFC of patients with OCD indicate a neurochemical imbalance in the excitatory neurotransmission that could be associated with the neurobiology of the disease and may be relevant for the pathophysiology of OCD.

Keywords: obsessive-compulsive disorder, magnetic resonance spectroscopy, prefrontal cortex, neurometabolic alterations, Glutamate, GABA

INTRODUCTION

Obsessive–compulsive disorder (OCD) is a psychiatric disease that affects 1–4% of the population (lifetime) around the world (1, 2). Although its pathophysiology remains not entirely understood, there is a consensus that OCD is characterized by abnormalities in the cortico-striato-thalamo-cortical (CSTC) circuitry. In the last decade, studies using proton magnetic resonance spectroscopy (^{1}H-MRS), the only technique that allows to non-invasively estimate the levels of brain neurochemicals *in vivo*, showed that patients with OCD could present altered glutamatergic (excitatory) and GABAergic (inhibitory) neurotransmission in the prefrontal cortex and striatal brain regions (3–8). However, inconclusive findings in the literature indicate that there is still a need for a thorough investigation (9).

The role of glutamate (Glu) signaling in the treatment of OCD has been investigated in therapeutic clinical trials in the literature (10–14), including positive randomized clinical trials that used glutamatergic agents as the main outcome or as an enhancer (15–18). On the other hand, augmentation studies with glutamatergic agents in patients with OCD did not show superiority to the simple administration of selective serotonin reuptake inhibitors (19, 20). In addition, candidate gene studies showed the involvement of genes coding for the glutamate signaling cascade, especially the DLGAP/SAPAP family genes (21, 22). Overall, these studies advanced the field by adding information on the neurobiological model of OCD, by testing modulation effects or associated genes, but they did not measure glutamate directly. Therefore, neurobiological research and, more specifically, *in vivo* neurochemical research on patients with OCD, is important to elucidate the glutamatergic hypothesis in OCD (11) and the role of other metabolites as well.

The most prominent neurobiological model of OCD involves abnormalities (typically hyperactivation) in the multiple and parallel CSTC circuits (22, 23). Generally, the role of gamma aminobutyric acid (GABA) in these circuits has been relatively understudied, but one hypothesis is that diminished levels of this metabolite in the prefrontal cortex (PFC) would be one of the reasons for the striatal dopaminergic and glutamatergic hyperactivity observed in patients with OCD (24). In this sense, two possible GABA paths are postulated: a direct path, in which GABA projections from the ventromedial PFC (vmPFC) reach the striatum, and a second one, indirectly, via projections to the orbitofrontal cortex.

Brain circuits related to fear and reward that encompass the vmPFC are relevant for the neurobiology of OCD and have been previously associated with the disorder both in theory and practice (25, 26). Structural, but mainly functional, abnormalities within the vmPFC were detected in imaging studies and could be related to alterations in the CSTC circuits described in the neuroimaging literature (22, 27). The vmPFC is thought to be involved with the "affective system," participating, for example, in affective behaviors as processing affects or rewards (26). Of note, this region has been shown to be crucial to the retention of extinction learning in fear conditioning paradigms. As the habituation promoted by one of the main psychotherapeutic treatments of OCD (cognitive behavioral therapy, with exposure, and response prevention techniques) is somehow similar to extinction as evaluated in fear conditioning paradigms, some authors have proposed that proper activation of the vmPFC could be implicated in the treatment response to psychotherapy among OCD patients (28). Therefore, due to its importance in the neurobiological model of OCD, we investigated the vmPFC in the present study.

^{1}H-MRS studies evaluating Glu concentrations in the brain of patients with OCD have found mixed results. Some of them show a reduction in Glu concentration in patients when compared to controls (29) while others have reported increased Glx (Glu + glutamine) levels (30). However, most of the findings did not report any differences (4, 6, 8, 9, 31). Therefore, despite the growing literature in the OCD ^{1}H-MRS field in recent years (14, 32), there is still no consensus on the role of the glutamatergic cycle in OCD. Regarding GABA, this is a much more difficult metabolite to detect, as it requires specific ^{1}H-MRS editing techniques. In a recent review of the literature that included only ^{1}H-MRS studies that used scan fields strength of 3 T, the authors concluded that most studies did not demonstrate any neurometabolic abnormalities in OCD patients when compared to healthy controls, although they indicated that altered GABA levels in the rostral anterior cingulate cortex (rACC) is one of the most consistent findings (9). Still, while they reported two studies showing lower GABA concentrations in rACC in adults with OCD (4, 6), a more recent study has found higher concentrations of this metabolite in patients with OCD in the ACC (7). Therefore, the current evidence is not sufficiently strong for elucidating the role of neurometabolites in OCD, particularly Glu and GABA, and further research is needed in this field.

Factors that can contribute to results heterogeneity among different studies include voxel size and anatomical placement and the inherent variability of the OCD population. Moreover, since conventional ^{1}H-MRS is not ideal to detect Glu, glutamine (Gln), and GABA due to their low signal and partial overlap with other metabolites, this could be considered a limitation

of the previous studies, since most of them were incapable of disentangling the specific signal from each metabolite. Hence, this study used a two-dimensional JPRESS ^{1}H-MRS sequence that allows the discrimination of overlapping metabolites by observing the differences in J-coupling (second dimension of the spectrum), leading to higher accuracy of all metabolites in the brain, including Glu, Gln, and GABA (33, 34).

The main objective of this study was to quantify specific metabolites (especially Glu/Cr and GABA/Cr) in the vmPFC of OCD patients and to compare them with HC. In our statistical model, we considered demographic data (such as age and sex) and also the fraction of gray matter (fGM) in the MRS voxel, aiming to control for possible confounders. Additionally, since alterations in Glu/Cr levels could be accompanied by corresponding GABA/Cr alterations [for example, see Scotti-Muzzi (35), which used the same ^{1}H-MRS technique to acquire the data], an imbalance in the Glu/GABA ratio between groups could also add information regarding the neurochemistry of OCD. Thus, we also explored the Glu/GABA ratio, which has not been systematically studied previously in the OCD field. We hypothesized that the current investigation could improve our comprehension of prior results with mixed findings, by studying a large sample of OCD patients with a ^{1}H-MRS sequence more specific for overlapping metabolites.

MATERIALS AND METHODS

Ethical Issues

This project was approved by the Ethics Committee for Analysis of Research Projects (CAPPesq) at Faculdade de Medicina da Universidade de São Paulo (FMUSP). All participants signed a written informed consent after a thorough description of the study and the assurance that their decision to participate would not interfere with their access to treatment. Participants received financial compensation for transportation and refreshments during the study.

Participants and Inclusion and Exclusion Criteria

Participants were recruited from 2014 to 2017, during a period of 3 years and 1 month. Inclusion criteria for OCD patients were the following: (a) age between 18 and 65 years; (b) primary diagnosis of OCD according to the Diagnostic and Statistical Manual of Mental Disorders, fourth edition (DSM-IV), confirmed by the Structured Clinical Interview for DSM-IV Axis I disorders (SCID-I); (c) Y-BOCS score $\geq$16 or $\geq$10 only for only obsessions or compulsions; and (d) to be on a stable medication regimen for the last 6 weeks or off medication. Exclusion criteria were the following: (a) IQ below 80; (b) comorbidity with schizophrenia or bipolar disorder; (c) any contraindication to MRI, such as pacemakers or cochlear implant, etc.; (d) claustrophobia or not being able to tolerate the exam; (e) past or current substance abuse or dependence; and (f) head trauma with loss of consciousness. HC had no history of physical or psychiatric disorders on the basis of the SCID interview and had to meet the same inclusion/exclusion criteria, with the exception of the OCD-related ones.

Clinical Measures

All participants were interviewed by experienced clinical psychologists and completed the same battery of clinical assessments with the standardized instruments described below. All interviews were conducted in person and lasted ∼2 h. To evaluate psychiatric disorders, the SCID-I (axis I) and an additional module for impulse-control disorders according to DSM-IV criteria were used for all participants (36). The OCD diagnosis was established by clinicians with long experience in OCD assessment and treatment (ACL, AM, JBD, RMFS, and RGS). The present Portuguese version of the SCID showed good interrater reliability (37).

OCD severity was measured using the Y-BOCS severity scale (38), which is a 10-item semistructured clinician-administered measure of obsession and compulsion severity. Each item can score from 0 to 4, with a maximum of 40 (20 for obsessions and 20 for compulsions). The Y-BOCS has been considered the gold-standard instrument for the assessment of OCD symptoms (38), with good psychometric properties including Brazilian samples evaluated in Portuguese (39).

Finally, the 21-item Beck Depression Inventory (BDI) (40) measures cognitive, behavioral, and somatic symptoms associated with depression. The Beck Anxiety Inventory (BAI) is a 21-question multiple choice, each answer being scored on a scale value of 0 (not at all) to 3 (severely), used for measuring the severity of anxiety in adults (41). Both scales were applied to all participants, they are consolidated scales that were translated into Brazilian Portuguese and validated in our environment previously (42).

Procedures

Image Acquisition

The entire MRI scan lasted ∼1 h, and the images were acquired on a Philips 3 T Achieva scanner (Philips Healthcare, Best, The Netherlands) using a 32-channel head coil. Spectroscopy was acquired with a two-dimensional JPRESS ^{1}H-MRS sequence (33), a technique based on a conventional PRESS spin echo (single voxel) that varies the echo time of the acquisition, encoding the J coupling evolution in an additional dimension. In other words, the ^{1}H-MRS signal is measured not only as a function of the chemical shift (expressed by the Larmor frequency, as in conventional one-dimensional spectroscopy) but also as a function of the coupling constant J in Hz. With the coupling constant J, it is possible to resolve the signals from overlapping multiplets, such as Glu and Gln. This sequence lasted ∼25 min and was obtained with the following parameters: the voxel was positioned in the ventromedial PFC (**Figure 1**) with a size of 30 mm (L–R) × 25 mm (I–S) × 25 mm (A–P); minimum echo time (TE) used was 31 ms, and TE was incremented in 100 steps of 2 ms each; for every time increment ΔTE, the maximum-echo sampling started the acquisition ΔTE/2 earlier with respect to the echo top, the repetition time (TR) was 1,600 ms, and 8 averages were acquired for each TE step. One non-water suppressed spectrum was also acquired at each TE. The number of points per spectrum was 1,024, and the spectral bandwidth was 2,000 Hz. An automatic second-order B0 shimming routine was used, and water suppression was achieved by VAPOR (43). Additionally, in

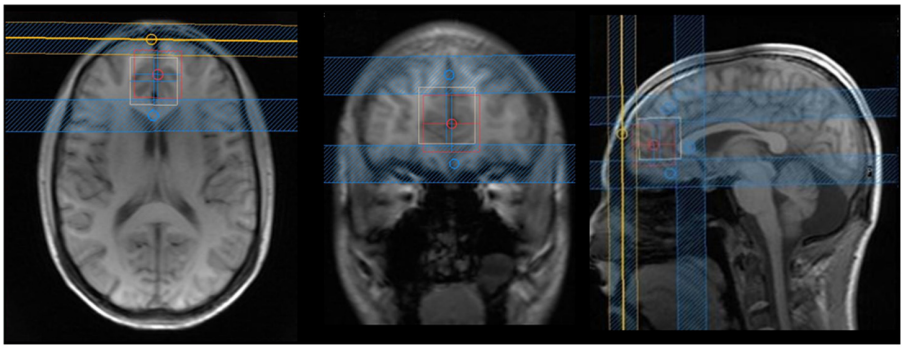

FIGURE 1 | Axial, coronal, and sagittal images from the voxel position in the ventromedial prefrontal cortex: blue lines are suppression bands, used in the Y- and Z-axes. We analyzed that only the voxel that was the overlap between the white and red squares in order to reduce effects of chemical shift voxel displacement. The following rationale was used: the bottom portion of the voxel was aligned with the anterior–posterior commissure; in the anterior/posterior axis, the corpus callosum was used as reference (just ahead of the genu of corpus callosum); and in the lateral axis, the voxel was situated in the most medial portion of the brain.

order to reduce the effect of chemical shift voxel displacement, four suppression bands were positioned at the voxel edges along the Y- and Z-axes, which present a more pronounced chemical shift artifact due to the use of 180-slice selective pulses (see **Figure 1**).

Data Processing

Metabolite quantification was obtained using Prior Knowledge Fitting (ProFit) version 2.0 running on Matlab R2011b (44). ProFit (34) works as an extension of LCModel (45) principles to fit 2D data sets. Fuchs et al. (44) improved the quantification program (ProFit, version 2.0) by introducing an experimentally acquired 2D macromolecular baseline into the fitting model and allowing for a more accurate and precise fit by accounting for the actual line shape and additional baseline distortions by self-deconvolution and spline modeling approach. An example of a ^{1}H-MRS JPRESS spectrum can be found in the supplementary files (**Supplementary Figure 1**).

The metabolite basis set used by ProFit includes spectra from a total of 18 brain metabolites. The metabolites of interest that were analyzed in this study were Glu, GABA, Gln, N-acetylaspartate (NAA), creatine (Cr), glutathione (GSH), choline (Cho), lactate (Lac), and myo-inositol (ml). The first two metabolites, and the ratio among them (Glu/GABA), were the main objective of this study. All the other metabolites described above were also extracted and quantified but analyzed as secondary outcomes. Basis set metabolite spectra were calculated with the GAMMA library (46) using the chemical shift and J-coupling values from the literature (47, 48). Quantitative results in ProFit are given in the form of ratios to Cr signal (met/Cr). These ratios are already corrected for T2 relaxation effects since ProFit automatically calculates T2 relaxation times for each metabolite from the signal obtained at the different TEs.

To determine the brain tissue composition contained in the MRS voxel of interest, three-dimensional volumetric T1 images were obtained using the 3D turbo field echo technique [fractional anisotropy (FA) = 8°; TE = 3.2 ms; TR = 7 ms; inversion time (TI) = 900 ms] with an isotropic voxel size of 1 mm^3. With the help of the voxel tissue segmentation tool incorporated into Gannet 3.0 software (49), percentages of white matter (WM), GM, and cerebrospinal fluid (CSF) were calculated for each voxel. The fraction of GM (fGM) contributing to the observed MRS signal was calculated as fGM = GM%/(GM% + WM%) and was inserted into the statistical model as a covariate.

The ProFit program also provides a Cramér–Rao lower bound (CRLB), a measure of the quality of the metabolite quantification for each metabolite (50). Metabolites with CRLBs above 20% were excluded from the statistical analysis.

Statistical Analysis

Two-sided independent *t*-tests and two-sided asymptotic Pearson chi-square, at the 5% significance level, were performed comparing demographic data between patients and HC. In addition, each metabolite was entered as a dependent variable in a univariate Generalized Linear Model (GLM) with group as the fixed factor and age, sex, and fGM as covariates. Finally, we performed GLM analyses only at the OCD group to investigate eventual associations between metabolic values and clinical data covarying for sex, age, and fGM. Statistical analysis was performed using Python version 3.6, and Bonferroni correction was applied considering the number of comparisons/metabolites analyzed in the study: separate corrections were performed for the main outcomes (three comparisons) and for the secondary outcomes (seven comparisons). The same rule was applied for the GLM seeking to evaluate the clinical associations; however, once we had three scales (Y-BOCS, BDI, and BAI) for each metabolite, corrections were performed for nine comparisons regarding the main outcomes and 21 comparisons for the secondary ones.

RESULTS

Demographic Group Comparisons

One hundred forty-five volunteers were scanned with the two-dimensional JPRESS ^{1}H-MRS sequence. Forty-four participants were excluded due to excessive movement or bad quality

TABLE 1 | Clinical and demographic variables in patients with obsessive-compulsive disorder and healthy controls.

	Patients ($n = 59$)	Controls ($n = 42$)	t/X^2	p-value
Age (SD)	35.1 (10.0)	33.4 (11.5)	0.78	0.435[b]
Sex, female (%)	37 (62.7)	23 (57.5)	0.80	0.427[b]
Y-BOCS (SD)	29.3 (6.7)	–	–	–
BDI (SD)	17.7 (10.1)	–	–	–
BAI (SD)	16.0 (9.9)	–	–	–
Medications SSRI or SRI[1] (%)	37 (62.7)	–	–	–
Other antidepressants[2] (%)	4 (5.1)	–	–	–
Benzodiazepines[3] (%)	4 (5.1)	–	–	–
Neuroleptics[4] (%)	12 (20.3)	–	–	–
Anticonvulsants[5] (%)	1 (1.7)	–	–	–
Stimulants[6] (%)	1 (1.7)	–	–	–
fGM (SD)	0.69 (0.07)	0.71 (0.09)	−1.20	0.234[a]

Y-BOCS, Yale-Brown Obsessive–Compulsive Scale; BDI, Beck Depression Inventory; BAI, Beck Anxiety Inventory; fGM, fractioned gray matter.
[1]Fluoxetine, fluvoxamine, paroxetine, sertraline, citalopram, escitalopram, clomipramine.
[2]Mirtazapine, venlafaxine, duloxetine.
[3]Clonazepam.
[4]Olanzapine, ziprasidone, quetiapine, aripiprazole.
[5]Gabapentin.
[6]Ritalin.
[a]Student's t-test for two independent samples (patients and healthy controls).
[b]Two-sided asymptotic significance, Pearson chi-square.

TABLE 2 | Ventromedial PFC metabolites levels in patients with obsessive-compulsive disorder and healthy controls.

	N	OCD	HC	Group-effect GLM	
		Mean (SD)	Mean (SD)	z	p-value
Primary outcomes					
Glu/Cr	101	0.70 (0.36)	0.77 (0.37)	2.540	0.011
GABA/Cr	91	0.29 (0.19)	0.30 (0.20)	−1.015	0.310
Glu/GABA	91	3.71 (3.68)	4.58 (5.37)	0.353	0.724
Secondary outcomes					
Gln/Cr	91	0.29 (0.15)	0.27 (0.13)	−0.658	0.511
Glu/Gln	91	2.96 (1.87)	3.23 (1.92)	1.821	0.069
NAA/Cr	101	1.05 (0.17)	1.04 (0.12)	1.578	0.110
GSH/Cr	101	0.26 (0.09)	0.26 (0.09)	0.028	0.977
Cho/Cr	101	0.16 (0.02)	0.16 (0.02)	0.021	0.983
Lac/Cr	39	0.15 (0.15)	0.14 (0.13)	−0.206	0.837
mI/Cr	101	0.43 (0.13)	0.43 (0.13)	0.096	0.923

Glu, glutamate; GABA, gamma aminobutyric acid; Gln, Glutamine; NAA, n-acetylaspartate; GSH, glutathione; Cho, choline; Lac, lactate; mI, myo-inositol, z, t-stats.

spectroscopy data. The final sample consisted of 101 participants: 59 patients with OCD and 42 healthy controls. Descriptives of demographic and clinical characteristics of both groups can be seen in **Table 1**: groups did not differ in age, sex, or gray matter fraction (fGM) in the voxel. It is worth mentioning that the mean Y-BOCS score was 29.3, which indicates a moderate to severe level of symptomatology according to Storch et al. (51) criteria. Regarding previous treatments, 42 patients have failed at least one selective serotonin reuptake inhibitor (SSRI), and 34 have failed to improve symptomatology after cognitive behavior therapy (CBT).

^{1}H-MRS Results

Mean metabolite ratios relative to Cr are listed in **Table 2** for each group. Due to CRLB above 20%, it was necessary to exclude 10 subjects for GABA and Gln and 62 subjects for Lac evaluation. Mean CRLB were 10.66% for GABA, 2.73% for Glu, 0.68% for Cr, 13.08% for Gln, 0.65% for NAA, 4.88% for GSH, 0.80% for Cho, 14.75% for Lac, and 2.99% for mI.

Generalized Linear Model

A summary of the group effect in the Generalized Linear Model (GLM) for each metabolite, together with the average for each group, is shown in **Table 2**. Multivariate regressions using GLM aimed to predict the variation in metabolites quantities using the following set of explanatory variables: (1) group, (2) sex, (3) age, and (4) fGM. We found a significant group effect for Glu/Cr, indicating that patients presented a lower concentration of this metabolite ($z = 2.540$; $p = 0.011$), a result that persisted after Bonferroni correction (**Figure 2**). On the other hand, GABA/Cr and the Glu/GABA ratio did not present any difference between groups (**Table 2**).

Regarding the secondary outcomes, none of the following models reached statistical significance or presented group effects: Gln/Cr, Glu/Gln, NAA/Cr, GSH/Cr, Cho/Cr, Lac/Cr, and mI/Cr (**Table 2**).

Association With Clinical Symptoms

None of the clinical measures were associated with the metabolites for the primary or secondary outcomes: severity of OCD (Y-BOCS scores) and depressive or anxiety symptoms (BDI and BAI scores) (**Supplementary Table 1**).

DISCUSSION

The present study used a two-dimensional JPRESS ^{1}H-MRS sequence to investigate specific metabolites in the ventromedial PFC (vmPFC) in one of the largest samples of patients with OCD reported to date. We found lower levels of Glu/Cr in patients compared with HC but no alterations in GABA/Cr or Glu/GABA ratio. We also did not observe any association of the metabolites with age or clinical symptoms nor group differences in the secondary outcomes.

Up to now, the literature regarding ^{1}H-MRS of vmPFC in patients with OCD has presented inconclusive findings. Results are especially inconsistent when metabolites are reported as Glx: some studies reported higher levels of Glx in OCD compared with controls (8, 30), while others showed lower levels of Glx in patients (52). However, the vast majority of studies reported no differences (4, 6, 53). One explanation for the mixed findings could be related to the fact that most studies could not separate the spectral peaks of Glu and Gln, leading to ambiguity. Recent ^{1}H-MRS techniques (as JPRESS) at high-field scanners (3T)

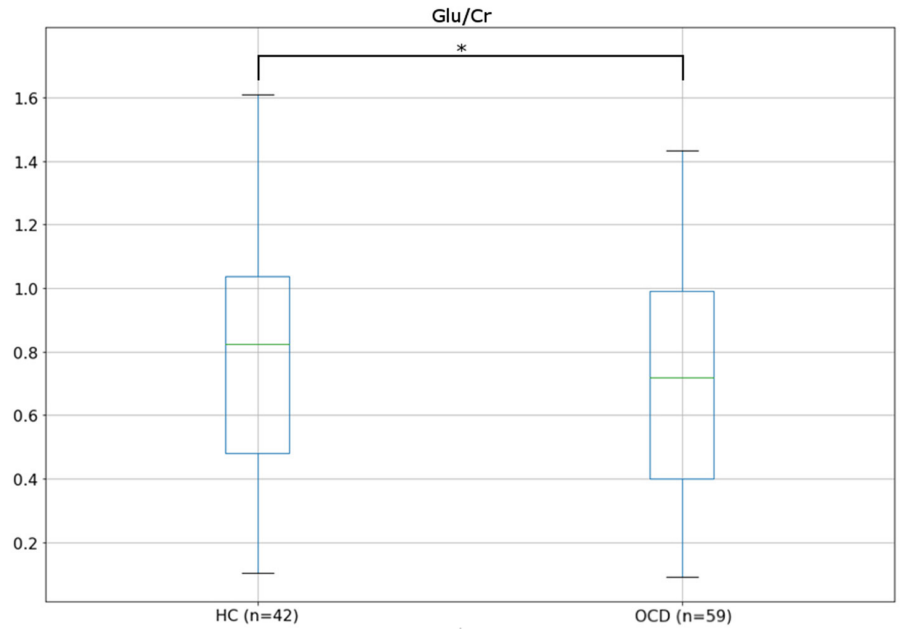

FIGURE 2 | Boxplots showing the distribution of Glu/Cr in healthy controls (HCs) and patients with obsessive–compulsive disorder (OCD).

are able to disentangle each metabolite concentration due to better spectral resolution, offering more precise results, i.e., Glu minimally contaminated by precursors and other metabolites.

Studies measuring Glu levels in adults with OCD and evaluating regions similar to ours have also found inconsistent results. While most of the literature found no differences in Glu values when comparing patients and controls (30, 53, 54), one study has found lower levels in the mPFC of OCD patients (29). Our results replicated, in a larger sample, the previous findings of Zhu et al. (29), who evaluated 13 patients with OCD. At first, these findings may seem contradictory, once the postulated hyperactivation of the CSTC would demand increased levels of Glu in frontal areas. However, it is noteworthy that no study using a 3T scan observed higher Glu values in the mPFC [for a review see Vester et al. (9)]. Moreover, the small sample size of previous studies ($n = 16$, 30, and 40) and the fact that only one study (53) used a JPRESS sequence could also account for the inconclusive results.

Lower levels of Glu in the vmPFC were also detected in children with OCD when compared to control youths (55, 56). While a straightforward comparison with these studies is difficult because of two main reasons, (1) a developing brain can be totally different in terms of functioning and neurochemistry from an adult brain and (2) both studies assessing children have used 1.5 T scans (and their samples were 20 and 14, respectively), it is possible that the brain mechanisms that underlie OCD symptoms could present similar pathophysiology, independently of age or developmental stage (57). In fact, our results support this view: even without having youth in our sample, we had participants with a wide age range. Although we tried to observe a pattern of association (reduction or increase) over the lifespan, we could not find age influences in any metabolite. In addition, this was a cross-sectional design study, which is not appropriate for this type of investigation.

The Glu alterations mentioned above and reported in our results may underlie the abnormalities in the frontostriatal circuits detected in OCD patients. The imbalance in Glu concentrations, especially in this frontal region, may reflect changes in the excitatory/inhibitory neurotransmission of the frontostriatal circuits, crucial in OCD pathophysiology, or even a compensatory mechanism. Finding similar results to ours, Rosenberg and colleagues (55), speculated that the pathophysiological model of OCD was associated with tonic–phasic dysregulation of Glu in CSTC circuits. Translating this hypothesis to our results, reduced tonic Glu levels in vmPFC could predispose to phasic Glu hyperactivity in the striatum and OFC. Although we did not measure metabolites concentrations in other areas, future studies should assess more than one voxel to have a greater view of the neurochemistry balance behind the CSTC circuitry in OCD patients. The clinical implication of a better understanding of the neurobiological model of the disease is relevant and useful. For example, a disrupted excitatory or inhibitory system in the vmPFC could be related to dysregulations in affective (26, 28) and cognitive systems (58), as reported in patients with OCD.

Overall, the lower levels in Glu/Cr presented by OCD patients support the glutamatergic hypothesis for OCD (10). The evidence for glutamatergic dysregulation in OCD has been increasingly strong in the literature (22), with alterations being detected in studies that analyzed neurochemical levels in the cerebrospinal fluid of unmedicated patients (59, 60) and also in ^{1}H-MRS studies (29), as previously mentioned. Therefore, even with most ^{1}H-MRS studies presenting negative results regarding Glu in several regions of the brain, we remember once more that most

of the previous studies were underpowered and did not have a proper ^{1}H-MRS sequence capable of separating Glu from Gln.

Regarding GABA/Cr, our findings are in line with other studies reporting no differences in vmPFC (5), including more recent studies that have used newer ^{1}H-MRS sequences capable of measuring those metabolites more precisely (9). Although part of the literature emphasizes GABAergic abnormalities in the vmPFC of patients with OCD, with two studies reporting lower levels (4, 6) and a more recent one reporting higher levels (7) of this metabolite, we could not find any difference between groups. In fact, looking at the means for each group, they were impressively similar. Comparing the studies, our sample was larger than two of the previous studies (4, 7), and although the study of Zhang et al. (6) had a larger sample than ours, the voxel position was not exactly in the same region: while they preferred to evaluate the orbitofrontal cortex, in our study, we positioned the voxel in a more superior location, delimited by a straight line between the anterior and posterior commissures. These factors may have influenced and diverged our results from the previous studies.

Our JPRESS sequence allowed us to measure the Glu/Gln ratio, differently from previous studies that mainly reported only Glx (4, 6, 29, 30). Although we could not find differences between patients with OCD and HC, this ratio is particularly informative and was previously shown to be associated with other psychiatric disorders, like depression (61), autistic traits (62), and schizophrenia (63). Therefore, new ^{1}H-MRS studies using pulse sequences that can distinguish Glu signals from Gln in OCD are warranted, not only to study their ratio but also to have a more precise and clear measure of each metabolite.

Regarding the secondary outcomes, our results also extend previous investigations of the involvement of these metabolites in the physiopathology of OCD: except for some studies that reported lower concentrations of NAA in the PFC of OCD patients (6, 64), most studies reported no alterations of Gln, NAA, GSH, Cho, Lac, or mI in the ventromedial PFC (29–31, 54, 65). Although this region is thought to be one of the most important of the cortico-striatal circuits involved with OCD symptoms, it seems that the evidence so far is insufficient to demonstrate alterations in other metabolites except Glu or GABA. Nevertheless, future studies with larger samples should investigate the longitudinal role of specific metabolites in OCD, whether they could be valid predictors of treatment response or if they could play a role in OCD symptoms improvement, as suggested in a recent umbrella review of biomarkers in OCD (58).

Even though we have found group effects in the Glu/Cr in this sample, none of the metabolites correlated with clinical symptoms, as measured by the Y-BOCS, BAI, or BDI, after a strict multiple comparisons correction, indicating that their levels are independent of clinical presentation or severity. Before correcting for multiple comparisons, GABA/Cr was associated with the severity of OCD symptoms and Glu/GABA with depression scores (regarding the mains outcomes), while Cho was associated with OCD and anxiety symptoms (secondary outcomes). With a sample of 59 patients with OCD, we cannot say that we were underpowered to observe correlations. On the other hand, the elevated number of comparisons does not allow us to interpret results without multiple comparison corrections. The literature offers mixed findings in this regard, with studies showing both positive (52) and negative (6) correlations of Glu (or Glx) and GABA in the vmPFC. However, previous studies did not control for multiple comparisons, and most ^{1}H-MRS studies in the OCD literature did not find metabolic–clinical associations (4, 7, 54, 65). Therefore, it is difficult to establish a pattern, as concluded by a recent review of the literature (9), but our results reinforce these negative findings.

Limitations of this study should be observed. First, we did not exclude patients with comorbid depression. On the other hand, BDI scores definitely differed between groups and were not associated with metabolites levels, suggesting that depressive symptoms were independent of those measures. Second, although most of our patients were medicated at the time of the scan, we admitted patients taking medications only if they were stable for at least 6 weeks. Nevertheless, this could have influenced our findings. Thus, we ran analyses without patients taking anticonvulsants and benzodiazepines, and the results remained the same. Finally, we used a unique and non-commercial pulse sequence of MRS that could separate Glu/Cr and Gln/Cr, which strengthens our study. However, this was a very long sequence (lasting ∼25 min), and thus, there was a higher chance that some subjects needed to be excluded from the analysis, simply because they moved their heads during this very long scanning. In addition, the voxel size was relatively large and positioned at the midline (as opposed to bilateral), encompassing diverse cortical subregions. Inevitably, the voxel contained also some white matter, which could affect results. In order to control for that, we verified that white matter portion was equal for both groups, and the gray matter fraction was considered in the statistical analysis.

To conclude, we found a group effect in the Glu/Cr concentration, which may indicate a neurochemical imbalance in the vmPFC of patients with OCD that could be associated with the corticostriatal dysregulation consistently implicated in the neurobiology of this disorder. It is hard to establish if the lower Glu/Cr levels found in patients with OCD in this study could be the cause or consequence of the disease or even related to any other pathophysiological process. They also could be the result of a compensatory system, as hypothesized before. Moreover, clinical severity of OCD, depression, and anxiety symptoms did not associate with metabolites levels, replicating previous studies. Our study sheds light on the relevance of further studying the glutamatergic system for understanding the neurobiology of the disease, for example, studies designed to test the predictive value of this metabolite and if/how it is affected by first-line treatments. It is possible that different OCD subtypes or patients that exhibit different clinical profiles would present different metabolite levels in the brain. Finally, future studies should evaluate other areas of the brain, particularly related to the CSTC circuits in patients with OCD.

Conflicts of Interest

All the authors declare that the research was conducted in the absence of any commercial or financial relationships that could be construed as a potential conflict of interest. Dr. Batistuzzo

confirms he had full access to all the data in the study and takes responsibility for the integrity of the data and the accuracy of the data analysis.

DATA AVAILABILITY STATEMENT

The raw data supporting the conclusions of this article will be made available by the authors, without undue reservation.

ETHICS STATEMENT

This study, involving human participants, was reviewed and approved by Ethics Committee for Analysis of Research Projects (CAPPesq) board, of the Faculdade de Medicina da Universidade de São Paulo (FMUSP). The patients/participants provided their written informed consent to participate in this study.

AUTHOR CONTRIBUTIONS

MB planned the study, acquired and analyzed the data, wrote, and reviewed the manuscript. BS analyzed the data, wrote, and reviewed the manuscript. RGS and EM reviewed the manuscript. AL, CC, AM, JD, and RS acquired the data and reviewed the manuscript. BP helped to analyze the data and reviewed the manuscript. MH planned the study, wrote, and reviewed the manuscript. MO planned the study, analyzed the data, wrote, and reviewed the manuscript. All authors contributed to the article and approved the submitted version.

FUNDING

This study was supported by the National Institute of Developmental Psychiatry for Children and Adolescents, the São Paulo Research Foundation (FAPESP grants nos. 2011/21357-9, 2013/08531-5, 2014/50917-0, 2016/05865-8) and the Brazilian National Council for Scientific and Technological Development (CNPq 465550/2014-2).

ACKNOWLEDGMENTS

We thank Dr. Anke Henning and her former group at ETH University, Zürich, Switzerland for sharing their JPRESS sequence with us.

SUPPLEMENTARY MATERIAL

The Supplementary Material for this article can be found online at: https://www.frontiersin.org/articles/10.3389/fpsyt.2021.668304/full#supplementary-material

REFERENCES

1. Ruscio AM, Stein DJ, Chiu WT, Kessler RC. The epidemiology of obsessive-compulsive disorder in the National Comorbidity Survey Replication. *Mol Psychiatry.* (2010) 15:53–63. doi: 10.1038/mp.2008.94
2. Andrade LH, Wang YP, Andreoni S, Silveira CM, Alexandrino-Silva C, Siu ER, et al. Mental disorders in megacities: findings from the São Paulo megacity mental health survey, Brazil. *PLoS ONE.* (2012) 7:e31879. doi: 10.1371/journal.pone.0031879
3. Aoki Y, Aoki A, Suwa H. Reduction of N-acetylaspartate in the medial prefrontal cortex correlated with symptom severity in obsessive-compulsive disorder: meta-analyses of (1)H-MRS studies. *Transl Psychiatry.* (2012) 2:e153. doi: 10.1038/tp.2012.78
4. Simpson HB, Shungu DC, Bender J, Mao X, Xu X, Slifstein M, et al. Investigation of cortical glutamate-glutamine and γ-aminobutyric acid in obsessive-compulsive disorder by proton magnetic resonance spectroscopy. *Neuropsychopharmacology.* (2012) 37:2684–92. doi: 10.1038/npp.2012.132
5. Brennan BP, Rauch SL, Jensen JE, Pope HG. A critical review of magnetic resonance spectroscopy studies of obsessive-compulsive disorder. *Biol Psychiatry.* (2013) 73:24–31. doi: 10.1016/j.biopsych.2012.06.023
6. Zhang Z, Fan Q, Bai Y, Wang Z, Zhang H, Xiao Z. Brain Gamma-Aminobutyric Acid (GABA) concentration of the prefrontal lobe in unmedicated patients with obsessive-compulsive disorder: a research of magnetic resonance spectroscopy. *Shanghai Arch Psychiatry.* (2016) 28:263–70. doi: 10.11919/j.issn.1002-0829.216043
7. Li Y, Zhang CC, Kathrin Weidacker, Zhang Y, He N, Jin H, et al. Investigation of anterior cingulate cortex gamma-aminobutyric acid and glutamate-glutamine levels in obsessive-compulsive disorder using magnetic resonance spectroscopy. *BMC Psychiatry.* (2019) 19:164. doi: 10.1186/s12888-019-2160-1
8. de Salles Andrade JB, Ferreira FM, Suo C, Yücel M, Frydman I, Monteiro M, et al. An MRI study of the metabolic and structural abnormalities in obsessive-compulsive disorder. *Front Hum Neurosci.* (2019) 13:186. doi: 10.3389/fnhum.2019.00186
9. Vester EL, de Joode NT, Vriend C, Pouwels PJW, van den Heuvel OA. Little evidence for neurometabolite alterations in obsessive-compulsive disorder - a systematic review of magnetic resonance spectroscopy studies at 3 Tesla. *J Obsessive-Compulsive Relat Disord.* (2020) 25:100523. doi: 10.1016/j.jocrd.2020.100523
10. Pittenger C, Bloch MH, Williams K. Glutamate abnormalities in obsessive compulsive disorder: neurobiology, pathophysiology, and treatment. *Pharmacol Ther.* (2011) 132:314–32. doi: 10.1016/j.pharmthera.2011.09.006
11. Wu K, Hanna GL, Rosenberg DR, Arnold PD. The role of glutamate signaling in the pathogenesis and treatment of obsessive-compulsive disorder. *Pharmacol Biochem Behav.* (2012) 100:726–35. doi: 10.1016/j.pbb.2011.10.007
12. Stewart SE, Mayerfeld C, Arnold PD, Crane JR, O'Dushlaine C, Fagerness JA, et al. Meta-analysis of association between obsessive-compulsive disorder and the 3' region of neuronal glutamate transporter gene SLC1A1. *Am J Med Genet B Neuropsychiatr Genet.* (2013) 162B:367–79. doi: 10.1002/ajmg.b.32137
13. Marinova Z, Chuang DM, Fineberg N. Glutamate-modulating drugs as a potential therapeutic strategy in obsessive-compulsive disorder. *Curr Neuropharmacol.* (2017) 15:977–95. doi: 10.2174/1570159X15666170320104237
14. Karthik S, Sharma LP, Narayanaswamy JC. Investigating the role of glutamate in obsessive-compulsive disorder: current perspectives. *Neuropsychiatr Dis Treat.* (2020) 16:1003–13. doi: 10.2147/NDT.S211703
15. Rodriguez CI, Kegeles LS, Levinson A, Feng T, Marcus SM, Vermes D, et al. Randomized controlled crossover trial of ketamine in obsessive-compulsive disorder: proof-of-concept. *Neuropsychopharmacology.* (2013) 38:2475–83. doi: 10.1038/npp.2013.150
16. Rodriguez CI, Kegeles LS, Levinson A, Ogden RT, Mao X, Milak MS, et al. *In vivo* effects of ketamine on glutamate-glutamine and gamma-aminobutyric acid in obsessive-compulsive disorder: proof of concept. *Psychiatry Res.* (2015) 233:141–7. doi: 10.1016/j.pscychresns.2015.06.001
17. Oliver G, Dean O, Camfield D, Blair-West S, Ng C, Berk M, et al. N-acetyl cysteine in the treatment of obsessive compulsive and related disorders: a systematic review. *Clin Psychopharmacol Neurosci.* (2015) 13:12–24. doi: 10.9758/cpn.2015.13.1.12

18. Li F, Welling MC, Johnson JA, Coughlin C, Mulqueen J, Jakubovski E, et al. N-Acetylcysteine for pediatric obsessive-compulsive disorder: a small pilot study. *J Child Adolesc Psychopharmacol.* (2020) 30:32–7. doi: 10.1089/cap.2019.0041
19. Costa DLC, Diniz JB, Requena G, Joaquim MA, Pittenger C, Bloch MH, et al. Randomized, double-blind, placebo-controlled trial of N-acetylcysteine augmentation for treatment-resistant obsessive-compulsive disorder. *J Clin Psychiatry.* (2017) 78:e766–73. doi: 10.4088/JCP.16m11101
20. Sheshachala K, Narayanaswamy JC. Glutamatergic augmentation strategies in obsessive-compulsive disorder. *Indian J Psychiatry.* (2019) 61(Suppl 1):S58–65. doi: 10.4103/psychiatry.IndianJPsychiatry_520_18
21. International Obsessive-Compulsive Disorder Foundation Genetics Collaborative (IOCDF-GC) and OCD Collaborative Genetics Association Studies (OCGAS). Revealing the complex genetic architecture of obsessive-compulsive disorder using meta-analysis. *Mol Psychiatry.* (2018) 23:1181–8. doi: 10.1038/mp.2017.154
22. Stein DJ, Costa DLC, Lochner C, Miguel EC, Reddy YCJ, Shavitt RG, et al. Obsessive-compulsive disorder. *Nat Rev Dis Primers.* (2019) 5:52. doi: 10.1038/s41572-019-0102-3
23. Shephard E, Stern ER, van den Heuvel OA, Costa DLC, Batistuzzo MC, Godoy PBG, et al. Toward a neurocircuit-based taxonomy to guide treatment of obsessive-compulsive disorder. *Mol Psychiatry.* (2021). doi: 10.1038/s41380-020-01007-8. [Epub ahead of print].
24. Dougherty DD, Brennan BP, Stewart SE, Wilhelm S, Widge AS, Rauch SL. Neuroscientifically informed formulation and treatment planning for patients with obsessive-compulsive disorder: a review. *JAMA Psychiatry.* (2018) 75:1081–7. doi: 10.1001/jamapsychiatry.2018.0930
25. Graybiel AM, Rauch SL. Toward a neurobiology of obsessive-compulsive disorder. *Neuron.* (2000) 28:343–7. doi: 10.1016/S0896-6273(00)00113-6
26. Milad MR, Rauch SL. Obsessive-compulsive disorder: beyond segregated cortico-striatal pathways. *Trends Cogn Sci.* (2012) 16:43–51. doi: 10.1016/j.tics.2011.11.003
27. van den Heuvel OA, Remijnse PL, Mataix-Cols D, Vrenken H, Groenewegen HJ, Uylings HB, et al. The major symptom dimensions of obsessive-compulsive disorder are mediated by partially distinct neural systems. *Brain.* (2009) 132:853–68. doi: 10.1093/brain/awn267
28. Milad MR, Rosenbaum BL, Simon NM. Neuroscience of fear extinction: implications for assessment and treatment of fear-based and anxiety related disorders. *Behav Res Ther.* (2014) 62:17–23. doi: 10.1016/j.brat.2014.08.006
29. Zhu Y, Fan Q, Han X, Zhang H, Chen J, Wang Z, et al. Decreased thalamic glutamate level in unmedicated adult obsessive-compulsive disorder patients detected by proton magnetic resonance spectroscopy. *J Affect Disord.* (2015) 178:193–200. doi: 10.1016/j.jad.2015.03.008
30. O'Neill J, Lai TM, Sheen C, Salgari GC, Ly R, Armstrong C, et al. Cingulate and thalamic metabolites in obsessive-compulsive disorder. *Psychiatry Res Neuroimaging.* (2016) 254:34–40. doi: 10.1016/j.pscychresns.2016.05.005
31. Yücel M, Harrison BJ, Wood SJ, Fornito A, Wellard RM, Pujol J, et al. Functional and biochemical alterations of the medial frontal cortex in obsessive-compulsive disorder. *Arch Gen Psychiatry.* (2007) 64:946–55. doi: 10.1001/archpsyc.64.8.946
32. Rajendram R, Kronenberg S, Burton CL, Arnold PD. Glutamate genetics in obsessive-compulsive disorder: a review. *J Can Acad Child Adolesc Psychiatry.* (2017) 26:205–13.
33. Schulte RF, Lange T, Beck J, Meier D, Boesiger P. Improved two-dimensional J-resolved spectroscopy. *NMR Biomed.* (2006) 19:264–70. doi: 10.1002/nbm.1027
34. Schulte RF, Boesiger P. ProFit: two-dimensional prior-knowledge fitting of J-resolved spectra. *NMR Biomed.* (2006) 19:255–63. doi: 10.1002/nbm.1026
35. Scotti-Muzzi E, Chile T, Moreno R, Pastorello BF, da Costa Leite C, Henning A, et al. ACC Glu/GABA ratio is decreased in euthymic bipolar disorder I patients: possible *in vivo* neurometabolite explanation for mood stabilization. *Eur Arch Psychiatry Clin Neurosci.* (2020) 271:537–47. doi: 10.1007/s00406-020-01096-0
36. First MB, Spitzer RL, Gibbon M, Williams JBW. *Structured Clinical Interview for DSM-IV Axis I Disorders. Patient Edition (SCID-I/P)*. New York, NY: Biometrics Research, New York State Psychiatric Institute (1998).
37. Gorenstein C, Andrade LHSG, Zuardi AW. *Escalas de avaliação clínica em psiquiatria e psicofarmacologia*. São Paulo: Lemos Editorial (2000).
38. Goodman WK, Price LH, Rasmussen SA, Mazure C, Fleischmann RL, Hill CL, et al. The yale-brown obsessive compulsive scale. *I.* development, use, and reliability. *Arch Gen Psychiatry.* (1989) 46:1006–11. doi: 10.1001/archpsyc.1989.01810110048007
39. Fatori D, Costa DL, Asbahr FR, Ferrão YA, Rosário MC, Miguel EC, et al. Is it time to change the gold standard of obsessive-compulsive disorder severity assessment? Factor structure of the Yale-Brown Obsessive-Compulsive Scale. *Aust N Z J Psychiatry.* (2020) 54:732–42. doi: 10.1177/0004867420924113
40. Beck AT, Ward CH, Mendelson M, Mock J, Erbaugh J. An inventory for measuring depression. *Arch Gen Psychiatry.* (1961) 4:561–71. doi: 10.1001/archpsyc.1961.01710120031004
41. Beck AT, Epstein N, Brown G, Steer RA. An inventory for measuring clinical anxiety: psychometric properties. *J Consult Clin Psychol.* (1988) 56:893–7. doi: 10.1037/0022-006X.56.6.893
42. Cunha JA. *Manual da versão em português das Escalas Beck*. São Paulo: Casa do Psicólogo (2001).
43. Tkác I, Starcuk Z, Choi IY, Gruetter R. *In vivo* 1H NMR spectroscopy of rat brain at 1 ms echo time. *Magn Reson Med.* (1999) 41:649–56.3. doi: 10.1002/(SICI)1522-2594(199904)41:4<649::AID-MRM2>3.0.CO;2-G
44. Fuchs A, Boesiger P, Schulte RF, Henning A. ProFit revisited. *Magn Reson Med.* (2014) 71:458–68. doi: 10.1002/mrm.24703
45. Provencher SW. Estimation of metabolite concentrations from localized *in vivo* proton NMR spectra. *Magn Reson Med.* (1993) 30:672–9. doi: 10.1002/mrm.1910300604
46. Smith SA, Levante TO, de Beer R, Luyten PR, van Ormondt D. Computer simulations in magnetic resonance. an object-oriented programming approach. *J Magnet Reson.* (1994) 106:75–105. doi: 10.1006/jmra.1994.1008
47. Fan TWM. Metabolite profiling by one- and two-dimensional NMR analysis of complex mixtures. *Prog Nuclear Magnet Reson Spectroscop.* (1996) 28:161–219. doi: 10.1016/0079-6565(96)90002-3
48. Govindaraju V, Young K, Maudsley AA. Proton NMR chemical shifts and coupling constants for brain metabolites. *NMR Biomed.* (2000) 13:129–53. doi: 10.1002/1099-1492(200005)13:3<129::AID-NBM619>3.0.CO;2-V
49. Edden RA, Puts NA, Harris AD, Barker PB, Evans CJ. Gannet: a batch-processing tool for the quantitative analysis of gamma-aminobutyric acid–edited MR spectroscopy spectra. *J Magn Reson Imaging.* (2014) 40:1445–52. doi: 10.1002/jmri.24478
50. Cavassila S, Deval S, Huegen C, van Ormondt D, Graveron-Demilly D. Cramér-Rao bounds: an evaluation tool for quantitation. *NMR Biomed.* (2001) 14:278–83. doi: 10.1002/nbm.701
51. Storch EA, De Nadai AS, Conceição do Rosário M, Shavitt RG, Torres AR, Ferrão YA, et al. Defining clinical severity in adults with obsessive-compulsive disorder. *Compr Psychiatry.* (2015) 63:30–5. doi: 10.1016/j.comppsych.2015.08.007
52. Yücel M, Wood SJ, Wellard RM, Harrison BJ, Fornito A, Pujol J, et al. Anterior cingulate glutamate-glutamine levels predict symptom severity in women with obsessive-compulsive disorder. *Aust N Z J Psychiatry.* (2008) 42:467–77. doi: 10.1080/00048670802050546
53. Brennan BP, Tkachenko O, Schwab ZJ, Juelich RJ, Ryan EM, Athey AJ, et al. An examination of rostral anterior cingulate cortex function and neurochemistry in obsessive-compulsive disorder. *Neuropsychopharmacology.* (2015) 40:1866–76. doi: 10.1038/npp.2015.36
54. Zurowski B, Kordon A, Weber-Fahr W, Voderholzer U, Kuelz AK, Freyer T, et al. Relevance of orbitofrontal neurochemistry for the outcome of cognitive-behavioural therapy in patients with obsessive-compulsive disorder. *Eur Arch Psychiatry Clin Neurosci.* (2012) 262:617–24. doi: 10.1007/s00406-012-0304-0
55. Rosenberg DR, Mirza Y, Russell A, Tang J, Smith JM, Banerjee SP, et al. Reduced anterior cingulate glutamatergic concentrations in childhood OCD and major depression versus healthy controls. *J Am Acad Child Adolesc Psychiatry.* (2004) 43:1146–53. doi: 10.1097/01.chi.0000132812.44664.2d
56. Arnold PD, Macmaster FP, Richter MA, Hanna GL, Sicard T, Burroughs E, et al. Glutamate receptor gene (GRIN2B) associated with reduced anterior cingulate glutamatergic concentration in

pediatric obsessive-compulsive disorder. *Psychiatry Res.* (2009) 172:136–9. doi: 10.1016/j.pscychresns.2009.02.005
57. Kalra SK, Swedo SE. Children with obsessive-compulsive disorder: are they just "little adults"? *J Clin Invest.* (2009) 119:737–46. doi: 10.1172/JCI37563
58. Fullana MA, Abramovitch A, Via E, López-Sola C, Goldberg X, Reina N, et al. Diagnostic biomarkers for obsessive-compulsive disorder: a reasonable quest or ignis fatuus? *Neurosci Biobehav Rev.* (2020) 118:504–13. doi: 10.1016/j.neubiorev.2020.08.008
59. Chakrabarty K, Bhattacharyya S, Christopher R, Khanna S. Glutamatergic dysfunction in OCD. *Neuropsychopharmacology.* (2005) 30:1735–40. doi: 10.1038/sj.npp.1300733
60. Bhattacharyya S, Khanna S, Chakrabarty K, Mahadevan A, Christopher R, Shankar SK. Anti-brain autoantibodies and altered excitatory neurotransmitters in obsessive-compulsive disorder. *Neuropsychopharmacology.* (2009) 34:2489–96. doi: 10.1038/npp.2009.77
61. Yüksel C, Öngür D. Magnetic resonance spectroscopy studies of glutamate-related abnormalities in mood disorders. *Biol Psychiatry.* (2010) 68:785–94. doi: 10.1016/j.biopsych.2010.06.016
62. Kondo HM, Lin IF. Excitation-inhibition balance and auditory multistable perception are correlated with autistic traits and schizotypy in a non-clinical population. *Sci Rep.* (2020) 10:8171. doi: 10.1038/s41598-020-65126-6
63. Bustillo JR, Chen H, Jones T, Lemke N, Abbott C, Qualls C, et al. Increased glutamine in patients undergoing long-term treatment for schizophrenia: a proton magnetic resonance spectroscopy study at 3 T. *JAMA Psychiatry.* (2014) 71:265–72. doi: 10.1001/jamapsychiatry.2013.3939
64. Tükel R, Aydin K, Ertekin E, Özyildirim S, Taravari V. Proton magnetic resonance spectroscopy in obsessive-compulsive disorder: evidence for reduced neuronal integrity in the anterior cingulate. *Psychiatry Res.* (2014) 224:275–80. doi: 10.1016/j.pscychresns.2014.08.012
65. Hatchondo L, Jaafari N, Langbour N, Maillochaud S, Herpe G, Guillevin R, et al. H magnetic resonance spectroscopy suggests neural membrane alteration in specific regions involved in obsessive-compulsive disorder. *Psychiatry Res Neuroimaging.* (2017) 269:48–53. doi: 10.1016/j.pscychresns.2017.08.010

Conflict of Interest: The authors declare that the research was conducted in the absence of any commercial or financial relationships that could be construed as a potential conflict of interest.

The reviewer JO'N declared a shared consortium with several of the authors, MB, MH, JD, and EM, at time of review.

frontiers in Psychiatry

BRIEF RESEARCH REPORT
published: 05 July 2021
doi: 10.3389/fpsyt.2021.656468

Cortical Glutamate and GABA Changes During Early Abstinence in Alcohol Dependence and Their Associations With Benzodiazepine Medication

Guoying Wang[1], Wolfgang Weber-Fahr[1], Ulrich Frischknecht[2,3], Derik Hermann[2,4], Falk Kiefer[2], Gabriele Ende[1] and Markus Sack[1]*

[1] Department of Neuroimaging, Central Institute of Mental Health, Mannheim Medical Faculty, University of Heidelberg, Mannheim, Germany, [2] Department of Addiction Medicine and Addictive Behavior, Central Institute of Mental Health, Mannheim Medical Faculty, University of Heidelberg, Mannheim, Germany, [3] German Institute of Addiction and Prevention Research, Catholic University of Applied Sciences, Cologne, Germany, [4] Therapieverbund Ludwigsmühle, Landau in der Pfalz, Germany

OPEN ACCESS

Edited by:
Richard Edden, Johns Hopkins University, United States

Reviewed by:
Eric C. Porges, University of Florida, United States
Muhammad Saleh, University of Maryland, United States

***Correspondence:**
Guoying Wang
guoying.wang@zi-mannheim.de

Specialty section:
This article was submitted to Psychopharmacology, a section of the journal Frontiers in Psychiatry

Received: *21 January 2021*
Accepted: *01 June 2021*
Published: *05 July 2021*

Citation:
Wang G, Weber-Fahr W, Frischknecht U, Hermann D, Kiefer F, Ende G and Sack M (2021) Cortical Glutamate and GABA Changes During Early Abstinence in Alcohol Dependence and Their Associations With Benzodiazepine Medication. Front. Psychiatry 12:656468. doi: 10.3389/fpsyt.2021.656468

In this report, we present cross-sectional and longitudinal findings from single-voxel MEGA-PRESS MRS of GABA as well as Glu, and Glu + glutamine (Glx) concentrations in the ACC of treatment-seeking alcohol-dependent patients (ADPs) during detoxification (first 2 weeks of abstinence). The focus of this study was to examine whether the amount of benzodiazepine administered to treat withdrawal symptoms was associated with longitudinal changes in Glu, Glx, and GABA. The tNAA levels served as an internal quality reference; in agreement with the vast majority of previous reports, these levels were initially decreased and normalized during the course of abstinence in ADPs. Our results on Glu and Glx support hyperglutamatergic functioning during alcohol withdrawal, by showing higher ACC Glu and Glx levels on the first day of detoxification in ADPs. Withdrawal severity is reflected in cumulative benzodiazepine requirements throughout the withdrawal period. The importance of withdrawal severity for the study of GABA and Glu changes in early abstinence is emphasized by the benzodiazepine-dependent Glu, Glx, and GABA changes observed during the course of abstinence.

Keywords: alcohol dependence, glutamate, GABA, benzodiazepine, withdrawal, N-acetylaspartate, 1H-MR-spectroscopy

INTRODUCTION

Although benzodiazepines (BZD) are often used in clinical management of alcohol withdrawal, little is known about their effects on cortical concentrations of gamma aminobutyric acid (GABA) and glutamate (Glu) in alcohol dependent patients (ADPs). The present study aimed to detect longitudinal changes of the Glu and GABA concentrations in the anterior cingulate cortex (ACC) during alcohol detoxification treatment, by using proton magnetic resonance spectroscopy (MRS). Furthermore, we hypothesized a potential role of BZD in these longitudinal dynamic changes.

The alcohol withdrawal syndrome is characterized by excessive glutamatergic neurotransmission and reduced GABA functioning as well as a reduced number of $GABA_A$

receptors which regulate the chloride channel, both indicated as key features of alcohol-dependent neuroplasticity (1–3). Our previous studies had focused on the excitatory neurotransmitter Glu and other brain metabolites [total N-acetylaspartate (tNAA), and total choline (tCh)] (4–6) during acute withdrawal and continued abstinence in non-medicated ADPs. The ACC was chosen as region of interest due to its important role in alcohol dependence and relapse. Our previous findings indicated that ACC Glu concentrations were elevated in non-medicated ADPs during acute withdrawal and normalized after 2 weeks of abstinence. In addition, a lower ACC NAA level due to chronic alcohol consumption and partial recovery during continued abstinence was observed repeatedly (7, 8).

GABA is the primary inhibitory neurotransmitter, and abnormalities in synaptic inhibition mediated by GABAergic neurons are associated with alcohol dependence (9). This GABAergic dysfunction leads to neuronal disinhibition, adding to the hyperarousal of hyperglutamatergic states which are thought to be the basis for alcohol withdrawal (10). Since cortical GABA concentrations are small and the peak is hidden under the creatine resonance without spectral editing, only a few MRS studies have reported on the effects of alcohol dependence on concentrations of GABA, showing non consistent results (10–12). Moreover, recent studies report that brain GABA levels in healthy subjects decreased after administration of BZD (13, 14). However, although BZD are the first-line pharmacological treatment of alcohol withdrawal symptoms by enhancing the activation of GABAergic neurons (2), their role in modulating brain GABA and Glu is still not clear.

This report presents cross-sectional and longitudinal findings of single voxel MEGA-PRESS MRS, focusing on absolute quantification of GABA, Glu, and Glu + glutamine (Glx) concentrations in the ACC of treatment-seeking ADPs during detoxification and early abstinence. Our primary focus of this study was to explore, whether the amount of BZD administered to ameliorate withdrawal symptoms was associated with the extent of longitudinal changes of Glu, Glx, and GABA.

METHODS

The present study comprised 20 ADPs and 22 age- and sex-matched healthy controls (HCs). Patients seeking voluntary treatment for their alcohol use disorders were recruited from a specialized inpatient treatment facility. All participants provided written informed consent before study participation. The study was approved by the Ethics committee of the Medical Faculty Mannheim, Heidelberg University (2007-234N-M).

Twenty (15 males, 5 females) ADPs were scanned twice with MRS at 3 T (Siemens, TimTrio systems), during alcohol withdrawal (TP1: day 1 of detoxification) and on day 14 of abstinence (TP2), respectively. HCs (18 males, 4 females) were scanned once. Of the 20 ADPs, 15 patients received BZD medication after the 1st MRS measurement. BZD doses varied according to withdrawal severity, assessed via Clinical Institute Withdrawal Assessment for alcohol (CIWA-Ar) until withdrawal symptoms had subsided (see **Table 1**). CIWA-Ar scores reflect the number and intensity of typical alcohol withdrawal symptoms (e.g., sweating, tremor, headache, nausea) assessed by trained personal. Scores above 10 typically indicate the need for BZD treatment to prevent seizures or delirium tremens. Diazepam was the only BZD used in the present sample.

MRS data was obtained using a MEGA-PRESS sequence (15) with TR/TE = 3,000/68 ms, 192 averages (96 "edit on," 96 "edit off"), voxel size 20 × 30 × 40 mm^3 as we had previously used in other studies (16). The MEGA-PRESS employed was based on the Siemens WIP package for VB15 which was ported to VB17 and expanded to include control of the reflection frequency. The editing pulse (gauss shape, duration: 20.36 ms, bandwidth: 44 Hz) was mirrored at 1.7 ppm, thus suppressing MM contributions in the GABA signal (17). Due to the low sensitivity of the GABA signal we chose a bigger voxel – suitable for GABA detection compared to our previous Glu study (4). For absolute quantification, an additional water-unsuppressed PRESS spectrum was acquired with TR/TE = 10,000/30 ms to minimize water relaxation effects. No other measurements except localizer and a 3D-anatomical MPRAGE were conducted preceding MEGA-PRESS spectroscopy.

The acquired raw data (Siemens' "twix" files) was post-processed via an in-house-developed algorithm written in MATLAB (The Mathworks Inc.). After reading the raw data, the single coil elements were phased and weighted. Weighting was based on coil SNR. The coil elements were then combined and the water-unsuppressed data was not further processed. The individual averages of the water-suppressed data were split in "edit on" and "edit off" and further processed separately but in the same manner. Correction of spectral misalignments was done by adjusting frequency and phase using a Nelder-Mead simplex algorithm (implemented in MATLAB's "fminsearch") minimizing the least square error between the single spectra and a template within a predefined area in the frequency domain. As template the very first obtained "edit on" and "edit off" spectra were chosen, respectively, and a frequency range of 2.1–5.8 ppm for alignment correction was selected, thus covering the water and metabolites signal except NAA. Furthermore, to minimize the influence of noise on the adjustment, the spectra underwent temporarily an apodization of 15Hz during correction. To identify outlier spectra, the absolute sum of square differences of all spectra to their median spectrum in a range of 1.85–4.2 ppm was calculated. Averages were excluded in case of a more than three scaled median absolute deviation (MATLAB's "isoutlier"). This procedure of finding outliers and redetermination of the median was repeatedly done until no more outliers were detected. Exclusion of spectra was always pairwise. Lastly, the two resulting "edit on" and "edit off" spectra were aligned to each other, subtracted and saved for further quantification.

Quantification was performed with LCModel (v6.3-1k) using a basis dataset which was created with VeSPA (https://scion.duhs.duke.edu/vespa/project) and the available "MEGA-PRESS" pulse sequence simulation. It includes the resonances of the following metabolites: GABA, Gln, Glu, GSH, NAA, Cr, NAAG, Eth, mI, Lac, Ala, Asp, Tau, Scyllo, GPC, PCr, PCh, Glyc (for difference spectrum: GABA, Gln, Glu, GSH, NAA, NAAG, Eth, Glyc). As recommended the option "SPTYPE = "mega-press-3"" was used

TABLE 1 | Characteristics and ACC metabolites concentrations of the ADP and HC samples.

	ADP (Mean ± SD)	HC (Mean ± SD)	F or *t*	*p*	Partial Eta Squared	Observed power
Age	45.70 ± 9.62	46.41 ± 11.67	0.214	0.345		
Male/Female	15/5	18/4	−0.27	0.789		
LDH_Total (g)	654,963 ± 301,312	55,481 ± 77,205	66.861	0.000	0.663	1.000
LDH_last 1 2Months (g)	66,842 ± 46,482	1,963 ± 2,117	16.529	0.000	0.327	0.977
Diazepam (mg)	59.00 ± 39.29	–				
CIWA_unmed (max)#	8.94 ± 4.63	–				
Glu TP1 (i.u.)	10.20 ± 1.14	9.56 ± 0.67	5.002	0.031	0.111	0.588
Glx TP1 (i.u.)	12.53 ± 1.19	11.86 ± 0.94	4.181	0.047	0.095	0.514
GABA TP1 (i.u.)	2.71± 0.77	2.70 ± 0.58	0.002	0.965	0.000	0.050
tNAA TP1 (i.u.)	13.41 ± 0.75	14.07 ± 0.64	9.261	0.004	0.188	0.844
tCr TP1 (i.u.)	12.23 ± 1.21	11.91 ± 1.14	0.805	0.375	0.020	0.141
Glu TP2 (i.u.)	9.80 ± 0.63					
Glx TP2 (i.u.)	12.31 ± 0.84					
GABA TP2 (i.u.)	2.55 ± 0.49					
tNAA TP2 (i.u.)	17.09 ± 0.91					
tCr TP2 (i.u.)	12.20 ± 0.82					

ADP, alcohol dependent Patients; HC, healthy controls; BDZs, benzodiazepine; HC, healthy controls; Mean ± SD, Mean ± Standard Deviation; Glu, glutamate; Glx, glutamate plus glutamine; GABA, gamma aminobutyric acid; tNAA, total N-acetylaspartate;LDH, Lifetime drinking history; CIWA, clinical institute withdrawal assessment for alcohol.
#CIWA_unmed (max): maximum CIWA score of non-medicated patients before BZDs were administered.
TP1 (day 1 of detoxification before BZDs were administered); TP2 (day 14 of abstinence).

for the difference spectra. Absolute quantification was done based on (18) with voxel tissue compartments calculated by "SegSpec" (19) and, thus, adjusted for chemical shift displacement. Water and metabolite relaxation values were taken from (12) and (20–22), respectively, whereby the latter were averaged for GM and WM. All spectra underwent visual inspection by MRS experts to rate spectral quality and identify any spectra of poor quality. Furthermore, all LCModel Cramér Rao Lower Bounds of the analyzed metabolite signals were < 20%. The voxel location as well as spectra are shown in **Figure 1**. The GABA levels were obtained from the "difference" spectra, all other reported metabolite levels from the "edit-off" spectra.

Statistics

Cross-sectional analysis of the absolute quantified metabolite levels were performed using multivariate analysis of variance (MANOVA) with group as between-subject factor and four dependent variables (GABA, Glu, Glx, tNAA). For longitudinal analysis repeated measurements ANOVA with total BZD dosage as covariate were used, followed by simple correlations between total BZD dosage and metabolites' respective difference values. We regarded *p*-values < 0.05 as significant. All second level analyses were preformed using SPSS (IBM SPSS Statistics 26).

To investigate the comparability of spectral quality and voxel location among groups and sessions, frequency drifts, linewidths evaluated by LCModel and voxel overlap were analyzed.

Although the hypothesis is clearly directed to Glu, we decided to present Glu and Glx since the MEGA-PRESS sequence is not optimal to distinguish both measures.

RESULTS

Cross-Sectional Group Comparisons on Day 1 of Detoxification (TP1)

On day 1 of detoxification, a MANOVA analysis yielded a significant lower ACC tNAA concentration [$F(1, 40) = 9.261$, $p = 0.004$, partial $\eta^2 = 0.188$), higher ACC Glu [$F(1,40) = 5.002$, $p = 0.031$, partial $\eta^2 = 0.111$] and higher Glx levels [$F(1,40) = 4.181$, $p = 0.047$, partial $\eta^2 = 0.095$] in ADPs compared to HCs. Neither tCr, nor GABA concentrations differed significantly between groups (all $p > 0.1$) (see **Table 1**).

Longitudinal Changes in ADPs of Glu, Glx and GABA Are Associated With BZD Dosage

Since we aimed to investigate the influence of BZD on the neurotransmitters Glu and GABA during detoxification and continued abstinence, we evaluated the correlation between the amount of BZD received for amelioration of withdrawal symptoms and Glu, Glx, and GABA levels. For this we used the subgroup of patients that received BZD ($n = 15$, 11 male, 4 female, age = 47.07 ± 8.34). Additionally, we used the amount of BZD as a covariate in a repeated measurements ANOVA analysis.

The amount of BZD received was negatively correlated with the change of Glx ($r = -0.762$, $p = 0.001$), Glu ($r = -0.718$, $p = 0.003$) and GABA ($r = -0.578$, $p = 0.024$) between TP1 and TP2 (TP2-TP1). No such relation was observed for tCr ($r = -0.345$, $p = 0.208$) and tNAA ($r = -0.128$, $p = 0.650$) although tNAA

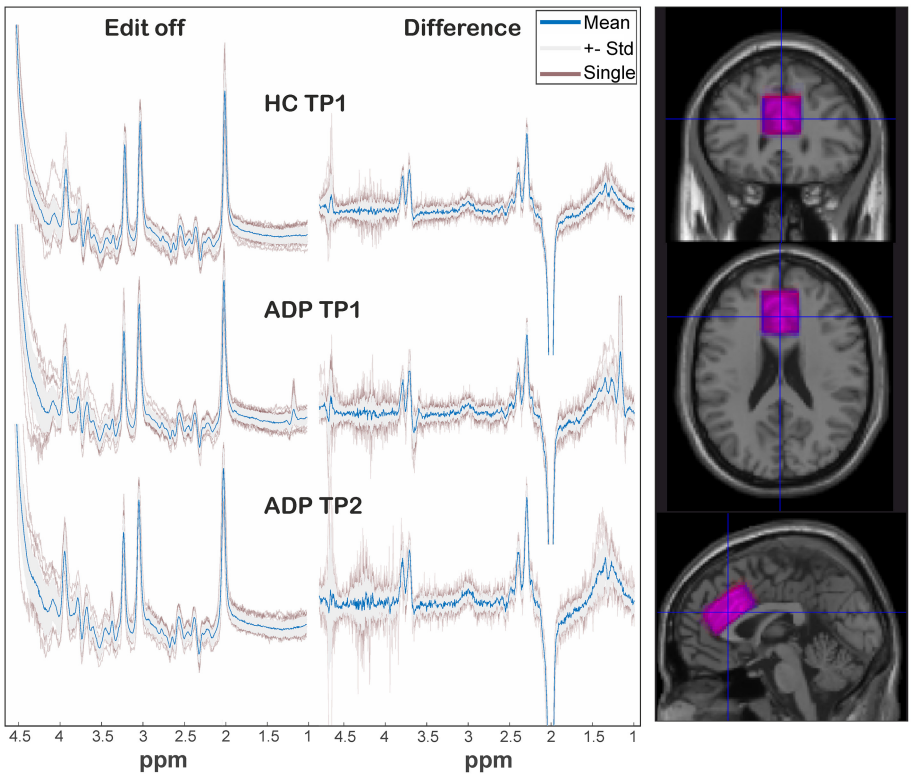

FIGURE 1 | On the left: representation of spectra among groups and sessions. The individual spectra (transparent red) are overlaid by the standard deviation (gray area) and corresponding mean spectrum (blue). On the right: overlap of mean voxel location of HC (blue) and ADP (red) at TP1 after transformation in a template space.

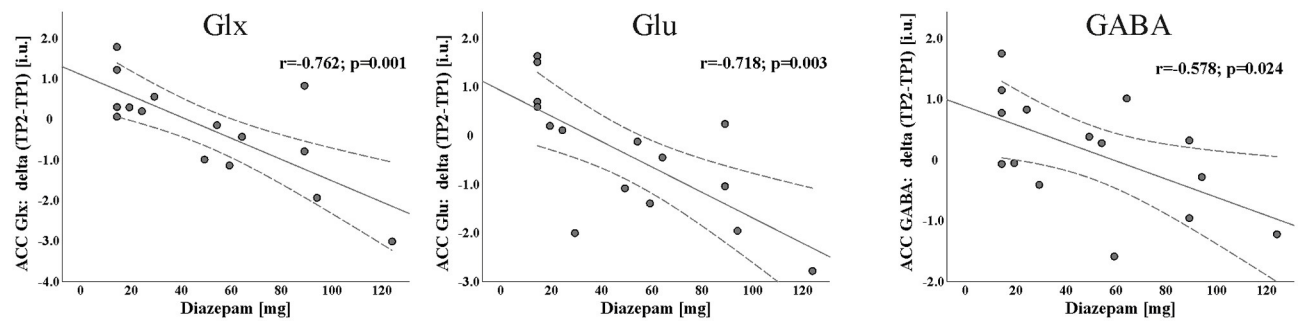

FIGURE 2 | Scatterplot with linear fit line of the significant negative association between Diazepam and longitudinal changes of Glx, Glu, and GABA concentrations during first 2 weeks of abstinence [day14 of abstinence (TP2) - day 1 of detoxification (TP1)].

levels increased significantly [$F(1, 13) = 9.563$, $p = 0.009$, partial $\eta^2 = 0.424$] in ADPs from TP1 to TP2 (see **Figure 2**).

We found a significant increase in GABA levels [$F(1, 13) = 6.147$, $p = 0.028$, partial $\eta^2 = 0.321$, TP1: 2.71 ± 0.82 i.u., TP2: 2.84 ± 0.36 i.u.] as well as significant decreases in Glx [$F(1, 13) = 8.799$, $p = 0.011$, partial $\eta^2 = 0.404$, TP1: 12.41 ± 1.18 i.u., TP2: 12.20 ± 0.88 i.u.] and Glu levels [$F(1, 13) = 4.758$, $p = 0.048$, partial $\eta^2 = 0.268$, TP1:10.12 ± 1.28 i.u., TP2: 9.74 ± 0.68 i.u.] after 2 weeks of abstinence in the 15 patients receiving BZD. BZD dosage showed a significant interaction effect with all three neurotransmitter measures (see **Figure 3**).

Comparability of Spectroscopic Measurements Between Groups

Figure 1 depicts a visual overview of acquired spectra and voxel overlap of HCs and ADPs at TP1. Analysis of standard deviations of individual frequency drifts [HC_{TP1}: 0.73 ± 0.33; ADP_{TP1}: 0.86 ± 0.24; ADP_{TP2}: 0.72 ± 0.29; mean ± SD (Hz)] and linewidths [HC_{TP1}: 0.0367 ± 0.0037; ADP_{TP1}: 0.038 ± 0.0046; ADP_{TP2}: 0.0387 ± 0.0067; mean ± SD (ppm)] revealed no significant differences (all $p > 0.1$). The calculated individual voxel overlap in ADPs between TP1 and TP2 yielded a mean coverage of 90

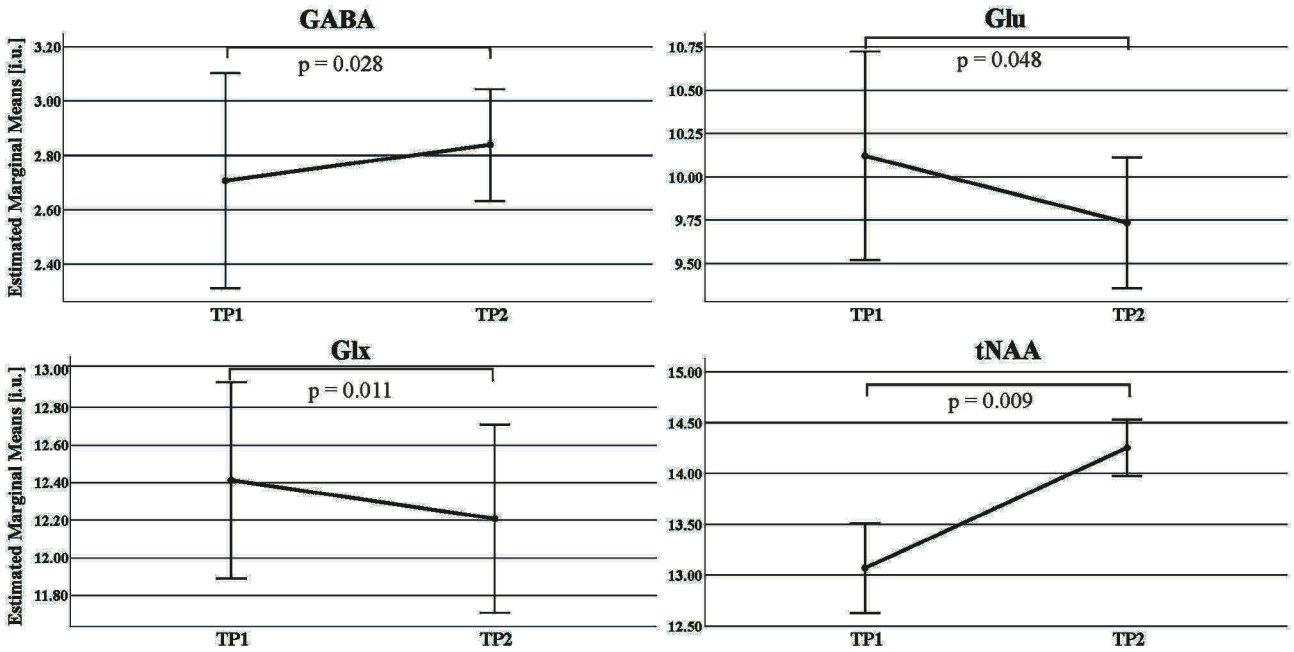

FIGURE 3 | Estimated Marginal Means and standard error of GABA, Glu, Glx, tNAA concentrations in the ACC in ADP across two MRS scans: TP1 (day 1 of detoxification); TP2 (day 14 of abstinence). Estimated marginal means: mean value adjusted for covariate (amount of Diazepam) in the repeated ANOVA model.

± 5 % (including one outlier with 78% coverage) and revealed no significant difference in bulk tissue fractions calculated as gray matter/(gray matter + white matter) (HC_{TP1}: 0.594 ± 0.031, ADP_{TP1}: 0.597 ± 0.046, ADP_{TP2}: 0.602 ± 0.045; mean ± SD).

DISCUSSION

In line with our previous findings, we found decreased tNAA on day 1 of detoxification in ADPs compared to HCs and a significant increase in tNAA levels during the first 2 weeks of abstinence in ADPs. This was repeatedly and robustly found before (7), which speaks for the plausibility of the sample and the data. Moreover, although the present study consists of patients with and without severe withdrawal symptoms, indicated by big variations in the CIWA score and the BZD values, patients at the first day of abstinence showed higher Glu and Glx concentrations in the ACC. However, in compliance with our previous findings from a different sample (4, 23) our results support the glutamate hyperexcitability hypothesis of alcoholism (24), representing an up-regulated glutamatergic activity during alcohol withdrawal as a consequence of counterbalancing the effects of chronic alcohol intake.

The correlation results indicate patients with greater decline in ACC GABA levels after 2 weeks of abstinence have received higher amounts of Diazepam. This is in line with previous MRS findings, showing a decrease in GABA levels after BZD administration in healthy subjects (13, 14). Notably, contrasting with previous studies indicating that BZD have no effects on Glx and Glu levels in HCs (25–27), our finding suggests that with higher total BZD dosages the patients received, ACC Glx and Glu levels declined to a bigger extent between TP1 and TP2. Unlike other studies, which mostly investigate Glx (Glu) level changes after acute administration of BZD, our sample received prolonged administration of BZD.

Moreover, when including total BZD dosage as a covariate, the Glx and Glu levels showed significant decreases between day 1 of detoxification and after 14 days of abstinence. This finding is in line with (4) showing elevated Glu levels during acute alcohol withdrawal and their amelioration within 2 weeks of abstinence. Opposite to our findings, Umhau et al. (28) reported a non-significant trend for an increase of Glu in a placebo-treatment abstinent ADPs group. This discrepancy may be driven by different baseline levels of Glu between the two studies. Instead of a measurement during acute withdrawal before BZD were administered, their first scan was on day 5 of abstinence, when some ADPs already had 4 days of BZD treatment. Moreover, as they did not include a healthy control group in their study, no conclusions on relative Glu levels at the beginning of treatment can be drawn.

Like in the study of Mon A, et al. (10), the group comparisons on day 1 of detoxification did not yield significant differences for GABA levels in our study. But our longitudinal analyses that included BZD dosage as covariate showed comparable patterns of GABA increase as did another MRS study in ADPs (11). The finding of a decrease in GABA after alcohol injection in healthy participants supports a GABA decrease as a result of alcohol consumption rather than withdrawal from alcohol (29).

The MRS detectable metabolite concentrations of Glx, Glu and GABA largely represent the signal from the respective

neurotransmitters stored in presynaptic vesicles (state-related intracellular levels) rather than representing transient synaptic activity. This background in mind, we assume that the inverse trajectories of Glu and GABA after 14 days of abstinence in ADPs are associated with withdrawal-induced imbalance and recovery from neuroadaptations in the glutamine/glutamate – GABA cycle (30) where glutamine acts as a precursor for the synthesis of Glu, which itself is the direct precursor of GABA.

Interactions between chronic alcohol exposure, receptor expressions and binding potentials are beyond the scope of this article and are not yet fully understood (31). In addition, glutamatergic and GABAergic system modulations after chronic ethanol exposure are suggested to last over 120 days or even the whole life (9, 32). We assume that after the BZD treatment cessation the "hyperexcitable withdrawal-like" neurochemical state can occur repeatedly in ADPs over the long-term abstinence. This might manifest in heightened Glu levels caused by exposure to alcohol-related cues (smell, pictures) or social stress. Further research is needed to elucidate this hypothesis.

A limitation of the used MM suppression scheme is its susceptibility to frequency drift. Although neither a significant difference between TP1 and TP2 in frequency drift nor its associations with spectral quality were found, numerical differences point to slightly more movement in ADPs at TP1. Therefore, as drift can induce both increases and decreases of the GABA signal (33), we cannot completely rule out that this affected our findings of increased GABA levels.

Despite the limitations of a small sample size and a voxel that is much bigger and contained more white matter compared to our previous study on Glu changes during alcohol withdrawal (4), our findings corroborate our own previous studies and those of other groups. Addressing the question raised by (11) our results furthermore indicate that withdrawal severity during the full period of withdrawal (reflected by cumulated BZD needs) has to be taken into account when investigating neurotransmitter changes in ADPs during early abstinence.

DATA AVAILABILITY STATEMENT

The raw data supporting the conclusions of this article will be made available by the authors, without undue reservation.

ETHICS STATEMENT

This study was reviewed and approved by the Ethics Committee of the Mannheim Medical Faculty of the Heidelberg University, Germany. All patients/participants provided their written informed consent to participate in this study.

AUTHOR CONTRIBUTIONS

GW was involved in data acquisition, statistical analysis, and writing of the manuscript. MS was responsible for MRS data, post-processing, and writing the manuscript. UF was involved in the planning of the study, patient recruitment and characterization, and interpretation of the results. WW-F was involved in statistical analysis and writing of the manuscript. GE was involved in the planning of the study, responsible for the supervision of the study, and coedited the manuscript. FK and DH were involved in the planning of the study and recruitment of ADP patients. All authors contributed to the article and approved the submitted version.

FUNDING

This study was supported by a grant from the Deutsche Forschungsgemeinschaft (DFG) to GE and FK within the SFB 636.

ACKNOWLEDGMENTS

We acknowledge Gunilla Oberthuer for her technical skills operating the scanner and obtaining the best possible shim and her social skills in handling the ADP patients and convincing them to endure the measurement.

REFERENCES

1. Brousse G, Arnaud B, Vorspan F, Richard D, Dissard A, Dubois M, et al. Alteration of glutamate/GABA balance during acute alcohol withdrawal in emergency department: a prospective analysis. *Alcohol Alcohol.* (2012) 47:501–8. doi: 10.1093/alcalc/ags078
2. Lejoyeux M, Solomon J, Ades J. Benzodiazepine treatment for alcohol-dependent patients. *Alcohol Alcohol.* (1998) 33:563–75. doi: 10.1093/alcalc/33.6.563
3. Sachdeva A, Choudhary M, Chandra M. Alcohol withdrawal syndrome: benzodiazepines and beyond. *J Clin Diagn Res.* (2015) 9:VE01–VE7. doi: 10.7860/JCDR/2015/13407.6538
4. Hermann D, Weber-Fahr W, Sartorius A, Hoerst M, Frischknecht U, Tunc-Skarka N, et al. Translational magnetic resonance spectroscopy reveals excessive central glutamate levels during alcohol withdrawal in humans and rats. *Biol Psychiatry.* (2012) 71:1015–21. doi: 10.1016/j.biopsych.2011.07.034
5. Frischknecht U, Hermann D, Tunc-Skarka N, Wang GY, Sack M, van Eijk J, et al. Negative association between MR-spectroscopic glutamate markers and gray matter volume after alcohol withdrawal in the hippocampus: a translational study in humans and rats. *Alcohol Clin Exp Res.* (2017) 41:323–33. doi: 10.1111/acer.13308
6. Ende G, Welzel H, Walter S, Weber-Fahr W, Diehl A, Hermann D, et al. Monitoring the effects of chronic alcohol consumption and abstinence on brain metabolism: a longitudinal proton magnetic resonance spectroscopy study. *Biol Psychiatry.* (2005) 58:974–80. doi: 10.1016/j.biopsych.2005.05.038
7. Meyerhoff DJ, Durazzo TC, Ende G. Chronic alcohol consumption, abstinence and relapse: brain proton magnetic resonance spectroscopy studies in animals and humans. *Curr Top Behav Neurosci.* (2013) 13:511–40. doi: 10.1007/978-3-642-28720-6_131
8. Zahr NM, Pfefferbaum A. Alcohol's effects on the brain: neuroimaging results in humans and animal models. *Alcohol Res.* (2017) 38:183–206.
9. Olsen RW, Liang J. Role of GABAA receptors in alcohol use disorders suggested by chronic intermittent ethanol (CIE) rodent model. *Mol Brain.* (2017) 10:45. doi: 10.1186/s13041-017-0325-8
10. Mon A, Durazzo TC, Meyerhoff DJ. Glutamate, GABA, and other cortical metabolite concentrations during early abstinence from alcohol and their associations with neurocognitive changes. *Drug Alcohol Depend.* (2012) 125:27–36. doi: 10.1016/j.drugalcdep.2012.03.012

11. Prisciandaro JJ, Schacht JP, Prescot AP, Brenner HM, Renshaw PF, Brown TR, et al. Intraindividual changes in brain GABA, glutamate, and glutamine during monitored abstinence from alcohol in treatment-naive individuals with alcohol use disorder. *Addict Biol.* (2020) 25:e12810. doi: 10.1111/adb.12810
12. Prisciandaro JJ, Schacht JP, Prescot AP, Renshaw PF, Brown TR, Anton RF. Brain glutamate, GABA, and glutamine levels and associations with recent drinking in treatment-naive individuals with alcohol use disorder versus light drinkers. *Alcohol Clin Exp Res.* (2019) 43:221–6. doi: 10.1111/acer.13931
13. Ferland MC, Therrien-Blanchet JM, Proulx S, Klees-Themens G, Bacon BA, Dang Vu TT, et al. Transcranial magnetic stimulation and H(1)-magnetic resonance spectroscopy measures of excitation and inhibition following lorazepam administration. *Neuroscience.* (2021) 452:235–46. doi: 10.1016/j.neuroscience.2020.11.011
14. Goddard AW, Mason GF, Appel M, Rothman DL, Gueorguieva R, Behar KL, et al. Impaired GABA neuronal response to acute benzodiazepine administration in panic disorder. *Am J Psychiatry.* (2004) 161:2186–93. doi: 10.1176/appi.ajp.161.12.2186
15. Mescher M, Merkle H, Kirsch J, Garwood M, Gruetter R. Simultaneous in vivo spectral editing and water suppression. *NMR Biomed.* (1998) 11:266–72. doi: 10.1002/(SICI)1099-1492(199810)11:6<266::AID-NBM530>3.0.CO;2-J
16. Aufhaus E, Weber-Fahr W, Sack M, Tunc-Skarka N, Oberthuer G, Hoerst M, et al. Absence of changes in GABA concentrations with age and gender in the human anterior cingulate cortex: a MEGA-PRESS study with symmetric editing pulse frequencies for macromolecule suppression. *Magn Reson Med.* (2013) 69:317–20. doi: 10.1002/mrm.24257
17. Henry PG, Dautry C, Hantraye P, Bloch G. Brain GABA editing without macromolecule contamination. *Magn Reson Med.* (2001) 45:517–20. doi: 10.1002/1522-2594(200103)45:3<517::AID-MRM1068>3.0.CO;2-6
18. Gasparovic C, Song T, Devier D, Bockholt HJ, Caprihan A, Mullins PG, et al. Use of tissue water as a concentration reference for proton spectroscopic imaging. *Magn Reson Med.* (2006) 55:1219–26. doi: 10.1002/mrm.20901
19. Weber-Fahr W, Ende G, Braus DF, Bachert P, Soher BJ, Henn FA, et al. A fully automated method for tissue segmentation and CSF-correction of proton MRSI metabolites corroborates abnormal hippocampal NAA in schizophrenia. *Neuroimage.* (2002) 16:49–60. doi: 10.1006/nimg.2002.1057
20. Mlynarik V, Gruber S, Moser E. Proton T (1) and T (2) relaxation times of human brain metabolites at 3 Tesla. *NMR Biomed.* (2001) 14:325–31. doi: 10.1002/nbm.713
21. Puts NA, Barker PB, Edden RA. Measuring the longitudinal relaxation time of GABA in vivo at 3 Tesla. *J Magn Reson Imaging.* (2013) 37:999–1003. doi: 10.1002/jmri.23817
22. Wyss PO, Bianchini C, Scheidegger M, Giapitzakis IA, Hock A, Fuchs A, et al. In vivo estimation of transverse relaxation time constant (T2) of 17 human brain metabolites at 3T. *Magn Reson Med.* (2018) 80:452–61. doi: 10.1002/mrm.27067
23. Streit F, Treutlein J, Frischknecht U, Hermann D, Mann K, Kiefer F, et al. Glutamate concentration in the anterior cingulate cortex in alcohol dependence: association with alcohol withdrawal and exploration of contribution from glutamatergic candidate genes. *Psychiatr Genet.* (2018) 28:94–5. doi: 10.1097/YPG.0000000000000202
24. Gass JT, Olive MF. Glutamatergic substrates of drug addiction and alcoholism. *Biochem Pharmacol.* (2008) 75:218–65. doi: 10.1016/j.bcp.2007.06.039
25. Brambilla P, Stanley JA, Nicoletti M, Harenski K, Wells KF, Mallinger AG, et al. 1H MRS brain measures and acute lorazepam administration in healthy human subjects. *Neuropsychopharmacology.* (2002) 26:546–51. doi: 10.1016/S0893-133X(01)00388-8
26. Henry ME, Jensen JE, Licata SC, Ravichandran C, Butman ML, Shanahan M, et al. The acute and late CNS glutamine response to benzodiazepine challenge: a pilot pharmacokinetic study using proton magnetic resonance spectroscopy. *Psychiatry Res.* (2010) 184:171–6. doi: 10.1016/j.pscychresns.2010.08.003
27. Yildiz A, Gokmen N, Kucukguclu S, Yurt A, Olson D, Rouse ED, et al. In vivo proton magnetic resonance spectroscopic examination of benzodiazepine action in humans. *Psychiatry Res.* (2010) 184:162–70. doi: 10.1016/j.pscychresns.2010.07.004
28. Umhau JC, Momenan R, Schwandt ML, Singley E, Lifshitz M, Doty L, et al. Effect of acamprosate on magnetic resonance spectroscopy measures of central glutamate in detoxified alcohol-dependent individuals: a randomized controlled experimental medicine study. *Arch Gen Psychiatry.* (2010) 67:1069–77. doi: 10.1001/archgenpsychiatry.2010.125
29. Gomez R, Behar KL, Watzl J, Weinzimer SA, Gulanski B, Sanacora G, et al. Intravenous ethanol infusion decreases human cortical gamma-aminobutyric acid and N-acetylaspartate as measured with proton magnetic resonance spectroscopy at 4 tesla. *Biol Psychiatry.* (2012) 71:239–46. doi: 10.1016/j.biopsych.2011.06.026
30. Walls AB, Waagepetersen HS, Bak LK, Schousboe A, Sonnewald U. The glutamine-glutamate/GABA cycle: function, regional differences in glutamate and GABA production and effects of interference with GABA metabolism. *Neurochem Res.* (2015) 40:402–9. doi: 10.1007/s11064-014-1473-1
31. Roberto M, Varodayan FP. Synaptic targets: chronic alcohol actions. *Neuropharmacology.* (2017) 122:85–99. doi: 10.1016/j.neuropharm.2017.01.013
32. Ron D, Wang J. The NMDA receptor and alcohol addiction. In: Van Dongen AM, editor. *Biology of the NMDA Receptor*. Boca Raton, FL: CRC Press/Taylor & Francis (2009).
33. Edden RA, Oeltzschner G, Harris AD, Puts NA, Chan KL, Boer VO, et al. Prospective frequency correction for macromolecule-suppressed GABA editing at 3T. *J Magn Reson Imaging.* (2016) 44:1474–82. doi: 10.1002/jmri.25304

Conflict of Interest: The authors declare that the research was conducted in the absence of any commercial or financial relationships that could be construed as a potential conflict of interest.

frontiers in Psychiatry

BRIEF RESEARCH REPORT
published: 03 December 2021
doi: 10.3389/fpsyt.2021.665347

Left Dorsolateral Prefrontal Cortex Glx/tCr Predicts Efficacy of High Frequency 4- to 6-Week rTMS Treatment and Is Associated With Symptom Improvement in Adults With Major Depressive Disorder: Findings From a Pilot Study

Pallab Bhattacharyya[1,2]*, *Amit Anand*[3], *Jian Lin*[1] and *Murat Altinay*[3]

[1] Cleveland Clinic, Imaging Institute, Cleveland, OH, United States, [2] Department of Radiology, Cleveland Clinic Lerner College of Medicine, Cleveland, OH, United States, [3] Cleveland Clinic, Neurological Institute, Cleveland, OH, United States

OPEN ACCESS

Edited by:
Maria Concepcion Garcia Otaduy, University of São Paulo, Brazil

Reviewed by:
Jeffrey A. Stanley, Wayne State University, United States
Frank P. MacMaster, University of Calgary, Canada

***Correspondence:**
Pallab Bhattacharyya
bhattap@ccf.org

Specialty section:
This article was submitted to Neuroimaging and Stimulation, a section of the journal Frontiers in Psychiatry

Received: 07 February 2021
Accepted: 08 November 2021
Published: 03 December 2021

Citation:
Bhattacharyya P, Anand A, Lin J and Altinay M (2021) Left Dorsolateral Prefrontal Cortex Glx/tCr Predicts Efficacy of High Frequency 4- to 6-Week rTMS Treatment and Is Associated With Symptom Improvement in Adults With Major Depressive Disorder: Findings From a Pilot Study. Front. Psychiatry 12:665347. doi: 10.3389/fpsyt.2021.665347

About 20–40% of estimated 121 million patients with major depressive disorder (MDD) are not adequately responsive to medication treatment. Repetitive transcranial magnetic stimulation (rTMS), a non-invasive, non-convulsive neuromodulation/neurostimulation method, has gained popularity in treatment of MDD. Because of the high cost involved in rTMS therapy, ability to predict the therapy effectiveness is both clinically and cost wise significant. This study seeks an imaging biomarker to predict efficacy of rTMS treatment using a standard high frequency 10-Hz 4- to 6-week protocol in adult population. Given the significance of excitatory and inhibitory neurotransmitters glutamate (Glu) and gamma aminobutyric acid (GABA) in the pathophysiology of MDD, and the involvement of the site of rTMS application, left dorsolateral prefrontal cortex (lDLPFC), in MDD, we explored lDLPFC Glx (Glu + glutamine) and GABA levels, measured by single voxel magnetic resonance spectroscopy (MRS) with total creatine (tCr; sum of creatine and phosphocreatine) as reference, as possible biomarkers of rTMS response prediction. Mescher-Garwood point-resolved spectroscopy (MEGA-PRESS) MRS data from 7 patients (40–74 y) were used in the study; 6 of these patients were scanned before and after 6 weeks of rTMS therapy. Findings from this study show inverse correlation between pretreatment lDLPFC Glx/tCr and (i) posttreatment depression score and (ii) change in depression score, suggesting higher Glx/tCr as a predictor of treatment efficacy. In addition association was observed between changes in depression scores and changes in Glx/tCr ratio. The preliminary findings did not show any such association between GABA/tCr and depression score.

Keywords: repetitive transcranial magnetic stimulation (rTMS), major depressive disorder (MDD), magnetic resonance spectroscopy (MRS), glutamate, gamma aminobutyric acid (GABA)

INTRODUCTION

Major depressive disorder (MDD), which has a lifetime prevalence of 15% (1), does not respond adequately to medication treatment in ∼20–40% of affected patients (2), and these patients have higher morbidity and mortality than those with disease that responds to medication (3, 4). Although electrical stimulation techniques such as electroconvulsive therapy (5–7), vagus nerve stimulation (8–10), and deep brain stimulation (11–13) are suitable for medication-resistant MDD, they are invasive in nature. Repetitive transcranial magnetic stimulation (rTMS), on the other hand, is a non-invasive, non-convulsive neuromodulation/neurostimulation method that has gained popularity for the treatment of MDD that is not responsive to medication (14–37). In particular, high-frequency (>5 Hz) rTMS applied to the left dorsolateral prefrontal cortex (lDLPFC) has been found to significantly decrease Hamilton Depression Rating Scale (HAM-D) scores in patients with medication-resistant MDD (38, 39). Standard and most optimal rTMS therapies are administered at a frequency of 10 Hz (40, 41) over 4–6 weeks (40).

In patients with MDD, rTMS has been reported to change the balance of excitation and inhibition in cortical networks (42, 43), and the antidepressant effect from rTMS has been attributed in part on modulation of the major excitatory neurotransmitter glutamate (Glu) and the major inhibitory neurotransmitter gamma aminobutyric acid (GABA) (44). Multiple studies have documented the involvement of these neurotransmitters in the pathophysiology of MDD (45–51). Changes in cortical Glu or Glx (Glu + glutamine) and GABA levels in patients with MDD have been investigated using *in vivo* magnetic resonance spectroscopy (MRS). In spite of some differences in acquisition (e.g., Mescher-Garwood point-resolved spectroscopy [MEGA-PRESS] vs. short echo time [TE] PRESS), analysis, and quantification methodologies (e.g., absolute levels vs. ratios), these studies have demonstrated a reduction in cortical Glu or Glx and GABA levels associated with MDD (45, 48–50, 52). More specifically, reduced PFC Glx level in patients with MDD has been reported in several studies (45, 53, 54). Researchers have suggested that dysfunction of the glutamatergic system and malfunction in Glu metabolism are contributing factors to the neurobiology and pathophysiology of MDD (55, 56), and the efficacy of glutamatergic agents (glutamatergic targets/receptors such as ketamine, mamantine, riluzole, dextromethorphan, AZD6765 etc.) for the treatment of MDD has been reported (56, 57). Studies have also shown that reduced cortical GABA level is associated with dysfunctional GABAergic interneurons and $GABA_A$ receptors; affected GABAergic transmission has been proposed as a mechanism of MDD (58–60). rTMS studies have shown deficits in cortical inhibition in adults with MDD (61, 62); while in children and adolescents increased excitatory cortical facilitation with unchanged cortical inhibition was observed (63).

Multiple *in vivo* studies of Glu and GABA modulation after rTMS in patients with MDD have been performed (58, 64–66). In one study using MEGA-PRESS, the medial prefrontal cortex (MPFC) Glu level was unchanged but the GABA level was elevated after 25 sessions of 10-Hz rTMS therapy applied at the lDLPFC (58). In another study using PRESS and involving 10 sessions of 20-Hz rTMS, an increase in Glu level was seen in the DLPFC, with no changes seen in the anterior cingulate cortex (64). In a short TE PRESS study of young adults treated with 10-Hz rTMS for 15 days, the lDLPFC Glu level was increased in responders but reduced in non-responders (65). Another study using MEGA-PRESS demonstrated an increase in DLPFC GABA level after 6 weeks of 10-Hz rTMS therapy (67).

The prefrontal cortex has been shown to be important in the pathogenesis of MDD (68, 69), and decreased activation of the cortical areas of the mood-regulating circuit has also been reported in patients with MDD (70, 71). More specifically, several studies have shown abnormalities in the DLPFC in patients with MDD (72–76), with affected patients demonstrating reduced levels of GABA and Glx (Glu + glutamine [Gln]) in the DLPFC (45, 77, 78). Lower metabolic activity in the DLPFC (79) as well as lower functional connectivity within the cognitive control network (80), a network that contains the DLPFC, has been reported in depression. In addition MDD is associated with reduced prefrontal cortex gray matter volume, cell counts and glucose metabolism (81). These abnormal (mostly left) prefrontal cortex activities in MDD therefore make the DLPFC a logical and popular rTMS target (73, 81–83).

Differences in Glu levels between responders and non-responders to antidepressants (84) and rTMS therapy (64, 65) suggest that Glu level is a predictor of therapy outcomes in MDD. More specifically, studies have demonstrated that responders to rTMS therapy have lower baseline DLPFC Glu levels than non-responders (64, 65), suggesting that baseline Glu level could be a predictor of response to rTMS therapy. However, most of these studies included only young adults or were carried out over a different period of time than the standard and optimal 4- to 6-week period (40). Thus, additional research is needed to establish an imaging biomarker that can be used to predict the success of rTMS treatment using a standard 10-Hz (40, 41) 4- to 6-week protocol in the adult population. Identifying such biomarker is significant from out of pocket patient expense also, since rTMS therapy is quite costly (can range from ∼6,000 to ∼$15,000 for 30 sessions in the USA depending on the location, center, applicable discounts and insurance coverage) and is often not covered by insurance.

In this longitudinal study, we measured Glx/tCr and GABA/tCr at the lDLPFC, the site of rTMS application, to determine whether the baseline measures of these could be used to predict outcomes after 6 weeks of 10-Hz rTMS therapy. To this end, we assessed the association between these baseline ratios (Glx/tCr and GABA/tCr) and change in 17-item Hamilton Depression (HAM-D) score after rTMS, as well as the association between the baseline ratios and posttreatment HAM-D score. In addition, we evaluated the Glx/tCr and GABA/tCr ratios to track recovery after rTMS therapy, i.e., we assessed the association between the changes of these ratios and HAM-D scores in response to rTMS therapy.

MATERIALS AND METHODS

The study was performed following an IRB-approved protocol. All patients provided written informed consent. We initially enrolled 12 patients (4 men; mean age, 53 y ± 15 y; range, 23–74 y) who had an HAM-D score >15 and who met the DSM-IV-TR (85) criteria for MDD inadequately responsive to at least one antidepressant despite treatment with an adequate dosage for at least 8 weeks (the indication for rTMS approved by the Food and Drug Administration). Patients were recruited from Center of Behavioral Health outpatient psychiatry clinic for mood disorders at our center. Two of these patients did not complete the study, undergoing only 1 MR imaging session and 3 patients had excessive motion during the pretreatment scan; thus, the final analysis consisted of 7 patients.

Of the 7 subjects included in the final analysis, 6 subjects were on antidepressants in combination with low dose 2nd generation neuroleptics ($n = 4$), mood stabilizers ($n = 2$), stimulants ($n = 2$) and other augmentation agents ($n = 2$). Low dose anti-anxiety medications were allowed per inclusion criteria ($n = 4$). Patients were asked to remain on the same dosages on all of the medications during the course of the rTMS treatment. No new medications and/or other non-medication treatment modalities were started at least 1 month before or during the acute rTMS series.

rTMS Protocol

rTMS was performed using a MagPro R-30 magnetic stimulator (MagVenture, Farum, Denmark) with "cool B-65" magnetic coil, a device that has been used effectively in previous studies (14, 86, 87). Each patient underwent rTMS therapy sessions 5 times per week for a total of 6 weeks (total of 30 rTMS sessions); we selected a duration of 6 weeks because previous studies have used 4–6 weeks of treatment to testy for rTMS effectiveness (14, 88, 89). Each session lasted ∼40 min and used the following parameters: frequency, 10 Hz; power, 120% of the motor threshold (i.e., minimum amount of energy needed to trigger thumb movement); duration of stimulus, 4 s; intertrain interval, 26 s; number of pulses per train, 75; and total number of pulses, 3,000. In order to locate the lDLPFC, first the left motor strip controlling the movements of the right thumb was located. The coil was then advanced 5 cm on to the anterior of the motor strip to target the lDLPFC. An experienced staff psychiatrist (MA) administered the rTMS and also performed HAM-D assessment at baseline and every 2 weeks.

MR Imaging

MR scans were performed on a Siemens 3T Prisma scanner (Erlangen, Germany) using a 20-channel coil head/neck coil. Each patient was scanned within 1 week before starting rTMS therapy (pretreatment scan) and within 1 week after the end of 6 weeks of therapy (posttreatment scan).

Each MR session consisted of the following scans: (1) Localizer scan to obtain scout images: scan time, 9 s; (2) Gradient recalled echo scan for field-mapping: 32 axial slices; thickness, 4 mm; field of view (FOV), 256 mm × 256 mm; dual echo times (TE1/TE2)/repetition time (TR)/flip angle (FA), 4.89 ms/7.35 ms/388 ms/60°; matrix, 64 × 64; bandwidth, 260 Hz; scan time, 36 s; (3) T1-weighted anatomical magnetization prepared rapid acquisition gradient echo (MPRAGE) scan: 120 axial slices; thickness, 1.2 mm; FOV, 256 mm × 256 mm; inversion time/TE/TR/FA, 1,900 ms/1.71 ms/900 ms/8°; matrix, 256 × 128; bandwidth, 62 kHz; scan time, 4 min 5 s; and (4) Mescher-Garwood point-resolved spectroscopy (MEGA-PRESS) scan for GABA and Glx measurement of a 2 × 2 × 2 cm^3 voxel in the lDLPFC: TR, 2,700 ms; TE, 68 ms; frequency-selective 180° pulses at 1.9 (ON-resonance) and 1.5 ppm (OFF-resonance, to minimize macromolecule contamination of GABA); minimum achievable frequency selective pulse bandwidth (∼44 Hz); number of averages, 128 per condition (ON-/OFF-resonance); weak water suppression (to use residual water fluctuation to assess patient motion); scan time, 10 min 53 s. A trained technologist ensured that the lDLPFC voxel locations (**Figure 1**) were closely matched between the pretreatment and posttreatment sessions. The patients bit onto a bite-bar during all scans to reduce head motion. For all spectroscopy scans, shimming was performed using the FASTESTMAP shimming routine (90).

MRS Data Analysis

Postprocessing of MRS data was performed using the MRUI software package (91) following the method described by Bhattacharyya et al. (92). Postprocessing consisted of zero-order phase correction and frequency shift correction of the individual subspectra using residual water as a reference, averaging the individually phase- and frequency-corrected spectra, residual water suppression with Hankel-Lanczos squares singular value decomposition (HLSVD) filter (93), apodization by a 5-Hz Gaussian filter, and zero filling The OFF-resonance spectrum was subtracted from the ON-resonance spectrum to obtain the final edited spectrum. Motion was identified retrospectively using residual water signal fluctuation as an indicator (92).

Next the ∼3.75-ppm Glx and 3.01-ppm GABA peaks from the edited spectrum were fitted as double Gaussian peaks using the AMARES algorithm (94) with zero-order phase correction. The 3.04-ppm creatine (tCr) peak was fitted similarly from the OFF-resonance spectrum. Glx/tCr and GABA/tCr levels were obtained from I_{Glx}/I_{tCr} and I_{GABA}/I_{tCr}, respectively, where I_{Glx}, I_{GABA}, and I_{tCr} represent areas of the Glx, GABA, and tCr fits, respectively. Edited spectral fitting was done by including the ∼2.3 ppm GABA+Glu and inverted NAA peaks as well, but that did not have any effect on I_{Glx} or I_{GABA}.

Statistical Analysis

Percent (%) changes in HAM-D score and Glx/Cr were determined using the expressions

$$\frac{(\text{Posttreatment HAMD}) - (\text{Pretreatment HAMD})}{\text{Pretreatment HAMD}} \times 100$$

and

$$\frac{\left(\text{Posttreatment Glx/Cr}\right) - (\text{Pretreatment Glx/Cr})}{\text{Pretreatment Glx/Cr}} \times 100 \quad (1)$$

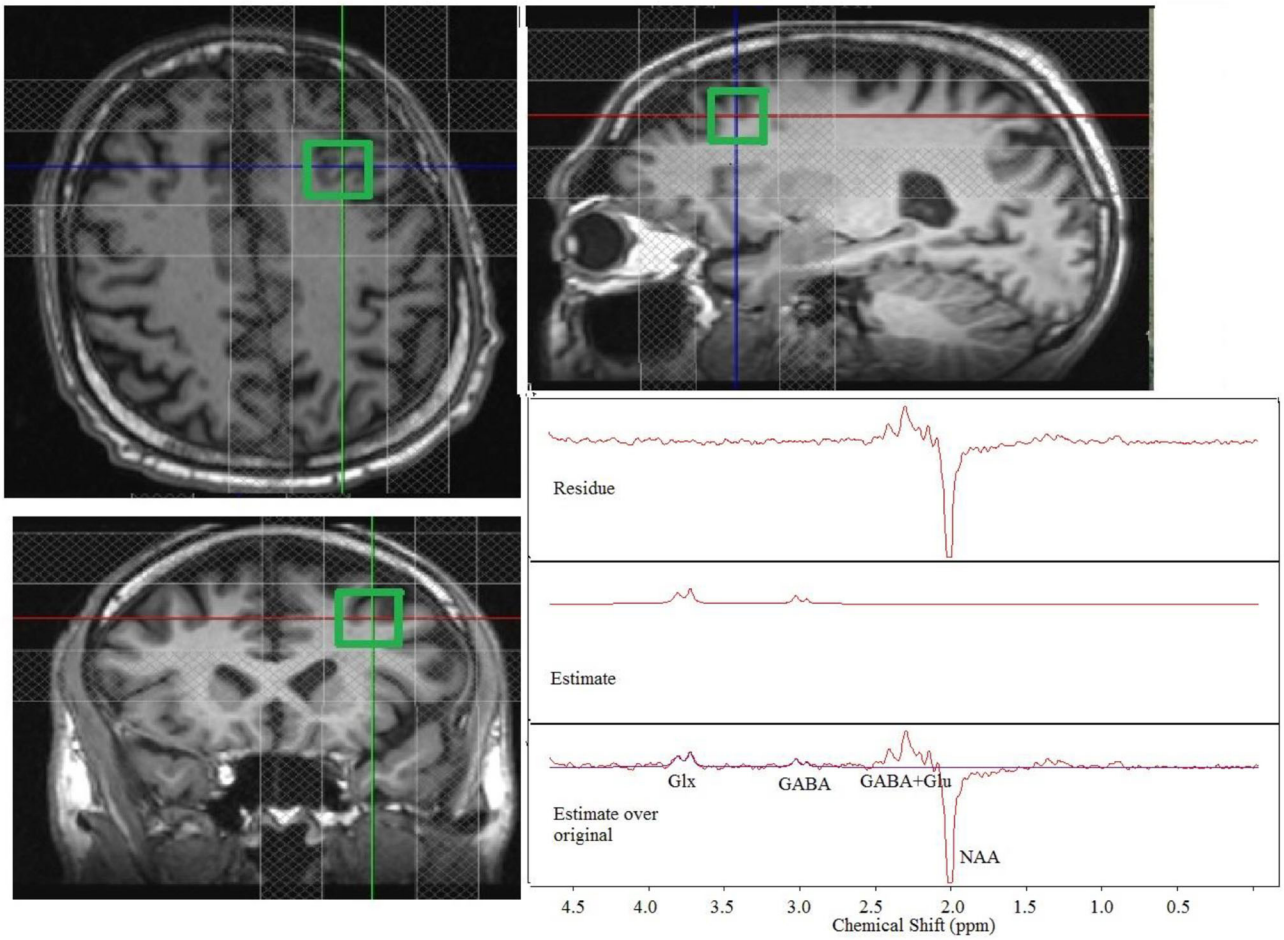

FIGURE 1 | Placement of a 2 × 2 × 2 cm^3 dorsolateral prefrontal cortex voxel with the outer volume suppression bands and representative single-patient MEGA-PRESS edited spectra (original, estimate and residue). Glx, glutamate + glutamine; GABA, gamma aminobutyric acid; Glu, glutamate.

respectively. Non-parametric Wilcoxon signed rank test was between pre- and posttreatment HAM-D scores. Spearman correlation coefficient was used to characterize the association between (1) pretreatment DLPFC Glx/tCr (and GABA/tCr) ratios and changes in HAM-D scores (from pretreatment to 6 weeks posttreatment) and (2) changes in DLPFC Glx/tCr (and GABA/tCr) ratios and changes in HAM-D scores.

RESULTS

Some MRS datasets had to be discarded because of excessive motion. A total of 3 patients had pretreatment scans that could not be used because of excessive motion, and 1 of these patients also had a posttreatment scan that could not be used because of excessive motion. Thus, 7 motion-free pretreatment scans and 6 motion-free posttreatment scans were used for analysis. A Representative single-patient edited spectra (original, estimate and residual spectra) at the lDLPFC are shown in **Figure 1**.

From Wilcoxon signed rank test, significant decrease in HAM-D scores was observed for the 10 patients who completed the study (pretreatment score, 20 ± 3; posttreatment score, 8 ± 6; $p = 0.006$). Of the 7 patients (age: 59 ± 13 y) with motion-free pretreatment scans the pretreatment and posttreatment HAM-D scores were 21 ± 3 and 11 ± 8, respectively ($p = 0.016$), while the pretreatment and posttreatment HAM-D scores for the 6 patients (age: 59 ± 13 y) with both motion-free scans were 20 ± 3 and 10 ± 8, respectively ($p = 0.031$).

Overall, no significant changes in Glx/tCr or GABA/tCr were observed as a result of rTMS therapy (**Table 1**). Inverse Spearman correlations were observed between (1) posttreatment HAM-D score and pretreatment lDLPFC Glx/tCr ($n = 7$; $p < 0.0005$) and (2) change in HAM-D score and pretreatment lDLPFC Glx/tCr ($n = 7$; $p = 0.001$; **Figures 2A,B**). No such significant correlations were observed between (1) posttreatment HAM-D score and pretreatment GABA/tCr ($n = 7$; $p = 0.66$) and (2) change in HAM-D score and pretreatment lDLPFC GABA/tCr ($n = 7$; $p = 0.39$). A significant correlation was observed between change in HAM-D score and change in Glx/tCr in the lDLPFC

TABLE 1 | Depression ratings, Glx and GABA levels before and after rTMS treatment.

Variable	Pretreatment value	Posttreatment value	*p*
HAM-D score ($n = 10$)	20 ± 3	11 ± 7	0.0007
Glx/tCr ($n = 6$)	0.21 ± 0.04	0.24 ± 0.05	0.21
GABA/tCr ($n = 6$)	0.11 ± 0.02	0.13 ± 0.06	0.20

Data are presented as mean ± SD. HAM-D, Hamilton Depression Rating Scale; Glx, glutamate + glutamine; tCr, total creatine; GABA, gamma aminobutyric acid.

($n = 6$; $p = 0.02$; **Figure 3**); no such association was observed between change in HAM-D score and change in GABA/tCr ($n = 6$; $p = 0.45$).

It should be pointed out that HAM-D scores were obtained every 2 weeks and similar analyses were run using the 4-week HAM-D scores. Significant decrease in HAM-D scores were observed in 7 patients with motion-free pretreatment scans (4-week HAM-D score $= 10 \pm 7$, $p = 0.022$). Similar to 6-week data, inverse Spearman correlations were seen between (1) 4-week HAM-D score and pretreatment lDLPFC Glx/tCr ($n = 7$; $p < 0.0005$) and (2) change in HAM-D score in 4 weeks and pretreatment lDLPFC Glx/tCr ($n = 7$; $p < 0.0005$).

DISCUSSION

In this study, patients treated with 6 weeks of 10-Hz rTMS targeting the lDLPFC demonstrated a decrease in HAM-D score; however, no overall changes in Glx/tCr or GABA/tCr ratios (averaged over 6 patients) were observed. One previous study reported no change in the MPFC Glu level after 25 sessions of 10-Hz rTMS therapy (58); however, an increase in MPFC GABA+ (GABA+macromolecule) level was observed. Although this previous study had a higher number of patients ($n = 23$) than the current study, the region of interest (MPFC) was different from the site of rTMS application (lDLPFC), which was evaluated in the current study.

In this study, patients with higher pretreatment Glx/tCr had lower posttreatment HAM-D scores and larger reductions in HAM-D score after 6 (as well as 4) weeks of rTMS. This finding, albeit from a small sample, is promising and suggests that lDLPFC Glu level may be a predictor of 4- to 6-week rTMS outcome. It should be noted that a higher baseline lDLPFC Glu level has also been previously reported in responders to antidepressant therapy (84), indicating that the predictive power of lDLPFC Glu level may not be limited to rTMS. On the other hand, a lower baseline Glu level has also been reported in youth responders to 3 weeks of rTMS (65), which is the opposite of what we observed in the current study. We speculate that this difference results from the difference in age groups between the studies. Cerebral Glu level has been reported to decrease with age (95); hence, in the older patient population as in this study (40–74 y for the patients who completed the study and had motion-free pretreatment scans), a higher pretreatment Glu level may favor the therapeutic action of rTMS. There was no overall change in Glx/tCr after rTMS. Our results indicate that while Glx/tCr in the lDLPFC increased in 4 patients and decreased in 2 patients, a decrease in HAM-D was associated with a lesser increase or larger decrease in Glx/tCr ratio.

Baseline GABA level in this preliminary study was not associated with response to rTMS therapy, and no previous studies have demonstrated evidence of such a relationship. Additionally, no association between baseline prefrontal cortex GABA level and improvement in MDD was observed in a study assessing ketamine infusion therapy (96). It is likely, therefore, that the baseline GABA level does not predict recovery from MDD irrespective of the treatment regimen.

Test-retest reliability of Glx/Cr and GABA/Cr measurements of a $2 \times 2 \times 2$ cm^3 voxel in the lDLPFC using MEGA-PRESS sequence was evaluated independently in our center as described in the **Supplementary Material**. The test-retest variability (9.2%) of Glx/Cr is less than that observed in response to rTMS treatment, while the corresponding GABA/Cr changes for two subjects were less than the variability (16.6%).

While a direct connection between Glx and excitatory neurotransmission is not obvious, it should be noted that Glx measured with the MEGA-PRESS sequence (97, 98) used in this study has been reported to contain mostly Glu with little or no Gln and is therefore considered a good measure of Glu (58, 99–101). Based upon those reports, we speculate that much of our findings pertain to the involvement of excitatory Glu in rTMS therapy. However, we do recognize that there could be a small contribution of Gln in the Glx peak.

A higher lDLPFC Cr in MDD than in healthy controls has been reported (102). In this study, Glx/tCr and GABA/tCr ratios are reported, with areas of the respective resonances in the MEGA-PRESS edited spectra normalized to tCr area from OFF-resonance spectra. For technical reasons, water-unsuppressed MEGA-PRESS scans were not incorporated in the protocol at the beginning of the study; however, those scans were added after the scans of the first 2 patients were completed. Normalizing Glx and GABA to tCr is a well-established method (103–105), and we validated this in our dataset by correlating Glx and GABA normalized to unsuppressed water with Glx/tCr and GABA/tCr from all studies with unsuppressed water acquisition (i.e., from both MRI sessions for patients who completed the study and from pretreatment visits for patients who dropped out after 1 MRI session). The 2 metrics were correlated ($p = 0.001$ for Glx and 0.0001 for GABA), which validated usage of ratio with respect to tCr for this patient population.

Lack of any observed association of GABA in this preliminary study should be treated with caution. It is possible that the main

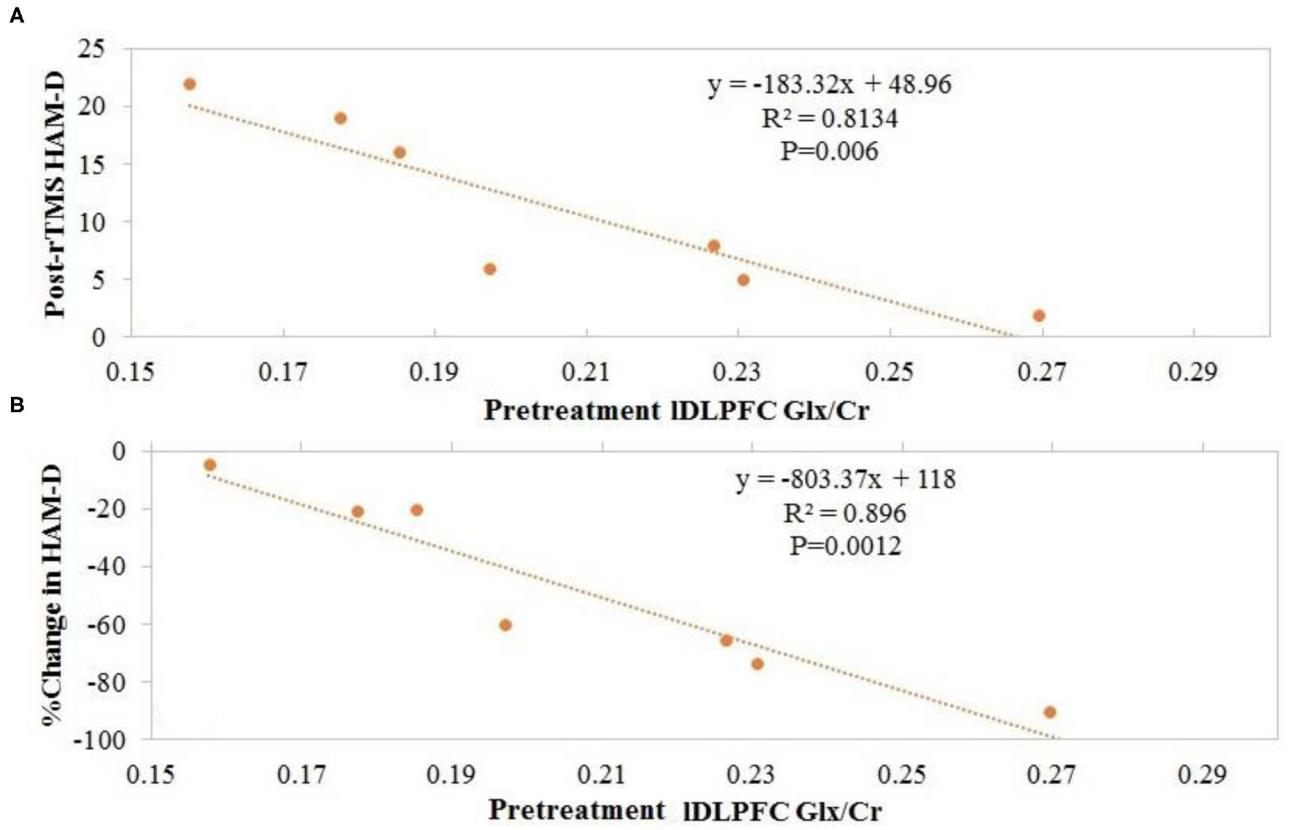

FIGURE 2 | Patients with higher pretreatment glutamate + glutamine (Glx)/total creatine (tCr) at the left dorsolateral prefrontal cortex (lDLPFC) demonstrated **(A)** lower posttreatment Hamilton Depression Rating Scale (HAM-D) scores and **(B)** greater change in HAM-D scores after repetitive transcranial magnetic stimulation (rTMS).

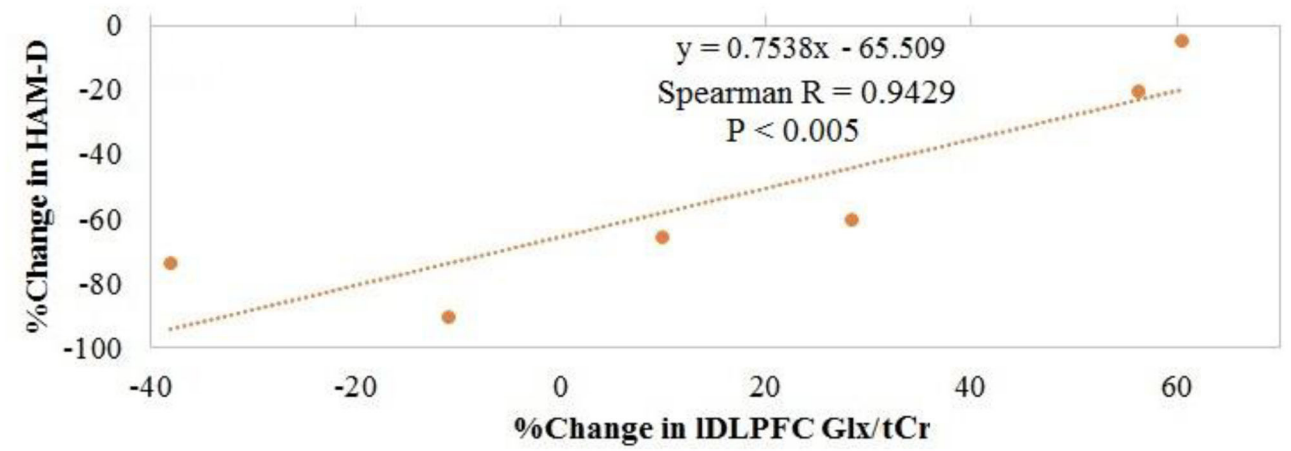

FIGURE 3 | Association between change in glutamate + glutamine (Glx)/total creatine (tCr) in the left dorsolateral prefrontal cortex and change in Hamilton Depression Rating Scale (HAM-D) score.

reason for the lack of any significant changes in GABA/tCr ratios or any correlations therewith in this study is the lack of statistical power with 6 subjects. Spectral fitting error was ∼30% worse in GABA than in case of Glx, which would result in lower sensitivity of detecting GABA association. Signal to noise ratio and fitting error can be improved with GABA+ acquisition (103), but our choice of macromolecule-minimized GABA accounts for any inter-subject macromolecule level differences (106).

This study had some limitations, including its small sample size. However, a power analysis with $n = 7$ yielded power of 0.95 and 0.85, respectively, for the inverse correlation observed between pretreatment lDLPFC Glx/tCr and change in HAM-D and posttreatment HAM-D, respectively. In addition, with $n = 6$ the study had power of 0.80 to detect 18% change in Glx/tCr ratio. The study also did not include a sham treatment population, which may raise questions regarding glutamatergic involvement in the improvement of MDD as an effect of rTMS. Use of the standard 5-cm rule for rTMS target selection is another limitation, as use of neuronavigation instead has been shown to ensure more reliable, precise, and consistent targeting of the desired brain region (107). Finally, low doses of neuroleptics, benzodiazepine (not more than 1–2 mg), and mood stabilizers were allowed in the study; we did not assess the potential effects of these medications on the study findings. However, for all medications a fixed dose for 4 weeks (6 weeks for benzodiazepines) before rTMS with no change in medication during rTMS treatment was followed as part of the study protocol to minimize any medication effect to the observations reported in this study. We have covered a wide range of age in this study. We hypothesize that while the baseline metabolite levels may be varying due to age and drug regimen, the change in those levels in 6 weeks (study period) will be due to rTMS therapy.

CONCLUSION

This study found that the most commonly used rTMS protocol (10 Hz, 4–6 weeks, lDLPFC target) did not significantly change lDLPFC Glx/tCr or GABA/tCr ratios in adults with MDD. Patients with higher pretreatment lDLPFC Glx/tCr ratio did respond better to rTMS therapy; they had a greater reduction in HAM-D score and a lower posttreatment HAM-D score. These findings suggest that excitatory Glu is associated with recovery from MDD and can potentially be used as a biomarker to predict response to rTMS treatment, whereas no such relationship between inhibitory GABA and MDD/rTMS outcome was observed in this preliminary study. The results of this pilot study should be interpreted with caution because of the small sample size and absence of a sham arm; further studies using larger sample sizes are needed to assess these preliminary results.

DATA AVAILABILITY STATEMENT

The raw data supporting the conclusions of this article will be made available by the authors, without undue reservation.

ETHICS STATEMENT

The studies involving human participants were reviewed and approved by Institutional Review Board, Cleveland Clinic. The patients/participants provided their written informed consent to participate in this study.

AUTHOR CONTRIBUTIONS

PB: MRI study design, planning, funding acquisition, MRI data analysis, and writing—original draft. AA: conceptualization, study design, writing—review, and editing. JL: MRI data processing. MA: patient recruitment and consenting, prescribing and administering rTMS, depression rating, writing—review, and editing. All authors contributed to the article and approved the submitted version.

FUNDING

Cleveland Clinic Research Program Committee partially funded this project.

ACKNOWLEDGMENTS

We are grateful to Sineyob Ahn from Siemens Healthineers for support with the MEGA-PRESS sequence used in this study. FASTESTMAP sequence, used for shimming, was developed by Edward J. Auerbach and Malgorzata Marjanska and were provided by the University of Minnesota under a C2P agreement. We also acknowledge Jennifer Bullen of Quantitative Health Sciences of Cleveland Clinic for her input in statistical analyses.

SUPPLEMENTARY MATERIAL

The Supplementary Material for this article can be found online at: https://www.frontiersin.org/articles/10.3389/fpsyt.2021.665347/full#supplementary-material

REFERENCES

1. Tundo A, de Filippis R, Proietti L. Pharmacologic approaches to treatment resistant depression: evidences and personal experience. *World J Psychiatry.* (2015) 5:330–41. doi: 10.5498/wjp.v5.i3.330
2. Fava M. Diagnosis and definition of treatment-resistant depression. *Biol Psychiatry.* (2003) 53:649–59. doi: 10.1016/S0006-3223(03)00231-2
3. Russell JM, Hawkins K, Ozminkowski RJ, Orsini L, Crown WH, Kennedy S, et al. The cost consequences of treatment-resistant depression. *J Clin Psychiatry.* (2004) 65:341–7. doi: 10.4088/JCP.v65n0309
4. Reutfors J, Andersson TM, Brenner P, Brandt L, DiBernardo A, Li G, et al. Mortality in treatment-resistant unipolar depression: a register-based cohort study in Sweden. *J Affect Disord.* (2018) 238:674–9. doi: 10.1016/j.jad.2018.06.030
5. Kellner C. Review: maintenance antidepressants reduce risk of relapse in the 6 months following ECT in people with major depression. *Evid Based Ment Health.* (2014) 17:8. doi: 10.1136/eb-2013-101663
6. de Vreede IM, Burger H, van Vliet IM. Prediction of response to ECT with routinely collected data in major depression. *J Affect Disord.* (2005) 86:323–7. doi: 10.1016/j.jad.2005.03.008
7. Ruedrich SL, Chu CC, Moore SL. ECT for major depression in a patient with acute brain trauma. *Am J Psychiatry.* (1983) 140:928–9. doi: 10.1176/ajp.140.7.928
8. Muller HH, Kornhuber J, Maler JM, Sperling W. The effects of stimulation parameters on clinical outcomes in patients with vagus nerve stimulation implants with major depression. *J Ect.* (2013) 29:e40–2. doi: 10.1097/YCT.0b013e318290f7ed

9. Conway CR, Chibnall JT, Gangwani S, Mintun MA, Price JL, Hershey T, et al. Pretreatment cerebral metabolic activity correlates with antidepressant efficacy of vagus nerve stimulation in treatment-resistant major depression: a potential marker for response? *J Affect Disord.* (2012) 139:283–90. doi: 10.1016/j.jad.2012.02.007
10. Cristancho P, Cristancho MA, Baltuch GH, Thase ME, O'Reardon JP. Effectiveness and safety of vagus nerve stimulation for severe treatment-resistant major depression in clinical practice after FDA approval: outcomes at 1 year. *J Clin Psychiatry.* (2011) 72:1376–82. doi: 10.4088/JCP.09m05888blu
11. Artigas F. Deep brain stimulation in major depression: plastic changes of 5-hydroxytryptamine neurons. *Biol Psychiatry.* (2014) 76:174–5. doi: 10.1016/j.biopsych.2014.05.008
12. Schlaepfer TE, Bewernick BH, Kayser S, Hurlemann R, Coenen VA. Deep brain stimulation of the human reward system for major depression–rationale, outcomes and outlook. *Neuropsychopharmacology.* (2014) 39:1303–14. doi: 10.1038/npp.2014.28
13. Schlaepfer TE, Bewernick BH. Deep brain stimulation for major depression. *Handb Clin Neurol.* (2013) 116:235–43. doi: 10.1016/B978-0-444-53497-2.00018-8
14. Bakker N, Shahab S, Giacobbe P, Blumberger DM, Daskalakis ZJ, Kennedy SH, et al. rTMS of the dorsomedial prefrontal cortex for major depression: safety, tolerability, effectiveness, and outcome predictors for 10 Hz versus intermittent theta-burst stimulation. *Brain Stimul.* (2015) 8:208–15. doi: 10.1016/j.brs.2014.11.002
15. De Raedt R, Vanderhasselt MA, Baeken C. Neurostimulation as an intervention for treatment resistant depression: from research on mechanisms towards targeted neurocognitive strategies. *Clin Psychol Rev.* (2015) 41:61–9. doi: 10.1016/j.cpr.2014.10.006
16. McGirr A, Van den Eynde F, Tovar-Perdomo S, Fleck MP, Berlim MT. Effectiveness and acceptability of accelerated repetitive transcranial magnetic stimulation (rTMS) for treatment-resistant major depressive disorder: an open label trial. *J Affect Disord.* (2015) 173:216–20. doi: 10.1016/j.jad.2014.10.068
17. Tortella G, Selingardi PM, Moreno ML, Veronezi BP, Brunoni AR. Does non-invasive brain stimulation improve cognition in major depressive disorder? A systematic review. *CNS Neurol Disord Drug Targets.* (2014) 13:1759–69. doi: 10.2174/1871527313666141130224431
18. Chung SW, Hoy KE, Fitzgerald PB. Theta-burst stimulation: a new form of tms treatment for depression? *Depress Anxiety.* (2015) 32:182–92. doi: 10.1002/da.22335
19. Boldt I, Eriks-Hoogland I, Brinkhof MW, de Bie R, Joggi D, von Elm E. Non-pharmacological interventions for chronic pain in people with spinal cord injury. *Cochrane Database Syst Rev.* (2014) 11:CD009177. doi: 10.1002/14651858.CD009177.pub2
20. Gaynes BN, Lloyd SW, Lux L, Gartlehner G, Hansen RA, Brode S, et al. Repetitive transcranial magnetic stimulation for treatment-resistant depression: a systematic review and meta-analysis. *J Clin Psychiatry.* (2014) 75:477–89; quiz 89. doi: 10.4088/JCP.13r08815
21. Leong K, Chan P, Grabovac A, Wilkins-Ho M, Perri M. Changes in mindfulness following repetitive transcranial magnetic stimulation for mood disorders. *Can J Psychiatry.* (2013) 58:687–91. doi: 10.1177/070674371305801206
22. Nakamura M. Therapeutic application of repetitive transcranial magnetic stimulation for major depression. *Seishin Shinkeigaku Zasshi.* (2012) 114:1231–49.
23. Lefaucheur JP, Andre-Obadia N, Poulet E, Devanne H, Haffen E, Londero A, et al. French guidelines on the use of repetitive transcranial magnetic stimulation (rTMS): safety and therapeutic indications. *Neurophysiol Clin.* (2011) 41:221–95. doi: 10.1016/j.neucli.2011.10.062
24. Foucher JR, Luck D, Chassagnon S, Offerlin-Meyer I, Pham BT. What is needed for rTMS to become a treatment?. *Encephale.* (2007) 33:982–9. doi: 10.1016/j.encep.2007.06.002
25. Fregni F, Marcolin MA, Myczkowski M, Amiaz R, Hasey G, Rumi DO, et al. Predictors of antidepressant response in clinical trials of transcranial magnetic stimulation. *Int J Neuropsychopharmacol.* (2006) 9:641–54. doi: 10.1017/S1461145705006280
26. Lam RW, Chan P, Wilkins-Ho M, Yatham LN. Repetitive transcranial magnetic stimulation for treatment-resistant depression: a systematic review and metaanalysis. *Can J Psychiatry.* (2008) 53:621–31. doi: 10.1177/070674370805300909
27. Pallanti S, Bernardi S. Neurobiology of repeated transcranial magnetic stimulation in the treatment of anxiety: a critical review. *Int Clin Psychopharmacol.* (2009) 24:163–73. doi: 10.1097/YIC.0b013e32832c2639
28. Richieri R, Adida M, Dumas R, Fakra E, Azorin JM, Pringuey D, et al. Affective disorders and repetitive transcranial magnetic stimulation: therapeutic innovations. *Encephale.* (2010) 36(Suppl. 6):S197–201. doi: 10.1016/S0013-7006(10)70057-9
29. Schutter DJ, van Honk J. A framework for targeting alternative brain regions with repetitive transcranial magnetic stimulation in the treatment of depression. *J Psychiatry Neurosci.* (2005) 30:91–7.
30. Fitzgerald P. Repetitive transcranial magnetic stimulation and electroconvulsive therapy: complementary or competitive therapeutic options in depression? *Australas Psychiatry.* (2004) 12:234–8. doi: 10.1080/j.1039-8562.2004.02113.x
31. Padberg F, Moller HJ. Repetitive transcranial magnetic stimulation: does it have potential in the treatment of depression? *CNS Drugs.* (2003) 17:383–403. doi: 10.2165/00023210-200317060-00002
32. Burt T, Lisanby SH, Sackeim HA. Neuropsychiatric applications of transcranial magnetic stimulation: a meta analysis. *Int J Neuropsychopharmacol.* (2002) 5:73–103. doi: 10.1017/S1461145702002791
33. McNamara B, Ray JL, Arthurs OJ, Boniface S. Transcranial magnetic stimulation for depression and other psychiatric disorders. *Psychol Med.* (2001) 31:1141–6. doi: 10.1017/S0033291701004378
34. Boutros NN, Berman RM, Hoffman R, Miano AP, Campbell D, Ilmoniemi R. Electroencephalogram and repetitive transcranial magnetic stimulation. *Depress Anxiety.* (2000) 12:166–9. doi: 10.1002/1520-6394(2000)12:3<166::AID-DA8>3.0.CO;2-M
35. Post RM, Kimbrell TA, McCann UD, Dunn RT, Osuch EA, Speer AM, et al. Repetitive transcranial magnetic stimulation as a neuropsychiatric tool: present status and future potential. *J Ect.* (1999) 15:39–59. doi: 10.1097/00124509-199903000-00005
36. O'Reardon JP, Solvason HB, Janicak PG, Sampson S, Isenberg KE, Nahas Z, et al. Efficacy and safety of transcranial magnetic stimulation in the acute treatment of major depression: a multisite randomized controlled trial. *Biol Psychiatry.* (2007) 62:1208–16. doi: 10.1016/j.biopsych.2007.01.018
37. Slotema CW, Blom JD, Hoek HW, Sommer IE. Should we expand the toolbox of psychiatric treatment methods to include Repetitive Transcranial Magnetic Stimulation (rTMS)? A meta-analysis of the efficacy of rTMS in psychiatric disorders. *J Clin Psychiatry.* (2010) 71:873–84. doi: 10.4088/JCP.08m04872gre
38. Brunelin J, Poulet E, Boeuve C, Zeroug-vial H, d'Amato T, Saoud M. Efficacy of repetitive transcranial magnetic stimulation (rTMS) in major depression: a review. *Encephale.* (2007) 33:126–34. doi: 10.1016/S0013-7006(07)91542-0
39. Rizvi S, Khan AM. Use of transcranial magnetic stimulation for depression. *Cureus.* (2019) 11:e4736. doi: 10.7759/cureus.4736
40. McClintock SM, Reti IM, Carpenter LL, McDonald WM, Dubin M, Taylor SF, et al. Consensus recommendations for the clinical application of repetitive transcranial magnetic stimulation (rTMS) in the treatment of depression. *J Clin Psychiatry.* (2018) 79:16cs10905. doi: 10.4088/JCP.16cs10905
41. Philip NS, Carpenter SL, Ridout SJ, Sanchez G, Albright SE, Tyrka AR, et al. 5Hz Repetitive transcranial magnetic stimulation to left prefrontal cortex for major depression. *J Affect Disord.* (2015) 186:13–7. doi: 10.1016/j.jad.2014.12.024
42. Fitzgerald PB, Fountain S, Daskalakis ZJ. A comprehensive review of the effects of rTMS on motor cortical excitability and inhibition. *Clin Neurophysiol.* (2006) 117:2584–96. doi: 10.1016/j.clinph.2006.06.712
43. Lenz M, Vlachos A. Releasing the cortical brake by non-invasive electromagnetic stimulation? rTMS induces LTD of GABAergic neurotransmission. *Front Neural Circuits.* (2016) 10:96. doi: 10.3389/fncir.2016.00096
44. Spronk D, Arns M, Fitzgerald PB. Repetitive transcranial magnetic stimulation in depression: protocols, mechanisms and new developments. In: Cohen, Evans E, editors. *Neuromodulation and Neurofeedback: Techniques and Applications* (2010).

45. Hasler G, van der Veen JW, Tumonis T, Meyers N, Shen J, Drevets WC. Reduced prefrontal glutamate/glutamine and gamma-aminobutyric acid levels in major depression determined using proton magnetic resonance spectroscopy. *Arch Gen Psychiatry.* (2007) 64:193–200. doi: 10.1001/archpsyc.64.2.193
46. Hashimoto K. Emerging role of glutamate in the pathophysiology of major depressive disorder. *Brain Res Rev.* (2009) 61:105–23. doi: 10.1016/j.brainresrev.2009.05.005
47. Bernard R, Kerman IA, Thompson RC, Jones EG, Bunney WE, Barchas JD, et al. Altered expression of glutamate signaling, growth factor, and glia genes in the locus coeruleus of patients with major depression. *Mol Psychiatry.* (2011) 16:634–46. doi: 10.1038/mp.2010.44
48. Rosenberg DR, Macmaster FP, Mirza Y, Smith JM, Easter PC, Banerjee SP, et al. Reduced anterior cingulate glutamate in pediatric major depression: a magnetic resonance spectroscopy study. *Biol Psychiatry.* (2005) 58:700–4. doi: 10.1016/j.biopsych.2005.05.007
49. Auer DP, Putz B, Kraft E, Lipinski B, Schill J, Holsboer F. Reduced glutamate in the anterior cingulate cortex in depression: an *in vivo* proton magnetic resonance spectroscopy study. *Biol Psychiatry.* (2000) 47:305–13. doi: 10.1016/S0006-3223(99)00159-6
50. Chang L, Cloak CC, Ernst T. Magnetic resonance spectroscopy studies of GABA in neuropsychiatric disorders. *J Clin Psychiatry.* (2003) 64(Suppl. 3):7–14.
51. Lener MS, Niciu MJ, Ballard ED, Park M, Park LT, Nugent AC, et al. Glutamate and gamma-aminobutyric acid systems in the pathophysiology of major depression and antidepressant response to ketamine. *Biol Psychiatry.* (2017) 81:886–97. doi: 10.1016/j.biopsych.2016.05.005
52. Rosenberg DR, Mirza Y, Russell A, Tang J, Smith JM, Banerjee SP, et al. Reduced anterior cingulate glutamatergic concentrations in childhood OCD and major depression versus healthy controls. *J Am Acad Child Adolesc Psychiatry.* (2004) 43:1146–53. doi: 10.1097/01.chi.0000132812.44664.2d
53. Arnone D, Mumuni AN, Jauhar S, Condon B, Cavanagh J. Indirect evidence of selective glial involvement in glutamate-based mechanisms of mood regulation in depression: meta-analysis of absolute prefrontal neurometabolic concentrations. *Eur Neuropsychopharmacol.* (2015) 25:1109–17. doi: 10.1016/j.euroneuro.2015.04.016
54. Yuksel C, Ongur D. Magnetic resonance spectroscopy studies of glutamate-related abnormalities in mood disorders. *Biol Psychiatry.* (2010) 68:785–94. doi: 10.1016/j.biopsych.2010.06.016
55. Sanacora G, Treccani G, Popoli M. Towards a glutamate hypothesis of depression: an emerging frontier of neuropsychopharmacology for mood disorders. *Neuropharmacology.* (2012) 62:63–77. doi: 10.1016/j.neuropharm.2011.07.036
56. Mathews DC, Henter ID, Zarate CA. Targeting the glutamatergic system to treat major depressive disorder: rationale and progress to date. *Drugs.* (2012) 72:1313–33. doi: 10.2165/11633130-000000000-00000
57. Jaso BA, Niciu MJ, Iadarola ND, Lally N, Richards EM, Park M, et al. Therapeutic modulation of glutamate receptors in major depressive disorder. *Curr Neuropharmacol.* (2017) 15:57–70. doi: 10.2174/1570159X14666160321123221
58. Dubin MJ, Mao X, Banerjee S, Goodman Z, Lapidus KA, Kang G, et al. Elevated prefrontal cortex GABA in patients with major depressive disorder after TMS treatment measured with proton magnetic resonance spectroscopy. *J Psychiatry Neurosci.* (2016) 41:E37–45. doi: 10.1503/jpn.150223
59. Fogaca MV, Duman RS. Cortical GABAergic dysfunction in stress and depression: new insights for therapeutic interventions. *Front Cell Neurosci.* (2019) 13:87. doi: 10.3389/fncel.2019.00087
60. Maciag D, Hughes J, O'Dwyer G, Pride Y, Stockmeier CA, Sanacora G, et al. Reduced density of calbindin immunoreactive GABAergic neurons in the occipital cortex in major depression: relevance to neuroimaging studies. *Biol Psychiatry.* (2010) 67:465–70. doi: 10.1016/j.biopsych.2009.10.027
61. Bajbouj M, Lisanby SH, Lang UE, Danker-Hopfe H, Heuser I, Neu P. Evidence for impaired cortical inhibition in patients with unipolar major depression. *Biol Psychiatry.* (2006) 59:395–400. doi: 10.1016/j.biopsych.2005.07.036
62. Levinson AJ, Fitzgerald PB, Favalli G, Blumberger DM, Daigle M, Daskalakis ZJ. Evidence of cortical inhibitory deficits in major depressive disorder. *Biol Psychiatry.* (2010) 67:458–64. doi: 10.1016/j.biopsych.2009.09.025
63. Croarkin PE, Nakonezny PA, Husain MM, Melton T, Buyukdura JS, Kennard BD, et al. Evidence for increased glutamatergic cortical facilitation in children and adolescents with major depressive disorder. *JAMA Psychiatry.* (2013) 70:291–9. doi: 10.1001/2013.jamapsychiatry.24
64. Luborzewski A, Schubert F, Seifert F, Danker-Hopfe H, Brakemeier EL, Schlattmann P, et al. Metabolic alterations in the dorsolateral prefrontal cortex after treatment with high-frequency repetitive transcranial magnetic stimulation in patients with unipolar major depression. *J Psychiatr Res.* (2007) 41:606–15. doi: 10.1016/j.jpsychires.2006.02.003
65. Yang XR, Kirton A, Wilkes TC, Pradhan S, Liu I, Jaworska N, et al. Glutamate alterations associated with transcranial magnetic stimulation in youth depression: a case series. *J ECT.* (2014) 30:242–7. doi: 10.1097/YCT.0000000000000094
66. Peng Z, Zhou C, Xue S, Bai J, Yu S, Li X, et al. Mechanism of repetitive transcranial magnetic stimulation for depression. *Shanghai Arch Psychiatry.* (2018) 30:84–92.
67. Levitt JG, Kalender G, O'Neill J, Diaz JP, Cook IA, Ginder N, et al. Dorsolateral prefrontal gamma-aminobutyric acid in patients with treatment-resistant depression after transcranial magnetic stimulation measured with magnetic resonance spectroscopy. *J Psychiatry Neurosci.* (2019) 44:386–94. doi: 10.1503/jpn.180230
68. Davidson RJ, Pizzagalli D, Nitschke JB, Putnam K. Depression: perspectives from affective neuroscience. *Annu Rev Psychol.* (2002) 53:545–74. doi: 10.1146/annurev.psych.53.100901.135148
69. Drevets WC. Functional neuroimaging studies of depression: the anatomy of melancholia. *Annu Rev Med.* (1998) 49:341–61. doi: 10.1146/annurev.med.49.1.341
70. Anand A, Shekhar A. Brain imaging studies in mood and anxiety disorders: special emphasis on the amygdala. *Ann N Y Acad Sci.* (2003) 985:370–88. doi: 10.1111/j.1749-6632.2003.tb07095.x
71. Drevets WC. Neuroimaging and neuropathological studies of depression: implications for the cognitive-emotional features of mood disorders. *Curr Opin Neurobiol.* (2001) 11:240–9. doi: 10.1016/S0959-4388(00)00203-8
72. Koenigs M, Grafman J. The functional neuroanatomy of depression: distinct roles for ventromedial and dorsolateral prefrontal cortex. *Behav Brain Res.* (2009) 201:239–43. doi: 10.1016/j.bbr.2009.03.004
73. Brunoni AR, Vanderhasselt MA. Working memory improvement with non-invasive brain stimulation of the dorsolateral prefrontal cortex: a systematic review and meta-analysis. *Brain Cogn.* (2014) 86:1–9. doi: 10.1016/j.bandc.2014.01.008
74. Fitzgerald PB, Oxley TJ, Laird AR, Kulkarni J, Egan GF, Daskalakis ZJ. An analysis of functional neuroimaging studies of dorsolateral prefrontal cortical activity in depression. *Psychiatry Res.* (2006) 148:33–45. doi: 10.1016/j.pscychresns.2006.04.006
75. Grimm S, Beck J, Schuepbach D, Hell D, Boesiger P, Bermpohl F, et al. Imbalance between left and right dorsolateral prefrontal cortex in major depression is linked to negative emotional judgment: an fMRI study in severe major depressive disorder. *Biol Psychiatry.* (2008) 63:369–76. doi: 10.1016/j.biopsych.2007.05.033
76. Oh DH, Oh D, Son H, Webster MJ, Weickert CS, Kim SH. An association between the reduced levels of SLC1A2 and GAD1 in the dorsolateral prefrontal cortex in major depressive disorder: possible involvement of an attenuated RAF/MEK/ERK signaling pathway. *J Neural Transm.* (2014) 121:783–92. doi: 10.1007/s00702-014-1189-z
77. Michael N, Gosling M, Reutemann M, Kersting A, Heindel W, Arolt V, et al. Metabolic changes after repetitive transcranial magnetic stimulation (rTMS) of the left prefrontal cortex: a sham-controlled proton magnetic resonance spectroscopy (1H MRS) study of healthy brain. *Eur J Neurosci.* (2003) 17:2462–8. doi: 10.1046/j.1460-9568.2003.02683.x
78. Michael N, Erfurth A, Ohrmann P, Arolt V, Heindel W, Pfleiderer B. Metabolic changes within the left dorsolateral prefrontal cortex occurring with electroconvulsive therapy in patients with treatment resistant unipolar depression. *Psychol Med.* (2003) 33:1277–84. doi: 10.1017/S0033291703007931

79. Drevets WC, Price JL, Simpson JR, Jr., Todd RD, Reich T, et al. Subgenual prefrontal cortex abnormalities in mood disorders. *Nature.* (1997) 386:824–7. doi: 10.1038/386824a0
80. Alexopoulos GS, Hoptman MJ, Kanellopoulos D, Murphy CF, Lim KO, Gunning FM. Functional connectivity in the cognitive control network and the default mode network in late-life depression. *J Affect Disord.* (2012) 139:56–65. doi: 10.1016/j.jad.2011.12.002
81. Drevets WC, Price JL, Furey ML. Brain structural and functional abnormalities in mood disorders: implications for neurocircuitry models of depression. *Brain Struct Funct.* (2008) 213:93–118. doi: 10.1007/s00429-008-0189-x
82. Cummings JL. Frontal-subcortical circuits and human behavior. *Arch Neurol.* (1993) 50:873–80. doi: 10.1001/archneur.1993.00540080076020
83. Mayberg HS. Modulating dysfunctional limbic-cortical circuits in depression: towards development of brain-based algorithms for diagnosis and optimised treatment. *Br Med Bull.* (2003) 65:193–207. doi: 10.1093/bmb/65.1.193
84. Grimm S, Luborzewski A, Schubert F, Merkl A, Kronenberg G, Colla M, et al. Region-specific glutamate changes in patients with unipolar depression. *J Psychiatr Res.* (2012) 46:1059–65. doi: 10.1016/j.jpsychires.2012.04.018
85. American Psychatric Association. *Diagnostic and Statistical Manual of Mental Disorders*. 4th Text Rev ed. Washington, DC: American Psychatric Association (2000).
86. Downar J, Geraci J, Salomons TV, Dunlop K, Wheeler S, McAndrews MP, et al. Anhedonia and reward-circuit connectivity distinguish nonresponders from responders to dorsomedial prefrontal repetitive transcranial magnetic stimulation in major depression. *Biol Psychiatry.* (2014) 76:176–85. doi: 10.1016/j.biopsych.2013.10.026
87. Salomons TV, Dunlop K, Kennedy SH, Flint A, Geraci J, Giacobbe P, et al. Resting-state cortico-thalamic-striatal connectivity predicts response to dorsomedial prefrontal rTMS in major depressive disorder. *Neuropsychopharmacology.* (2014) 39:488–98. doi: 10.1038/npp.2013.222
88. Fitzgerald PB, Huntsman S, Gunewardene R, Kulkarni J, Daskalakis ZJ. A randomized trial of low-frequency right-prefrontal-cortex transcranial magnetic stimulation as augmentation in treatment-resistant major depression. *Int J Neuropsychopharmacol.* (2006) 9:655–66. doi: 10.1017/S1461145706007176
89. Januel D, Dumortier G, Verdon CM, Stamatiadis L, Saba G, Cabaret W, et al. A double-blind sham controlled study of right prefrontal repetitive transcranial magnetic stimulation (rTMS): therapeutic and cognitive effect in medication free unipolar depression during 4 weeks. *Prog Neuropsychopharmacol Biol Psychiatry.* (2006) 30:126–30. doi: 10.1016/j.pnpbp.2005.08.016
90. Gruetter R. Automatic, localized *in vivo* adjustment of all first- and second-order shim coils. *Magn Reson Med.* (1993) 29:804–11. doi: 10.1002/mrm.1910290613
91. Naressi A, Couturier C, Devos JM, Janssen M, Mangeat C, de Beer R, et al. Java-based graphical user interface for the MRUI quantitation package. *Magma.* (2001) 12:141–52. doi: 10.1007/BF02668096
92. Bhattacharyya PK, Phillips MD, Stone LA, Bermel RA, Lowe MJ. Sensorimotor cortex gamma-aminobutyric acid concentration correlates with impaired performance in patients with MS. *AJNR Am J Neuroradiol.* (2013) 34:1733–9. doi: 10.3174/ajnr.A3483
93. Pijnappel WWF, Van den Boogaart A, De Beer R, Van Ormondt D. SVD-based quantification of magnetic resonance signals. *J Magn Reson.* (1992) 97:122–4. doi: 10.1016/0022-2364(92)90241-X
94. Vanhamme L, van den Boogaart A, Van Huffel S. Improved method for accurate and efficient quantification of MRS data with use of prior knowledge. *J Magn Reson.* (1997) 129:35–43. doi: 10.1006/jmre.1997.1244
95. Chang L, Jiang CS, Ernst T. Effects of age and sex on brain glutamate and other metabolites. *Magn Reson Imaging.* (2009) 27:142–5. doi: 10.1016/j.mri.2008.06.002
96. Salvadore G, van der Veen JW, Zhang Y, Marenco S, Machado-Vieira R, Baumann J, et al. An investigation of amino-acid neurotransmitters as potential predictors of clinical improvement to ketamine in depression. *Int J Neuropsychopharmacol.* (2012) 15:1063–72. doi: 10.1017/S1461145711001593
97. Mescher M, Merkle H, Kirsch J, Garwood M, Gruetter R. Simultaneous *in vivo* spectral editing and water suppression. *NMR Biomed.* (1998) 11:266–72. doi: 10.1002/(SICI)1099-1492(199810)11:6<266::AID-NBM530>3.0.CO;2-J
98. Terpstra M, Ugurbil K, Gruetter R. Direct *in vivo* measurement of human cerebral GABA concentration using MEGA-editing at 7 Tesla. *Magn Reson Med.* (2002) 47:1009–12. doi: 10.1002/mrm.10146
99. Milak MS, Proper CJ, Mulhern ST, Parter AL, Kegeles LS, Ogden RT, et al. A pilot *in vivo* proton magnetic resonance spectroscopy study of amino acid neurotransmitter response to ketamine treatment of major depressive disorder. *Mol Psychiatry.* (2016) 21:320–7. doi: 10.1038/mp.2015.83
100. Cleve M, Gussew A, Reichenbach JR. *In vivo* detection of acute pain-induced changes of GABA+ and Glx in the human brain by using functional 1H MEGA-PRESS MR spectroscopy. *Neuroimage.* (2015) 105:67–75. doi: 10.1016/j.neuroimage.2014.10.042
101. de la Fuente-Sandoval C, Reyes-Madrigal F, Mao X, Leon-Ortiz P, Rodriguez-Mayoral O, Solis-Vivanco R, et al. Cortico-striatal GABAergic and glutamatergic dysregulations in subjects at ultra-high risk for psychosis investigated with proton magnetic resonance spectroscopy. *Int J Neuropsychopharmacol.* (2015) 19:pyv105. doi: 10.1093/ijnp/pyv105
102. Yang XR, Langevin LM, Jaworska N, Kirton A, Lebel RM, Harris AD, et al. Proton spectroscopy study of the dorsolateral prefrontal cortex in youth with familial depression. *Psychiatry Clin Neurosci.* (2016) 70:269–77. doi: 10.1111/pcn.12392
103. Mikkelsen M, Barker PB, Bhattacharyya PK, Brix MK, Buur PF, Cecil KM, et al. Big GABA: edited MR spectroscopy at 24 research sites. *Neuroimage.* (2017) 159:32–45. doi: 10.1016/j.neuroimage.2017.07.021
104. Ramadan S, Lin A, Stanwell P. Glutamate and glutamine: a review of *in vivo* MRS in the human brain. *NMR Biomed.* (2013) 26:1630–46. doi: 10.1002/nbm.3045
105. Goto N, Yoshimura R, Kakeda S, Nishimura J, Moriya J, Hayashi K, et al. Six-month treatment with atypical antipsychotic drugs decreased frontal-lobe levels of glutamate plus glutamine in early-stage first-episode schizophrenia. *Neuropsychiatr Dis Treat.* (2012) 8:119–22. doi: 10.2147/NDT.S25582
106. Bhattacharyya PK. Macromolecule contamination in GABA editing using MEGA-PRESS should be properly accounted for. *Neuroimage.* (2014) 84:1111–2. doi: 10.1016/j.neuroimage.2013.08.050
107. Ahdab R, Ayache SS, Brugieres P, Goujon C, Lefaucheur JP. Comparison of "standard" and "navigated" procedures of TMS coil positioning over motor, premotor and prefrontal targets in patients with chronic pain and depression. *Neurophysiol Clin.* (2010) 40:27–36. doi: 10.1016/j.neucli.2010.01.001

Conflict of Interest: The authors declare that the research was conducted in the absence of any commercial or financial relationships that could be construed as a potential conflict of interest.

Publisher's Note: All claims expressed in this article are solely those of the authors and do not necessarily represent those of their affiliated organizations, or those of the publisher, the editors and the reviewers. Any product that may be evaluated in this article, or claim that may be made by its manufacturer, is not guaranteed or endorsed by the publisher.

Advantages of publishing in Frontiers

OPEN ACCESS
Articles are free to read for greatest visibility and readership

FAST PUBLICATION
Around 90 days from submission to decision

HIGH QUALITY PEER-REVIEW
Rigorous, collaborative, and constructive peer-review

TRANSPARENT PEER-REVIEW
Editors and reviewers acknowledged by name on published articles

Frontiers
Avenue du Tribunal-Fédéral 34
1005 Lausanne | Switzerland

Visit us: www.frontiersin.org
Contact us: frontiersin.org/about/contact

REPRODUCIBILITY OF RESEARCH
Support open data and methods to enhance research reproducibility

DIGITAL PUBLISHING
Articles designed for optimal readership across devices

FOLLOW US
@frontiersin

IMPACT METRICS
Advanced article metrics track visibility across digital media

EXTENSIVE PROMOTION
Marketing and promotion of impactful research

LOOP RESEARCH NETWORK
Our network increases your article's readership